

Draft November 13, 2018

The *Chandra* ACIS Survey of M 33 (ChASeM33): The final source catalog

R. Tüllmann¹, T. J. Gaetz¹, P. P. Plucinsky¹, K. D. Kuntz^{2,3}, B. F. Williams⁴, W. Pietsch⁵, F. Haberl⁵, K. S. Long⁶, W. P. Blair², M. Sasaki⁷, P. F. Winkler⁸, P. Challis¹, T. G. Pannuti⁹, R. J. Edgar¹, D. J. Helfand¹⁰, J. P. Hughes¹¹, R. P. Kirshner¹, T. Mazeh¹², and A. Shporer^{13,14}

ABSTRACT

This study presents the final source catalog of the *Chandra* ACIS Survey of M 33 (ChASeM33). With a total exposure time of 1.4 Ms, ChASeM33 covers

¹Harvard-Smithsonian Center for Astrophysics, 60 Garden Street, Cambridge, MA 02138; rtuellmann@cfa.harvard.edu

²Department of Physics and Astronomy, Johns Hopkins University, 3400 North Charles Street, Baltimore, MD 21218

³NASA Goddard Space Flight Center, Code 662, Greenbelt, MD 20771

⁴Astronomy Department, University of Washington, Seattle, WA 98195

⁵Max-Planck-Institut für Extraterrestrische Physik, Giessenbachstraße, 85741 Garching, Germany

⁶Space Telescope Science Institute, 3700 San Martin Drive, Baltimore, MD 21218

⁷Institut für Astronomie und Astrophysik, Eberhard Karls Universität, Tübingen, Germany

⁸Department of Physics, Middlebury College, Middlebury, VT 05753

⁹Space Science Center, 235 Martindale Drive, Morehead State University, Morehead, KY 40351

¹⁰Columbia Astrophysics Laboratory, 550 W. 120th St., New York, NY 10027

¹¹Department of Physics and Astronomy, Rutgers University, 136 Frelinghuysen Road, Piscataway, NJ 08854-8019

¹²School of Physics and Astronomy, Raymond and Beverly Sackler Faculty of Exact Sciences, Tel Aviv University, Tel Aviv, Israel 69978

¹³Las Cumbres Observatory Global Telescope Network, 6740 Cortona Drive, Santa Barbara, CA 93117, USA

¹⁴Department of Physics, Broida Hall, University of California, Santa Barbara, CA 93106, USA

~70% of the D_{25} isophote ($R \approx 4.0$ kpc) of M 33 and provides the deepest, most complete, and detailed look at a spiral galaxy in X-rays. The source catalog includes 662 sources, reaches a limiting unabsorbed luminosity of $\sim 2.4 \times 10^{34}$ erg s $^{-1}$ in the 0.35–8.0 keV energy band, and contains source positions, source net counts, fluxes and significances in several energy bands, and information on source variability. The analysis challenges posed by ChASeM33 and the techniques adopted to address these challenges are discussed. To constrain the nature of the detected X-ray source, hardness ratios were constructed and spectra were fit for 254 sources, followup MMT spectra of 116 sources were acquired, and cross-correlations with previous X-ray catalogs and other multi-wavelength data were generated. Based on this effort, 183 of the 662 ChASeM33 sources could be identified. Finally, the luminosity function for the detected point sources as well as the one for the X-ray binaries in M 33 is presented. mk78The luminosity functions in the soft band (0.5–2.0 keV) and the hard band (2.0–8.0 keV) have a limiting luminosity at the 90% completeness limit of 4.0×10^{34} erg s $^{-1}$ and 1.6×10^{35} erg s $^{-1}$ (for $D = 817$ kpc), respectively, which is significantly lower than what was reported by previous X-ray binary population studies in galaxies more distant than M33. The resulting distribution is consistent with a dominant population of high mass X-ray binaries as would be expected for M33.

Subject headings: surveys — binaries: general — galaxies: individual (M 33) — supernova remnants — X-rays: galaxies

1. Introduction

The *Chandra* ACIS survey of M33 (ChASeM33) is a very deep X-ray survey of M 33, the nearest late-type face-on spiral galaxy, comprising a total of 1.4 Ms of observing time. M 33 is located at a distance of about 817 kpc (Freedman et al. 2001) and is viewed at an intermediate inclination angle of $i = 56^\circ \pm 1^\circ$ (Zaritsky et al. 1989). The corresponding Galactic foreground column density is $N_H = 6.0 \times 10^{20}$ cm $^{-2}$ (Dickey & Lockman 1990) which is relatively low. These properties make M 33 a prime target to exploit *Chandra*'s high spatial resolution to gain new insights on the X-ray properties and the evolution of spiral galaxies. A detailed discussion of ChASeM33, its scientific goals, the survey layout as well as the observing strategy was provided by Plucinsky et al. (2008). They also provided initial science results based on the data collected during the first half of the observing cycle (from September 2005 through July 2006), such as the first version of the X-ray source catalog, hardness ratios of the X-ray sources, and an evaluation of the diffuse X-ray emission

in the giant H II region NGC 604 and of the X-ray emitting SNRs in the southern spiral arm.

In the present study, we make use of all ChASeM33 observations and two archival observations to generate the final ChASeM33 point source catalog of M33. The full survey covers about 70% of the area enclosed by the D_{25} B-band isophote (Fig. 1) and reaches a radial angular extent of $\sim 18'$ which corresponds to ~ 4 kpc for the assumed distance to M33. Our survey attains an unabsorbed limiting luminosity of 2.4×10^{34} erg s $^{-1}$ in the 0.35–8.0 keV energy band which makes ChASeM33 the deepest and spatially best resolved X-ray survey of any galaxy so far.

The X-ray source population of M33 was first surveyed by the *Einstein* X-ray observatory (Long et al. 1981; Markert & Rallis 1983; Trinchieri et al. 1988), revealing 17 sources and a significant diffuse component to the emission. Subsequent observations carried out with *ROSAT* increased the number of known X-ray sources significantly (Schulman & Bregman 1995; Long et al. 1996) culminating in the catalog provided by Haberl & Pietsch (2001, HP01 hereafter) of 184 discrete X-ray sources located within 50' of the nucleus to a limiting unabsorbed luminosity $L_X(0.12 - 2.48 \text{ keV}) \approx 2 \times 10^{35}$ erg s $^{-1}$. The more recent *XMM-Newton* surveys from Pietsch et al. (2004, PMH04 hereafter) and Misanovic et al. (2006, MPH06 hereafter) cover sources located within a radius of $\sim 32'$ from the center of the galaxy, raised the total number of sources detected within the M33 field of view (FOV) to 447 and reached a limiting unabsorbed luminosity as low as $L_X(0.2 - 4.5 \text{ keV}) \approx 1 \times 10^{35}$ erg s $^{-1}$. Lastly, an initial study of 261 discrete X-ray sources detected by *Chandra* towards M33 – for a field that covered a 0.16 square degree region including the center of the galaxy (ObsIDs 786, and 1730) and a field northwest of the center which covers the giant H II region NGC604 (ObsID 2023) – was provided by Grimm et al. (2005, G05 hereafter). The limiting unabsorbed luminosity claimed by G05 is $L_X(0.35 - 8.0 \text{ keV}) \approx 2 \times 10^{34}$ erg s $^{-1}$ which is comparable to our survey's limit, because G05 used a lower significance threshold for their source detection. A brief overview of the previous X-ray surveys of M33 is presented in Table 1.

The limiting luminosity attained by ChASeM33 is significantly lower than that for comparable surveys of other galaxies, such as the *ROSAT* surveys of the Local Group galaxy M31 (Capaccioli et al. 1989; Supper et al. 2001), the Small Magellanic Cloud (SMC, Kahabka et al. 1999) and the *Chandra* surveys of spiral galaxies located outside of the Local Group, such as M101 (Pence et al. 2001; Kuntz & Snowden 2010).

For all of these surveys, a significant number of background AGN and foreground stars were detected which contaminated the sources that are in fact native to M33, such as X-ray binaries (XRBs), supersoft sources (SSSs) or SNRs. Perhaps with the exception of *Chandra*, the relatively poor spatial resolution of the aforementioned X-ray satellites has certainly introduced a severe source confusion bias into the existing data which also hampered the

cross-correlation of the X-ray sources with those observed at different wavelengths. In M 33 this is particularly true for regions where source crowding is an issue, such as the nucleus and NGC604. Therefore, for a reliable source identification which might ultimately affect the shape of the luminosity function (LF) of the discrete sources, high spatial resolution is essential.

Before and after the publication of the ChASeM33 firstlook paper by Plucinsky et al. (2008) our collaboration exploited this complex data set and published results related to the primary objectives of ChASeM33. These are: (1) an investigation of the SNR population in M 33 (Gaetz et al. 2007; Long et al. 2010), (2) the establishment of the morphology and physical parameters of extended sources such as the giant H II-regions NGC 604, and IC 131 as well as the large-scale hot gas in the spiral arms (Tüllmann et al. 2008, 2009; Kuntz et al. 2011), (3) the detection and analysis of X-ray binaries (Pietsch et al. 2006, 2009) and transient sources (Williams et al. 2008), and (4) the detection of all X-ray sources down to the sensitivity limit and the location of possible counterparts including stars and background AGN (Plucinsky et al. 2008). The searches for such counterparts help us to identify and properly classify X-ray sources unassociated with M 33, which in turn allows us to construct the intrinsic X-ray LF of M 33. In the present paper, we concentrate on science objective (4).

The organization of this paper is as follows. In Section 2 we provide detailed information on data reduction and on the generation of the final source catalog. Although this paper concentrates on the discrete X-ray sources in M 33, we also discuss the criteria which need to be met to classify a source as “extended” (Sect. 2.3.2). In Section 3 the main results of our survey are presented and discussed, covering topics ranging from basic source properties (3.1), a source cross-correlation with other catalogs (3.2), hardness ratios (3.3), an analysis of time variable (3.4) and supersoft sources (3.5), a spectral X-ray analysis of the 15 brightest sources (3.6), to the X-ray LF and radial source distribution of M 33 (3.7). The paper concludes with a summary and the main conclusions in Section 4.

2. Observations and Data Reduction

2.1. Observations

ChASeM33 was designed to provide two uninterrupted observations of the seven survey fields, each with an integration time of 100 ks (see Plucinsky et al. 2008, for details). The individual observations per field were separated by 5–13 months depending on field to allow for an investigation of the time variability of the X-ray sources. In some cases, as for example

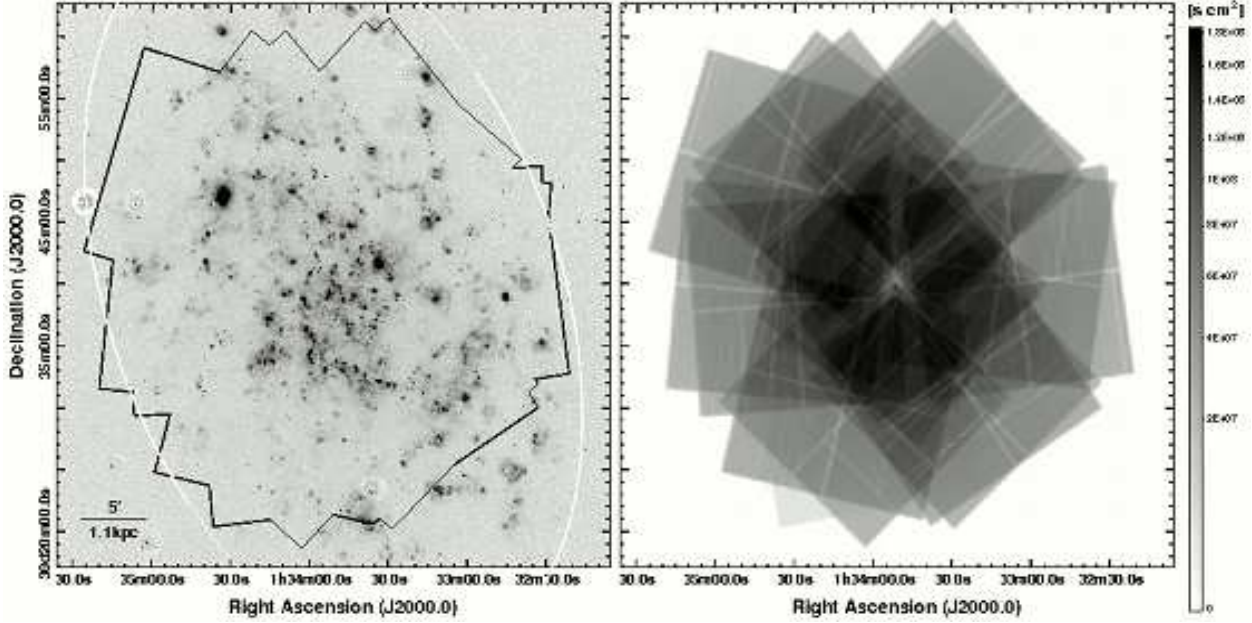


Fig. 1.— Left panel: Total coverage (black solid line) of the ChASeM33 and archival pointings together with the D_{25} ellipse are shown on an continuum-subtracted H α image (McNeil & Winkler 2006). Right panel: Merged exposure map shown on a square root scale in the 0.35 – 8.0 keV energy band. Only ACIS-I CCDs 0-3 have been used for the analysis.

for Fields 5 and 6, scheduling constraints required a larger number of shorter observations. In addition to the ChASeM33 observations, we also utilized two archival ACIS-I observations of M33 (ObsIDs 1730 and 2023), one centered on the nucleus and one centered on the giant H II region NGC 604. The results presented here use the full survey data obtained during September 2005 to November 2006. All observations were performed with ACIS-I as the primary instrument in VFAINT mode, except ObsID 2023 which was observed in FAINT mode. The coverage of the survey is shown in Fig. 1 together with the merged exposure map of the ChASeM33 and the archival ACIS-I observations 1730 and 2023. The exposure map was binned by 1 pixel (or $0''.492$). A journal of observations is given in Table 2.

As can be seen from Fig. 1, the merged exposure map is non-uniform due to different pointing directions and roll angles with a relative minimum at the center of the field of view. This minimum occurs because only Field 1 and ObsID 1730 cover the central part of M33; the other observations either omit this area or the area around the nucleus was later masked out (see below).

The merging process combines source data from different off-axis angles for which the point spread function (PSF), response, and effective area may all be significantly different. It

is therefore possible that the sensitivity and angular resolution for such sources is significantly degraded and requires that the source detection and characterization be done not only on the merged data, but on the individual fields and epochs as well. For extracting the final source catalog only data from the ACIS-I chips I0-I3 were included because the best imaging performance was essential to achieve the highest sensitivity to point sources. The S-array CCDs (S2 & S3) were sufficiently far off-axis to suffer from reduced sensitivity and severe source crowding.

2.2. Data Reduction

Data reduction was carried out with CIAO v4.0.1 and CALDB v3.4.2. The first step in processing the data was the visual inspection, identification, and rejection of spurious features such as hot pixels and bad columns in the level=1 eventlists and bias maps. None of the M33 data sets showed any of the rare large-scale distortions of the bias maps. We decided to generate our own bad pixel files as the standard bad column screening applied by the pipeline to the level=1 data products appeared to be too aggressive. In contrast to the diffuse X-ray emission, point sources typically have much smaller extraction regions and higher signal-to-noise (S/N) ratios. Therefore, a less conservative bad column screening with a slightly higher background should not seriously affect the source statistics, but would restore a significant fraction of the chip for source detection. We considered all warm columns which contributed more than 10% to the total counts within a column of a source’s extraction region for a given epoch to be ‘bad’, i.e., a threshold of $85 \text{ cts col}^{-1} 100 \text{ ks}^{-1}$ for the front illuminated chips (I-array) had to be exceeded. The observation-specific bad pixel files were updated with the new bad column lists and as a result 3%–15% of the chip area which was previously contained in “warm” columns could be put back into the eventlists, including the neighboring columns next to the ones previously flagged as ‘bad’.

We next ran `acis_process_events`, filtered on the background flags for the VFAINT mode to improve the background rejection efficiency, corrected for bad pixels/columns, charge transfer inefficiency (CTI), and time-dependent gain variations, and removed the pixel randomization. The eventlist was then filtered for grades=0,2,3,4,6, status=0, and pipeline-provided good time intervals. Next, we checked for background flares by creating a background light curve from the source-free eventlists of the ACIS-I3 chip. We applied an iterative sigma-clipping algorithm (`lc_clean`¹) to remove time intervals with count rates more than 3σ from the mean of each iteration, until all count rates were less than 3σ above

¹see http://cxc.harvard.edu/ciao/ahelp/lc_clean.py.html

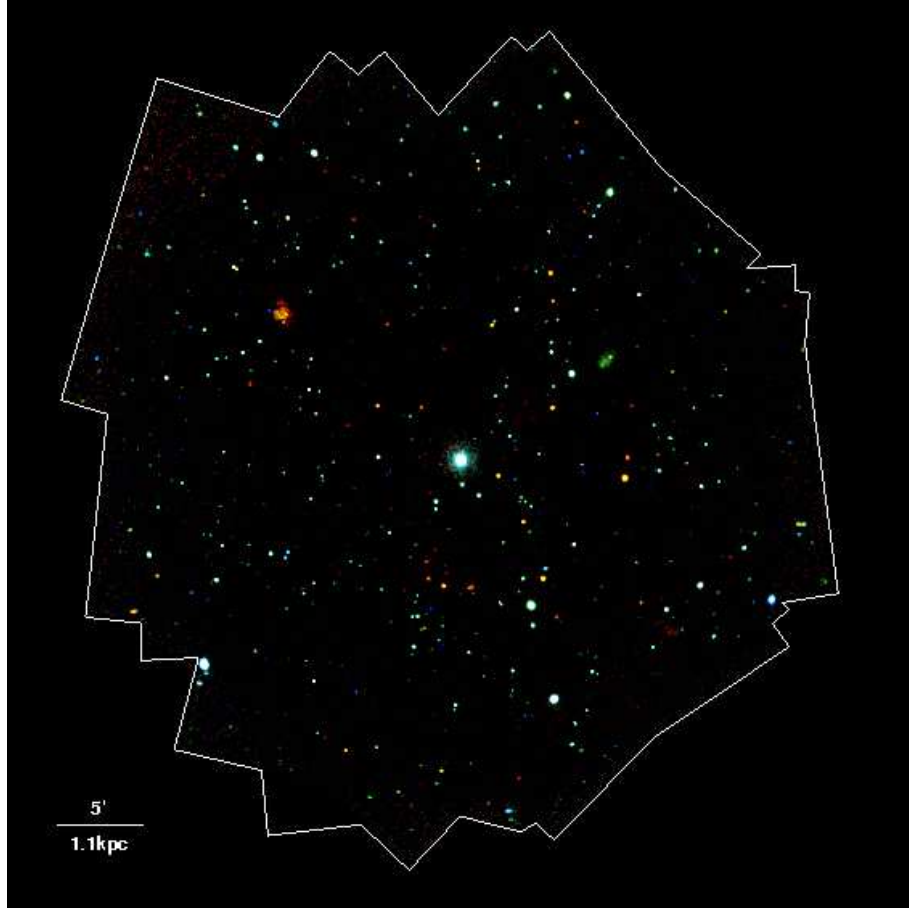


Fig. 2.— Multicolor exposure-corrected X-ray mosaic constructed from the full survey data. Red represents soft X-ray emission in the 0.35–1.0 keV energy band, green represents medium hard X-rays (1.0–2.0 keV), and blue denotes hard X-rays in the range of 2.0–8.0 keV.

the mean. The resulting effective exposure times are listed in the last column of Table 2. The same steps were also applied to ObsID 2023, except that `check_vf_pha` was set to 'no'. All ObsIDs were checked for known processing offsets in the aspect solution using the aspect corrector² and any offsets found were corrected.

Transfer streaks from bright sources were removed from the individual level=2 event lists by masking out appropriately-sized regions. If a source was affected by the transfer streak in one of the observations, the analysis for this source was carried out without that observation. The resulting event lists were merged for each epoch (e1, e2) and field (e1+e2,

²http://cxc.harvard.edu/ciao/threads/arcsec_correction/index.html#aspcalc

see Table 2) and images were created in the following energy bands (keV): 0.35–8.0, 0.35–1.0, 1.0–2.0, 2.0–8.0 with bin sizes of 1, 2, 3, and 4. To create exposure-corrected images, appropriate exposure maps were constructed using `mkinstmap` and `mkexpmap` in CIAO using the same mask regions as for the corresponding event lists. For the instrument maps, spectral weights were computed assuming a power-law spectrum with $\Gamma = 1.9$ that is typical of XRBs and AGN. An average N_{H} of $1 \times 10^{21} \text{ cm}^{-2}$ was assumed for the total line of sight H I column density (Newton 1980), while the absorption in M 33 was determined from a weighted 21 cm H I map (D. Thilker, priv. comm.) to be $\sim 0.4 \times 10^{21} \text{ cm}^{-2}$.

The composite X-ray image of M 33 is shown in Fig. 2. Soft X-rays (0.35–1.0 keV) are displayed in red, medium hard X-ray emission (1.0–2.0 keV) is shown in green, and hard X-rays (2.0–8.0 keV) are represented in blue. In addition to a large number of point sources, the most prominent feature in this image is the nucleus of M 33, M 33 X-8, a stellar black hole candidate which is the brightest steady ultra luminous X-ray source in the Local Group (e.g., Dubus et al. 2004; Weng et al. 2009). The extended reddish source to the NE is NGC 604, the second largest H II region in the Local Group (Tüllmann et al. 2008) and the elongated greenish emission to the NW of the nucleus is IC 131, an enigmatic giant H II region with an unusually hard X-ray spectrum (Tüllmann et al. 2009).

2.3. Source Catalog Creation

The general idea behind our source detection strategy is to use `wavdetect` (Freeman et al. 2002) to determine the positions of potential source candidates and to input these positions to `ACIS Extract` (Broos et al. 2002, AE hereafter), which is designed to determine the actual significance of a point source, allowing for variations in exposure time and PSF in different exposures. Therefore, we deliberately created an initial source list that included many more sources than we expected to be statistically significant. We applied an iterative procedure in which the source candidate list was filtered with increasing source significance thresholds and the output was checked for potentially lost sources. The screening process continued until only a small number of spurious sources was present in the final source list (see below for details).

2.3.1. Point sources

We used the CIAO tool `wavdetect` (Freeman et al. 2002) to identify candidate sources in an image by correlating it with a "Mexican Hat" wavelet function using different scale

sizes to account for sources located at different off-axis angles. For each scale size, the input image is correlated with the wavelet function and pixels with a sufficiently high correlation coefficient are removed as 'source' pixels (the removal of source pixels from the image is called "cleansing"). In order to decide on reasonable values for the source significance (*sigthresh*) and cleansing thresholds (*bkgthresh*), the maximum number of cleansing iterations per scale (*maxiter*), and spatial scale sizes (*scale*), we used fields 3 and 4 (epochs 1, 2, and 1+2, see Plucinsky et al. 2008, for their locations) as testbeds for a series of **wavdetect** runs in which we evaluated several combinations of these parameters. Based on these tests, we decided to run **wavdetect** with *sigthresh* = 10^{-4} , to include a substantial number of unreal sources (~ 100 per 1 Mpix) but also to catch all real sources, *bkgthresh* = 10^{-2} (see Freeman et al. 2002), and *maxiter* = 5, to avoid background contamination by additional source counts. All other parameters were left at their default values. If we, for example, would have chosen values for *sigthresh* $\leq 10^{-6}$, we would have lost a handful of potentially real sources (see also Nandra et al. 2005), which supports our decision to not let **wavdetect** do the source culling. We also tested to what extent different binnings affect the number of sources found by **wavdetect**. For this purpose it is important to keep in mind that the wavelet 'scales' match the pixel size for each binning. If we, e.g., wanted to search for sources with a radius of 4 pixels, we used *scales* = 4 and *bin* = 1, and compared the number of potential sources with the one for *scales* = 1 and *bin* = 4. We found that the 'bin=1(8), scale=64(8)' lists did not contain any additional statistically significant sources that were not already included in the lists with lower bin/scale sizes. However, up to 3 source candidates with 9–31 counts were detected in the remaining lists with higher bin sizes that were not in the lower binned data. Therefore, we chose to run **wavdetect** on images with bin sizes of 1, 2, 3, and 4 and *scale* sizes that ranged from 1 to 32 pixels (in a power-of-2 sequence) in each of the subbands. With these parameters we are also able to detect extended sources on spatial scales of up to $\sim 1'$ which are needed to include giant H II regions like NGC 604 or IC 131 (see Sect. 2.3.2).

As can be seen from the multicolor composite image shown in Fig.2, some sources show rather soft X-ray emission which is typical for SNRs, H II regions or supersoft sources. Others emit much harder X-rays as one would expect from AGN or X-ray binaries. Therefore, we ran the source detection in several energy bands that are tailored to the different kinds of sources. We adopted the following energy bands (in keV): 0.35-8.0, 0.35-1.0, 1.0-2.0, 2.0-8.0. Finally, we ran **wavdetect** on all ChASeM33 fields on each individual epoch (e1, e2, and e1+2) in four different energy bands and binnings as well as on the two archival fields (ObsIDs 1730, 2023), resulting in a total of 368 source candidate lists. Because many of the sources in the various lists are duplicates of one another and to save substantial processing time later in AE, the different **wavdetect** source candidate lists were merged sequentially according to the

following scheme: 1) Match the sources among different binnings of the same field, epoch, and energy, choosing for each source the position belonging to the detection at the smallest binning (this method assures the best centroiding of the source and the matching creates a single list for each energy of each epoch of each field). 2) Match the sources among different energies for the same field and epoch, choosing for each source the position belonging to the detection with the highest significance (detections with the highest significances tend to have the higher count rates with respect to the background, and thus better centroiding; a single list for each epoch of each field is created). 3) Match the sources among different epochs of the same field, choosing for each source the position belonging to the detection with the highest significance (this matching creates a single list for each field). 4) Match the sources among different fields/archival ObsIDs, choosing for each source the position belonging to the detection with the smallest PSF (this matching creates a single list for the entire galaxy).

PSF sizes and source significances were taken from `wavdetect` output (parameters `psf_size` and `src_significance`). The resulting merged `wavdetect` source list contained positions of about 9700 source candidates and was used as the input to `AE`.

`AE` is a multi-purpose source extraction and characterization tool which determines source and background count rates and calculates fluxes and source significances for all source candidates within a number of user-specified energy bands. Among other tasks, it also extracts and groups spectra, generates the appropriate response matrices, and constructs lightcurves and checks for time variability (see Broos et al. 2002, 2010, for details). An important feature of `AE` is its ability to produce source and background extraction regions by simulating the *Chandra* PSF at a given source position, i.e., off-axis and azimuthal angle. This capability is essential for sources in overlapping fields as for each individual observation a different extraction region is required in order to optimize the S/N for that source. Moreover, `AE` can shrink the source extraction regions so that they do not overlap. This is important when source crowding is an issue, as for example for the circumnuclear region or NGC 604.

For the ChASeM33 First Look Catalog (Plucinsky et al. 2008, FLC hereafter) we adopted a traditional S/N ratio estimate (`src_significance`) to distinguish between real and false source detections. Because this criterion seemed to be too conservative (a 3σ source had to have 15 counts in the case of infinitesimally low background and therefore biases the sample towards higher count rates), we have chosen the Poisson probability of not being a source (`prob_no_source`, `pns` hereafter) provided by `AE` as our new threshold criterion, which also takes the uncertainty of the local background estimate into account. `pns` represents the Poisson probability that all of the counts within the source extraction region are actually from the background, i.e., source candidates with low probabilities are most likely real sources

and vice versa. Source pruning was done by filtering the source candidate list iteratively with decreasing pns thresholds until a suitably low false source detection rate was reached. This false source detection rate was determined by a number of `wavdetect` and `AE` test runs on the eventlist for field 4 (epoch 2) from which all sources were removed and for which pixel coordinates were randomized, to smooth out possible residuals from the source removal and to get a uniform background. We determined that pns values around $\simeq 10^{-6}$ provided a suitably low false detection rate in agreement with the work of Nandra et al. (2005) and Georgakakis et al. (2008). We decided to adopt their value of $pns = 4 \times 10^{-6}$ which results in ~ 0.5 false detections per 1 Mpix.

As the source extraction and characterization in `AE` works only on eventlists we had to merge the aspect solution files for each field and epoch using the CIAO tools `dmmerge` and `dmsort`. Due to scheduling constraints, ObsID 7208, which is part of Field 6 epoch 1, has a significantly different roll angle and much lower exposure, which is why we decided to analyze this observation separately. The merging process substantially reduced the number of `AE` runs from 27 to 17. `AE` was run first on each individual field and epoch (including ObsIDs 1730, 2023, and 7208) using the full list of ~ 9700 sources and with no pns filter applied in order to get a first estimate of the pns value for each source candidate. Source and background extraction regions were created with the `ae_make_catalog` recipe, using 90% of the PSF at a primary energy of 1.49 keV ($psf_frac = 0.9$) and setting *mask_fraction* and *mask_multiplier* to 0.95, and 1.2, respectively. The latter two parameters control the size of the inner radius of the background region (see Broos et al. (2002) for details). The outer radius of the background annulus was allowed to expand until a minimum of 50 background counts in each background region was achieved (*min_num_cts* = 50). Next, `ae_standard_extraction` was executed which extracts the source eventlists and source and background spectra. Source properties, such as the pns and flux values, were computed in the 0.5–8.0, 0.5–2.0, 2.0–8.0, 0.35–8.0, 0.35–1.1, 1.1–2.6, 2.6–8.0, and 0.35–2.0 keV energy bands. These bands were adopted for the FLC (Plucinsky et al. 2008) and the ChASeM33 SNR catalog (Long et al. 2010, L10 hereafter); some of these bands were also used by other major X-ray surveys, such as ChaMP (Kim et al. 2007) and the CDF-N (Alexander et al. 2003). After that we applied the `/merge_observations` stage which generated a composite PSF for each source candidate from all observations, a merged spectrum, a merged auxiliary response file (ARF), a merged response matrix file (RMF), and a merged source eventlist. In the final step the `/collate_filename` stage was run which combined all source parameters and properties into a single FITS table (hereafter simply called output).

Due to the liberal choice of *sigthres* in `wavdetect`, the majority of sources in the full initial list are unreal and source crowding poses a serious issue. The vast number of sources seriously reduces the available background area and because of the large-scale diffuse X-

ray emission in M33, the average background could be artificially raised and result in a systematic underestimate of the p_{ns} value for every source. Therefore, the output from the first AE iteration was filtered with $p_{ns} = 10^{-2}$, a value of which we were certain that no real sources will be lost, and AE was run a second time to restore the background area and to get revised source properties. This filtered source list contained 1800 sources which is still a factor of ~ 5 higher than the total number of sources in the FLC and further filtering was applied as described below.

We overlaid the region files for each field generated by AE onto the corresponding eventlists and we checked if any obvious sources were missed or displaced as a consequence of the merging of the `wavdetect` source lists. It turned out that 8 sources were lost/displaced and all, except one, were detected by `wavdetect`, implying that they were lost during the merging process. The source candidate which was not detected by `wavdetect` was a special case, as it is a faint source more than 8' off-axis which is located between two very bright X-ray sources. The missed source was accounted for in the next AE run by adopting appropriate center coordinates. The displaced sources, however, raised doubts whether the adopted merging scheme for the `wavdetect` sourcelists was the correct one. Instead of using the position of the most significant source for merging the different bin sizes, we alternatively used the position of the lowest binning. Although this solved the issue with the missed sources, there were new cases for which the previous combination was more appropriate. We therefore decided to modify the positions of the source candidates by hand, which resulted in the repositioning of 36 relatively faint sources.

We also created thumbnail catalogs for all observations of each source and its neighbors and overplotted source and background regions together with the estimated p_{ns} value, net counts, and off-axis angle. By visually inspecting these catalogs, we deleted obviously misidentified source candidates, e.g., multiply identified sources or those for which the PSF contours were systematically offset from the obvious source position in one observation and which were not present in other observations. Both issues are residuals from the merging process where `wavdetect` source lists for different binnings and sources at different off-axis angles were combined. Even with a reduced number of 1800 source candidates, a handful of cases existed in which source crowding was an issue. This typically occurred in the off-axis data in which the PSF was larger than in the on-axis data. If a less-significant source was located close enough to a more significant source such that the extraction region of the more significant source was decreased to less than 66% of the PSF size, the less significant source was removed for that observation. The on-axis data for the less significant source were retained for the characterization of the source. In case a source looked dubious but was isolated and its extraction region did not affect neighboring sources, it was kept. The screening process removed a total of 154 sources from the AE output list and was done by three

team members individually in order to compensate for subjective biases. This approach was always used when source candidates had to be added, removed, or repositioned.

The nucleus, because of heavy pile-up, was treated specially. We included only the on-axis pointings for imaging, and only the off-axis pointings for the spectral analysis. In the on-axis Field 1 observations as well as in ObsID 1730 pile-up is most pronounced and the source has a highly peculiar “Mexican hat”-like shape. As a consequence, `wavdetect` reported 31 source candidates within a radius of $24''$, which almost all looked spurious. We therefore replaced all sources within that region with a single source region centered on the position of the nucleus and carried out a separate AE run on F1e1, F1e2, and ObsID 1730 with a p_{ns} value of 10^{-2} . Because of the pile-up and a heavily distorted PSF in the on-axis pointings, we cannot tell whether any of these replaced sources are real. For the separate AE run, 30 sources within $1.7'$ from the nucleus were considered and those which did not pass the p_{ns} threshold were removed from the source directory tree. This step fortunately removed the source crowding around the nucleus in the off-axis pointings (F4e2 and F6e1). As pile-up is less pronounced in these observations, the spectroscopic analysis of the nucleus was only carried out with these two off-axis pointings.

Next the full AE output was filtered with a $p_{ns} = 10^{-3}$ to further reduce source crowding and to remove other spurious sources, yielding 918 source candidates. Sources which did not pass the $p_{ns} = 10^{-3}$ filter were visually examined to ensure that potentially real sources (e.g., transient sources) were not erroneously removed. This number had to be trimmed down further as the source list still contained a substantial number of spurious source candidates. For the source screening process, the following nine energy bands were considered (in keV): $0.5 - 8.0$, $0.5 - 2.0$, $2.0 - 8.0$, $0.5 - 1.0$, $1.0 - 2.0$, $2.0 - 4.0$, $4.0 - 8.0$, $0.35 - 1.0$, and $0.35 - 8.0$. We decided to include a source if [1] the p_{ns} value in any of the nine energy bands is $\leq 10^{-5}$ for the combined data set or [2] the p_{ns} of a source which was rejected by [1] is $\leq 10^{-5}$ in any individual ObsID and in any of the nine energy bands. Criterion [2] should catch potential transient sources and by including the energy bands mentioned before, we account for different types of sources with different spectral energy distributions. If we would have considered merely the $0.35 - 8.0$ keV band, $\sim 3\%$ of significant sources would have been lost. A sanity check was carried out to ensure that no potentially real sources were missed by examining again those source candidates which did not pass the p_{ns} threshold. This latest screened list contained 721 source candidates. Further trimming was necessary as the visual inspection of the catalogs still indicated a significant number of false sources. We applied the same two p_{ns} criteria as mentioned above and ran AE with the final p_{ns} value of 4×10^{-6} . The analysis of the thumbnail images of those sources in the catalog and those who did not pass the final p_{ns} filter indicated, that no obvious source candidates were lost and that source crowding was no longer an issue. However, three more corrective actions were taken.

First, there were sources which were located at or which extended beyond the chip edges, so that only a fraction of the source photons was collected. The extraction regions of these far off-axis sources were heavily distorted and would have caused incorrect *pns* and flux values due to zero or strongly reduced exposure. Therefore, those observations were removed from the source directory tree, provided there was more than one observation left for this source. Second, sources on transfer streaks had to be dealt with. There were 9 sources covering, at least partly, the masked-out region of the transfer streaks. By narrowing down the width of the mask region, 4 sources could be fully restored and for the remaining 5 sources, we had to remove the corresponding observations from the source candidate list. Third, new source and background extraction regions for the extended sources in M33 had to be created in order to obtain proper estimates of the source properties (see Sect. 2.3.2 for details). With these modifications applied, AE was run a second time with a *pns* value of 4×10^{-6} , but this time enabling the `/fit_spectra` and `/timing` stages in AE.

As this source list has been tailored such that each source has proper extraction and background regions, we can now examine how the source properties, such as *flux2*³ and *net_cnts*, change if the number of background counts within the background extraction region increases from 50 to 100. This was tested by running AE on the final source list and setting *bkg_cnts* to 100 and comparing the results with the corresponding 50 counts source list. One general trend emerged, namely, sources with 100 counts in the background extraction region tended to have slightly higher source net counts and fluxes than the ones with 50 background counts. This could mean that the background is higher closer to the sources due to diffuse emission in M33. As the difference between the two AE test runs is < 10% and therefore less than the uncertainty in the flux calibration, we continued to work with *bkg_cnts* = 50.

Now that source crowding issues have been solved by iterative pruning of the source list and because the spatial resolution of *Chandra* will be unrivaled in the coming decades, we decided to spend extra time on improving source positions. For this purpose we ran the `/check_positions` stage of AE which provides three additional position estimates. Besides simply adopting the position from `wavdetect` (method catalog), a mean peak position is calculated by centroiding on the merged data (method mean), a correlation between the merged image and the merged PSF is carried out (method corr), and the merged image is reconstructed using a Maximum Likelihood algorithm and finding the peak in the reconstructed image (method ML, see Broos et al. 2002, for details). If the individual observations for a given source suggested different position estimates, the observation for which the source

³*flux2* computes the flux by assuming a mean ARF in the band of interest and dividing the net counts in that band by the mean ARF (see the AE manual for details)

was closest to on-axis and/or had the lowest p_{ns} was chosen to determine the position of the source. In case the estimates were very close to each other, the original position from `wavdetect` was kept and if none of the estimates was preferred, an appropriate position of the source’s center was determined by eye. In order to provide consistent results between L10 and this work, we adopted the same positions and extraction regions used by L10. The source repositioning required rerunning `ae_make_catalog`, `ae_standard_extraction` as well as the `/fit_spectra`, `/merge_observations`, and `/collated_filename` stages of AE.

The positional uncertainties provided by AE were sometimes unreasonably small ($\sim 0.01''$), since systematic errors such as aspect reconstruction are not considered. To achieve a more accurate positional uncertainty, we applied the following strategy: 1) If there is only one observation for a given source, the distances between the adopted catalog position and those suggested by the other three methods (mean, corr, ML) are calculated. The positional uncertainty is then simply the average distance to the catalog position. 2) If there are two or more observations for a given source, all observations are used to calculate the average distance for each position estimate with respect to the catalog position. The most discrepant position estimate is discarded and the average positional uncertainty is determined from the two remaining position estimates. 3) If the uncertainty is less than $0.5''$, the positional uncertainty was set to $0.5''$. This value is taken from the CXC absolute astrometric accuracy web page⁴ and also accounts for a possible systematic shift which might have been introduced by the merging of the different fields. To see how our astrometric accuracy compares to other X-ray catalogs, such as the ChaMP survey (Kim et al. 2007), we computed a histogram using the values for the positional uncertainties listed in column (5) of Table 3 and compared it to that provided by (Kim et al. 2007). Both histograms are in good agreement; their distribution peaks at $0.7''$, ours at $0.6''$ and also shows outliers well above $1''$. Our largest positional error of $3.5''$ is for a faint source (#179) that is far off-axis.

2.3.2. Extended sources

Although all sources in the catalog presented here were detected in our point source search, some of them are actually extended. Our approach to determining this was as follows: we used the energy-filtered eventlists (0.35-2keV), subtracted the point sources, created (if necessary) custom-made ellipse regions to include the remaining counts for those sources which showed obvious excess counts, and calculated the number of source counts from the polygon region (N_p) provided by AE and the total number of counts within the ellipse region

⁴<http://cxc.harvard.edu/cal/ASPECT/celmon/>

(N_e) .

A necessary condition for a source to be extended is that $\zeta = 1 - (N_p/N_e) > (1 - psf_frac)$ in epoch 1 or 2 ($psf_frac = 0.9$). However, for the source to be ‘confidently’ or ‘possibly’ extended, we calculate the 3σ uncertainty and include a term which accounts for the uncertainty within the PSF model (here set to 1%). Therefore, if $\zeta > 0.1 + 3\sqrt{d\zeta^2 + 0.01^2}$, with $d\zeta = \zeta\sqrt{1/N_p + 1/N_e}$, then the source is ‘confidently’ extended, else if $\zeta \leq 0.1 + 3\sqrt{d\zeta^2 + 0.01^2}$, the source is ‘possibly’ extended. If $\zeta \leq 0.1$ the source is not extended.

Most of the extended source candidates were observed multiple times, which means that they can have different extension flags. In the extreme case in one observation a source can be confidently extended, in another it could be not extended. We applied the following merging scheme if the sources had different flags in different observations: if the source was confidently/possibly extended (or vice versa), the source was flagged as possibly extended. If the source was not extended/possibly extended (or vice versa), the source was flagged as possibly extended. For all possibly and confidently extended sources in the FLC or in the SNR study (L10), we estimated an intrinsic source size using an elliptical region. To account for the varying PSF with off-axis angle and roll, the ellipse was “puffed out” using the appropriate AE-generated PSF polygon region (see L10 for more details on this procedure). These regions, together with new source and background eventlists and exposure maps replaced the original point source data. For consistency, we adopted the Long et al. regions for extended sources when available. In Table 9 (see Appendix A) the column labeled “Extended” flags each source either as not extended (=0), extended (=1), or possibly extended (=2). Among the 70 extended source candidates are the 23 extended SNRs listed in L10. L10 detected 82 (58) SNRs at 2σ (3σ). We did not detect all of them due to our initial requirement, that the source had to be detected as a point source.

It should be noted that the 3σ criterion plus a relatively low uncertainty in the PSF model (<5%) provides the best source classification compared to 3σ and 5σ criteria which neglect uncertainties in the PSF model. A 5σ -screening especially appears to be problematic as clearly extended objects would have been downgraded from confidently to possibly extended.

3. Results and Discussion

3.1. The Source Catalog

The final ChASeM33 source catalog contains 662 sources⁵. Their positions and properties, such as the source significances (p_{ns} values), net counts, and photon fluxes (in eight different energy bands) are listed in Tables 3, 4, 5, and 6. We will use this information to carry out a detailed spectral analysis of the 15 brightest X-ray sources (excluding the SNRs studied by L10 and X-7, the eclipsing XRB studied by Pietsch et al. (2006)), to create hardness ratio diagrams to learn about the different source populations in M 33 (SNRs, XRBs, etc.), and to create an X-ray LF. For the latter we first have to cross-reference the ChASeM33 sources with the other catalogs and observations from other wavelengths to screen out sources which are definitely not associated with M 33 and to identify sources which may be in M 33. Finally, we search for time-variable sources and supersoft X-ray sources.

3.2. Comparisons with other Catalogs and other Wavelengths

We cross-correlated the final ChASeM33 source catalog with the FLC, the *XMM-Newton* catalogs of M 33 from PMH04 and MPH06, the *Chandra* catalog from G05, the SNR catalog from L10, the 2MASS All-Sky Catalog of Point Sources (Cutri et al. 2003), and the USNO-B1.0 catalog (Monet et al. 2003). We also utilized optical follow-up spectroscopy of 116 X-ray sources obtained with the Hectospec spectrograph (Fabricant et al. 2008) attached to the MMT to search for and identify possible counterparts. Because there is a significant number of X-ray sources that are neither listed in the above catalogs, nor covered by our spectroscopic follow-up observations, we also used multi-wavelength imaging data to attempt to determine the nature of each source.

3.2.1. Comparison to other X-ray catalogs

Although the final ChASeM33 X-ray catalog and the earlier FLC are based on many of the same observations, the reduction and analysis techniques are very different. Of the 394 sources in the FLC, only one is missing from the current catalog, source FLC 191, which is in the highly confused nuclear region which we replaced by a single extraction region (cf. Sect. 2.3.1). Some of the FLC sources have substantial offsets from the current catalog

⁵The source catalog is also available in FITS format at: http://hea-www.harvard.edu/vlp_m33_public/

position as those sources were detected in FLC only at large off-axis angles. As a result, the positions reported here are to be preferred from those in the FLC.

There has been a substantial effort to observe the entire disk of M 33 with a somewhat shallower *XMM-Newton* survey by PMH04 and MPH06. Of the 233 sources listed by PMH04 which fall within the ChASeM33 FOV, 217 appear in our catalog. Of those that remain, 7 appear coincident with diffuse emission (PHM-89, 101, 125=IC 131, 170, 266, 299=NGC 604, and 365) but were detected as a single source. Three others are in regions with low *Chandra* exposure (280, 281, and 352). Of the remaining 6 PHM04 sources that ought to have been detected (52, 223, 245, 313, 328, and 332), all but one (PMH-245) have *XMM* fluxes near the detection limit of the PMH04 survey (10^{-15} erg s $^{-1}$ cm $^{-2}$) and may well be false detections. It appears likely that PMH-245 is a transient source.

Of the 39 sources in MPH06 that are not in PMH04, 26 fall in the ChASeM33 FOV. Of these, three match ChASeM33 sources. Two additional sources were associated with bright H II regions (one inside NGC604 and one in NGC595) where source crowding and confusion with the large-scale diffuse X-ray emission is an issue. Another four sources fall in regions with strong diffuse emission. None of the 17 remaining sources have obvious counterparts, diffuse or otherwise in the ChASeM33 data. Since the MPH06 catalog was constructed only from individual observations rather than stacked data, the detection limit is slightly higher. Of the 17 unmatched sources, about half are fainter than 2×10^{-15} erg s $^{-1}$ cm $^{-2}$, near the detection limit. The other half should have been detected in our survey, and hence are likely transient or variable sources.

We detect 211 of the 261 sources cataloged by G05 in their analysis of early *Chandra* observations of M 33. One source is covered by the S2 chip and therefore outside the ChASeM33 FOV. The remaining 49 source candidates have no obvious ChASeM33 counterparts, neither in the individual event lists, nor in the merged ones. As already discussed by Plucinsky et al. (2008), the main reason for this discrepancy is clearly the liberal source selection criteria chosen by G05 (they demanded only a detection by `wavdetect` at any significance level). Forty four of these 49 sources were filtered out during our iterative source pruning process while 5 sources were not even considered to be candidates in our `wavdetect` runs. It is therefore possible that most, if not all of the 49 sources listed in the G05 catalog are actually spurious sources. Moreover, the reason why the G05 survey, which is much shallower than ChASeM33, apparently reaches a similar limiting sensitivity is that G05 used source significances provided by `wavdetect`. The source with the lowest number of net counts in G05 is CXO J013400.7+304138, which has 1.7 net counts in the 2.0–8.0 keV band. The source was not detected by G05, neither in their soft band (0.3–2.0 keV) nor in their broad band (0.3–8.0 keV). There are other sources in the G05 catalog that have for example 2.8

and 2.9 net counts. Such sources did not pass our source significance threshold. Our results of the cross-correlation are summarized in Table 9.

3.2.2. Comparison with optical follow-up spectroscopy and other multi-wavelength data

The 662 sources represent a wide variety of objects, ranging from foreground stars to XRBs, SNRs, and H II regions in M 33, to background AGN. Most of the sources are faint, and therefore, to make progress in understanding the nature of the sources, we have begun an optical spectroscopy study of 116 of the 662 ChASeM33 sources using Hectospec, a fiber-fed spectrograph attached to the MMT. The fibers were positioned such, that, if there was an optical counterpart to the X-ray source, the fiber was put at the position of the optical source. If no optical emission was present the fiber was put down at the position of the X-ray source. The spectra cover the wavelength range from 3700Å to 9150Å and were obtained with a fiber diameter of 1''.5, which provides a resolution of 6.2Å. This resolution is sufficient to classify all of the spectroscopically observed sources. Standard data reduction techniques were applied and spectrophotometric standard stars were used to flux calibrate the spectra and to correct for the wavelength-dependent instrument response.

Since we do not yet have spectra of the majority of sources, we have also attempted to gain some idea of the nature of the sources by examining additional multi-wavelength data including archival imagery from *Spitzer* (3.6, 4.5, 5.8, 8.0 μ m), 2MASS (J, H, K), CFHT MegaCam (u, g, r), HST (f435w, f555w, f814w), data from the Local Group Galaxies Survey (LGGS, Massey et al. 2006), such as U, B, V, R, I, H α , [O III], and [S II] images, as well as archival *Galex* (NUV, FUV) and *Swift*/UVOT (UVW2, UVM2, UVW1) data.

The infrared data are sensitive to Milky Way stars, red giants, and associations of older stars in M 33, galaxies, and background AGN. Similarly, the USNO catalog is sensitive to Milky Way stars, compact clusters in M 33 and AGN, with the further selection that the USNO survey excludes the central disk of M 33. The high spatial resolution of the optical data, especially of the HST data, provides a sensitive tool to search for optical counterparts to the X-ray sources, while the UV emission is a good tracer of the young stellar population in M 33 and of AGN-type background sources.

Combining the results from the spectral analysis and the imaging analysis, we divided the X-ray sources with counterparts into the following seven groups: (1) foreground stars (FSs), (2) stellar sources in M 33 (i.e. objects with star-like spectra, such as stellar associations), (3) QSOs/AGN (sources with broad and redshifted emission lines), (4) galaxies (i.e. obviously extended sources with redshifted emission lines, but no broadened emission

line components as typically seen in QSOs/AGN), (5) XRBs (including known XRBs and XRB candidates from HP01, PMH04, MHP06, and W08), (6) SNRs (SNR-like spectra, to be distinguished from H II regions by significantly stronger [S II] emission lines), and (7) non-stellar sources (everything which is not classified as stellar, but looked extended in the LGGS/MCam/HST data and did not match any of the other classes).

As a result of this effort, we have suggested classifications for 183 ChASeM33 sources. Among them are 23 foreground stars, 40 stellar sources (of which 2 are classified as globular clusters, GC hereafter), 20 QSOs and AGN, 21 galaxies, 14 XRBs, 45 SNRs (those from L10), and 20 non-stellar objects (see Table 9, column “Source type” for details). Considering the uncertainty associated with the positional coincidence of a source at X-ray and at other wavelengths, we do not expect every source to be classified correctly. However, we are confident that the bulk of sources are identified correctly. Fig. 3 shows the spatial distribution of the afore mentioned source classes across the FOV. The distribution of SNRs nicely follows the spiral arms of M 33, while the observed AGN candidates seem to be located in the outskirts of this galaxy. We have optical spectra for all stellar sources, except one GC source, and it is conceivable that there is a significant number of XRBs among the 39 sources whose spectra are indistinguishable from other stellar sources.

A clear separation between foreground stars and sources with stellar-like spectra (e.g., globular clusters or star-forming regions in M 33) and background AGN can be accomplished by plotting X-ray to optical flux ratios vs. X-ray colors as shown in Fig. 4. These plots contain 229 of the 662 ChASeM33 sources and are those for which an optical counterpart could be identified.

We note that there may be a small systematic shift between the coordinate systems of the ChASeM33 catalog and the other surveys mentioned above. These shifts are below the typical ChASeM33 source positional error of $0.^{\circ}5$, and could arise from small (some $0.^{\circ}1$), systematic positional errors of each data set. Based on sources with well known optical counterparts in the LGGS, we find that the ChASeM33 positions are systematically offset by $-0.^{\circ}4$ in RA and $-0.^{\circ}2$ in Dec relative to the LGGS ones. We also cross-correlated ChASeM33 with the USNO-B1.0 and 2MASS All Sky point source catalogs (48 and 78 matches, respectively). The mean offset between the ChASeM33 sources and the matched USNO (2MASS) sources was $\Delta\text{RA} = 0.^{\circ}12$ ($0.^{\circ}11$) and $\Delta\text{dec} = -0.^{\circ}06$ ($-0.^{\circ}07$), respectively.

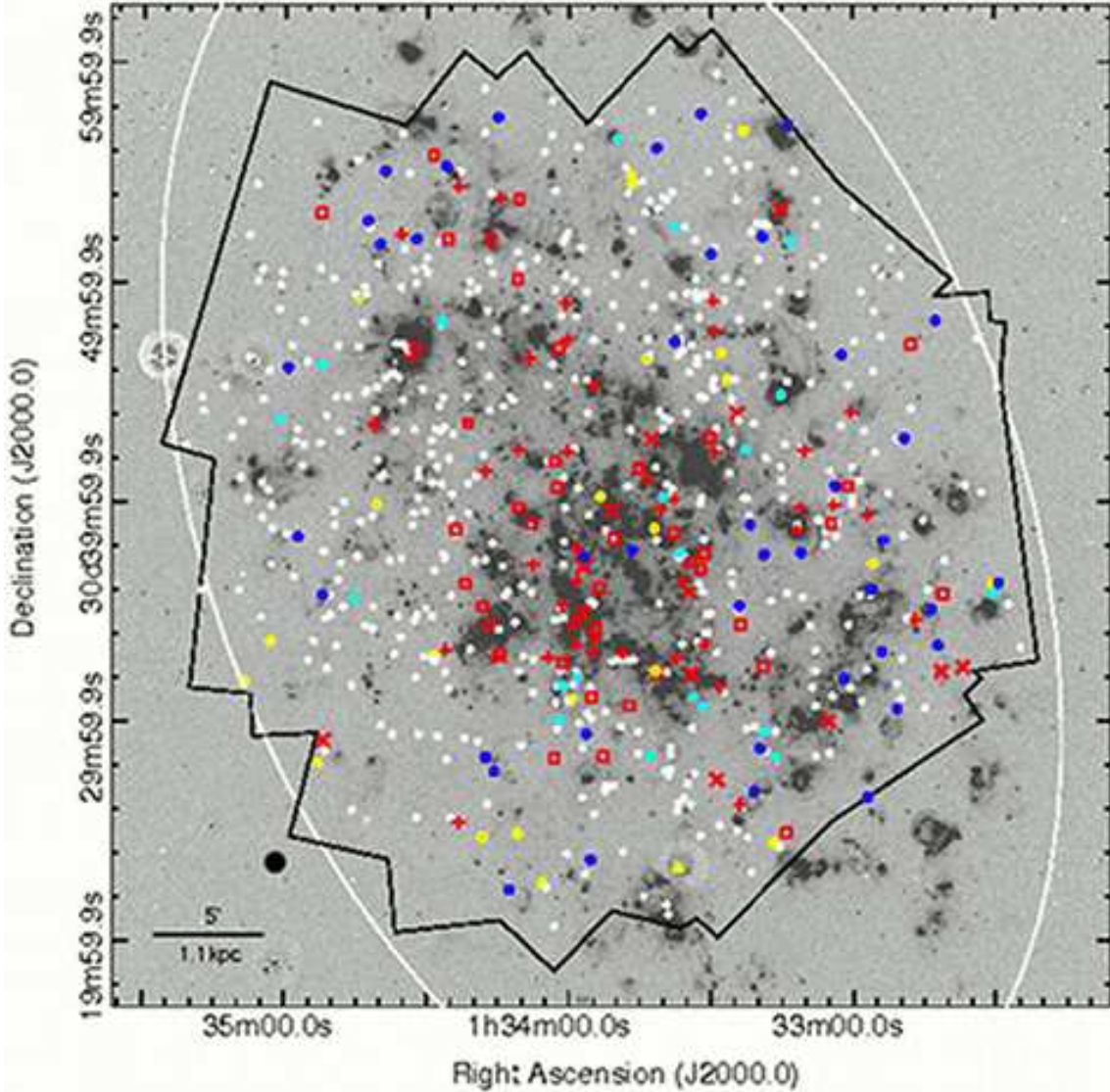


Fig. 3.— ChASeM33 sources overplotted on the same image as shown in the left panel of Fig. 1. Red sources are considered to be located in M 33 (crosses represent SNRs from L10, “x” symbols are known XRBs and XRB candidates, and squares are stellar sources). Blue circles stand for QSOs, AGN, and background galaxies, cyan circles are for non-stellar sources, yellow circles represent FSs, and unidentified sources are plotted in white.

3.2.3. Comparison with sources in globular clusters

Given the long-standing interest in the X-ray globular cluster LF for spiral galaxies, we attempted to find the discrete X-ray sources associated with GCs by cross-correlating our source list with the (mostly non-overlapping) catalogs of GCs in M 33 from Sarajedini & Mancone

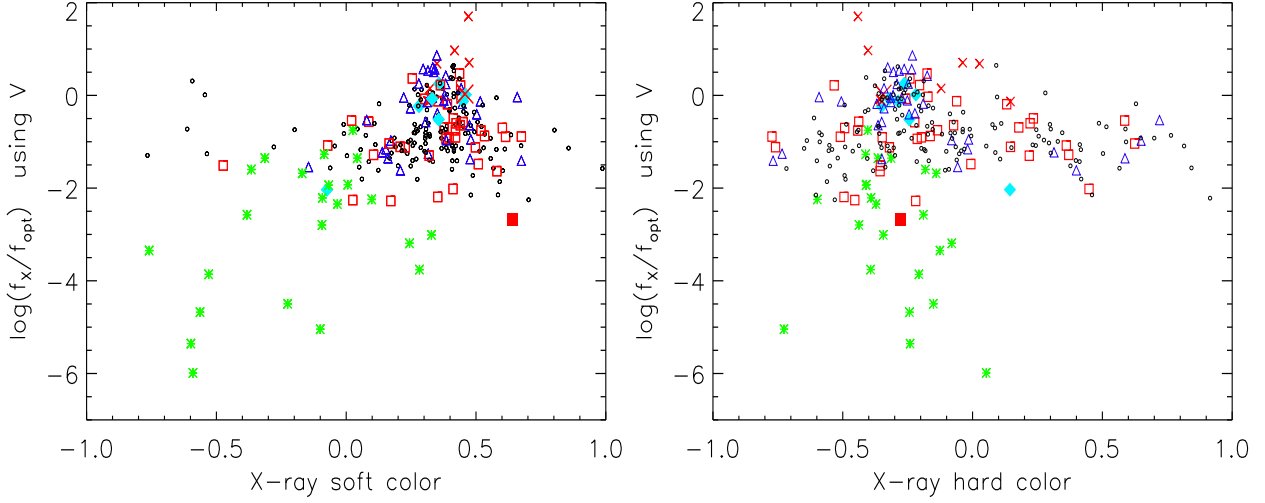


Fig. 4.— X-ray (0.35–8 keV) to optical (V band) flux ratios as a function of soft ($M-S)/(S+M+H)$ and hard ($H-M)/(S+M+H)$ X-ray color. A similar symbol/color scheme as in Fig. 3 was adopted, again using red symbols for sources which are considered to be in M33 (the large red cross represents the nucleus of M33, while the solid red square denotes one of the two globular clusters). Green asterisks are FSs, blue triangles represent galaxies, QSO, and AGN, cyan diamonds are non-stellar sources, and black sources have no suggested identifications. The sources plotted here are a subset of the X-ray catalog, as not every X-ray source has an optical counterpart in the LGGS data.

(2007, SM07 hereafter) and Zloczewski et al. (2008, ZKH08 hereafter). For the ZKH08 catalog, which was created from the CFHT Megacam survey of M33 and covers the outer part of our survey region, we selected only sources that were likely to be clusters (their type 1 and 2) and accepted as matches those X-ray sources that were located within 1 FWHM of the cluster center. The SM07 catalog, which is a heterogeneous collection of older catalogs and covers the bulk of our survey region, does not list a cluster size, so we used the mean cluster size from ZKH08 (1''.8). We selected all sources listed as cluster candidates in that catalog, and accepted as matches those X-ray sources within 1''.8 of the cluster center, roughly the same criterion used for the ZKH08 catalog. Between these two lists we found two potential matches. ChASeM33 source number 393 is well matched to the GC SMS275 (which was verified with the Megacam and HST data) and ChASeM33 source number 511 which is matched to cluster 04-6-013 from the ZKH08 catalog.

The ZKH08 catalog also contains a listing of background galaxies that were discarded from their cluster sample. We cross-correlated the X-ray source list with the ZKH08 galaxy list using the same criterion as above and found five matches (ChASeM33 source numbers 15=Zea20-6-037, 24=Zea21-6-004, 46=Zea26-3-007, 105=Zea30-6-023, and 433=Zea25-

1-011). Of those, ChASeM33 sources 46 and 105 show near coincidences with background galaxies in the HST images. Six non-GC sources in the SM07 catalog were matched to our X-ray sources (ChASeM33 sources 197=SMS107, 236=SMS133, 326=SMS213, 345=SMS230, 444=SMS356, and 455=SMS362), all of which were listed as being of an unknown nature. Source 345 is clearly a background galaxy, and number 444 and 455 both coincide with the nuclei of background galaxies.

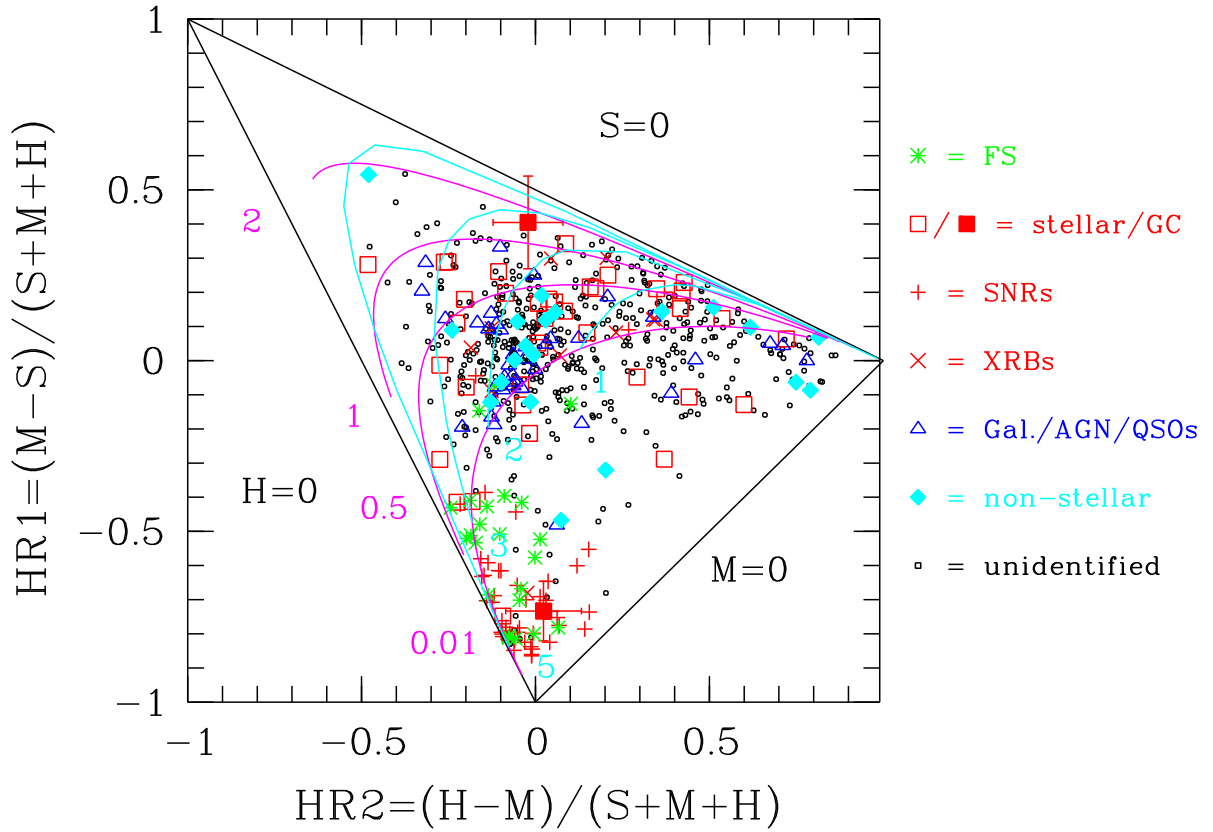


Fig. 5.— Hardness ratio plot using a Bayesian approach (Park et al. 2006). SNRs are from L10, whereas XRBs/candidates are taken from HP01, PMH04, MPH06, and W08. The magenta lines are trajectories for absorbed power-law models ($-1 \leq \Gamma \leq 6$) for which the N_{H} was fixed at 0.01, 0.5, 1.0, and $2.0 \times 10^{22} \text{ cm}^{-2}$, while the cyan-colored trajectories assume a variable column density ($10^{20} \text{ cm}^{-2} \leq N_{\text{H}} \leq 10^{24} \text{ cm}^{-2}$), but constant photon indices of 1, 2, 3, and 5. Representative error bars are shown for the two identified GCs.

3.3. Hardness ratios

We compute hardness ratios (HRs) using a definition similar to that described in Prestwich et al. (2009), except that we extract source and background counts in the “soft” (S , 0.35–1.1keV), “medium” (M , 1.1–2.6keV), and “hard” (H , 2.6–8.0keV) energy bands. These bands are identical to the ones used for the FLC and help to separate the soft sources (FSs and SNRs) from the hard sources (AGN). Two different HRs are computed: $HR1 = (M - S)/(S + M + H)$, and $HR2 = (H - M)/(S + M + H)$. We use a Bayesian approach which accounts for the fact that source and background counts are non-negative. Although the *BEHR* code (Park et al. 2006) does not directly handle this form for the HRs, we adapt an approach described in a Chandra Source Catalog memo⁶ and evaluate the HRs based on the merged AE data for each source.

For each energy band, the inputs are source region counts, background region counts, a factor accounting for the ratio of the source and background extraction areas and efficiencies (AE’s “backscale” parameter), and a factor converting from counts to flux (exposure time multiplied by the mean of the ARF over the extraction region). The BEHR code is run twice, once for S and M , and again for S and H ; an option is set to save the “draws” for the posterior probability distributions of the two fluxes. We set the “burnin” parameter to 50000 and the “total draws” parameter to 100000. This provides 50000 samples from the probability distributions for the fluxes. Combining the results from the two BEHR runs, we obtain 50000 samples from the probability distributions for the S , M , and H fluxes. Using these distributions, we obtain 50000 values for HR1 and HR2. The HR value is obtained as the mean of the distribution, and the credible interval is evaluated based on the 68.2% equal-tails estimates (i.e., 0.682/2 of the samples have values below the lower limit, and 0.682/2 of the samples have values above the upper limit).

In Fig. 5 we plot the HR2 values vs. the HR1 values for all of the sources. The limiting photon fluxes are indicated by solid black lines (the triangle): $S = 0$ (upper left to right center), $M = 0$ (right center to bottom center), and $H = 0$ (bottom center to upper left). Two distinctive regions with an enhanced source density are visible: one which contains the bulk of (mostly unidentified) sources around $(HR2, HR2) \sim (0.0, 0.1)$, and one at about $(HR2, HR1) \sim (-0.1, -0.8)$, following the $H = 0$ line. The first clump of sources near the center of the diagram appears to be a combination of XRBs, stellar and non-stellar sources, and background AGN. These objects appear to have N_{H} values between 0.01 and $0.5 \times 10^{22} \text{ cm}^{-2}$ and photon indices between 1.0 and 2.5. The majority of the unidentified sources in our survey are in this clump, indicating that most of them are likely to be XRBs

⁶http://cxc.harvard.edu/csc/memos/files/IEvans_HardnessRatios.pdf

or AGN.

The stretch of sources in the second clump with $HR1 < -0.5$ along $H = 0$ seems to be predominantly occupied by the L10 SNRs and foreground stars which tend to have significantly softer spectra. An estimate of the N_{H} or the photon index for sources located around $(HR2, HR1) = (-0.1; -0.8)$ and $(HR2, HR1) = (0.5; 0.2)$ is not possible as the model solutions in these regions become degenerate.

3.4. Time variable sources in ChASeM33

The full ChASeM33 source catalog was systematically searched for sources which show significant long and short-term variability in the 0.35–8.0keV energy band. To check for variability, we applied a 5σ variability threshold, defined as $\eta = (\text{flux}_{\text{max}} - \text{flux}_{\text{min}})/\Delta\text{flux}$ across all observations (long-term variability) and a Kolmogorov-Smirnov (KS) test probing the probability ξ of the source being constant within a single observation (short-term variability). The KS test is part of AE and compares a uniform count rate model to the distribution of source event time stamps. The flux error Δflux is calculated using the Gehrels approximation (Gehrels 1986) which is more appropriate for low count data. To see how much the sources vary in flux, we calculated a variability factor defined as $\text{flux}_{\text{max}}/\text{flux}_{\text{min}}$, i.e. the ratio of the maximum flux to the minimum flux for a given source.

Conservatively, we consider any source with $\eta \geq 5$ or $\xi \leq 5.7 \times 10^{-7}$ (5σ equivalent) to be variable. We only used KS test results from observations when the source had >20 counts and was $<8'$ off-axis. In determining η , we only used observations where the source was $<8'$ off-axis, in order to avoid problems with background contamination where the PSF is very large. From our detailed spectral analysis (see Section 3.6) we identified two additional sources at off-axis angles $>8'$ which also show time variability. These two sources are #561 (X-9a) and #612 (X-10).

To test the robustness of our variability thresholds, we used the L10 SNR sample. Since SNRs should not be time-variable, these tests provide a check against spurious variability detections. As a result, the SNR with the highest long-term variability, L10-039, has a variability index of $\eta=4.2$ while the KS test for the SNR with the highest likelihood for short-term variability, L10-081, yields a ξ of 0.025. These values are well outside of our high-confidence variability threshold.

The results of our variability analysis are shown in the column named 'Variability' of Table 9, where high-confidence variables are shown in bold typeface. According to our conservative criteria, 38 sources are time-variable, 35 (7) are variable on short (long) time

scales, 4 show both types of variability. We note that η and ξ remain undefined if there are not enough observations in which a source has >20 counts (KS test minimum) and/or is $<8'$ off axis (KS and variability index maximum). The variability factor $flux_{max}/flux_{min}$ remains undetermined if the faintest observation had a flux ≤ 0 or where there were fewer than 2 reliable flux measurements. If we are less conservative and set our variability criteria to values just outside of the range covered by the SNR sample ($\eta > 4.2$ and $\xi < 0.025$), 73 sources are time-variable, 49 (42) are variable on short (long) time scales, and 17 sources show both. We want to point out that the variability analysis is not optimized to find transient sources. Because the transients in M33 are typically faint, can be far off-axis, and can sometimes only be detected in the unmerged observations (Williams et al. 2008), such transient sources may be too faint to pass our variability criteria. Running the transient identification routine from Williams et al. (2008) on the full catalog yielded 2 new transient candidates, 013345.24+304135.0 and 013420.91+303319.0.

3.5. Supersoft X-ray sources

Although the front-illuminated ACIS-I chips are not the ideal choice to search for supersoft sources, we checked whether we detected any of the 12 SSSs reported by PMH04 and MPH06. It turned out that three sources are outside the ChASeM33 FOV, three are located at the border of the FOV and are not detected (faint *XMM* sources), while the remaining six sources are well within the ChASeM33 FOV but are not detected. Among these six objects one source is detected with *XMM-Newton* but is located in a region of diffuse emission and is most likely not a point source, while PMH04 source 247 (source 207 in MPH06) is a transient source named XRT-6 (Williams et al. 2008, W08 hereafter) which is only detected in an ACIS-S observation (ObsID 786) which was intentionally excluded from our analysis. Table 10 provides a brief summary of the cross-identified SSSs.

The seven sources from MPH06 that are not reported in PMH04 are sources that are only detected by MPH06 as faint sources in one observation of the *XMM* M33 raster. PMH04, however, analyzed integrated images of the entire raster which are less sensitive for this type of source (due to the higher background) and therefore might have missed these sources. Besides lower sensitivity of ACIS-I for SSSs, the transient behavior of the sources might also be an additional reason why none of the *XMM* SSSs are detected by *Chandra*.

To see if we can detect new SSSs besides the ones reported by PMH04 and MPH06, the entire ChASeM33 catalog was searched using criteria similar to the ones introduced by Kong et al. (2002). We used the soft hardness ratio defined as $HR1 = (m - s)/(s + m + h)$ based on *net_cnts* in the bands $s=0.35 - 1.1\text{keV}$, $m = 1.1 - 2.6\text{keV}$, $h = 2.6 - 8\text{keV}$ and selected

all sources with a hardness ratio $HR1 < -0.5$. Among the 11 sources which passed the filter, eight sources are identified as L10 SNRs, two with stars, and one source is most likely a patch of diffuse X-ray emission in the giant H II region NGC 604. We detected no new SSSs in our sample.

3.6. X-ray Spectral Analysis

Spectra were extracted by AE using the CIAO tool `dmextract`. Response products were created by AE using the CIAO tools `mkacisrmf` and `mkarf`. For sources observed in more than one observation, summed spectra were created and weighted response products were created by weighting by the exposure times for the individual observations and using the `ftools addrmf` and `addirf`. The spectra were grouped using the grouping algorithm in AE which allows the user to specify an energy range over which the grouping should be performed (0.35–8.0 keV in our case) and to specify a minimum signal-to-noise threshold to be achieved in each spectral bin in the net (background-subtracted) spectrum. We specified a minimum signal-to-noise threshold of 2.0 for each spectral bin and a minimum of 8 spectral bins for a spectrum to be considered for spectral fitting. 254 of the 662 sources had a sufficient number of counts to satisfy both of these criteria. The majority of these sources (163 of 254) had a minimum signal to noise ratio of 3.0 or larger in each spectral bin and 8 or more spectral bins, thereby approaching the regime in which Gaussian statistics are a good approximation. Given this grouping scheme, we used the reduced χ^2 statistic as a measure of the goodness of fit.

The grouped spectra for 254 of the 662 sources were automatically fit in AE with an absorbed power-law model and, alternatively, with an absorbed *apec* model (Smith et al. 2001). The Galactic absorption was modeled with the *tbabs* model (Wilms et al. 2000) by freezing the Galactic N_{H} at $6 \times 10^{20} \text{ cm}^{-2}$ (Dickey & Lockman 1990). For the absorption component internal to M33, we assumed a *tbvarabs* model with relative elemental abundances for elements heavier than He set to 0.5 (see Rosolowsky & Simon (2008) and references therein). This component was allowed to vary during the fit. In order to determine the best-fit model, models which predicted unreasonably high photon indices ($\Gamma > 4.0$) and plasma temperatures ($kT > 6.0 \text{ keV}$) were rejected. To distinguish between a power-law and a thermal plasma model, we checked which model provided the best fit to the spectrum (e.g., if there were indications for emission features, the thermal model was adopted). If both model fits appeared to be reasonable (a common occurrence for sources with only a few hundred counts), the one with the lower reduced χ^2 value was chosen. The best-fit model and parameters are listed in Table 7.

Because these simplistic single component models sometimes provide a poor fit, we also used multi-component models for sources which have a sufficiently large number of counts to warrant fitting with more detailed spectral models. There are 15 sources in the ChASeM33 catalog which have more than 2,000 net counts in the 0.35–8.0 keV band. Most of these sources (13/15) are the well-known *Einstein* sources, including of course the nucleus of M 33, which has the largest number of counts. Four of these sources have already been fit with more complicated spectral models and the results were published in earlier papers from the ChASeM33 project (see Pietsch et al. 2006; Gaetz et al. 2007, L10). For the remainder, we examined the one component fits for the sources looking for structure in the residuals which might suggest a better, more complicated model. We experimented with more complex models which added additional components such as an accretion disk model (`diskbb` in `XSPEC`) and/or multiple thermal components. For some of the sources we were able to identify a model which improved the fit significantly compared to the single component power-law or thermal models. Below, we comment on the sources with the largest number of net counts, moving from highest number of counts to lowest number of counts.

013350.89+303936.6 (X-8, the Nucleus): The nucleus is the brightest X-ray source in M 33 and has been suggested to be a binary system containing an accreting stellar mass black hole ($\gtrsim 5M_{\odot}$) with a variable accretion disk (e.g., Dubus & Rutledge 2002; La Parola et al. 2003; Weng et al. 2009). Spectral analysis of the nucleus requires special care as the source is so bright that pileup is a significant concern. The F1e1, F1e2, and ObsID 1730 data are not useful for spectral analysis because the nucleus is severely piled-up distorting the spectral shape. The other ChASeM33 pointings were arranged when possible to place the nucleus near the edge or just off of the CCD to eliminate the transfer streak from affecting the data in the region of interest. However, for two observations, F4e2 and F6e1, the nucleus was on the chip and far enough from the chip edge so that the source did not move on and off the CCD as the satellite dithered. The source was 9°0 and 9°8 off-axis respectively in the F4e2 and F6e1 observations which reduced the effects of pileup. There are 163,938 counts in the combined spectrum.

The one component fits are poor; the thermal model resulted in a reduced χ^2 of 2.93 and the non-thermal model resulted in a reduced χ^2 of 3.40. Dubus & Rutledge (2002) fit the S3 spectrum of X-8 from ObsID 787, in which the source is positioned 7°7 off-axis, with an absorbed disk blackbody model. La Parola et al. (2003) analyzed the S3 data from ObsID 2023 in which X-8 was 12° off-axis and found that the fit improved with the addition of a power-law component, a thermal component, and a broad Gaussian centered at 0.96 keV. We fit the data with a model similar to that of La Parola et al. (2003), specifically a thermal component (`apec`), plus a Gaussian, plus a disk blackbody component (`diskbb`), and a non-thermal component (`pow`) model. In our initial fits the `apec` component was unconstrained

and went to unreasonably low temperatures and high normalizations. We therefore set the temperature of the `apec` component to the value determined by La Parola et al. (2003) of $kT=0.18\text{ keV}$ since they analyzed data from the BI CCD (S3) which is more sensitive at energies below 1.0 keV . This fit resulted in a reduced χ^2 of 1.02 for 237 degrees of freedom (DOF). The results are summarized in Table 8 for this fit and the other sources. The thermal component has a low normalization and contributed only to the lowest few channels. The vast majority of the flux is contained in the disk blackbody and power-law components. Our fit resulted in a central energy for the Gaussian of $1.15_{-0.06}^{+0.05}\text{ keV}$ which is somewhat higher than the value which La Parola et al. (2003) derived, $0.96_{-0.10}^{+0.03}\text{ keV}$. Future observations of X-8 with high-resolution spectrometers would be useful to characterize this feature.

We examined the F4e2 and F6e1 spectra independently to search for variability between the epochs. We fit each spectrum with the model described above and determined that the fit values of all of the parameters were consistent with each other at the 90% confidence level. The normalization of the disk blackbody component was 20% higher in F4e2 than in F6e1, but this was only significant at the 1σ confidence level. These different normalizations for F4e2 and F6e1 imply values for the inner radius of the accretion disk of $R_{in}(\cos\theta)^{1/2} = 62.9\text{ km}$ in F4e2 and $R_{in}(\cos\theta)^{1/2} = 57.4\text{ km}$ in F6e1. The large range of allowed values for the parameters is partially due to the complexity of the multi-component model we have adopted in which some parameters can be strongly coupled to other parameters. The best-fit value of the power-law index varied from 0.77 for F4e2 to 1.18 for F6e1, but again this difference was only significant at the 1σ confidence level. Although there is a clear variation in the total flux of X-8 between these two observations, it is not possible to ascribe the variability to just one component in our assumed spectral model. The power-law index for the combined observations is $\Gamma = 1.20_{-0.40}^{+0.29}$. Our results are consistent with X-8 being an accreting black hole with a variable accretion disk. The combined spectrum is displayed in Figure 6 together with those for the other sources.

013334.13+303211.3 (X-7): Detailed spectral fits and a timing analysis of X-7 have been carried out by Pietsch et al. (2006). The source is an eclipsing black hole X-ray binary (see also Orosz et al. 2007) and was fit with a `diskbb` model.

013328.69+302723.6 (X-6): There are a total of 47082 counts in the combined spectrum of X-6 from F5e1, F5e2, F6e1, and ObsID 7208. The one component fits are poor; the thermal model resulted in a reduced χ^2 of 1.41 and the non-thermal model resulted in a reduced χ^2 of 1.58. We fit this spectrum with a disk blackbody and a power-law model which resulted in a small improvement in the reduced χ^2 to 1.35 with 242 DOF. This fit is still formally unacceptable but we were unable to find any other model combinations which fit the data better. The source showed some evidence of variability in the ChASeM33 data sets,

the long-term variability index η is 3.9 which is below our threshold of 5.0 to be classified as confidently variable. There was no evidence for short-term variability. The long-term variability may be part of the explanation for the relatively poor fit to the combined spectrum. We fit the F5e1, F5e2, and F6e1 spectra separately since they had between 13706 and 16108 counts, but we did not fit ObsID 7208 separately since it only had 1899 counts. The disk blackbody plus power-law model results in better fits to the F5e1, F5e2, and F6e1 spectra with reduced χ^2 values of 1.17, 1.11, and 1.07 respectively. All of the fit parameters are consistent with each other across the epochs at the 2σ confidence level. X-6 is located in an uncrowded region of the galaxy with no obvious optical, IR, or UV counterpart. We conclude that this source is most likely an XRB in M33 since the disk blackbody model fits the spectrum best and there is a marginal indication of variability. Future studies to characterize the variability of this source in X-rays and to determine its optical counterpart are needed to confirm the classification as an XRB.

013324.40+304402.4 (X-5): There are a total of 33863 counts in the combined spectrum of X-5 from F1e1, F1e2, F3e1, F3e2, F4e1, F4e2, and ObsID 1730. The one component fits are poor; the thermal model resulted in a reduced χ^2 of 1.53 and the non-thermal model resulted in a reduced χ^2 of 1.58. The fit with the disk blackbody and power-law model improved the reduced χ^2 to 1.21 for 239 DOF. This source is clearly variable, as the count rate varied by $\sim 33\%$ between F3e1 and ObsID 1730. The long-term variability index η is 8.8, but there is no indication of short-term variability. We attempted to determine spectral differences between the various epochs but since there were only about ~ 5000 counts in a spectrum for an epoch we were unsuccessful. Similar to X-6, this source is in an uncrowded region with no obvious optical, IR, or UV counterpart. We conclude that this source is most likely an XRB in M33 since the disk blackbody model fits the spectrum best and there is convincing evidence for variability.

013451.85+302909.7 (X-10): There are a total of 26303 counts in the combined spectrum of X-10 from F6e1 and F6e2. The one component fits are acceptable; the thermal model resulted in a reduced χ^2 of 1.01 and the non-thermal model resulted in a reduced χ^2 of 1.04. The fit with the disk blackbody and power-law model improved the reduced χ^2 slightly to 0.99 for 236 DOF. There is significant evidence for both long-term and short-term variability ($\eta = 12.5$ and $\xi = 6.62 \times 10^{-10}$). X-10 is located in an uncrowded region on the eastern side of the galaxy near the border of the D₂₅ isophote. There is no optical counterpart, but there is some faint emission in the 2MASS J band which might be a counterpart. We conclude that this source is an XRB in M33 given its nonthermal X-ray spectrum and its short-term variability.

013315.16+305318.2 (X-4): There are a total of 23117 counts in the combined spec-

trum of X-4 from F3e1 and F3e2. The one component fits are poor; the thermal model resulted in a reduced χ^2 of 2.22 and the non-thermal model resulted in a reduced χ^2 of 2.03. The fit with the disk blackbody and power-law model improved the reduced χ^2 significantly to 1.13 for 239 DOF. There is no evidence for variability between these two epochs (η is 0.6 and ξ is 1.48×10^{-2}). We conclude that this source is most likely an XRB in M 33, since the quality of the fit improved dramatically for the disk blackbody plus power-law model. Future studies should try to detect and characterize any variability in X-rays and to determine the optical counterpart to confirm the classification as an XRB.

013311.75+303841.5 (X-3): X-3 is the brightest SNR in M 33 (G98-21, see Gordon et al. (1998)) and a detailed analysis of the spectrum was presented in Gaetz et al. (2007).

013425.80+305518.1 (X-9b): There are a total of 9064 counts in the combined spectrum of X-9b from F2e2, F2e1, and ObsID 2023. The one component thermal model resulted in a reduced χ^2 of 1.15 and is unacceptable, but the one component nonthermal model resulted in a reduced χ^2 of 1.00 and is acceptable. The two component disk blackbody and power-law model also resulted in a reduced χ^2 of 1.00 (for 236 DOF) and therefore does not significantly improve the fit. Based on these results, we conclude that the power-law model is the best fit to the data. The source is highly variable with the flux changing by a factor of three between F2e2 and ObsID 2023. The long-term variability index η is 38.7. Unfortunately, there are not enough counts in a given epoch to search for spectral variability between the epochs (1943 counts in F2e2 and 4578 counts in ObsID 2023). The source has a clear counterpart in the optical and the IR. It is bright in all of the *Spitzer* and 2MASS bands. We conclude that this source is most likely an AGN or an XRB since the non-thermal model fits the spectrum best with a spectral index of 1.87 typical of AGN and XRBs, there is evidence for long-term variability, and the source has a bright optical and IR counterpart. Followup optical spectroscopy would be useful in distinguishing between an AGN and XRB.

013253.89+303311.8 (X-2): There are a total of 4891 counts in the combined spectrum of X-2 from F4e1, F4e2, F5e1, and F5e2. The one component fits are acceptable; the thermal model resulted in a reduced χ^2 of 1.05 and the non-thermal model resulted in a reduced χ^2 of 0.91. The fit with the disk blackbody and power-law model only improved the reduced χ^2 to 0.90 for 165 DOF. Based on these results, we conclude that the power-law model is the best fit to the data. The source is variable with the flux changing by $\sim 30\%$ between F4e2 and F5e1 (η is 7.2). Unfortunately, there are not enough counts in a given epoch to search for spectral variability between the epochs (1430 counts in F4e2 and 1167 counts in F5e1). The source has a bright optical counterpart for which we acquired an MMT spectrum. The optical spectrum is consistent with an AGN at a redshift of 0.49. The optical source was also identified as variable in the Canada-France-Hawaii Telescope (CFHT)

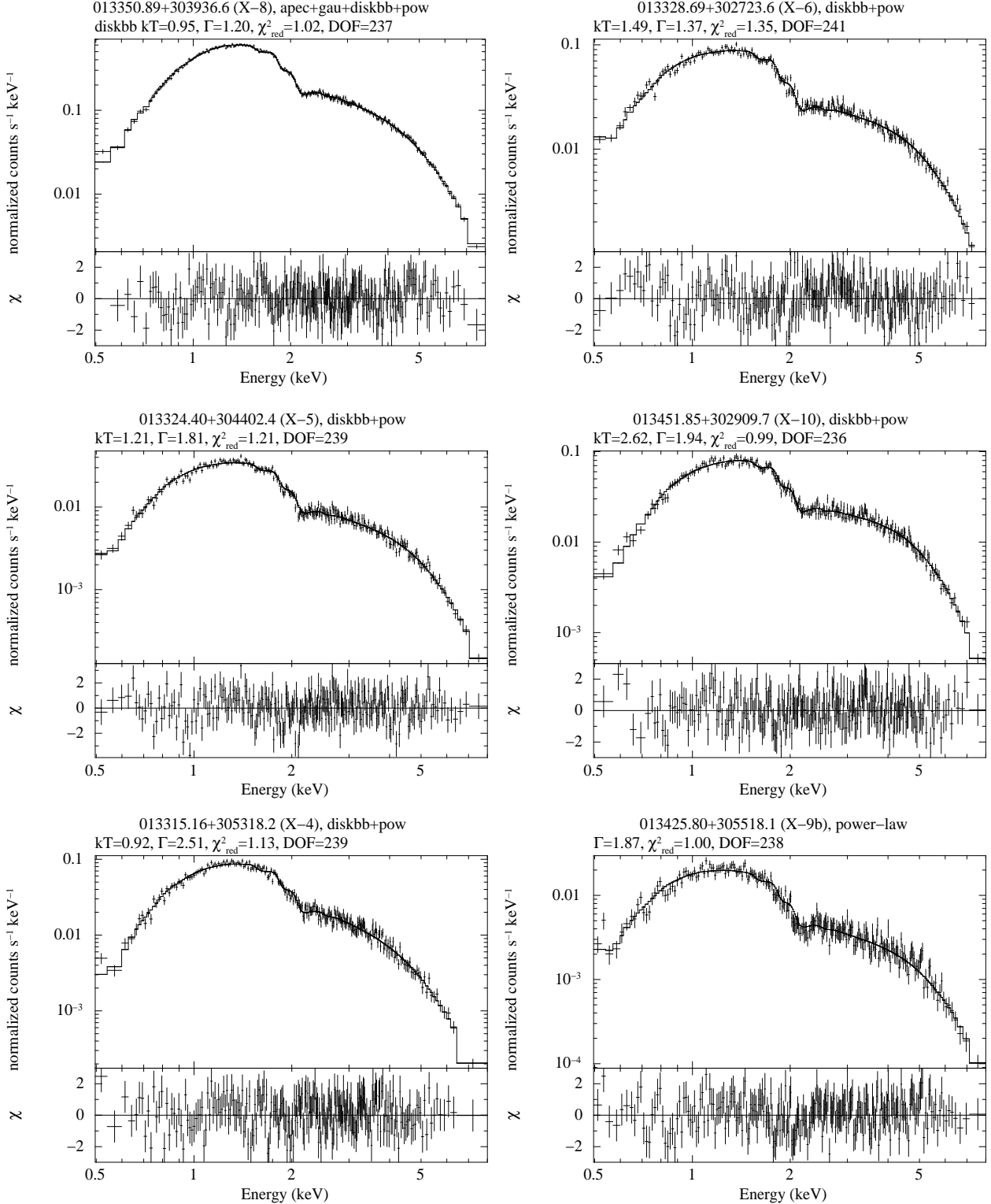


Fig. 6.— Spectra and refined spectral fits for the brightest ChASeM33 sources. The best-fit model is either a disk blackbody plus non-thermal model (`diskbb+pow`) or a simple power-law model (`pow`), except for the nucleus, which requires a third component (`apec`) in addition to the `diskbb` and `pow` components. The column density is modeled by a two component absorption model, consisting of the Galactic column density and the one internal to M 33.

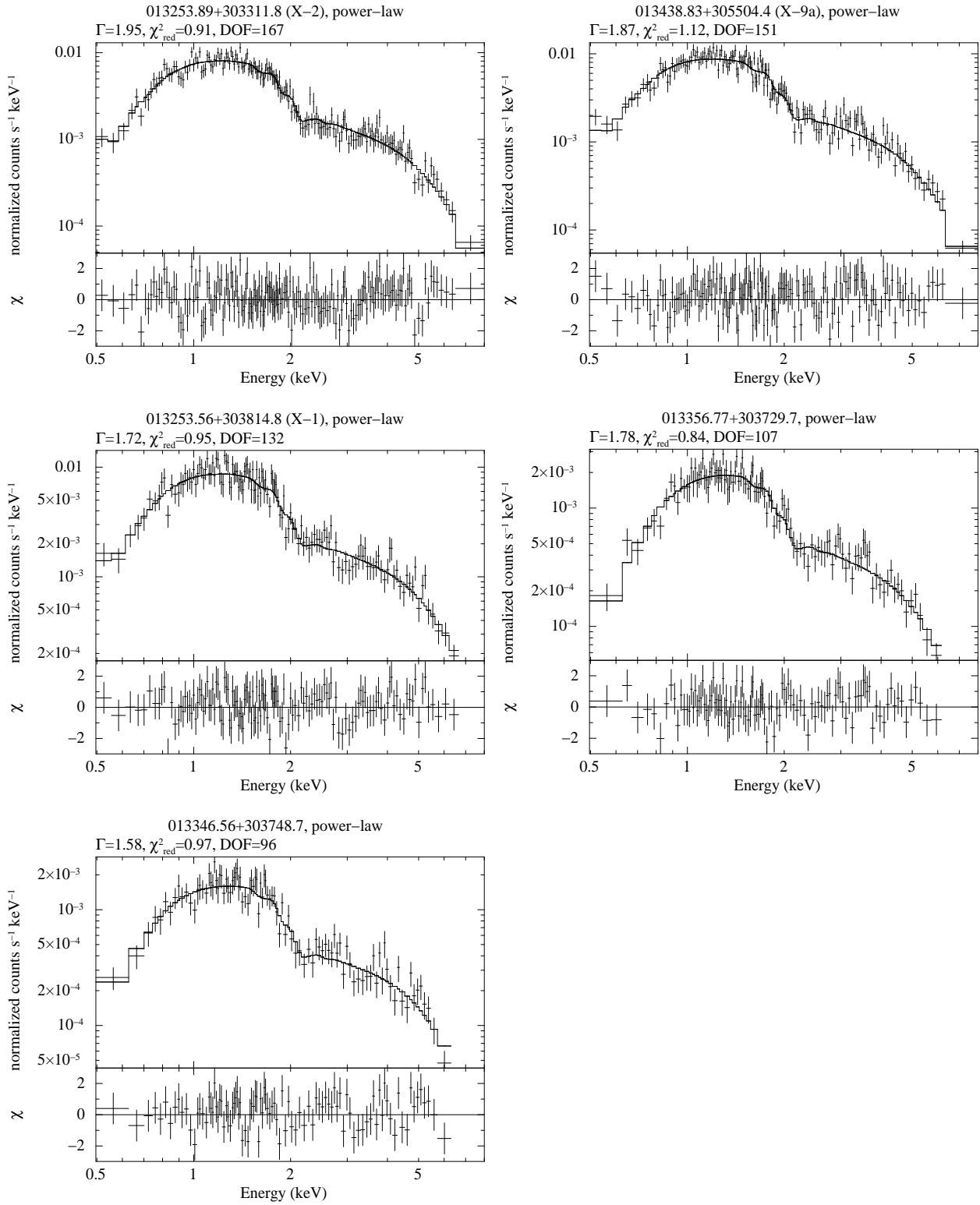


Fig. 6.— Continued.

survey of M 33 (Hartman et al. 2006) as source CFHT 250850. We conclude that this source is certainly an AGN given its non-thermal spectrum with a spectral index of 1.95, long-term variability in X-rays, and its optical spectrum and redshift of $z = 0.49$.

013438.83+305504.4 (X-9a): There are a total of 4044 counts in the combined spectrum of X-9a from ObsID 2023, F2e2, and F2e1. The one component fits are reasonable, but not formally acceptable. The thermal model resulted in a reduced χ^2 of 1.15 and the non-thermal model resulted in a reduced χ^2 of 1.12. The fit with the disk blackbody and power-law model resulted in no improvement in the reduced χ^2 (1.12 for 149 DOF). Based on these results, the power-law model is the best fit to the data. The source is clearly variable as the long-term variability index η is 11.9, but there is no evidence for short-term variability. The source has a bright counterpart in the optical, IR, and UV. Our MMT spectrum of the source is consistent with an AGN at a redshift of $z = 0.89$. We conclude that this source is certainly an AGN given its non-thermal X-ray spectrum with a spectral index of 1.87, X-ray long-term variability, and redshifted spectrum.

013331.25+303333.4 (X-14): X-14 is the second brightest SNR in M 33 (G98-31, see Gordon et al. (1998)) and a detailed analysis of the spectrum was presented by L10.

013253.56+303814.8 (X-1): There are a total of 2808 counts in the combined spectrum of X-1 from F4e1 and F4e2. The one component fits are acceptable; the thermal model resulted in a reduced χ^2 of 0.97 and the non-thermal model resulted in a reduced χ^2 of 0.95. The fit with the disk blackbody and power-law model resulted in no improvement in the reduced χ^2 (0.96 for 130 DOF). Based on these results, the power-law model is the best fit to the data. The source showed only marginal evidence for long-term variability (η is 4.3). The source has a bright counterpart in the optical and IR. Our MMT spectrum of the source is consistent with an AGN at a redshift of $z = 0.37$. The source is also identified with the optical variable CFHT 250829. We conclude that this source is certainly an AGN given its non-thermal X-ray spectrum with a spectral index of 1.74, redshift, and variability in the optical.

013356.77+303729.7: There are a total of 2434 counts in the combined spectrum of 013356.77+303729.7 from ObsID 1730, ObsID 7208, F1e1, F1e2, F5e1, F5e2, F6e1, F6e2, and F7e2. This source was not detected by *Einstein*. The combined exposure in the ChASeM33 survey is over 700 ks, so it is perhaps not surprising that ChASeM33 detected this source while *Einstein* did not. The one component fits are acceptable; the thermal model resulted in a reduced χ^2 of 0.83 and the non-thermal model resulted in a reduced χ^2 of 0.84. The fit with the disk blackbody and power-law model resulted in no improvement in the reduced χ^2 (0.85 for 105 DOF). Based on these results, we have a slight preference for the thermal model. However, the source is clearly variable as the flux varied from ObsID 1730 to F1e1

by a factor of 6 (η is 5.7). Based on the variability, we have a slight preference for the non-thermal model. The source is located in a crowded region, so the optical counterpart is not secure. There is a variable source, CFHT 235490, inside the error circle for the X-ray source. We conclude that this source is most likely an AGN or an XRB since the non-thermal model fits the spectrum as well as the thermal model, the best-fit spectral index is 1.82, and there is convincing evidence for long-term variability.

013354.91+303310.9 (X-13): X-13 is the third brightest SNR in M 33 (G98-55, see Gordon et al. (1998)). A detailed analysis of the spectrum was presented by L10.

013346.56+303748.7: There are a total of 2195 counts in the combined spectrum of 013346.56+303748.7 from ObsID 1730, ObsID 7208, F1e1, F1e2, F4e2, F5e1, F5e2, F6e1, and F6e2. This source was not detected by *Einstein*. The combined exposure in the ChASeM33 survey is over 700 ks, so it is perhaps not surprising that ChASeM33 detected this source while *Einstein* did not. The one component fits are acceptable; the thermal model resulted in a reduced χ^2 of 0.99 and the non-thermal model resulted in a reduced χ^2 of 0.97. The fit with the disk blackbody and power-law model resulted in no improvement in the reduced χ^2 (0.99 for 94 DOF). The source is clearly variable as the flux varied from F5e1 to F1e2 by a factor of 3 (η is 11.8). Based on the variability, we have a slight preference for the non-thermal model. The source is close to the nucleus of the galaxy and is located in a crowded region. A secure optical counterpart cannot be identified. We conclude that this source is most likely an AGN or an XRB since the non-thermal model fits the spectrum as well as the thermal model, the best-fit value for the spectral index is 1.61, and there is convincing evidence for long-term variability.

3.7. The X-ray Luminosity Function of M 33

3.7.1. Conversion of Photon Flux to Energy Flux

Both the radial profile determination and the log N –log S relations discussed below require estimates for the energy flux, S , of a source. AE provides a photon flux estimate (the *flux2* column) based on the source *net_cts*, exposure, and the mean ARF in the given energy band (assuming a spectrum with a flat photon index). To obtain the energy flux, some information about the intrinsic spectrum of the object is required. There are multiple ways of measuring the flux in a given energy band that could be used. One could use fluxes calculated from the raw count rate using a single ad hoc spectral model (which can be done for all of our sources), or one could use fluxes which are calculated from the raw count rate using a simple spectral model derived from the hardness ratios (which can be done for all but

the dimmest sources). Alternatively, one could use fluxes derived from spectral fits (which can be done only for the brightest third of our sources). Applying different count rate to flux conversions, particularly at different flux levels, can introduce biases and spurious features in the $\log N$ – $\log S$ distribution. As a result, we decided to convert photon fluxes to energy fluxes using an absorbed powerlaw spectral model with $\Gamma = 1.9$ and $N_{\text{H}} = 6 \times 10^{20} \text{ cm}^{-2}$, which is considered to be representative for all sources (standard model hereafter). This kind of model appears to be appropriate for XRBs in M33 and background AGN which dominate at the lower flux levels. The model would be inappropriate for really hard/soft sources (where we would overestimate/underestimate the flux). The flux estimate could be off by as much as a factor of two if the spectrum is significantly different than the assumed one. However, the standard model seems to be a good choice for the majority of sources so that the net effect is not that large and does not bias the $\log N$ – $\log S$ relation systematically to higher or lower fluxes.

3.7.2. Sensitivity Maps

For the following analyses, we require sensitivity maps which provide, for each point in the survey area, the energy flux level at which a source would be detectable. Sensitivity maps consistent with the AE selection criteria are, in the absence of a high density of sources, relatively straight-forward to generate. For each point in the source image we calculated the size of the source extraction region and the corresponding local background rate. From these quantities one can calculate the number of counts required within the exposure for which the *pns* falls below 4×10^{-6} . Based on the standard model, the count rate is then converted to the corresponding energy flux and luminosity. Of course, multiple exposures and field centers are a complication. We combined all data for each field and calculated sensitivity maps for the individual fields. We then combined the sensitivity maps for all of the fields. If at a point in the region of overlap there are several different measures of the sensitivity, $[S_0, S_1, \dots, S_n]$, the resulting sensitivity was taken to be $\text{Min}(\text{Min}([S_0, S_1, \dots, S_n]), (\sum_N S_i^2)^{1/2})$, i.e., either the best individual field sensitivity at that point, or the sensitivity of the summed data, whichever was smaller. Since we excluded the region around the nucleus from our standard source detection and characterization, we set the exposure within a radius of $24''$ from the nucleus to zero. The sensitivity limit of $10^{-7} \text{ photons cm}^{-2} \text{ s}^{-1}$ corresponds to completeness limits of 34%, 51%, and 66% for semi-major axes of $30'$, $20'$, and $10'$, respectively. In other words, 34% of the sky area of the sensitivity map within $30'$ has a value $\geq 10^{-7} \text{ photons cm}^{-2} \text{ s}^{-1}$ and likewise for the other semi-major axes mentioned. The resulting sensitivity maps for the standard model in the soft and hard energy band are shown in Figure 7.

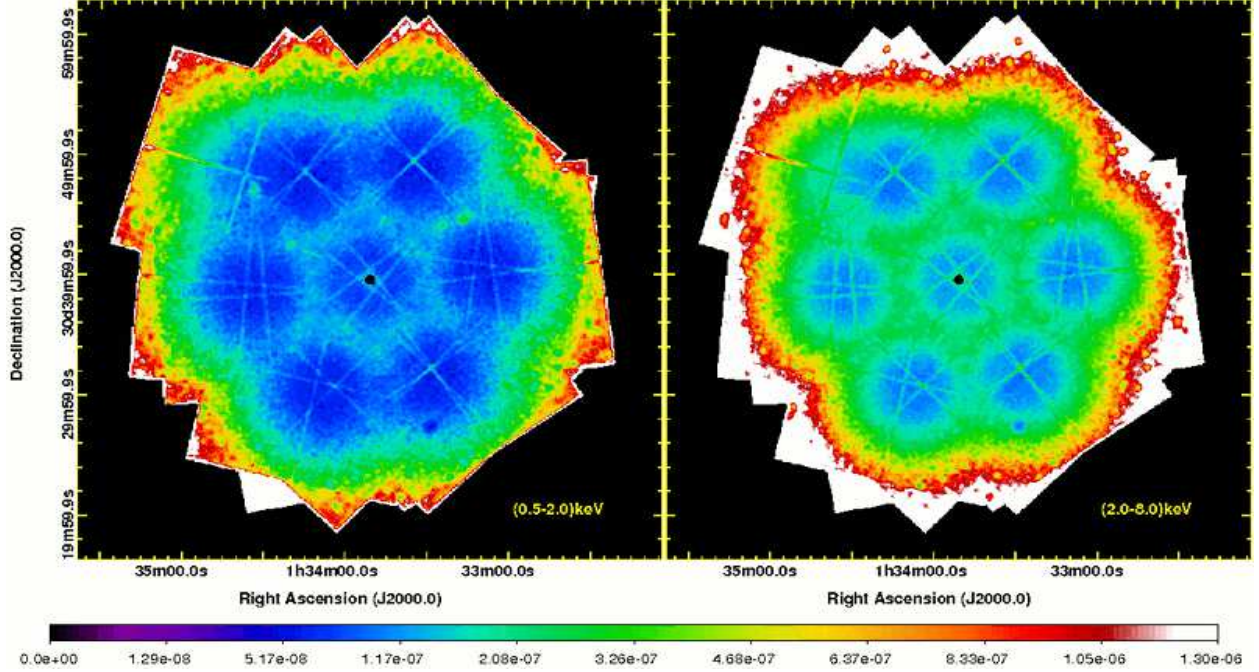


Fig. 7.— Sensitivity map (in units of photons s^{-1} cm^{-2} , square root scale) created in the 0.5–2.0 keV (left) and 2.0–8.0 keV energy band (right), assuming that each source can be represented by a power-law of $\Gamma = 1.9$ and an average column density of $N_H = 6 \times 10^{20} \text{ cm}^{-2}$. Since we excluded the region around the nucleus from our standard source detection and characterization, we set the exposure within a radius of 24'' from the nucleus to zero.

3.7.3. Radial source distribution

Direct multi-wavelength detection of counterparts to the X-ray sources allows the classification of X-ray sources and provides a means to discriminate between sources in M 33 and those in either the foreground or background (see §3.2). Such a detection scheme is limited in that some objects in M 33 or faint background sources, are unlikely to be detected and classified in such multi-wavelength studies. As a consequence, the nature of a significant number of sources will remain ambiguous. Statistical tests on the spatial distribution of the sources, however, can constrain directly the number of sources in M 33, as well as providing useful information for the construction of the log N –log S distribution and the LF of M 33.

The galactocentric profile was created by summing the number of sources within ellipses concentric with the D_{25} contour within $\Delta \log(S) = 0.1$ intervals, forming a two dimensional histogram. Each bin of this histogram was divided by the area within the annulus over which sources within the flux interval could have been detected. Histogram bins for which that area was less than one tenth of the total area of the annulus were eliminated from

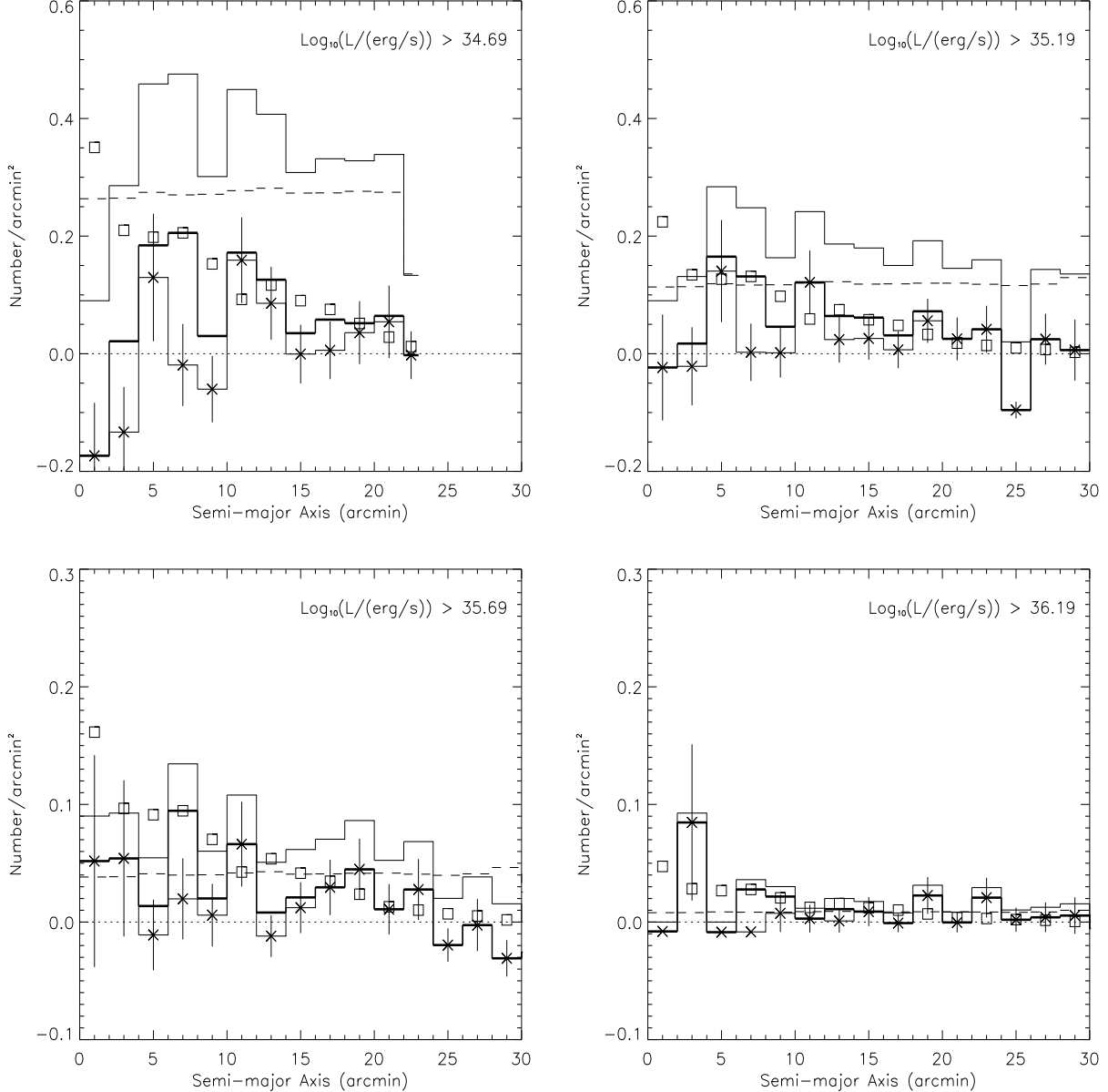


Fig. 8.— The galactocentric source density profiles in the 0.5–2.0 keV energy band. In each panel, the *top histogram* represents the total number of sources greater than the indicated luminosity after the removal of foreground stars. The *dashed histogram* is the expected number of background AGN, the *thick histogram* addresses the number of sources after the removal of the expected number of background AGN, while the *bottom histogram (with error bars)* represents the number of sources after the removal of the expected number of background AGN and the removal of the known SNRs. *Open boxes* follow a scaled profile of the *Galex FUV* surface brightness.

further use. The resulting galactocentric profiles are shown in Figure 8 for four different luminosity levels. The only sources removed before these histograms were constructed were the foreground stars. They are few in number and it is unlikely that a significant number of them was missed.

At each flux level the raw number of sources generally decreases with galactocentric radius. We used the cumulative $\log N$ – $\log S$ distribution of Cappelluti et al. (2009) and a map of the total hydrogen nucleon column density ($N(\text{HI})+2X\text{N}(\text{CO})$, where $X=2 \times 10^{20} \text{ cm}^{-2}$) to calculate the expected number of AGN at each location after their flux has been reduced by foreground galactic absorption and absorption by the disk of M 33. The expected contribution is shown by the dashed line in Figure 8. In each case the expected contribution from background AGN is nearly flat at most galactocentric radii, with an increase at the largest radii at the edge of the H I disk.

Subtracting the expected number of AGN from the total profile leaves the same downward trend with radius (the thick histogram in Figure 8). The identification of M 33 SNRs has been well studied (e.g. by L10) though the completeness of their SNR catalog is not clear. As most of the SNRs included in our source catalog are point-like, the completeness for the set of SNRs in our catalog will be similar to that of the other point sources. After the removal of the SNRs, the profile becomes significantly flatter, though there is still a positive signal. Although the majority of sources are in M 33, there could still be some AGN in those bins.

Figure 8 reveals also some significant features at $\sim 7'$ and $\sim 12'$. While the excess of sources at the smaller radius could correspond to prominent spiral arms tangent to the ellipses concentric with the D_{25} ellipse, the feature at the larger radius seems to be due to aggregations of faint sources.

3.7.4. The $\log N$ – $\log S$ relation and the M 33 X-ray Luminosity Function

For a survey covering the total geometric area A , the cumulative number of sources $N(> S)$ can be evaluated by summing over all sources with fluxes exceeding S , weighted by the survey area, $A(S)$, over which a source with flux S could have been detected:

$$N(> S) = \sum_{i,S_i>S} \frac{1}{A(S_i)}. \quad (1)$$

Here, S is the energy flux in units of $\text{erg cm}^{-2} \text{s}^{-1}$, and $A(S)$ survey area over which a source with flux S could have been detected. $N(> S)$ and the corresponding differential

form ($N(S)$) thus have units of sources per solid angle, or in our case, sources deg $^{-2}$. Note that the $A(S)$ factor would account for survey completeness if the sources were distributed uniformly. Although the LF could vary, the number of sources is not sufficient to show a significant difference at low fluxes between the inner and outer halves of the area covered by the survey. As a practical matter, we terminate the low flux end of the distribution when $A(S)/A$ falls below 10% of the total geometric area of the survey. The sensitivity maps calculated above (§3.7.2; see Fig. 7) allow the area function, $A(S)$ to be evaluated, by summing the sensitivity map over the regions where a source with flux S would satisfy our p_{ns} detection criterion. If $N(> S)$ is given, the differential version can be evaluated as:

$$N(S) \Delta S = \frac{N(> [S + \Delta S]) - N(> S)}{\Delta S} \quad (2)$$

By itself, the cumulative or differential log N –log S relation is of limited utility for the heterogeneous collections of M 33 objects mixed with foreground stars and background AGN. Our aim is to dissect the log N –log S distribution to extract the LF for the M 33 point source population. Two components, the foreground stars and the SNRs in M 33, are well in hand, and their contribution can be evaluated directly. However, because M 33 subtends a large solid angle on the sky, the contamination by background AGN is a serious issue. We start with the differential log N –log S distribution, because the variation of the components is easier to discern.

In Fig. 9, we show the differential log N –log S relation for the soft (0.5–2 keV) and hard (2–8 keV) bands in the left and right panels, respectively. We start by subtracting foreground stars and SNR contributions from the total source distribution, resulting in a combination of M 33 point sources and background AGN.

Subtracting the AGN contribution requires some care, since the AGN dominate strongly at lower flux values. For each $1'' \times 1''$ pixel of our image, we calculated the differential log N –log S relation of the background AGN. We accounted for M 33 absorption by evaluating $e^{-\sigma N(H)}[S, S + \delta S]$, where $N(H)$ is the total hydrogen (nucleon) column density ($N(\text{HI}) + 2X\text{N(CO)}$) for that pixel. For the AGN log N –log S , we adopted the distribution provided by Cappelluti et al. (2009), which nicely confirms the earlier work from Harrison et al. (2003).

In Fig. 10 we present the cumulative X-ray LF for all sources detected in the FOV corrected for absorption and contributions due to background AGN. We used vertical black lines to mark the flux for which $\int N(S)dS / \int N(S)(A/A(S))dS \sim 0.9$, i.e. the level at which the survey is $\sim 90\%$ complete. The cumulative log N –log S for the AGN (blue line in Fig. 10) was obtained by summing the AGN differential log N –log S in the same manner as the measured differential log N –log S . The cumulative log N –log S for the AGN was then

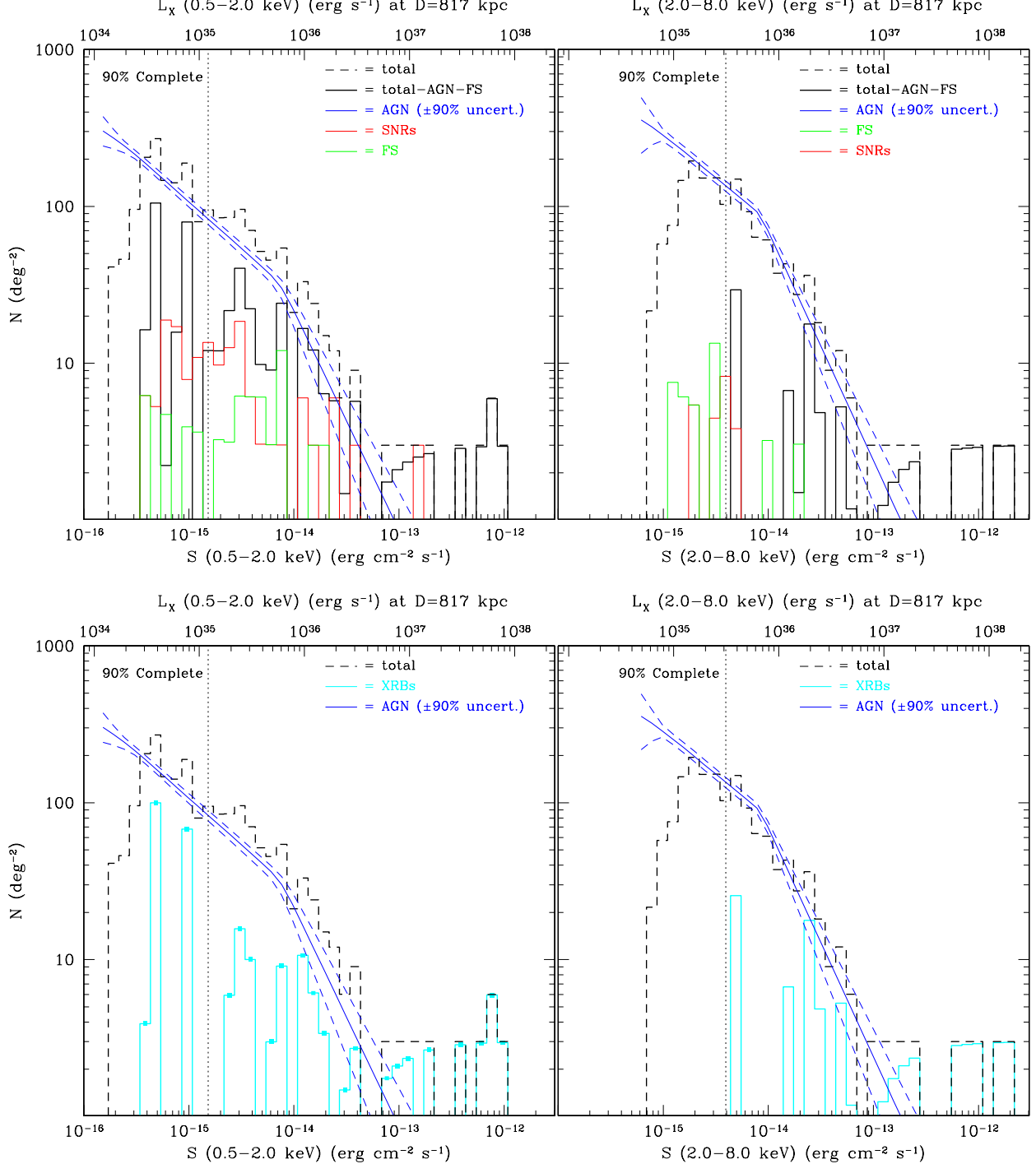


Fig. 9.— Differential X-ray log N -log S for M33 in the soft (0.5–2.0 keV) and hard (2.0–8.0 keV) energy band. The uncertainty of the AGN model from Cappelluti et al. (2009) was evaluated for a 90% Poisson error. The corresponding X-ray luminosities (assuming the objects are in M33) are shown on top of each panel.

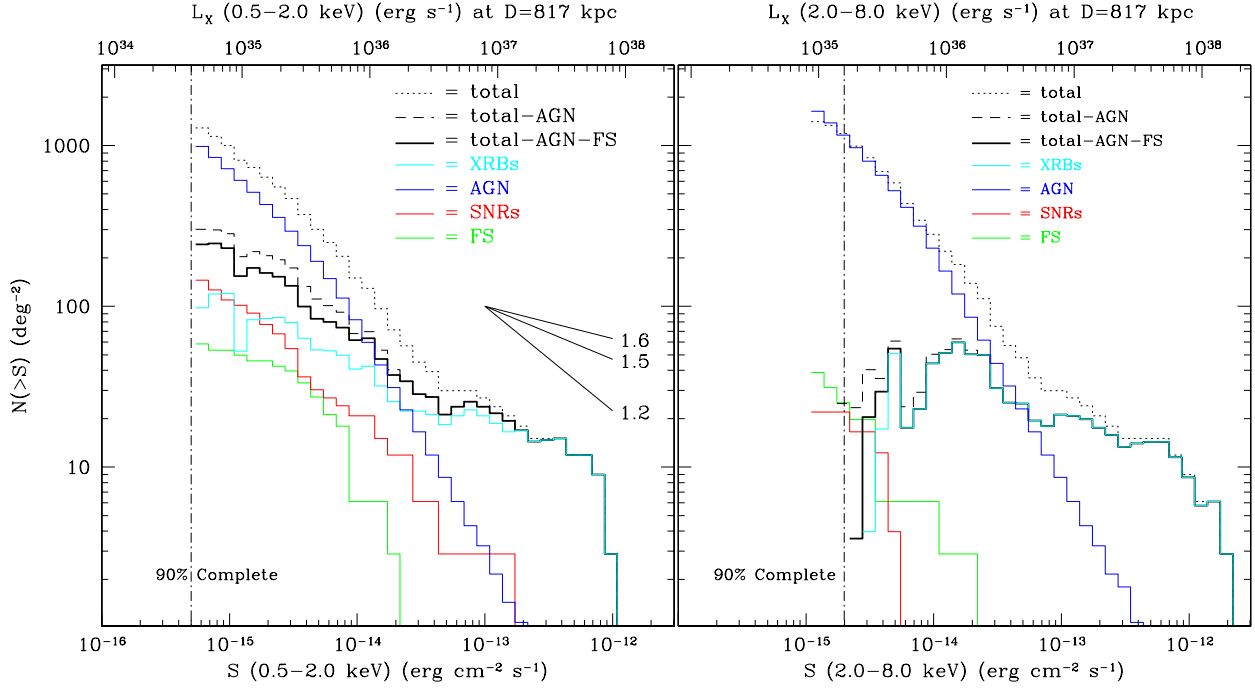


Fig. 10.— Cumulative X-ray log N –log S for M 33 in the soft (0.5–2.0 keV) and hard (2.0–8.0 keV) energy band. For the AGN log N –log S , the model from Cappelluti et al. (2009) was assumed. The solid black histogram corresponds to the sources we think are in M 33, while the solid cyan line reflects the XRBs (after SNRs have been subtracted). The three black lines represent different cumulative slopes for the HMXBs.

subtracted from the uncorrected log N –log S to give the background-corrected cumulative log N –log S for M 33 (black dashed line in Fig. 10). The cyan curve is what remains left after contributions from SNRs and FSs are removed, i.e., the distribution for sources in M 33. By converting the fluxes to luminosities (based on the assumed M 33 distance), the corresponding M 33 X-ray LF is obtained.

There are four sources of uncertainty in deriving the X-ray LF. The first uncertainty is due to Poisson statistics for X-ray source numbers which become increasingly important at higher luminosities and dominate over the other sources of uncertainty at most luminosities. The second uncertainty is due to intrinsic source variability. Zezas et al. (2007) have shown that in the case of the Antennae, where there is a strongly time-varying population, the LF from a single epoch is statistically consistent with the mean of multi-epoch measurements. Our LF is formed from at least two epochs of observation and should therefore be a reasonable representation of the mean LF. The third uncertainty is due to the sensitivity calculation. Although this uncertainty produces only small changes in $A(S)$, it produces a large change

in the expected number of background AGN, because the number of AGN increases rapidly at low fluxes. This effect is insignificant at higher fluxes, but becomes significant below the flux at which AGN start to dominate ($S \lesssim 5 \times 10^{-15} \text{ erg cm}^{-2} \text{ s}^{-1}$ in the 2.0-8.0 keV band).

The fourth uncertainty is due to the uncertainty in the AGN log N –log S relation. The Cappelluti et al. (2009) log N –log S distribution was derived from a deep (2deg^2) field and is consistent with the deeper Chandra Deep Field-South (CDF-S). Given the depth and FOV of the CDF-S compared to ChASeM33, the uncertainty in the shape of the AGN log N –log S distribution should be a smaller effect than the Poisson uncertainty in the number of expected sources (i.e., the normalization) in the M 33 FOV. To determine the magnitude of the normalization uncertainty we used the Cappelluti et al. (2009) parametrization of the AGN log N –log S relation to simulate the expected number of AGN within the FOV as a function of flux. At each flux level we determined the limits containing 90% of 10^4 Monte Carlo simulations. We then propagated these limits through our model of the absorption due to M 33 to determine the uncertainty in the AGN subtraction due to the uncertainty of the normalization. To determine the magnitude of the effect of the uncertainty in the shape of the AGN log N –log S , we fit the data from the Cappelluti et al. (2009) cumulative log N –log S . We then found the 90% uncertainty interval for each parameter individually, allowing all the other parameters to vary. The envelope formed by the log N –log S derived from the individual parameter limits is smaller (by roughly a factor of two at most fluxes) than the envelope due to the normalization uncertainty. We show the effect of the normalization error in Figure 9 rather than the uncertainty due to the shape of the log N –log S . This relative uncertainty becomes larger at higher fluxes where the total number of AGN becomes insignificant.

From the cumulative log N –log S we see that the source density of X-ray sources in M 33 is relatively low. Even at the lowest fluxes the source density is $< 0.1 \text{ arcmin}^{-2}$ (4.6 kpc^{-2}), which is significantly lower than the surface density of background sources. The cumulative log N –log S of the sources in M 33 is also significantly flatter than that of the background, so that the surface density contributions are equivalent at $f_X \simeq 10^{-14} \text{ erg s}^{-1} \text{ cm}^{-2}$ ($L_X \simeq 10^{36} \text{ erg s}^{-1}$ for objects in M 33). When the SNRs and FSs are removed from the M 33 source LF, the function becomes even flatter.

The number of HMXBs should correlate with the star formation rate (Grimm et al. 2003) and the number of LMXBs should correlate with the total stellar mass (Gilfanov 2004). We adopt a star formation rate for M 33 of $0.45 \pm 0.10 M_\odot/\text{yr}$ from Verley et al. (2009) and a stellar mass of $4.5 \times 10^9 M_\odot$ (Corbelli 2003). In order to scale from values determined for the Milky Way, we adopt a stellar mass of the Milky Way of $5.0 \times 10^{10} M_\odot$ (Hammer et al. 2007) and a range of star formation rates from $0.68 - 5.0 M_\odot$ (Smith et al.

1978; Robitaille & Whitney 2010). Given the star formation rate and total stellar mass of M33 we expect that HMXBs will dominate over LMXBs for luminosities larger than $L_X > 10^{36}$ erg s $^{-1}$, but the expected number of HMXBs and LMXBs is roughly equal for luminosities larger than $L_X > 10^{37}$ erg s $^{-1}$ given the steeper slope of the HMXB LF. The estimates of the XRB cumulative LFs in Figure 10 suggest a rather flat slope. Grimm et al. (2002) predict a slope of 1.6 for HMXBs and 1.2 for LMXBs based on the populations in the Milky Way. Our estimate of the slope is 1.5 based on the soft band luminosity function, but the uncertainties are large given the large uncertainty in the AGN model.

There are several methods for estimating the number of HMXBs, LMXBs, and total XRBs expected in M33. We have examined the predictions from three methods: (1) simply scaling from the observed population in the MW (Grimm et al. 2002), (2) population synthesis modeling for HMXBs Dalton & Sarazin (1995), and (3) “universal” LFs for HMXBs (Grimm et al. 2003) and LMXBs (Gilfanov 2004) based on the analysis of *Chandra* data of nearby galaxies. We compare the expected number of total XRBs (where total is the sum of the HMXBs and LMXBs) to the number of XRBs derived from the ChASeM33 survey LFs in three luminosity ranges ($L_X > 10^{38}$, 10^{37} , & 10^{36} erg s $^{-1}$), except for the Dalton & Sarazin (1995) results which only predict the number of HMXBs. The energy band from 2.0-10.0 keV has been used traditionally for the luminosity of XRBs, so we converted our 2.0-8.0 keV band fluxes to the broader band assuming a disk blackbody plus power-law model appropriate for XRBs.

We estimate that in the ChASeM33 source catalog there are 2/7/16 XRBs more luminous than $L_X > 10^{38}/10^{37}/10^{36}$ erg s $^{-1}$ respectively. We scaled the expected numbers by the star formation rate and stellar mass of M33 and also by a factor of 0.7 to account for the fact that the ChASeM33 survey only covers 70% of the area of the galaxy within the D₂₅ isophote. Using the LFs for HMXBs and LMXBs in the Milky Way derived by Grimm et al. (2002), we would expect (0.6-1.0)/(2.4-4.2)/(6.4-14.3) XRBs more luminous than $L_X > 10^{38}/10^{37}/10^{36}$ erg s $^{-1}$ respectively, where the range of values is due to the assumed range of star formation rates for the Milky Way. The Dalton & Sarazin (1995) models predict 1–6 HMXBs with $L_X > 10^{37}$ erg s $^{-1}$ and 4–26 HMXBs with $L_X > 10^{36}$ erg s $^{-1}$ (they made no predictions for $L_X > 10^{38}$ erg s $^{-1}$). Finally, the universal LFs of Grimm et al. (2003) and Gilfanov (2004) predict a total number of XRBs more luminous than $L_X > 10^{38}/10^{37}/10^{36}$ erg s $^{-1}$ of 2.3/11.4/39.0 respectively.

Our estimates and the model predictions agree to within a factor of \sim 3. The predictions based on the Milky Way populations are lower than our estimates for M33, while the predictions from the universal LFs are higher than our estimates for M33. Given the rather crude scaling by star formation rate and total stellar mass, the inherent uncertainty in the

universal LFs (estimated to be 50%), and the partial coverage of M 33 by the ChASeM33 survey, agreement to within a factor of ~ 3 is not surprising. Agreement to this level indicates that the processes which control the formation and evolution of XRBs in M 33 are not radically different from the Milky Way, M31, and other nearby galaxies.

4. Summary and Conclusions

We have presented the final version of the X-ray point source catalog in the framework of the ChASeM33 project. ChASeM33 is the deepest and spatially best resolved X-ray survey of any galaxy so far. A total of 662 sources were detected of which at least 100 could be identified to be located in M 33. The faintest detected point source in the $0.35 - 8.0$ keV energy band (#501) has an unabsorbed energy (photon) flux of 2.79×10^{-16} erg s $^{-1}$ cm $^{-2}$ (1.42×10^{-7} photons s $^{-1}$ cm $^{-2}$) if we adopt our standard model with $\Gamma = 1.9$ and an N_{H} of 6×10^{20} cm $^{-2}$. If this source is located in M 33, its luminosity would be 2.2×10^{34} erg s $^{-1}$. By far the brightest source in M 33 is the nucleus (#318) with a total unabsorbed energy (photon) flux of 1.5×10^{-11} erg s $^{-1}$ cm $^{-2}$ (6.2×10^{-3} photons s $^{-1}$ cm $^{-2}$), which translates into a luminosity of about 1.2×10^{39} erg s $^{-1}$, making this object the brightest single X-ray source in the Local Group.

Neither of the supersoft X-ray sources reported by PMH07 and MPH06 were detected nor did we detect new candidates. This, however, is not surprising as the sensitivity of the front-illuminated ACIS-I chips is insufficient for such studies. Among the 38 ChASeM33 sources which are time-variable, 35 (7) are variable on short (long) time scales, while 4 show both types of variability.

Based on optical follow-up spectroscopy, the analysis of multi-wavelength data, and the cross correlation with other catalogs, we were able to identify counterparts for 183 of the 662 X-ray sources. Most sources, which appear to be located within M 33, seem to be well aligned with the spiral arms of this galaxy. By means of hardness ratio diagrams we could identify two distinct regions, one covered by SNRs and foreground stars and one region which is populated by the bulk of (yet unidentified) sources. The majority of unidentified sources are likely background galaxies/AGN.

We were able to perform detailed spectral fits to the 15 sources with the largest number of net counts (11 in this paper and 4 in previous papers). The detailed spectral fits confirmed or supported the classification of 5 of the 11 sources as XRBs when the variability is also considered. Three of the 11 sources are confirmed AGN based on the X-ray spectra, X-ray variability, and measured redshift, while 3 of the 11 sources are most likely AGN based on

the X-ray spectra and variability.

We presented the differential log N –log S of all the sources in the ChASeM33 in the 0.5–2.0 keV and 2.0–8.0 keV bands. Taking advantage of the 183 source classifications, we were able to create differential log N –log S functions for the foreground stars and SNRs in M 33. We modeled the contribution of background AGN and subtracted it from the total log N –log S along with the foreground stars and SNRs to generate a log N –log S of the XRBs and unidentified sources which could be in M 33. The largest uncertainty in creating a log N –log S of the XRBs and unclassified sources in M 33 is the model of the AGN contribution. We therefore explored the sensitivity of our result for a range of AGN models. We then created cumulative LFs for the SNRs and XRBs and unidentified sources in M 33. The slope of the LF for XRBs is closer to 1.6, the expected value for a dominant HMXB population. Additionally, the number of candidate XRBs above 10^{35} erg s $^{-1}$, 10^{36} erg s $^{-1}$, and 10^{37} erg s $^{-1}$ agrees to within a factor of three with the number of XRBs in the Milky Way after scaling by stellar mass and star formation rate, the number of HMXBs predicted by population synthesis models, and the number derived from universal luminosity functions based on XRBs in other nearby galaxies.

Support for this work was provided by the National Aeronautics and Space Administration through *Chandra* Award Number G06-7073A issued by the *Chandra* X-ray Observatory Center, which is operated by the Smithsonian Astrophysical Observatory and on behalf of the National Aeronautics Space and Administration under contract NAS8-03060. RT, PPP, TJG, and RJE acknowledge support under NASA contract NAS8-03060. This work has made use of SAOImage DS9, developed by the Smithsonian Astrophysical Observatory (Joye & Mandel 2003), the XSPEC spectral fitting package (Arnaud 1996), the FUNTOOLS utilities package, the HEASARC FTOOLS package, the CIAO (*Chandra* Interactive Analysis of Observations) package, and ACIS Extract, the source extraction and characterization tool developed and maintained by Pat Broos. Sincere thanks to Pat Broos for answering our questions regarding AE and for maintaining this important tool and to David Thilker for kindly providing the H I map of M 33. We also acknowledge the heroic effort of the anonymous referee for a careful reading of the manuscript and several comments that helped to improve the paper.

A. APPENDIX

This section provides all tables which contain the basic ChASeM33 catalog data. Table 3 lists basic properties for each source, such as source position, its positional uncertainty,

exposure time, and size of the source and background region. In Table 4 we provide the merged p_{ns} values for each source in eight different energy bands, while Tables 5 and 6 list the corresponding net counts and photon fluxes in these bands.

In Table 7 we provide the results of the spectral analysis of sources with 8 or more spectral groups. We list the best-fit model together with the best-fit parameters, as well as deabsorbed X-ray luminosities in the 0.35–2.0 keV and 0.35–8.0 keV energy bands. As some of the source spectra have more than 2000 counts, we fit those sources with more complex models. These results are listed in Table 8.

The results of the cross correlation of the ChASeM33 data with other multi-wavelength spectrophotometric data are given in Table 9 together with $H\alpha$ surface brightnesses and results from our variability analysis of the X-ray sources. Finally, Table 10 provides the cross-identifications of the SSSs between the ChASeM33 catalog and the catalogs from PMH04 and MPH06.

Table 1. Summary of Prior X-ray Surveys of M 33

Observatory	Number of Detected Sources	Limiting Unabsorbed Luminosity (10^{35} ergs/sec) ^a	References
<i>Einstein</i>	17 ^b	–	(1), (2), (3)
<i>ROSAT</i>	184 ^c	~2.0	(4), (5), (6)
<i>XMM-Newton</i>	447 ^d	~1.0	(7), (8)
<i>Chandra</i>	261 ^e	~0.2	(9)

Note. — ^aFor the *ROSAT*, *XMM-Newton*, and *Chandra* observations, the corresponding energy ranges are 0.12-2.48 keV, 0.2-4.5 keV, and 0.35-8.0 keV, respectively. ^bSignificant component of diffuse emission detected. ^cTotal number of sources located within ~50' of nucleus. ^dTotal number of sources within ~32' of nucleus. ^eTotal number of sources in a 0.16 square degree field including the nucleus and a field northwest of the center that included NGC 604. Summary of References: (1) – Long et al. (1981), (2) – Markert & Rallis (1983), (3) – Trinchieri et al. (1988), (4) – Schulman & Bregman (1995), (5) – Long et al. (1996), (6) – Haberl & Pietsch (2001), (7) – Pietsch et al. (2004), (8) – Misanovic et al. (2006), (9) – Grimm et al. (2005).

Table 2. List of all ChASeM33 and archival observations.

ObsID	Field No.	Epoch	Pointing direction		Obs. start date	Roll angle [°]	Exposure (cleaned) [ks]
			RA (J2000.0)	Dec (J2000.0)			
6376	1	e1	01:33:51.143	+30:39:20.54	2006/03/03	308.48	94.3
6377	1	e2	01:33:50.182	+30:39:51.29	2006/09/25	142.01	93.2
6378	2	e1	01:34:13.208	+30:48:02.91	2005/09/21	140.21	95.5
6379	2	e2	01:34:13.468	+30:48:04.21	2006/09/04	127.88	54.3
7402	2	e2	01:34:13.470	+30:48:04.17	2006/09/07	127.88	45.2
6380	3	e1	01:33:33.310	+30:48:55.50	2005/09/23	140.21	90.5
6381	3	e2	01:33:33.475	+30:48:56.44	2006/09/12	132.17	99.6
6382	4	e1	01:33:08.204	+30:40:10.59	2005/11/23	262.21	72.7
7226	4	e1	01:33:08.211	+30:40:10.55	2005/11/26	262.21	25.2
6383	4	e2	01:33:09.206	+30:40:40.97	2006/06/15	97.80	91.9
7170	5	e1	01:33:27.204	+30:31:39.31	2005/09/26	145.71	41.5
7171	5	e1	01:33:27.205	+30:31:39.29	2005/09/29	145.71	38.2
6384	5	e1	01:33:27.210	+30:31:39.25	2005/10/01	145.71	22.2
6385	5	e2	01:33:27.402	+30:31:40.64	2006/09/18	135.75	90.4
6386	6	e1	01:34:06.489	+30:30:26.69	2005/10/31	224.21	14.8
7196	6	e1	01:34:06.500	+30:30:26.73	2005/11/02	224.21	23.0
7197	6	e1	01:34:06.501	+30:30:26.62	2005/11/03	224.21	12.8
7198	6	e1	01:34:06.505	+30:30:26.82	2005/11/05	224.21	22.0
7199	6	e1	01:34:06.489	+30:30:26.78	2005/11/06	224.21	14.8
7208	6	e1	01:34:06.992	+30:30:18.96	2005/11/21	259.45	11.7
6387	6	e2	01:34:07.920	+30:30:49.21	2006/06/26	103.21	78.3
7344	6	e2	01:34:07.921	+30:30:49.31	2006/07/01	103.21	21.7
6388	7	e1	01:34:33.542	+30:39:00.27	2006/06/09	94.87	89.7
6389	7	e2	01:34:32.547	+30:38:29.65	2006/11/28	265.72	96.8
1730	archival	ObsID	01:33:50.953	+30:39:57.27	2000/07/12	108.58	47.3
2023	archival	ObsID	01:34:34.630	+30:47:58.17	2001/07/06	106.55	89.4

Table 3. ChASeM33 source list.

Source No. (1)	Source ID (2)	RA (J2000) [$^{\circ}$] (3)	Dec (J2000) [$^{\circ}$] (4)	Positional Error [$''$] (5)	No. of obs. (6)	Total exposure [s] (7)	Total exp. map value [$s\ cm^2$] (8)	R_{src} [sky pixel] (9)	R_{bkg} [$'$] (10)	θ (11)
1	013224.55+303322.3	23.102333	30.55622	2.34	1	96659	1.316e+07	24.3	66.1	11.6
2	013227.18+303521.0	23.113250	30.58919	1.17	1	96659	1.795e+07	18.3	56.7	10.1
3	013229.23+303618.6	23.121792	30.60517	0.74	1	96659	1.797e+07	15.8	44.8	9.2
4	013229.31+304514.0	23.122138	30.75389	1.40	1	96662	1.439e+07	17.5	50.1	9.8
5	013230.28+303548.1	23.126172	30.59671	0.97	1	96659	1.876e+07	15.6	43.4	9.3
6	013230.54+303618.0	23.127250	30.60500	1.44	1	96659	1.885e+07	15.4	42.0	9.0
7	013232.83+304027.9	23.136833	30.67442	1.43	2	187395	2.958e+07	11.9	33.2	7.7
8	013233.76+304726.7	23.140678	30.79077	1.62	2	187398	3.506e+07	19.7	67.6	10.3
9	013236.34+304045.4	23.151458	30.67928	1.06	2	187395	2.932e+07	9.9	32.0	7.0
10	013236.84+303229.0	23.153500	30.54139	0.68	2	185890	3.063e+07	20.6	54.8	10.6
11	013240.62+303721.2	23.169250	30.62258	0.50	2	187404	3.987e+07	8.9	33.6	6.8
12	013240.86+303550.3	23.170271	30.59732	0.50	2	187404	3.877e+07	11.2	33.6	7.5
13	013241.32+303217.7	23.172208	30.53825	1.19	4	377183	6.091e+07	18.7	68.5	10.0
14	013242.07+303329.0	23.175292	30.55806	0.97	3	276635	5.272e+07	16.6	41.5	9.3
15	013242.46+304815.0	23.176917	30.80419	0.83	3	276767	5.042e+07	19.1	49.8	10.0
16	013243.41+303506.2	23.180875	30.58506	0.50	2	187404	3.874e+07	11.4	30.5	7.6
17	013244.17+303559.7	23.184042	30.59992	1.00	2	187404	3.979e+07	9.5	34.1	6.9
18	013244.77+303037.4	23.186542	30.51039	2.05	2	189779	3.265e+07	16.0	46.8	9.2
19	013245.06+303911.3	23.187750	30.65314	0.50	2	187404	4.071e+07	6.0	29.5	5.2
20	013246.72+303437.7	23.194688	30.57715	1.32	3	276635	5.058e+07	12.3	69.2	7.9
21	013247.65+304414.7	23.198542	30.73742	0.54	2	187398	3.348e+07	7.1	30.0	5.9
22	013247.71+304711.1	23.198792	30.78642	0.50	3	276767	5.280e+07	14.5	42.4	8.7
23	013248.66+303441.3	23.202750	30.57814	0.55	4	377183	7.123e+07	12.1	39.7	7.9
24	013249.08+304253.5	23.204528	30.71488	0.50	2	187398	3.580e+07	5.1	32.9	4.9
25	013249.39+303829.6	23.205829	30.64156	0.50	2	187404	4.288e+07	4.8	30.8	4.6
26	013249.63+303250.7	23.206792	30.54742	0.51	4	377183	7.163e+07	13.7	37.7	8.4

Table 3—Continued

Source No.	Source ID	RA (J2000) [$^{\circ}$]	Dec (J2000) [$^{\circ}$]	Positional Error [$''$]	No. of obs.	Total exposure [s]	Total exp. map value [$s\ cm^2$]	R_{src} [sky pixel]	R_{bkg} [$''$]	θ
(1)	(2)	(3)	(4)	(5)	(6)	(7)	(8)	(9)	(10)	(11)
27	013249.84+303102.3	23.207667	30.51731	0.50	2	189779	3.314e+07	12.8	41.3	8.1
28	013249.87+305018.9	23.207828	30.83859	0.50	2	187757	3.421e+07	16.8	42.4	9.4
29	013250.71+303035.3	23.211292	30.50983	0.50	2	189779	3.375e+07	12.0	35.8	8.0
30	013250.71+303144.1	23.211292	30.52892	0.56	2	189779	3.625e+07	11.9	35.8	7.9
31	013250.86+304252.8	23.211917	30.71467	0.50	2	187398	4.030e+07	4.6	29.8	4.6
32	013251.87+305132.6	23.216125	30.85906	1.29	2	187757	3.255e+07	16.4	47.4	9.3
33	013252.50+304023.9	23.218750	30.67331	0.50	2	187395	1.988e+07	3.4	36.5	3.5
34	013253.20+303809.1	23.221693	30.63587	0.50	2	187404	3.941e+07	3.8	25.8	4.0
35	013253.56+303814.8	23.223167	30.63747	0.50	2	187404	4.022e+07	3.7	25.8	3.9
36	013253.82+304732.6	23.224250	30.79239	1.14	4	375155	7.314e+07	13.1	44.3	8.2
37	013253.89+303311.8	23.224542	30.55328	0.50	4	377183	7.144e+07	11.3	45.6	7.6
38	013253.90+305017.8	23.224598	30.83830	0.50	2	187757	3.541e+07	14.2	38.4	8.6
39	013255.06+305038.9	23.229417	30.84414	0.94	2	187757	3.209e+07	13.8	42.9	8.4
40	013255.33+304215.8	23.230546	30.70440	0.50	2	187398	4.218e+07	3.0	29.7	3.4
41	013255.45+304842.3	23.231056	30.81176	0.50	4	375155	7.176e+07	13.7	35.6	8.4
42	013255.66+304557.8	23.231917	30.76606	0.50	3	276767	5.871e+07	9.7	36.0	6.9
43	013255.74+303712.1	23.232250	30.62003	0.50	2	187404	4.342e+07	4.1	31.2	4.3
44	013256.03+303559.8	23.233481	30.59995	0.50	4	377183	7.883e+07	8.9	31.2	6.5
45	013256.20+303547.6	23.234167	30.59656	0.50	4	377183	7.873e+07	8.9	31.2	6.5
46	013256.94+302633.9	23.237256	30.44276	1.16	1	100548	7.952e+06	12.6	47.6	8.3
47	013257.07+303222.8	23.237792	30.53967	0.57	4	377183	6.608e+07	11.2	41.3	7.5
48	013257.07+303927.0	23.237792	30.65752	0.50	2	187404	4.507e+07	2.3	32.6	2.7
49	013257.51+304314.8	23.239655	30.72078	0.50	2	187398	4.316e+07	3.3	32.6	3.7
50	013258.16+304936.2	23.242346	30.82675	0.52	2	187757	3.499e+07	11.0	35.6	7.6
51	013258.17+303056.2	23.242414	30.51562	0.50	2	189779	3.051e+07	7.7	29.7	6.3
52	013258.54+303547.1	23.243958	30.59642	1.30	4	377183	8.043e+07	8.1	32.6	6.2

Table 3—Continued

Source No.	Source ID	RA (J2000) [$^{\circ}$]	Dec (J2000) [$^{\circ}$]	Positional Error [$''$]	No. of obs.	Total exposure [s]	Total exp. map value [$s\ cm^2$]	R_{src} [sky pixel]	R_{bkg} [$^{\prime}$]	θ
(1)	(2)	(3)	(4)	(5)	(6)	(7)	(8)	(9)	(10)	(11)
53	013258.63+304059.4	23.244329	30.68319	0.50	2	187398	4.590e+07	2.0	32.6	2.3
54	013259.67+305326.4	23.248625	30.89067	0.50	2	187757	3.755e+07	14.3	39.8	8.5
55	013259.71+304718.8	23.248792	30.78858	0.64	4	375155	7.665e+07	10.4	33.0	7.3
56	013300.07+303957.2	23.250292	30.66589	0.50	2	187404	4.546e+07	1.9	34.6	1.9
57	013300.12+304136.6	23.250528	30.69353	0.50	2	187398	4.599e+07	2.0	34.6	2.2
58	013300.19+304009.5	23.250792	30.66931	0.50	3	280473	4.817e+07	6.6	26.7	5.2
59	013300.42+304408.1	23.251750	30.73559	0.91	2	187398	4.355e+07	3.9	38.7	4.1
60	013300.43+303133.4	23.251792	30.52597	0.58	2	189779	3.404e+07	6.7	32.9	5.8
61	013300.88+303424.8	23.253667	30.57358	0.72	4	377183	7.348e+07	8.0	32.9	6.3
62	013300.88+304520.8	23.253667	30.75578	0.50	4	375155	8.011e+07	8.8	33.5	6.4
63	013301.03+304043.1	23.254292	30.67864	0.50	3	280467	4.947e+07	8.9	33.5	4.9
64	013301.93+303158.1	23.258042	30.53283	0.50	3	286438	5.773e+07	8.8	32.9	6.4
65	013302.33+304643.1	23.259734	30.77865	0.50	4	375155	7.550e+07	9.2	34.0	6.8
66	013302.41+304328.6	23.260065	30.72463	0.50	2	187398	4.515e+07	3.0	29.5	3.3
67	013303.52+303827.3	23.264708	30.64092	0.50	6	562306	1.038e+08	11.9	29.7	7.1
68	013303.55+303903.8	23.264833	30.65106	0.50	5	473082	9.315e+07	10.6	29.7	6.4
69	013303.68+304043.9	23.265365	30.67888	0.50	4	372521	6.420e+07	11.0	31.3	5.8
70	013304.03+303953.6	23.266796	30.66491	0.50	2	187404	3.604e+07	1.7	33.2	1.2
71	013304.15+304006.7	23.267292	30.66853	0.50	2	187408	3.083e+07	1.6	33.2	1.1
72	013304.36+303112.1	23.268167	30.52003	0.50	2	189779	3.763e+07	5.1	33.0	5.0
73	013304.53+303903.7	23.268904	30.65104	0.50	2	187404	2.870e+07	1.9	28.7	1.8
74	013304.78+304124.1	23.269937	30.69005	0.50	3	280467	6.099e+07	6.2	33.2	3.6
75	013304.90+302835.6	23.270417	30.47656	0.83	2	189779	3.795e+07	6.8	32.2	5.7
76	013305.14+303001.4	23.271456	30.50041	0.50	2	189779	3.355e+07	5.4	27.9	5.0
77	013305.62+303840.4	23.273458	30.64457	0.50	6	562306	1.170e+08	10.4	33.2	6.3
78	013305.79+303804.7	23.274125	30.63464	0.50	6	562306	1.152e+08	10.1	33.2	6.4

Table 3—Continued

Source No. (1)	Source ID (2)	RA (J2000) [$^{\circ}$] (3)	Dec (J2000) [$^{\circ}$] (4)	Positional Error [$''$] (5)	No. of obs. (6)	Total exposure [s] (7)	Total exp. map value [$s\ cm^2$] (8)	R_{src} [sky pixel] (9)	R_{bkg} [$'$] (10)	θ (11)
79	013306.22+305109.2	23.275917	30.85256	0.66	2	187757	4.074e+07	7.7	31.9	6.2
80	013306.82+303909.7	23.278445	30.65272	0.50	2	187404	4.646e+07	1.7	33.2	1.3
81	013307.06+303910.4	23.279417	30.65289	0.50	2	187404	4.656e+07	1.7	33.2	1.3
82	013307.39+303912.3	23.280792	30.65344	0.50	2	187404	4.660e+07	1.7	33.2	1.2
83	013307.51+305343.5	23.281292	30.89544	0.50	2	187757	3.887e+07	10.8	31.9	7.3
84	013307.72+305235.5	23.282167	30.87653	1.20	2	187757	3.701e+07	8.8	35.7	6.6
85	013307.77+302827.0	23.282409	30.47417	0.50	2	189779	3.753e+07	6.2	36.6	5.3
86	013307.81+303044.6	23.282583	30.51239	0.50	2	189779	3.950e+07	4.1	31.7	4.3
87	013307.90+303316.1	23.282955	30.55449	0.76	4	377183	8.195e+07	7.2	27.5	5.7
88	013307.96+303219.5	23.283167	30.53875	0.75	3	286438	6.187e+07	6.6	32.2	5.4
89	013308.23+305047.5	23.284292	30.84653	0.50	2	187757	4.152e+07	6.8	35.7	5.7
90	013308.35+304803.4	23.284792	30.80097	0.50	4	375161	6.450e+07	9.1	25.3	6.5
91	013308.50+303134.7	23.285417	30.52633	0.50	3	286438	5.884e+07	7.0	32.2	5.4
92	013308.80+304525.4	23.286667	30.75708	0.85	5	421871	6.811e+07	9.5	35.7	6.6
93	013309.10+303422.5	23.287917	30.57292	0.50	4	377183	8.359e+07	6.3	32.2	5.4
94	013310.17+304221.9	23.292413	30.70611	0.56	2	187395	4.063e+07	2.0	33.2	2.0
95	013310.51+303539.9	23.293792	30.59442	0.53	4	377190	8.325e+07	5.8	31.0	5.1
96	013310.56+304228.5	23.294030	30.70792	0.50	2	187395	3.574e+07	2.1	34.7	2.2
97	013310.72+303734.6	23.294667	30.62628	0.50	4	377183	8.336e+07	5.3	30.1	4.8
98	013310.92+303741.7	23.295500	30.62825	0.50	5	470252	1.034e+08	5.4	30.1	5.5
99	013311.08+304929.7	23.296167	30.82494	0.50	2	187757	4.026e+07	4.8	37.0	4.8
100	013311.09+303943.7	23.296246	30.66214	1.20	6	562306	1.050e+08	10.1	31.3	6.1
101	013311.67+303858.8	23.298625	30.64967	0.50	6	562306	1.183e+08	8.6	26.0	5.7
102	013311.75+303841.5	23.298992	30.64487	0.50	6	562306	1.193e+08	8.5	22.5	5.7
103	013312.31+305504.5	23.301292	30.91792	0.76	2	187766	2.988e+07	11.7	37.0	7.6
104	013313.12+305150.4	23.304708	30.86400	0.50	2	187757	3.996e+07	5.9	32.3	5.2

Table 3—Continued

Source No. (1)	Source ID (2)	RA (J2000) [$^{\circ}$] (3)	Dec (J2000) [$^{\circ}$] (4)	Positional Error [$''$] (5)	No. of obs. (6)	Total exposure [s] (7)	Total exp. map value [$s\ cm^2$] (8)	R_{src} [sky pixel] (9)	R_{bkg} [$^{\prime}$] (10)	θ (11)
105	013313.48+305709.6	23.306167	30.95269	1.54	1	89378	1.576e+07	15.7	52.3	9.3
106	013313.82+304530.5	23.307611	30.75849	0.50	5	421877	8.174e+07	7.6	31.9	5.8
107	013313.86+303552.2	23.307787	30.59785	0.50	5	470252	1.029e+08	7.1	31.9	5.6
108	013314.17+302459.0	23.309055	30.41639	0.50	2	189772	3.698e+07	10.6	33.9	7.3
109	013314.32+304236.7	23.309667	30.71022	0.50	8	707554	1.441e+08	10.5	31.9	6.7
110	013314.68+304012.2	23.311167	30.67008	0.50	7	609013	1.286e+08	9.3	27.6	5.9
111	013315.05+304059.4	23.312748	30.68317	0.50	7	609013	1.099e+08	10.7	30.9	6.7
112	013315.10+304453.0	23.312917	30.74808	0.50	5	421877	8.978e+07	7.1	17.3	5.6
113	013315.16+305318.2	23.313167	30.88839	0.50	2	187766	3.866e+07	7.4	33.5	5.9
114	013315.18+304138.0	23.313250	30.69389	0.64	6	519798	1.114e+08	9.1	29.9	5.8
115	013315.22+304937.9	23.313448	30.82721	0.50	2	187757	4.377e+07	3.5	31.4	4.0
116	013315.58+302418.2	23.314917	30.40506	0.57	2	189772	3.631e+07	12.1	40.6	7.8
117	013316.21+302934.1	23.317583	30.49281	0.60	3	276194	4.465e+07	9.1	35.1	5.7
118	013316.30+302823.8	23.317917	30.47328	0.50	2	189772	3.152e+07	4.0	34.5	4.0
119	013316.69+302429.4	23.319542	30.40817	0.50	2	189772	3.672e+07	11.0	43.9	7.5
120	013317.29+303530.4	23.322042	30.59178	0.50	6	562293	1.154e+08	7.4	29.9	5.8
121	013317.30+303308.9	23.322095	30.55249	0.50	4	377170	6.900e+07	5.9	31.0	4.5
122	013317.91+305236.3	23.324625	30.87675	0.50	2	187766	3.095e+07	5.6	27.2	5.0
123	013317.94+304900.1	23.324750	30.81672	0.50	3	278498	6.212e+07	6.1	27.2	4.8
124	013318.33+304200.6	23.326386	30.70017	0.50	8	707554	1.485e+08	9.4	28.9	6.4
125	013318.34+302840.4	23.326417	30.47789	0.50	2	189772	3.989e+07	3.2	33.2	3.6
126	013318.45+304716.5	23.326875	30.78792	0.50	4	375158	8.162e+07	6.6	28.8	5.3
127	013318.70+302934.0	23.327917	30.49278	0.50	2	186963	2.836e+07	12.5	82.7	7.0
128	013318.71+303736.5	23.327992	30.62681	0.50	7	609006	1.287e+08	7.2	27.1	5.7
129	013318.79+305241.0	23.328328	30.87806	0.50	2	187766	3.803e+07	5.5	28.8	4.9
130	013318.87+303229.9	23.328636	30.54164	0.50	4	372853	7.557e+07	8.0	30.1	5.1

Table 3—Continued

Source No. (1)	Source ID (2)	RA (J2000) [$^{\circ}$] (3)	Dec (J2000) [$^{\circ}$] (4)	Positional Error [$''$] (5)	No. of obs. (6)	Total exposure [s] (7)	Total exp. map value [$s\ cm^2$] (8)	R_{src} [sky pixel] (9)	R_{bkg} [$'$] (10)	θ (11)
131	013318.91+304546.0	23.328792	30.76278	0.50	5	421877	8.482e+07	7.1	32.2	5.6
132	013319.06+305205.0	23.329458	30.86806	0.50	2	187757	3.370e+07	4.6	25.5	4.4
133	013319.61+302847.8	23.331729	30.47997	0.50	3	276187	5.862e+07	7.5	30.1	5.2
134	013319.91+305102.0	23.332978	30.85056	0.50	2	187757	4.477e+07	3.3	28.5	3.6
135	013320.33+305241.6	23.334735	30.87824	0.50	2	187766	3.395e+07	5.1	35.1	4.7
136	013320.80+302948.0	23.336667	30.49669	0.50	3	276187	5.045e+07	7.5	32.0	4.8
137	013320.83+304335.6	23.336792	30.72656	0.51	7	607000	1.296e+08	7.6	33.8	5.9
138	013320.95+302648.8	23.337292	30.44689	0.50	2	189772	4.044e+07	5.6	30.4	5.0
139	013321.34+305218.9	23.338917	30.87192	0.50	2	187766	4.191e+07	4.5	29.8	4.3
140	013321.48+302309.8	23.339500	30.38606	1.95	2	189772	3.409e+07	14.4	39.2	8.6
141	013321.70+303858.4	23.340417	30.64958	0.50	7	609013	1.323e+08	7.0	31.3	5.6
142	013321.94+303923.0	23.341458	30.65639	0.50	7	609013	1.172e+08	7.4	27.1	5.7
143	013321.94+305520.6	23.341458	30.92239	0.69	2	187766	4.029e+07	9.4	33.3	6.9
144	013322.24+302445.6	23.342708	30.41267	0.50	3	201282	3.861e+07	10.2	34.0	7.2
145	013322.33+304011.2	23.343042	30.66978	0.50	5	419234	9.472e+07	5.3	25.4	4.7
146	013322.45+304224.1	23.343583	30.70672	0.50	9	796779	1.612e+08	9.8	28.4	6.7
147	013322.48+302942.6	23.343667	30.49519	0.50	3	276187	6.062e+07	6.1	28.0	4.2
148	013322.92+304010.3	23.345512	30.66953	0.50	6	519788	1.134e+08	6.0	24.6	5.3
149	013323.11+305653.9	23.346292	30.94831	1.38	2	187766	3.777e+07	13.0	38.1	8.3
150	013323.62+305001.2	23.348417	30.83367	0.50	3	285899	5.904e+07	7.9	27.0	4.7
151	013323.65+303426.6	23.348553	30.57406	0.50	7	609006	1.098e+08	7.7	28.0	5.6
152	013323.65+302607.0	23.348583	30.43528	0.50	2	189772	3.983e+07	6.5	34.2	5.5
153	013323.84+302613.5	23.349363	30.43709	0.50	2	189772	4.002e+07	6.3	34.2	5.5
154	013323.93+303517.5	23.349735	30.58820	0.50	7	609006	1.247e+08	7.3	29.6	5.7
155	013323.94+304820.4	23.349750	30.80567	0.50	4	372817	7.973e+07	8.6	27.0	5.3
156	013324.07+304347.3	23.350333	30.72981	0.64	7	607000	1.313e+08	7.3	21.7	5.8

Table 3—Continued

Source No. (1)	Source ID (2)	RA (J2000) [$^{\circ}$] (3)	Dec (J2000) [$^{\circ}$] (4)	Positional Error [$''$] (5)	No. of obs. (6)	Total exposure [s] (7)	Total exp. map value [$s\ cm^2$] (8)	R_{src} [sky pixel] (9)	R_{bkg} [$'$] (10)	θ (11)
157	013324.15+303503.4	23.350625	30.58428	0.50	7	609006	1.247e+08	7.4	29.6	5.7
158	013324.40+304402.4	23.351667	30.73400	0.50	7	607000	1.297e+08	7.3	14.9	5.8
159	013324.46+302504.5	23.351917	30.41794	0.50	3	201282	3.977e+07	9.4	36.0	6.8
160	013324.49+305346.6	23.352042	30.89628	0.50	2	187766	4.258e+07	6.0	29.2	5.2
161	013324.88+304536.0	23.353667	30.76000	0.50	6	513935	1.101e+08	7.6	29.2	5.8
162	013324.90+305508.9	23.353750	30.91914	0.50	2	187766	4.005e+07	8.4	32.6	6.5
163	013325.38+305814.8	23.355750	30.97078	0.85	2	187766	3.594e+07	16.9	56.8	9.5
164	013325.39+304246.1	23.355792	30.71283	0.57	8	696224	1.470e+08	8.7	29.5	6.2
165	013325.48+303619.1	23.356167	30.60531	0.50	8	707734	1.438e+08	8.2	29.5	6.1
166	013325.54+304440.7	23.356417	30.74464	0.50	7	607000	1.223e+08	7.4	27.5	5.8
167	013325.56+303647.7	23.356500	30.61325	0.50	8	707734	1.446e+08	8.5	32.9	6.2
168	013326.05+304119.2	23.358542	30.68867	0.50	9	796769	1.551e+08	9.6	26.7	6.7
169	013326.28+305639.8	23.359500	30.94439	0.85	2	187766	3.820e+07	11.7	37.6	7.9
170	013326.36+305533.1	23.359866	30.92588	0.56	2	187766	3.995e+07	9.2	32.6	6.8
171	013326.50+304535.7	23.360417	30.75994	0.50	7	607006	1.267e+08	8.0	28.2	6.0
172	013326.92+305012.5	23.362167	30.83683	0.50	3	285899	6.441e+07	6.9	28.2	4.2
173	013327.20+304911.4	23.363345	30.81984	0.50	5	470959	9.218e+07	10.6	28.2	4.8
174	013327.20+303119.8	23.363356	30.52219	0.50	6	431069	9.117e+07	9.2	30.0	5.8
175	013327.76+304647.3	23.365667	30.77981	0.50	7	608253	1.281e+08	9.6	28.2	6.3
176	013328.08+303135.0	23.367013	30.52640	0.50	7	524148	1.084e+08	9.9	33.5	5.3
177	013328.18+302518.0	23.367417	30.42167	1.04	3	201282	4.125e+07	8.7	31.4	6.5
178	013328.43+304221.3	23.368468	30.70594	0.50	6	508612	1.101e+08	6.3	38.6	5.4
179	013328.63+305930.9	23.369292	30.99192	3.46	2	187766	3.201e+07	20.4	58.0	10.6
180	013328.69+302723.6	23.369542	30.45658	0.50	4	287697	6.141e+07	7.6	20.1	5.6
181	013328.72+304322.5	23.369708	30.72292	0.50	8	696224	1.441e+08	8.4	33.6	6.2
182	013328.76+303309.3	23.369845	30.55259	0.50	9	713613	1.442e+08	10.0	28.4	6.2

Table 3—Continued

Source No. (1)	Source ID (2)	RA (J2000) [$^{\circ}$] (3)	Dec (J2000) [$^{\circ}$] (4)	Positional Error [$''$] (5)	No. of obs. (6)	Total exposure [s] (7)	Total exp. map value [$s\ cm^2$] (8)	R_{src} [sky pixel] (9)	R_{bkg} [$'$] (10)	θ (11)
183	013328.96+304743.5	23.370671	30.79542	1.14	6	561534	1.116e+08	10.0	29.1	6.1
184	013329.04+304216.9	23.371025	30.70471	0.50	7	607000	1.316e+08	6.7	36.8	5.6
185	013329.16+305134.9	23.371500	30.85972	0.50	2	187766	4.529e+07	2.5	30.9	2.8
186	013329.29+304537.4	23.372042	30.76039	0.50	7	607006	1.262e+08	7.9	26.7	5.9
187	013329.29+304508.4	23.372082	30.75235	0.50	7	607006	1.305e+08	7.6	26.7	5.9
188	013329.45+304910.7	23.372729	30.81966	0.68	5	470959	9.475e+07	10.1	34.4	5.6
189	013329.61+304521.8	23.373409	30.75606	0.50	4	375158	7.977e+07	5.9	28.0	5.0
190	013329.83+305118.0	23.374292	30.85500	0.50	3	285909	6.323e+07	6.9	31.3	4.6
191	013330.10+303456.7	23.375417	30.58242	0.50	7	609016	1.292e+08	7.2	28.4	5.6
192	013330.19+304255.6	23.375792	30.71547	0.69	8	696224	1.435e+08	8.0	30.4	6.1
193	013330.40+304641.9	23.376667	30.77831	0.50	7	608253	1.276e+08	9.1	27.1	6.1
194	013330.43+305503.6	23.376833	30.91767	0.70	2	187766	4.032e+07	7.7	30.3	6.2
195	013330.64+303404.1	23.377667	30.56781	0.50	10	805674	1.709e+08	9.2	31.8	6.4
196	013330.82+303455.2	23.378458	30.58200	0.50	10	805668	1.581e+08	8.3	31.8	6.3
197	013331.25+303333.4	23.380225	30.55928	0.50	10	805674	1.589e+08	10.3	32.8	6.7
198	013331.26+304445.7	23.380250	30.74603	0.50	7	607006	1.324e+08	7.2	26.2	5.8
199	013331.30+304928.2	23.380417	30.82450	0.50	5	470959	1.000e+08	9.6	22.7	5.3
200	013331.32+303402.2	23.380500	30.56728	0.50	3	282857	6.486e+07	4.2	31.8	3.8
201	013331.37+303816.9	23.380741	30.63805	0.50	8	707394	1.460e+08	8.3	25.3	6.0
202	013331.39+303737.4	23.380833	30.62708	0.50	8	707734	1.468e+08	7.7	30.7	5.9
203	013331.64+303042.9	23.381860	30.51192	0.50	7	526215	1.097e+08	8.9	31.8	5.5
204	013331.72+303556.1	23.382167	30.59894	0.50	9	719243	1.451e+08	8.0	31.8	6.0
205	013331.86+304011.7	23.382750	30.66994	0.50	9	796769	1.676e+08	8.9	26.3	6.3
206	013331.99+305741.0	23.383292	30.96139	0.80	2	187766	3.788e+07	14.6	38.0	8.8
207	013332.19+303656.8	23.384125	30.61578	0.50	9	719243	1.538e+08	7.8	27.9	5.9
208	013332.20+304446.7	23.384167	30.74631	0.50	7	607006	1.291e+08	7.1	23.3	5.7

Table 3—Continued

Source No. (1)	Source ID (2)	RA (J2000) [$^{\circ}$] (3)	Dec (J2000) [$^{\circ}$] (4)	Positional Error [$''$] (5)	No. of obs. (6)	Total exposure [s] (7)	Total exp. map value [$s\ cm^2$] (8)	R_{src} [sky pixel] (9)	R_{bkg} [$'$] (10)	θ (11)
209	013332.22+302448.8	23.384250	30.41356	1.12	3	201282	4.066e+07	9.8	34.4	7.1
210	013332.23+303955.5	23.384292	30.66544	0.50	9	796769	1.692e+08	8.9	27.9	6.3
211	013332.41+304824.5	23.385083	30.80681	0.50	6	563017	1.172e+08	10.0	27.6	5.7
212	013332.57+303617.4	23.385735	30.60484	0.75	9	719243	1.498e+08	7.9	28.5	6.0
213	013332.71+303339.3	23.386292	30.56094	0.50	10	805677	1.540e+08	10.1	31.5	6.6
214	013332.81+304633.3	23.386720	30.77592	0.50	8	701325	1.468e+08	9.6	27.6	6.4
215	013332.89+304916.3	23.387042	30.82122	0.50	5	470959	7.612e+07	11.6	51.5	6.5
216	013333.00+304618.5	23.387518	30.77182	0.50	8	701325	1.501e+08	9.3	25.8	6.3
217	013333.07+305009.8	23.387792	30.83606	0.50	4	380227	6.495e+07	8.9	35.6	5.3
218	013333.13+305155.5	23.388083	30.86542	0.77	3	285909	6.383e+07	6.9	28.9	4.9
219	013333.28+304932.5	23.388700	30.82570	0.50	5	470959	8.316e+07	10.2	40.9	6.1
220	013333.43+302739.8	23.389292	30.46106	0.50	4	287697	6.244e+07	6.4	27.6	5.3
221	013333.71+303109.6	23.390498	30.51934	0.50	8	622875	1.147e+08	11.4	38.2	6.8
222	013333.93+302943.9	23.391398	30.49553	0.50	6	479503	1.007e+08	8.3	33.8	5.5
223	013334.04+304710.1	23.391863	30.78615	0.50	8	706396	1.498e+08	10.2	28.9	6.4
224	013334.12+303714.9	23.392167	30.62081	0.50	9	719243	1.435e+08	8.0	29.3	6.0
225	013334.13+303211.3	23.392234	30.53648	0.50	8	622884	1.305e+08	9.3	17.2	5.9
226	013334.24+302616.6	23.392667	30.43797	0.90	3	198473	3.927e+07	9.8	34.3	6.8
227	013334.51+304555.0	23.393792	30.76528	0.50	8	701325	1.506e+08	8.8	28.9	6.3
228	013334.54+303556.1	23.393926	30.59894	0.50	10	805668	1.559e+08	8.9	27.6	6.3
229	013334.93+302711.4	23.395542	30.45317	0.50	5	386424	7.613e+07	8.1	29.7	6.1
230	013335.02+304404.7	23.395917	30.73464	0.80	7	607006	1.362e+08	7.0	28.9	5.7
231	013335.02+304931.8	23.395917	30.82550	0.50	6	563027	7.219e+07	14.7	48.1	8.3
232	013335.45+305231.4	23.397714	30.87540	0.50	3	285909	5.767e+07	6.6	32.3	5.0
233	013335.50+303729.3	23.397958	30.62481	0.50	9	719243	1.502e+08	7.9	25.7	5.9
234	013335.65+302632.2	23.398542	30.44228	0.50	5	386424	7.500e+07	9.0	33.2	6.5

Table 3—Continued

Source No. (1)	Source ID (2)	RA (J2000) [$^{\circ}$] (3)	Dec (J2000) [$^{\circ}$] (4)	Positional Error [$''$] (5)	No. of obs. (6)	Total exposure [s] (7)	Total exp. map value [$s\ cm^2$] (8)	R_{src} [sky pixel] (9)	R_{bkg} [$'$] (10)	θ (11)
235	013335.83+304655.4	23.399292	30.78208	0.50	9	799468	1.681e+08	10.2	28.0	6.6
236	013335.90+303627.4	23.399600	30.60762	0.50	10	805668	1.478e+08	8.9	37.2	6.4
237	013336.04+303332.9	23.400189	30.55914	0.50	10	805677	1.653e+08	9.4	24.6	6.4
238	013336.40+303742.7	23.401685	30.62853	0.50	9	719243	1.475e+08	7.3	25.6	5.9
239	013336.51+304722.8	23.402125	30.78969	1.01	7	609736	1.295e+08	8.6	28.0	5.9
240	013336.70+303729.6	23.402917	30.62489	0.50	8	707734	1.472e+08	7.3	28.2	5.8
241	013336.84+304757.3	23.403500	30.79925	0.50	7	609736	1.273e+08	9.4	28.0	5.8
242	013336.91+302321.5	23.403792	30.38931	0.50	3	201282	3.750e+07	14.5	40.9	8.6
243	013336.91+304641.4	23.403833	30.77819	0.50	9	799468	1.681e+08	9.8	28.0	6.5
244	013336.99+302618.2	23.404125	30.43839	0.61	5	386424	8.016e+07	9.5	36.9	6.8
245	013337.08+303253.5	23.404538	30.54820	0.50	9	714945	1.522e+08	8.6	36.6	6.0
246	013337.12+302558.5	23.404667	30.43292	0.79	5	386424	7.941e+07	10.0	36.6	7.0
247	013337.39+305232.9	23.405792	30.87581	0.50	3	285909	6.370e+07	7.0	28.0	5.3
248	013337.52+304718.7	23.406339	30.78853	0.50	9	799468	1.668e+08	10.3	28.0	6.5
249	013337.75+304009.1	23.407300	30.66922	1.05	9	796769	1.669e+08	9.1	48.1	6.2
250	013337.90+303837.2	23.407917	30.64369	0.50	9	709885	1.537e+08	8.4	29.4	5.9
251	013337.96+304023.8	23.408167	30.67328	0.50	7	606991	1.332e+08	6.6	31.2	5.5
252	013337.99+304035.6	23.408292	30.67656	0.50	9	796769	1.679e+08	8.4	27.0	6.3
253	013337.99+304926.0	23.408333	30.82389	0.50	6	563027	1.115e+08	10.3	30.1	6.0
254	013338.15+305407.6	23.408963	30.90213	0.61	2	187766	4.083e+07	6.2	37.3	5.3
255	013338.50+302851.2	23.410458	30.48089	0.50	6	479503	1.002e+08	8.3	33.2	5.9
256	013338.53+302750.1	23.410542	30.46392	0.50	5	386424	8.370e+07	6.9	33.2	5.6
257	013338.56+302829.7	23.410667	30.47492	0.50	6	479503	9.969e+07	8.9	33.2	6.1
258	013338.62+304343.7	23.410917	30.72881	0.88	7	607006	1.361e+08	7.0	26.1	5.7
259	013338.97+302734.8	23.412375	30.45969	0.50	5	386424	8.335e+07	7.2	37.1	5.8
260	013339.01+302115.0	23.412542	30.35417	1.34	1	100548	1.658e+07	22.2	86.0	10.7

Table 3—Continued

Source No. (1)	Source ID (2)	RA (J2000) [$^{\circ}$] (3)	Dec (J2000) [$^{\circ}$] (4)	Positional Error [$''$] (5)	No. of obs. (6)	Total exposure [s] (7)	Total exp. map value [$s\ cm^2$] (8)	R_{src} [sky pixel] (9)	R_{bkg} [$'$] (10)	θ (11)
261	013339.18+303216.5	23.413250	30.53792	0.50	9	714945	1.515e+08	8.8	30.4	6.1
262	013339.22+304049.9	23.413438	30.68054	0.50	8	696215	1.383e+08	8.5	29.7	5.9
263	013339.40+305347.6	23.414167	30.89656	0.50	2	187766	4.151e+07	5.5	32.7	5.0
264	013339.46+302140.8	23.414447	30.36136	0.86	1	100548	1.698e+07	20.0	57.5	10.3
265	013339.62+302745.7	23.415117	30.46272	0.50	5	386424	8.240e+07	6.9	32.3	5.7
266	013339.79+304350.3	23.415833	30.73064	0.58	8	701325	1.445e+08	7.6	32.7	5.9
267	013339.97+304015.4	23.416542	30.67097	0.50	9	796769	1.629e+08	9.5	24.8	6.2
268	013340.09+304323.1	23.417056	30.72310	0.50	7	607006	1.351e+08	7.0	31.7	5.6
269	013340.15+305352.5	23.417292	30.89794	0.50	2	187766	4.060e+07	5.9	31.7	5.2
270	013340.66+303940.8	23.419421	30.66135	0.88	10	808279	1.610e+08	9.8	48.1	6.3
271	013340.75+304408.8	23.419792	30.73578	0.50	8	701325	1.501e+08	8.0	31.3	6.1
272	013340.81+303524.2	23.420042	30.59006	0.50	10	805677	1.717e+08	8.5	32.7	6.2
273	013341.02+305322.2	23.420958	30.88950	0.86	4	380227	6.824e+07	8.9	31.3	6.3
274	013341.26+303213.4	23.421917	30.53706	0.50	8	618286	1.346e+08	6.7	29.1	5.6
275	013341.35+305607.9	23.422292	30.93553	0.50	2	187766	4.004e+07	10.7	35.0	7.4
276	013341.47+303815.9	23.422792	30.63775	0.50	10	808612	1.591e+08	9.1	29.9	6.0
277	013341.56+304136.4	23.423205	30.69345	0.50	7	606994	1.300e+08	7.1	25.9	5.4
278	013341.62+303220.1	23.423417	30.53892	0.50	6	433147	9.759e+07	5.3	28.2	4.8
279	013341.90+303848.8	23.424620	30.64690	0.50	9	709885	1.459e+08	8.7	25.9	5.8
280	013342.05+304852.6	23.425248	30.81462	0.50	6	563027	1.179e+08	9.0	27.7	5.8
281	013342.54+304253.3	23.427250	30.71483	0.50	7	607006	1.316e+08	7.3	29.0	5.7
282	013342.55+305750.1	23.427292	30.96394	0.55	2	187766	3.685e+07	15.7	41.2	9.1
283	013342.77+304642.5	23.428222	30.77848	0.50	8	702808	1.428e+08	7.9	25.2	6.0
284	013342.85+302826.6	23.428542	30.47406	0.50	6	479503	1.005e+08	8.6	32.3	6.1
285	013342.97+305341.7	23.429042	30.89492	0.50	4	380227	7.294e+07	9.6	30.9	6.7
286	013343.30+304724.5	23.430451	30.79014	0.50	8	702808	1.332e+08	9.5	35.1	6.4

Table 3—Continued

Source No. (1)	Source ID (2)	RA (J2000) [$^{\circ}$] (3)	Dec (J2000) [$^{\circ}$] (4)	Positional Error [$''$] (5)	No. of obs. (6)	Total exposure [s] (7)	Total exp. map value [$s\ cm^2$] (8)	R_{src} [sky pixel] (9)	R_{bkg} [$'$] (10)	θ (11)
287	013343.39+304630.6	23.430792	30.77517	0.50	9	799468	1.604e+08	9.2	29.9	6.5
288	013343.48+304103.7	23.431196	30.68438	0.54	7	606994	1.334e+08	7.8	28.9	5.3
289	013343.76+305313.2	23.432345	30.88701	0.66	4	380227	8.131e+07	9.1	31.0	6.4
290	013343.98+304955.5	23.433265	30.83211	0.56	6	563027	1.152e+08	9.6	31.0	6.1
291	013344.17+302205.4	23.434042	30.36817	2.36	1	98727	1.812e+07	19.9	54.6	10.1
292	013344.41+305437.1	23.435042	30.91031	0.59	2	187766	4.185e+07	7.8	31.0	6.2
293	013345.21+302933.9	23.438375	30.49275	0.50	6	479503	9.405e+07	7.5	33.4	5.6
294	013345.24+304135.0	23.438500	30.69306	0.55	7	606997	1.168e+08	8.6	27.7	5.9
295	013345.38+302833.8	23.439107	30.47606	0.50	6	479503	9.394e+07	8.5	28.9	6.1
296	013346.29+303251.6	23.442875	30.54767	0.50	8	618286	1.248e+08	6.6	30.8	5.5
297	013346.48+305223.0	23.443667	30.87308	0.50	4	380224	7.730e+07	7.7	34.7	5.9
298	013346.54+305430.8	23.443958	30.90856	0.52	4	380230	6.781e+07	10.6	34.7	7.2
299	013346.56+303748.7	23.444031	30.63021	0.50	9	709018	1.493e+08	8.8	27.3	5.8
300	013346.78+304318.0	23.444917	30.72169	0.50	9	799484	1.617e+08	8.5	28.6	6.1
301	013346.81+305452.8	23.445042	30.91469	0.50	2	187766	4.120e+07	8.8	33.6	6.6
302	013347.20+303045.1	23.446667	30.51253	0.50	7	571573	1.238e+08	7.6	28.0	5.7
303	013347.50+305403.8	23.447917	30.90106	0.50	4	380230	7.955e+07	10.2	29.1	7.0
304	013347.56+304042.9	23.448186	30.67860	0.50	6	510334	1.117e+08	7.7	26.4	4.8
305	013347.83+303249.2	23.449330	30.54702	0.50	8	618286	1.323e+08	6.5	33.5	5.5
306	013347.91+305516.2	23.449650	30.92119	0.80	2	187766	3.950e+07	10.3	33.5	7.1
307	013348.46+302406.0	23.451917	30.40169	0.56	4	297184	5.604e+07	12.5	35.0	8.0
308	013348.50+303307.8	23.452090	30.55219	1.23	8	618286	1.330e+08	6.3	58.1	5.4
309	013348.91+302946.7	23.453792	30.49633	0.50	6	479512	1.039e+08	6.9	32.5	5.4
310	013349.00+304758.7	23.454201	30.79964	0.50	7	612076	1.304e+08	7.7	26.5	5.8
311	013349.27+303249.8	23.455292	30.54717	0.50	8	618286	1.308e+08	6.5	32.5	5.5
312	013349.78+305631.7	23.457440	30.94215	0.50	2	187766	3.656e+07	13.4	35.3	8.4

Table 3—Continued

Source No. (1)	Source ID (2)	RA (J2000) [$^{\circ}$] (3)	Dec (J2000) [$^{\circ}$] (4)	Positional Error [$''$] (5)	No. of obs. (6)	Total exposure [s] (7)	Total exp. map value [$s\ cm^2$] (8)	R_{src} [sky pixel] (9)	R_{bkg} [$'$] (10)	θ (11)
313	013350.05+305023.3	23.458542	30.83981	0.59	5	472285	1.022e+08	7.2	24.9	5.5
314	013350.49+302705.8	23.460376	30.45162	0.50	5	386408	8.395e+07	7.5	28.1	5.9
315	013350.50+304858.7	23.460417	30.81631	0.50	7	612076	1.319e+08	8.3	30.6	6.0
316	013350.50+303821.4	23.460443	30.63930	0.53	8	618286	1.163e+08	7.8	22.8	6.0
317	013350.74+303245.4	23.461417	30.54597	0.85	9	713856	1.470e+08	8.0	32.9	6.0
318	013350.89+303936.6	23.462083	30.66017	0.50	2	177147	3.166e+07	15.7	91.0	9.3
319	013351.13+303823.7	23.463042	30.63994	0.50	3	231836	4.444e+07	1.7	23.1	1.4
320	013352.12+302706.5	23.467167	30.45181	0.50	5	386408	7.908e+07	7.4	32.1	5.8
321	013352.13+303844.5	23.467227	30.64572	0.50	8	667127	1.336e+08	10.4	21.3	6.1
322	013352.27+303029.9	23.467792	30.50831	0.50	7	571573	1.220e+08	7.9	31.6	5.7
323	013352.35+302651.6	23.468125	30.44769	0.50	5	386408	8.039e+07	8.0	29.6	6.1
324	013352.63+302825.2	23.469292	30.47367	0.50	5	386424	6.230e+07	6.5	29.6	5.3
325	013353.32+304015.8	23.472204	30.67107	0.50	4	327412	5.862e+07	6.0	19.3	3.5
326	013353.53+305719.9	23.473042	30.95553	3.38	1	98387	1.890e+07	16.5	56.1	9.4
327	013353.69+303605.6	23.473726	30.60156	0.50	9	713856	1.558e+08	7.7	23.7	5.8
328	013354.28+303347.8	23.476175	30.56330	1.15	9	713856	1.524e+08	7.6	55.3	5.9
329	013354.47+303414.5	23.476980	30.57070	0.50	9	713856	1.550e+08	7.4	27.6	5.9
330	013354.52+303523.7	23.477167	30.58994	0.50	9	713856	1.541e+08	7.1	30.9	5.8
331	013354.64+302549.0	23.477667	30.43028	0.50	4	285860	4.940e+07	7.7	33.2	6.0
332	013354.69+304518.4	23.477883	30.75513	0.73	8	707636	1.453e+08	8.4	44.3	6.1
333	013354.76+304722.8	23.478167	30.78967	0.50	7	612076	1.344e+08	7.1	27.1	5.6
334	013354.91+303310.9	23.478794	30.55305	0.50	9	713856	1.548e+08	7.8	26.8	5.9
335	013355.14+303108.3	23.479764	30.51898	0.50	8	667143	1.400e+08	9.1	26.8	6.1
336	013355.21+303010.1	23.480042	30.50281	0.50	7	571573	1.131e+08	8.6	29.4	5.9
337	013355.24+303528.6	23.480167	30.59128	0.50	9	713856	1.537e+08	7.0	27.0	5.8
338	013355.30+303134.6	23.480417	30.52628	0.50	9	713856	1.408e+08	8.7	26.8	6.1

Table 3—Continued

Source No. (1)	Source ID (2)	RA (J2000) [$^{\circ}$] (3)	Dec (J2000) [$^{\circ}$] (4)	Positional Error [$''$] (5)	No. of obs. (6)	Total exposure [s] (7)	Total exp. map value [$s\ cm^2$] (8)	R_{src} [sky pixel] (9)	R_{bkg} [$'$] (10)	θ (11)
339	013355.39+302343.7	23.480833	30.39550	0.50	3	196636	3.942e+07	10.7	32.8	7.4
340	013355.75+303924.9	23.482292	30.65692	0.50	5	413821	9.101e+07	6.8	21.3	4.2
341	013356.02+304404.7	23.483451	30.73466	0.50	9	796178	1.582e+08	9.2	32.1	6.4
342	013356.06+303024.7	23.483591	30.50687	0.50	7	571573	1.095e+08	8.9	34.1	6.0
343	013356.23+304935.6	23.484292	30.82658	0.64	7	653650	1.349e+08	9.0	27.8	6.2
344	013356.28+304535.7	23.484500	30.75994	0.50	9	796172	1.456e+08	10.0	31.6	6.7
345	013356.32+302928.2	23.484667	30.49117	0.59	7	571573	1.140e+08	9.6	25.9	6.2
346	013356.53+302305.2	23.485542	30.38478	0.50	3	196636	3.821e+07	12.0	36.6	7.9
347	013356.77+303729.7	23.486542	30.62492	0.50	9	713840	1.465e+08	8.8	28.5	6.0
348	013356.82+303706.7	23.486750	30.61853	0.50	9	713840	1.480e+08	8.5	28.8	6.0
349	013356.96+303458.6	23.487371	30.58297	0.50	6	428504	9.744e+07	5.4	39.1	4.9
350	013357.13+302849.3	23.488048	30.48037	0.50	5	377921	7.712e+07	7.6	26.3	4.8
351	013357.15+302634.1	23.488125	30.44281	0.50	4	285860	5.797e+07	6.4	29.4	5.4
352	013357.19+305135.3	23.488292	30.85983	0.50	5	468520	8.989e+07	8.2	32.5	6.1
353	013357.79+302956.6	23.490792	30.49906	0.50	7	571573	1.176e+08	9.1	29.4	5.9
354	013357.97+305610.2	23.491542	30.93619	1.81	3	290852	5.646e+07	15.0	55.1	8.8
355	013358.01+304039.1	23.491740	30.67754	0.50	7	608415	1.232e+08	8.1	24.8	5.4
356	013358.03+303201.2	23.491792	30.53369	0.50	9	713856	1.384e+08	9.5	25.4	6.4
357	013358.07+303754.5	23.491979	30.63182	0.89	8	612594	1.304e+08	7.2	27.0	5.2
358	013358.23+303438.2	23.492652	30.57730	0.50	9	713856	1.506e+08	7.6	30.2	5.9
359	013358.38+303219.8	23.493254	30.53884	0.50	9	713856	1.521e+08	8.7	24.6	6.1
360	013358.42+303624.2	23.493429	30.60674	0.69	10	802372	1.466e+08	9.0	30.2	6.4
361	013358.43+304827.7	23.493476	30.80772	0.50	8	700369	1.484e+08	8.8	27.0	6.1
362	013358.50+303332.2	23.493780	30.55896	0.50	9	713856	1.523e+08	7.9	32.6	6.0
363	013358.65+304228.5	23.494375	30.70792	0.50	7	608419	1.197e+08	8.1	32.7	5.9
364	013358.72+304538.0	23.494667	30.76056	0.50	9	796188	1.588e+08	9.7	33.8	6.6

Table 3—Continued

Source No. (1)	Source ID (2)	RA (J2000) [$^{\circ}$] (3)	Dec (J2000) [$^{\circ}$] (4)	Positional Error [$''$] (5)	No. of obs. (6)	Total exposure [s] (7)	Total exp. map value [$s\ cm^2$] (8)	R_{src} [sky pixel] (9)	R_{bkg} [$'$] (10)	θ (11)
365	013358.83+305004.2	23.495155	30.83452	0.50	5	468520	1.014e+08	6.4	28.6	5.3
366	013359.02+303425.2	23.495958	30.57367	0.57	9	755676	1.538e+08	8.2	30.5	6.2
367	013359.05+303143.6	23.496042	30.52878	0.50	8	667143	1.264e+08	9.9	30.5	6.4
368	013359.47+303101.0	23.497792	30.51697	0.50	7	571573	1.237e+08	7.1	30.5	5.5
369	013400.19+305216.2	23.500792	30.87117	0.70	5	468524	9.697e+07	8.6	30.6	6.3
370	013400.28+303057.2	23.501204	30.51590	0.50	9	755676	1.504e+08	9.0	30.5	6.4
371	013400.30+304219.3	23.501288	30.70538	1.20	7	608419	1.301e+08	7.2	33.1	5.6
372	013400.31+304724.0	23.501321	30.79002	0.89	8	700369	1.527e+08	7.9	40.0	5.9
373	013400.37+302400.6	23.501542	30.40017	0.50	3	196636	4.094e+07	9.0	30.5	6.8
374	013400.60+304904.1	23.502500	30.81782	0.67	8	700369	1.476e+08	9.0	28.4	6.2
375	013400.61+305202.3	23.502542	30.86733	0.73	5	468524	9.850e+07	8.0	31.7	6.2
376	013400.65+305019.5	23.502727	30.83876	0.50	5	468520	1.051e+08	6.3	28.3	5.2
377	013400.75+303944.9	23.503137	30.66248	0.50	7	600506	1.309e+08	8.1	27.0	5.4
378	013400.91+303812.9	23.503792	30.63694	0.50	8	612594	1.332e+08	7.3	25.3	5.3
379	013400.97+304107.5	23.504042	30.68544	0.50	7	608419	1.297e+08	7.3	27.0	5.4
380	013401.03+303445.0	23.504333	30.57917	0.71	10	802388	1.651e+08	8.6	26.9	6.3
381	013401.12+303136.9	23.504667	30.52692	0.50	9	755676	1.489e+08	10.3	26.7	6.6
382	013401.12+303710.7	23.504667	30.61964	0.76	9	713151	1.545e+08	8.0	26.0	5.9
383	013401.12+305153.7	23.504667	30.86492	0.50	5	468524	9.914e+07	7.3	33.6	6.1
384	013401.16+303242.3	23.504841	30.54511	0.50	10	802388	1.688e+08	9.3	29.8	6.3
385	013401.34+303520.2	23.505604	30.58896	1.23	6	428507	8.230e+07	4.9	54.5	4.9
386	013401.63+304829.7	23.506792	30.80825	0.50	8	700369	1.482e+08	8.6	33.3	6.0
387	013401.66+303517.0	23.506917	30.58806	0.50	10	802392	1.571e+08	5.7	37.3	6.4
388	013401.69+303221.5	23.507042	30.53931	0.50	10	802388	1.679e+08	9.7	26.3	6.4
389	013402.03+303004.8	23.508490	30.50136	0.50	6	478479	9.138e+07	8.7	26.3	5.3
390	013402.10+304702.7	23.508761	30.78410	0.50	10	884465	1.825e+08	10.0	28.9	6.6

Table 3—Continued

Source No. (1)	Source ID (2)	RA (J2000) [$^{\circ}$] (3)	Dec (J2000) [$^{\circ}$] (4)	Positional Error [$''$] (5)	No. of obs. (6)	Total exposure [s] (7)	Total exp. map value [$s\ cm^2$] (8)	R_{src} [sky pixel] (9)	R_{bkg} [$'$] (10)	θ (11)
391	013402.37+303136.2	23.509904	30.52674	0.50	9	755676	1.551e+08	9.8	26.3	6.4
392	013402.41+302940.4	23.510042	30.49456	0.50	5	386418	8.252e+07	6.3	29.5	4.3
393	013402.44+304040.5	23.510167	30.67792	0.50	8	694821	1.502e+08	8.7	29.2	5.9
394	013402.71+303052.7	23.511292	30.51464	0.50	9	755676	1.312e+08	13.3	36.8	7.6
395	013402.82+305412.4	23.511771	30.90347	0.50	5	468524	9.880e+07	11.8	30.2	7.7
396	013402.83+304940.5	23.511792	30.82794	0.50	6	515240	1.179e+08	7.0	26.1	5.4
397	013402.85+303439.0	23.511903	30.57752	0.50	10	802392	1.703e+08	8.5	31.2	6.3
398	013402.86+304151.2	23.511917	30.69756	0.50	7	608419	1.289e+08	7.0	29.6	5.5
399	013402.92+302042.6	23.512167	30.34517	2.22	1	86398	1.593e+07	18.0	50.2	9.8
400	013403.06+302821.5	23.512750	30.47264	0.50	4	285860	6.272e+07	5.3	31.2	4.1
401	013403.28+305815.8	23.513667	30.97106	2.07	1	94321	1.770e+07	19.8	62.6	10.4
402	013403.34+304618.2	23.513958	30.77173	0.50	10	884481	1.778e+08	9.8	31.3	6.5
403	013403.49+305641.3	23.514583	30.94481	1.02	2	192464	3.834e+07	14.8	39.2	8.9
404	013404.26+303257.0	23.517754	30.54918	1.06	10	802388	1.644e+08	9.4	34.9	6.3
405	013404.43+304153.4	23.518463	30.69817	0.60	8	696709	1.363e+08	7.3	33.1	5.7
406	013404.48+304520.8	23.518667	30.75578	0.61	10	884475	1.873e+08	9.1	26.8	6.4
407	013404.71+302227.9	23.519625	30.37442	0.50	3	196636	3.959e+07	12.9	55.2	8.2
408	013405.05+305557.2	23.521042	30.93258	0.66	2	192464	3.866e+07	12.4	35.5	8.1
409	013405.68+302239.2	23.523667	30.37756	0.50	3	196636	4.002e+07	12.3	43.7	8.0
410	013406.58+305105.9	23.527417	30.85164	0.50	5	468524	8.604e+07	7.8	34.7	6.0
411	013407.42+303121.0	23.530917	30.52250	0.50	9	755666	1.429e+08	11.7	26.7	6.7
412	013407.50+303249.4	23.531250	30.54706	0.50	10	802388	1.656e+08	9.9	32.7	6.5
413	013407.50+303708.0	23.531250	30.61889	0.87	8	612594	1.361e+08	6.5	34.4	5.4
414	013407.63+303902.4	23.531792	30.65067	0.50	9	793548	1.662e+08	8.7	29.8	6.3
415	013407.81+303553.9	23.532542	30.59831	0.50	9	713151	1.508e+08	7.9	30.7	6.1
416	013408.32+303851.7	23.534667	30.64772	0.50	9	793548	1.484e+08	9.0	28.1	6.5

Table 3—Continued

Source No.	Source ID	RA (J2000) [$^{\circ}$]	Dec (J2000) [$^{\circ}$]	Positional Error [$''$]	No. of obs.	Total exposure [s]	Total exp. map value [$s\ cm^2$]	R_{src} [sky pixel]	R_{bkg} [$''$]	θ
(1)	(2)	(3)	(4)	(5)	(6)	(7)	(8)	(9)	(10)	(11)
417	013408.36+304633.2	23.534871	30.77589	0.50	10	884475	1.756e+08	10.2	26.7	6.5
418	013409.22+304848.3	23.538417	30.81342	0.50	6	515240	1.157e+08	7.0	29.9	4.8
419	013409.65+303259.8	23.540249	30.54995	0.50	10	802388	1.542e+08	10.4	28.3	6.7
420	013409.70+303612.3	23.540417	30.60342	0.50	9	713148	1.514e+08	7.8	32.1	6.0
421	013409.91+305045.3	23.541333	30.84594	0.50	5	468524	9.911e+07	7.0	29.9	5.2
422	013410.03+302856.2	23.541792	30.48228	0.50	3	196636	4.766e+07	1.8	27.8	1.8
423	013410.42+305346.2	23.543417	30.89619	0.50	4	370133	7.879e+07	10.1	29.9	7.0
424	013410.51+303946.4	23.543792	30.66289	0.50	10	881838	1.747e+08	10.1	27.9	6.7
425	013410.54+303218.8	23.543917	30.53858	0.66	9	755672	1.433e+08	11.3	35.2	6.9
426	013410.69+305123.1	23.544542	30.85644	0.50	5	468524	1.001e+08	7.7	29.0	5.9
427	013410.69+304224.0	23.544571	30.70667	0.50	8	696699	1.385e+08	7.2	32.7	5.7
428	013410.78+305010.2	23.544917	30.83619	0.50	6	515243	1.066e+08	8.6	35.5	5.7
429	013410.84+302455.8	23.545167	30.41550	0.50	3	196636	4.360e+07	6.8	30.5	5.8
430	013411.33+303432.2	23.547220	30.57562	0.50	10	802372	1.686e+08	9.4	26.4	6.6
431	013411.80+304437.2	23.549167	30.74369	0.50	8	696709	1.469e+08	7.4	31.3	5.8
432	013412.46+304447.4	23.551958	30.74650	0.50	8	696709	1.465e+08	7.6	31.3	5.8
433	013412.54+302222.0	23.552250	30.37278	0.75	2	97908	1.942e+07	13.0	37.4	8.2
434	013412.93+303555.1	23.553875	30.59864	0.50	7	520530	1.157e+08	6.4	32.3	5.5
435	013413.41+303546.2	23.555875	30.59617	0.50	8	612591	1.296e+08	6.6	32.3	5.6
436	013413.81+304423.3	23.557578	30.73981	0.50	8	696709	1.540e+08	7.4	31.3	5.8
437	013413.98+303706.6	23.558279	30.61852	0.84	8	612587	1.355e+08	6.7	25.3	5.6
438	013414.40+305351.9	23.560033	30.89776	0.77	3	280757	6.236e+07	8.1	70.1	6.3
439	013414.42+303303.8	23.560087	30.55107	0.50	8	663596	1.287e+08	10.1	28.0	6.9
440	013414.83+303412.3	23.561814	30.57009	0.50	10	802372	1.650e+08	10.1	28.0	6.8
441	013414.92+305731.1	23.562167	30.95864	1.95	2	192464	3.722e+07	16.5	55.4	9.5
442	013415.07+304748.8	23.562833	30.79689	0.50	6	515252	1.073e+08	7.9	27.7	4.6

Table 3—Continued

Source No. (1)	Source ID (2)	RA (J2000) [$^{\circ}$] (3)	Dec (J2000) [$^{\circ}$] (4)	Positional Error [$''$] (5)	No. of obs. (6)	Total exposure [s] (7)	Total exp. map value [$s\ cm^2$] (8)	R_{src} [sky pixel] (9)	R_{bkg} [$'$] (10)	θ (11)
443	013415.56+303259.9	23.564863	30.54998	0.85	7	563032	1.151e+08	8.4	39.0	6.3
444	013415.72+302745.4	23.565511	30.46262	0.50	3	196630	4.549e+07	3.1	33.8	3.4
445	013416.09+305025.6	23.567042	30.84047	0.50	6	515243	1.117e+08	8.9	31.0	5.7
446	013416.18+303808.9	23.567417	30.63581	0.50	10	805061	1.635e+08	9.5	30.1	6.5
447	013416.32+305403.7	23.568035	30.90103	0.50	3	280757	6.009e+07	8.5	39.3	6.4
448	013416.50+305156.5	23.568783	30.86571	0.80	5	468524	9.972e+07	9.1	39.3	6.3
449	013416.68+304410.7	23.569500	30.73631	0.50	8	696709	1.533e+08	7.4	29.8	5.8
450	013416.76+305101.8	23.569856	30.85050	0.50	5	468524	1.039e+08	8.2	29.8	5.8
451	013416.87+304544.2	23.570292	30.76228	0.50	7	603637	1.337e+08	7.6	25.8	5.5
452	013417.08+303426.6	23.571167	30.57408	0.50	9	713148	1.491e+08	9.5	29.2	6.6
453	013417.16+302616.5	23.571500	30.43792	0.60	3	196630	4.393e+07	5.2	35.8	4.9
454	013417.17+304843.8	23.571542	30.81217	0.50	6	515249	1.010e+08	9.1	34.7	5.5
455	013417.56+302823.9	23.573167	30.47333	0.50	3	196639	4.533e+07	2.8	31.0	3.2
456	013417.61+304123.3	23.573383	30.68981	0.97	8	696696	1.516e+08	7.4	56.1	5.9
457	013417.62+305649.8	23.573417	30.94717	0.93	2	192464	3.879e+07	14.9	39.4	8.8
458	013417.65+303723.3	23.573542	30.62314	0.70	9	706902	1.494e+08	8.8	28.0	6.2
459	013417.77+305848.9	23.574042	30.98025	2.43	2	192464	3.326e+07	20.9	70.0	10.8
460	013418.01+304208.9	23.575077	30.70249	0.50	8	696696	1.458e+08	7.2	31.3	5.9
461	013418.16+303516.0	23.575667	30.58778	0.50	8	612591	1.326e+08	7.4	25.7	5.9
462	013418.22+302446.1	23.575917	30.41281	0.50	3	196630	3.266e+07	8.1	36.8	6.3
463	013418.58+304710.1	23.577417	30.78614	0.50	6	514403	1.046e+08	8.6	30.3	5.2
464	013419.17+302907.1	23.579875	30.48531	0.50	3	196639	4.734e+07	2.5	24.9	3.0
465	013419.32+304942.4	23.580500	30.82847	0.50	6	515243	1.044e+08	9.3	30.3	5.8
466	013419.71+304111.8	23.582137	30.68664	0.50	8	696696	1.500e+08	7.7	31.3	6.0
467	013419.77+303718.9	23.582404	30.62193	0.50	9	706902	1.493e+08	9.2	31.3	6.3
468	013420.91+303319.0	23.587125	30.55528	0.50	5	380745	8.699e+07	5.5	24.9	4.9

Table 3—Continued

Source No. (1)	Source ID (2)	RA (J2000) [$^{\circ}$] (3)	Dec (J2000) [$^{\circ}$] (4)	Positional Error [$''$] (5)	No. of obs. (6)	Total exposure [s] (7)	Total exp. map value [$s\ cm^2$] (8)	R_{src} [sky pixel] (9)	R_{bkg} [$'$] (10)	θ (11)
469	013420.96+305002.7	23.587357	30.83409	0.50	5	468524	1.015e+08	8.8	33.9	5.5
470	013421.09+304932.3	23.587893	30.82565	0.50	5	468530	9.119e+07	9.2	28.7	5.6
471	013421.15+303930.7	23.588125	30.65853	0.50	9	795423	1.660e+08	9.8	27.1	6.5
472	013421.25+304335.4	23.588542	30.72650	0.50	8	696699	1.464e+08	7.5	29.7	5.9
473	013421.30+304051.8	23.588773	30.68106	0.50	8	696696	1.500e+08	8.0	33.2	6.0
474	013421.43+304449.0	23.589292	30.74697	0.50	7	603637	1.343e+08	7.4	31.1	5.6
475	013421.83+303618.2	23.590970	30.60508	0.50	8	612587	1.343e+08	7.7	26.3	5.9
476	013422.01+302915.4	23.591721	30.48762	0.50	3	196639	4.680e+07	3.1	30.8	3.5
477	013422.68+304623.9	23.594500	30.77331	0.68	6	511570	1.017e+08	7.3	34.4	5.2
478	013422.68+305504.1	23.594500	30.91781	0.70	3	280757	5.930e+07	10.7	34.8	7.4
479	013423.22+302524.8	23.596779	30.42357	0.50	3	196630	4.154e+07	8.0	73.9	6.3
480	013423.27+305423.9	23.596970	30.90665	1.68	3	280757	6.000e+07	9.2	60.3	6.7
481	013423.68+303833.2	23.598667	30.64258	0.50	7	608978	1.140e+08	8.6	30.3	6.3
482	013423.86+303847.6	23.599417	30.64656	0.50	8	697268	1.406e+08	9.5	27.4	6.2
483	013424.55+304307.1	23.602292	30.71864	0.50	7	603637	1.357e+08	7.2	30.6	5.8
484	013424.67+304022.0	23.602792	30.67278	0.50	9	795423	1.670e+08	9.9	30.6	6.5
485	013424.79+303914.1	23.603292	30.65392	0.50	8	697264	1.399e+08	10.2	30.6	6.5
486	013424.85+303543.5	23.603542	30.59542	0.50	7	520530	1.143e+08	7.5	30.6	5.7
487	013424.94+302539.6	23.603917	30.42767	0.50	3	196630	4.147e+07	8.2	33.5	6.3
488	013425.33+304159.7	23.605583	30.69992	0.50	8	696696	1.497e+08	8.2	28.6	6.1
489	013425.38+303131.5	23.605750	30.52542	0.50	5	380739	8.422e+07	7.2	26.5	5.5
490	013425.43+305159.6	23.605992	30.86658	0.50	3	280757	6.087e+07	5.0	36.1	4.6
491	013425.75+302817.9	23.607292	30.47164	0.50	3	196639	4.274e+07	4.7	32.5	4.6
492	013425.80+305518.1	23.607500	30.92172	0.50	3	280757	5.726e+07	11.5	41.6	7.7
493	013425.87+303316.8	23.607796	30.55467	1.08	5	380745	8.350e+07	6.0	42.5	5.2
494	013426.11+303216.5	23.608792	30.53792	0.50	5	380745	8.001e+07	6.6	31.4	5.4

Table 3—Continued

Source No. (1)	Source ID (2)	RA (J2000) [$^{\circ}$] (3)	Dec (J2000) [$^{\circ}$] (4)	Positional Error [$''$] (5)	No. of obs. (6)	Total exposure [s] (7)	Total exp. map value [$s\ cm^2$] (8)	R_{src} [sky pixel] (9)	R_{bkg} [$'$] (10)	θ (11)
495	013426.14+303726.6	23.608917	30.62406	0.50	8	612587	1.323e+08	8.6	26.0	5.9
496	013426.32+304324.8	23.609667	30.72358	0.50	7	603637	1.321e+08	7.4	29.4	5.8
497	013426.53+304446.2	23.610542	30.74619	0.50	7	603637	1.359e+08	7.6	29.4	5.8
498	013426.56+303738.1	23.610708	30.62725	0.50	8	612587	1.284e+08	8.9	30.9	5.9
499	013426.71+304812.8	23.611292	30.80356	0.50	3	280764	6.912e+07	2.3	29.4	2.5
500	013426.80+304050.4	23.611678	30.68069	0.50	8	696696	1.463e+08	9.0	30.9	6.2
501	013426.82+304803.6	23.611757	30.80102	0.50	3	280764	6.916e+07	2.4	25.5	2.5
502	013426.98+304313.4	23.612417	30.72039	0.50	7	603637	1.327e+08	7.5	31.2	5.8
503	013427.22+305151.9	23.613417	30.86444	0.50	3	280757	5.281e+07	5.0	27.0	4.6
504	013427.28+304421.9	23.613667	30.73944	0.57	7	603637	1.343e+08	7.7	30.2	5.8
505	013427.61+302921.0	23.615042	30.48917	0.50	3	196636	4.198e+07	4.6	30.4	4.6
506	013427.88+304138.1	23.616167	30.69394	0.50	8	696696	1.471e+08	8.7	31.6	6.2
507	013428.21+303248.0	23.617542	30.54669	0.50	5	380729	7.285e+07	6.5	34.0	5.4
508	013428.24+304319.4	23.617667	30.72208	0.50	7	603637	1.334e+08	7.9	34.6	6.0
509	013428.33+303653.3	23.618083	30.61483	0.50	8	612587	1.115e+08	9.5	34.2	6.3
510	013428.48+303301.5	23.618667	30.55042	0.50	5	380729	7.144e+07	6.5	34.5	5.5
511	013428.59+305548.1	23.619125	30.93003	2.33	3	280761	5.812e+07	13.1	41.5	8.3
512	013428.69+304054.3	23.619583	30.68175	0.50	8	696696	1.510e+08	9.6	30.2	6.3
513	013428.87+303450.0	23.620333	30.58056	0.50	7	520507	9.594e+07	8.8	34.5	6.3
514	013428.94+303251.1	23.620605	30.54753	0.50	5	380729	7.980e+07	6.7	29.9	5.5
515	013429.01+304249.7	23.620875	30.71381	0.50	7	603634	1.280e+08	8.0	35.3	6.0
516	013429.10+304212.9	23.621268	30.70359	0.50	7	603634	1.297e+08	8.4	35.3	6.1
517	013429.74+305026.3	23.623917	30.84064	0.50	3	280764	6.429e+07	3.7	25.6	3.7
518	013429.95+305107.4	23.624833	30.85206	0.50	3	280757	5.425e+07	4.4	28.7	4.1
519	013430.14+303511.7	23.625617	30.58659	0.50	7	520507	1.059e+08	8.4	29.9	6.0
520	013430.36+303937.1	23.626500	30.66033	0.52	7	602949	1.122e+08	11.6	73.6	6.9

Table 3—Continued

Source No. (1)	Source ID (2)	RA (J2000) [$^{\circ}$] (3)	Dec (J2000) [$^{\circ}$] (4)	Positional Error [$''$] (5)	No. of obs. (6)	Total exposure [s] (7)	Total exp. map value [$s\ cm^2$] (8)	R_{src} [sky pixel] (9)	R_{bkg} [$'$] (10)	θ (11)
521	013430.49+305042.4	23.627070	30.84512	0.50	3	280764	6.802e+07	4.1	27.1	4.0
522	013430.61+303259.7	23.627542	30.54994	0.50	5	380729	8.358e+07	6.8	33.4	5.7
523	013430.91+304510.1	23.628792	30.75283	0.50	5	464850	1.021e+08	5.9	36.8	5.0
524	013431.62+302927.1	23.631775	30.49086	0.50	3	196636	4.447e+07	6.1	27.6	5.4
525	013431.71+304128.0	23.632156	30.69112	0.50	7	603630	1.304e+08	9.0	34.7	6.2
526	013431.86+304110.1	23.632750	30.68614	0.50	7	603630	1.320e+08	9.2	33.0	6.1
527	013431.87+304011.7	23.632792	30.66994	0.50	8	697261	1.460e+08	11.2	33.0	6.6
528	013432.02+303454.1	23.633417	30.58172	0.50	6	427445	9.622e+07	7.7	28.5	5.8
529	013432.11+302538.6	23.633792	30.42739	0.50	3	196639	3.870e+07	10.6	34.9	7.3
530	013432.16+305158.7	23.634000	30.86631	0.57	3	280761	5.059e+07	6.5	28.3	5.4
531	013432.23+304958.9	23.634304	30.83304	0.50	3	280764	6.571e+07	3.7	28.3	3.6
532	013432.26+303201.2	23.634417	30.53367	0.50	5	380723	7.589e+07	8.0	37.8	6.2
533	013432.56+303436.8	23.635667	30.57689	0.50	6	427445	9.597e+07	8.1	30.3	5.9
534	013432.59+305035.4	23.635833	30.84319	0.50	3	280764	6.248e+07	4.4	33.3	4.2
535	013432.60+304704.1	23.635868	30.78448	0.50	4	369290	7.947e+07	4.7	15.8	3.8
536	013432.65+304318.5	23.636042	30.72181	0.50	6	556914	1.233e+08	7.9	33.8	6.0
537	013432.74+303930.1	23.636417	30.65838	0.50	7	602946	1.269e+08	10.7	29.3	6.1
538	013432.98+303857.4	23.637417	30.64928	0.50	6	514659	1.081e+08	10.2	29.3	5.5
539	013433.02+304639.1	23.637600	30.77754	0.50	5	464854	8.872e+07	5.9	23.7	4.5
540	013433.64+305459.6	23.640167	30.91658	0.90	3	280761	5.716e+07	12.0	33.9	7.8
541	013433.88+304652.7	23.641167	30.78131	0.50	3	280761	6.715e+07	3.6	12.0	3.4
542	013434.30+304701.7	23.642917	30.78383	1.04	4	369290	8.035e+07	5.1	10.4	4.1
543	013434.60+305132.5	23.644167	30.85903	0.50	3	280767	6.400e+07	5.9	29.4	5.0
544	013435.06+304439.3	23.646114	30.74427	0.50	5	464847	9.395e+07	6.4	29.4	5.3
545	013435.09+304712.0	23.646220	30.78668	0.50	4	369290	8.297e+07	5.8	14.7	4.4
546	013435.14+305646.1	23.646458	30.94614	0.58	2	186439	3.033e+07	16.4	43.4	9.2

Table 3—Continued

Source No. (1)	Source ID (2)	RA (J2000) [$^{\circ}$] (3)	Dec (J2000) [$^{\circ}$] (4)	Positional Error [$''$] (5)	No. of obs. (6)	Total exposure [s] (7)	Total exp. map value [$s\ cm^2$] (8)	R_{src} [sky pixel] (9)	R_{bkg} [$'$] (10)	θ (11)
547	013435.32+303726.9	23.647167	30.62414	0.50	6	434099	9.027e+07	9.5	37.1	5.6
548	013435.38+304946.7	23.647417	30.82964	0.50	3	280767	5.234e+07	5.0	37.4	4.5
549	013435.40+305212.6	23.647534	30.87019	1.28	3	280761	5.870e+07	6.6	45.6	5.5
550	013435.50+303352.4	23.647917	30.56456	0.61	5	380729	8.482e+07	7.6	33.3	5.9
551	013436.01+304542.5	23.650042	30.76181	0.86	5	464854	1.060e+08	6.8	32.4	5.3
552	013436.04+303450.0	23.650167	30.58056	0.50	6	427445	9.436e+07	8.9	27.6	6.2
553	013436.43+304713.8	23.651792	30.78717	0.50	4	369290	8.563e+07	6.2	25.5	4.6
554	013436.67+304315.6	23.652802	30.72102	0.50	6	556905	1.211e+08	8.8	30.9	6.2
555	013436.76+303307.0	23.653167	30.55197	0.50	5	380729	8.227e+07	8.4	30.4	6.3
556	013436.91+304552.3	23.653792	30.76453	0.50	5	464854	1.054e+08	5.8	31.2	5.4
557	013437.17+302927.7	23.654875	30.49103	0.69	3	196636	4.280e+07	8.5	30.4	6.6
558	013437.53+304551.5	23.656402	30.76432	0.50	5	464854	1.045e+08	6.5	34.9	5.5
559	013437.74+303721.5	23.657250	30.62264	0.50	6	434102	8.109e+07	11.1	28.9	6.4
560	013438.72+304539.3	23.661356	30.76093	0.50	5	464854	1.046e+08	7.3	34.9	5.6
561	013438.83+305504.4	23.661792	30.91789	0.50	3	280761	4.419e+07	13.3	27.6	8.1
562	013438.89+304117.4	23.662042	30.68819	0.50	3	272383	6.461e+07	4.6	30.6	4.1
563	013439.66+304110.6	23.665250	30.68628	0.50	4	364441	8.195e+07	6.7	30.6	5.5
564	013439.69+302950.7	23.665375	30.49744	0.50	4	292190	5.473e+07	11.4	31.3	7.6
565	013439.84+305144.3	23.666000	30.86231	0.50	3	280767	6.175e+07	7.5	33.8	5.8
566	013440.18+305050.6	23.667417	30.84739	1.00	3	280767	6.407e+07	6.4	29.3	5.3
567	013440.42+304154.5	23.668421	30.69847	0.50	4	364441	7.993e+07	8.5	30.5	5.8
568	013440.48+303954.9	23.668667	30.66526	0.50	4	371110	7.609e+07	8.8	29.6	5.3
569	013440.63+304513.2	23.669292	30.75369	1.77	5	464854	9.280e+07	8.3	31.4	6.1
570	013440.73+304336.4	23.669729	30.72679	0.62	5	464847	1.009e+08	6.2	37.5	5.8
571	013440.81+304410.2	23.670042	30.73617	0.51	5	464854	1.016e+08	7.5	35.1	5.8
572	013441.10+304328.3	23.671254	30.72454	1.58	5	464847	1.018e+08	7.7	39.2	5.9

Table 3—Continued

Source No. (1)	Source ID (2)	RA (J2000) [$^{\circ}$] (3)	Dec (J2000) [$^{\circ}$] (4)	Positional Error [$''$] (5)	No. of obs. (6)	Total exposure [s] (7)	Total exp. map value [$s\ cm^2$] (8)	R_{src} [sky pixel] (9)	R_{bkg} [$'$] (10)	θ (11)
573	013441.26+303516.4	23.671917	30.58789	0.50	5	341040	7.431e+07	9.5	26.4	6.2
574	013441.32+303921.8	23.672167	30.65606	0.50	3	282820	4.851e+07	8.3	29.6	4.9
575	013441.43+303415.7	23.672625	30.57103	0.50	5	380732	7.809e+07	9.1	29.6	6.5
576	013442.07+305228.8	23.675292	30.87469	0.50	3	280767	6.150e+07	9.1	30.8	6.7
577	013442.43+305249.5	23.676792	30.88042	0.50	3	280767	6.068e+07	9.7	31.8	6.9
578	013442.70+304927.5	23.677917	30.82433	0.50	3	280767	6.524e+07	6.2	31.8	5.0
579	013442.79+304505.6	23.678292	30.75156	0.50	5	464854	1.008e+08	7.2	35.5	6.1
580	013442.92+304459.8	23.678842	30.74995	0.50	1	88290	2.235e+07	3.2	35.5	3.5
581	013443.00+303423.0	23.679167	30.57306	0.50	4	294324	6.238e+07	8.3	28.6	6.1
582	013443.12+304948.6	23.679667	30.83017	0.50	3	280767	6.550e+07	6.7	30.8	5.2
583	013443.41+304808.7	23.680904	30.80242	0.50	3	280761	6.300e+07	6.1	26.6	4.8
584	013444.02+303906.6	23.683438	30.65184	0.50	2	184099	4.465e+07	2.1	28.6	2.4
585	013444.23+304920.3	23.684292	30.82233	0.51	3	280767	6.536e+07	6.8	32.6	5.3
586	013444.38+304702.9	23.684917	30.78414	0.50	4	369290	8.313e+07	8.1	28.3	5.9
587	013444.62+305535.0	23.685917	30.92639	0.78	1	88296	1.790e+07	12.0	40.0	7.9
588	013444.71+303732.9	23.686313	30.62581	0.50	2	184090	4.456e+07	2.4	28.6	2.8
589	013444.99+304927.7	23.687461	30.82437	0.50	3	280767	6.406e+07	6.9	28.3	5.4
590	013445.34+303539.4	23.688921	30.59430	1.66	4	294324	6.092e+07	8.0	29.9	5.8
591	013445.62+302559.5	23.690108	30.43321	1.05	1	98720	1.945e+07	16.6	52.8	9.5
592	013445.76+303138.8	23.690673	30.52747	0.50	4	369219	7.620e+07	12.4	44.7	8.0
593	013446.78+304448.9	23.694917	30.74694	0.50	5	464854	1.014e+08	9.4	31.6	6.7
594	013447.35+304001.3	23.697292	30.66703	0.50	2	184093	4.363e+07	3.1	31.8	3.3
595	013447.62+303514.3	23.698417	30.58733	0.50	3	195597	4.322e+07	5.4	29.7	5.0
596	013448.12+303714.4	23.700500	30.62069	0.50	2	184090	4.300e+07	3.2	29.7	3.6
597	013448.37+304313.2	23.701569	30.72034	0.50	3	272383	6.115e+07	6.6	33.2	5.6
598	013448.63+303627.0	23.702629	30.60752	0.50	2	184090	4.207e+07	3.9	30.7	4.1

Table 3—Continued

Source No. (1)	Source ID (2)	RA (J2000) [$^{\circ}$] (3)	Dec (J2000) [$^{\circ}$] (4)	Positional Error [$''$] (5)	No. of obs. (6)	Total exposure [s] (7)	Total exp. map value [$s\ cm^2$] (8)	R_{src} [sky pixel] (9)	R_{bkg} [$'$] (10)	θ (11)
599	013448.63+304706.7	23.702640	30.78520	0.50	4	369290	7.508e+07	9.6	31.6	6.6
600	013449.00+303328.6	23.704208	30.55797	0.50	2	184090	3.479e+07	8.0	29.8	6.3
601	013449.04+304446.8	23.704344	30.74636	0.50	5	464854	9.884e+07	10.1	31.6	6.9
602	013449.36+303857.0	23.705667	30.64917	0.50	2	184099	4.071e+07	3.2	28.8	3.5
603	013449.51+305011.9	23.706292	30.83664	0.91	3	280767	6.201e+07	9.6	27.4	6.6
604	013449.58+303935.0	23.706609	30.65975	0.50	2	184093	2.798e+07	3.6	30.1	3.7
605	013450.35+303452.5	23.709801	30.58127	0.50	2	184090	3.250e+07	6.2	35.3	5.4
606	013450.40+303545.3	23.710000	30.59592	0.50	2	184090	3.296e+07	4.9	30.6	4.8
607	013451.01+303226.5	23.712542	30.54072	0.66	2	184090	3.742e+07	10.5	31.9	7.4
608	013451.10+304356.7	23.712917	30.73244	0.50	3	272383	5.801e+07	7.6	30.6	6.1
609	013451.31+303444.1	23.713792	30.57892	0.50	2	184090	4.069e+07	6.6	35.7	5.6
610	013451.37+302841.0	23.714083	30.47806	0.80	1	98720	1.964e+07	17.6	61.3	9.6
611	013451.73+303745.9	23.715542	30.62944	0.61	2	184090	3.714e+07	4.1	39.1	4.1
612	013451.85+302909.7	23.716042	30.48603	0.50	2	185129	3.212e+07	17.7	48.4	9.7
613	013451.94+304615.8	23.716417	30.77106	0.50	5	464854	8.971e+07	11.8	34.2	7.5
614	013452.00+303547.6	23.716676	30.59656	0.50	2	184090	4.200e+07	5.6	37.8	5.0
615	013452.24+305309.2	23.717708	30.88589	0.70	1	88296	2.045e+07	8.2	34.2	6.4
616	013452.34+305038.4	23.718122	30.84401	0.80	3	280767	5.903e+07	11.3	50.4	7.4
617	013452.52+304242.5	23.718849	30.71183	0.50	3	272383	5.885e+07	7.6	36.3	6.0
618	013452.89+302809.5	23.720375	30.46933	1.46	1	98720	1.855e+07	18.2	54.2	10.0
619	013453.25+305717.7	23.721875	30.95492	1.19	1	88296	1.779e+07	19.3	51.0	10.1
620	013453.81+303341.8	23.724234	30.56162	0.50	2	184090	3.729e+07	9.0	32.8	6.7
621	013454.94+303248.9	23.728917	30.54694	0.50	2	184090	3.504e+07	11.1	36.6	7.6
622	013455.30+304624.3	23.730417	30.77342	0.50	5	464854	9.026e+07	13.2	31.3	8.0
623	013455.90+304814.5	23.732917	30.80403	0.50	3	280761	6.084e+07	11.6	31.3	7.5
624	013456.08+304237.9	23.733667	30.71053	0.50	3	272383	5.840e+07	8.6	34.0	6.6

Table 3—Continued

Source No. (1)	Source ID (2)	RA (J2000) [$^{\circ}$] (3)	Dec (J2000) [$^{\circ}$] (4)	Positional Error [$''$] (5)	No. of obs. (6)	Total exposure [s] (7)	Total exp. map value [$s\ cm^2$] (8)	R_{src} [sky pixel] (9)	R_{bkg} [$'$] (10)	θ (11)
625	013456.26+304139.4	23.734417	30.69428	0.59	3	272383	5.789e+07	8.7	31.8	6.5
626	013457.21+303825.5	23.738375	30.64044	0.50	2	184099	3.880e+07	6.1	38.9	5.2
627	013457.33+304319.4	23.738875	30.72206	0.55	3	272383	5.947e+07	9.4	33.8	6.9
628	013457.76+304247.9	23.740667	30.71331	0.50	3	272383	5.821e+07	9.3	33.7	6.8
629	013458.06+303637.5	23.741917	30.61044	0.79	2	184090	3.743e+07	7.0	33.7	5.8
630	013458.51+304707.1	23.743792	30.78533	0.50	4	369290	7.450e+07	14.0	32.8	8.5
631	013459.25+304607.6	23.746890	30.76878	0.50	4	370532	7.462e+07	14.1	32.8	8.4
632	013459.65+303833.6	23.748542	30.64267	0.50	2	184099	3.784e+07	7.0	32.1	5.7
633	013500.54+305028.7	23.752250	30.84133	0.50	2	182618	3.878e+07	13.9	32.8	8.1
634	013500.76+304952.7	23.753167	30.83131	1.82	2	182611	2.805e+07	15.6	69.9	8.8
635	013500.97+304348.1	23.754083	30.73003	0.50	3	272383	5.724e+07	11.2	32.8	7.6
636	013501.09+304847.4	23.754542	30.81317	0.85	3	280761	5.790e+07	14.8	32.8	8.6
637	013502.58+303849.8	23.760750	30.64717	0.82	2	184099	3.896e+07	8.5	31.1	6.4
638	013502.70+303950.1	23.761250	30.66394	0.50	2	184093	2.944e+07	8.9	34.8	6.5
639	013502.80+303710.8	23.761708	30.61969	0.50	2	184090	3.965e+07	8.9	32.6	6.6
640	013503.04+303340.7	23.762667	30.56133	0.69	2	184090	3.675e+07	13.1	40.0	8.2
641	013503.28+304559.1	23.763704	30.76644	0.50	3	272383	5.503e+07	14.3	32.8	8.5
642	013503.46+304033.8	23.764417	30.67606	0.51	2	184093	3.910e+07	9.5	33.6	6.8
643	013504.54+304443.0	23.768917	30.74528	0.50	3	272383	5.485e+07	13.6	36.6	8.4
644	013504.72+304054.9	23.769667	30.68192	0.50	2	184093	3.802e+07	10.6	35.2	7.2
645	013504.75+303919.1	23.769792	30.65531	0.50	2	184099	3.902e+07	9.8	30.5	6.8
646	013504.78+305034.5	23.769958	30.84292	1.03	1	88296	1.923e+07	10.3	36.6	7.0
647	013504.99+303445.5	23.770792	30.57931	0.50	2	184090	3.454e+07	12.5	34.1	8.0
648	013505.66+305006.4	23.773602	30.83513	0.55	2	182611	2.895e+07	18.3	70.8	9.5
649	013505.83+305428.9	23.774296	30.90805	1.44	1	88296	1.441e+07	16.4	45.3	9.3
650	013507.31+305208.8	23.780466	30.86913	0.86	1	88296	1.903e+07	13.0	39.3	8.2

Table 3—Continued

Source No. (1)	Source ID (2)	RA (J2000) [$^{\circ}$] (3)	Dec (J2000) [$^{\circ}$] (4)	Positional Error [$''$] (5)	No. of obs. (6)	Total exposure [s] (7)	Total exp. map value [$s\ cm^2$] (8)	R_{src} [sky pixel] (9)	R_{bkg} [$'$] (10)	θ (11)
651	013507.51+304636.5	23.781292	30.77683	1.45	2	176819	3.336e+07	15.1	39.3	8.8
652	013507.75+304009.4	23.782325	30.66928	0.97	2	184093	3.710e+07	11.9	38.1	7.6
653	013508.44+303150.4	23.785167	30.53067	2.65	1	88535	1.649e+07	20.6	50.3	10.4
654	013509.10+304341.8	23.787917	30.72828	0.62	3	272383	5.484e+07	15.4	46.0	9.0
655	013509.30+304108.4	23.788750	30.68569	1.03	2	184093	3.482e+07	12.8	43.9	8.2
656	013509.55+303600.6	23.789792	30.60019	0.98	1	88535	1.854e+07	13.4	37.2	8.3
657	013511.08+304256.9	23.796167	30.71581	1.51	2	176819	3.173e+07	16.2	43.1	9.2
658	013512.72+304515.8	23.803000	30.75439	1.24	2	176819	3.338e+07	16.7	40.3	9.4
659	013517.08+304409.3	23.821167	30.73592	1.56	1	88290	1.829e+07	18.1	53.3	9.9
660	013517.38+303601.5	23.822417	30.60042	1.69	1	88535	8.149e+06	17.2	59.7	9.9
661	013517.47+304446.7	23.822792	30.74631	1.61	1	88290	1.837e+07	17.1	46.1	9.7
662	013520.83+304237.0	23.836833	30.71028	1.79	1	88290	1.652e+07	22.5	86.3	11.3

(2): The source ID also contains the source coordinates (J2000.0). (5): The positional uncertainty is a simple error circle (in $''$) around RA and Dec. (7): Total exposure in all observations. (8): Sum of mean exposure map values in source region for all observations. (9) and (10): Average radius of the source and background extraction region (1 sky pixel = $0''.492$). (11): Average off-axis angle.

Table 4. Merged pns values for different energy bands[†].

Source No	$pns[1]$ [0.5–8.0keV]	$pns[2]$ [0.5–2.0keV]	$pns[3]$ [2.0–8.0keV]	$pns[4]$ [0.35–8.0keV]	$pns[5]$ [0.35–1.1keV]	$pns[6]$ [1.1–2.6keV]	$pns[7]$ [2.6–8.0keV]	$pns[8]$ [0.35–2.0keV]
1	<1.0e-10	1.8e-10	1.9e-04	<1.0e-10	8.7e-02	<1.0e-10	2.3e-03	2.7e-10
2	1.7e-06	7.4e-06	5.6e-03	1.7e-06	4.0e-02	6.0e-05	1.4e-02	7.4e-06
3	<1.0e-10	<1.0e-10	<1.0e-10	<1.0e-10	3.2e-10	<1.0e-10	4.9e-10	<1.0e-10
4	1.4e-09	<1.0e-10	3.6e-02	1.4e-09	1.7e-04	1.2e-10	2.6e-01	<1.0e-10
5	<1.0e-10	<1.0e-10	4.8e-07	<1.0e-10	2.4e-03	<1.0e-10	2.0e-05	<1.0e-10
6	<1.0e-10	<1.0e-10	4.2e-01	<1.0e-10	<1.0e-10	<1.0e-10	8.0e-01	<1.0e-10
7	1.7e-06	2.4e-06	4.8e-03	2.2e-06	3.5e-01	1.5e-05	5.6e-03	4.0e-06
8	2.8e-04	<1.0e-10	8.2e-01	3.4e-04	<1.0e-10	5.7e-02	8.6e-01	<1.0e-10
9	9.0e-04	2.8e-06	4.4e-01	5.5e-04	8.4e-03	8.0e-04	3.8e-01	1.5e-06
10	<1.0e-10	<1.0e-10	<1.0e-10	<1.0e-10	<1.0e-10	<1.0e-10	<1.0e-10	<1.0e-10
11	2.7e-06	<1.0e-10	7.4e-01	4.2e-06	1.0e-04	5.7e-07	6.6e-01	<1.0e-10
12	<1.0e-10	<1.0e-10	1.2e-05	<1.0e-10	3.3e-08	<1.0e-10	1.5e-02	<1.0e-10
13	<1.0e-10	<1.0e-10	<1.0e-10	<1.0e-10	4.7e-02	<1.0e-10	<1.0e-10	1.1e-10
14	<1.0e-10	<1.0e-10	4.5e-06	<1.0e-10	5.8e-04	<1.0e-10	2.9e-06	<1.0e-10
15	<1.0e-10	<1.0e-10	1.1e-06	<1.0e-10	2.6e-09	<1.0e-10	7.3e-06	<1.0e-10
16	<1.0e-10	<1.0e-10	<1.0e-10	<1.0e-10	<1.0e-10	<1.0e-10	<1.0e-10	<1.0e-10
17	1.5e-07	1.7e-04	1.3e-04	3.8e-07	4.9e-01	3.5e-06	1.5e-03	5.7e-04
18	4.2e-08	4.4e-10	1.5e-02	4.1e-08	2.6e-02	3.8e-08	2.3e-02	7.6e-10
19	<1.0e-10	<1.0e-10	9.6e-05	<1.0e-10	2.3e-06	1.5e-09	1.8e-04	<1.0e-10
20	1.2e-05	1.2e-09	2.3e-01	4.1e-06	1.1e-10	2.3e-02	2.7e-01	2.3e-10
21	<1.0e-10	<1.0e-10	1.8e-08	<1.0e-10	9.4e-07	<1.0e-10	6.4e-07	<1.0e-10
22	<1.0e-10	<1.0e-10	2.1e-02	<1.0e-10	<1.0e-10	<1.0e-10	1.2e-01	<1.0e-10
23	7.7e-09	5.2e-09	2.8e-03	7.6e-09	2.1e-02	1.0e-06	1.7e-03	7.1e-09
24	<1.0e-10	<1.0e-10	<1.0e-10	<1.0e-10	7.0e-09	<1.0e-10	1.8e-06	<1.0e-10
25	<1.0e-10	<1.0e-10	<1.0e-10	<1.0e-10	<1.0e-10	<1.0e-10	<1.0e-10	<1.0e-10
26	<1.0e-10	<1.0e-10	6.6e-10	<1.0e-10	3.7e-04	<1.0e-10	4.2e-06	<1.0e-10
27	1.6e-07	3.3e-04	7.5e-05	4.8e-07	4.4e-01	8.5e-06	5.5e-04	1.3e-03

Table 4—Continued

Source No	<i>pns</i> [1] [0.5–8.0keV]	<i>pns</i> [2] [0.5–2.0keV]	<i>pns</i> [3] [2.0–8.0keV]	<i>pns</i> [4] [0.35–8.0keV]	<i>pns</i> [5] [0.35–1.1keV]	<i>pns</i> [6] [1.1–2.6keV]	<i>pns</i> [7] [2.6–8.0keV]	<i>pns</i> [8] [0.35–2.0keV]
28	<1.0e-10	<1.0e-10	9.9e-08	<1.0e-10	8.7e-09	<1.0e-10	4.4e-07	<1.0e-10
29	<1.0e-10	<1.0e-10	<1.0e-10	<1.0e-10	<1.0e-10	<1.0e-10	8.1e-10	<1.0e-10
30	<1.0e-10	8.8e-10	1.5e-04	1.3e-10	1.9e-03	4.1e-07	8.4e-04	6.4e-09
31	<1.0e-10	<1.0e-10	9.7e-03	<1.0e-10	4.8e-04	<1.0e-10	1.6e-02	<1.0e-10
32	<1.0e-10	4.0e-10	3.3e-05	<1.0e-10	6.5e-02	<1.0e-10	7.8e-04	1.1e-09
33	<1.0e-10	<1.0e-10	<1.0e-10	<1.0e-10	<1.0e-10	<1.0e-10	<1.0e-10	<1.0e-10
34	<1.0e-10	8.1e-04	1.5e-08	<1.0e-10	4.0e-02	2.6e-02	3.2e-09	1.0e-03
35	<1.0e-10	<1.0e-10	<1.0e-10	<1.0e-10	<1.0e-10	<1.0e-10	<1.0e-10	<1.0e-10
36	9.3e-07	3.1e-06	3.3e-03	1.0e-07	3.5e-03	7.1e-06	8.6e-03	1.5e-07
37	<1.0e-10	<1.0e-10	<1.0e-10	<1.0e-10	<1.0e-10	<1.0e-10	<1.0e-10	<1.0e-10
38	<1.0e-10	<1.0e-10	<1.0e-10	<1.0e-10	8.2e-04	<1.0e-10	<1.0e-10	<1.0e-10
39	3.9e-05	1.5e-04	1.5e-02	5.6e-05	5.0e-01	3.8e-04	1.0e-02	2.9e-04
40	<1.0e-10	<1.0e-10	<1.0e-10	<1.0e-10	<1.0e-10	<1.0e-10	<1.0e-10	<1.0e-10
41	<1.0e-10	2.3e-03	<1.0e-10	<1.0e-10	2.0e-01	1.0e-03	<1.0e-10	2.2e-03
42	2.4e-07	2.7e-05	8.8e-04	1.7e-07	9.2e-03	7.7e-04	9.3e-04	1.9e-05
43	7.1e-10	<1.0e-10	3.5e-01	1.5e-09	<1.0e-10	6.1e-02	6.5e-01	<1.0e-10
44	<1.0e-10	2.4e-02	<1.0e-10	<1.0e-10	5.5e-01	5.7e-04	<1.0e-10	3.6e-02
45	1.9e-03	4.9e-05	3.2e-01	1.4e-03	7.6e-02	2.0e-04	3.6e-01	4.6e-05
46	4.0e-10	5.8e-05	1.6e-06	9.3e-10	4.9e-01	5.0e-06	1.7e-05	1.4e-04
47	5.0e-09	2.3e-06	1.1e-04	2.6e-09	3.3e-02	7.6e-08	2.6e-03	1.4e-06
48	<1.0e-10	<1.0e-10	5.1e-01	<1.0e-10	<1.0e-10	<1.0e-10	6.8e-01	<1.0e-10
49	<1.0e-10	1.4e-10	<1.0e-10	<1.0e-10	1.4e-04	<1.0e-10	6.9e-08	<1.0e-10
50	9.1e-09	3.9e-06	1.1e-04	1.8e-09	4.0e-02	1.1e-06	4.2e-04	5.2e-07
51	<1.0e-10	<1.0e-10	4.0e-04	<1.0e-10	1.6e-01	<1.0e-10	7.2e-04	1.1e-10
52	6.3e-08	2.1e-01	2.4e-08	4.2e-08	7.8e-01	4.3e-03	1.2e-07	1.5e-01
53	<1.0e-10	<1.0e-10	<1.0e-10	<1.0e-10	6.0e-02	<1.0e-10	<1.0e-10	<1.0e-10
54	<1.0e-10	<1.0e-10	<1.0e-10	<1.0e-10	<1.0e-10	<1.0e-10	<1.0e-10	<1.0e-10

Table 4—Continued

Source No	<i>pns</i> [1] [0.5–8.0keV]	<i>pns</i> [2] [0.5–2.0keV]	<i>pns</i> [3] [2.0–8.0keV]	<i>pns</i> [4] [0.35–8.0keV]	<i>pns</i> [5] [0.35–1.1keV]	<i>pns</i> [6] [1.1–2.6keV]	<i>pns</i> [7] [2.6–8.0keV]	<i>pns</i> [8] [0.35–2.0keV]
55	2.9e-05	7.4e-08	1.5e-01	5.3e-05	1.3e-02	2.4e-07	5.2e-01	4.0e-07
56	<1.0e-10	<1.0e-10	4.4e-06	<1.0e-10	<1.0e-10	1.4e-09	2.2e-05	<1.0e-10
57	6.2e-08	1.8e-08	4.7e-02	6.8e-08	5.0e-02	6.4e-07	3.8e-02	2.3e-08
58	<1.0e-10	<1.0e-10	2.4e-04	<1.0e-10	4.8e-03	<1.0e-10	6.1e-04	<1.0e-10
59	<1.0e-10	<1.0e-10	6.1e-04	<1.0e-10	<1.0e-10	<1.0e-10	2.0e-03	<1.0e-10
60	<1.0e-10	<1.0e-10	2.1e-06	<1.0e-10	3.0e-04	<1.0e-10	4.4e-05	<1.0e-10
61	<1.0e-10	<1.0e-10	<1.0e-10	<1.0e-10	2.8e-03	<1.0e-10	<1.0e-10	<1.0e-10
62	<1.0e-10	7.6e-03	<1.0e-10	<1.0e-10	3.9e-01	1.1e-03	<1.0e-10	5.9e-03
63	<1.0e-10	<1.0e-10	<1.0e-10	<1.0e-10	<1.0e-10	<1.0e-10	<1.0e-10	<1.0e-10
64	<1.0e-10	<1.0e-10	<1.0e-10	<1.0e-10	<1.0e-10	<1.0e-10	<1.0e-10	<1.0e-10
65	1.5e-10	4.9e-10	8.6e-04	3.4e-10	2.8e-04	1.1e-05	8.2e-04	2.3e-09
66	7.2e-07	2.3e-01	6.5e-07	9.7e-07	1.0e+00	7.8e-07	2.0e-02	2.6e-01
67	1.3e-02	1.6e-01	2.6e-02	2.3e-02	9.6e-01	2.3e-02	3.4e-02	2.8e-01
68	<1.0e-10	<1.0e-10	<1.0e-10	<1.0e-10	<1.0e-10	<1.0e-10	<1.0e-10	<1.0e-10
69	1.9e-04	2.3e-09	5.1e-01	3.2e-04	2.1e-03	4.9e-06	6.2e-01	1.3e-08
70	<1.0e-10	<1.0e-10	9.4e-01	<1.0e-10	<1.0e-10	6.6e-07	9.6e-01	<1.0e-10
71	<1.0e-10	<1.0e-10	<1.0e-10	<1.0e-10	4.2e-02	<1.0e-10	<1.0e-10	<1.0e-10
72	1.5e-08	1.2e-09	7.1e-02	4.6e-09	2.8e-09	1.9e-02	1.4e-01	4.0e-10
73	<1.0e-10	2.3e-07	<1.0e-10	<1.0e-10	1.0e+00	<1.0e-10	1.2e-10	2.7e-07
74	<1.0e-10	<1.0e-10	<1.0e-10	<1.0e-10	<1.0e-10	<1.0e-10	<1.0e-10	<1.0e-10
75	5.6e-08	2.5e-04	2.8e-05	9.6e-08	1.3e-01	1.9e-05	9.0e-04	5.8e-04
76	<1.0e-10	<1.0e-10	<1.0e-10	<1.0e-10	1.3e-08	<1.0e-10	<1.0e-10	<1.0e-10
77	<1.0e-10	1.0e-02	1.0e-10	<1.0e-10	2.9e-01	7.1e-04	2.0e-09	2.4e-02
78	<1.0e-10	2.5e-01	<1.0e-10	<1.0e-10	9.2e-02	1.4e-01	<1.0e-10	3.4e-01
79	5.9e-07	3.3e-03	4.1e-05	8.2e-07	7.9e-02	8.7e-04	7.2e-04	4.9e-03
80	3.6e-05	3.0e-03	2.9e-03	4.2e-05	5.3e-02	5.8e-02	2.4e-03	3.9e-03
81	3.6e-05	3.1e-03	2.9e-03	4.2e-05	1.0e+00	1.6e-03	2.4e-03	4.1e-03

Table 4—Continued

Source No	<i>pns</i> [1] [0.5–8.0keV]	<i>pns</i> [2] [0.5–2.0keV]	<i>pns</i> [3] [2.0–8.0keV]	<i>pns</i> [4] [0.35–8.0keV]	<i>pns</i> [5] [0.35–1.1keV]	<i>pns</i> [6] [1.1–2.6keV]	<i>pns</i> [7] [2.6–8.0keV]	<i>pns</i> [8] [0.35–2.0keV]
82	<1.0e-10	<1.0e-10	1.4e-05	<1.0e-10	9.8e-07	<1.0e-10	3.0e-02	<1.0e-10
83	4.0e-07	1.0e-02	9.4e-06	4.5e-07	3.5e-01	1.2e-03	8.6e-05	1.2e-02
84	9.8e-04	4.6e-05	1.6e-01	4.4e-04	2.4e-01	1.4e-05	2.6e-01	1.2e-05
85	4.0e-07	1.2e-02	9.5e-06	4.0e-07	3.4e-01	3.0e-03	3.6e-05	1.2e-02
86	3.9e-07	1.6e-04	3.8e-04	4.6e-07	1.1e-03	2.2e-03	5.2e-03	2.1e-04
87	9.2e-07	1.5e-04	7.5e-04	6.5e-07	8.7e-02	4.2e-04	7.7e-04	1.0e-04
88	<1.0e-10	<1.0e-10	1.8e-01	<1.0e-10	<1.0e-10	<1.0e-10	2.8e-01	<1.0e-10
89	<1.0e-10	<1.0e-10	3.4e-03	<1.0e-10	1.8e-07	<1.0e-10	1.3e-02	<1.0e-10
90	<1.0e-10	<1.0e-10	<1.0e-10	<1.0e-10	<1.0e-10	<1.0e-10	<1.0e-10	<1.0e-10
91	2.0e-08	1.4e-05	1.1e-04	4.5e-08	2.2e-01	1.0e-04	5.3e-05	4.7e-05
92	<1.0e-10	<1.0e-10	6.5e-03	<1.0e-10	3.5e-05	<1.0e-10	5.1e-02	<1.0e-10
93	<1.0e-10	<1.0e-10	<1.0e-10	<1.0e-10	<1.0e-10	<1.0e-10	<1.0e-10	<1.0e-10
94	<1.0e-10	<1.0e-10	5.6e-01	<1.0e-10	<1.0e-10	1.2e-02	4.2e-01	<1.0e-10
95	<1.0e-10	<1.0e-10	6.3e-03	<1.0e-10	8.3e-04	2.0e-10	3.0e-02	<1.0e-10
96	<1.0e-10	<1.0e-10	<1.0e-10	<1.0e-10	1.0e+00	<1.0e-10	<1.0e-10	1.7e-10
97	<1.0e-10	7.3e-03	<1.0e-10	<1.0e-10	5.1e-01	1.7e-04	<1.0e-10	7.7e-03
98	<1.0e-10	9.8e-05	<1.0e-10	<1.0e-10	9.6e-02	4.1e-09	1.8e-10	1.1e-05
99	<1.0e-10	<1.0e-10	<1.0e-10	<1.0e-10	1.3e-05	<1.0e-10	<1.0e-10	<1.0e-10
100	<1.0e-10	<1.0e-10	4.3e-01	<1.0e-10	<1.0e-10	<1.0e-10	5.8e-01	<1.0e-10
101	5.9e-04	4.2e-05	1.4e-01	1.0e-03	1.8e-02	2.7e-04	3.6e-01	1.5e-04
102	<1.0e-10	<1.0e-10	<1.0e-10	<1.0e-10	<1.0e-10	<1.0e-10	1.6e-04	<1.0e-10
103	<1.0e-10	1.6e-07	1.2e-07	<1.0e-10	8.6e-02	9.3e-07	2.3e-07	2.2e-07
104	2.1e-07	3.6e-09	7.6e-02	3.2e-07	1.0e+00	<1.0e-10	3.3e-01	1.0e-08
105	<1.0e-10	<1.0e-10	7.7e-04	<1.0e-10	6.9e-03	<1.0e-10	9.1e-03	<1.0e-10
106	6.4e-07	6.2e-02	8.4e-07	9.8e-07	7.7e-02	7.2e-02	5.1e-06	7.9e-02
107	<1.0e-10	<1.0e-10	3.9e-03	<1.0e-10	1.9e-02	<1.0e-10	7.9e-03	<1.0e-10
108	<1.0e-10	5.4e-05	<1.0e-10	<1.0e-10	8.5e-01	5.1e-09	<1.0e-10	1.6e-04

Table 4—Continued

Source No	<i>pns</i> [1] [0.5–8.0keV]	<i>pns</i> [2] [0.5–2.0keV]	<i>pns</i> [3] [2.0–8.0keV]	<i>pns</i> [4] [0.35–8.0keV]	<i>pns</i> [5] [0.35–1.1keV]	<i>pns</i> [6] [1.1–2.6keV]	<i>pns</i> [7] [2.6–8.0keV]	<i>pns</i> [8] [0.35–2.0keV]
109	<1.0e-10	3.2e-02	<1.0e-10	<1.0e-10	6.1e-01	9.1e-03	<1.0e-10	7.1e-02
110	5.5e-02	6.9e-01	1.9e-02	5.1e-02	8.7e-01	1.3e-01	4.0e-02	6.4e-01
111	3.9e-09	3.0e-01	4.9e-10	1.8e-08	9.5e-01	1.1e-04	3.5e-07	4.8e-01
112	<1.0e-10	<1.0e-10	<1.0e-10	<1.0e-10	<1.0e-10	<1.0e-10	3.0e-08	<1.0e-10
113	<1.0e-10	<1.0e-10	<1.0e-10	<1.0e-10	<1.0e-10	<1.0e-10	<1.0e-10	<1.0e-10
114	1.9e-04	3.0e-05	6.5e-02	8.9e-05	1.0e-02	3.0e-06	3.7e-01	1.1e-05
115	<1.0e-10	<1.0e-10	3.2e-03	<1.0e-10	2.4e-06	<1.0e-10	9.0e-03	<1.0e-10
116	4.4e-07	1.4e-02	7.9e-06	6.2e-07	1.0e+00	1.6e-05	6.3e-04	1.9e-02
117	4.4e-03	5.7e-02	2.2e-02	3.3e-03	3.6e-01	8.4e-02	1.1e-02	4.0e-02
118	1.0e-07	4.5e-07	1.0e-02	1.2e-07	8.1e-06	5.2e-03	3.3e-02	6.4e-07
119	1.5e-06	<1.0e-10	4.3e-01	2.3e-06	5.2e-08	1.3e-04	5.2e-01	<1.0e-10
120	1.3e-04	3.3e-05	6.9e-02	3.1e-04	3.6e-01	2.9e-05	1.0e-01	1.9e-04
121	<1.0e-10	<1.0e-10	<1.0e-10	<1.0e-10	4.9e-03	<1.0e-10	2.6e-10	<1.0e-10
122	<1.0e-10	<1.0e-10	<1.0e-10	<1.0e-10	<1.0e-10	<1.0e-10	<1.0e-10	<1.0e-10
123	<1.0e-10	<1.0e-10	<1.0e-10	<1.0e-10	1.5e-01	<1.0e-10	<1.0e-10	<1.0e-10
124	<1.0e-10	<1.0e-10	<1.0e-10	<1.0e-10	6.6e-01	<1.0e-10	<1.0e-10	<1.0e-10
125	<1.0e-10	<1.0e-10	<1.0e-10	<1.0e-10	<1.0e-10	<1.0e-10	<1.0e-10	<1.0e-10
126	<1.0e-10	<1.0e-10	2.0e-08	<1.0e-10	4.5e-07	<1.0e-10	4.8e-06	<1.0e-10
127	7.0e-09	2.8e-02	2.0e-08	8.0e-09	9.8e-01	1.0e-04	6.7e-08	3.0e-02
128	6.8e-06	2.3e-02	6.1e-05	5.9e-06	1.1e-01	6.2e-03	3.7e-04	1.9e-02
129	1.7e-08	4.7e-04	8.1e-06	2.0e-08	1.2e-02	1.5e-04	5.5e-04	5.6e-04
130	<1.0e-10	<1.0e-10	2.4e-06	<1.0e-10	1.4e-02	<1.0e-10	1.2e-05	<1.0e-10
131	<1.0e-10	3.5e-01	<1.0e-10	<1.0e-10	7.3e-01	6.8e-03	<1.0e-10	4.6e-01
132	<1.0e-10	<1.0e-10	<1.0e-10	<1.0e-10	<1.0e-10	<1.0e-10	<1.0e-10	<1.0e-10
133	<1.0e-10	<1.0e-10	<1.0e-10	<1.0e-10	<1.0e-10	<1.0e-10	<1.0e-10	<1.0e-10
134	<1.0e-10	<1.0e-10	<1.0e-10	<1.0e-10	<1.0e-10	<1.0e-10	<1.0e-10	<1.0e-10
135	<1.0e-10	7.8e-09	2.2e-05	<1.0e-10	4.3e-03	1.0e-09	1.3e-03	1.5e-09

Table 4—Continued

Source No	<i>pns</i> [1] [0.5–8.0keV]	<i>pns</i> [2] [0.5–2.0keV]	<i>pns</i> [3] [2.0–8.0keV]	<i>pns</i> [4] [0.35–8.0keV]	<i>pns</i> [5] [0.35–1.1keV]	<i>pns</i> [6] [1.1–2.6keV]	<i>pns</i> [7] [2.6–8.0keV]	<i>pns</i> [8] [0.35–2.0keV]
136	2.8e-10	1.1e-06	2.7e-05	3.5e-10	3.0e-02	2.4e-08	1.4e-03	1.4e-06
137	3.2e-06	2.1e-10	3.5e-01	1.4e-06	1.6e-04	2.6e-06	3.9e-01	<1.0e-10
138	<1.0e-10	<1.0e-10	<1.0e-10	<1.0e-10	<1.0e-10	<1.0e-10	<1.0e-10	<1.0e-10
139	<1.0e-10	<1.0e-10	1.0e+00	<1.0e-10	<1.0e-10	1.5e-06	1.0e+00	<1.0e-10
140	4.2e-09	7.1e-07	1.2e-04	6.2e-09	7.3e-01	1.4e-09	2.7e-03	2.0e-06
141	<1.0e-10	<1.0e-10	<1.0e-10	<1.0e-10	2.7e-05	<1.0e-10	<1.0e-10	<1.0e-10
142	<1.0e-10	<1.0e-10	<1.0e-10	<1.0e-10	<1.0e-10	<1.0e-10	<1.0e-10	<1.0e-10
143	<1.0e-10	<1.0e-10	<1.0e-10	<1.0e-10	2.5e-02	<1.0e-10	<1.0e-10	<1.0e-10
144	<1.0e-10	<1.0e-10	1.2e-05	<1.0e-10	2.9e-06	<1.0e-10	4.3e-04	<1.0e-10
145	<1.0e-10	2.3e-10	2.8e-05	<1.0e-10	1.0e-04	1.1e-06	1.4e-04	1.6e-09
146	4.6e-08	5.2e-01	1.1e-09	1.5e-07	2.8e-01	5.3e-01	1.5e-09	6.4e-01
147	<1.0e-10	<1.0e-10	9.8e-03	<1.0e-10	7.7e-03	<1.0e-10	8.6e-02	<1.0e-10
148	<1.0e-10	6.6e-03	1.6e-09	<1.0e-10	3.4e-01	2.3e-04	1.6e-08	5.0e-03
149	<1.0e-10	<1.0e-10	8.3e-01	<1.0e-10	<1.0e-10	2.6e-06	7.5e-01	<1.0e-10
150	<1.0e-10	2.6e-01	<1.0e-10	<1.0e-10	6.6e-01	1.9e-03	<1.0e-10	3.1e-01
151	3.8e-07	<1.0e-10	1.6e-01	2.0e-07	8.7e-03	1.6e-09	2.7e-01	<1.0e-10
152	<1.0e-10	<1.0e-10	<1.0e-10	<1.0e-10	4.0e-06	<1.0e-10	<1.0e-10	<1.0e-10
153	<1.0e-10	<1.0e-10	3.2e-01	<1.0e-10	<1.0e-10	9.3e-07	3.5e-01	<1.0e-10
154	<1.0e-10	<1.0e-10	<1.0e-10	<1.0e-10	<1.0e-10	<1.0e-10	<1.0e-10	<1.0e-10
155	<1.0e-10	<1.0e-10	<1.0e-10	<1.0e-10	<1.0e-10	<1.0e-10	<1.0e-10	<1.0e-10
156	<1.0e-10	5.8e-02	<1.0e-10	<1.0e-10	8.5e-01	2.8e-03	<1.0e-10	6.4e-02
157	2.0e-10	4.6e-10	1.0e-03	6.4e-10	3.6e-02	<1.0e-10	7.8e-02	4.2e-09
158	<1.0e-10	<1.0e-10	<1.0e-10	<1.0e-10	<1.0e-10	<1.0e-10	<1.0e-10	<1.0e-10
159	<1.0e-10	<1.0e-10	<1.0e-10	<1.0e-10	<1.0e-10	<1.0e-10	<1.0e-10	<1.0e-10
160	1.5e-05	1.2e-07	2.1e-01	2.1e-05	1.5e-01	8.6e-08	4.9e-01	2.9e-07
161	<1.0e-10	<1.0e-10	<1.0e-10	<1.0e-10	1.2e-07	<1.0e-10	4.1e-08	<1.0e-10
162	<1.0e-10	<1.0e-10	<1.0e-10	<1.0e-10	1.6e-03	<1.0e-10	<1.0e-10	<1.0e-10

Table 4—Continued

Source No	<i>pns</i> [1] [0.5–8.0keV]	<i>pns</i> [2] [0.5–2.0keV]	<i>pns</i> [3] [2.0–8.0keV]	<i>pns</i> [4] [0.35–8.0keV]	<i>pns</i> [5] [0.35–1.1keV]	<i>pns</i> [6] [1.1–2.6keV]	<i>pns</i> [7] [2.6–8.0keV]	<i>pns</i> [8] [0.35–2.0keV]
163	<1.0e-10	<1.0e-10	<1.0e-10	<1.0e-10	<1.0e-10	<1.0e-10	<1.0e-10	<1.0e-10
164	1.7e-07	2.0e-09	2.7e-02	4.7e-07	6.7e-03	1.4e-05	1.5e-02	2.1e-08
165	<1.0e-10	<1.0e-10	3.3e-10	<1.0e-10	7.6e-09	<1.0e-10	8.1e-10	<1.0e-10
166	<1.0e-10	<1.0e-10	<1.0e-10	<1.0e-10	<1.0e-10	<1.0e-10	<1.0e-10	<1.0e-10
167	2.3e-04	1.0e-01	5.2e-04	4.2e-04	6.4e-01	8.4e-02	3.2e-04	1.6e-01
168	2.7e-09	1.8e-04	2.5e-06	6.3e-09	4.5e-01	1.3e-08	3.3e-04	4.3e-04
169	3.2e-05	4.5e-06	4.7e-02	2.5e-05	1.1e-01	5.9e-05	3.0e-02	4.7e-06
170	1.1e-08	1.4e-04	1.6e-05	1.7e-09	4.6e-02	1.0e-04	2.2e-05	1.7e-05
171	7.9e-05	5.9e-09	4.7e-01	1.0e-04	9.1e-05	1.3e-03	4.0e-01	2.1e-08
172	1.6e-07	7.9e-02	2.2e-07	3.1e-07	8.5e-01	6.7e-02	2.3e-08	1.1e-01
173	2.8e-02	1.4e-01	6.2e-02	2.7e-02	7.4e-01	1.6e-03	3.0e-01	1.4e-01
174	1.0e-06	3.9e-04	4.0e-04	9.5e-08	5.3e-03	6.8e-04	7.9e-04	2.3e-05
175	<1.0e-10	<1.0e-10	2.6e-05	<1.0e-10	<1.0e-10	<1.0e-10	5.2e-03	<1.0e-10
176	<1.0e-10	<1.0e-10	4.8e-01	<1.0e-10	<1.0e-10	1.3e-05	2.6e-01	<1.0e-10
177	<1.0e-10	4.2e-03	5.5e-10	<1.0e-10	5.6e-02	2.5e-02	6.0e-10	6.8e-03
178	<1.0e-10	<1.0e-10	8.0e-06	<1.0e-10	2.4e-06	<1.0e-10	1.1e-04	<1.0e-10
179	<1.0e-10	<1.0e-10	1.1e-05	<1.0e-10	2.4e-01	<1.0e-10	4.6e-04	<1.0e-10
180	<1.0e-10	<1.0e-10	<1.0e-10	<1.0e-10	<1.0e-10	<1.0e-10	<1.0e-10	<1.0e-10
181	<1.0e-10	<1.0e-10	<1.0e-10	<1.0e-10	<1.0e-10	<1.0e-10	<1.0e-10	<1.0e-10
182	1.2e-05	8.6e-06	2.9e-02	5.3e-06	5.2e-02	4.7e-06	5.9e-02	3.1e-06
183	<1.0e-10	<1.0e-10	3.7e-01	<1.0e-10	<1.0e-10	<1.0e-10	5.2e-01	<1.0e-10
184	<1.0e-10	<1.0e-10	5.2e-02	<1.0e-10	<1.0e-10	<1.0e-10	3.3e-01	<1.0e-10
185	3.4e-10	1.3e-08	1.3e-03	4.4e-10	1.0e+00	<1.0e-10	8.2e-03	2.0e-08
186	<1.0e-10	<1.0e-10	<1.0e-10	<1.0e-10	<1.0e-10	<1.0e-10	<1.0e-10	<1.0e-10
187	<1.0e-10	<1.0e-10	<1.0e-10	<1.0e-10	<1.0e-10	<1.0e-10	<1.0e-10	<1.0e-10
188	<1.0e-10	<1.0e-10	8.0e-03	<1.0e-10	<1.0e-10	<1.0e-10	1.2e-01	<1.0e-10
189	<1.0e-10	<1.0e-10	8.0e-10	<1.0e-10	5.5e-06	<1.0e-10	2.1e-05	<1.0e-10

Table 4—Continued

Source No	<i>pns</i> [1] [0.5–8.0keV]	<i>pns</i> [2] [0.5–2.0keV]	<i>pns</i> [3] [2.0–8.0keV]	<i>pns</i> [4] [0.35–8.0keV]	<i>pns</i> [5] [0.35–1.1keV]	<i>pns</i> [6] [1.1–2.6keV]	<i>pns</i> [7] [2.6–8.0keV]	<i>pns</i> [8] [0.35–2.0keV]
190	<1.0e-10	<1.0e-10	<1.0e-10	<1.0e-10	<1.0e-10	<1.0e-10	<1.0e-10	<1.0e-10
191	2.4e-04	8.4e-01	4.4e-06	3.8e-04	8.6e-01	8.5e-01	7.7e-07	8.8e-01
192	<1.0e-10	<1.0e-10	8.1e-03	<1.0e-10	7.7e-02	<1.0e-10	3.6e-02	<1.0e-10
193	<1.0e-10	<1.0e-10	<1.0e-10	<1.0e-10	3.3e-06	<1.0e-10	<1.0e-10	<1.0e-10
194	9.8e-10	<1.0e-10	9.7e-03	1.8e-09	4.6e-03	1.6e-07	7.7e-03	<1.0e-10
195	<1.0e-10	<1.0e-10	<1.0e-10	<1.0e-10	<1.0e-10	<1.0e-10	<1.0e-10	<1.0e-10
196	<1.0e-10	<1.0e-10	1.3e-03	<1.0e-10	1.1e-03	<1.0e-10	8.4e-03	<1.0e-10
197	<1.0e-10	<1.0e-10	2.6e-05	<1.0e-10	<1.0e-10	<1.0e-10	9.9e-03	<1.0e-10
198	4.3e-09	1.4e-04	4.6e-06	2.5e-09	7.2e-04	2.9e-03	3.2e-05	8.2e-05
199	<1.0e-10	<1.0e-10	<1.0e-10	<1.0e-10	5.6e-01	<1.0e-10	1.3e-10	2.6e-10
200	<1.0e-10	2.7e-05	2.5e-08	<1.0e-10	1.0e+00	1.3e-10	9.1e-07	5.8e-05
201	3.6e-05	3.4e-06	5.0e-02	9.5e-05	1.5e-01	2.4e-05	7.5e-02	2.8e-05
202	<1.0e-10	<1.0e-10	3.1e-07	<1.0e-10	1.1e-02	<1.0e-10	2.7e-05	<1.0e-10
203	2.8e-06	3.6e-01	2.9e-07	9.0e-06	9.8e-01	1.3e-02	1.2e-06	5.2e-01
204	1.0e-08	9.1e-08	1.3e-03	7.1e-09	9.9e-03	6.4e-06	1.1e-03	7.0e-08
205	<1.0e-10	2.7e-10	2.5e-04	<1.0e-10	3.2e-04	3.5e-06	1.2e-04	2.3e-10
206	<1.0e-10	<1.0e-10	<1.0e-10	<1.0e-10	<1.0e-10	<1.0e-10	<1.0e-10	<1.0e-10
207	<1.0e-10	3.7e-02	<1.0e-10	<1.0e-10	2.9e-01	1.2e-07	<1.0e-10	4.2e-02
208	<1.0e-10	<1.0e-10	2.5e-02	<1.0e-10	5.1e-06	<1.0e-10	4.4e-01	<1.0e-10
209	1.0e-04	1.6e-01	1.6e-04	1.6e-04	4.7e-01	6.0e-05	5.3e-02	2.2e-01
210	<1.0e-10	<1.0e-10	<1.0e-10	<1.0e-10	<1.0e-10	<1.0e-10	<1.0e-10	<1.0e-10
211	5.9e-07	1.3e-09	4.4e-02	4.3e-07	1.4e-02	2.3e-06	2.7e-02	1.2e-09
212	2.0e-08	<1.0e-10	3.9e-02	4.6e-08	9.9e-04	8.6e-08	7.5e-02	2.6e-10
213	4.8e-10	2.1e-04	3.8e-07	1.4e-09	3.4e-02	6.5e-03	1.3e-07	5.7e-04
214	<1.0e-10	5.3e-02	<1.0e-10	<1.0e-10	3.1e-01	2.0e-05	<1.0e-10	9.4e-02
215	<1.0e-10	<1.0e-10	<1.0e-10	<1.0e-10	9.9e-09	<1.0e-10	<1.0e-10	<1.0e-10
216	<1.0e-10	6.2e-09	5.0e-05	<1.0e-10	1.1e-01	<1.0e-10	3.9e-03	4.9e-09

Table 4—Continued

Source No	<i>pns</i> [1] [0.5–8.0keV]	<i>pns</i> [2] [0.5–2.0keV]	<i>pns</i> [3] [2.0–8.0keV]	<i>pns</i> [4] [0.35–8.0keV]	<i>pns</i> [5] [0.35–1.1keV]	<i>pns</i> [6] [1.1–2.6keV]	<i>pns</i> [7] [2.6–8.0keV]	<i>pns</i> [8] [0.35–2.0keV]
217	1.9e-03	2.6e-02	1.9e-02	2.4e-03	6.0e-01	6.2e-02	4.4e-03	3.5e-02
218	2.0e-02	2.0e-01	3.7e-02	1.4e-02	1.5e-01	4.0e-02	1.5e-01	1.2e-01
219	2.4e-10	2.6e-07	2.0e-05	3.5e-10	5.9e-02	2.2e-06	3.7e-05	6.0e-07
220	1.7e-06	1.1e-01	1.6e-06	2.4e-06	8.2e-01	2.3e-03	2.0e-05	1.3e-01
221	<1.0e-10	<1.0e-10	<1.0e-10	<1.0e-10	<1.0e-10	<1.0e-10	<1.0e-10	<1.0e-10
222	3.0e-08	4.3e-06	2.3e-04	1.8e-08	1.4e-02	5.4e-06	1.8e-03	3.3e-06
223	4.3e-05	2.1e-07	1.2e-01	5.1e-05	3.9e-02	9.3e-05	6.5e-02	5.5e-07
224	<1.0e-10	<1.0e-10	<1.0e-10	<1.0e-10	<1.0e-10	<1.0e-10	<1.0e-10	<1.0e-10
225	<1.0e-10	<1.0e-10	<1.0e-10	<1.0e-10	<1.0e-10	<1.0e-10	<1.0e-10	<1.0e-10
226	5.5e-06	5.3e-04	1.3e-03	7.4e-06	3.5e-02	4.2e-02	3.4e-04	8.3e-04
227	1.1e-06	4.3e-06	6.0e-03	3.4e-06	1.6e-01	1.6e-07	6.3e-02	2.7e-05
228	<1.0e-10	<1.0e-10	3.2e-10	<1.0e-10	<1.0e-10	<1.0e-10	6.0e-08	<1.0e-10
229	<1.0e-10	<1.0e-10	5.7e-06	<1.0e-10	5.2e-04	<1.0e-10	4.8e-05	<1.0e-10
230	5.0e-06	5.3e-03	2.0e-04	1.5e-06	4.7e-02	1.9e-02	1.1e-04	1.3e-03
231	<1.0e-10	3.6e-09	3.7e-08	<1.0e-10	8.8e-03	6.9e-08	6.9e-08	3.0e-09
232	5.7e-04	8.5e-03	1.1e-02	1.0e-03	8.4e-01	1.8e-03	1.7e-02	2.1e-02
233	<1.0e-10	<1.0e-10	<1.0e-10	<1.0e-10	<1.0e-10	<1.0e-10	<1.0e-10	<1.0e-10
234	<1.0e-10	8.8e-07	<1.0e-10	<1.0e-10	5.5e-01	<1.0e-10	<1.0e-10	4.9e-07
235	<1.0e-10	2.7e-07	<1.0e-10	<1.0e-10	1.3e-01	<1.0e-10	<1.0e-10	5.5e-07
236	<1.0e-10	<1.0e-10	2.8e-04	<1.0e-10	<1.0e-10	<1.0e-10	1.0e-03	<1.0e-10
237	<1.0e-10	<1.0e-10	<1.0e-10	<1.0e-10	<1.0e-10	<1.0e-10	<1.0e-10	<1.0e-10
238	<1.0e-10	<1.0e-10	<1.0e-10	<1.0e-10	<1.0e-10	<1.0e-10	<1.0e-10	<1.0e-10
239	7.3e-03	2.9e-01	7.1e-03	5.4e-03	2.6e-01	7.3e-02	2.9e-02	2.1e-01
240	<1.0e-10	<1.0e-10	<1.0e-10	<1.0e-10	1.8e-04	<1.0e-10	<1.0e-10	<1.0e-10
241	<1.0e-10	<1.0e-10	<1.0e-10	<1.0e-10	4.6e-01	<1.0e-10	4.4e-08	<1.0e-10
242	<1.0e-10	<1.0e-10	1.2e-01	<1.0e-10	<1.0e-10	3.3e-02	2.9e-02	<1.0e-10
243	7.0e-06	1.6e-02	9.6e-05	4.3e-06	5.2e-01	2.8e-04	5.3e-04	9.2e-03

Table 4—Continued

Source No	<i>pns</i> [1] [0.5–8.0keV]	<i>pns</i> [2] [0.5–2.0keV]	<i>pns</i> [3] [2.0–8.0keV]	<i>pns</i> [4] [0.35–8.0keV]	<i>pns</i> [5] [0.35–1.1keV]	<i>pns</i> [6] [1.1–2.6keV]	<i>pns</i> [7] [2.6–8.0keV]	<i>pns</i> [8] [0.35–2.0keV]
244	2.7e-07	2.4e-06	1.9e-03	4.2e-07	3.1e-02	3.0e-05	5.2e-03	5.5e-06
245	<1.0e-10	<1.0e-10	7.9e-01	<1.0e-10	<1.0e-10	2.8e-10	7.6e-01	<1.0e-10
246	4.3e-05	3.6e-06	6.7e-02	7.3e-05	1.2e-01	1.7e-06	2.2e-01	1.2e-05
247	<1.0e-10	1.1e-06	<1.0e-10	<1.0e-10	1.8e-01	3.0e-09	1.1e-09	4.7e-06
248	<1.0e-10	<1.0e-10	<1.0e-10	<1.0e-10	<1.0e-10	<1.0e-10	<1.0e-10	<1.0e-10
249	<1.0e-10	<1.0e-10	7.8e-02	<1.0e-10	<1.0e-10	4.8e-03	6.8e-02	<1.0e-10
250	<1.0e-10	<1.0e-10	<1.0e-10	<1.0e-10	8.1e-04	<1.0e-10	<1.0e-10	<1.0e-10
251	<1.0e-10	1.3e-08	<1.0e-10	<1.0e-10	3.2e-02	<1.0e-10	<1.0e-10	2.8e-08
252	<1.0e-10	<1.0e-10	<1.0e-10	<1.0e-10	7.8e-01	<1.0e-10	<1.0e-10	<1.0e-10
253	<1.0e-10	<1.0e-10	1.1e-04	<1.0e-10	8.8e-02	<1.0e-10	1.4e-03	<1.0e-10
254	2.0e-08	1.9e-09	2.0e-02	4.8e-08	5.0e-01	<1.0e-10	1.0e-01	1.5e-08
255	<1.0e-10	<1.0e-10	<1.0e-10	<1.0e-10	<1.0e-10	<1.0e-10	<1.0e-10	<1.0e-10
256	<1.0e-10	<1.0e-10	<1.0e-10	<1.0e-10	2.5e-09	<1.0e-10	<1.0e-10	<1.0e-10
257	1.3e-04	3.0e-05	5.1e-02	2.3e-04	1.5e-01	9.4e-04	4.3e-02	1.3e-04
258	1.7e-10	2.6e-09	7.2e-04	1.6e-10	1.5e-02	3.7e-08	6.1e-04	3.0e-09
259	<1.0e-10	<1.0e-10	<1.0e-10	<1.0e-10	3.6e-06	<1.0e-10	1.8e-10	<1.0e-10
260	2.0e-04	2.5e-07	4.4e-01	2.7e-04	1.0e-02	1.9e-07	9.3e-01	5.2e-07
261	2.2e-04	4.1e-07	3.1e-01	2.9e-04	1.4e-03	2.2e-04	4.4e-01	1.1e-06
262	<1.0e-10	<1.0e-10	<1.0e-10	<1.0e-10	<1.0e-10	<1.0e-10	<1.0e-10	<1.0e-10
263	<1.0e-10	<1.0e-10	<1.0e-10	<1.0e-10	<1.0e-10	<1.0e-10	<1.0e-10	<1.0e-10
264	<1.0e-10	<1.0e-10	<1.0e-10	<1.0e-10	4.1e-06	<1.0e-10	<1.0e-10	<1.0e-10
265	<1.0e-10	1.6e-03	1.1e-09	<1.0e-10	1.7e-01	9.4e-06	6.5e-07	6.0e-03
266	<1.0e-10	<1.0e-10	3.9e-10	<1.0e-10	2.4e-03	<1.0e-10	1.3e-07	<1.0e-10
267	1.2e-02	2.6e-02	9.6e-02	1.1e-02	4.4e-02	1.4e-01	1.1e-01	2.1e-02
268	<1.0e-10	<1.0e-10	<1.0e-10	<1.0e-10	<1.0e-10	<1.0e-10	<1.0e-10	<1.0e-10
269	<1.0e-10	<1.0e-10	3.2e-06	<1.0e-10	<1.0e-10	<1.0e-10	2.8e-03	<1.0e-10
270	1.5e-09	1.2e-09	5.3e-03	2.5e-09	<1.0e-10	2.1e-02	1.3e-02	3.3e-09

|
85
|

Table 4—Continued

Source No	<i>pns</i> [1] [0.5–8.0keV]	<i>pns</i> [2] [0.5–2.0keV]	<i>pns</i> [3] [2.0–8.0keV]	<i>pns</i> [4] [0.35–8.0keV]	<i>pns</i> [5] [0.35–1.1keV]	<i>pns</i> [6] [1.1–2.6keV]	<i>pns</i> [7] [2.6–8.0keV]	<i>pns</i> [8] [0.35–2.0keV]
271	1.2e-07	1.3e-08	2.4e-02	2.6e-07	1.9e-01	3.4e-08	1.6e-02	5.9e-08
272	<1.0e-10	<1.0e-10	5.4e-06	<1.0e-10	<1.0e-10	<1.0e-10	5.0e-03	<1.0e-10
273	2.0e-05	2.8e-01	9.2e-06	1.4e-05	6.2e-01	9.1e-03	1.3e-04	2.0e-01
274	<1.0e-10	<1.0e-10	<1.0e-10	<1.0e-10	<1.0e-10	<1.0e-10	<1.0e-10	<1.0e-10
275	<1.0e-10	<1.0e-10	<1.0e-10	<1.0e-10	<1.0e-10	<1.0e-10	<1.0e-10	<1.0e-10
276	1.9e-01	5.3e-01	1.4e-01	2.6e-01	8.9e-01	3.3e-01	1.2e-01	6.6e-01
277	<1.0e-10	<1.0e-10	<1.0e-10	<1.0e-10	<1.0e-10	<1.0e-10	<1.0e-10	<1.0e-10
278	<1.0e-10	<1.0e-10	4.6e-09	<1.0e-10	<1.0e-10	<1.0e-10	2.6e-06	<1.0e-10
279	<1.0e-10	<1.0e-10	<1.0e-10	<1.0e-10	<1.0e-10	<1.0e-10	2.4e-04	<1.0e-10
280	<1.0e-10	1.5e-07	<1.0e-10	<1.0e-10	6.8e-01	<1.0e-10	<1.0e-10	1.9e-07
281	<1.0e-10	<1.0e-10	<1.0e-10	<1.0e-10	<1.0e-10	<1.0e-10	<1.0e-10	<1.0e-10
282	<1.0e-10	<1.0e-10	<1.0e-10	<1.0e-10	<1.0e-10	<1.0e-10	<1.0e-10	<1.0e-10
283	<1.0e-10	<1.0e-10	<1.0e-10	<1.0e-10	<1.0e-10	<1.0e-10	<1.0e-10	<1.0e-10
284	<1.0e-10	1.8e-01	<1.0e-10	<1.0e-10	1.8e-01	1.4e-01	<1.0e-10	2.4e-01
285	<1.0e-10	<1.0e-10	<1.0e-10	<1.0e-10	4.7e-05	<1.0e-10	<1.0e-10	<1.0e-10
286	4.5e-08	5.6e-02	1.2e-07	7.7e-08	4.4e-02	2.6e-01	7.9e-08	7.5e-02
287	<1.0e-10	<1.0e-10	1.8e-06	<1.0e-10	<1.0e-10	<1.0e-10	1.3e-03	<1.0e-10
288	2.7e-06	<1.0e-10	8.3e-01	6.1e-07	1.1e-08	1.2e-07	8.9e-01	<1.0e-10
289	1.0e-04	1.4e-07	2.6e-01	8.5e-05	7.7e-04	3.3e-05	5.3e-01	1.5e-07
290	1.8e-05	2.9e-01	6.7e-06	5.3e-05	7.6e-01	2.5e-02	5.9e-05	4.6e-01
291	2.7e-08	1.5e-06	6.8e-04	1.9e-08	3.4e-06	6.2e-03	1.5e-03	1.1e-06
292	5.1e-06	2.9e-06	2.4e-02	6.9e-07	8.0e-03	8.4e-06	5.2e-02	1.9e-07
293	<1.0e-10	<1.0e-10	1.5e-08	<1.0e-10	7.2e-04	4.3e-10	4.7e-08	<1.0e-10
294	3.4e-07	5.3e-02	6.3e-07	1.7e-07	3.8e-02	1.2e-02	1.7e-05	3.0e-02
295	<1.0e-10	<1.0e-10	<1.0e-10	<1.0e-10	1.5e-03	<1.0e-10	3.7e-09	<1.0e-10
296	1.6e-06	3.3e-04	7.5e-04	1.1e-06	1.5e-01	6.4e-07	3.3e-02	2.4e-04
297	<1.0e-10	<1.0e-10	<1.0e-10	<1.0e-10	7.8e-05	<1.0e-10	<1.0e-10	<1.0e-10

Table 4—Continued

Source No	<i>pns</i> [1] [0.5–8.0keV]	<i>pns</i> [2] [0.5–2.0keV]	<i>pns</i> [3] [2.0–8.0keV]	<i>pns</i> [4] [0.35–8.0keV]	<i>pns</i> [5] [0.35–1.1keV]	<i>pns</i> [6] [1.1–2.6keV]	<i>pns</i> [7] [2.6–8.0keV]	<i>pns</i> [8] [0.35–2.0keV]
298	<1.0e-10	<1.0e-10	8.0e-01	<1.0e-10	<1.0e-10	<1.0e-10	7.8e-01	<1.0e-10
299	<1.0e-10	<1.0e-10	<1.0e-10	<1.0e-10	<1.0e-10	<1.0e-10	<1.0e-10	<1.0e-10
300	2.3e-07	8.3e-05	2.8e-04	6.3e-07	1.2e-01	1.1e-06	1.1e-02	3.2e-04
301	<1.0e-10	<1.0e-10	<1.0e-10	<1.0e-10	<1.0e-10	<1.0e-10	<1.0e-10	<1.0e-10
302	<1.0e-10	<1.0e-10	8.8e-01	2.8e-10	6.6e-10	<1.0e-10	8.4e-01	<1.0e-10
303	2.7e-10	1.5e-07	4.5e-05	1.1e-09	1.5e-02	1.0e-06	6.5e-04	1.4e-06
304	<1.0e-10	1.0e-06	8.0e-06	<1.0e-10	3.0e-02	4.4e-09	3.6e-04	1.6e-07
305	<1.0e-10	<1.0e-10	<1.0e-10	<1.0e-10	2.8e-02	<1.0e-10	<1.0e-10	<1.0e-10
306	8.6e-10	5.9e-10	5.1e-03	2.4e-09	8.7e-01	<1.0e-10	4.7e-02	3.9e-09
307	<1.0e-10	<1.0e-10	7.7e-09	<1.0e-10	3.6e-02	<1.0e-10	1.1e-05	<1.0e-10
308	<1.0e-10	<1.0e-10	1.3e-02	<1.0e-10	<1.0e-10	<1.0e-10	9.2e-03	<1.0e-10
309	<1.0e-10	<1.0e-10	<1.0e-10	<1.0e-10	<1.0e-10	<1.0e-10	<1.0e-10	<1.0e-10
310	<1.0e-10	2.0e-03	<1.0e-10	<1.0e-10	9.5e-02	1.3e-05	<1.0e-10	4.4e-03
311	1.0e-06	1.6e-01	5.7e-07	1.9e-06	4.3e-01	1.9e-01	2.1e-07	2.1e-01
312	<1.0e-10	<1.0e-10	<1.0e-10	<1.0e-10	9.2e-10	<1.0e-10	<1.0e-10	<1.0e-10
313	3.5e-02	9.1e-07	9.5e-01	4.2e-02	2.2e-01	8.7e-06	9.5e-01	2.3e-06
314	1.6e-05	5.1e-09	2.2e-01	2.5e-05	4.4e-03	8.0e-07	4.1e-01	2.3e-08
315	2.8e-06	3.4e-04	1.1e-03	2.7e-06	7.2e-03	4.4e-02	4.0e-04	3.7e-04
316	<1.0e-10	<1.0e-10	<1.0e-10	<1.0e-10	<1.0e-10	<1.0e-10	<1.0e-10	<1.0e-10
317	<1.0e-10	<1.0e-10	9.2e-08	<1.0e-10	2.0e-02	<1.0e-10	8.1e-07	<1.0e-10
318	<1.0e-10	<1.0e-10	<1.0e-10	<1.0e-10	<1.0e-10	<1.0e-10	<1.0e-10	<1.0e-10
319	3.3e-10	4.2e-09	6.3e-03	4.2e-10	1.0e-03	7.9e-09	2.6e-01	5.9e-09
320	<1.0e-10	<1.0e-10	<1.0e-10	<1.0e-10	<1.0e-10	<1.0e-10	<1.0e-10	<1.0e-10
321	9.7e-02	5.3e-01	4.6e-02	1.2e-01	8.0e-01	2.7e-01	6.3e-02	5.9e-01
322	4.5e-09	<1.0e-10	2.4e-01	2.0e-09	4.9e-07	3.9e-10	4.6e-01	<1.0e-10
323	<1.0e-10	<1.0e-10	<1.0e-10	<1.0e-10	5.5e-08	<1.0e-10	<1.0e-10	<1.0e-10
324	4.0e-09	4.1e-09	4.0e-03	6.1e-09	2.1e-04	1.8e-06	2.4e-02	9.9e-09

Table 4—Continued

Source No	<i>pns</i> [1] [0.5–8.0keV]	<i>pns</i> [2] [0.5–2.0keV]	<i>pns</i> [3] [2.0–8.0keV]	<i>pns</i> [4] [0.35–8.0keV]	<i>pns</i> [5] [0.35–1.1keV]	<i>pns</i> [6] [1.1–2.6keV]	<i>pns</i> [7] [2.6–8.0keV]	<i>pns</i> [8] [0.35–2.0keV]
325	2.8e-05	5.1e-06	9.1e-02	5.0e-05	2.2e-06	2.8e-02	1.9e-01	1.4e-05
326	6.8e-07	1.3e-04	4.2e-04	1.8e-06	1.6e-01	2.5e-03	3.4e-04	6.1e-04
327	<1.0e-10	<1.0e-10	<1.0e-10	<1.0e-10	9.9e-05	<1.0e-10	<1.0e-10	<1.0e-10
328	7.3e-10	<1.0e-10	8.1e-01	6.3e-10	<1.0e-10	3.7e-03	8.7e-01	<1.0e-10
329	<1.0e-10	<1.0e-10	1.8e-04	<1.0e-10	4.6e-02	<1.0e-10	9.6e-03	<1.0e-10
330	<1.0e-10	9.9e-08	3.8e-05	<1.0e-10	3.7e-04	3.9e-06	5.4e-04	1.3e-07
331	<1.0e-10	2.2e-08	1.2e-05	<1.0e-10	3.1e-02	<1.0e-10	1.0e-02	5.9e-08
332	<1.0e-10	<1.0e-10	5.1e-01	<1.0e-10	<1.0e-10	2.2e-02	5.4e-01	<1.0e-10
333	<1.0e-10	<1.0e-10	7.1e-07	<1.0e-10	<1.0e-10	<1.0e-10	1.6e-04	<1.0e-10
334	<1.0e-10	<1.0e-10	5.0e-02	<1.0e-10	<1.0e-10	<1.0e-10	9.0e-01	<1.0e-10
335	<1.0e-10	<1.0e-10	<1.0e-10	<1.0e-10	4.0e-08	<1.0e-10	<1.0e-10	<1.0e-10
336	<1.0e-10	5.7e-08	<1.0e-10	<1.0e-10	4.1e-02	<1.0e-10	<1.0e-10	2.0e-07
337	<1.0e-10	8.6e-04	<1.0e-10	<1.0e-10	9.3e-01	4.4e-07	<1.0e-10	3.1e-03
338	<1.0e-10	<1.0e-10	2.0e-03	1.9e-10	2.5e-03	<1.0e-10	2.1e-02	<1.0e-10
339	<1.0e-10	<1.0e-10	<1.0e-10	<1.0e-10	<1.0e-10	<1.0e-10	<1.0e-10	<1.0e-10
340	1.0e-03	1.5e-02	1.7e-02	9.0e-04	4.3e-01	8.1e-04	5.2e-02	1.3e-02
341	2.5e-05	3.3e-04	6.0e-03	3.0e-05	3.8e-02	1.1e-04	5.0e-02	4.8e-04
342	<1.0e-10	<1.0e-10	<1.0e-10	<1.0e-10	1.2e-08	<1.0e-10	<1.0e-10	<1.0e-10
343	5.2e-03	1.4e-02	5.5e-02	5.1e-03	1.0e-01	7.0e-03	1.6e-01	1.5e-02
344	2.9e-06	1.2e-05	5.6e-03	2.0e-06	1.3e-02	8.6e-05	1.5e-02	8.6e-06
345	2.2e-06	1.1e-07	2.9e-02	2.2e-06	1.4e-06	4.5e-03	6.6e-02	1.9e-07
346	<1.0e-10	<1.0e-10	<1.0e-10	<1.0e-10	1.2e-02	<1.0e-10	<1.0e-10	<1.0e-10
347	<1.0e-10	<1.0e-10	<1.0e-10	<1.0e-10	<1.0e-10	<1.0e-10	<1.0e-10	<1.0e-10
348	<1.0e-10	<1.0e-10	<1.0e-10	<1.0e-10	<1.0e-10	<1.0e-10	<1.0e-10	<1.0e-10
349	1.4e-04	1.5e-08	6.3e-01	1.1e-04	5.1e-07	2.4e-02	5.5e-01	1.5e-08
350	1.7e-02	1.1e-05	7.5e-01	2.5e-02	7.0e-02	4.7e-05	9.4e-01	4.7e-05
351	1.1e-08	1.6e-03	1.5e-06	1.9e-08	1.0e+00	2.5e-05	4.0e-06	2.9e-03

Table 4—Continued

Source No	<i>pns</i> [1] [0.5–8.0keV]	<i>pns</i> [2] [0.5–2.0keV]	<i>pns</i> [3] [2.0–8.0keV]	<i>pns</i> [4] [0.35–8.0keV]	<i>pns</i> [5] [0.35–1.1keV]	<i>pns</i> [6] [1.1–2.6keV]	<i>pns</i> [7] [2.6–8.0keV]	<i>pns</i> [8] [0.35–2.0keV]
352	<1.0e-10	<1.0e-10	<1.0e-10	<1.0e-10	<1.0e-10	<1.0e-10	<1.0e-10	<1.0e-10
353	<1.0e-10	<1.0e-10	1.1e-03	<1.0e-10	7.0e-05	<1.0e-10	1.1e-02	<1.0e-10
354	3.8e-08	4.3e-03	1.8e-06	3.7e-09	1.3e-02	8.6e-03	1.3e-06	3.3e-04
355	5.1e-10	3.4e-08	2.8e-04	1.2e-09	1.2e-02	1.2e-06	7.4e-04	1.3e-07
356	<1.0e-10	3.7e-05	<1.0e-10	<1.0e-10	6.2e-01	<1.0e-10	<1.0e-10	2.0e-04
357	2.1e-06	<1.0e-10	4.5e-01	2.0e-06	<1.0e-10	7.7e-02	6.0e-01	<1.0e-10
358	<1.0e-10	8.6e-04	<1.0e-10	<1.0e-10	2.8e-02	1.5e-02	<1.0e-10	9.2e-04
359	1.5e-04	3.5e-01	3.7e-05	2.3e-04	6.2e-01	7.2e-01	1.3e-06	4.3e-01
360	4.8e-05	1.4e-08	3.6e-01	4.1e-05	3.4e-09	7.1e-03	6.4e-01	1.4e-08
361	<1.0e-10	5.7e-09	<1.0e-10	<1.0e-10	3.9e-01	<1.0e-10	<1.0e-10	9.7e-08
362	<1.0e-10	<1.0e-10	3.4e-01	<1.0e-10	<1.0e-10	<1.0e-10	6.4e-01	<1.0e-10
363	7.9e-04	4.6e-06	3.6e-01	2.8e-04	3.4e-04	3.0e-03	3.5e-01	7.8e-07
364	2.3e-04	1.3e-01	3.9e-04	2.0e-04	7.5e-02	6.4e-02	2.8e-03	1.1e-01
365	<1.0e-10	<1.0e-10	<1.0e-10	<1.0e-10	<1.0e-10	<1.0e-10	<1.0e-10	<1.0e-10
366	<1.0e-10	<1.0e-10	2.4e-02	<1.0e-10	<1.0e-10	<1.0e-10	5.1e-02	<1.0e-10
367	<1.0e-10	<1.0e-10	8.4e-05	<1.0e-10	2.5e-04	<1.0e-10	5.4e-04	<1.0e-10
368	<1.0e-10	<1.0e-10	2.2e-04	<1.0e-10	<1.0e-10	<1.0e-10	8.7e-02	<1.0e-10
369	<1.0e-10	4.3e-02	<1.0e-10	<1.0e-10	5.4e-01	4.9e-02	<1.0e-10	5.8e-02
370	<1.0e-10	<1.0e-10	<1.0e-10	<1.0e-10	<1.0e-10	<1.0e-10	1.9e-09	<1.0e-10
371	<1.0e-10	<1.0e-10	5.3e-01	<1.0e-10	<1.0e-10	<1.0e-10	7.6e-01	<1.0e-10
372	<1.0e-10	<1.0e-10	6.2e-02	<1.0e-10	<1.0e-10	<1.0e-10	8.5e-02	<1.0e-10
373	<1.0e-10	<1.0e-10	1.0e-02	<1.0e-10	1.5e-04	<1.0e-10	4.1e-02	<1.0e-10
374	1.3e-06	<1.0e-10	8.4e-01	1.2e-06	<1.0e-10	3.1e-05	9.0e-01	<1.0e-10
375	<1.0e-10	<1.0e-10	3.8e-01	<1.0e-10	<1.0e-10	8.8e-05	6.3e-01	<1.0e-10
376	4.5e-07	7.3e-07	1.3e-02	1.3e-07	1.1e-08	4.2e-01	8.8e-03	1.5e-07
377	2.2e-04	2.5e-06	3.3e-01	3.5e-04	2.9e-03	3.3e-03	2.8e-01	7.1e-06
378	3.4e-05	4.5e-01	1.9e-06	7.0e-05	9.4e-01	5.0e-02	2.8e-06	5.5e-01

Table 4—Continued

Source No	<i>pns</i> [1] [0.5–8.0keV]	<i>pns</i> [2] [0.5–2.0keV]	<i>pns</i> [3] [2.0–8.0keV]	<i>pns</i> [4] [0.35–8.0keV]	<i>pns</i> [5] [0.35–1.1keV]	<i>pns</i> [6] [1.1–2.6keV]	<i>pns</i> [7] [2.6–8.0keV]	<i>pns</i> [8] [0.35–2.0keV]
379	<1.0e-10	1.6e-05	<1.0e-10	<1.0e-10	8.7e-02	1.0e-06	<1.0e-10	6.3e-06
380	2.3e-06	3.0e-04	1.1e-03	1.8e-06	1.9e-01	1.4e-03	2.0e-04	2.4e-04
381	<1.0e-10	<1.0e-10	<1.0e-10	<1.0e-10	<1.0e-10	<1.0e-10	<1.0e-10	<1.0e-10
382	6.7e-03	7.3e-04	3.3e-01	9.8e-03	3.0e-01	1.0e-03	3.2e-01	1.6e-03
383	1.4e-04	2.5e-04	2.1e-02	4.0e-04	4.6e-02	1.2e-03	7.9e-02	2.1e-03
384	<1.0e-10	<1.0e-10	<1.0e-10	<1.0e-10	<1.0e-10	<1.0e-10	<1.0e-10	<1.0e-10
385	2.0e-08	2.2e-07	2.3e-03	5.9e-09	8.6e-08	1.6e-02	4.6e-03	5.1e-08
386	<1.0e-10	<1.0e-10	<1.0e-10	<1.0e-10	<1.0e-10	<1.0e-10	<1.0e-10	<1.0e-10
387	<1.0e-10	<1.0e-10	<1.0e-10	<1.0e-10	5.9e-05	<1.0e-10	<1.0e-10	<1.0e-10
388	<1.0e-10	<1.0e-10	<1.0e-10	<1.0e-10	1.3e-10	<1.0e-10	<1.0e-10	<1.0e-10
389	<1.0e-10	<1.0e-10	<1.0e-10	<1.0e-10	<1.0e-10	<1.0e-10	<1.0e-10	<1.0e-10
390	<1.0e-10	<1.0e-10	3.2e-09	<1.0e-10	1.1e-05	<1.0e-10	1.8e-04	<1.0e-10
391	<1.0e-10	<1.0e-10	<1.0e-10	<1.0e-10	<1.0e-10	<1.0e-10	<1.0e-10	<1.0e-10
392	<1.0e-10	<1.0e-10	6.2e-10	<1.0e-10	2.4e-08	<1.0e-10	8.5e-07	<1.0e-10
393	<1.0e-10	<1.0e-10	1.7e-08	<1.0e-10	5.7e-01	<1.0e-10	1.2e-06	<1.0e-10
394	<1.0e-10	1.6e-01	<1.0e-10	<1.0e-10	2.5e-01	4.4e-02	<1.0e-10	1.9e-01
395	<1.0e-10	<1.0e-10	<1.0e-10	<1.0e-10	<1.0e-10	<1.0e-10	6.1e-10	<1.0e-10
396	<1.0e-10	<1.0e-10	<1.0e-10	<1.0e-10	2.9e-03	<1.0e-10	<1.0e-10	<1.0e-10
397	<1.0e-10	<1.0e-10	<1.0e-10	<1.0e-10	5.1e-05	<1.0e-10	<1.0e-10	<1.0e-10
398	<1.0e-10	<1.0e-10	<1.0e-10	<1.0e-10	1.7e-09	<1.0e-10	<1.0e-10	<1.0e-10
399	5.1e-06	9.4e-07	1.4e-02	1.7e-06	1.1e-02	3.8e-06	3.7e-02	2.6e-07
400	1.9e-09	1.4e-08	1.6e-03	2.6e-09	1.8e-01	4.2e-10	9.9e-03	2.5e-08
401	1.4e-07	7.0e-04	2.7e-05	9.3e-08	7.3e-01	7.8e-05	5.3e-05	4.3e-04
402	9.2e-06	2.5e-03	6.1e-04	2.3e-05	1.2e-01	3.5e-02	3.3e-04	7.8e-03
403	<1.0e-10	<1.0e-10	6.5e-07	<1.0e-10	4.1e-08	<1.0e-10	5.4e-05	<1.0e-10
404	1.5e-10	<1.0e-10	3.3e-02	<1.0e-10	<1.0e-10	7.3e-02	7.9e-02	<1.0e-10
405	<1.0e-10	<1.0e-10	5.7e-04	<1.0e-10	5.5e-04	<1.0e-10	1.2e-02	<1.0e-10

Table 4—Continued

Source No	<i>pns</i> [1] [0.5–8.0keV]	<i>pns</i> [2] [0.5–2.0keV]	<i>pns</i> [3] [2.0–8.0keV]	<i>pns</i> [4] [0.35–8.0keV]	<i>pns</i> [5] [0.35–1.1keV]	<i>pns</i> [6] [1.1–2.6keV]	<i>pns</i> [7] [2.6–8.0keV]	<i>pns</i> [8] [0.35–2.0keV]
406	2.0e-03	3.5e-01	1.2e-03	1.8e-03	2.6e-01	4.6e-01	8.6e-04	3.1e-01
407	2.9e-08	4.2e-03	1.3e-06	2.3e-08	7.4e-01	1.6e-05	1.9e-05	3.2e-03
408	<1.0e-10	<1.0e-10	<1.0e-10	<1.0e-10	<1.0e-10	<1.0e-10	<1.0e-10	<1.0e-10
409	<1.0e-10	<1.0e-10	9.9e-04	<1.0e-10	<1.0e-10	<1.0e-10	2.0e-02	<1.0e-10
410	<1.0e-10	1.1e-01	<1.0e-10	<1.0e-10	1.2e-01	2.6e-01	<1.0e-10	1.4e-01
411	<1.0e-10	<1.0e-10	8.4e-09	<1.0e-10	2.8e-02	<1.0e-10	1.3e-06	<1.0e-10
412	<1.0e-10	6.6e-02	<1.0e-10	<1.0e-10	6.5e-01	5.6e-07	1.5e-09	4.8e-02
413	5.8e-07	<1.0e-10	6.4e-01	1.1e-07	<1.0e-10	8.5e-02	7.5e-01	<1.0e-10
414	<1.0e-10	<1.0e-10	<1.0e-10	<1.0e-10	1.2e-01	<1.0e-10	<1.0e-10	<1.0e-10
415	<1.0e-10	<1.0e-10	<1.0e-10	<1.0e-10	<1.0e-10	<1.0e-10	<1.0e-10	<1.0e-10
416	<1.0e-10	<1.0e-10	<1.0e-10	<1.0e-10	8.5e-02	<1.0e-10	<1.0e-10	<1.0e-10
417	<1.0e-10	<1.0e-10	1.7e-01	<1.0e-10	<1.0e-10	<1.0e-10	3.2e-01	<1.0e-10
418	5.5e-07	2.2e-06	5.2e-03	1.2e-06	8.7e-02	5.5e-05	6.1e-03	8.8e-06
419	<1.0e-10	<1.0e-10	<1.0e-10	<1.0e-10	<1.0e-10	<1.0e-10	<1.0e-10	<1.0e-10
420	<1.0e-10	<1.0e-10	<1.0e-10	<1.0e-10	7.8e-02	<1.0e-10	1.3e-10	<1.0e-10
421	<1.0e-10	<1.0e-10	<1.0e-10	<1.0e-10	<1.0e-10	<1.0e-10	<1.0e-10	<1.0e-10
422	4.0e-08	1.9e-07	5.7e-03	5.3e-08	3.6e-03	7.6e-06	3.4e-02	3.8e-07
423	<1.0e-10	<1.0e-10	<1.0e-10	<1.0e-10	<1.0e-10	<1.0e-10	<1.0e-10	<1.0e-10
424	<1.0e-10	<1.0e-10	<1.0e-10	<1.0e-10	<1.0e-10	<1.0e-10	<1.0e-10	<1.0e-10
425	6.7e-03	1.3e-02	7.3e-02	1.0e-02	5.3e-01	1.3e-02	7.7e-02	2.6e-02
426	5.3e-09	1.9e-07	5.2e-04	1.5e-08	1.6e-01	3.5e-05	7.4e-05	1.0e-06
427	<1.0e-10	<1.0e-10	6.7e-04	<1.0e-10	<1.0e-10	<1.0e-10	9.0e-02	<1.0e-10
428	<1.0e-10	2.9e-04	<1.0e-10	<1.0e-10	8.4e-01	<1.0e-10	<1.0e-10	4.4e-04
429	<1.0e-10	<1.0e-10	<1.0e-10	<1.0e-10	<1.0e-10	<1.0e-10	1.2e-08	<1.0e-10
430	2.6e-07	<1.0e-10	1.1e-01	2.1e-07	5.4e-03	1.2e-08	1.3e-01	<1.0e-10
431	<1.0e-10	2.3e-02	<1.0e-10	<1.0e-10	8.0e-01	4.0e-09	2.0e-07	3.1e-02
432	<1.0e-10	3.3e-05	<1.0e-10	<1.0e-10	8.3e-01	<1.0e-10	1.6e-07	5.2e-05

Table 4—Continued

Source No	<i>pns</i> [1] [0.5–8.0keV]	<i>pns</i> [2] [0.5–2.0keV]	<i>pns</i> [3] [2.0–8.0keV]	<i>pns</i> [4] [0.35–8.0keV]	<i>pns</i> [5] [0.35–1.1keV]	<i>pns</i> [6] [1.1–2.6keV]	<i>pns</i> [7] [2.6–8.0keV]	<i>pns</i> [8] [0.35–2.0keV]
433	<1.0e-10	<1.0e-10	5.1e-02	<1.0e-10	3.9e-02	<1.0e-10	5.3e-02	<1.0e-10
434	<1.0e-10	<1.0e-10	1.1e-06	<1.0e-10	1.7e-03	<1.0e-10	2.8e-03	<1.0e-10
435	<1.0e-10	<1.0e-10	1.9e-06	<1.0e-10	3.0e-04	<1.0e-10	7.6e-05	<1.0e-10
436	<1.0e-10	1.5e-04	<1.0e-10	<1.0e-10	3.5e-02	3.0e-09	1.7e-08	2.3e-05
437	4.7e-06	4.6e-07	7.0e-02	3.5e-06	2.3e-05	4.2e-03	1.0e-01	3.6e-07
438	<1.0e-10	<1.0e-10	9.0e-02	<1.0e-10	<1.0e-10	1.3e-03	3.9e-02	<1.0e-10
439	<1.0e-10	<1.0e-10	1.2e-09	<1.0e-10	1.5e-05	<1.0e-10	6.1e-07	<1.0e-10
440	<1.0e-10	<1.0e-10	<1.0e-10	<1.0e-10	<1.0e-10	<1.0e-10	7.6e-07	<1.0e-10
441	2.9e-08	8.1e-08	3.0e-03	5.3e-08	9.0e-02	3.5e-06	1.7e-03	2.3e-07
442	<1.0e-10	3.7e-07	9.9e-10	<1.0e-10	5.8e-01	4.8e-10	4.4e-09	2.7e-07
443	3.9e-03	1.8e-05	4.1e-01	4.3e-03	6.5e-07	3.8e-01	4.5e-01	3.6e-05
444	<1.0e-10	<1.0e-10	<1.0e-10	<1.0e-10	9.5e-03	<1.0e-10	<1.0e-10	<1.0e-10
445	2.3e-04	5.6e-08	3.5e-01	5.4e-04	4.1e-03	2.2e-05	5.8e-01	7.3e-07
446	1.3e-10	4.9e-10	6.0e-04	3.1e-10	2.8e-01	<1.0e-10	3.3e-02	2.4e-09
447	<1.0e-10	<1.0e-10	<1.0e-10	<1.0e-10	1.3e-03	<1.0e-10	<1.0e-10	<1.0e-10
448	<1.0e-10	<1.0e-10	3.8e-01	<1.0e-10	<1.0e-10	3.1e-09	8.5e-01	<1.0e-10
449	3.0e-10	4.1e-09	3.3e-04	2.0e-10	1.5e-03	1.7e-05	1.1e-04	4.1e-09
450	<1.0e-10	<1.0e-10	<1.0e-10	<1.0e-10	<1.0e-10	<1.0e-10	<1.0e-10	<1.0e-10
451	1.3e-08	4.5e-08	1.7e-03	1.4e-08	1.0e-01	3.2e-07	1.4e-03	7.0e-08
452	<1.0e-10	<1.0e-10	<1.0e-10	<1.0e-10	7.7e-03	<1.0e-10	<1.0e-10	<1.0e-10
453	<1.0e-10	3.9e-03	<1.0e-10	<1.0e-10	3.3e-01	2.0e-05	<1.0e-10	9.3e-04
454	3.9e-08	4.1e-03	1.8e-06	5.9e-08	1.8e-01	5.0e-04	1.6e-05	5.9e-03
455	<1.0e-10	2.0e-03	<1.0e-10	<1.0e-10	1.3e-01	6.8e-05	7.5e-10	2.6e-03
456	<1.0e-10	<1.0e-10	1.1e-01	<1.0e-10	<1.0e-10	2.0e-02	5.2e-02	<1.0e-10
457	<1.0e-10	<1.0e-10	9.3e-07	<1.0e-10	2.4e-03	1.0e-10	4.5e-06	<1.0e-10
458	4.2e-08	4.2e-06	4.1e-04	1.8e-07	4.7e-03	1.6e-05	1.0e-02	3.9e-05
459	9.5e-07	2.2e-09	6.9e-02	1.1e-06	1.1e-01	3.6e-09	1.6e-01	4.5e-09

Table 4—Continued

Source No	$pns[1]$ [0.5–8.0keV]	$pns[2]$ [0.5–2.0keV]	$pns[3]$ [2.0–8.0keV]	$pns[4]$ [0.35–8.0keV]	$pns[5]$ [0.35–1.1keV]	$pns[6]$ [1.1–2.6keV]	$pns[7]$ [2.6–8.0keV]	$pns[8]$ [0.35–2.0keV]
460	8.6e-09	5.3e-06	1.1e-04	4.1e-09	3.8e-01	<1.0e-10	1.6e-02	2.5e-06
461	<1.0e-10	1.0e-09	5.7e-09	<1.0e-10	3.0e-03	9.5e-09	2.6e-09	<1.0e-10
462	<1.0e-10	<1.0e-10	1.8e-07	<1.0e-10	<1.0e-10	<1.0e-10	2.0e-02	<1.0e-10
463	1.6e-02	2.6e-01	2.1e-02	2.0e-02	8.5e-01	1.5e-01	1.3e-02	3.2e-01
464	<1.0e-10	<1.0e-10	4.3e-03	<1.0e-10	5.0e-03	<1.0e-10	1.1e-01	<1.0e-10
465	<1.0e-10	<1.0e-10	<1.0e-10	<1.0e-10	4.5e-07	<1.0e-10	<1.0e-10	<1.0e-10
466	6.0e-07	5.4e-02	1.5e-06	5.5e-07	3.5e-01	8.5e-03	5.4e-06	4.7e-02
467	<1.0e-10	<1.0e-10	1.4e-04	<1.0e-10	2.9e-08	<1.0e-10	6.9e-03	<1.0e-10
468	<1.0e-10	<1.0e-10	<1.0e-10	<1.0e-10	1.1e-05	<1.0e-10	<1.0e-10	<1.0e-10
469	<1.0e-10	2.1e-06	<1.0e-10	<1.0e-10	3.9e-02	1.4e-07	<1.0e-10	1.1e-05
470	<1.0e-10	<1.0e-10	<1.0e-10	<1.0e-10	7.2e-02	<1.0e-10	<1.0e-10	<1.0e-10
471	<1.0e-10	<1.0e-10	<1.0e-10	<1.0e-10	<1.0e-10	<1.0e-10	<1.0e-10	<1.0e-10
472	1.3e-06	1.5e-01	9.7e-07	1.8e-06	9.4e-01	2.1e-03	4.1e-06	1.7e-01
473	1.7e-09	<1.0e-10	4.2e-02	4.9e-09	5.5e-03	5.8e-09	3.3e-02	<1.0e-10
474	1.0e-06	3.0e-08	2.4e-02	2.9e-06	5.0e-02	2.7e-06	3.6e-02	3.7e-07
475	<1.0e-10	5.6e-05	<1.0e-10	<1.0e-10	3.2e-01	1.0e-10	5.0e-10	1.5e-05
476	<1.0e-10	<1.0e-10	2.9e-02	<1.0e-10	7.0e-04	<1.0e-10	1.1e-01	<1.0e-10
477	5.0e-02	1.9e-01	9.4e-02	6.3e-02	4.5e-01	3.8e-01	5.8e-02	2.5e-01
478	8.9e-09	<1.0e-10	2.0e-01	4.9e-10	2.2e-05	1.0e-09	2.0e-01	<1.0e-10
479	2.7e-04	9.5e-06	9.6e-02	5.1e-04	1.8e-08	6.9e-01	1.1e-01	5.0e-05
480	3.5e-09	<1.0e-10	2.3e-01	1.7e-09	<1.0e-10	1.5e-03	3.2e-01	<1.0e-10
481	<1.0e-10	<1.0e-10	<1.0e-10	<1.0e-10	<1.0e-10	<1.0e-10	4.7e-09	<1.0e-10
482	<1.0e-10	<1.0e-10	<1.0e-10	<1.0e-10	<1.0e-10	<1.0e-10	<1.0e-10	<1.0e-10
483	<1.0e-10	<1.0e-10	<1.0e-10	<1.0e-10	<1.0e-10	<1.0e-10	<1.0e-10	<1.0e-10
484	<1.0e-10	1.8e-07	2.1e-09	<1.0e-10	6.3e-01	5.9e-10	3.8e-08	2.3e-06
485	<1.0e-10	<1.0e-10	<1.0e-10	<1.0e-10	1.8e-05	<1.0e-10	<1.0e-10	<1.0e-10
486	2.6e-05	1.0e-09	3.6e-01	6.4e-05	1.5e-01	2.9e-10	7.3e-01	1.7e-08

Table 4—Continued

Source No	<i>pns</i> [1] [0.5–8.0keV]	<i>pns</i> [2] [0.5–2.0keV]	<i>pns</i> [3] [2.0–8.0keV]	<i>pns</i> [4] [0.35–8.0keV]	<i>pns</i> [5] [0.35–1.1keV]	<i>pns</i> [6] [1.1–2.6keV]	<i>pns</i> [7] [2.6–8.0keV]	<i>pns</i> [8] [0.35–2.0keV]
487	<1.0e-10	<1.0e-10	<1.0e-10	<1.0e-10	2.0e-07	<1.0e-10	6.7e-10	<1.0e-10
488	<1.0e-10	<1.0e-10	<1.0e-10	<1.0e-10	<1.0e-10	<1.0e-10	<1.0e-10	<1.0e-10
489	<1.0e-10	1.3e-04	<1.0e-10	<1.0e-10	1.0e-01	3.4e-09	<1.0e-10	1.5e-04
490	2.4e-09	7.2e-10	1.3e-02	4.2e-09	1.0e-03	1.2e-08	1.5e-01	2.3e-09
491	<1.0e-10	<1.0e-10	<1.0e-10	<1.0e-10	<1.0e-10	<1.0e-10	<1.0e-10	<1.0e-10
492	<1.0e-10	<1.0e-10	<1.0e-10	<1.0e-10	<1.0e-10	<1.0e-10	<1.0e-10	<1.0e-10
493	<1.0e-10	<1.0e-10	<1.0e-10	<1.0e-10	<1.0e-10	<1.0e-10	6.8e-09	<1.0e-10
494	<1.0e-10	<1.0e-10	1.0e-03	<1.0e-10	1.9e-01	<1.0e-10	1.6e-03	<1.0e-10
495	4.5e-10	<1.0e-10	6.2e-03	2.8e-10	3.8e-02	<1.0e-10	8.8e-02	<1.0e-10
496	1.0e-03	4.2e-07	5.3e-01	1.8e-03	1.8e-05	1.6e-02	6.8e-01	2.6e-06
497	<1.0e-10	<1.0e-10	<1.0e-10	<1.0e-10	<1.0e-10	<1.0e-10	<1.0e-10	<1.0e-10
498	<1.0e-10	<1.0e-10	<1.0e-10	<1.0e-10	<1.0e-10	<1.0e-10	<1.0e-10	<1.0e-10
499	<1.0e-10	<1.0e-10	<1.0e-10	<1.0e-10	<1.0e-10	<1.0e-10	<1.0e-10	<1.0e-10
500	4.0e-07	4.6e-04	1.4e-04	2.6e-07	3.8e-01	1.9e-05	4.0e-04	2.8e-04
501	1.3e-04	2.8e-06	5.1e-01	1.5e-04	9.5e-04	5.6e-03	4.3e-01	4.2e-06
502	<1.0e-10	<1.0e-10	<1.0e-10	<1.0e-10	<1.0e-10	<1.0e-10	<1.0e-10	<1.0e-10
503	5.9e-03	2.0e-03	2.1e-01	2.6e-04	6.8e-06	1.4e-01	3.6e-01	2.1e-05
504	<1.0e-10	<1.0e-10	5.1e-10	<1.0e-10	3.0e-07	<1.0e-10	3.8e-07	<1.0e-10
505	<1.0e-10	<1.0e-10	<1.0e-10	<1.0e-10	<1.0e-10	<1.0e-10	<1.0e-10	<1.0e-10
506	3.2e-06	4.8e-01	1.8e-07	8.3e-06	5.2e-01	3.0e-01	4.9e-07	6.1e-01
507	<1.0e-10	<1.0e-10	<1.0e-10	<1.0e-10	<1.0e-10	<1.0e-10	<1.0e-10	<1.0e-10
508	2.1e-07	1.1e-03	3.4e-05	4.7e-07	1.6e-01	5.5e-03	2.7e-05	2.8e-03
509	1.3e-03	1.8e-03	5.8e-02	3.5e-03	8.3e-01	6.5e-07	4.5e-01	1.0e-02
510	<1.0e-10	<1.0e-10	1.4e-01	<1.0e-10	<1.0e-10	1.5e-05	1.5e-01	<1.0e-10
511	7.7e-06	2.1e-09	2.7e-01	5.9e-06	<1.0e-10	7.3e-02	3.4e-01	2.8e-09
512	2.5e-03	8.2e-03	4.7e-02	2.1e-03	1.7e-02	9.0e-02	5.6e-02	7.0e-03
513	3.0e-07	1.2e-03	4.4e-05	3.3e-07	7.0e-01	1.2e-04	4.8e-05	1.4e-03

Table 4—Continued

Source No	<i>pns</i> [1] [0.5–8.0keV]	<i>pns</i> [2] [0.5–2.0keV]	<i>pns</i> [3] [2.0–8.0keV]	<i>pns</i> [4] [0.35–8.0keV]	<i>pns</i> [5] [0.35–1.1keV]	<i>pns</i> [6] [1.1–2.6keV]	<i>pns</i> [7] [2.6–8.0keV]	<i>pns</i> [8] [0.35–2.0keV]
514	9.8e-07	3.2e-06	5.1e-03	1.4e-06	1.2e-01	1.5e-06	3.0e-02	6.8e-06
515	<1.0e-10	<1.0e-10	6.3e-09	<1.0e-10	<1.0e-10	<1.0e-10	6.5e-09	<1.0e-10
516	<1.0e-10	<1.0e-10	<1.0e-10	<1.0e-10	<1.0e-10	<1.0e-10	2.6e-06	<1.0e-10
517	<1.0e-10	<1.0e-10	<1.0e-10	<1.0e-10	<1.0e-10	<1.0e-10	<1.0e-10	<1.0e-10
518	<1.0e-10	<1.0e-10	<1.0e-10	<1.0e-10	4.1e-01	<1.0e-10	<1.0e-10	<1.0e-10
519	<1.0e-10	9.1e-07	<1.0e-10	<1.0e-10	6.9e-01	1.1e-09	<1.0e-10	9.3e-07
520	4.3e-04	3.5e-01	1.4e-04	2.6e-04	3.3e-01	4.1e-02	1.2e-03	2.4e-01
521	<1.0e-10	<1.0e-10	1.4e-05	<1.0e-10	5.9e-04	1.1e-08	1.3e-05	<1.0e-10
522	<1.0e-10	<1.0e-10	6.1e-03	1.5e-10	7.0e-03	1.7e-09	4.7e-03	<1.0e-10
523	<1.0e-10	<1.0e-10	4.8e-09	<1.0e-10	4.6e-07	<1.0e-10	7.2e-05	<1.0e-10
524	3.9e-03	7.6e-04	2.5e-01	4.1e-03	1.0e+00	2.0e-04	2.8e-01	8.6e-04
525	3.4e-07	<1.0e-10	1.1e-01	1.4e-07	4.6e-04	1.9e-06	7.0e-02	<1.0e-10
526	4.6e-05	4.0e-06	5.5e-02	5.2e-05	2.6e-03	3.6e-04	1.3e-01	6.8e-06
527	3.1e-05	2.0e-02	3.5e-04	3.8e-05	7.2e-02	5.5e-02	6.0e-04	2.4e-02
528	<1.0e-10	<1.0e-10	<1.0e-10	<1.0e-10	<1.0e-10	<1.0e-10	<1.0e-10	<1.0e-10
529	4.1e-06	2.6e-04	9.0e-04	4.3e-07	3.2e-03	1.7e-04	4.7e-03	1.1e-05
530	<1.0e-10	<1.0e-10	<1.0e-10	<1.0e-10	<1.0e-10	<1.0e-10	<1.0e-10	<1.0e-10
531	<1.0e-10	1.7e-08	1.4e-09	<1.0e-10	5.7e-02	7.0e-07	3.4e-10	3.4e-08
532	<1.0e-10	<1.0e-10	<1.0e-10	<1.0e-10	4.1e-08	<1.0e-10	1.5e-09	<1.0e-10
533	<1.0e-10	<1.0e-10	<1.0e-10	<1.0e-10	<1.0e-10	<1.0e-10	<1.0e-10	<1.0e-10
534	<1.0e-10	<1.0e-10	<1.0e-10	<1.0e-10	3.5e-01	<1.0e-10	<1.0e-10	<1.0e-10
535	<1.0e-10	<1.0e-10	7.9e-03	<1.0e-10	<1.0e-10	<1.0e-10	1.0e-01	<1.0e-10
536	<1.0e-10	<1.0e-10	1.8e-04	<1.0e-10	2.3e-06	<1.0e-10	4.1e-04	<1.0e-10
537	<1.0e-10	4.4e-02	<1.0e-10	<1.0e-10	7.1e-01	3.8e-03	<1.0e-10	1.1e-01
538	<1.0e-10	<1.0e-10	<1.0e-10	<1.0e-10	2.5e-01	<1.0e-10	<1.0e-10	<1.0e-10
539	<1.0e-10	<1.0e-10	2.8e-01	<1.0e-10	<1.0e-10	<1.0e-10	6.3e-01	<1.0e-10
540	<1.0e-10	8.4e-04	<1.0e-10	<1.0e-10	4.4e-01	1.2e-07	<1.0e-10	1.9e-03

Table 4—Continued

Source No	<i>pns</i> [1] [0.5–8.0keV]	<i>pns</i> [2] [0.5–2.0keV]	<i>pns</i> [3] [2.0–8.0keV]	<i>pns</i> [4] [0.35–8.0keV]	<i>pns</i> [5] [0.35–1.1keV]	<i>pns</i> [6] [1.1–2.6keV]	<i>pns</i> [7] [2.6–8.0keV]	<i>pns</i> [8] [0.35–2.0keV]
541	3.9e-08	5.8e-08	1.1e-01	1.4e-08	8.9e-04	3.0e-07	3.8e-01	1.9e-08
542	7.3e-06	4.4e-09	9.9e-01	5.6e-06	2.4e-08	7.6e-02	9.5e-01	3.3e-09
543	<1.0e-10	<1.0e-10	<1.0e-10	<1.0e-10	1.1e-03	<1.0e-10	<1.0e-10	<1.0e-10
544	<1.0e-10	<1.0e-10	<1.0e-10	<1.0e-10	6.5e-04	<1.0e-10	<1.0e-10	<1.0e-10
545	2.9e-09	1.1e-05	4.7e-05	5.2e-09	2.8e-04	1.7e-02	3.7e-05	2.0e-05
546	<1.0e-10	<1.0e-10	<1.0e-10	<1.0e-10	2.2e-02	<1.0e-10	<1.0e-10	<1.0e-10
547	3.0e-04	2.8e-01	1.8e-04	3.5e-04	4.0e-01	1.1e-01	5.4e-04	2.9e-01
548	<1.0e-10	<1.0e-10	<1.0e-10	<1.0e-10	9.9e-08	<1.0e-10	<1.0e-10	<1.0e-10
549	1.5e-05	1.1e-07	1.0e-01	7.4e-06	<1.0e-10	8.2e-01	6.8e-02	4.8e-08
550	8.4e-07	7.8e-03	2.5e-05	1.5e-06	5.0e-01	7.0e-04	1.7e-04	1.5e-02
551	9.9e-02	8.8e-03	6.3e-01	7.6e-02	3.4e-03	2.9e-01	6.6e-01	5.4e-03
552	<1.0e-10	<1.0e-10	<1.0e-10	<1.0e-10	<1.0e-10	<1.0e-10	<1.0e-10	<1.0e-10
553	<1.0e-10	1.4e-10	<1.0e-10	<1.0e-10	9.4e-03	<1.0e-10	<1.0e-10	1.2e-10
554	7.0e-09	4.9e-05	1.4e-05	1.3e-08	8.1e-01	6.4e-09	6.2e-04	1.2e-04
555	<1.0e-10	2.8e-10	7.1e-10	<1.0e-10	9.8e-04	4.2e-09	4.5e-09	<1.0e-10
556	2.0e-03	2.7e-02	1.9e-02	3.2e-03	3.9e-02	5.1e-01	1.0e-02	4.9e-02
557	1.4e-09	8.1e-02	3.6e-09	1.7e-09	3.7e-01	6.8e-05	3.9e-06	9.4e-02
558	1.4e-07	8.4e-02	1.5e-07	1.5e-07	7.6e-01	9.5e-04	1.5e-06	7.4e-02
559	<1.0e-10	1.8e-09	3.4e-08	<1.0e-10	1.5e-01	<1.0e-10	1.6e-06	1.8e-10
560	<1.0e-10	<1.0e-10	<1.0e-10	<1.0e-10	<1.0e-10	<1.0e-10	<1.0e-10	<1.0e-10
561	<1.0e-10	<1.0e-10	<1.0e-10	<1.0e-10	<1.0e-10	<1.0e-10	<1.0e-10	<1.0e-10
562	<1.0e-10	7.6e-07	3.6e-10	<1.0e-10	2.1e-01	<1.0e-10	3.2e-07	3.5e-06
563	6.4e-08	1.0e-02	1.4e-06	5.8e-08	7.5e-01	1.0e-04	6.3e-06	9.1e-03
564	<1.0e-10	<1.0e-10	1.9e-10	<1.0e-10	<1.0e-10	<1.0e-10	1.5e-07	<1.0e-10
565	<1.0e-10	<1.0e-10	<1.0e-10	<1.0e-10	<1.0e-10	<1.0e-10	<1.0e-10	<1.0e-10
566	5.8e-08	5.2e-05	1.1e-04	1.5e-07	7.1e-02	1.6e-05	1.7e-03	2.2e-04
567	1.2e-03	3.5e-04	1.0e-01	5.6e-04	4.3e-04	1.2e-01	6.5e-02	1.2e-04

Table 4—Continued

Source No	<i>pns</i> [1] [0.5–8.0keV]	<i>pns</i> [2] [0.5–2.0keV]	<i>pns</i> [3] [2.0–8.0keV]	<i>pns</i> [4] [0.35–8.0keV]	<i>pns</i> [5] [0.35–1.1keV]	<i>pns</i> [6] [1.1–2.6keV]	<i>pns</i> [7] [2.6–8.0keV]	<i>pns</i> [8] [0.35–2.0keV]
568	3.9e-02	7.7e-04	5.6e-01	4.9e-02	1.0e-02	4.1e-02	7.0e-01	2.0e-03
569	2.4e-05	4.0e-02	1.5e-04	3.5e-05	7.9e-02	1.2e-02	2.3e-03	5.6e-02
570	1.8e-05	<1.0e-10	4.2e-01	1.4e-05	1.6e-10	9.7e-02	2.8e-01	<1.0e-10
571	<1.0e-10	<1.0e-10	<1.0e-10	<1.0e-10	<1.0e-10	<1.0e-10	1.3e-10	<1.0e-10
572	<1.0e-10	<1.0e-10	4.7e-01	<1.0e-10	<1.0e-10	7.1e-04	2.5e-01	<1.0e-10
573	<1.0e-10	<1.0e-10	<1.0e-10	<1.0e-10	1.6e-02	<1.0e-10	<1.0e-10	<1.0e-10
574	<1.0e-10	2.0e-10	<1.0e-10	<1.0e-10	8.2e-01	<1.0e-10	5.0e-09	1.5e-09
575	<1.0e-10	<1.0e-10	<1.0e-10	<1.0e-10	2.9e-01	<1.0e-10	<1.0e-10	<1.0e-10
576	<1.0e-10	<1.0e-10	<1.0e-10	<1.0e-10	<1.0e-10	<1.0e-10	<1.0e-10	<1.0e-10
577	<1.0e-10	<1.0e-10	<1.0e-10	<1.0e-10	<1.0e-10	<1.0e-10	<1.0e-10	<1.0e-10
578	3.8e-04	1.4e-02	6.9e-03	4.7e-04	5.1e-01	1.2e-03	2.7e-02	1.8e-02
579	<1.0e-10	<1.0e-10	<1.0e-10	<1.0e-10	<1.0e-10	<1.0e-10	<1.0e-10	<1.0e-10
580	1.4e-06	2.9e-06	4.2e-02	2.0e-06	9.6e-03	3.5e-04	3.4e-02	5.2e-06
581	<1.0e-10	1.3e-06	4.3e-07	<1.0e-10	2.8e-01	<1.0e-10	3.5e-04	5.1e-06
582	3.7e-10	2.2e-09	1.1e-03	3.7e-10	1.3e-03	8.1e-08	7.4e-03	2.1e-09
583	<1.0e-10	5.1e-03	<1.0e-10	<1.0e-10	2.8e-02	4.2e-04	<1.0e-10	1.6e-03
584	<1.0e-10	9.5e-04	1.4e-09	<1.0e-10	1.1e-01	9.3e-03	5.6e-10	1.4e-03
585	<1.0e-10	<1.0e-10	8.9e-07	<1.0e-10	<1.0e-10	<1.0e-10	2.1e-02	<1.0e-10
586	<1.0e-10	<1.0e-10	<1.0e-10	<1.0e-10	1.3e-08	<1.0e-10	1.5e-10	<1.0e-10
587	<1.0e-10	<1.0e-10	<1.0e-10	<1.0e-10	<1.0e-10	<1.0e-10	<1.0e-10	<1.0e-10
588	<1.0e-10	<1.0e-10	<1.0e-10	<1.0e-10	4.3e-03	<1.0e-10	1.4e-10	<1.0e-10
589	<1.0e-10	<1.0e-10	<1.0e-10	<1.0e-10	<1.0e-10	<1.0e-10	<1.0e-10	<1.0e-10
590	7.7e-03	1.4e-03	2.1e-01	6.2e-03	2.1e-01	4.7e-03	2.0e-01	1.1e-03
591	1.1e-06	1.3e-07	1.6e-02	3.0e-06	3.9e-01	3.2e-10	2.0e-01	1.3e-06
592	1.6e-09	1.7e-08	5.9e-04	7.2e-09	1.3e-01	1.1e-05	1.2e-04	2.3e-07
593	<1.0e-10	<1.0e-10	<1.0e-10	<1.0e-10	<1.0e-10	<1.0e-10	2.4e-06	<1.0e-10
594	<1.0e-10	<1.0e-10	<1.0e-10	<1.0e-10	<1.0e-10	<1.0e-10	<1.0e-10	<1.0e-10

Table 4—Continued

Source No	<i>pns</i> [1] [0.5–8.0keV]	<i>pns</i> [2] [0.5–2.0keV]	<i>pns</i> [3] [2.0–8.0keV]	<i>pns</i> [4] [0.35–8.0keV]	<i>pns</i> [5] [0.35–1.1keV]	<i>pns</i> [6] [1.1–2.6keV]	<i>pns</i> [7] [2.6–8.0keV]	<i>pns</i> [8] [0.35–2.0keV]
595	<1.0e-10	<1.0e-10	<1.0e-10	<1.0e-10	<1.0e-10	<1.0e-10	<1.0e-10	<1.0e-10
596	<1.0e-10	<1.0e-10	<1.0e-10	<1.0e-10	4.3e-08	<1.0e-10	<1.0e-10	<1.0e-10
597	<1.0e-10	8.7e-05	<1.0e-10	<1.0e-10	2.4e-01	4.1e-05	<1.0e-10	8.4e-05
598	<1.0e-10	<1.0e-10	1.1e-07	<1.0e-10	4.6e-04	<1.0e-10	2.0e-04	<1.0e-10
599	9.8e-08	2.3e-03	8.1e-06	1.8e-07	6.7e-01	9.3e-05	7.0e-05	4.9e-03
600	<1.0e-10	<1.0e-10	<1.0e-10	<1.0e-10	<1.0e-10	<1.0e-10	<1.0e-10	<1.0e-10
601	<1.0e-10	<1.0e-10	<1.0e-10	<1.0e-10	<1.0e-10	<1.0e-10	<1.0e-10	<1.0e-10
602	<1.0e-10	2.6e-10	7.0e-07	<1.0e-10	2.3e-02	<1.0e-10	2.2e-05	5.5e-10
603	5.6e-08	3.7e-06	1.1e-03	4.5e-08	3.4e-02	1.4e-05	1.8e-03	3.2e-06
604	1.2e-06	1.7e-03	1.6e-04	1.4e-06	1.0e+00	1.7e-04	6.7e-04	2.1e-03
605	4.9e-08	5.0e-05	1.3e-04	5.9e-08	3.7e-01	7.3e-05	7.2e-05	6.5e-05
606	<1.0e-10	<1.0e-10	<1.0e-10	<1.0e-10	1.0e+00	<1.0e-10	<1.0e-10	<1.0e-10
607	<1.0e-10	3.3e-02	<1.0e-10	<1.0e-10	1.0e+00	2.4e-08	3.3e-10	7.4e-02
608	<1.0e-10	<1.0e-10	<1.0e-10	<1.0e-10	<1.0e-10	<1.0e-10	<1.0e-10	<1.0e-10
609	4.6e-07	1.8e-08	5.2e-02	2.5e-07	5.1e-04	3.0e-06	1.6e-01	1.6e-08
610	1.3e-06	3.6e-06	1.0e-02	1.9e-06	3.3e-03	1.1e-04	3.2e-02	7.0e-06
611	2.0e-06	2.5e-01	2.5e-06	2.3e-06	1.0e+00	6.9e-03	5.3e-05	2.6e-01
612	<1.0e-10	<1.0e-10	<1.0e-10	<1.0e-10	<1.0e-10	<1.0e-10	<1.0e-10	<1.0e-10
613	<1.0e-10	<1.0e-10	<1.0e-10	<1.0e-10	<1.0e-10	<1.0e-10	<1.0e-10	<1.0e-10
614	<1.0e-10	<1.0e-10	1.0e-09	<1.0e-10	6.4e-02	<1.0e-10	1.9e-06	<1.0e-10
615	<1.0e-10	<1.0e-10	1.2e-02	<1.0e-10	7.7e-03	<1.0e-10	2.9e-01	<1.0e-10
616	8.8e-06	4.0e-02	5.5e-05	2.3e-05	9.7e-01	2.6e-04	7.3e-04	9.4e-02
617	<1.0e-10	6.8e-09	7.6e-06	<1.0e-10	2.1e-02	1.5e-09	4.4e-04	6.8e-08
618	<1.0e-10	<1.0e-10	<1.0e-10	<1.0e-10	<1.0e-10	<1.0e-10	<1.0e-10	<1.0e-10
619	<1.0e-10	<1.0e-10	1.4e-10	<1.0e-10	6.4e-08	<1.0e-10	7.2e-06	<1.0e-10
620	2.8e-05	6.6e-01	4.2e-06	5.3e-05	1.0e+00	1.0e-01	1.6e-05	7.5e-01
621	<1.0e-10	6.5e-10	<1.0e-10	<1.0e-10	1.0e+00	<1.0e-10	<1.0e-10	1.1e-09

Table 4—Continued

Source No	<i>pns</i> [1] [0.5–8.0keV]	<i>pns</i> [2] [0.5–2.0keV]	<i>pns</i> [3] [2.0–8.0keV]	<i>pns</i> [4] [0.35–8.0keV]	<i>pns</i> [5] [0.35–1.1keV]	<i>pns</i> [6] [1.1–2.6keV]	<i>pns</i> [7] [2.6–8.0keV]	<i>pns</i> [8] [0.35–2.0keV]
622	<1.0e-10	3.6e-10	<1.0e-10	<1.0e-10	2.8e-02	<1.0e-10	<1.0e-10	1.3e-10
623	<1.0e-10	<1.0e-10	4.5e-06	<1.0e-10	2.4e-05	<1.0e-10	1.2e-02	<1.0e-10
624	5.3e-07	3.6e-02	2.8e-06	1.0e-06	1.0e+00	3.1e-03	1.2e-06	5.6e-02
625	2.8e-09	6.9e-10	1.1e-02	1.7e-09	3.1e-03	7.2e-09	3.5e-02	4.7e-10
626	<1.0e-10	<1.0e-10	<1.0e-10	<1.0e-10	<1.0e-10	<1.0e-10	<1.0e-10	<1.0e-10
627	2.9e-09	<1.0e-10	2.2e-02	4.5e-09	1.3e-05	1.4e-07	1.6e-01	1.1e-10
628	<1.0e-10	2.9e-01	<1.0e-10	<1.0e-10	8.7e-01	4.2e-02	<1.0e-10	4.2e-01
629	7.4e-08	8.2e-02	1.1e-07	1.5e-07	1.0e+00	3.3e-03	3.0e-07	1.2e-01
630	<1.0e-10	<1.0e-10	<1.0e-10	<1.0e-10	1.7e-07	<1.0e-10	<1.0e-10	<1.0e-10
631	9.1e-05	1.0e-07	2.1e-01	1.2e-04	8.2e-02	1.5e-07	4.3e-01	2.9e-07
632	<1.0e-10	<1.0e-10	5.1e-06	<1.0e-10	3.6e-03	<1.0e-10	9.3e-05	<1.0e-10
633	<1.0e-10	<1.0e-10	<1.0e-10	<1.0e-10	8.1e-10	<1.0e-10	<1.0e-10	<1.0e-10
634	5.9e-05	1.1e-03	5.9e-03	1.4e-04	1.7e-01	2.2e-04	4.9e-02	4.1e-03
635	<1.0e-10	<1.0e-10	<1.0e-10	<1.0e-10	<1.0e-10	<1.0e-10	<1.0e-10	<1.0e-10
636	3.8e-03	1.1e-03	1.4e-01	4.1e-03	1.7e-01	1.6e-02	8.6e-02	1.6e-03
637	9.7e-09	2.2e-05	4.8e-05	1.7e-08	1.0e+00	1.7e-10	9.2e-03	5.1e-05
638	1.0e-10	2.6e-07	1.4e-05	1.8e-10	2.9e-01	<1.0e-10	2.6e-03	6.8e-07
639	<1.0e-10	<1.0e-10	<1.0e-10	<1.0e-10	5.6e-08	<1.0e-10	<1.0e-10	<1.0e-10
640	<1.0e-10	<1.0e-10	5.9e-03	<1.0e-10	<1.0e-10	<1.0e-10	1.4e-02	<1.0e-10
641	2.5e-05	3.3e-02	1.8e-04	1.8e-05	1.7e-01	7.9e-02	7.9e-05	2.3e-02
642	<1.0e-10	1.4e-01	<1.0e-10	<1.0e-10	6.2e-01	1.0e-04	2.0e-09	8.0e-02
643	1.8e-06	1.4e-03	2.0e-04	1.5e-06	1.3e-01	3.1e-03	2.1e-04	1.1e-03
644	9.3e-08	1.9e-07	2.3e-03	7.0e-08	1.8e-02	3.4e-08	5.6e-02	2.2e-07
645	<1.0e-10	1.9e-07	<1.0e-10	<1.0e-10	1.6e-02	1.0e-10	8.2e-07	3.8e-07
646	1.6e-05	6.1e-07	2.3e-01	9.9e-06	7.6e-05	2.7e-04	7.1e-01	4.9e-07
647	<1.0e-10	<1.0e-10	<1.0e-10	<1.0e-10	<1.0e-10	<1.0e-10	<1.0e-10	<1.0e-10
648	<1.0e-10	<1.0e-10	<1.0e-10	<1.0e-10	5.7e-03	<1.0e-10	<1.0e-10	<1.0e-10

Table 4—Continued

Source No	<i>pns</i> [1] [0.5–8.0keV]	<i>pns</i> [2] [0.5–2.0keV]	<i>pns</i> [3] [2.0–8.0keV]	<i>pns</i> [4] [0.35–8.0keV]	<i>pns</i> [5] [0.35–1.1keV]	<i>pns</i> [6] [1.1–2.6keV]	<i>pns</i> [7] [2.6–8.0keV]	<i>pns</i> [8] [0.35–2.0keV]
649	1.8e-08	9.5e-06	2.9e-04	3.1e-08	1.0e-02	5.7e-04	2.5e-04	2.0e-05
650	<1.0e-10	9.6e-08	<1.0e-10	<1.0e-10	8.7e-03	1.6e-07	1.5e-09	3.6e-07
651	2.8e-02	7.0e-03	2.8e-01	8.3e-03	2.2e-03	3.7e-02	4.3e-01	7.5e-04
652	3.4e-09	1.3e-09	2.8e-03	5.0e-09	7.7e-02	3.6e-09	1.6e-02	3.1e-09
653	<1.0e-10	<1.0e-10	8.9e-07	<1.0e-10	<1.0e-10	<1.0e-10	9.2e-06	<1.0e-10
654	<1.0e-10	<1.0e-10	6.5e-10	<1.0e-10	3.9e-02	<1.0e-10	2.2e-08	<1.0e-10
655	3.1e-06	4.7e-02	1.6e-05	8.2e-07	6.1e-03	3.7e-04	4.0e-03	1.2e-02
656	<1.0e-10	<1.0e-10	6.9e-04	<1.0e-10	8.9e-05	<1.0e-10	2.8e-03	<1.0e-10
657	<1.0e-10	<1.0e-10	2.1e-07	<1.0e-10	6.3e-02	<1.0e-10	1.1e-04	<1.0e-10
658	7.6e-04	1.5e-06	3.2e-01	8.8e-04	5.4e-01	3.6e-06	2.5e-01	3.7e-06
659	1.4e-06	1.5e-06	1.2e-02	2.6e-06	1.0e-01	7.0e-06	2.4e-02	8.8e-06
660	1.3e-06	1.7e-09	6.4e-02	2.7e-06	1.2e-01	7.9e-06	2.6e-02	2.3e-08
661	<1.0e-10	<1.0e-10	<1.0e-10	<1.0e-10	2.0e-01	<1.0e-10	<1.0e-10	<1.0e-10
662	5.7e-05	2.1e-07	2.5e-01	6.7e-05	4.0e-03	2.0e-05	4.1e-01	6.7e-07

[†]The *pns* value is the Poission probability of not being a source. *pns* values smaller than 1.0e-10 have been replaced by <1.0e-10. All these cases are highly significant detections.

Table 5. Total net counts in different energy bands[†].

Source No	<i>net_cnts</i> [1] [0.5–8.0keV]	<i>net_cnts</i> [2] [0.5–2.0keV]	<i>net_cnts</i> [3] [2.0–8.0keV]	<i>net_cnts</i> [4] [0.35–8.0keV]	<i>net_cnts</i> [5] [0.35–1.1keV]	<i>net_cnts</i> [6] [1.1–2.6keV]	<i>net_cnts</i> [7] [2.6–8.0keV]	<i>net_cnts</i> [8] [0.35–2.0keV]
1	47.6 ^{+9.9} _{-8.8}	27.6 ^{+7.1} _{-6.0}	20.0 ^{+7.6} _{-6.5}	47.5 ^{+9.9} _{-8.8}	3.9 ^{+4.1} _{-2.9}	29.0 ^{+7.1} _{-6.0}	14.6 ^{+6.9} _{-5.8}	27.4 ^{+7.1} _{-6.0}
2	28.1 ^{+8.3} _{-7.2}	15.5 ^{+5.8} _{-4.6}	12.6 ^{+6.6} _{-5.5}	28.1 ^{+8.3} _{-7.2}	3.9 ^{+3.7} _{-2.4}	14.3 ^{+5.8} _{-4.7}	9.8 ^{+6.0} _{-4.9}	15.5 ^{+5.8} _{-4.6}
3	101.1 ^{+12.0} _{-10.9}	57.1 ^{+8.9} _{-7.8}	44.0 ^{+8.6} _{-7.5}	102.1 ^{+12.0} _{-10.9}	17.7 ^{+5.5} _{-4.3}	53.5 ^{+8.7} _{-7.6}	30.8 ^{+7.7} _{-6.5}	58.1 ^{+9.0} _{-7.9}
4	32.8 ^{+8.1} _{-7.0}	25.1 ^{+6.4} _{-5.3}	7.6 ^{+5.6} _{-4.5}	32.8 ^{+8.1} _{-7.0}	7.9 ^{+4.2} _{-3.0}	22.1 ^{+6.2} _{-5.0}	2.8 ^{+4.9} _{-3.7}	25.1 ^{+6.4} _{-5.3}
5	48.9 ^{+9.0} _{-7.9}	26.8 ^{+6.5} _{-5.4}	22.1 ^{+6.8} _{-5.7}	49.5 ^{+9.0} _{-7.9}	5.2 ^{+3.7} _{-2.4}	27.2 ^{+6.6} _{-5.5}	17.1 ^{+6.2} _{-5.1}	27.4 ^{+6.6} _{-5.5}
6	74.4 ^{+10.8} _{-9.7}	73.1 ^{+9.8} _{-8.7}	1.3 ^{+5.2} _{-4.1}	76.1 ^{+10.9} _{-9.8}	35.6 ^{+7.3} _{-6.2}	43.0 ^{+7.8} _{-6.7}	-2.5 ^{+4.6} _{-3.4}	74.8 ^{+9.9} _{-8.9}
7	24.0 ^{+7.5} _{-6.4}	12.4 ^{+5.0} _{-3.9}	11.5 ^{+6.1} _{-5.0}	23.8 ^{+7.5} _{-6.4}	0.9 ^{+2.7} _{-1.3}	12.4 ^{+5.2} _{-4.0}	10.5 ^{+5.8} _{-4.7}	12.3 ^{+5.0} _{-3.9}
8	25.7 ^{+9.4} _{-8.3}	30.4 ^{+7.4} _{-6.3}	-4.7 ^{+6.5} _{-5.4}	25.6 ^{+9.4} _{-8.4}	25.4 ^{+6.7} _{-5.6}	5.5 ^{+4.8} _{-3.7}	-5.3 ^{+6.1} _{-5.0}	30.3 ^{+7.5} _{-6.4}
9	12.4 ^{+5.9} _{-4.7}	11.5 ^{+4.9} _{-3.7}	0.8 ^{+4.1} _{-2.9}	13.1 ^{+6.0} _{-4.8}	4.5 ^{+3.6} _{-2.4}	7.5 ^{+4.3} _{-3.1}	1.1 ^{+3.9} _{-2.7}	12.3 ^{+5.0} _{-3.9}
10	1419.1 ^{+39.5} _{-38.5}	593.9 ^{+25.7} _{-24.6}	825.2 ^{+30.6} _{-29.6}	1424.2 ^{+39.6} _{-38.6}	129.9 ^{+12.7} _{-11.7}	628.0 ^{+26.4} _{-25.4}	666.2 ^{+27.6} _{-26.6}	598.9 ^{+25.8} _{-24.8}
11	17.7 ^{+6.2} _{-5.1}	18.9 ^{+5.7} _{-4.6}	-1.2 ^{+3.5} _{-2.3}	17.5 ^{+6.2} _{-5.1}	7.5 ^{+4.1} _{-3.0}	10.6 ^{+4.6} _{-3.4}	-0.6 ^{+3.5} _{-2.3}	18.7 ^{+5.7} _{-4.6}
12	68.9 ^{+10.3} _{-9.2}	49.9 ^{+8.4} _{-7.3}	19.0 ^{+6.7} _{-5.6}	68.2 ^{+10.3} _{-9.2}	14.8 ^{+5.3} _{-4.1}	44.8 ^{+8.0} _{-6.9}	8.5 ^{+5.5} _{-4.3}	49.1 ^{+8.4} _{-7.3}
13	102.5 ^{+14.1} _{-13.1}	35.7 ^{+8.2} _{-7.2}	66.9 ^{+12.0} _{-11.0}	101.9 ^{+14.2} _{-13.1}	5.7 ^{+4.8} _{-3.7}	40.7 ^{+8.7} _{-7.6}	55.5 ^{+11.1} _{-10.0}	35.0 ^{+8.3} _{-7.2}
14	90.4 ^{+13.0} _{-12.0}	58.0 ^{+9.6} _{-8.5}	32.4 ^{+9.5} _{-8.4}	89.9 ^{+13.1} _{-12.0}	12.1 ^{+5.6} _{-4.5}	47.4 ^{+9.0} _{-7.9}	30.3 ^{+8.9} _{-7.8}	57.5 ^{+9.7} _{-8.6}
15	114.8 ^{+14.2} _{-13.2}	77.4 ^{+10.6} _{-9.5}	37.5 ^{+10.2} _{-9.1}	117.4 ^{+14.4} _{-13.3}	22.5 ^{+6.5} _{-5.3}	64.2 ^{+10.1} _{-9.1}	30.7 ^{+9.2} _{-8.2}	79.9 ^{+10.8} _{-9.7}
16	396.5 ^{+21.4} _{-20.4}	235.2 ^{+16.5} _{-15.5}	161.3 ^{+14.3} _{-13.2}	396.3 ^{+21.4} _{-20.4}	53.9 ^{+8.5} _{-7.4}	205.9 ^{+15.6} _{-14.6}	136.6 ^{+13.2} _{-12.2}	235.0 ^{+16.5} _{-15.5}
17	21.0 ^{+6.6} _{-5.5}	8.5 ^{+4.5} _{-3.3}	12.5 ^{+5.5} _{-4.4}	20.6 ^{+6.6} _{-5.5}	0.4 ^{+2.7} _{-1.3}	10.8 ^{+4.7} _{-3.6}	9.3 ^{+5.0} _{-3.9}	8.1 ^{+4.5} _{-3.3}
18	35.6 ^{+9.1} _{-8.0}	23.6 ^{+6.5} _{-5.4}	11.9 ^{+7.0} _{-5.9}	35.9 ^{+9.2} _{-8.1}	4.9 ^{+4.0} _{-2.8}	20.9 ^{+6.4} _{-5.2}	10.1 ^{+6.5} _{-5.4}	24.0 ^{+6.6} _{-5.5}
19	26.4 ^{+6.6} _{-5.5}	17.9 ^{+5.4} _{-4.3}	8.5 ^{+4.4} _{-3.3}	26.2 ^{+6.6} _{-5.5}	7.3 ^{+4.0} _{-2.8}	11.1 ^{+4.6} _{-3.4}	7.8 ^{+4.3} _{-3.1}	17.7 ^{+5.4} _{-4.3}
20	46.5 ^{+13.2} _{-12.1}	39.6 ^{+9.3} _{-8.3}	6.9 ^{+9.9} _{-8.9}	49.6 ^{+13.4} _{-12.3}	32.5 ^{+7.9} _{-6.9}	11.8 ^{+7.4} _{-6.3}	5.3 ^{+9.1} _{-8.1}	42.7 ^{+9.6} _{-8.6}
21	39.7 ^{+7.8} _{-6.7}	23.4 ^{+6.1} _{-5.0}	16.2 ^{+5.6} _{-4.5}	39.5 ^{+7.8} _{-6.7}	8.2 ^{+4.1} _{-2.9}	18.4 ^{+5.6} _{-4.4}	12.9 ^{+5.1} _{-4.0}	23.3 ^{+6.1} _{-5.0}
22	89.7 ^{+12.1} _{-11.1}	77.9 ^{+10.3} _{-9.2}	11.8 ^{+7.3} _{-6.2}	91.5 ^{+12.3} _{-11.2}	38.6 ^{+7.6} _{-6.5}	46.5 ^{+8.5} _{-7.4}	6.4 ^{+6.5} _{-5.4}	79.7 ^{+10.4} _{-9.4}
23	42.2 ^{+10.1} _{-9.0}	25.4 ^{+7.1} _{-6.0}	16.8 ^{+7.8} _{-6.7}	42.5 ^{+10.1} _{-9.1}	6.3 ^{+4.7} _{-3.5}	19.9 ^{+6.5} _{-5.4}	16.4 ^{+7.4} _{-6.3}	25.7 ^{+7.2} _{-6.1}
24	61.1 ^{+9.3} _{-8.2}	39.8 ^{+7.5} _{-6.4}	21.3 ^{+6.2} _{-5.1}	61.0 ^{+9.3} _{-8.2}	9.5 ^{+4.3} _{-3.1}	37.8 ^{+7.3} _{-6.2}	13.7 ^{+5.4} _{-4.2}	39.7 ^{+7.5} _{-6.4}
25	90.4 ^{+9.6} _{-9.6}	55.2 ^{+8.5} _{-7.5}	35.2 ^{+7.1} _{-6.1}	90.2 ^{+10.7} _{-9.6}	16.6 ^{+5.2} _{-4.1}	47.2 ^{+8.0} _{-6.9}	26.4 ^{+6.4} _{-5.3}	55.0 ^{+8.5} _{-7.5}
26	99.5 ^{+13.3} _{-12.3}	53.6 ^{+9.3} _{-8.2}	45.9 ^{+10.2} _{-9.1}	99.9 ^{+13.4} _{-12.4}	11.5 ^{+5.3} _{-4.2}	57.7 ^{+9.5} _{-8.4}	30.6 ^{+9.1} _{-8.0}	54.0 ^{+9.4} _{-8.3}
27	27.7 ^{+7.9} _{-6.8}	10.5 ^{+5.0} _{-3.9}	17.3 ^{+6.6} _{-5.5}	26.9 ^{+7.9} _{-6.8}	0.7 ^{+3.3} _{-2.0}	12.1 ^{+5.0} _{-3.9}	14.1 ^{+6.2} _{-5.1}	9.7 ^{+5.1} _{-3.9}

Table 5—Continued

Source No	<i>net_cnts</i> [1] [0.5–8.0keV]	<i>net_cnts</i> [2] [0.5–2.0keV]	<i>net_cnts</i> [3] [2.0–8.0keV]	<i>net_cnts</i> [4] [0.35–8.0keV]	<i>net_cnts</i> [5] [0.35–1.1keV]	<i>net_cnts</i> [6] [1.1–2.6keV]	<i>net_cnts</i> [7] [2.6–8.0keV]	<i>net_cnts</i> [8] [0.35–2.0keV]
28	123.3 ^{+13.7} _{-12.6}	89.2 ^{+10.9} _{-9.9}	34.1 ^{+8.9} _{-7.8}	122.8 ^{+13.7} _{-12.6}	19.7 ^{+6.0} _{-4.8}	73.9 ^{+10.2} _{-9.1}	29.3 ^{+8.2} _{-7.1}	88.7 ^{+10.9} _{-9.9}
29	171.0 ^{+14.8} _{-13.7}	116.6 ^{+12.1} _{-11.0}	54.4 ^{+9.3} _{-8.2}	170.3 ^{+14.8} _{-13.7}	26.9 ^{+6.5} _{-5.4}	114.8 ^{+12.0} _{-10.9}	28.7 ^{+7.4} _{-6.3}	115.9 ^{+12.1} _{-11.0}
30	37.5 ^{+8.6} _{-7.5}	20.3 ^{+6.0} _{-4.9}	17.1 ^{+6.7} _{-5.6}	36.9 ^{+8.6} _{-7.5}	6.8 ^{+4.2} _{-3.0}	16.6 ^{+5.7} _{-4.6}	13.5 ^{+6.1} _{-5.0}	19.8 ^{+6.0} _{-4.9}
31	19.6 ^{+5.8} _{-4.7}	15.3 ^{+5.1} _{-4.0}	4.3 ^{+3.6} _{-2.4}	19.6 ^{+5.8} _{-4.7}	3.7 ^{+3.2} _{-1.9}	12.3 ^{+4.7} _{-3.6}	3.6 ^{+3.4} _{-2.2}	15.3 ^{+5.1} _{-4.0}
32	46.9 ^{+9.8} _{-8.7}	23.8 ^{+6.5} _{-5.4}	23.1 ^{+7.9} _{-6.8}	47.1 ^{+9.8} _{-8.8}	3.5 ^{+3.7} _{-2.5}	26.8 ^{+6.9} _{-5.8}	16.8 ^{+7.1} _{-6.0}	24.0 ^{+6.6} _{-5.5}
33	65.4 ^{+9.2} _{-8.1}	41.9 ^{+7.5} _{-6.5}	23.5 ^{+6.0} _{-4.9}	65.4 ^{+9.2} _{-8.1}	8.9 ^{+4.1} _{-2.9}	39.8 ^{+7.4} _{-6.3}	16.6 ^{+5.2} _{-4.1}	41.8 ^{+7.5} _{-6.5}
34	15.9 ^{+5.3} _{-4.2}	4.3 ^{+3.4} _{-2.2}	11.5 ^{+4.7} _{-3.6}	15.8 ^{+5.3} _{-4.2}	1.7 ^{+2.7} _{-1.3}	2.4 ^{+2.9} _{-1.6}	11.7 ^{+4.7} _{-3.6}	4.3 ^{+3.4} _{-2.2}
35	2768.4 ^{+53.7} _{-52.7}	1811.7 ^{+43.6} _{-42.6}	956.7 ^{+32.1} _{-31.1}	2790.9 ^{+54.0} _{-52.9}	607.3 ^{+25.7} _{-24.7}	1486.2 ^{+39.6} _{-38.6}	697.4 ^{+27.6} _{-26.5}	1834.2 ^{+43.9} _{-42.9}
36	34.2 ^{+9.5} _{-8.4}	17.6 ^{+6.2} _{-5.1}	16.5 ^{+7.8} _{-6.7}	38.1 ^{+9.8} _{-8.7}	7.8 ^{+4.7} _{-3.5}	16.7 ^{+6.1} _{-5.0}	13.6 ^{+7.3} _{-6.2}	21.6 ^{+6.7} _{-5.5}
37	4762.1 ^{+70.7} _{-69.6}	3285.0 ^{+58.5} _{-57.5}	1477.1 ^{+40.3} _{-39.3}	4783.9 ^{+70.8} _{-69.8}	1052.6 ^{+33.6} _{-32.6}	2647.6 ^{+52.7} _{-51.7}	1083.7 ^{+34.8} _{-33.7}	3306.8 ^{+58.8} _{-57.7}
38	99.5 ^{+12.1} _{-11.1}	50.3 ^{+8.6} _{-7.5}	49.3 ^{+9.2} _{-8.1}	99.2 ^{+12.1} _{-11.1}	7.9 ^{+4.4} _{-3.2}	57.4 ^{+9.1} _{-8.1}	33.9 ^{+7.9} _{-6.8}	49.9 ^{+8.6} _{-7.5}
39	19.8 ^{+7.1} _{-6.0}	10.8 ^{+5.0} _{-3.9}	9.0 ^{+5.7} _{-4.6}	19.5 ^{+7.1} _{-6.0}	0.4 ^{+2.7} _{-1.4}	9.9 ^{+4.9} _{-3.8}	9.2 ^{+5.6} _{-4.4}	10.5 ^{+5.0} _{-3.9}
40	150.8 ^{+13.4} _{-12.4}	89.4 ^{+10.5} _{-9.5}	61.4 ^{+9.0} _{-7.9}	150.8 ^{+13.4} _{-12.4}	24.6 ^{+6.1} _{-5.0}	88.4 ^{+10.5} _{-9.4}	37.7 ^{+7.3} _{-6.2}	89.3 ^{+10.5} _{-9.5}
41	86.5 ^{+12.7} _{-11.7}	12.3 ^{+6.1} _{-4.9}	74.2 ^{+11.6} _{-10.5}	86.9 ^{+12.8} _{-11.7}	2.9 ^{+4.3} _{-3.1}	13.7 ^{+6.3} _{-5.1}	70.3 ^{+11.1} _{-10.0}	12.6 ^{+6.2} _{-5.1}
42	26.0 ^{+7.6} _{-6.6}	13.4 ^{+5.5} _{-4.4}	12.7 ^{+6.0} _{-4.8}	26.7 ^{+7.7} _{-6.6}	4.9 ^{+3.8} _{-2.6}	9.8 ^{+5.0} _{-3.9}	11.9 ^{+5.7} _{-4.6}	14.0 ^{+5.6} _{-4.5}
43	13.4 ^{+5.0} _{-3.8}	12.6 ^{+4.7} _{-3.6}	0.8 ^{+2.7} _{-1.3}	13.3 ^{+5.0} _{-3.8}	11.7 ^{+4.6} _{-3.4}	1.6 ^{+2.7} _{-1.3}	-0.0 ^{+2.3} _{-0.8}	12.5 ^{+4.7} _{-3.6}
44	57.8 ^{+10.1} _{-9.0}	6.5 ^{+4.8} _{-3.6}	51.3 ^{+9.3} _{-8.3}	57.4 ^{+10.1} _{-9.0}	0.1 ^{+3.3} _{-2.0}	10.0 ^{+5.0} _{-3.9}	47.2 ^{+8.9} _{-7.9}	6.0 ^{+4.8} _{-3.6}
45	15.9 ^{+7.3} _{-6.2}	13.5 ^{+5.6} _{-4.5}	2.3 ^{+5.3} _{-4.2}	16.8 ^{+7.4} _{-6.4}	4.1 ^{+4.2} _{-3.0}	11.0 ^{+5.1} _{-4.0}	1.7 ^{+5.0} _{-3.8}	14.5 ^{+5.8} _{-4.7}
46	20.5 ^{+6.1} _{-5.0}	8.3 ^{+4.3} _{-3.1}	12.3 ^{+5.0} _{-3.9}	20.3 ^{+6.1} _{-5.0}	0.4 ^{+2.3} _{-0.9}	10.1 ^{+4.6} _{-3.4}	9.8 ^{+4.6} _{-3.4}	8.0 ^{+4.3} _{-3.1}
47	38.0 ^{+9.3} _{-8.2}	18.0 ^{+6.3} _{-5.1}	20.0 ^{+7.5} _{-6.4}	39.6 ^{+9.5} _{-8.4}	5.3 ^{+4.3} _{-3.2}	20.6 ^{+6.4} _{-5.3}	13.7 ^{+6.7} _{-5.6}	19.6 ^{+6.5} _{-5.4}
48	78.7 ^{+10.4} _{-9.3}	78.3 ^{+10.0} _{-8.9}	0.3 ^{+3.9} _{-2.7}	80.3 ^{+10.5} _{-9.5}	63.9 ^{+9.1} _{-8.0}	17.1 ^{+5.5} _{-4.3}	-0.7 ^{+3.5} _{-2.3}	80.0 ^{+10.1} _{-9.0}
49	21.8 ^{+5.9} _{-4.8}	9.6 ^{+4.3} _{-3.1}	12.2 ^{+4.7} _{-3.6}	22.7 ^{+6.0} _{-4.9}	3.8 ^{+3.2} _{-1.9}	10.6 ^{+4.4} _{-3.3}	8.3 ^{+4.1} _{-2.9}	10.5 ^{+4.4} _{-3.3}
50	27.0 ^{+7.4} _{-6.3}	12.2 ^{+5.0} _{-3.9}	14.8 ^{+6.1} _{-5.0}	28.8 ^{+7.6} _{-6.5}	3.4 ^{+3.4} _{-2.2}	13.1 ^{+5.1} _{-4.0}	12.3 ^{+5.6} _{-4.5}	13.9 ^{+5.3} _{-4.1}
51	26.2 ^{+6.8} _{-5.7}	17.1 ^{+5.5} _{-4.3}	9.1 ^{+4.7} _{-3.6}	25.9 ^{+6.8} _{-5.7}	1.7 ^{+3.0} _{-1.7}	16.3 ^{+5.3} _{-4.2}	7.9 ^{+4.5} _{-3.3}	16.8 ^{+5.5} _{-4.3}
52	28.6 ^{+7.9} _{-6.9}	2.4 ^{+3.9} _{-2.7}	26.2 ^{+7.4} _{-6.3}	29.2 ^{+8.0} _{-6.9}	-0.9 ^{+2.7} _{-1.4}	7.5 ^{+4.6} _{-3.5}	22.6 ^{+6.9} _{-5.8}	3.0 ^{+4.0} _{-2.8}
53	22.5 ^{+5.9} _{-4.8}	8.9 ^{+4.1} _{-2.9}	13.6 ^{+4.8} _{-3.7}	22.5 ^{+5.9} _{-4.8}	0.9 ^{+2.3} _{-0.8}	9.9 ^{+4.3} _{-3.1}	11.7 ^{+4.6} _{-3.4}	8.9 ^{+4.1} _{-2.9}
54	158.9 ^{+14.7} _{-13.6}	95.9 ^{+11.2} _{-10.1}	63.0 ^{+10.2} _{-9.2}	157.9 ^{+14.7} _{-13.6}	29.9 ^{+6.8} _{-5.7}	80.8 ^{+10.5} _{-9.4}	47.2 ^{+9.1} _{-8.0}	94.9 ^{+11.2} _{-10.1}

Table 5—Continued

Source No	<i>net_cnts</i> [1] [0.5–8.0keV]	<i>net_cnts</i> [2] [0.5–2.0keV]	<i>net_cnts</i> [3] [2.0–8.0keV]	<i>net_cnts</i> [4] [0.35–8.0keV]	<i>net_cnts</i> [5] [0.35–1.1keV]	<i>net_cnts</i> [6] [1.1–2.6keV]	<i>net_cnts</i> [7] [2.6–8.0keV]	<i>net_cnts</i> [8] [0.35–2.0keV]
55	24.1 ^{+8.1} _{-7.1}	19.0 ^{+6.1} _{-5.0}	5.1 ^{+6.0} _{-4.9}	23.4 ^{+8.2} _{-7.1}	5.2 ^{+4.0} _{-2.8}	18.0 ^{+6.0} _{-4.9}	0.2 ^{+5.3} _{-4.1}	18.3 ^{+6.1} _{-5.0}
56	16.5 ^{+5.2} _{-4.1}	10.9 ^{+4.4} _{-3.3}	5.6 ^{+3.6} _{-2.4}	17.5 ^{+5.3} _{-4.2}	6.0 ^{+3.6} _{-2.4}	6.8 ^{+3.8} _{-2.6}	4.7 ^{+3.4} _{-2.2}	11.9 ^{+4.6} _{-3.4}
57	7.5 ^{+4.0} _{-2.8}	5.9 ^{+3.6} _{-2.4}	1.7 ^{+2.7} _{-1.3}	7.5 ^{+4.0} _{-2.8}	1.0 ^{+2.3} _{-0.8}	4.9 ^{+3.4} _{-2.2}	1.7 ^{+2.7} _{-1.3}	5.9 ^{+3.6} _{-2.4}
58	39.1 ^{+8.2} _{-7.2}	25.5 ^{+6.4} _{-5.3}	13.6 ^{+5.9} _{-4.8}	39.0 ^{+8.2} _{-7.2}	4.0 ^{+3.4} _{-2.2}	23.1 ^{+6.2} _{-5.1}	11.8 ^{+5.6} _{-4.5}	25.4 ^{+6.4} _{-5.3}
59	76.0 ^{+11.0} _{-9.9}	60.3 ^{+9.3} _{-8.2}	15.7 ^{+6.7} _{-5.6}	76.8 ^{+11.0} _{-10.0}	34.2 ^{+7.2} _{-6.1}	29.5 ^{+7.0} _{-5.9}	13.1 ^{+6.3} _{-5.2}	61.1 ^{+9.3} _{-8.2}
60	29.7 ^{+6.9} _{-5.8}	17.7 ^{+5.5} _{-4.3}	11.9 ^{+5.0} _{-3.8}	29.4 ^{+6.9} _{-5.8}	5.2 ^{+3.6} _{-2.4}	14.8 ^{+5.1} _{-4.0}	9.4 ^{+4.6} _{-3.4}	17.5 ^{+5.5} _{-4.3}
61	64.1 ^{+9.9} _{-8.8}	31.0 ^{+7.0} _{-5.9}	33.1 ^{+7.6} _{-6.5}	63.7 ^{+9.9} _{-8.8}	6.3 ^{+4.1} _{-3.0}	29.9 ^{+6.8} _{-5.7}	27.4 ^{+7.0} _{-5.9}	30.6 ^{+7.0} _{-5.9}
62	45.0 ^{+9.0} _{-7.9}	6.3 ^{+4.3} _{-3.1}	38.7 ^{+8.3} _{-7.3}	46.0 ^{+9.1} _{-8.1}	0.9 ^{+3.2} _{-2.0}	8.2 ^{+4.6} _{-3.4}	36.8 ^{+8.0} _{-7.0}	7.3 ^{+4.6} _{-3.5}
63	450.9 ^{+23.3} _{-22.3}	224.5 ^{+16.3} _{-15.3}	226.4 ^{+17.2} _{-16.2}	453.6 ^{+23.4} _{-22.4}	43.3 ^{+8.0} _{-6.9}	244.1 ^{+16.9} _{-15.9}	166.1 ^{+15.1} _{-14.1}	227.1 ^{+16.4} _{-15.4}
64	1284.4 ^{+37.5} _{-36.4}	792.4 ^{+29.5} _{-28.4}	492.0 ^{+23.8} _{-22.8}	1291.2 ^{+37.6} _{-36.6}	229.9 ^{+16.5} _{-15.4}	680.3 ^{+27.4} _{-26.3}	380.9 ^{+21.1} _{-20.1}	799.2 ^{+29.6} _{-28.6}
65	35.7 ^{+8.5} _{-7.4}	21.7 ^{+6.3} _{-5.2}	14.0 ^{+6.4} _{-5.3}	35.2 ^{+8.5} _{-7.4}	8.4 ^{+4.5} _{-3.3}	13.8 ^{+5.5} _{-4.4}	13.1 ^{+6.1} _{-5.0}	21.2 ^{+6.3} _{-5.2}
66	8.1 ^{+4.1} _{-2.9}	0.7 ^{+2.3} _{-0.8}	7.4 ^{+4.0} _{-2.8}	8.1 ^{+4.1} _{-2.9}	-0.1 ^{+1.9} _{-0.9}	5.7 ^{+3.6} _{-2.4}	2.5 ^{+2.9} _{-1.6}	0.7 ^{+2.3} _{-0.8}
67	19.5 ^{+10.3} _{-9.3}	4.7 ^{+5.8} _{-4.7}	14.8 ^{+9.1} _{-8.0}	17.8 ^{+10.4} _{-9.4}	-4.5 ^{+3.5} _{-2.3}	9.3 ^{+6.2} _{-5.1}	13.0 ^{+8.5} _{-7.5}	3.0 ^{+5.9} _{-4.8}
68	676.5 ^{+28.4} _{-27.4}	432.6 ^{+22.2} _{-21.2}	243.9 ^{+18.3} _{-17.3}	679.3 ^{+28.5} _{-27.5}	104.8 ^{+11.8} _{-10.7}	410.7 ^{+21.7} _{-20.7}	163.8 ^{+15.6} _{-14.5}	435.4 ^{+22.4} _{-21.3}
69	25.5 ^{+9.2} _{-8.1}	25.3 ^{+7.0} _{-5.9}	0.2 ^{+6.6} _{-5.5}	24.7 ^{+9.2} _{-8.1}	9.1 ^{+5.0} _{-3.9}	16.9 ^{+6.1} _{-5.0}	-1.2 ^{+6.1} _{-5.0}	24.5 ^{+7.0} _{-5.9}
70	37.5 ^{+8.1} _{-7.0}	41.2 ^{+7.7} _{-6.6}	-3.6 ^{+3.3} _{-2.1}	37.3 ^{+8.1} _{-7.0}	28.6 ^{+6.6} _{-5.5}	12.6 ^{+5.0} _{-3.9}	-3.9 ^{+3.1} _{-1.8}	40.9 ^{+7.7} _{-6.6}
71	21.8 ^{+5.8} _{-4.7}	7.9 ^{+4.0} _{-2.8}	13.8 ^{+4.8} _{-3.7}	21.8 ^{+5.8} _{-4.7}	1.0 ^{+2.3} _{-0.8}	7.9 ^{+4.0} _{-2.8}	12.9 ^{+4.7} _{-3.6}	7.9 ^{+4.0} _{-2.8}
72	13.6 ^{+5.1} _{-4.0}	11.1 ^{+4.6} _{-3.4}	2.5 ^{+3.2} _{-1.9}	14.5 ^{+5.2} _{-4.1}	10.3 ^{+4.4} _{-3.3}	2.5 ^{+2.9} _{-1.6}	1.7 ^{+2.9} _{-1.6}	12.0 ^{+4.7} _{-3.6}
73	15.6 ^{+5.1} _{-4.0}	4.9 ^{+3.4} _{-2.2}	10.7 ^{+4.4} _{-3.3}	15.6 ^{+5.1} _{-4.0}	-0.1 ^{+1.9} _{-0.0}	7.9 ^{+4.0} _{-2.8}	7.8 ^{+4.0} _{-2.8}	4.9 ^{+3.4} _{-2.2}
74	169.8 ^{+15.0} _{-14.0}	113.3 ^{+12.0} _{-11.0}	56.5 ^{+9.7} _{-8.6}	170.4 ^{+15.0} _{-14.0}	23.5 ^{+6.3} _{-5.2}	100.4 ^{+11.4} _{-10.4}	46.5 ^{+8.9} _{-7.8}	113.9 ^{+12.1} _{-11.0}
75	17.6 ^{+5.9} _{-4.8}	6.0 ^{+3.8} _{-2.6}	11.6 ^{+5.1} _{-4.0}	17.4 ^{+5.9} _{-4.8}	1.4 ^{+2.7} _{-1.3}	7.8 ^{+4.1} _{-2.9}	8.2 ^{+4.6} _{-3.4}	5.8 ^{+3.8} _{-2.6}
76	173.6 ^{+14.3} _{-13.3}	85.9 ^{+10.4} _{-9.3}	87.7 ^{+10.5} _{-9.5}	174.5 ^{+14.4} _{-13.3}	9.4 ^{+4.3} _{-3.1}	100.0 ^{+11.1} _{-10.0}	65.1 ^{+9.2} _{-8.2}	86.8 ^{+10.4} _{-9.4}
77	61.8 ^{+12.1} _{-11.1}	10.9 ^{+6.3} _{-5.2}	50.9 ^{+10.8} _{-9.8}	60.7 ^{+12.2} _{-11.2}	2.2 ^{+4.6} _{-3.4}	15.5 ^{+6.8} _{-5.7}	43.0 ^{+10.0} _{-8.9}	9.8 ^{+6.4} _{-5.3}
78	90.4 ^{+13.0} _{-11.9}	3.0 ^{+5.2} _{-4.1}	87.4 ^{+12.2} _{-11.2}	89.4 ^{+13.0} _{-12.0}	4.3 ^{+4.5} _{-3.4}	4.7 ^{+5.5} _{-4.4}	80.4 ^{+11.7} _{-10.6}	2.1 ^{+5.4} _{-4.3}
79	17.3 ^{+6.0} _{-4.9}	5.3 ^{+3.8} _{-2.6}	12.0 ^{+5.2} _{-4.1}	17.2 ^{+6.0} _{-4.9}	2.1 ^{+3.0} _{-1.6}	6.3 ^{+4.0} _{-2.8}	8.8 ^{+4.7} _{-3.6}	5.1 ^{+3.8} _{-2.6}
80	4.7 ^{+3.4} _{-2.2}	1.9 ^{+2.7} _{-1.3}	2.7 ^{+2.9} _{-1.6}	4.6 ^{+3.4} _{-2.2}	0.9 ^{+2.3} _{-0.8}	0.9 ^{+2.3} _{-0.8}	2.7 ^{+2.9} _{-1.6}	1.9 ^{+2.7} _{-1.3}
81	4.7 ^{+3.4} _{-2.2}	1.9 ^{+2.7} _{-1.3}	2.7 ^{+2.9} _{-1.6}	4.6 ^{+3.4} _{-2.2}	-0.1 ^{+1.9} _{-0.0}	1.9 ^{+2.7} _{-1.3}	2.7 ^{+2.9} _{-1.6}	1.9 ^{+2.7} _{-1.3}

Table 5—Continued

Source No	<i>net_cnts</i> [1] [0.5–8.0keV]	<i>net_cnts</i> [2] [0.5–2.0keV]	<i>net_cnts</i> [3] [2.0–8.0keV]	<i>net_cnts</i> [4] [0.35–8.0keV]	<i>net_cnts</i> [5] [0.35–1.1keV]	<i>net_cnts</i> [6] [1.1–2.6keV]	<i>net_cnts</i> [7] [2.6–8.0keV]	<i>net_cnts</i> [8] [0.35–2.0keV]
82	18.6 ^{+5.4} _{-4.3}	13.9 ^{+4.8} _{-3.7}	4.7 ^{+3.4} _{-2.2}	18.6 ^{+5.4} _{-4.3}	3.9 ^{+3.2} _{-1.9}	12.9 ^{+4.7} _{-3.6}	1.7 ^{+2.7} _{-1.3}	13.9 ^{+4.8} _{-3.7}
83	24.9 ^{+7.4} _{-6.3}	6.3 ^{+4.4} _{-3.2}	18.6 ^{+6.6} _{-5.5}	24.8 ^{+7.4} _{-6.3}	0.9 ^{+2.7} _{-1.3}	8.8 ^{+4.8} _{-3.6}	15.1 ^{+6.1} _{-5.0}	6.2 ^{+4.4} _{-3.2}
84	10.7 ^{+5.4} _{-4.3}	7.7 ^{+4.1} _{-3.0}	3.1 ^{+4.2} _{-3.0}	11.7 ^{+5.5} _{-4.4}	1.1 ^{+2.7} _{-1.3}	8.6 ^{+4.3} _{-3.1}	1.9 ^{+3.8} _{-2.6}	8.6 ^{+4.3} _{-3.1}
85	13.5 ^{+5.2} _{-4.1}	3.2 ^{+3.2} _{-1.9}	10.3 ^{+4.7} _{-3.6}	13.5 ^{+5.2} _{-4.1}	0.6 ^{+2.3} _{-0.8}	4.1 ^{+3.4} _{-2.2}	8.8 ^{+4.4} _{-3.3}	3.2 ^{+3.2} _{-1.9}
86	10.3 ^{+4.6} _{-3.4}	4.6 ^{+3.4} _{-2.2}	5.8 ^{+3.8} _{-2.6}	10.3 ^{+4.6} _{-3.4}	2.8 ^{+2.9} _{-1.6}	3.5 ^{+3.2} _{-1.9}	4.0 ^{+3.4} _{-2.2}	4.5 ^{+3.4} _{-2.2}
87	22.9 ^{+7.2} _{-6.1}	10.5 ^{+5.0} _{-3.9}	12.4 ^{+5.8} _{-4.7}	23.5 ^{+7.3} _{-6.2}	2.8 ^{+3.4} _{-2.2}	9.1 ^{+4.7} _{-3.6}	11.6 ^{+5.6} _{-4.5}	11.2 ^{+5.1} _{-4.0}
88	119.2 ^{+13.3} _{-12.2}	114.4 ^{+12.2} _{-11.1}	4.8 ^{+6.1} _{-5.0}	121.7 ^{+13.4} _{-12.4}	92.5 ^{+11.0} _{-9.9}	26.2 ^{+6.9} _{-5.8}	3.0 ^{+5.7} _{-4.6}	116.9 ^{+12.4} _{-11.3}
89	26.6 ^{+6.7} _{-5.6}	20.0 ^{+5.7} _{-4.5}	6.6 ^{+4.3} _{-3.1}	26.5 ^{+6.7} _{-5.6}	8.4 ^{+4.1} _{-2.9}	13.1 ^{+4.8} _{-3.7}	5.1 ^{+4.0} _{-2.8}	19.9 ^{+5.7} _{-4.5}
90	514.2 ^{+24.1} _{-23.1}	353.8 ^{+20.0} _{-18.9}	160.4 ^{+14.2} _{-13.2}	517.8 ^{+24.2} _{-23.2}	109.7 ^{+11.6} _{-10.6}	301.4 ^{+18.6} _{-17.5}	106.7 ^{+11.9} _{-10.8}	357.3 ^{+20.1} _{-19.1}
91	25.4 ^{+7.3} _{-6.2}	11.4 ^{+5.0} _{-3.8}	14.1 ^{+5.9} _{-4.8}	25.0 ^{+7.3} _{-6.2}	1.7 ^{+3.2} _{-1.9}	9.7 ^{+4.7} _{-3.6}	13.7 ^{+5.7} _{-4.6}	11.0 ^{+5.0} _{-3.9}
92	43.6 ^{+9.1} _{-8.0}	32.6 ^{+7.3} _{-6.2}	11.0 ^{+6.1} _{-5.0}	42.6 ^{+9.1} _{-8.0}	10.6 ^{+4.9} _{-3.7}	25.5 ^{+6.8} _{-5.7}	6.5 ^{+5.4} _{-4.3}	31.7 ^{+7.3} _{-6.2}
93	137.2 ^{+13.2} _{-12.2}	83.2 ^{+10.3} _{-9.3}	54.1 ^{+8.9} _{-7.9}	137.1 ^{+13.2} _{-12.2}	23.7 ^{+6.1} _{-5.0}	80.5 ^{+10.2} _{-9.1}	33.0 ^{+7.4} _{-6.3}	83.0 ^{+10.3} _{-9.3}
94	44.7 ^{+8.6} _{-7.5}	44.8 ^{+8.0} _{-6.9}	-0.1 ^{+4.1} _{-2.9}	44.3 ^{+8.6} _{-7.5}	37.7 ^{+7.3} _{-6.2}	5.7 ^{+4.2} _{-3.0}	0.9 ^{+4.1} _{-2.9}	44.4 ^{+8.0} _{-6.9}
95	25.6 ^{+6.8} _{-5.7}	18.6 ^{+5.7} _{-4.6}	7.0 ^{+4.6} _{-3.4}	25.5 ^{+6.8} _{-5.7}	5.6 ^{+3.8} _{-2.6}	15.1 ^{+5.2} _{-4.1}	4.8 ^{+4.1} _{-3.0}	18.5 ^{+5.7} _{-4.6}
96	19.6 ^{+5.6} _{-4.4}	6.9 ^{+3.8} _{-2.6}	12.7 ^{+4.7} _{-3.6}	19.6 ^{+5.6} _{-4.4}	-0.1 ^{+1.9} _{-0.0}	10.9 ^{+4.4} _{-3.3}	8.8 ^{+4.1} _{-2.9}	6.9 ^{+3.8} _{-2.6}
97	34.3 ^{+7.6} _{-6.5}	4.9 ^{+3.8} _{-2.6}	29.4 ^{+7.0} _{-5.9}	34.3 ^{+7.6} _{-6.5}	0.3 ^{+2.3} _{-0.8}	8.4 ^{+4.4} _{-3.3}	25.6 ^{+6.6} _{-5.5}	4.9 ^{+3.8} _{-2.6}
98	41.0 ^{+8.4} _{-7.3}	10.1 ^{+4.9} _{-3.7}	30.8 ^{+7.3} _{-6.2}	42.8 ^{+8.5} _{-7.4}	2.3 ^{+3.2} _{-1.9}	17.2 ^{+5.7} _{-4.6}	23.3 ^{+6.6} _{-5.5}	11.9 ^{+5.1} _{-4.0}
99	49.1 ^{+8.2} _{-7.1}	26.7 ^{+6.3} _{-5.2}	22.5 ^{+6.0} _{-4.9}	50.1 ^{+8.3} _{-7.2}	4.8 ^{+3.4} _{-2.2}	25.6 ^{+6.2} _{-5.1}	19.7 ^{+5.7} _{-4.5}	27.6 ^{+6.4} _{-5.3}
100	422.5 ^{+24.2} _{-23.2}	420.3 ^{+22.2} _{-21.2}	2.2 ^{+10.5} _{-9.5}	437.3 ^{+24.6} _{-23.6}	356.9 ^{+20.4} _{-19.3}	81.7 ^{+11.6} _{-10.5}	-1.3 ^{+9.5} _{-8.4}	435.1 ^{+22.6} _{-21.6}
101	24.2 ^{+9.4} _{-8.3}	17.6 ^{+6.6} _{-5.5}	6.6 ^{+7.2} _{-6.2}	23.1 ^{+9.4} _{-8.3}	7.3 ^{+5.0} _{-3.9}	13.6 ^{+5.9} _{-4.8}	2.3 ^{+6.5} _{-5.5}	16.5 ^{+6.6} _{-5.5}
102	9111.5 ^{+97.2} _{-96.1}	8996.9 ^{+96.1} _{-95.1}	114.6 ^{+15.1} _{-14.1}	9254.3 ^{+97.9} _{-96.9}	6931.2 ^{+84.5} _{-83.4}	2289.1 ^{+49.2} _{-48.2}	34.0 ^{+11.3} _{-10.3}	9139.7 ^{+96.9} _{-95.9}
103	36.3 ^{+8.1} _{-7.0}	14.9 ^{+5.4} _{-4.2}	21.4 ^{+6.6} _{-5.5}	36.2 ^{+8.1} _{-7.0}	2.1 ^{+3.0} _{-1.7}	15.5 ^{+5.6} _{-4.5}	18.6 ^{+6.1} _{-5.0}	14.8 ^{+5.4} _{-4.2}
104	13.1 ^{+5.1} _{-4.0}	10.3 ^{+4.4} _{-3.3}	2.8 ^{+3.4} _{-2.2}	13.0 ^{+5.1} _{-4.0}	-0.4 ^{+1.9} _{-0.0}	12.4 ^{+4.7} _{-3.6}	1.0 ^{+2.9} _{-1.6}	10.2 ^{+4.4} _{-3.3}
105	32.0 ^{+7.6} _{-6.5}	20.2 ^{+5.8} _{-4.7}	11.8 ^{+5.6} _{-4.4}	31.9 ^{+7.6} _{-6.5}	4.2 ^{+3.4} _{-2.2}	19.4 ^{+5.7} _{-4.6}	8.3 ^{+5.1} _{-4.0}	20.1 ^{+5.8} _{-4.7}
106	24.2 ^{+7.4} _{-6.4}	4.7 ^{+4.5} _{-3.3}	19.4 ^{+6.5} _{-5.4}	23.9 ^{+7.4} _{-6.4}	2.9 ^{+3.4} _{-2.2}	4.3 ^{+4.3} _{-3.2}	16.7 ^{+6.1} _{-5.0}	4.4 ^{+4.5} _{-3.3}
107	47.4 ^{+9.2} _{-8.2}	35.5 ^{+7.4} _{-6.3}	11.9 ^{+6.3} _{-5.1}	46.6 ^{+9.2} _{-8.2}	4.5 ^{+3.8} _{-2.6}	32.1 ^{+7.2} _{-6.1}	10.0 ^{+5.8} _{-4.7}	34.7 ^{+7.4} _{-6.3}
108	45.5 ^{+8.8} _{-7.7}	10.7 ^{+4.9} _{-3.7}	34.8 ^{+7.8} _{-6.7}	45.1 ^{+8.8} _{-7.7}	-0.9 ^{+2.4} _{-0.9}	17.7 ^{+5.7} _{-4.6}	28.3 ^{+7.1} _{-6.0}	10.3 ^{+4.9} _{-3.7}

Table 5—Continued

Source No	<i>net_cnts</i> [1] [0.5–8.0keV]	<i>net_cnts</i> [2] [0.5–2.0keV]	<i>net_cnts</i> [3] [2.0–8.0keV]	<i>net_cnts</i> [4] [0.35–8.0keV]	<i>net_cnts</i> [5] [0.35–1.1keV]	<i>net_cnts</i> [6] [1.1–2.6keV]	<i>net_cnts</i> [7] [2.6–8.0keV]	<i>net_cnts</i> [8] [0.35–2.0keV]
109	128.7 ^{+15.0} _{-13.9}	8.7 ^{+6.1} _{-5.0}	120.0 ^{+14.1} _{-13.0}	127.3 ^{+15.0} _{-14.0}	-0.5 ^{+4.3} _{-3.1}	11.1 ^{+6.3} _{-5.2}	116.7 ^{+13.6} _{-12.6}	7.3 ^{+6.2} _{-5.1}
110	11.8 ^{+8.7} _{-7.7}	-1.4 ^{+4.5} _{-3.4}	13.2 ^{+7.9} _{-6.8}	12.3 ^{+8.9} _{-7.8}	-2.6 ^{+3.5} _{-2.3}	4.6 ^{+5.2} _{-4.0}	10.3 ^{+7.3} _{-6.2}	-0.9 ^{+4.8} _{-3.7}
111	47.0 ^{+10.8} _{-9.8}	2.3 ^{+4.8} _{-3.7}	44.8 ^{+10.1} _{-9.0}	45.3 ^{+10.8} _{-9.8}	-3.4 ^{+3.0} _{-1.8}	15.5 ^{+6.3} _{-5.2}	33.3 ^{+9.1} _{-8.1}	0.6 ^{+4.8} _{-3.7}
112	131.5 ^{+14.2} _{-13.1}	92.4 ^{+11.8} _{-10.7}	39.2 ^{+8.6} _{-7.5}	134.2 ^{+14.3} _{-13.2}	35.3 ^{+7.8} _{-6.7}	72.9 ^{+10.6} _{-9.5}	26.0 ^{+7.3} _{-6.2}	95.0 ^{+11.9} _{-10.9}
113	22937.5 ^{+152.7} _{-151.7}	15923.6 ^{+127.3} _{-126.3}	7013.9 ^{+85.0} _{-84.0}	22987.8 ^{+152.9} _{-151.9}	3829.1 ^{+63.0} _{-62.0}	14650.8 ^{+122.2} _{-121.2}	4507.8 ^{+68.3} _{-67.3}	15973.9 ^{+127.5} _{-126.5}
114	25.6 ^{+9.2} _{-8.2}	16.3 ^{+6.2} _{-5.1}	9.3 ^{+7.4} _{-6.3}	27.5 ^{+9.4} _{-8.4}	6.8 ^{+4.6} _{-3.5}	18.6 ^{+6.4} _{-5.3}	2.1 ^{+6.4} _{-5.3}	18.2 ^{+6.5} _{-5.4}
115	21.7 ^{+5.9} _{-4.8}	17.6 ^{+5.3} _{-4.2}	4.1 ^{+3.4} _{-2.2}	21.6 ^{+5.9} _{-4.8}	4.8 ^{+3.4} _{-2.2}	13.6 ^{+4.8} _{-3.7}	3.2 ^{+3.2} _{-1.9}	17.6 ^{+5.3} _{-4.2}
116	26.6 ^{+7.8} _{-6.7}	6.1 ^{+4.4} _{-3.2}	20.5 ^{+7.0} _{-5.9}	26.3 ^{+7.8} _{-6.7}	-1.1 ^{+1.9} _{-0.0}	13.4 ^{+5.4} _{-4.3}	14.0 ^{+6.2} _{-5.1}	5.8 ^{+4.4} _{-3.2}
117	14.5 ^{+7.3} _{-6.2}	5.1 ^{+4.6} _{-3.5}	9.4 ^{+6.2} _{-5.1}	15.2 ^{+7.3} _{-6.3}	1.1 ^{+3.4} _{-2.2}	4.2 ^{+4.3} _{-3.2}	9.9 ^{+6.0} _{-4.9}	5.8 ^{+4.8} _{-3.6}
118	9.8 ^{+4.4} _{-3.3}	6.6 ^{+3.8} _{-2.6}	3.2 ^{+3.2} _{-1.9}	9.8 ^{+4.4} _{-3.3}	4.8 ^{+3.4} _{-2.2}	2.7 ^{+2.9} _{-1.6}	2.3 ^{+2.9} _{-1.6}	6.6 ^{+3.8} _{-2.6}
119	22.3 ^{+7.1} _{-6.0}	21.3 ^{+6.0} _{-4.9}	1.0 ^{+4.6} _{-3.4}	22.0 ^{+7.1} _{-6.0}	11.9 ^{+4.7} _{-3.6}	9.9 ^{+4.8} _{-3.6}	0.2 ^{+4.3} _{-3.1}	21.0 ^{+6.0} _{-4.9}
120	21.7 ^{+8.0} _{-6.9}	14.5 ^{+5.8} _{-4.7}	7.2 ^{+6.2} _{-5.1}	20.6 ^{+8.0} _{-7.0}	1.2 ^{+3.7} _{-2.4}	13.7 ^{+5.6} _{-4.5}	5.8 ^{+5.8} _{-4.6}	13.4 ^{+5.8} _{-4.7}
121	55.7 ^{+9.2} _{-8.1}	25.1 ^{+6.4} _{-5.3}	30.5 ^{+7.3} _{-6.2}	55.4 ^{+9.2} _{-8.1}	4.6 ^{+3.6} _{-2.4}	27.5 ^{+6.6} _{-5.5}	23.3 ^{+6.6} _{-5.5}	24.9 ^{+6.4} _{-5.3}
122	135.9 ^{+12.8} _{-11.8}	82.7 ^{+10.2} _{-9.1}	53.2 ^{+8.5} _{-7.4}	135.8 ^{+12.8} _{-11.8}	14.7 ^{+5.0} _{-3.8}	77.8 ^{+9.9} _{-8.9}	43.4 ^{+7.8} _{-6.7}	82.6 ^{+10.2} _{-9.1}
123	71.4 ^{+10.1} _{-9.0}	25.0 ^{+6.4} _{-5.3}	46.4 ^{+8.4} _{-7.3}	71.1 ^{+10.1} _{-9.0}	2.1 ^{+3.2} _{-1.9}	32.7 ^{+7.0} _{-5.9}	36.4 ^{+7.6} _{-6.5}	24.7 ^{+6.4} _{-5.3}
124	254.3 ^{+18.7} _{-17.7}	59.9 ^{+9.7} _{-8.6}	194.3 ^{+16.4} _{-15.4}	252.3 ^{+18.7} _{-17.7}	-0.8 ^{+4.1} _{-2.9}	90.3 ^{+11.2} _{-10.1}	162.8 ^{+15.2} _{-14.1}	57.9 ^{+9.7} _{-8.6}
125	65.0 ^{+9.2} _{-8.1}	39.7 ^{+7.4} _{-6.3}	25.3 ^{+6.2} _{-5.1}	65.0 ^{+9.2} _{-8.1}	10.8 ^{+4.4} _{-3.3}	36.8 ^{+7.1} _{-6.1}	17.4 ^{+5.3} _{-4.2}	39.7 ^{+7.4} _{-6.3}
126	53.3 ^{+9.1} _{-8.0}	32.2 ^{+7.0} _{-5.9}	21.2 ^{+6.5} _{-5.4}	54.2 ^{+9.1} _{-8.1}	10.4 ^{+4.6} _{-3.4}	27.9 ^{+6.6} _{-5.5}	15.9 ^{+5.9} _{-4.8}	33.1 ^{+7.1} _{-6.0}
127	33.2 ^{+8.5} _{-7.4}	6.5 ^{+4.9} _{-3.8}	26.6 ^{+7.5} _{-6.4}	33.1 ^{+8.5} _{-7.4}	-2.9 ^{+2.4} _{-1.0}	11.8 ^{+5.3} _{-4.1}	24.2 ^{+7.1} _{-6.0}	6.4 ^{+4.9} _{-3.8}
128	25.4 ^{+8.1} _{-7.1}	6.9 ^{+5.0} _{-3.9}	18.5 ^{+7.0} _{-5.9}	25.9 ^{+8.2} _{-7.1}	3.5 ^{+4.2} _{-3.0}	7.1 ^{+4.6} _{-3.4}	15.2 ^{+6.5} _{-5.4}	7.4 ^{+5.2} _{-4.0}
129	16.1 ^{+5.6} _{-4.4}	5.8 ^{+3.8} _{-2.6}	10.4 ^{+4.7} _{-3.6}	16.1 ^{+5.6} _{-4.4}	2.6 ^{+2.9} _{-1.6}	6.6 ^{+4.0} _{-2.8}	6.9 ^{+4.1} _{-3.0}	5.7 ^{+3.8} _{-2.6}
130	55.1 ^{+10.2} _{-9.1}	30.1 ^{+7.2} _{-6.1}	25.0 ^{+7.8} _{-6.7}	56.1 ^{+10.3} _{-9.2}	5.5 ^{+4.2} _{-3.0}	29.1 ^{+7.1} _{-6.0}	21.5 ^{+7.3} _{-6.2}	31.1 ^{+7.4} _{-6.3}
131	46.9 ^{+8.7} _{-7.6}	1.1 ^{+3.4} _{-2.2}	45.8 ^{+8.4} _{-7.3}	46.3 ^{+8.7} _{-7.6}	-0.6 ^{+2.7} _{-1.3}	5.4 ^{+4.0} _{-2.8}	41.5 ^{+8.0} _{-6.9}	0.6 ^{+3.4} _{-2.2}
132	120.9 ^{+12.1} _{-11.1}	67.4 ^{+9.3} _{-8.2}	53.5 ^{+8.5} _{-7.4}	120.8 ^{+12.1} _{-11.1}	9.6 ^{+4.3} _{-3.1}	70.3 ^{+9.5} _{-8.4}	40.8 ^{+7.5} _{-6.5}	67.3 ^{+9.3} _{-8.2}
133	488.1 ^{+23.8} _{-22.7}	303.6 ^{+18.7} _{-17.7}	184.5 ^{+15.3} _{-14.3}	488.6 ^{+23.8} _{-22.8}	74.2 ^{+10.0} _{-8.9}	290.5 ^{+18.3} _{-17.3}	123.9 ^{+12.9} _{-11.8}	304.1 ^{+18.7} _{-17.7}
134	124.8 ^{+12.3} _{-11.2}	71.7 ^{+9.5} _{-8.5}	53.1 ^{+8.4} _{-7.3}	125.8 ^{+12.3} _{-11.3}	21.9 ^{+5.8} _{-4.7}	61.7 ^{+8.9} _{-7.9}	42.2 ^{+7.6} _{-6.5}	72.7 ^{+9.6} _{-8.5}
135	17.0 ^{+5.4} _{-4.3}	9.3 ^{+4.3} _{-3.1}	7.6 ^{+4.1} _{-2.9}	17.9 ^{+5.6} _{-4.4}	2.7 ^{+2.9} _{-1.6}	10.3 ^{+4.4} _{-3.3}	4.9 ^{+3.6} _{-2.4}	10.3 ^{+4.4} _{-3.3}

Table 5—Continued

Source No	<i>net_cnts</i> [1] [0.5–8.0keV]	<i>net_cnts</i> [2] [0.5–2.0keV]	<i>net_cnts</i> [3] [2.0–8.0keV]	<i>net_cnts</i> [4] [0.35–8.0keV]	<i>net_cnts</i> [5] [0.35–1.1keV]	<i>net_cnts</i> [6] [1.1–2.6keV]	<i>net_cnts</i> [7] [2.6–8.0keV]	<i>net_cnts</i> [8] [0.35–2.0keV]
136	34.8 ^{+8.4} _{-7.3}	17.3 ^{+6.0} _{-4.9}	17.5 ^{+6.5} _{-5.4}	34.6 ^{+8.4} _{-7.3}	4.6 ^{+4.0} _{-2.8}	18.2 ^{+5.9} _{-4.8}	11.9 ^{+5.8} _{-4.7}	17.1 ^{+6.0} _{-4.9}
137	27.2 ^{+8.4} _{-7.3}	25.1 ^{+6.8} _{-5.8}	2.1 ^{+5.5} _{-4.4}	28.6 ^{+8.5} _{-7.4}	10.0 ^{+4.9} _{-3.7}	17.1 ^{+6.1} _{-5.0}	1.4 ^{+5.1} _{-3.9}	26.5 ^{+7.0} _{-5.9}
138	97.9 ^{+11.1} _{-10.0}	62.1 ^{+9.0} _{-7.9}	35.7 ^{+7.2} _{-6.1}	97.7 ^{+11.1} _{-10.0}	15.5 ^{+5.1} _{-4.0}	59.1 ^{+8.8} _{-7.7}	23.1 ^{+6.1} _{-5.0}	62.0 ^{+9.0} _{-7.9}
139	38.3 ^{+7.5} _{-6.4}	40.2 ^{+7.5} _{-6.4}	-1.8 ^{+1.9} _{-0.0}	39.2 ^{+7.5} _{-6.5}	33.5 ^{+6.9} _{-5.8}	7.3 ^{+4.0} _{-2.8}	-1.6 ^{+1.9} _{-0.0}	41.1 ^{+7.5} _{-6.5}
140	35.7 ^{+8.8} _{-7.7}	16.5 ^{+5.8} _{-4.6}	19.2 ^{+7.2} _{-6.1}	35.8 ^{+8.8} _{-7.8}	-0.6 ^{+2.8} _{-1.4}	23.4 ^{+6.6} _{-5.4}	13.0 ^{+6.4} _{-5.3}	16.6 ^{+5.9} _{-4.7}
141	261.7 ^{+17.9} _{-16.9}	26.9 ^{+6.8} _{-5.7}	234.8 ^{+16.9} _{-15.9}	262.8 ^{+18.0} _{-16.9}	10.7 ^{+4.9} _{-3.7}	31.4 ^{+7.3} _{-6.2}	220.7 ^{+16.3} _{-15.3}	28.1 ^{+7.0} _{-5.9}
142	176.4 ^{+15.2} _{-14.2}	96.5 ^{+11.2} _{-10.1}	79.9 ^{+10.9} _{-9.9}	175.7 ^{+15.2} _{-14.2}	20.4 ^{+5.9} _{-4.8}	98.6 ^{+11.4} _{-10.3}	56.8 ^{+9.5} _{-8.5}	95.8 ^{+11.2} _{-10.2}
143	196.9 ^{+15.4} _{-14.4}	36.8 ^{+7.3} _{-6.2}	160.1 ^{+14.0} _{-13.0}	196.7 ^{+15.4} _{-14.4}	3.1 ^{+3.2} _{-1.9}	56.3 ^{+8.7} _{-7.7}	137.4 ^{+13.1} _{-12.0}	36.6 ^{+7.3} _{-6.2}
144	70.1 ^{+10.3} _{-9.2}	52.3 ^{+8.6} _{-7.5}	17.8 ^{+6.4} _{-5.3}	69.7 ^{+10.3} _{-9.2}	10.3 ^{+4.6} _{-3.4}	46.9 ^{+8.2} _{-7.1}	12.5 ^{+5.7} _{-4.6}	51.9 ^{+8.6} _{-7.5}
145	29.2 ^{+7.2} _{-6.2}	15.7 ^{+5.3} _{-4.2}	13.5 ^{+5.6} _{-4.5}	28.9 ^{+7.2} _{-6.2}	6.7 ^{+4.0} _{-2.8}	10.8 ^{+4.7} _{-3.6}	11.3 ^{+5.2} _{-4.1}	15.4 ^{+5.3} _{-4.2}
146	49.5 ^{+11.8} _{-10.8}	0.2 ^{+5.2} _{-4.1}	49.4 ^{+11.0} _{-10.0}	48.2 ^{+11.9} _{-10.8}	2.2 ^{+4.5} _{-3.4}	0.1 ^{+5.2} _{-4.1}	45.9 ^{+10.5} _{-9.4}	-1.2 ^{+5.4} _{-4.2}
147	33.7 ^{+7.8} _{-6.7}	25.9 ^{+6.6} _{-5.5}	7.8 ^{+5.0} _{-3.9}	33.4 ^{+7.8} _{-6.7}	5.5 ^{+4.0} _{-2.8}	23.6 ^{+6.2} _{-5.1}	4.3 ^{+4.5} _{-3.3}	25.6 ^{+6.6} _{-5.5}
148	31.9 ^{+7.9} _{-6.8}	6.3 ^{+4.3} _{-3.1}	25.6 ^{+7.1} _{-6.0}	32.5 ^{+8.0} _{-6.9}	1.0 ^{+3.0} _{-1.7}	9.3 ^{+4.7} _{-3.6}	22.2 ^{+6.7} _{-5.6}	6.8 ^{+4.5} _{-3.3}
149	63.0 ^{+10.0} _{-8.9}	65.8 ^{+9.5} _{-8.4}	-2.8 ^{+4.2} _{-3.0}	63.5 ^{+10.1} _{-9.0}	51.6 ^{+8.4} _{-7.3}	13.6 ^{+5.3} _{-4.1}	-1.7 ^{+4.2} _{-3.0}	66.2 ^{+9.5} _{-8.4}
150	59.8 ^{+10.7} _{-9.6}	2.4 ^{+4.5} _{-3.4}	57.4 ^{+10.0} _{-9.0}	59.4 ^{+10.7} _{-9.6}	-0.4 ^{+3.0} _{-1.7}	10.6 ^{+5.5} _{-4.4}	49.1 ^{+9.4} _{-8.3}	2.0 ^{+4.5} _{-3.4}
151	30.8 ^{+8.7} _{-7.6}	26.0 ^{+6.9} _{-5.8}	4.9 ^{+6.0} _{-4.9}	32.1 ^{+8.8} _{-7.8}	6.9 ^{+4.6} _{-3.5}	22.3 ^{+6.5} _{-5.4}	2.9 ^{+5.4} _{-4.3}	27.2 ^{+7.1} _{-6.0}
152	109.4 ^{+11.7} _{-10.7}	54.7 ^{+8.5} _{-7.5}	54.7 ^{+8.7} _{-7.6}	109.3 ^{+11.7} _{-10.7}	6.5 ^{+3.8} _{-2.6}	54.4 ^{+8.5} _{-7.5}	48.4 ^{+8.2} _{-7.1}	54.6 ^{+8.5} _{-7.5}
153	48.2 ^{+9.2} _{-8.1}	46.0 ^{+8.2} _{-7.1}	2.2 ^{+5.0} _{-3.9}	47.9 ^{+9.2} _{-8.1}	29.0 ^{+6.6} _{-5.5}	17.2 ^{+6.0} _{-4.8}	1.7 ^{+4.6} _{-3.4}	45.7 ^{+8.2} _{-7.1}
154	1324.5 ^{+38.0} _{-37.0}	871.5 ^{+30.7} _{-29.7}	453.1 ^{+23.0} _{-22.0}	1337.5 ^{+38.2} _{-37.2}	299.0 ^{+18.5} _{-17.5}	695.4 ^{+27.6} _{-26.6}	343.1 ^{+20.2} _{-19.2}	884.4 ^{+31.0} _{-29.9}
155	480.9 ^{+24.1} _{-23.1}	278.9 ^{+18.2} _{-17.1}	202.0 ^{+16.5} _{-15.4}	486.2 ^{+24.3} _{-23.2}	66.1 ^{+9.7} _{-8.7}	269.9 ^{+17.9} _{-16.9}	150.2 ^{+14.5} _{-13.4}	284.3 ^{+18.4} _{-17.3}
156	57.7 ^{+11.8} _{-10.8}	8.8 ^{+6.9} _{-5.8}	48.8 ^{+10.1} _{-9.0}	57.4 ^{+11.8} _{-10.8}	-2.3 ^{+3.5} _{-2.3}	15.9 ^{+7.5} _{-6.4}	43.8 ^{+9.4} _{-8.3}	8.6 ^{+6.9} _{-5.8}
157	38.0 ^{+8.9} _{-7.9}	23.2 ^{+6.6} _{-5.5}	14.8 ^{+6.7} _{-5.6}	37.2 ^{+8.9} _{-7.9}	4.8 ^{+4.2} _{-3.0}	26.3 ^{+6.8} _{-5.7}	6.2 ^{+5.6} _{-4.5}	22.4 ^{+6.6} _{-5.5}
158	33458.8 ^{+184.6} _{-183.6}	21604.6 ^{+148.4} _{-147.4}	11854.2 ^{+110.4} _{-109.4}	33578.6 ^{+184.9} _{-183.9}	5981.8 ^{+78.6} _{-77.6}	19114.2 ^{+139.7} _{-138.7}	8482.5 ^{+93.6} _{-92.6}	21724.4 ^{+148.8} _{-147.8}
159	373.5 ^{+20.7} _{-19.6}	227.3 ^{+16.2} _{-15.2}	146.2 ^{+13.5} _{-12.5}	373.1 ^{+20.7} _{-19.6}	58.3 ^{+8.8} _{-7.7}	211.2 ^{+15.7} _{-14.6}	103.7 ^{+11.6} _{-10.5}	226.9 ^{+16.2} _{-15.2}
160	11.9 ^{+5.1} _{-4.0}	9.9 ^{+4.4} _{-3.3}	1.9 ^{+3.4} _{-2.2}	11.7 ^{+5.1} _{-4.0}	1.4 ^{+2.7} _{-1.3}	10.0 ^{+4.4} _{-3.3}	0.4 ^{+3.0} _{-1.7}	9.8 ^{+4.4} _{-3.3}
161	79.2 ^{+11.0} _{-10.0}	46.8 ^{+8.4} _{-7.3}	32.5 ^{+7.9} _{-6.8}	79.6 ^{+11.1} _{-10.0}	13.3 ^{+5.1} _{-4.0}	42.5 ^{+8.1} _{-7.0}	23.7 ^{+7.0} _{-5.9}	47.1 ^{+8.4} _{-7.4}
162	183.8 ^{+14.9} _{-13.8}	16.7 ^{+5.3} _{-4.2}	167.2 ^{+14.2} _{-13.2}	183.6 ^{+14.9} _{-13.8}	4.4 ^{+3.4} _{-2.2}	27.9 ^{+6.6} _{-5.5}	151.4 ^{+13.5} _{-12.5}	16.4 ^{+5.3} _{-4.2}

Table 5—Continued

Source No	<i>net_cnts[1]</i> [0.5–8.0keV]	<i>net_cnts[2]</i> [0.5–2.0keV]	<i>net_cnts[3]</i> [2.0–8.0keV]	<i>net_cnts[4]</i> [0.35–8.0keV]	<i>net_cnts[5]</i> [0.35–1.1keV]	<i>net_cnts[6]</i> [1.1–2.6keV]	<i>net_cnts[7]</i> [2.6–8.0keV]	<i>net_cnts[8]</i> [0.35–2.0keV]
163	815.9 ^{+30.7} _{-29.6}	633.9 ^{+26.6} _{-25.5}	182.1 ^{+16.1} _{-15.1}	822.8 ^{+30.8} _{-29.8}	217.7 ^{+16.1} _{-15.0}	493.5 ^{+23.6} _{-22.6}	111.6 ^{+13.3} _{-12.3}	640.7 ^{+26.7} _{-25.7}
164	41.3 ^{+10.6} _{-9.5}	28.7 ^{+7.6} _{-6.5}	12.6 ^{+8.0} _{-6.9}	40.0 ^{+10.6} _{-9.5}	8.5 ^{+5.2} _{-4.0}	17.9 ^{+6.5} _{-5.4}	13.5 ^{+7.8} _{-6.7}	27.3 ^{+7.6} _{-6.5}
165	117.7 ^{+13.8} _{-12.7}	75.2 ^{+10.4} _{-9.3}	42.5 ^{+9.7} _{-8.6}	119.3 ^{+13.9} _{-12.9}	21.1 ^{+6.4} _{-5.3}	59.3 ^{+9.5} _{-8.4}	38.8 ^{+9.2} _{-8.2}	76.8 ^{+10.6} _{-9.5}
166	144.8 ^{+14.0} _{-13.0}	90.9 ^{+11.0} _{-10.0}	53.9 ^{+9.4} _{-8.3}	144.3 ^{+14.0} _{-13.0}	28.7 ^{+6.7} _{-5.6}	75.7 ^{+10.2} _{-9.2}	39.9 ^{+8.3} _{-7.2}	90.4 ^{+11.0} _{-10.0}
167	27.5 ^{+9.9} _{-8.8}	5.5 ^{+5.5} _{-4.4}	22.0 ^{+8.7} _{-7.6}	26.4 ^{+9.9} _{-8.8}	-0.6 ^{+3.9} _{-2.7}	5.7 ^{+5.4} _{-4.3}	21.3 ^{+8.2} _{-7.2}	4.4 ^{+5.5} _{-4.4}
168	51.9 ^{+11.6} _{-10.5}	19.0 ^{+7.3} _{-6.3}	32.9 ^{+9.5} _{-8.5}	51.4 ^{+11.7} _{-10.7}	0.9 ^{+4.8} _{-3.7}	28.3 ^{+7.7} _{-6.6}	22.3 ^{+8.5} _{-7.4}	18.5 ^{+7.5} _{-6.4}
169	19.6 ^{+7.0} _{-5.9}	12.7 ^{+5.1} _{-4.0}	6.9 ^{+5.5} _{-4.3}	20.2 ^{+7.1} _{-6.0}	2.7 ^{+3.5} _{-2.2}	10.2 ^{+4.8} _{-3.6}	7.3 ^{+5.3} _{-4.2}	13.3 ^{+5.3} _{-4.1}
170	23.3 ^{+6.8} _{-5.7}	9.2 ^{+4.6} _{-3.4}	14.1 ^{+5.6} _{-4.5}	25.1 ^{+7.0} _{-5.9}	2.8 ^{+3.2} _{-1.9}	9.3 ^{+4.6} _{-3.4}	13.0 ^{+5.4} _{-4.2}	11.0 ^{+4.9} _{-3.7}
171	23.1 ^{+8.2} _{-7.2}	22.4 ^{+6.6} _{-5.5}	0.8 ^{+5.7} _{-4.6}	23.1 ^{+8.3} _{-7.2}	10.8 ^{+5.0} _{-3.9}	10.9 ^{+5.5} _{-4.4}	1.4 ^{+5.3} _{-4.2}	22.3 ^{+6.7} _{-5.6}
172	31.1 ^{+8.6} _{-7.5}	4.7 ^{+4.6} _{-3.5}	26.4 ^{+7.7} _{-6.6}	30.5 ^{+8.6} _{-7.5}	-1.4 ^{+2.7} _{-1.4}	4.9 ^{+4.6} _{-3.5}	27.0 ^{+7.5} _{-6.5}	4.1 ^{+4.6} _{-3.5}
173	14.6 ^{+9.1} _{-8.0}	4.5 ^{+5.3} _{-4.2}	10.1 ^{+7.9} _{-6.8}	14.9 ^{+9.2} _{-8.1}	-1.2 ^{+3.5} _{-2.2}	12.7 ^{+6.2} _{-5.1}	3.4 ^{+7.0} _{-5.9}	4.9 ^{+5.5} _{-4.4}
174	33.8 ^{+9.5} _{-8.4}	14.7 ^{+6.4} _{-5.3}	19.1 ^{+7.7} _{-6.6}	37.5 ^{+9.7} _{-8.7}	8.4 ^{+5.0} _{-3.9}	12.5 ^{+5.8} _{-4.7}	16.6 ^{+7.2} _{-6.1}	18.4 ^{+6.7} _{-5.6}
175	220.1 ^{+17.6} _{-16.6}	191.0 ^{+15.4} _{-14.4}	29.1 ^{+9.3} _{-8.3}	225.7 ^{+17.8} _{-16.8}	108.4 ^{+11.8} _{-10.8}	100.7 ^{+11.7} _{-10.7}	16.7 ^{+8.2} _{-7.1}	196.7 ^{+15.6} _{-14.6}
176	169.1 ^{+18.4} _{-17.4}	168.3 ^{+15.5} _{-14.5}	0.9 ^{+10.6} _{-9.6}	172.8 ^{+18.6} _{-17.6}	136.6 ^{+13.6} _{-12.5}	29.9 ^{+9.3} _{-8.2}	6.3 ^{+10.2} _{-9.1}	171.9 ^{+15.8} _{-14.7}
177	29.8 ^{+7.4} _{-6.3}	6.2 ^{+4.2} _{-3.0}	23.7 ^{+6.7} _{-5.6}	29.6 ^{+7.4} _{-6.3}	2.7 ^{+3.2} _{-1.9}	4.3 ^{+3.8} _{-2.6}	22.6 ^{+6.5} _{-5.4}	5.9 ^{+4.2} _{-3.0}
178	42.1 ^{+8.4} _{-7.4}	26.2 ^{+6.6} _{-5.5}	15.9 ^{+6.0} _{-4.9}	42.7 ^{+8.5} _{-7.4}	10.7 ^{+4.7} _{-3.6}	19.8 ^{+5.9} _{-4.8}	12.3 ^{+5.5} _{-4.3}	26.9 ^{+6.6} _{-5.5}
179	72.0 ^{+12.0} _{-10.9}	43.1 ^{+8.6} _{-7.5}	28.9 ^{+8.9} _{-7.9}	70.6 ^{+12.0} _{-10.9}	2.6 ^{+4.3} _{-3.1}	47.6 ^{+8.9} _{-7.8}	20.4 ^{+8.0} _{-6.9}	41.7 ^{+8.6} _{-7.5}
180	46491.4 ^{+217.0} _{-215.9}	27184.6 ^{+166.1} _{-165.1}	19306.9 ^{+140.2} _{-139.2}	46746.2 ^{+217.6} _{-216.5}	8350.8 ^{+92.5} _{-91.5}	23733.7 ^{+155.3} _{-154.2}	14661.7 ^{+122.4} _{-121.3}	27439.3 ^{+166.9} _{-165.8}
181	330.4 ^{+20.6} _{-19.5}	227.9 ^{+16.6} _{-15.6}	102.5 ^{+12.8} _{-11.8}	335.3 ^{+20.7} _{-19.7}	89.0 ^{+11.0} _{-9.9}	168.6 ^{+14.5} _{-13.5}	77.7 ^{+11.4} _{-10.4}	232.8 ^{+16.8} _{-15.8}
182	38.4 ^{+11.3} _{-10.3}	24.8 ^{+8.0} _{-7.0}	13.6 ^{+8.6} _{-7.5}	40.7 ^{+11.5} _{-10.5}	6.6 ^{+5.4} _{-4.3}	23.8 ^{+7.7} _{-6.6}	10.4 ^{+8.0} _{-6.9}	27.1 ^{+8.3} _{-7.2}
183	282.7 ^{+20.5} _{-19.5}	279.3 ^{+18.5} _{-17.4}	3.4 ^{+9.8} _{-8.7}	291.0 ^{+20.8} _{-19.8}	210.7 ^{+15.9} _{-14.9}	80.2 ^{+11.4} _{-10.3}	0.1 ^{+8.9} _{-7.9}	287.6 ^{+18.8} _{-17.7}
184	1719.3 ^{+43.2} _{-42.2}	1707.8 ^{+42.6} _{-41.5}	11.5 ^{+8.3} _{-7.2}	1757.5 ^{+43.7} _{-42.6}	1338.9 ^{+37.8} _{-36.7}	415.6 ^{+21.8} _{-20.8}	3.0 ^{+7.0} _{-5.9}	1746.1 ^{+43.0} _{-42.0}
185	10.3 ^{+4.4} _{-3.3}	6.8 ^{+3.8} _{-2.6}	3.6 ^{+3.2} _{-1.9}	10.3 ^{+4.4} _{-3.3}	-0.1 ^{+1.9} _{-0.0}	7.8 ^{+4.0} _{-2.8}	2.6 ^{+2.9} _{-1.6}	6.7 ^{+3.8} _{-2.6}
186	492.2 ^{+23.8} _{-22.8}	281.0 ^{+18.0} _{-17.0}	211.2 ^{+16.2} _{-15.2}	493.5 ^{+23.8} _{-22.8}	74.2 ^{+9.9} _{-8.8}	265.5 ^{+17.6} _{-16.5}	153.8 ^{+14.0} _{-13.0}	282.3 ^{+18.1} _{-17.0}
187	1644.9 ^{+42.2} _{-41.2}	1066.4 ^{+33.9} _{-32.9}	578.6 ^{+25.8} _{-24.8}	1656.2 ^{+42.4} _{-41.4}	374.8 ^{+20.6} _{-19.5}	855.1 ^{+30.5} _{-29.5}	426.3 ^{+22.5} _{-21.4}	1077.6 ^{+34.1} _{-33.1}
188	769.6 ^{+31.2} _{-30.1}	743.6 ^{+29.0} _{-27.9}	26.0 ^{+12.3} _{-11.3}	785.8 ^{+31.5} _{-30.5}	583.5 ^{+25.6} _{-24.6}	190.5 ^{+16.0} _{-14.9}	11.9 ^{+11.1} _{-10.0}	759.8 ^{+29.3} _{-28.3}
189	37.7 ^{+7.7} _{-6.6}	18.4 ^{+5.6} _{-4.4}	19.3 ^{+6.0} _{-4.9}	40.6 ^{+7.9} _{-6.8}	7.2 ^{+4.0} _{-2.8}	21.7 ^{+5.9} _{-4.8}	11.7 ^{+5.1} _{-4.0}	21.3 ^{+5.9} _{-4.8}

Table 5—Continued

Source No	<i>net_cnts</i> [1] [0.5–8.0keV]	<i>net_cnts</i> [2] [0.5–2.0keV]	<i>net_cnts</i> [3] [2.0–8.0keV]	<i>net_cnts</i> [4] [0.35–8.0keV]	<i>net_cnts</i> [5] [0.35–1.1keV]	<i>net_cnts</i> [6] [1.1–2.6keV]	<i>net_cnts</i> [7] [2.6–8.0keV]	<i>net_cnts</i> [8] [0.35–2.0keV]
190	188.0 ^{+15.5} _{-14.5}	134.8 ^{+12.9} _{-11.8}	53.2 ^{+9.4} _{-8.3}	188.8 ^{+15.5} _{-14.5}	53.3 ^{+8.5} _{-7.4}	100.0 ^{+11.4} _{-10.3}	35.5 ^{+8.1} _{-7.0}	135.6 ^{+12.9} _{-11.9}
191	19.5 ^{+7.6} _{-6.6}	-2.2 ^{+3.5} _{-2.2}	21.7 ^{+7.2} _{-6.1}	19.0 ^{+7.6} _{-6.6}	-1.8 ^{+3.0} _{-1.7}	-1.8 ^{+3.0} _{-1.7}	22.6 ^{+7.1} _{-6.0}	-2.7 ^{+3.5} _{-2.3}
192	53.8 ^{+11.0} _{-9.9}	39.0 ^{+8.3} _{-7.2}	14.8 ^{+7.8} _{-6.7}	52.1 ^{+11.0} _{-9.9}	4.9 ^{+4.8} _{-3.6}	36.9 ^{+8.0} _{-6.9}	10.3 ^{+7.2} _{-6.1}	37.3 ^{+8.3} _{-7.2}
193	185.8 ^{+16.2} _{-15.2}	88.0 ^{+11.1} _{-10.0}	97.8 ^{+12.4} _{-11.4}	188.9 ^{+16.4} _{-15.3}	15.3 ^{+5.7} _{-4.6}	96.0 ^{+11.4} _{-10.4}	77.5 ^{+11.3} _{-10.3}	91.1 ^{+11.3} _{-10.2}
194	21.2 ^{+6.3} _{-5.2}	14.8 ^{+5.1} _{-4.0}	6.5 ^{+4.5} _{-3.3}	21.0 ^{+6.3} _{-5.2}	3.4 ^{+3.2} _{-1.9}	11.4 ^{+4.7} _{-3.6}	6.2 ^{+4.3} _{-3.1}	14.6 ^{+5.1} _{-4.0}
195	1918.6 ^{+46.1} _{-45.1}	643.1 ^{+27.2} _{-26.2}	1275.5 ^{+37.8} _{-36.8}	1922.4 ^{+46.2} _{-45.2}	52.4 ^{+9.8} _{-8.8}	847.4 ^{+30.6} _{-29.6}	1022.6 ^{+34.0} _{-33.0}	646.9 ^{+27.3} _{-26.3}
196	56.3 ^{+10.9} _{-9.8}	38.2 ^{+8.1} _{-7.0}	18.1 ^{+7.9} _{-6.8}	57.4 ^{+11.0} _{-9.9}	10.6 ^{+5.4} _{-4.3}	33.4 ^{+7.5} _{-6.4}	13.4 ^{+7.3} _{-6.2}	39.3 ^{+8.2} _{-7.2}
197	2969.8 ^{+56.8} _{-55.8}	2927.2 ^{+55.6} _{-54.6}	42.5 ^{+12.6} _{-11.5}	3010.7 ^{+57.2} _{-56.2}	1979.2 ^{+45.8} _{-44.8}	1009.5 ^{+33.4} _{-32.4}	21.9 ^{+10.9} _{-9.8}	2968.1 ^{+56.0} _{-55.0}
198	33.5 ^{+8.5} _{-7.5}	11.9 ^{+5.4} _{-4.2}	21.7 ^{+7.2} _{-6.1}	34.7 ^{+8.7} _{-7.6}	8.3 ^{+4.6} _{-3.4}	8.0 ^{+4.7} _{-3.6}	18.3 ^{+6.8} _{-5.7}	13.0 ^{+5.6} _{-4.5}
199	89.3 ^{+12.8} _{-11.8}	29.8 ^{+7.5} _{-6.4}	59.5 ^{+10.9} _{-9.9}	88.9 ^{+12.9} _{-11.8}	0.0 ^{+3.5} _{-2.3}	44.5 ^{+8.6} _{-7.5}	44.5 ^{+9.9} _{-8.8}	29.5 ^{+7.5} _{-6.5}
200	23.7 ^{+6.5} _{-5.4}	8.3 ^{+4.3} _{-3.1}	15.4 ^{+5.5} _{-4.3}	23.5 ^{+6.5} _{-5.4}	-1.5 ^{+1.9} _{-0.0}	12.9 ^{+4.8} _{-3.7}	12.1 ^{+5.0} _{-3.8}	8.1 ^{+4.3} _{-3.1}
201	31.7 ^{+10.1} _{-9.1}	20.8 ^{+7.0} _{-5.9}	10.9 ^{+8.0} _{-6.9}	30.1 ^{+10.2} _{-9.1}	3.7 ^{+4.6} _{-3.5}	17.5 ^{+6.5} _{-5.4}	8.9 ^{+7.4} _{-6.4}	19.2 ^{+7.0} _{-5.9}
202	63.1 ^{+11.2} _{-10.1}	33.1 ^{+7.9} _{-6.8}	30.0 ^{+8.5} _{-7.4}	65.1 ^{+11.3} _{-10.3}	7.7 ^{+5.0} _{-3.9}	35.1 ^{+7.8} _{-6.7}	22.3 ^{+7.7} _{-6.6}	35.1 ^{+8.1} _{-7.0}
203	35.0 ^{+10.0} _{-9.0}	1.8 ^{+5.1} _{-3.9}	33.2 ^{+9.1} _{-8.1}	33.4 ^{+10.0} _{-9.0}	-4.7 ^{+3.0} _{-1.8}	9.2 ^{+5.7} _{-4.6}	28.9 ^{+8.5} _{-7.4}	0.2 ^{+5.1} _{-4.0}
204	44.0 ^{+10.5} _{-9.5}	25.1 ^{+7.4} _{-6.3}	18.8 ^{+8.1} _{-7.0}	45.0 ^{+10.6} _{-9.6}	7.5 ^{+4.9} _{-3.7}	19.6 ^{+6.8} _{-5.7}	17.9 ^{+7.7} _{-6.7}	26.1 ^{+7.5} _{-6.4}
205	61.3 ^{+12.2} _{-11.2}	35.6 ^{+8.6} _{-7.5}	25.6 ^{+9.4} _{-8.3}	62.6 ^{+12.4} _{-11.3}	14.2 ^{+6.2} _{-5.0}	23.6 ^{+7.6} _{-6.5}	24.9 ^{+8.8} _{-7.8}	37.0 ^{+8.8} _{-7.7}
206	177.3 ^{+15.4} _{-14.4}	113.5 ^{+12.1} _{-11.0}	63.8 ^{+10.3} _{-9.2}	178.8 ^{+15.5} _{-14.4}	32.7 ^{+7.1} _{-6.0}	100.4 ^{+11.5} _{-10.4}	45.7 ^{+9.0} _{-7.9}	115.0 ^{+12.1} _{-11.1}
207	123.9 ^{+13.9} _{-12.8}	7.4 ^{+5.6} _{-4.5}	116.5 ^{+13.1} _{-12.0}	124.0 ^{+13.9} _{-12.9}	1.9 ^{+4.0} _{-2.8}	22.3 ^{+6.9} _{-5.8}	99.8 ^{+12.2} _{-11.1}	7.5 ^{+5.7} _{-4.6}
208	38.2 ^{+8.7} _{-7.6}	29.8 ^{+7.0} _{-5.9}	8.4 ^{+5.8} _{-4.7}	38.6 ^{+8.7} _{-7.7}	11.7 ^{+5.0} _{-3.8}	25.9 ^{+6.6} _{-5.5}	0.9 ^{+4.8} _{-3.6}	30.1 ^{+7.1} _{-6.0}
209	15.3 ^{+6.2} _{-5.1}	2.2 ^{+3.4} _{-2.2}	13.1 ^{+5.7} _{-4.6}	15.0 ^{+6.2} _{-5.1}	0.4 ^{+2.7} _{-1.3}	9.4 ^{+4.6} _{-3.4}	5.2 ^{+4.6} _{-3.5}	1.9 ^{+3.4} _{-2.2}
210	339.7 ^{+21.3} _{-20.2}	213.3 ^{+16.4} _{-15.4}	126.4 ^{+14.2} _{-13.2}	340.9 ^{+21.4} _{-20.3}	58.2 ^{+9.5} _{-8.4}	190.4 ^{+15.5} _{-14.5}	92.4 ^{+12.6} _{-11.5}	214.5 ^{+16.5} _{-15.5}
211	41.9 ^{+11.0} _{-10.0}	29.7 ^{+7.7} _{-6.6}	12.2 ^{+8.5} _{-7.4}	42.9 ^{+11.1} _{-10.1}	7.3 ^{+4.9} _{-3.8}	23.0 ^{+7.3} _{-6.3}	12.6 ^{+8.0} _{-6.9}	30.7 ^{+7.9} _{-6.8}
212	40.7 ^{+10.1} _{-9.0}	30.5 ^{+7.6} _{-6.5}	10.3 ^{+7.3} _{-6.2}	39.9 ^{+10.1} _{-9.0}	9.9 ^{+5.1} _{-4.0}	22.1 ^{+6.8} _{-5.7}	7.9 ^{+6.8} _{-5.7}	29.6 ^{+7.6} _{-6.5}
213	58.4 ^{+12.3} _{-11.3}	20.3 ^{+7.8} _{-6.7}	38.1 ^{+10.1} _{-9.1}	57.4 ^{+12.4} _{-11.3}	7.9 ^{+5.8} _{-4.7}	12.9 ^{+6.9} _{-5.8}	36.6 ^{+9.6} _{-8.5}	19.3 ^{+7.8} _{-6.8}
214	110.3 ^{+13.6} _{-12.6}	6.6 ^{+5.5} _{-4.3}	103.7 ^{+12.8} _{-11.8}	109.3 ^{+13.6} _{-12.6}	1.6 ^{+3.9} _{-2.7}	17.6 ^{+6.5} _{-5.4}	90.1 ^{+12.1} _{-11.0}	5.6 ^{+5.5} _{-4.3}
215	181.6 ^{+16.1} _{-15.1}	102.4 ^{+11.7} _{-10.7}	79.2 ^{+11.7} _{-10.7}	182.7 ^{+16.2} _{-15.2}	21.2 ^{+6.3} _{-5.2}	100.8 ^{+11.6} _{-10.5}	60.7 ^{+10.6} _{-9.6}	103.5 ^{+11.8} _{-10.8}
216	54.2 ^{+11.3} _{-10.2}	27.0 ^{+7.4} _{-6.3}	27.3 ^{+9.1} _{-8.1}	54.8 ^{+11.3} _{-10.3}	3.8 ^{+4.4} _{-3.2}	33.7 ^{+7.8} _{-6.7}	17.2 ^{+8.2} _{-7.1}	27.5 ^{+7.5} _{-6.4}

Table 5—Continued

Source No	<i>net_cnts</i> [1] [0.5–8.0keV]	<i>net_cnts</i> [2] [0.5–2.0keV]	<i>net_cnts</i> [3] [2.0–8.0keV]	<i>net_cnts</i> [4] [0.35–8.0keV]	<i>net_cnts</i> [5] [0.35–1.1keV]	<i>net_cnts</i> [6] [1.1–2.6keV]	<i>net_cnts</i> [7] [2.6–8.0keV]	<i>net_cnts</i> [8] [0.35–2.0keV]
217	15.7 ^{+7.3} _{-6.2}	6.3 ^{+4.8} _{-3.6}	9.4 ^{+6.1} _{-5.0}	15.7 ^{+7.4} _{-6.3}	-0.1 ^{+3.3} _{-2.0}	4.8 ^{+4.5} _{-3.3}	11.0 ^{+6.0} _{-4.8}	6.3 ^{+4.9} _{-3.8}
218	9.5 ^{+6.2} _{-5.1}	2.2 ^{+3.6} _{-2.4}	7.2 ^{+5.5} _{-4.4}	10.3 ^{+6.3} _{-5.1}	2.0 ^{+3.2} _{-1.9}	4.3 ^{+4.0} _{-2.8}	3.9 ^{+4.9} _{-3.8}	3.0 ^{+3.8} _{-2.6}
219	44.7 ^{+10.0} _{-8.9}	20.0 ^{+6.4} _{-5.3}	24.7 ^{+8.2} _{-7.1}	44.8 ^{+10.0} _{-9.0}	4.1 ^{+4.0} _{-2.8}	18.4 ^{+6.3} _{-5.2}	22.3 ^{+7.8} _{-6.7}	20.0 ^{+6.5} _{-5.4}
220	18.1 ^{+6.3} _{-5.2}	2.8 ^{+3.6} _{-2.4}	15.3 ^{+5.7} _{-4.6}	17.9 ^{+6.3} _{-5.2}	-0.7 ^{+2.3} _{-0.9}	6.4 ^{+4.1} _{-3.0}	12.2 ^{+5.2} _{-4.1}	2.6 ^{+3.6} _{-2.4}
221	1434.2 ^{+40.4} _{-39.4}	749.7 ^{+29.2} _{-28.1}	684.5 ^{+28.6} _{-27.6}	1434.6 ^{+40.5} _{-39.5}	152.8 ^{+14.3} _{-13.2}	751.8 ^{+29.1} _{-28.0}	530.1 ^{+25.4} _{-24.4}	750.2 ^{+29.2} _{-28.2}
222	39.6 ^{+9.9} _{-8.8}	18.3 ^{+6.4} _{-5.3}	21.4 ^{+8.1} _{-7.0}	41.1 ^{+10.1} _{-9.0}	6.6 ^{+4.6} _{-3.5}	18.2 ^{+6.4} _{-5.3}	16.3 ^{+7.4} _{-6.3}	19.7 ^{+6.7} _{-5.6}
223	33.5 ^{+10.7} _{-9.6}	25.3 ^{+7.5} _{-6.4}	8.2 ^{+8.2} _{-7.1}	33.6 ^{+10.8} _{-9.7}	6.1 ^{+4.9} _{-3.8}	17.4 ^{+6.7} _{-5.6}	10.1 ^{+8.0} _{-6.9}	25.4 ^{+7.6} _{-6.6}
224	520.3 ^{+24.7} _{-23.7}	287.1 ^{+18.3} _{-17.3}	233.1 ^{+17.2} _{-16.2}	523.0 ^{+24.8} _{-23.8}	52.7 ^{+8.8} _{-7.7}	281.1 ^{+18.1} _{-17.1}	189.3 ^{+15.7} _{-14.7}	289.9 ^{+18.5} _{-17.4}
225	53831.4 ^{+233.6} _{-232.5}	37109.0 ^{+193.9} _{-192.9}	16722.3 ^{+130.8} _{-129.8}	54045.4 ^{+234.0} _{-233.0}	10214.9 ^{+102.3} _{-101.3}	32793.5 ^{+182.4} _{-181.4}	11036.9 ^{+106.6} _{-105.6}	37323.1 ^{+194.5} _{-193.5}
226	18.9 ^{+6.6} _{-5.5}	8.0 ^{+4.5} _{-3.3}	10.9 ^{+5.5} _{-4.4}	18.7 ^{+6.6} _{-5.5}	2.9 ^{+3.2} _{-1.9}	4.0 ^{+3.8} _{-2.6}	11.8 ^{+5.5} _{-4.4}	7.8 ^{+4.5} _{-3.3}
227	36.3 ^{+10.1} _{-9.0}	20.8 ^{+7.0} _{-5.9}	15.5 ^{+7.9} _{-6.8}	34.9 ^{+10.1} _{-9.0}	3.4 ^{+4.5} _{-3.4}	22.8 ^{+7.0} _{-5.9}	8.7 ^{+7.0} _{-5.9}	19.4 ^{+7.0} _{-5.9}
228	172.6 ^{+16.2} _{-15.1}	127.0 ^{+13.1} _{-12.1}	45.5 ^{+10.2} _{-9.1}	174.2 ^{+16.3} _{-15.2}	41.9 ^{+8.3} _{-7.2}	96.5 ^{+11.7} _{-10.6}	35.7 ^{+9.3} _{-8.2}	128.6 ^{+13.3} _{-12.2}
229	56.7 ^{+9.8} _{-8.7}	35.8 ^{+7.4} _{-6.3}	20.9 ^{+7.1} _{-6.0}	56.3 ^{+9.8} _{-8.7}	7.0 ^{+4.1} _{-3.0}	32.2 ^{+7.2} _{-6.1}	17.1 ^{+6.5} _{-5.4}	35.4 ^{+7.4} _{-6.3}
230	22.9 ^{+7.5} _{-6.4}	7.2 ^{+4.6} _{-3.4}	15.7 ^{+6.5} _{-5.4}	24.6 ^{+7.7} _{-6.6}	3.9 ^{+3.8} _{-2.6}	5.2 ^{+4.1} _{-3.0}	15.5 ^{+6.3} _{-5.2}	8.8 ^{+4.9} _{-3.7}
231	71.5 ^{+12.5} _{-11.5}	29.6 ^{+7.8} _{-6.7}	41.9 ^{+10.3} _{-9.3}	72.5 ^{+12.6} _{-11.5}	8.3 ^{+5.2} _{-4.0}	25.8 ^{+7.4} _{-6.3}	38.4 ^{+9.8} _{-8.7}	30.6 ^{+7.9} _{-6.9}
232	13.8 ^{+6.2} _{-5.1}	5.3 ^{+4.0} _{-2.8}	8.5 ^{+5.4} _{-4.2}	13.3 ^{+6.2} _{-5.1}	-0.8 ^{+2.3} _{-0.9}	6.9 ^{+4.3} _{-3.1}	7.2 ^{+5.0} _{-3.9}	4.8 ^{+4.0} _{-2.8}
233	296.0 ^{+19.5} _{-18.4}	203.9 ^{+15.8} _{-14.8}	92.2 ^{+12.0} _{-11.0}	296.8 ^{+19.5} _{-18.5}	59.6 ^{+9.3} _{-8.3}	179.4 ^{+14.8} _{-13.8}	57.8 ^{+10.1} _{-9.1}	204.6 ^{+15.9} _{-14.9}
234	98.0 ^{+12.1} _{-11.1}	17.8 ^{+6.1} _{-5.0}	80.2 ^{+10.9} _{-9.8}	98.7 ^{+12.2} _{-11.1}	0.2 ^{+3.0} _{-1.7}	38.7 ^{+7.9} _{-6.8}	59.9 ^{+9.6} _{-8.6}	18.5 ^{+6.2} _{-5.1}
235	93.0 ^{+13.6} _{-12.5}	26.9 ^{+7.8} _{-6.7}	66.1 ^{+11.6} _{-10.5}	93.2 ^{+13.6} _{-12.6}	4.4 ^{+5.0} _{-3.8}	36.9 ^{+8.3} _{-7.2}	51.9 ^{+10.6} _{-9.5}	27.2 ^{+8.0} _{-6.9}
236	1025.6 ^{+36.0} _{-34.9}	983.5 ^{+33.4} _{-32.4}	42.2 ^{+14.1} _{-13.0}	1041.0 ^{+36.3} _{-35.2}	618.7 ^{+26.6} _{-25.6}	388.2 ^{+22.2} _{-21.1}	34.1 ^{+12.8} _{-11.7}	998.8 ^{+33.7} _{-32.7}
237	935.7 ^{+32.8} _{-31.8}	596.8 ^{+26.0} _{-25.0}	338.8 ^{+20.7} _{-19.6}	941.1 ^{+32.9} _{-31.9}	159.4 ^{+14.3} _{-13.2}	549.7 ^{+24.9} _{-23.9}	232.0 ^{+17.5} _{-16.5}	602.3 ^{+26.2} _{-25.1}
238	304.1 ^{+19.5} _{-18.5}	173.4 ^{+14.7} _{-13.7}	130.7 ^{+13.5} _{-12.4}	304.8 ^{+19.6} _{-18.5}	30.3 ^{+7.3} _{-6.2}	170.5 ^{+14.5} _{-13.5}	104.0 ^{+12.2} _{-11.1}	174.1 ^{+14.8} _{-13.8}
239	16.9 ^{+8.6} _{-7.5}	2.3 ^{+4.8} _{-3.7}	14.6 ^{+7.6} _{-6.5}	17.9 ^{+8.7} _{-7.6}	2.1 ^{+4.0} _{-2.8}	5.2 ^{+4.9} _{-3.8}	10.6 ^{+7.0} _{-5.9}	3.3 ^{+5.1} _{-3.9}
240	137.3 ^{+14.1} _{-13.0}	80.3 ^{+10.6} _{-9.5}	57.0 ^{+10.0} _{-8.9}	138.3 ^{+14.2} _{-13.1}	11.8 ^{+5.4} _{-4.2}	81.0 ^{+10.5} _{-9.4}	45.5 ^{+9.1} _{-8.0}	81.3 ^{+10.7} _{-9.6}
241	86.7 ^{+12.8} _{-11.8}	36.4 ^{+8.2} _{-7.1}	50.2 ^{+10.4} _{-9.4}	87.9 ^{+12.9} _{-11.9}	0.7 ^{+4.1} _{-2.9}	52.0 ^{+9.3} _{-8.2}	35.3 ^{+9.1} _{-8.1}	37.7 ^{+8.4} _{-7.3}
242	44.7 ^{+9.3} _{-8.2}	39.4 ^{+7.8} _{-6.7}	5.4 ^{+5.7} _{-4.6}	47.0 ^{+9.4} _{-8.4}	33.3 ^{+7.2} _{-6.1}	5.6 ^{+4.5} _{-3.4}	8.1 ^{+5.7} _{-4.6}	41.6 ^{+8.0} _{-7.0}
243	38.6 ^{+11.1} _{-10.1}	9.9 ^{+6.2} _{-5.1}	28.7 ^{+9.8} _{-8.7}	40.1 ^{+11.3} _{-10.2}	0.2 ^{+4.1} _{-2.9}	16.7 ^{+6.8} _{-5.7}	23.2 ^{+9.0} _{-7.9}	11.4 ^{+6.5} _{-5.4}

Table 5—Continued

Source No	<i>net_cnts</i> [1] [0.5–8.0keV]	<i>net_cnts</i> [2] [0.5–2.0keV]	<i>net_cnts</i> [3] [2.0–8.0keV]	<i>net_cnts</i> [4] [0.35–8.0keV]	<i>net_cnts</i> [5] [0.35–1.1keV]	<i>net_cnts</i> [6] [1.1–2.6keV]	<i>net_cnts</i> [7] [2.6–8.0keV]	<i>net_cnts</i> [8] [0.35–2.0keV]
244	30.6 ^{+8.6} _{-7.5}	15.9 ^{+5.8} _{-4.7}	14.7 ^{+6.9} _{-5.8}	30.2 ^{+8.6} _{-7.5}	4.6 ^{+4.0} _{-2.8}	13.7 ^{+5.6} _{-4.5}	11.9 ^{+6.4} _{-5.3}	15.5 ^{+5.8} _{-4.7}
245	128.9 ^{+20.2} _{-19.2}	138.1 ^{+16.2} _{-15.1}	-9.2 ^{+12.9} _{-11.8}	133.6 ^{+20.5} _{-19.5}	82.1 ^{+12.7} _{-11.6}	58.8 ^{+12.3} _{-11.2}	-7.3 ^{+11.9} _{-10.9}	142.8 ^{+16.5} _{-15.5}
246	23.7 ^{+8.2} _{-7.1}	16.2 ^{+5.9} _{-4.8}	7.5 ^{+6.3} _{-5.2}	23.1 ^{+8.2} _{-7.1}	2.8 ^{+3.6} _{-2.4}	16.5 ^{+5.9} _{-4.8}	3.8 ^{+5.7} _{-4.6}	15.6 ^{+5.9} _{-4.8}
247	46.7 ^{+9.0} _{-7.9}	12.3 ^{+5.0} _{-3.8}	34.5 ^{+8.0} _{-6.9}	46.9 ^{+9.1} _{-8.0}	1.9 ^{+3.2} _{-2.0}	18.3 ^{+5.8} _{-4.7}	26.7 ^{+7.2} _{-6.1}	12.5 ^{+5.1} _{-4.0}
248	1740.8 ^{+44.0} _{-43.0}	1147.7 ^{+35.3} _{-34.2}	593.1 ^{+27.0} _{-26.0}	1751.3 ^{+44.2} _{-43.2}	355.6 ^{+20.3} _{-19.3}	936.7 ^{+32.0} _{-31.0}	459.1 ^{+24.1} _{-23.0}	1158.2 ^{+35.5} _{-34.5}
249	120.1 ^{+21.5} _{-20.5}	99.1 ^{+15.1} _{-14.0}	21.0 ^{+16.0} _{-15.0}	125.5 ^{+21.9} _{-20.8}	79.5 ^{+12.5} _{-11.5}	25.7 ^{+11.6} _{-10.5}	20.3 ^{+14.8} _{-13.8}	104.4 ^{+15.5} _{-14.5}
250	190.7 ^{+16.8} _{-15.7}	75.6 ^{+10.7} _{-9.6}	115.1 ^{+13.4} _{-12.4}	190.5 ^{+16.8} _{-15.8}	12.4 ^{+5.8} _{-4.7}	96.0 ^{+11.6} _{-10.5}	82.1 ^{+11.7} _{-10.7}	75.4 ^{+10.8} _{-9.7}
251	81.5 ^{+11.4} _{-10.4}	23.1 ^{+6.8} _{-5.7}	58.4 ^{+9.7} _{-8.6}	81.1 ^{+11.4} _{-10.4}	4.9 ^{+4.2} _{-3.0}	26.8 ^{+6.9} _{-5.8}	49.5 ^{+9.0} _{-8.0}	22.7 ^{+6.8} _{-5.7}
252	153.2 ^{+15.5} _{-14.5}	37.9 ^{+8.6} _{-7.5}	115.3 ^{+13.4} _{-12.4}	153.2 ^{+15.5} _{-14.5}	-1.7 ^{+3.7} _{-2.5}	66.9 ^{+10.2} _{-9.1}	88.0 ^{+12.0} _{-11.0}	37.9 ^{+8.6} _{-7.6}
253	63.3 ^{+12.1} _{-11.0}	36.0 ^{+8.2} _{-7.1}	27.4 ^{+9.4} _{-8.4}	62.7 ^{+12.1} _{-11.1}	4.6 ^{+4.7} _{-3.5}	37.9 ^{+8.3} _{-7.3}	20.3 ^{+8.6} _{-7.5}	35.4 ^{+8.3} _{-7.2}
254	15.5 ^{+5.5} _{-4.3}	11.1 ^{+4.6} _{-3.4}	4.4 ^{+3.8} _{-2.6}	15.3 ^{+5.5} _{-4.3}	0.3 ^{+2.3} _{-0.8}	12.3 ^{+4.7} _{-3.6}	2.6 ^{+3.4} _{-2.2}	10.9 ^{+4.6} _{-3.4}
255	570.9 ^{+25.7} _{-24.7}	376.5 ^{+20.7} _{-19.7}	194.3 ^{+16.0} _{-14.9}	575.5 ^{+25.9} _{-24.8}	103.8 ^{+11.5} _{-10.4}	318.8 ^{+19.2} _{-18.2}	152.9 ^{+14.3} _{-13.3}	381.1 ^{+20.9} _{-19.8}
256	88.7 ^{+11.2} _{-10.1}	55.1 ^{+8.7} _{-7.7}	33.6 ^{+7.6} _{-6.6}	89.7 ^{+11.2} _{-10.2}	13.3 ^{+5.0} _{-3.8}	49.0 ^{+8.3} _{-7.2}	27.4 ^{+7.1} _{-6.0}	56.1 ^{+8.8} _{-7.7}
257	25.9 ^{+9.2} _{-8.1}	16.1 ^{+6.2} _{-5.1}	9.8 ^{+7.3} _{-6.3}	25.3 ^{+9.2} _{-8.2}	3.0 ^{+4.0} _{-2.8}	12.8 ^{+6.0} _{-4.9}	9.5 ^{+6.9} _{-5.8}	15.5 ^{+6.3} _{-5.2}
258	38.5 ^{+9.0} _{-7.9}	23.6 ^{+6.8} _{-5.7}	14.9 ^{+6.6} _{-5.5}	39.0 ^{+9.1} _{-8.0}	6.4 ^{+4.6} _{-3.5}	18.4 ^{+6.0} _{-4.9}	14.2 ^{+6.3} _{-5.2}	24.1 ^{+6.9} _{-5.8}
259	74.1 ^{+10.5} _{-9.5}	41.2 ^{+7.8} _{-6.7}	33.0 ^{+7.7} _{-6.7}	75.1 ^{+10.6} _{-9.5}	10.1 ^{+4.6} _{-3.4}	37.8 ^{+7.5} _{-6.4}	27.2 ^{+7.2} _{-6.1}	42.1 ^{+7.9} _{-6.8}
260	22.4 ^{+8.3} _{-7.2}	21.3 ^{+6.7} _{-5.5}	1.1 ^{+5.7} _{-4.6}	22.0 ^{+8.3} _{-7.2}	5.9 ^{+4.2} _{-3.0}	21.4 ^{+6.7} _{-5.5}	-5.3 ^{+4.5} _{-3.4}	20.9 ^{+6.7} _{-5.6}
261	30.3 ^{+10.6} _{-9.6}	26.5 ^{+7.8} _{-6.8}	3.7 ^{+7.8} _{-6.7}	29.9 ^{+10.7} _{-9.6}	11.8 ^{+5.8} _{-4.7}	16.8 ^{+6.8} _{-5.7}	1.3 ^{+7.2} _{-6.1}	26.2 ^{+7.9} _{-6.8}
262	532.0 ^{+25.2} _{-24.2}	305.5 ^{+19.1} _{-18.0}	226.4 ^{+17.2} _{-16.1}	531.3 ^{+25.2} _{-24.2}	74.4 ^{+10.1} _{-9.1}	292.5 ^{+18.6} _{-17.6}	164.3 ^{+15.0} _{-13.9}	304.8 ^{+19.1} _{-18.0}
263	403.9 ^{+21.2} _{-20.2}	224.3 ^{+16.0} _{-15.0}	179.6 ^{+14.5} _{-13.5}	405.8 ^{+21.2} _{-20.2}	54.7 ^{+8.5} _{-7.4}	208.2 ^{+15.5} _{-14.4}	142.9 ^{+13.1} _{-12.0}	226.2 ^{+16.1} _{-15.1}
264	202.2 ^{+16.3} _{-15.3}	74.7 ^{+10.3} _{-9.2}	127.5 ^{+13.2} _{-12.2}	202.7 ^{+16.4} _{-15.3}	14.1 ^{+5.3} _{-4.2}	84.7 ^{+10.8} _{-9.7}	103.9 ^{+12.1} _{-11.0}	75.2 ^{+10.3} _{-9.3}
265	31.3 ^{+7.7} _{-6.6}	7.5 ^{+4.4} _{-3.3}	23.8 ^{+6.8} _{-5.7}	30.5 ^{+7.7} _{-6.6}	1.9 ^{+3.2} _{-1.9}	10.9 ^{+4.9} _{-3.7}	17.7 ^{+6.1} _{-5.0}	6.7 ^{+4.5} _{-3.3}
266	99.3 ^{+12.6} _{-11.6}	63.5 ^{+9.8} _{-8.8}	35.8 ^{+8.6} _{-7.6}	100.3 ^{+12.7} _{-11.7}	10.4 ^{+5.5} _{-4.4}	61.9 ^{+9.4} _{-8.3}	27.9 ^{+7.9} _{-6.9}	64.5 ^{+9.9} _{-8.9}
267	21.4 ^{+11.1} _{-10.0}	11.3 ^{+7.3} _{-6.2}	10.1 ^{+8.9} _{-7.9}	22.2 ^{+11.2} _{-10.1}	7.4 ^{+5.8} _{-4.6}	5.8 ^{+6.4} _{-5.3}	9.0 ^{+8.3} _{-7.2}	12.0 ^{+7.4} _{-6.4}
268	363.0 ^{+20.8} _{-19.8}	217.3 ^{+16.1} _{-15.0}	145.8 ^{+13.8} _{-12.8}	364.8 ^{+20.8} _{-19.8}	60.1 ^{+9.1} _{-8.0}	195.5 ^{+15.3} _{-14.3}	109.2 ^{+12.2} _{-11.2}	219.0 ^{+16.1} _{-15.1}
269	37.4 ^{+7.5} _{-6.4}	26.2 ^{+6.3} _{-5.2}	11.2 ^{+4.9} _{-3.7}	37.3 ^{+7.5} _{-6.4}	10.6 ^{+4.4} _{-3.3}	20.9 ^{+5.8} _{-4.7}	5.8 ^{+4.0} _{-2.8}	26.1 ^{+6.3} _{-5.2}
270	108.9 ^{+21.8} _{-20.8}	71.0 ^{+14.6} _{-13.6}	37.8 ^{+16.8} _{-15.7}	108.5 ^{+22.0} _{-21.0}	56.0 ^{+11.6} _{-10.6}	21.3 ^{+11.9} _{-10.8}	31.3 ^{+15.5} _{-14.5}	70.7 ^{+14.9} _{-13.8}

Table 5—Continued

Source No	<i>net_cnts</i> [1] [0.5–8.0keV]	<i>net_cnts</i> [2] [0.5–2.0keV]	<i>net_cnts</i> [3] [2.0–8.0keV]	<i>net_cnts</i> [4] [0.35–8.0keV]	<i>net_cnts</i> [5] [0.35–1.1keV]	<i>net_cnts</i> [6] [1.1–2.6keV]	<i>net_cnts</i> [7] [2.6–8.0keV]	<i>net_cnts</i> [8] [0.35–2.0keV]
271	36.2 ^{+9.5} _{-8.5}	25.5 ^{+7.2} _{-6.1}	10.8 ^{+6.9} _{-5.8}	35.4 ^{+9.5} _{-8.5}	2.9 ^{+4.3} _{-3.2}	21.6 ^{+6.6} _{-5.5}	10.9 ^{+6.6} _{-5.6}	24.7 ^{+7.2} _{-6.1}
272	235.5 ^{+18.2} _{-17.2}	203.8 ^{+16.0} _{-14.9}	31.7 ^{+9.5} _{-8.4}	235.5 ^{+18.2} _{-17.2}	58.3 ^{+9.3} _{-8.3}	160.5 ^{+14.3} _{-13.3}	16.7 ^{+8.2} _{-7.1}	203.8 ^{+16.0} _{-15.0}
273	19.8 ^{+7.1} _{-6.0}	1.7 ^{+3.6} _{-2.4}	18.1 ^{+6.5} _{-5.4}	20.5 ^{+7.1} _{-6.0}	-0.1 ^{+2.7} _{-1.3}	6.1 ^{+4.3} _{-3.1}	14.4 ^{+6.0} _{-4.9}	2.4 ^{+3.8} _{-2.6}
274	413.3 ^{+21.9} _{-20.9}	164.2 ^{+14.1} _{-13.1}	249.1 ^{+17.3} _{-16.3}	413.3 ^{+21.9} _{-20.9}	30.0 ^{+7.0} _{-5.9}	161.5 ^{+13.9} _{-12.9}	221.9 ^{+16.4} _{-15.3}	164.2 ^{+14.2} _{-13.1}
275	156.8 ^{+14.1} _{-13.1}	105.1 ^{+11.5} _{-10.4}	51.7 ^{+8.9} _{-7.9}	157.7 ^{+14.2} _{-13.1}	27.6 ^{+6.5} _{-5.4}	88.0 ^{+10.7} _{-9.6}	42.1 ^{+8.2} _{-7.1}	106.0 ^{+11.5} _{-10.5}
276	7.8 ^{+9.8} _{-8.8}	0.0 ^{+6.1} _{-5.0}	7.8 ^{+8.2} _{-7.2}	6.0 ^{+9.8} _{-8.8}	-4.1 ^{+4.4} _{-3.2}	2.3 ^{+5.7} _{-4.6}	7.8 ^{+7.8} _{-6.7}	-1.8 ^{+6.1} _{-5.0}
277	382.3 ^{+21.9} _{-20.9}	232.3 ^{+16.9} _{-15.9}	150.1 ^{+14.6} _{-13.5}	383.1 ^{+22.0} _{-20.9}	37.4 ^{+8.2} _{-7.1}	234.2 ^{+16.8} _{-15.8}	111.4 ^{+12.8} _{-11.7}	233.0 ^{+17.0} _{-15.9}
278	179.5 ^{+14.7} _{-13.7}	160.7 ^{+13.8} _{-12.8}	18.8 ^{+6.0} _{-4.9}	185.0 ^{+15.0} _{-13.9}	83.4 ^{+10.3} _{-9.3}	88.1 ^{+10.5} _{-9.5}	13.4 ^{+5.3} _{-4.2}	166.2 ^{+14.1} _{-13.0}
279	1451.1 ^{+40.3} _{-39.3}	1377.8 ^{+38.6} _{-37.5}	73.3 ^{+12.8} _{-11.7}	1480.8 ^{+40.8} _{-39.7}	957.8 ^{+32.2} _{-31.2}	493.9 ^{+23.8} _{-22.8}	29.1 ^{+10.2} _{-9.2}	1407.5 ^{+39.0} _{-38.0}
280	116.3 ^{+14.0} _{-12.9}	24.4 ^{+7.2} _{-6.2}	91.9 ^{+12.4} _{-11.4}	117.0 ^{+14.1} _{-13.0}	-0.8 ^{+3.7} _{-2.5}	42.3 ^{+8.6} _{-7.5}	75.5 ^{+11.4} _{-10.3}	25.1 ^{+7.4} _{-6.3}
281	822.1 ^{+30.2} _{-29.2}	330.9 ^{+19.4} _{-18.4}	491.2 ^{+23.6} _{-22.6}	823.6 ^{+30.2} _{-29.2}	24.8 ^{+6.5} _{-5.4}	414.9 ^{+21.5} _{-20.5}	383.8 ^{+21.1} _{-20.0}	332.4 ^{+19.5} _{-18.5}
282	227.6 ^{+17.4} _{-16.4}	145.5 ^{+13.6} _{-12.5}	82.1 ^{+11.6} _{-10.5}	228.4 ^{+17.5} _{-16.5}	46.7 ^{+8.3} _{-7.2}	127.7 ^{+13.0} _{-11.9}	54.1 ^{+9.9} _{-8.8}	146.3 ^{+13.7} _{-12.6}
283	380.6 ^{+21.3} _{-20.3}	223.9 ^{+16.3} _{-15.3}	156.8 ^{+14.4} _{-13.3}	382.7 ^{+21.4} _{-20.4}	48.8 ^{+8.4} _{-7.3}	207.9 ^{+15.7} _{-14.7}	126.1 ^{+13.1} _{-12.0}	225.9 ^{+16.4} _{-15.4}
284	52.1 ^{+10.6} _{-9.5}	3.6 ^{+4.9} _{-3.8}	48.4 ^{+9.8} _{-8.7}	51.5 ^{+10.7} _{-9.6}	2.7 ^{+4.0} _{-2.8}	4.3 ^{+5.1} _{-3.9}	44.5 ^{+9.3} _{-8.3}	3.0 ^{+5.1} _{-3.9}
285	154.9 ^{+14.2} _{-13.2}	98.0 ^{+11.2} _{-10.2}	56.9 ^{+9.5} _{-8.4}	155.6 ^{+14.3} _{-13.2}	8.9 ^{+4.4} _{-3.3}	98.9 ^{+11.3} _{-10.2}	47.8 ^{+8.8} _{-7.7}	98.6 ^{+11.3} _{-10.2}
286	41.8 ^{+10.4} _{-9.3}	6.3 ^{+5.3} _{-4.2}	35.5 ^{+9.4} _{-8.3}	41.4 ^{+10.4} _{-9.4}	5.2 ^{+4.5} _{-3.3}	2.8 ^{+4.9} _{-3.8}	33.5 ^{+8.9} _{-7.9}	5.9 ^{+5.4} _{-4.3}
287	1176.0 ^{+36.4} _{-35.4}	1137.0 ^{+35.1} _{-34.1}	39.0 ^{+10.7} _{-9.6}	1198.4 ^{+36.8} _{-35.8}	905.3 ^{+31.3} _{-30.3}	270.5 ^{+18.1} _{-17.1}	22.6 ^{+9.3} _{-8.2}	1159.4 ^{+35.5} _{-34.4}
288	57.6 ^{+15.0} _{-13.9}	66.1 ^{+11.8} _{-10.7}	-8.5 ^{+10.0} _{-8.9}	62.2 ^{+15.2} _{-14.2}	34.5 ^{+8.8} _{-7.7}	37.7 ^{+9.8} _{-8.8}	-10.0 ^{+9.1} _{-8.0}	70.7 ^{+12.1} _{-11.0}
289	20.7 ^{+7.7} _{-6.6}	17.5 ^{+5.9} _{-4.8}	3.2 ^{+5.6} _{-4.5}	21.2 ^{+7.7} _{-6.7}	7.4 ^{+4.3} _{-3.1}	13.7 ^{+5.6} _{-4.5}	0.1 ^{+4.8} _{-3.7}	18.0 ^{+6.0} _{-4.9}
290	35.4 ^{+10.8} _{-9.7}	2.6 ^{+5.3} _{-4.2}	32.8 ^{+9.8} _{-8.8}	33.6 ^{+10.8} _{-9.7}	-1.7 ^{+3.9} _{-2.7}	8.8 ^{+6.0} _{-4.9}	26.5 ^{+9.0} _{-7.9}	0.8 ^{+5.3} _{-4.2}
291	33.9 ^{+8.7} _{-7.6}	17.8 ^{+6.1} _{-5.0}	16.1 ^{+6.9} _{-5.8}	34.6 ^{+8.8} _{-7.7}	11.9 ^{+4.9} _{-3.7}	8.7 ^{+5.1} _{-4.0}	14.0 ^{+6.5} _{-5.4}	18.5 ^{+6.2} _{-5.1}
292	14.9 ^{+5.7} _{-4.6}	9.5 ^{+4.4} _{-3.3}	5.4 ^{+4.3} _{-3.1}	16.8 ^{+5.9} _{-4.8}	3.4 ^{+3.2} _{-1.9}	9.3 ^{+4.4} _{-3.3}	4.1 ^{+4.0} _{-2.8}	11.3 ^{+4.7} _{-3.6}
293	55.2 ^{+9.9} _{-8.8}	27.9 ^{+7.0} _{-5.9}	27.3 ^{+7.6} _{-6.5}	55.6 ^{+9.9} _{-8.9}	8.3 ^{+4.6} _{-3.4}	23.2 ^{+6.6} _{-5.5}	24.1 ^{+7.1} _{-6.0}	28.3 ^{+7.1} _{-6.0}
294	38.6 ^{+10.2} _{-9.2}	7.2 ^{+5.9} _{-4.7}	31.3 ^{+8.9} _{-7.8}	39.9 ^{+10.4} _{-9.3}	5.6 ^{+4.6} _{-3.5}	9.8 ^{+6.0} _{-4.8}	24.6 ^{+8.2} _{-7.1}	8.6 ^{+6.1} _{-5.0}
295	99.0 ^{+12.6} _{-11.6}	49.9 ^{+8.9} _{-7.8}	49.1 ^{+9.6} _{-8.5}	99.1 ^{+12.7} _{-11.6}	8.9 ^{+4.9} _{-3.7}	57.6 ^{+9.3} _{-8.2}	32.6 ^{+8.4} _{-7.3}	50.0 ^{+9.0} _{-7.9}
296	25.3 ^{+7.8} _{-6.7}	11.7 ^{+5.5} _{-4.4}	13.5 ^{+6.2} _{-5.1}	25.9 ^{+7.9} _{-6.8}	2.7 ^{+3.8} _{-2.6}	16.2 ^{+5.8} _{-4.7}	6.9 ^{+5.3} _{-4.1}	12.3 ^{+5.6} _{-4.5}
297	63.6 ^{+9.7} _{-8.7}	34.6 ^{+7.2} _{-6.1}	29.0 ^{+7.2} _{-6.1}	63.3 ^{+9.7} _{-8.7}	7.5 ^{+4.1} _{-3.0}	29.1 ^{+6.7} _{-5.6}	26.7 ^{+6.9} _{-5.8}	34.3 ^{+7.2} _{-6.1}

Table 5—Continued

Source No	<i>net_cnts[1]</i> [0.5–8.0keV]	<i>net_cnts[2]</i> [0.5–2.0keV]	<i>net_cnts[3]</i> [2.0–8.0keV]	<i>net_cnts[4]</i> [0.35–8.0keV]	<i>net_cnts[5]</i> [0.35–1.1keV]	<i>net_cnts[6]</i> [1.1–2.6keV]	<i>net_cnts[7]</i> [2.6–8.0keV]	<i>net_cnts[8]</i> [0.35–2.0keV]
298	$144.4^{+14.0}_{-12.9}$	$147.4^{+13.4}_{-12.3}$	$-3.0^{+4.9}_{-3.8}$	$147.0^{+14.1}_{-13.0}$	$116.1^{+11.9}_{-10.9}$	$33.3^{+7.4}_{-6.3}$	$-2.4^{+4.6}_{-3.4}$	$150.0^{+13.5}_{-12.5}$
299	$2035.3^{+47.5}_{-46.5}$	$1252.4^{+37.0}_{-36.0}$	$782.8^{+30.4}_{-29.3}$	$2048.5^{+47.6}_{-46.6}$	$377.0^{+21.0}_{-20.0}$	$1075.8^{+34.4}_{-33.4}$	$595.7^{+26.7}_{-25.6}$	$1265.7^{+37.3}_{-36.2}$
300	$40.9^{+10.6}_{-9.5}$	$18.0^{+6.9}_{-5.8}$	$22.9^{+8.6}_{-7.6}$	$39.6^{+10.6}_{-9.5}$	$4.1^{+4.6}_{-3.5}$	$21.7^{+7.0}_{-5.9}$	$13.9^{+7.7}_{-6.6}$	$16.7^{+6.9}_{-5.8}$
301	$204.2^{+15.7}_{-14.6}$	$141.6^{+13.0}_{-12.0}$	$62.6^{+9.5}_{-8.4}$	$205.0^{+15.7}_{-14.7}$	$46.9^{+8.0}_{-6.9}$	$114.2^{+11.9}_{-10.8}$	$43.8^{+8.2}_{-7.1}$	$142.4^{+13.1}_{-12.0}$
302	$44.6^{+9.9}_{-8.8}$	$49.8^{+8.6}_{-7.5}$	$-5.2^{+5.6}_{-4.5}$	$43.5^{+9.9}_{-8.8}$	$18.9^{+5.9}_{-4.8}$	$28.8^{+7.1}_{-6.0}$	$-4.2^{+5.3}_{-4.2}$	$48.7^{+8.6}_{-7.6}$
303	$37.7^{+8.9}_{-7.8}$	$18.2^{+6.0}_{-4.9}$	$19.5^{+7.1}_{-6.0}$	$36.8^{+8.9}_{-7.8}$	$5.2^{+4.0}_{-2.8}$	$16.9^{+5.9}_{-4.8}$	$14.7^{+6.5}_{-5.4}$	$17.3^{+6.0}_{-4.9}$
304	$56.5^{+11.7}_{-10.7}$	$26.8^{+8.0}_{-6.9}$	$29.7^{+9.1}_{-8.1}$	$59.0^{+11.9}_{-10.8}$	$6.9^{+5.2}_{-4.0}$	$31.0^{+8.1}_{-7.0}$	$21.1^{+8.2}_{-7.1}$	$29.3^{+8.2}_{-7.2}$
305	$108.6^{+12.4}_{-11.3}$	$50.7^{+8.7}_{-7.6}$	$57.9^{+9.4}_{-8.4}$	$108.1^{+12.4}_{-11.3}$	$4.9^{+4.1}_{-3.0}$	$55.0^{+8.9}_{-7.8}$	$48.2^{+8.7}_{-7.6}$	$50.3^{+8.7}_{-7.6}$
306	$29.6^{+7.6}_{-6.6}$	$20.1^{+6.0}_{-4.9}$	$9.6^{+5.4}_{-4.3}$	$29.1^{+7.6}_{-6.6}$	$-1.0^{+2.4}_{-0.9}$	$24.7^{+6.5}_{-5.4}$	$5.5^{+4.7}_{-3.5}$	$19.6^{+6.0}_{-4.9}$
307	$60.3^{+10.3}_{-9.3}$	$29.4^{+7.1}_{-6.0}$	$31.0^{+8.1}_{-7.0}$	$60.5^{+10.4}_{-9.3}$	$5.2^{+4.4}_{-3.2}$	$34.2^{+7.3}_{-6.3}$	$21.1^{+7.2}_{-6.1}$	$29.5^{+7.2}_{-6.1}$
308	$465.1^{+27.8}_{-26.8}$	$435.9^{+24.2}_{-23.2}$	$29.2^{+14.5}_{-13.5}$	$476.3^{+28.2}_{-27.1}$	$349.3^{+21.2}_{-20.2}$	$98.7^{+14.2}_{-13.1}$	$28.4^{+13.5}_{-12.5}$	$447.1^{+24.6}_{-23.5}$
309	$754.0^{+29.0}_{-27.9}$	$492.7^{+23.4}_{-22.3}$	$261.3^{+17.8}_{-16.8}$	$758.7^{+29.0}_{-28.0}$	$134.8^{+12.8}_{-11.7}$	$449.0^{+22.4}_{-21.3}$	$174.8^{+14.9}_{-13.9}$	$497.3^{+23.5}_{-22.5}$
310	$90.8^{+12.0}_{-11.0}$	$10.5^{+5.5}_{-4.4}$	$80.3^{+11.1}_{-10.0}$	$90.1^{+12.0}_{-11.0}$	$3.5^{+4.0}_{-2.8}$	$14.9^{+5.8}_{-4.7}$	$71.6^{+10.5}_{-9.5}$	$9.8^{+5.5}_{-4.4}$
311	$25.2^{+7.7}_{-6.7}$	$3.0^{+4.2}_{-3.0}$	$22.1^{+7.0}_{-5.9}$	$24.7^{+7.7}_{-6.7}$	$0.7^{+3.2}_{-1.9}$	$2.6^{+4.0}_{-2.8}$	$21.4^{+6.8}_{-5.7}$	$2.5^{+4.2}_{-3.0}$
312	$170.8^{+15.2}_{-14.1}$	$103.6^{+11.7}_{-10.6}$	$67.1^{+10.3}_{-9.3}$	$170.4^{+15.2}_{-14.1}$	$22.0^{+6.3}_{-5.1}$	$98.6^{+11.4}_{-10.3}$	$49.8^{+9.2}_{-8.1}$	$103.2^{+11.7}_{-10.6}$
313	$10.5^{+7.2}_{-6.2}$	$17.1^{+6.0}_{-4.9}$	$-6.5^{+4.8}_{-3.7}$	$10.1^{+7.2}_{-6.2}$	$2.0^{+3.6}_{-2.4}$	$14.1^{+5.6}_{-4.5}$	$-6.1^{+4.5}_{-3.4}$	$16.6^{+6.0}_{-4.9}$
314	$18.8^{+6.8}_{-5.7}$	$15.9^{+5.5}_{-4.3}$	$2.9^{+4.8}_{-3.6}$	$18.5^{+6.8}_{-5.7}$	$5.1^{+3.8}_{-2.6}$	$12.2^{+5.0}_{-3.8}$	$1.1^{+4.3}_{-3.2}$	$15.6^{+5.5}_{-4.3}$
315	$32.0^{+9.4}_{-8.3}$	$14.5^{+6.3}_{-5.2}$	$17.5^{+7.6}_{-6.5}$	$32.6^{+9.5}_{-8.4}$	$8.5^{+5.2}_{-4.0}$	$6.2^{+5.0}_{-3.9}$	$17.9^{+7.3}_{-6.2}$	$15.1^{+6.5}_{-5.4}$
316	$690.9^{+29.1}_{-28.1}$	$429.3^{+22.7}_{-21.6}$	$261.6^{+18.9}_{-17.9}$	$694.7^{+29.2}_{-28.1}$	$123.5^{+12.8}_{-11.8}$	$381.7^{+21.5}_{-20.4}$	$189.4^{+16.4}_{-15.3}$	$433.1^{+22.8}_{-21.7}$
317	$75.3^{+11.9}_{-10.8}$	$41.8^{+8.4}_{-7.4}$	$33.5^{+9.0}_{-7.9}$	$75.2^{+11.9}_{-10.9}$	$7.1^{+5.0}_{-3.9}$	$39.9^{+8.2}_{-7.1}$	$28.2^{+8.3}_{-7.2}$	$41.7^{+8.5}_{-7.4}$
318	$162779.9^{+405.0}_{-404.0}$	$102642.4^{+321.7}_{-320.7}$	$60137.5^{+246.7}_{-245.7}$	$163148.7^{+405.4}_{-404.4}$	$23331.4^{+153.9}_{-152.9}$	$97985.8^{+314.3}_{-313.3}$	$41831.6^{+206.0}_{-205.0}$	$103011.2^{+322.3}_{-321.3}$
319	$10.3^{+4.4}_{-3.3}$	$7.7^{+4.0}_{-2.8}$	$2.6^{+2.9}_{-1.6}$	$10.3^{+4.4}_{-3.3}$	$2.8^{+2.9}_{-1.6}$	$6.8^{+3.8}_{-2.6}$	$0.7^{+2.3}_{-0.8}$	$7.7^{+4.0}_{-2.8}$
320	$791.9^{+29.7}_{-28.7}$	$535.2^{+24.3}_{-23.3}$	$256.7^{+17.7}_{-16.7}$	$797.9^{+29.8}_{-28.8}$	$179.8^{+14.6}_{-13.6}$	$425.0^{+21.8}_{-20.8}$	$193.0^{+15.6}_{-14.6}$	$541.2^{+24.5}_{-23.4}$
321	$16.9^{+14.2}_{-13.1}$	$-0.1^{+9.0}_{-7.9}$	$17.1^{+11.5}_{-10.4}$	$15.5^{+14.2}_{-13.2}$	$-3.6^{+5.6}_{-4.5}$	$5.2^{+9.1}_{-8.0}$	$14.0^{+10.4}_{-9.4}$	$-1.6^{+9.1}_{-8.0}$
322	$42.8^{+10.2}_{-9.1}$	$38.4^{+8.1}_{-7.0}$	$4.3^{+6.9}_{-5.8}$	$44.2^{+10.3}_{-9.2}$	$16.3^{+5.8}_{-4.7}$	$26.9^{+7.2}_{-6.1}$	$0.9^{+6.1}_{-5.0}$	$39.8^{+8.2}_{-7.2}$
323	$124.5^{+12.9}_{-11.8}$	$74.4^{+9.9}_{-8.8}$	$50.0^{+8.9}_{-7.8}$	$123.8^{+12.9}_{-11.8}$	$14.2^{+5.2}_{-4.1}$	$70.7^{+9.6}_{-8.5}$	$39.0^{+8.1}_{-7.0}$	$73.8^{+9.9}_{-8.8}$
324	$20.4^{+6.3}_{-5.2}$	$13.2^{+5.0}_{-3.8}$	$7.3^{+4.6}_{-3.4}$	$20.3^{+6.3}_{-5.2}$	$5.9^{+3.8}_{-2.6}$	$9.4^{+4.4}_{-3.3}$	$5.0^{+4.1}_{-3.0}$	$13.0^{+5.0}_{-3.8}$

Table 5—Continued

Source No	<i>net_cnts</i> [1] [0.5–8.0keV]	<i>net_cnts</i> [2] [0.5–2.0keV]	<i>net_cnts</i> [3] [2.0–8.0keV]	<i>net_cnts</i> [4] [0.35–8.0keV]	<i>net_cnts</i> [5] [0.35–1.1keV]	<i>net_cnts</i> [6] [1.1–2.6keV]	<i>net_cnts</i> [7] [2.6–8.0keV]	<i>net_cnts</i> [8] [0.35–2.0keV]
325	28.5 ^{+9.3} _{-8.2}	21.3 ^{+7.1} _{-6.1}	7.2 ^{+6.6} _{-5.5}	27.7 ^{+9.3} _{-8.2}	14.8 ^{+5.6} _{-4.5}	8.6 ^{+6.0} _{-4.9}	4.4 ^{+5.9} _{-4.8}	20.6 ^{+7.1} _{-6.1}
326	27.4 ^{+8.0} _{-6.9}	11.2 ^{+5.1} _{-3.9}	16.3 ^{+6.8} _{-5.6}	26.6 ^{+8.0} _{-6.9}	2.2 ^{+3.3} _{-2.0}	9.0 ^{+5.0} _{-3.8}	15.5 ^{+6.5} _{-5.3}	10.3 ^{+5.1} _{-3.9}
327	124.4 ^{+13.9} _{-12.9}	68.9 ^{+10.1} _{-9.1}	55.5 ^{+10.2} _{-9.1}	124.5 ^{+14.0} _{-12.9}	13.4 ^{+5.7} _{-4.6}	69.4 ^{+10.0} _{-8.9}	41.7 ^{+9.2} _{-8.1}	69.0 ^{+10.2} _{-9.1}
328	85.9 ^{+17.7} _{-16.6}	95.3 ^{+13.8} _{-12.8}	-9.4 ^{+11.7} _{-10.6}	87.5 ^{+17.9} _{-16.8}	77.6 ^{+12.0} _{-10.9}	20.7 ^{+9.4} _{-8.4}	-10.8 ^{+10.7} _{-9.7}	96.9 ^{+14.1} _{-13.0}
329	59.2 ^{+10.7} _{-9.7}	39.4 ^{+8.2} _{-7.1}	19.8 ^{+7.6} _{-6.5}	57.8 ^{+10.7} _{-9.7}	5.6 ^{+4.8} _{-3.6}	40.3 ^{+8.0} _{-6.9}	11.9 ^{+6.7} _{-5.6}	37.9 ^{+8.2} _{-7.1}
330	43.0 ^{+9.6} _{-8.6}	22.4 ^{+6.9} _{-5.8}	20.6 ^{+7.4} _{-6.3}	43.8 ^{+9.7} _{-8.7}	10.0 ^{+5.0} _{-3.9}	18.3 ^{+6.4} _{-5.3}	15.5 ^{+6.7} _{-5.6}	23.2 ^{+7.0} _{-5.9}
331	28.8 ^{+7.3} _{-6.3}	13.0 ^{+5.0} _{-3.8}	15.8 ^{+6.0} _{-4.9}	28.6 ^{+7.3} _{-6.3}	2.9 ^{+3.2} _{-1.9}	17.9 ^{+5.6} _{-4.4}	7.7 ^{+5.0} _{-3.9}	12.8 ^{+5.0} _{-3.8}
332	95.0 ^{+14.9} _{-13.8}	94.8 ^{+12.5} _{-11.5}	0.1 ^{+8.7} _{-7.7}	92.5 ^{+15.0} _{-13.9}	81.2 ^{+11.3} _{-10.3}	11.6 ^{+7.2} _{-6.1}	-0.3 ^{+8.1} _{-7.1}	92.3 ^{+12.6} _{-11.6}
333	103.3 ^{+12.3} _{-11.2}	79.6 ^{+10.3} _{-9.3}	23.8 ^{+7.4} _{-6.3}	103.9 ^{+12.3} _{-11.3}	25.9 ^{+6.6} _{-5.5}	62.0 ^{+9.2} _{-8.2}	16.0 ^{+6.5} _{-5.4}	80.1 ^{+10.4} _{-9.3}
334	2054.5 ^{+47.6} _{-46.6}	2039.3 ^{+46.7} _{-45.6}	15.1 ^{+10.5} _{-9.4}	2093.1 ^{+48.1} _{-47.1}	1614.1 ^{+41.5} _{-40.5}	488.4 ^{+23.9} _{-22.8}	-9.4 ^{+8.3} _{-7.3}	2077.9 ^{+47.1} _{-46.1}
335	187.4 ^{+16.8} _{-15.8}	111.7 ^{+12.3} _{-11.3}	75.7 ^{+12.0} _{-11.0}	192.2 ^{+16.9} _{-15.9}	20.8 ^{+6.4} _{-5.3}	116.5 ^{+12.4} _{-11.3}	54.9 ^{+10.8} _{-9.8}	116.6 ^{+12.5} _{-11.5}
336	148.3 ^{+15.0} _{-13.9}	24.0 ^{+7.1} _{-6.0}	124.3 ^{+13.6} _{-12.6}	147.6 ^{+15.0} _{-13.9}	5.0 ^{+4.3} _{-3.2}	33.0 ^{+7.8} _{-6.7}	109.6 ^{+12.8} _{-11.8}	23.2 ^{+7.1} _{-6.0}
337	53.5 ^{+10.3} _{-9.2}	12.9 ^{+6.0} _{-4.9}	40.7 ^{+8.9} _{-7.8}	52.3 ^{+10.3} _{-9.2}	-3.3 ^{+3.3} _{-2.0}	19.0 ^{+6.3} _{-5.2}	36.6 ^{+8.4} _{-7.3}	11.6 ^{+6.0} _{-4.9}
338	54.6 ^{+11.5} _{-10.4}	34.9 ^{+8.2} _{-7.1}	19.7 ^{+8.6} _{-7.6}	53.9 ^{+11.5} _{-10.4}	10.3 ^{+5.5} _{-4.4}	30.8 ^{+7.7} _{-6.6}	12.7 ^{+7.8} _{-6.7}	34.2 ^{+8.2} _{-7.1}
339	137.5 ^{+13.4} _{-12.4}	108.8 ^{+11.7} _{-10.7}	28.7 ^{+7.3} _{-6.2}	137.9 ^{+13.5} _{-12.4}	33.9 ^{+7.2} _{-6.1}	76.1 ^{+10.1} _{-9.0}	27.8 ^{+7.0} _{-5.9}	109.1 ^{+11.8} _{-10.7}
340	23.3 ^{+9.4} _{-8.4}	11.0 ^{+6.6} _{-5.5}	12.3 ^{+7.3} _{-6.3}	23.7 ^{+9.5} _{-8.4}	1.0 ^{+4.5} _{-3.4}	14.2 ^{+6.4} _{-5.3}	8.6 ^{+6.7} _{-5.6}	11.4 ^{+6.7} _{-5.6}
341	33.4 ^{+10.4} _{-9.4}	16.4 ^{+6.8} _{-5.7}	17.1 ^{+8.5} _{-7.4}	33.4 ^{+10.5} _{-9.4}	6.3 ^{+5.0} _{-3.9}	16.7 ^{+6.6} _{-5.5}	10.3 ^{+7.6} _{-6.5}	16.3 ^{+6.9} _{-5.8}
342	266.0 ^{+18.5} _{-17.5}	128.9 ^{+13.0} _{-11.9}	137.1 ^{+13.8} _{-12.8}	266.5 ^{+18.5} _{-17.5}	18.9 ^{+6.0} _{-4.9}	139.4 ^{+13.3} _{-12.3}	108.2 ^{+12.5} _{-11.4}	129.5 ^{+13.0} _{-11.9}
343	21.4 ^{+10.0} _{-9.0}	9.9 ^{+6.1} _{-5.0}	11.6 ^{+8.5} _{-7.5}	21.8 ^{+10.2} _{-9.1}	4.5 ^{+4.8} _{-3.6}	10.5 ^{+6.0} _{-4.9}	6.8 ^{+7.8} _{-6.7}	10.2 ^{+6.3} _{-5.2}
344	42.1 ^{+11.6} _{-10.6}	22.7 ^{+7.6} _{-6.5}	19.4 ^{+9.3} _{-8.3}	43.4 ^{+11.8} _{-10.7}	8.7 ^{+5.5} _{-4.4}	19.6 ^{+7.3} _{-6.2}	15.2 ^{+8.6} _{-7.5}	24.0 ^{+7.9} _{-6.8}
345	37.4 ^{+10.5} _{-9.4}	24.7 ^{+7.3} _{-6.2}	12.7 ^{+8.2} _{-7.1}	37.9 ^{+10.6} _{-9.6}	17.1 ^{+6.0} _{-4.9}	11.5 ^{+6.2} _{-5.1}	9.4 ^{+7.5} _{-6.4}	25.2 ^{+7.5} _{-6.4}
346	96.7 ^{+11.7} _{-10.6}	40.9 ^{+7.8} _{-6.7}	55.7 ^{+9.3} _{-8.2}	97.8 ^{+11.8} _{-10.7}	5.3 ^{+4.0} _{-2.8}	50.5 ^{+8.4} _{-7.3}	42.0 ^{+8.3} _{-7.3}	42.1 ^{+7.9} _{-6.9}
347	2266.4 ^{+50.0} _{-49.0}	1425.6 ^{+39.4} _{-38.3}	840.7 ^{+31.5} _{-30.4}	2279.8 ^{+50.1} _{-49.1}	404.4 ^{+21.6} _{-20.6}	1249.6 ^{+36.9} _{-35.9}	625.8 ^{+27.5} _{-26.4}	1439.0 ^{+39.5} _{-38.5}
348	821.8 ^{+31.4} _{-30.4}	429.5 ^{+22.7} _{-21.6}	392.3 ^{+22.4} _{-21.4}	828.5 ^{+31.6} _{-30.5}	131.5 ^{+13.3} _{-12.3}	398.7 ^{+21.8} _{-20.7}	298.3 ^{+19.8} _{-18.7}	436.2 ^{+22.8} _{-21.8}
349	31.4 ^{+10.7} _{-9.6}	33.0 ^{+8.5} _{-7.5}	-1.6 ^{+7.1} _{-6.0}	32.6 ^{+10.8} _{-9.8}	24.1 ^{+7.3} _{-6.3}	8.7 ^{+5.9} _{-4.8}	-0.3 ^{+6.8} _{-5.7}	34.2 ^{+8.8} _{-7.7}
350	12.7 ^{+7.6} _{-6.5}	15.4 ^{+5.9} _{-4.8}	-2.7 ^{+5.5} _{-4.3}	11.9 ^{+7.6} _{-6.5}	3.5 ^{+3.8} _{-2.6}	14.2 ^{+5.8} _{-4.7}	-5.9 ^{+4.7} _{-3.6}	14.6 ^{+5.9} _{-4.8}
351	22.3 ^{+6.7} _{-5.6}	6.0 ^{+4.0} _{-2.8}	16.3 ^{+5.9} _{-4.8}	22.0 ^{+6.7} _{-5.6}	-1.2 ^{+1.9} _{-0.0}	8.3 ^{+4.3} _{-3.1}	14.9 ^{+5.7} _{-4.6}	5.8 ^{+4.0} _{-2.8}

Table 5—Continued

Source No	<i>net_cnts</i> [1] [0.5–8.0keV]	<i>net_cnts</i> [2] [0.5–2.0keV]	<i>net_cnts</i> [3] [2.0–8.0keV]	<i>net_cnts</i> [4] [0.35–8.0keV]	<i>net_cnts</i> [5] [0.35–1.1keV]	<i>net_cnts</i> [6] [1.1–2.6keV]	<i>net_cnts</i> [7] [2.6–8.0keV]	<i>net_cnts</i> [8] [0.35–2.0keV]
352	164.9 ^{+14.6} _{-13.6}	104.9 ^{+11.6} _{-10.6}	60.0 ^{+9.6} _{-8.5}	167.1 ^{+14.8} _{-13.7}	34.1 ^{+7.3} _{-6.3}	85.3 ^{+10.5} _{-9.4}	47.7 ^{+8.8} _{-7.7}	107.1 ^{+11.8} _{-10.7}
353	73.6 ^{+11.9} _{-10.9}	53.7 ^{+9.2} _{-8.1}	19.9 ^{+8.3} _{-7.3}	73.6 ^{+12.0} _{-10.9}	12.3 ^{+5.4} _{-4.2}	47.4 ^{+8.6} _{-7.6}	14.0 ^{+7.7} _{-6.6}	53.8 ^{+9.2} _{-8.2}
354	42.2 ^{+10.3} _{-9.3}	10.5 ^{+5.7} _{-4.6}	31.7 ^{+9.1} _{-8.0}	46.3 ^{+10.6} _{-9.6}	6.1 ^{+4.4} _{-3.2}	10.1 ^{+5.8} _{-4.7}	30.1 ^{+8.7} _{-7.6}	14.6 ^{+6.2} _{-5.1}
355	49.7 ^{+10.9} _{-9.9}	27.7 ^{+7.7} _{-6.6}	22.0 ^{+8.4} _{-7.3}	48.8 ^{+10.9} _{-9.9}	7.6 ^{+5.0} _{-3.9}	22.5 ^{+7.2} _{-6.1}	18.7 ^{+7.8} _{-6.7}	26.8 ^{+7.7} _{-6.6}
356	356.5 ^{+21.9} _{-20.9}	23.7 ^{+8.1} _{-7.0}	332.8 ^{+20.7} _{-19.6}	354.5 ^{+21.9} _{-20.9}	-0.8 ^{+4.7} _{-3.6}	47.4 ^{+9.4} _{-8.4}	307.8 ^{+19.8} _{-18.8}	21.7 ^{+8.1} _{-7.0}
357	47.1 ^{+12.6} _{-11.5}	45.7 ^{+9.8} _{-8.8}	1.4 ^{+8.5} _{-7.4}	47.6 ^{+12.6} _{-11.6}	40.9 ^{+8.7} _{-7.6}	7.9 ^{+6.8} _{-5.7}	-1.3 ^{+7.6} _{-6.6}	46.2 ^{+10.0} _{-8.9}
358	63.5 ^{+11.8} _{-10.8}	15.7 ^{+6.9} _{-5.8}	47.8 ^{+10.1} _{-9.1}	64.0 ^{+11.9} _{-10.9}	8.0 ^{+5.7} _{-4.5}	9.3 ^{+5.9} _{-4.8}	46.8 ^{+9.7} _{-8.6}	16.2 ^{+7.1} _{-6.0}
359	29.6 ^{+10.2} _{-9.2}	2.0 ^{+5.4} _{-4.3}	27.7 ^{+9.1} _{-8.1}	28.8 ^{+10.2} _{-9.2}	-0.5 ^{+4.0} _{-2.9}	-1.7 ^{+4.7} _{-3.5}	31.0 ^{+9.0} _{-7.9}	1.1 ^{+5.4} _{-4.3}
360	39.7 ^{+12.3} _{-11.2}	36.5 ^{+9.2} _{-8.1}	3.2 ^{+8.8} _{-7.8}	40.4 ^{+12.4} _{-11.3}	29.0 ^{+7.7} _{-6.6}	13.4 ^{+7.1} _{-6.0}	-2.0 ^{+8.0} _{-6.9}	37.2 ^{+9.3} _{-8.2}
361	102.2 ^{+13.5} _{-12.4}	30.5 ^{+8.0} _{-6.9}	71.7 ^{+11.4} _{-10.3}	100.7 ^{+13.5} _{-12.5}	1.4 ^{+4.8} _{-3.7}	39.6 ^{+8.3} _{-7.3}	59.7 ^{+10.5} _{-9.4}	29.0 ^{+8.1} _{-7.0}
362	312.8 ^{+22.9} _{-21.9}	308.0 ^{+20.3} _{-19.3}	4.8 ^{+11.4} _{-10.4}	324.4 ^{+23.3} _{-22.2}	222.9 ^{+17.4} _{-16.3}	104.4 ^{+13.0} _{-11.9}	-2.8 ^{+10.3} _{-9.3}	319.7 ^{+20.7} _{-19.7}
363	21.6 ^{+8.7} _{-7.7}	19.4 ^{+6.7} _{-5.6}	2.2 ^{+6.3} _{-5.2}	23.9 ^{+8.9} _{-7.9}	11.0 ^{+5.3} _{-4.1}	10.8 ^{+5.7} _{-4.6}	2.2 ^{+5.9} _{-4.8}	21.8 ^{+7.0} _{-5.9}
364	31.9 ^{+11.1} _{-10.1}	5.6 ^{+6.1} _{-5.0}	26.2 ^{+9.8} _{-8.7}	32.6 ^{+11.2} _{-10.2}	5.4 ^{+5.0} _{-3.9}	7.1 ^{+6.0} _{-4.9}	20.1 ^{+9.0} _{-8.0}	6.3 ^{+6.3} _{-5.2}
365	775.1 ^{+29.4} _{-28.3}	447.7 ^{+22.4} _{-21.3}	327.3 ^{+19.7} _{-18.6}	776.7 ^{+29.4} _{-28.4}	104.1 ^{+11.5} _{-10.4}	413.3 ^{+21.5} _{-20.5}	259.4 ^{+17.7} _{-16.7}	449.4 ^{+22.4} _{-21.4}
366	177.5 ^{+18.5} _{-17.5}	159.1 ^{+15.6} _{-14.6}	18.4 ^{+10.7} _{-9.6}	181.1 ^{+18.7} _{-17.7}	104.6 ^{+12.9} _{-11.8}	62.7 ^{+10.9} _{-9.8}	13.8 ^{+9.7} _{-8.7}	162.7 ^{+15.9} _{-14.8}
367	76.4 ^{+12.7} _{-11.7}	49.3 ^{+9.3} _{-8.3}	27.2 ^{+9.3} _{-8.2}	79.4 ^{+12.9} _{-11.8}	13.7 ^{+6.0} _{-4.8}	44.2 ^{+8.9} _{-7.8}	21.5 ^{+8.5} _{-7.4}	52.3 ^{+9.6} _{-8.5}
368	152.9 ^{+14.4} _{-13.4}	135.9 ^{+13.1} _{-12.1}	17.0 ^{+6.9} _{-5.8}	156.2 ^{+14.6} _{-13.5}	80.5 ^{+10.3} _{-9.3}	70.0 ^{+9.8} _{-8.8}	5.8 ^{+5.5} _{-4.4}	139.2 ^{+13.3} _{-12.2}
369	45.8 ^{+9.3} _{-8.3}	5.2 ^{+4.5} _{-3.3}	40.6 ^{+8.6} _{-7.5}	45.7 ^{+9.4} _{-8.3}	0.2 ^{+3.2} _{-2.0}	5.1 ^{+4.5} _{-3.3}	40.5 ^{+8.4} _{-7.3}	5.1 ^{+4.6} _{-3.5}
370	159.5 ^{+15.8} _{-14.8}	108.6 ^{+12.3} _{-11.2}	50.9 ^{+10.6} _{-9.6}	159.3 ^{+15.8} _{-14.8}	30.2 ^{+7.3} _{-6.2}	87.8 ^{+11.3} _{-10.3}	41.4 ^{+9.7} _{-8.6}	108.4 ^{+12.3} _{-11.3}
371	203.4 ^{+19.0} _{-18.0}	203.6 ^{+16.7} _{-15.6}	-0.2 ^{+9.8} _{-8.8}	205.0 ^{+19.1} _{-18.1}	158.5 ^{+14.6} _{-13.6}	51.6 ^{+10.2} _{-9.1}	-5.2 ^{+8.8} _{-7.7}	205.2 ^{+16.9} _{-15.8}
372	143.2 ^{+19.3} _{-18.3}	124.5 ^{+14.5} _{-13.4}	18.8 ^{+13.5} _{-12.4}	142.5 ^{+19.5} _{-18.4}	59.8 ^{+10.6} _{-9.6}	67.0 ^{+11.7} _{-10.7}	15.7 ^{+12.6} _{-11.6}	123.7 ^{+14.7} _{-13.6}
373	36.2 ^{+7.9} _{-6.8}	28.5 ^{+6.6} _{-5.5}	7.7 ^{+5.0} _{-3.9}	36.1 ^{+7.9} _{-6.8}	6.7 ^{+4.0} _{-2.8}	24.1 ^{+6.3} _{-5.2}	5.2 ^{+4.5} _{-3.3}	28.3 ^{+6.6} _{-5.5}
374	55.1 ^{+14.1} _{-13.0}	63.2 ^{+11.0} _{-10.0}	-8.2 ^{+9.4} _{-8.4}	55.9 ^{+14.2} _{-13.2}	39.6 ^{+8.7} _{-7.6}	26.2 ^{+8.7} _{-7.6}	-9.9 ^{+8.6} _{-7.5}	64.1 ^{+11.2} _{-10.2}
375	40.0 ^{+8.7} _{-7.6}	38.5 ^{+7.6} _{-6.5}	1.5 ^{+4.9} _{-3.8}	41.9 ^{+8.9} _{-7.8}	32.4 ^{+7.1} _{-6.0}	10.3 ^{+4.9} _{-3.7}	-0.7 ^{+4.4} _{-3.2}	40.4 ^{+7.9} _{-6.8}
376	24.0 ^{+7.4} _{-6.3}	15.7 ^{+5.7} _{-4.6}	8.3 ^{+5.4} _{-4.3}	25.6 ^{+7.5} _{-6.4}	16.4 ^{+5.6} _{-4.5}	0.7 ^{+3.2} _{-1.9}	8.5 ^{+5.3} _{-4.1}	17.3 ^{+5.9} _{-4.8}
377	30.0 ^{+10.5} _{-9.5}	27.0 ^{+8.2} _{-7.2}	3.0 ^{+7.3} _{-6.2}	29.3 ^{+10.6} _{-9.5}	12.1 ^{+6.2} _{-5.1}	13.5 ^{+6.7} _{-5.7}	3.7 ^{+6.8} _{-5.7}	26.2 ^{+8.3} _{-7.2}
378	28.9 ^{+9.4} _{-8.4}	0.9 ^{+5.1} _{-3.9}	28.0 ^{+8.4} _{-7.4}	27.9 ^{+9.4} _{-8.4}	-4.0 ^{+3.5} _{-2.3}	6.2 ^{+5.2} _{-4.0}	25.7 ^{+8.0} _{-6.9}	-0.2 ^{+5.1} _{-3.9}

Table 5—Continued

Source No	<i>net_cnts</i> [1] [0.5–8.0keV]	<i>net_cnts</i> [2] [0.5–2.0keV]	<i>net_cnts</i> [3] [2.0–8.0keV]	<i>net_cnts</i> [4] [0.35–8.0keV]	<i>net_cnts</i> [5] [0.35–1.1keV]	<i>net_cnts</i> [6] [1.1–2.6keV]	<i>net_cnts</i> [7] [2.6–8.0keV]	<i>net_cnts</i> [8] [0.35–2.0keV]
379	54.9 ^{+10.2} _{-9.1}	15.8 ^{+6.0} _{-4.9}	39.1 ^{+8.7} _{-7.7}	56.3 ^{+10.3} _{-9.2}	3.4 ^{+3.8} _{-2.6}	18.2 ^{+6.2} _{-5.1}	34.7 ^{+8.3} _{-7.2}	17.2 ^{+6.2} _{-5.1}
380	35.6 ^{+10.1} _{-9.1}	17.1 ^{+7.0} _{-5.9}	18.5 ^{+7.9} _{-6.9}	36.4 ^{+10.2} _{-9.2}	3.3 ^{+4.8} _{-3.6}	13.1 ^{+6.3} _{-5.1}	20.1 ^{+7.7} _{-6.6}	17.9 ^{+7.2} _{-6.1}
381	852.3 ^{+32.0} _{-30.9}	617.2 ^{+26.4} _{-25.4}	235.1 ^{+18.7} _{-17.7}	856.2 ^{+32.1} _{-31.0}	147.2 ^{+13.7} _{-12.7}	555.7 ^{+25.1} _{-24.1}	153.3 ^{+15.9} _{-14.9}	621.2 ^{+26.5} _{-25.5}
382	18.7 ^{+9.2} _{-8.2}	15.9 ^{+6.9} _{-5.8}	2.9 ^{+6.8} _{-5.7}	17.8 ^{+9.2} _{-8.2}	2.2 ^{+4.8} _{-3.7}	12.8 ^{+6.0} _{-4.9}	2.8 ^{+6.4} _{-5.3}	14.9 ^{+6.9} _{-5.8}
383	17.8 ^{+7.0} _{-5.9}	9.3 ^{+4.7} _{-3.6}	8.5 ^{+5.7} _{-4.6}	16.7 ^{+7.0} _{-5.9}	3.9 ^{+3.8} _{-2.6}	7.2 ^{+4.3} _{-3.1}	5.6 ^{+5.3} _{-4.2}	8.2 ^{+4.7} _{-3.6}
384	348.5 ^{+21.4} _{-20.4}	170.1 ^{+14.8} _{-13.8}	178.4 ^{+16.0} _{-15.0}	346.1 ^{+21.4} _{-20.4}	40.9 ^{+8.3} _{-7.2}	163.2 ^{+14.5} _{-13.5}	142.0 ^{+14.5} _{-13.5}	167.7 ^{+14.8} _{-13.8}
385	51.4 ^{+11.9} _{-10.9}	31.3 ^{+8.6} _{-7.6}	20.1 ^{+8.9} _{-7.8}	54.1 ^{+12.1} _{-11.1}	26.5 ^{+7.6} _{-6.5}	10.3 ^{+6.3} _{-5.2}	17.2 ^{+8.3} _{-7.2}	34.0 ^{+8.9} _{-7.8}
386	421.4 ^{+23.2} _{-22.2}	278.0 ^{+18.3} _{-17.3}	143.4 ^{+15.0} _{-13.9}	420.5 ^{+23.3} _{-22.2}	73.6 ^{+10.2} _{-9.2}	234.5 ^{+17.0} _{-15.9}	112.4 ^{+13.6} _{-12.5}	277.2 ^{+18.4} _{-17.3}
387	169.9 ^{+15.8} _{-14.8}	72.9 ^{+10.5} _{-9.5}	97.0 ^{+12.4} _{-11.4}	171.1 ^{+15.9} _{-14.9}	15.8 ^{+6.2} _{-5.1}	77.7 ^{+10.5} _{-9.5}	77.6 ^{+11.3} _{-10.2}	74.1 ^{+10.6} _{-9.6}
388	195.3 ^{+17.2} _{-16.2}	113.9 ^{+12.6} _{-11.5}	81.5 ^{+12.4} _{-11.3}	193.4 ^{+17.2} _{-16.2}	27.1 ^{+7.1} _{-6.0}	105.4 ^{+12.2} _{-11.1}	60.9 ^{+11.1} _{-10.1}	112.0 ^{+12.6} _{-11.5}
389	1125.8 ^{+35.4} _{-34.4}	719.3 ^{+28.1} _{-27.1}	406.6 ^{+22.2} _{-21.2}	1130.4 ^{+35.5} _{-34.5}	206.1 ^{+15.7} _{-14.6}	610.7 ^{+26.1} _{-25.0}	313.6 ^{+19.8} _{-18.7}	723.8 ^{+28.2} _{-27.2}
390	138.4 ^{+16.0} _{-15.0}	85.6 ^{+11.5} _{-10.5}	52.8 ^{+11.8} _{-10.7}	139.0 ^{+16.1} _{-15.1}	18.7 ^{+6.6} _{-5.5}	90.9 ^{+11.6} _{-10.6}	29.4 ^{+10.2} _{-9.2}	86.2 ^{+11.6} _{-10.6}
391	540.2 ^{+26.3} _{-25.3}	284.1 ^{+18.6} _{-17.6}	256.1 ^{+19.2} _{-18.2}	541.1 ^{+26.4} _{-25.3}	42.8 ^{+8.5} _{-7.4}	313.3 ^{+19.4} _{-18.4}	185.0 ^{+16.8} _{-15.8}	285.1 ^{+18.7} _{-17.7}
392	76.4 ^{+10.7} _{-9.7}	46.7 ^{+8.1} _{-7.1}	29.7 ^{+7.7} _{-6.6}	76.9 ^{+10.8} _{-9.7}	13.0 ^{+5.0} _{-3.8}	43.5 ^{+8.0} _{-6.9}	20.4 ^{+6.7} _{-5.6}	47.2 ^{+8.2} _{-7.1}
393	87.9 ^{+13.1} _{-12.0}	47.5 ^{+9.2} _{-8.1}	40.3 ^{+9.9} _{-8.9}	87.4 ^{+13.1} _{-12.1}	-0.2 ^{+4.2} _{-3.1}	55.9 ^{+9.5} _{-8.5}	31.6 ^{+9.1} _{-8.0}	47.0 ^{+9.3} _{-8.2}
394	96.0 ^{+14.9} _{-13.9}	5.9 ^{+6.9} _{-5.8}	90.2 ^{+13.7} _{-12.6}	95.6 ^{+15.0} _{-14.0}	3.1 ^{+5.4} _{-4.2}	9.9 ^{+7.2} _{-6.1}	82.6 ^{+12.9} _{-11.8}	5.4 ^{+7.1} _{-6.0}
395	194.9 ^{+16.5} _{-15.5}	133.5 ^{+13.1} _{-12.0}	61.4 ^{+10.7} _{-9.7}	197.7 ^{+16.6} _{-15.6}	39.5 ^{+7.8} _{-6.7}	117.8 ^{+12.4} _{-11.4}	40.4 ^{+9.3} _{-8.3}	136.3 ^{+13.3} _{-12.2}
396	528.0 ^{+24.7} _{-23.7}	129.9 ^{+12.9} _{-11.8}	398.1 ^{+21.5} _{-20.5}	527.4 ^{+24.7} _{-23.7}	9.0 ^{+5.0} _{-3.9}	185.3 ^{+14.9} _{-13.9}	333.1 ^{+19.8} _{-18.8}	129.3 ^{+12.9} _{-11.9}
397	136.7 ^{+14.6} _{-13.6}	85.3 ^{+11.1} _{-10.1}	51.4 ^{+10.1} _{-9.0}	136.2 ^{+14.6} _{-13.6}	15.5 ^{+6.1} _{-5.0}	79.5 ^{+10.6} _{-9.6}	41.2 ^{+9.3} _{-8.2}	84.9 ^{+11.2} _{-10.1}
398	407.6 ^{+21.9} _{-20.8}	128.9 ^{+12.8} _{-11.8}	278.7 ^{+18.2} _{-17.2}	410.1 ^{+21.9} _{-20.9}	19.5 ^{+6.0} _{-4.9}	150.6 ^{+13.6} _{-12.6}	240.1 ^{+17.0} _{-16.0}	131.4 ^{+12.9} _{-11.9}
399	21.7 ^{+7.1} _{-6.0}	12.3 ^{+4.9} _{-3.7}	9.3 ^{+5.8} _{-4.6}	23.3 ^{+7.3} _{-6.2}	4.1 ^{+3.5} _{-2.2}	12.0 ^{+4.9} _{-3.7}	7.3 ^{+5.4} _{-4.3}	14.0 ^{+5.2} _{-4.0}
400	24.6 ^{+6.9} _{-5.8}	15.1 ^{+5.3} _{-4.2}	9.5 ^{+5.1} _{-4.0}	24.4 ^{+6.9} _{-5.8}	1.6 ^{+2.9} _{-1.6}	15.8 ^{+5.3} _{-4.2}	7.1 ^{+4.7} _{-3.6}	14.9 ^{+5.3} _{-4.2}
401	28.7 ^{+8.0} _{-6.9}	8.7 ^{+4.6} _{-3.5}	20.0 ^{+7.1} _{-6.0}	29.4 ^{+8.1} _{-7.0}	-0.3 ^{+2.4} _{-0.9}	11.7 ^{+5.2} _{-4.0}	18.0 ^{+6.7} _{-5.6}	9.5 ^{+4.8} _{-3.6}
402	40.7 ^{+11.7} _{-10.7}	14.9 ^{+7.1} _{-6.0}	25.8 ^{+9.9} _{-8.8}	39.2 ^{+11.8} _{-10.8}	4.7 ^{+5.2} _{-4.0}	9.1 ^{+6.5} _{-5.4}	25.3 ^{+9.4} _{-8.3}	13.4 ^{+7.2} _{-6.1}
403	75.6 ^{+11.4} _{-10.3}	45.9 ^{+8.4} _{-7.3}	29.8 ^{+8.4} _{-7.3}	76.2 ^{+11.5} _{-10.4}	16.5 ^{+5.5} _{-4.4}	37.7 ^{+7.8} _{-6.7}	22.0 ^{+7.7} _{-6.6}	46.5 ^{+8.4} _{-7.3}
404	91.3 ^{+18.0} _{-17.0}	68.5 ^{+12.4} _{-11.3}	22.8 ^{+13.7} _{-12.7}	95.1 ^{+18.3} _{-17.3}	67.9 ^{+11.2} _{-10.1}	11.0 ^{+8.8} _{-7.7}	16.2 ^{+12.7} _{-11.6}	72.4 ^{+12.8} _{-11.7}
405	60.5 ^{+10.4} _{-9.3}	44.8 ^{+8.4} _{-7.4}	15.7 ^{+6.8} _{-5.7}	59.5 ^{+10.4} _{-9.3}	10.3 ^{+5.1} _{-4.0}	39.3 ^{+7.9} _{-6.8}	9.9 ^{+6.0} _{-4.9}	43.8 ^{+8.4} _{-7.4}

Table 5—Continued

Source No	<i>net_cnts</i> [1] [0.5–8.0keV]	<i>net_cnts</i> [2] [0.5–2.0keV]	<i>net_cnts</i> [3] [2.0–8.0keV]	<i>net_cnts</i> [4] [0.35–8.0keV]	<i>net_cnts</i> [5] [0.35–1.1keV]	<i>net_cnts</i> [6] [1.1–2.6keV]	<i>net_cnts</i> [7] [2.6–8.0keV]	<i>net_cnts</i> [8] [0.35–2.0keV]
406	$24.8^{+10.4}_{-9.4}$	$2.1^{+5.4}_{-4.3}$	$22.7^{+9.4}_{-8.3}$	$25.4^{+10.5}_{-9.5}$	$2.4^{+4.5}_{-3.3}$	$0.8^{+5.1}_{-4.0}$	$22.2^{+9.0}_{-7.9}$	$2.6^{+5.7}_{-4.6}$
407	$29.0^{+7.9}_{-6.9}$	$8.2^{+4.9}_{-3.8}$	$20.7^{+6.8}_{-5.7}$	$29.5^{+8.0}_{-6.9}$	$-0.6^{+2.7}_{-1.4}$	$13.6^{+5.5}_{-4.4}$	$16.6^{+6.2}_{-5.1}$	$8.8^{+5.0}_{-3.9}$
408	$120.9^{+12.8}_{-11.7}$	$79.3^{+10.2}_{-9.1}$	$41.6^{+8.5}_{-7.4}$	$123.0^{+12.9}_{-11.9}$	$25.7^{+6.4}_{-5.3}$	$61.8^{+9.2}_{-8.1}$	$35.6^{+7.9}_{-6.8}$	$81.4^{+10.4}_{-9.3}$
409	$72.1^{+10.4}_{-9.3}$	$59.5^{+9.0}_{-7.9}$	$12.5^{+6.0}_{-4.8}$	$73.7^{+10.5}_{-9.4}$	$31.4^{+6.8}_{-5.7}$	$34.6^{+7.2}_{-6.2}$	$7.7^{+5.3}_{-4.2}$	$61.1^{+9.1}_{-8.1}$
410	$38.3^{+8.8}_{-7.7}$	$4.0^{+4.5}_{-3.3}$	$34.3^{+8.0}_{-6.9}$	$38.1^{+8.8}_{-7.8}$	$3.5^{+4.2}_{-3.0}$	$1.8^{+3.6}_{-2.4}$	$32.8^{+7.7}_{-6.7}$	$3.8^{+4.6}_{-3.5}$
411	$113.0^{+15.0}_{-13.9}$	$62.1^{+10.1}_{-9.0}$	$50.9^{+11.6}_{-10.6}$	$110.7^{+15.0}_{-13.9}$	$7.8^{+5.6}_{-4.4}$	$64.3^{+10.2}_{-9.1}$	$38.6^{+10.6}_{-9.5}$	$59.9^{+10.1}_{-9.0}$
412	$67.4^{+12.6}_{-11.6}$	$7.3^{+6.1}_{-5.0}$	$60.1^{+11.5}_{-10.4}$	$68.3^{+12.7}_{-11.7}$	$-0.8^{+4.2}_{-3.1}$	$23.0^{+7.1}_{-6.1}$	$46.1^{+10.5}_{-9.4}$	$8.2^{+6.3}_{-5.2}$
413	$43.3^{+11.3}_{-10.2}$	$45.2^{+9.1}_{-8.0}$	$-1.9^{+7.4}_{-6.4}$	$46.9^{+11.5}_{-10.5}$	$44.3^{+8.5}_{-7.5}$	$6.3^{+5.8}_{-4.7}$	$-3.6^{+6.7}_{-5.6}$	$48.9^{+9.4}_{-8.3}$
414	$135.9^{+14.9}_{-13.8}$	$44.7^{+8.9}_{-7.8}$	$91.2^{+12.5}_{-11.4}$	$135.8^{+14.9}_{-13.9}$	$4.0^{+4.7}_{-3.5}$	$57.0^{+9.4}_{-8.3}$	$74.8^{+11.5}_{-10.5}$	$44.6^{+8.9}_{-7.9}$
415	$431.2^{+22.8}_{-21.7}$	$288.9^{+18.5}_{-17.4}$	$142.3^{+14.0}_{-13.0}$	$437.6^{+22.9}_{-21.9}$	$109.7^{+11.9}_{-10.9}$	$230.7^{+16.6}_{-15.5}$	$97.2^{+12.0}_{-10.9}$	$295.2^{+18.7}_{-17.6}$
416	$141.0^{+14.8}_{-13.7}$	$34.8^{+8.1}_{-7.0}$	$106.2^{+12.8}_{-11.8}$	$140.5^{+14.8}_{-13.8}$	$4.8^{+4.8}_{-3.6}$	$50.0^{+9.0}_{-7.9}$	$85.7^{+11.7}_{-10.6}$	$34.3^{+8.2}_{-7.1}$
417	$300.9^{+22.5}_{-21.4}$	$290.4^{+19.5}_{-18.5}$	$10.5^{+11.9}_{-10.9}$	$309.5^{+22.8}_{-21.7}$	$241.3^{+17.5}_{-16.5}$	$63.4^{+11.2}_{-10.1}$	$4.9^{+10.9}_{-9.8}$	$299.0^{+19.8}_{-18.8}$
418	$27.3^{+8.1}_{-7.0}$	$15.7^{+5.8}_{-4.7}$	$11.6^{+6.3}_{-5.1}$	$26.7^{+8.1}_{-7.0}$	$3.1^{+3.6}_{-2.4}$	$13.3^{+5.6}_{-4.5}$	$10.3^{+5.8}_{-4.7}$	$15.1^{+5.8}_{-4.7}$
419	$326.5^{+21.0}_{-20.0}$	$185.1^{+15.5}_{-14.5}$	$141.4^{+14.8}_{-13.8}$	$329.8^{+21.2}_{-20.1}$	$44.8^{+8.7}_{-7.6}$	$179.4^{+15.2}_{-14.1}$	$105.7^{+13.2}_{-12.1}$	$188.4^{+15.7}_{-14.7}$
420	$97.0^{+12.5}_{-11.4}$	$48.8^{+8.8}_{-7.8}$	$48.3^{+9.4}_{-8.4}$	$97.0^{+12.5}_{-11.5}$	$4.7^{+4.6}_{-3.5}$	$57.4^{+9.1}_{-8.1}$	$34.9^{+8.4}_{-7.3}$	$48.7^{+8.9}_{-7.8}$
421	$611.0^{+26.5}_{-25.5}$	$391.1^{+21.1}_{-20.1}$	$219.9^{+16.7}_{-15.7}$	$610.5^{+26.6}_{-25.5}$	$95.3^{+11.2}_{-10.1}$	$361.6^{+20.4}_{-19.3}$	$153.7^{+14.3}_{-13.3}$	$390.6^{+21.2}_{-20.1}$
422	$7.5^{+4.0}_{-2.8}$	$4.9^{+3.4}_{-2.2}$	$2.7^{+2.9}_{-1.6}$	$7.5^{+4.0}_{-2.8}$	$1.9^{+2.7}_{-1.3}$	$3.9^{+3.2}_{-1.9}$	$1.7^{+2.7}_{-1.3}$	$4.9^{+3.4}_{-2.2}$
423	$177.6^{+15.5}_{-14.4}$	$115.4^{+12.2}_{-11.2}$	$62.2^{+10.2}_{-9.1}$	$179.6^{+15.6}_{-14.5}$	$39.0^{+7.7}_{-6.6}$	$93.4^{+11.1}_{-10.1}$	$47.2^{+9.1}_{-8.0}$	$117.4^{+12.4}_{-11.3}$
424	$1838.1^{+44.8}_{-43.8}$	$1217.5^{+36.3}_{-35.3}$	$620.7^{+26.9}_{-25.9}$	$1847.1^{+44.9}_{-43.9}$	$450.9^{+22.6}_{-21.6}$	$921.0^{+31.7}_{-30.7}$	$475.2^{+23.8}_{-22.7}$	$1226.4^{+36.5}_{-35.5}$
425	$22.6^{+10.8}_{-9.7}$	$11.3^{+6.7}_{-5.6}$	$11.3^{+9.0}_{-8.0}$	$21.6^{+10.9}_{-9.8}$	$0.1^{+4.5}_{-3.4}$	$11.3^{+6.7}_{-5.6}$	$10.1^{+8.3}_{-7.3}$	$10.3^{+6.8}_{-5.7}$
426	$34.5^{+8.7}_{-7.6}$	$18.5^{+6.1}_{-5.0}$	$16.0^{+6.8}_{-5.7}$	$33.7^{+8.7}_{-7.6}$	$2.5^{+3.6}_{-2.4}$	$14.1^{+5.7}_{-4.6}$	$17.1^{+6.6}_{-5.5}$	$17.8^{+6.1}_{-5.0}$
427	$844.8^{+31.2}_{-30.2}$	$820.7^{+30.1}_{-29.0}$	$24.1^{+9.4}_{-8.3}$	$867.5^{+31.6}_{-30.6}$	$686.3^{+27.5}_{-26.5}$	$172.1^{+14.8}_{-13.8}$	$9.0^{+7.9}_{-6.8}$	$843.4^{+30.5}_{-29.5}$
428	$86.9^{+12.0}_{-10.9}$	$14.0^{+6.1}_{-4.9}$	$72.9^{+10.8}_{-9.7}$	$86.9^{+12.0}_{-11.0}$	$-2.0^{+3.3}_{-2.0}$	$34.8^{+7.8}_{-6.7}$	$54.1^{+9.5}_{-8.4}$	$14.0^{+6.2}_{-5.1}$
429	$93.6^{+11.0}_{-9.9}$	$70.5^{+9.5}_{-8.5}$	$23.1^{+6.3}_{-5.2}$	$94.4^{+11.0}_{-10.0}$	$26.0^{+6.3}_{-5.2}$	$52.7^{+8.4}_{-7.3}$	$15.6^{+5.5}_{-4.3}$	$71.3^{+9.6}_{-8.5}$
430	$47.5^{+12.0}_{-10.9}$	$38.2^{+8.7}_{-7.7}$	$9.3^{+8.8}_{-7.7}$	$48.3^{+12.1}_{-11.0}$	$10.2^{+5.7}_{-4.6}$	$30.2^{+8.1}_{-7.0}$	$7.9^{+8.2}_{-7.1}$	$39.0^{+8.9}_{-7.8}$
431	$46.1^{+9.8}_{-8.7}$	$7.5^{+5.3}_{-4.2}$	$38.6^{+8.7}_{-7.7}$	$45.9^{+9.9}_{-8.8}$	$-1.7^{+3.5}_{-2.3}$	$21.4^{+6.4}_{-5.3}$	$26.3^{+7.7}_{-6.6}$	$7.3^{+5.4}_{-4.3}$
432	$54.1^{+10.4}_{-9.3}$	$14.5^{+5.8}_{-4.7}$	$39.6^{+9.1}_{-8.0}$	$54.2^{+10.4}_{-9.4}$	$-1.5^{+3.0}_{-1.7}$	$26.5^{+6.8}_{-5.7}$	$29.2^{+8.2}_{-7.1}$	$14.6^{+5.9}_{-4.8}$

Table 5—Continued

Source No	<i>net_cnts</i> [1] [0.5–8.0keV]	<i>net_cnts</i> [2] [0.5–2.0keV]	<i>net_cnts</i> [3] [2.0–8.0keV]	<i>net_cnts</i> [4] [0.35–8.0keV]	<i>net_cnts</i> [5] [0.35–1.1keV]	<i>net_cnts</i> [6] [1.1–2.6keV]	<i>net_cnts</i> [7] [2.6–8.0keV]	<i>net_cnts</i> [8] [0.35–2.0keV]
433	$30.7^{+7.5}_{-6.4}$	$25.4^{+6.4}_{-5.3}$	$5.3^{+4.7}_{-3.5}$	$31.5^{+7.5}_{-6.4}$	$2.9^{+3.2}_{-1.9}$	$23.6^{+6.2}_{-5.1}$	$5.0^{+4.5}_{-3.3}$	$26.2^{+6.5}_{-5.4}$
434	$52.1^{+9.1}_{-8.1}$	$33.8^{+7.2}_{-6.1}$	$18.2^{+6.3}_{-5.2}$	$52.6^{+9.2}_{-8.1}$	$6.5^{+4.1}_{-3.0}$	$36.7^{+7.4}_{-6.3}$	$9.4^{+5.2}_{-4.1}$	$34.3^{+7.3}_{-6.2}$
435	$50.4^{+9.1}_{-8.1}$	$32.0^{+7.2}_{-6.1}$	$18.4^{+6.4}_{-5.3}$	$50.0^{+9.1}_{-8.1}$	$8.1^{+4.4}_{-3.3}$	$28.2^{+6.7}_{-5.6}$	$13.8^{+5.8}_{-4.7}$	$31.6^{+7.2}_{-6.1}$
436	$52.7^{+10.1}_{-9.0}$	$13.1^{+5.7}_{-4.6}$	$39.6^{+8.8}_{-7.7}$	$55.1^{+10.2}_{-9.2}$	$5.1^{+4.3}_{-3.1}$	$20.9^{+6.3}_{-5.2}$	$29.1^{+7.9}_{-6.8}$	$15.5^{+6.0}_{-4.9}$
437	$22.5^{+7.4}_{-6.3}$	$16.8^{+5.9}_{-4.8}$	$5.8^{+5.3}_{-4.1}$	$23.1^{+7.5}_{-6.4}$	$11.2^{+5.0}_{-3.8}$	$7.3^{+4.6}_{-3.4}$	$4.6^{+4.9}_{-3.7}$	$17.4^{+6.0}_{-4.9}$
438	$71.5^{+13.7}_{-12.6}$	$60.4^{+10.5}_{-9.4}$	$11.1^{+9.4}_{-8.4}$	$73.9^{+13.9}_{-12.8}$	$43.6^{+8.9}_{-7.8}$	$16.7^{+7.3}_{-6.3}$	$13.6^{+9.1}_{-8.0}$	$62.8^{+10.8}_{-9.7}$
439	$108.9^{+13.9}_{-12.9}$	$63.6^{+10.0}_{-8.9}$	$45.3^{+10.3}_{-9.3}$	$107.3^{+13.9}_{-12.9}$	$15.9^{+6.0}_{-4.9}$	$57.2^{+9.5}_{-8.4}$	$34.3^{+9.5}_{-8.4}$	$62.0^{+10.0}_{-8.9}$
440	$227.6^{+18.7}_{-17.7}$	$165.0^{+14.9}_{-13.8}$	$62.6^{+12.0}_{-11.0}$	$228.3^{+18.7}_{-17.7}$	$59.3^{+9.7}_{-8.6}$	$130.3^{+13.4}_{-12.3}$	$38.7^{+10.4}_{-9.4}$	$165.7^{+14.9}_{-13.9}$
441	$39.4^{+9.8}_{-8.7}$	$23.4^{+6.9}_{-5.8}$	$16.0^{+7.5}_{-6.5}$	$38.9^{+9.8}_{-8.7}$	$4.0^{+4.2}_{-3.1}$	$19.0^{+6.5}_{-5.4}$	$15.8^{+7.2}_{-6.1}$	$22.8^{+6.9}_{-5.8}$
442	$56.6^{+10.5}_{-9.5}$	$20.6^{+6.6}_{-5.5}$	$36.0^{+8.8}_{-7.7}$	$57.7^{+10.7}_{-9.6}$	$-0.1^{+3.5}_{-2.2}$	$25.6^{+7.0}_{-5.9}$	$32.2^{+8.3}_{-7.2}$	$21.6^{+6.8}_{-5.7}$
443	$28.7^{+12.5}_{-11.5}$	$26.5^{+8.6}_{-7.5}$	$2.2^{+9.7}_{-8.6}$	$28.7^{+12.6}_{-11.6}$	$25.3^{+7.6}_{-6.6}$	$2.1^{+6.5}_{-5.5}$	$1.4^{+8.9}_{-7.8}$	$26.5^{+8.8}_{-7.8}$
444	$61.0^{+8.9}_{-7.9}$	$12.7^{+4.7}_{-3.6}$	$48.3^{+8.1}_{-7.0}$	$61.0^{+8.9}_{-7.9}$	$1.9^{+2.7}_{-1.3}$	$11.7^{+4.6}_{-3.4}$	$47.4^{+8.0}_{-6.9}$	$12.7^{+4.7}_{-3.6}$
445	$24.9^{+9.1}_{-8.1}$	$22.4^{+6.8}_{-5.7}$	$2.6^{+6.8}_{-5.7}$	$23.6^{+9.1}_{-8.1}$	$8.2^{+4.9}_{-3.7}$	$16.0^{+6.1}_{-5.0}$	$-0.6^{+6.1}_{-5.0}$	$21.0^{+6.8}_{-5.7}$
446	$59.6^{+12.3}_{-11.2}$	$35.3^{+8.6}_{-7.5}$	$24.3^{+9.4}_{-8.4}$	$58.5^{+12.3}_{-11.2}$	$2.5^{+4.8}_{-3.7}$	$43.6^{+8.9}_{-7.8}$	$12.5^{+8.2}_{-7.2}$	$34.2^{+8.6}_{-7.5}$
447	$55.6^{+9.2}_{-8.1}$	$23.9^{+6.3}_{-5.2}$	$31.7^{+7.3}_{-6.3}$	$56.3^{+9.3}_{-8.2}$	$6.1^{+4.0}_{-2.8}$	$22.6^{+6.1}_{-5.0}$	$27.6^{+6.9}_{-5.8}$	$24.7^{+6.4}_{-5.3}$
448	$138.8^{+17.7}_{-16.6}$	$135.4^{+14.4}_{-13.3}$	$3.4^{+10.9}_{-9.9}$	$145.2^{+17.9}_{-16.9}$	$111.4^{+12.6}_{-11.5}$	$42.7^{+10.0}_{-8.9}$	$-8.9^{+9.6}_{-8.5}$	$141.7^{+14.7}_{-13.7}$
449	$39.3^{+9.2}_{-8.1}$	$21.8^{+6.5}_{-5.4}$	$17.5^{+7.1}_{-6.1}$	$40.4^{+9.3}_{-8.3}$	$8.4^{+4.7}_{-3.6}$	$14.3^{+5.7}_{-4.6}$	$17.7^{+6.9}_{-5.8}$	$22.9^{+6.7}_{-5.6}$
450	$465.4^{+23.8}_{-22.7}$	$282.2^{+18.2}_{-17.1}$	$183.2^{+16.0}_{-14.9}$	$465.1^{+23.8}_{-22.8}$	$54.8^{+8.8}_{-7.8}$	$278.5^{+18.1}_{-17.1}$	$131.9^{+13.9}_{-12.8}$	$281.9^{+18.2}_{-17.2}$
451	$40.1^{+9.8}_{-8.8}$	$23.0^{+6.9}_{-5.8}$	$17.1^{+7.7}_{-6.6}$	$40.3^{+9.9}_{-8.8}$	$3.7^{+4.2}_{-3.0}$	$20.1^{+6.5}_{-5.4}$	$16.5^{+7.3}_{-6.3}$	$23.2^{+7.0}_{-5.9}$
452	$313.8^{+20.4}_{-19.4}$	$144.6^{+14.0}_{-12.9}$	$169.2^{+15.5}_{-14.5}$	$312.5^{+20.4}_{-19.4}$	$10.2^{+5.9}_{-4.8}$	$176.7^{+14.9}_{-13.9}$	$125.7^{+13.7}_{-12.7}$	$143.3^{+14.0}_{-12.9}$
453	$21.3^{+6.0}_{-4.9}$	$3.4^{+3.2}_{-1.9}$	$17.9^{+5.6}_{-4.4}$	$22.2^{+6.1}_{-5.0}$	$0.6^{+2.3}_{-0.8}$	$6.3^{+3.8}_{-2.6}$	$15.3^{+5.2}_{-4.1}$	$4.3^{+3.4}_{-2.2}$
454	$39.2^{+9.9}_{-8.8}$	$10.8^{+5.8}_{-4.7}$	$28.4^{+8.5}_{-7.4}$	$39.1^{+10.0}_{-8.9}$	$3.0^{+4.3}_{-3.2}$	$12.7^{+5.8}_{-4.7}$	$23.4^{+7.9}_{-6.8}$	$10.7^{+6.0}_{-4.8}$
455	$14.1^{+5.0}_{-3.8}$	$2.8^{+2.9}_{-1.6}$	$11.4^{+4.6}_{-3.4}$	$14.1^{+5.0}_{-3.8}$	$0.9^{+2.3}_{-0.8}$	$3.8^{+3.2}_{-1.9}$	$9.4^{+4.3}_{-3.1}$	$2.7^{+2.9}_{-1.6}$
456	$150.3^{+20.2}_{-19.2}$	$134.5^{+15.2}_{-14.2}$	$15.8^{+14.0}_{-13.0}$	$155.6^{+20.6}_{-19.5}$	$119.6^{+13.7}_{-12.6}$	$16.5^{+9.5}_{-8.4}$	$19.5^{+13.3}_{-12.2}$	$139.8^{+15.6}_{-14.6}$
457	$54.6^{+10.1}_{-9.0}$	$27.6^{+6.9}_{-5.8}$	$27.0^{+7.9}_{-6.8}$	$55.4^{+10.1}_{-9.0}$	$7.3^{+4.4}_{-3.2}$	$24.3^{+6.5}_{-5.4}$	$23.7^{+7.5}_{-6.4}$	$28.5^{+7.0}_{-5.9}$
458	$43.8^{+10.7}_{-9.7}$	$21.5^{+7.1}_{-6.1}$	$22.3^{+8.6}_{-7.5}$	$42.0^{+10.8}_{-9.7}$	$9.1^{+5.3}_{-4.1}$	$18.6^{+6.7}_{-5.6}$	$14.2^{+7.8}_{-6.7}$	$19.7^{+7.2}_{-6.1}$
459	$38.2^{+10.3}_{-9.3}$	$28.5^{+7.5}_{-6.4}$	$9.7^{+7.8}_{-6.7}$	$38.3^{+10.4}_{-9.3}$	$4.0^{+4.4}_{-3.2}$	$28.3^{+7.5}_{-6.4}$	$6.0^{+7.0}_{-5.9}$	$28.6^{+7.6}_{-6.5}$

Table 5—Continued

Source No	<i>net_cnts</i> [1] [0.5–8.0keV]	<i>net_cnts</i> [2] [0.5–2.0keV]	<i>net_cnts</i> [3] [2.0–8.0keV]	<i>net_cnts</i> [4] [0.35–8.0keV]	<i>net_cnts</i> [5] [0.35–1.1keV]	<i>net_cnts</i> [6] [1.1–2.6keV]	<i>net_cnts</i> [7] [2.6–8.0keV]	<i>net_cnts</i> [8] [0.35–2.0keV]
460	31.7 ^{+8.3} _{-7.2}	14.8 ^{+5.7} _{-4.6}	16.9 ^{+6.7} _{-5.6}	33.0 ^{+8.5} _{-7.4}	1.0 ^{+3.4} _{-2.2}	23.2 ^{+6.4} _{-5.3}	8.8 ^{+5.7} _{-4.6}	16.1 ^{+5.9} _{-4.8}
461	52.2 ^{+9.8} _{-8.7}	23.4 ^{+6.7} _{-5.6}	28.8 ^{+7.7} _{-6.7}	54.8 ^{+9.9} _{-8.9}	8.0 ^{+4.7} _{-3.6}	19.4 ^{+6.1} _{-5.0}	27.4 ^{+7.4} _{-6.3}	26.0 ^{+6.9} _{-5.8}
462	118.3 ^{+12.2} _{-11.1}	102.8 ^{+11.2} _{-10.2}	15.5 ^{+5.6} _{-4.4}	122.3 ^{+12.4} _{-11.3}	64.2 ^{+9.1} _{-8.0}	53.0 ^{+8.4} _{-7.3}	5.1 ^{+4.1} _{-3.0}	106.8 ^{+11.4} _{-10.4}
463	15.0 ^{+8.6} _{-7.5}	2.6 ^{+4.8} _{-3.6}	12.4 ^{+7.6} _{-6.5}	14.4 ^{+8.6} _{-7.5}	-2.1 ^{+3.2} _{-2.0}	3.9 ^{+4.8} _{-3.6}	12.7 ^{+7.3} _{-6.2}	2.0 ^{+4.8} _{-3.6}
464	13.1 ^{+4.8} _{-3.7}	9.8 ^{+4.3} _{-3.1}	3.4 ^{+3.2} _{-1.9}	13.1 ^{+4.8} _{-3.7}	1.9 ^{+2.7} _{-1.3}	9.8 ^{+4.3} _{-3.1}	1.4 ^{+2.7} _{-1.3}	9.8 ^{+4.3} _{-3.1}
465	161.8 ^{+15.7} _{-14.6}	84.6 ^{+11.0} _{-9.9}	77.3 ^{+11.7} _{-10.7}	163.1 ^{+15.7} _{-14.7}	17.7 ^{+6.0} _{-4.9}	85.9 ^{+11.1} _{-10.0}	59.5 ^{+10.6} _{-9.5}	85.8 ^{+11.1} _{-10.0}
466	30.3 ^{+8.7} _{-7.6}	5.6 ^{+4.9} _{-3.8}	24.7 ^{+7.7} _{-6.6}	30.7 ^{+8.8} _{-7.7}	1.3 ^{+3.6} _{-2.4}	7.9 ^{+5.0} _{-3.9}	21.5 ^{+7.2} _{-6.1}	6.0 ^{+5.0} _{-3.9}
467	94.0 ^{+12.9} _{-11.9}	70.5 ^{+10.3} _{-9.3}	23.5 ^{+8.5} _{-7.5}	93.1 ^{+13.0} _{-11.9}	21.7 ^{+6.6} _{-5.5}	56.8 ^{+9.4} _{-8.3}	14.6 ^{+7.6} _{-6.5}	69.6 ^{+10.4} _{-9.3}
468	93.8 ^{+11.2} _{-10.1}	45.2 ^{+8.0} _{-6.9}	48.7 ^{+8.5} _{-7.4}	95.6 ^{+11.3} _{-10.2}	8.5 ^{+4.3} _{-3.1}	51.7 ^{+8.4} _{-7.3}	35.4 ^{+7.5} _{-6.4}	46.9 ^{+8.1} _{-7.1}
469	71.6 ^{+11.9} _{-10.8}	19.1 ^{+6.5} _{-5.4}	52.5 ^{+10.4} _{-9.3}	70.6 ^{+11.9} _{-10.8}	5.0 ^{+4.3} _{-3.2}	23.3 ^{+7.1} _{-6.0}	42.3 ^{+9.5} _{-8.4}	18.1 ^{+6.5} _{-5.4}
470	344.3 ^{+21.1} _{-20.0}	116.8 ^{+12.6} _{-11.6}	227.5 ^{+17.4} _{-16.3}	345.0 ^{+21.1} _{-20.1}	5.0 ^{+4.7} _{-3.5}	180.6 ^{+15.1} _{-14.0}	159.4 ^{+15.0} _{-13.9}	117.5 ^{+12.7} _{-11.7}
471	237.0 ^{+18.4} _{-17.4}	149.2 ^{+13.9} _{-12.9}	87.8 ^{+12.7} _{-11.6}	238.1 ^{+18.5} _{-17.4}	44.6 ^{+8.4} _{-7.3}	129.0 ^{+13.1} _{-12.0}	64.5 ^{+11.3} _{-10.3}	150.3 ^{+14.0} _{-13.0}
472	29.3 ^{+8.6} _{-7.6}	3.5 ^{+4.5} _{-3.3}	25.8 ^{+7.8} _{-6.8}	29.2 ^{+8.7} _{-7.6}	-2.6 ^{+2.7} _{-1.4}	9.4 ^{+5.1} _{-4.0}	22.5 ^{+7.4} _{-6.3}	3.4 ^{+4.6} _{-3.5}
473	40.3 ^{+9.6} _{-8.5}	31.2 ^{+7.5} _{-6.4}	9.1 ^{+6.7} _{-5.6}	39.4 ^{+9.6} _{-8.5}	7.6 ^{+4.8} _{-3.6}	22.8 ^{+6.7} _{-5.6}	9.0 ^{+6.4} _{-5.3}	30.3 ^{+7.5} _{-6.4}
474	29.8 ^{+8.7} _{-7.6}	19.5 ^{+6.2} _{-5.1}	10.3 ^{+6.7} _{-5.6}	28.8 ^{+8.7} _{-7.6}	4.5 ^{+4.2} _{-3.0}	15.7 ^{+5.8} _{-4.7}	8.7 ^{+6.3} _{-5.2}	18.5 ^{+6.2} _{-5.1}
475	56.2 ^{+10.2} _{-9.2}	13.3 ^{+5.6} _{-4.5}	42.9 ^{+9.1} _{-8.0}	57.7 ^{+10.3} _{-9.3}	1.3 ^{+3.4} _{-2.2}	23.1 ^{+6.5} _{-5.4}	33.4 ^{+8.3} _{-7.2}	14.8 ^{+5.8} _{-4.7}
476	13.1 ^{+4.8} _{-3.7}	10.7 ^{+4.4} _{-3.3}	2.4 ^{+2.9} _{-1.6}	13.1 ^{+4.8} _{-3.7}	2.8 ^{+2.9} _{-1.6}	8.8 ^{+4.1} _{-2.9}	1.5 ^{+2.7} _{-1.3}	10.7 ^{+4.4} _{-3.3}
477	9.3 ^{+7.0} _{-5.9}	2.9 ^{+4.3} _{-3.2}	6.4 ^{+6.1} _{-5.0}	8.7 ^{+7.0} _{-5.9}	0.6 ^{+3.2} _{-2.0}	1.2 ^{+4.2} _{-3.0}	6.9 ^{+5.7} _{-4.6}	2.3 ^{+4.3} _{-3.2}
478	32.6 ^{+8.4} _{-7.3}	28.8 ^{+6.9} _{-5.8}	3.9 ^{+5.5} _{-4.4}	36.2 ^{+8.7} _{-7.6}	11.6 ^{+5.0} _{-3.9}	21.1 ^{+6.2} _{-5.1}	3.5 ^{+5.1} _{-4.0}	32.4 ^{+7.3} _{-6.2}
479	27.9 ^{+10.0} _{-9.0}	18.9 ^{+6.6} _{-5.5}	9.1 ^{+8.1} _{-7.0}	26.7 ^{+10.0} _{-9.0}	20.1 ^{+6.2} _{-5.1}	-1.3 ^{+4.4} _{-3.3}	7.9 ^{+7.6} _{-6.6}	17.7 ^{+6.7} _{-5.6}
480	56.3 ^{+12.4} _{-11.3}	50.6 ^{+9.5} _{-8.4}	5.7 ^{+8.6} _{-7.6}	58.9 ^{+12.6} _{-11.6}	40.4 ^{+8.4} _{-7.4}	14.8 ^{+6.8} _{-5.7}	3.6 ^{+7.9} _{-6.9}	53.2 ^{+9.9} _{-8.8}
481	108.6 ^{+13.0} _{-11.9}	67.1 ^{+9.7} _{-8.7}	41.5 ^{+9.2} _{-8.2}	113.1 ^{+13.2} _{-12.1}	23.0 ^{+6.3} _{-5.2}	57.5 ^{+9.2} _{-8.1}	32.6 ^{+8.4} _{-7.3}	71.6 ^{+10.0} _{-9.0}
482	400.7 ^{+22.3} _{-21.3}	235.8 ^{+16.9} _{-15.8}	164.9 ^{+15.3} _{-14.2}	400.7 ^{+22.4} _{-21.3}	63.9 ^{+9.5} _{-8.4}	209.4 ^{+16.0} _{-14.9}	127.5 ^{+13.7} _{-12.6}	235.9 ^{+16.9} _{-15.9}
483	238.3 ^{+17.3} _{-16.2}	141.1 ^{+13.2} _{-12.2}	97.2 ^{+11.8} _{-10.7}	238.7 ^{+17.3} _{-16.3}	32.0 ^{+7.1} _{-6.0}	135.1 ^{+12.9} _{-11.9}	71.7 ^{+10.4} _{-9.3}	141.5 ^{+13.3} _{-12.2}
484	71.6 ^{+12.5} _{-11.5}	25.0 ^{+7.4} _{-6.3}	46.6 ^{+10.6} _{-9.6}	70.2 ^{+12.6} _{-11.5}	-0.6 ^{+4.1} _{-2.9}	32.0 ^{+8.0} _{-6.9}	38.9 ^{+9.8} _{-8.7}	23.6 ^{+7.5} _{-6.4}
485	163.4 ^{+15.7} _{-14.7}	74.5 ^{+10.5} _{-9.4}	88.9 ^{+12.3} _{-11.2}	165.6 ^{+15.9} _{-14.8}	16.4 ^{+6.2} _{-5.1}	76.1 ^{+10.5} _{-9.5}	73.1 ^{+11.2} _{-10.2}	76.7 ^{+10.7} _{-9.7}
486	22.5 ^{+7.8} _{-6.7}	20.6 ^{+6.2} _{-5.1}	1.9 ^{+5.4} _{-4.3}	21.6 ^{+7.8} _{-6.7}	2.5 ^{+3.6} _{-2.4}	21.0 ^{+6.2} _{-5.1}	-1.9 ^{+4.7} _{-3.5}	19.6 ^{+6.2} _{-5.1}

Table 5—Continued

Source No	<i>net_cnts</i> [1] [0.5–8.0keV]	<i>net_cnts</i> [2] [0.5–2.0keV]	<i>net_cnts</i> [3] [2.0–8.0keV]	<i>net_cnts</i> [4] [0.35–8.0keV]	<i>net_cnts</i> [5] [0.35–1.1keV]	<i>net_cnts</i> [6] [1.1–2.6keV]	<i>net_cnts</i> [7] [2.6–8.0keV]	<i>net_cnts</i> [8] [0.35–2.0keV]
487	72.0 ^{+9.9} _{-8.9}	40.1 ^{+7.5} _{-6.5}	31.9 ^{+7.2} _{-6.1}	72.0 ^{+9.9} _{-8.9}	9.1 ^{+4.3} _{-3.1}	43.4 ^{+7.8} _{-6.7}	19.5 ^{+6.0} _{-4.9}	40.1 ^{+7.5} _{-6.5}
488	432.2 ^{+22.8} _{-21.8}	312.3 ^{+19.1} _{-18.0}	119.9 ^{+13.2} _{-12.2}	432.3 ^{+22.8} _{-21.8}	86.9 ^{+10.7} _{-9.6}	264.6 ^{+17.6} _{-16.6}	80.8 ^{+11.3} _{-10.3}	312.3 ^{+19.1} _{-18.1}
489	57.7 ^{+9.7} _{-8.6}	10.0 ^{+4.9} _{-3.7}	47.7 ^{+8.8} _{-7.8}	57.7 ^{+9.7} _{-8.6}	2.3 ^{+3.2} _{-1.9}	17.3 ^{+5.7} _{-4.6}	38.1 ^{+8.1} _{-7.0}	10.0 ^{+4.9} _{-3.7}
490	16.5 ^{+5.6} _{-4.4}	11.9 ^{+4.7} _{-3.6}	4.6 ^{+3.8} _{-2.6}	16.4 ^{+5.6} _{-4.4}	4.3 ^{+3.4} _{-2.2}	10.1 ^{+4.4} _{-3.3}	2.0 ^{+3.2} _{-1.9}	11.8 ^{+4.7} _{-3.6}
491	363.8 ^{+20.2} _{-19.1}	253.4 ^{+17.0} _{-15.9}	110.3 ^{+11.6} _{-10.6}	365.7 ^{+20.2} _{-19.2}	76.7 ^{+9.8} _{-8.8}	210.3 ^{+15.6} _{-14.5}	78.7 ^{+10.0} _{-8.9}	255.4 ^{+17.0} _{-16.0}
492	8874.4 ^{+95.6} _{-94.6}	5952.1 ^{+78.4} _{-77.3}	2922.4 ^{+55.5} _{-54.5}	8934.1 ^{+96.0} _{-95.0}	1882.6 ^{+44.6} _{-43.6}	4888.9 ^{+71.1} _{-70.1}	2162.6 ^{+48.0} _{-47.0}	6011.7 ^{+78.8} _{-77.8}
493	222.5 ^{+18.0} _{-17.0}	153.7 ^{+14.1} _{-13.1}	68.8 ^{+11.9} _{-10.9}	222.8 ^{+18.1} _{-17.1}	49.8 ^{+8.8} _{-7.7}	128.9 ^{+13.2} _{-12.1}	44.0 ^{+10.3} _{-9.2}	154.0 ^{+14.2} _{-13.1}
494	36.2 ^{+7.9} _{-6.9}	25.3 ^{+6.4} _{-5.3}	10.9 ^{+5.5} _{-4.4}	36.0 ^{+7.9} _{-6.9}	1.6 ^{+2.9} _{-1.6}	24.6 ^{+6.3} _{-5.2}	9.9 ^{+5.2} _{-4.1}	25.2 ^{+6.4} _{-5.3}
495	44.2 ^{+10.0} _{-9.0}	30.0 ^{+7.4} _{-6.4}	14.2 ^{+7.4} _{-6.3}	45.3 ^{+10.1} _{-9.1}	5.3 ^{+4.5} _{-3.3}	32.8 ^{+7.5} _{-6.4}	7.1 ^{+6.5} _{-5.4}	31.1 ^{+7.6} _{-6.5}
496	17.4 ^{+7.6} _{-6.5}	17.4 ^{+6.0} _{-4.9}	0.0 ^{+5.3} _{-4.2}	16.6 ^{+7.6} _{-6.5}	11.4 ^{+5.0} _{-3.9}	6.7 ^{+4.8} _{-3.6}	-1.4 ^{+4.8} _{-3.7}	16.6 ^{+6.0} _{-4.9}
497	436.4 ^{+22.7} _{-21.7}	295.4 ^{+18.4} _{-17.4}	141.0 ^{+13.9} _{-12.9}	442.7 ^{+22.8} _{-21.8}	117.5 ^{+12.1} _{-11.0}	225.2 ^{+16.3} _{-15.3}	100.1 ^{+12.0} _{-11.0}	301.7 ^{+18.6} _{-17.6}
498	317.1 ^{+20.0} _{-18.9}	214.2 ^{+16.2} _{-15.1}	102.9 ^{+12.4} _{-11.4}	320.7 ^{+20.1} _{-19.0}	91.8 ^{+11.0} _{-10.0}	156.7 ^{+14.0} _{-12.9}	72.2 ^{+10.8} _{-9.8}	217.8 ^{+16.3} _{-15.3}
499	95.1 ^{+10.8} _{-9.8}	58.7 ^{+8.7} _{-7.7}	36.4 ^{+7.1} _{-6.1}	95.1 ^{+10.8} _{-9.8}	16.8 ^{+5.2} _{-4.1}	50.7 ^{+8.2} _{-7.1}	27.5 ^{+6.4} _{-5.3}	58.6 ^{+8.7} _{-7.7}
500	37.3 ^{+10.0} _{-8.9}	14.9 ^{+6.5} _{-5.4}	22.4 ^{+8.2} _{-7.1}	38.4 ^{+10.1} _{-9.0}	1.2 ^{+4.0} _{-2.9}	18.2 ^{+6.6} _{-5.5}	18.9 ^{+7.6} _{-6.5}	16.0 ^{+6.6} _{-5.5}
501	5.9 ^{+3.8} _{-2.6}	5.6 ^{+3.6} _{-2.4}	0.3 ^{+2.3} _{-0.8}	5.9 ^{+3.8} _{-2.6}	2.8 ^{+2.9} _{-1.6}	2.7 ^{+2.9} _{-1.6}	0.4 ^{+2.3} _{-0.8}	5.6 ^{+3.6} _{-2.4}
502	943.4 ^{+32.2} _{-31.1}	620.8 ^{+26.1} _{-25.1}	322.7 ^{+19.5} _{-18.5}	954.8 ^{+32.3} _{-31.3}	216.6 ^{+15.9} _{-14.9}	498.5 ^{+23.5} _{-22.5}	239.7 ^{+17.0} _{-16.0}	632.1 ^{+26.3} _{-25.3}
503	5.9 ^{+4.1} _{-2.9}	4.2 ^{+3.4} _{-2.2}	1.7 ^{+3.2} _{-1.9}	8.6 ^{+4.6} _{-3.4}	6.4 ^{+3.8} _{-2.6}	1.4 ^{+2.7} _{-1.3}	0.9 ^{+2.9} _{-1.6}	7.0 ^{+4.0} _{-2.8}
504	99.3 ^{+12.6} _{-11.5}	61.2 ^{+9.4} _{-8.3}	38.1 ^{+9.0} _{-8.0}	101.5 ^{+12.7} _{-11.7}	14.9 ^{+5.5} _{-4.3}	58.8 ^{+9.3} _{-8.2}	27.9 ^{+8.1} _{-7.0}	63.4 ^{+9.6} _{-8.5}
505	51.6 ^{+8.4} _{-7.3}	28.5 ^{+6.5} _{-5.4}	23.1 ^{+6.1} _{-5.0}	52.5 ^{+8.5} _{-7.4}	10.7 ^{+4.4} _{-3.3}	23.3 ^{+6.0} _{-4.9}	18.4 ^{+5.6} _{-4.4}	29.3 ^{+6.5} _{-5.4}
506	31.9 ^{+9.4} _{-8.3}	0.6 ^{+4.5} _{-3.4}	31.4 ^{+8.7} _{-7.6}	30.8 ^{+9.4} _{-8.3}	0.3 ^{+3.7} _{-2.5}	2.1 ^{+4.5} _{-3.4}	28.4 ^{+8.2} _{-7.2}	-0.6 ^{+4.5} _{-3.4}
507	228.0 ^{+16.4} _{-15.4}	129.4 ^{+12.5} _{-11.5}	98.6 ^{+11.3} _{-10.2}	229.8 ^{+16.5} _{-15.5}	38.7 ^{+7.4} _{-6.3}	117.6 ^{+12.0} _{-10.9}	73.5 ^{+9.9} _{-8.9}	131.3 ^{+12.6} _{-11.6}
508	31.6 ^{+8.8} _{-7.7}	10.6 ^{+5.4} _{-4.2}	21.0 ^{+7.5} _{-6.4}	30.8 ^{+8.8} _{-7.7}	2.7 ^{+3.8} _{-2.6}	8.6 ^{+5.1} _{-4.0}	19.5 ^{+7.0} _{-6.0}	9.8 ^{+5.4} _{-4.2}
509	21.0 ^{+8.8} _{-7.7}	11.9 ^{+5.9} _{-4.8}	9.1 ^{+7.1} _{-6.0}	19.1 ^{+8.8} _{-7.8}	-2.0 ^{+3.5} _{-2.3}	20.2 ^{+6.6} _{-5.5}	0.9 ^{+6.0} _{-4.9}	10.0 ^{+6.0} _{-4.8}
510	32.6 ^{+7.4} _{-6.3}	29.6 ^{+6.7} _{-5.6}	2.9 ^{+4.0} _{-2.8}	33.4 ^{+7.5} _{-6.4}	21.8 ^{+5.9} _{-4.8}	9.0 ^{+4.4} _{-3.3}	2.7 ^{+3.8} _{-2.6}	30.5 ^{+6.8} _{-5.7}
511	28.5 ^{+8.8} _{-7.7}	25.1 ^{+6.9} _{-5.8}	3.4 ^{+6.1} _{-5.0}	29.4 ^{+8.9} _{-7.8}	21.7 ^{+6.1} _{-5.0}	5.4 ^{+5.0} _{-3.8}	2.2 ^{+5.7} _{-4.6}	26.0 ^{+7.1} _{-6.0}
512	21.9 ^{+9.6} _{-8.5}	11.1 ^{+6.3} _{-5.2}	10.8 ^{+7.8} _{-6.7}	22.6 ^{+9.7} _{-8.6}	7.3 ^{+5.0} _{-3.9}	5.9 ^{+5.7} _{-4.6}	9.3 ^{+7.2} _{-6.1}	11.8 ^{+6.5} _{-5.4}
513	29.2 ^{+8.3} _{-7.3}	9.7 ^{+5.1} _{-4.0}	19.4 ^{+7.1} _{-6.0}	29.4 ^{+8.4} _{-7.3}	-0.6 ^{+3.0} _{-1.7}	12.4 ^{+5.5} _{-4.4}	17.6 ^{+6.7} _{-5.6}	10.0 ^{+5.3} _{-4.1}

Table 5—Continued

Source No	<i>net_cnts</i> [1] [0.5–8.0keV]	<i>net_cnts</i> [2] [0.5–2.0keV]	<i>net_cnts</i> [3] [2.0–8.0keV]	<i>net_cnts</i> [4] [0.35–8.0keV]	<i>net_cnts</i> [5] [0.35–1.1keV]	<i>net_cnts</i> [6] [1.1–2.6keV]	<i>net_cnts</i> [7] [2.6–8.0keV]	<i>net_cnts</i> [8] [0.35–2.0keV]
514	19.2 ^{+6.5} _{-5.4}	10.6 ^{+4.7} _{-3.6}	8.6 ^{+5.1} _{-4.0}	19.0 ^{+6.5} _{-5.4}	1.9 ^{+2.9} _{-1.6}	11.5 ^{+4.9} _{-3.7}	5.7 ^{+4.6} _{-3.4}	10.4 ^{+4.7} _{-3.6}
515	91.5 ^{+11.9} _{-10.8}	61.0 ^{+9.3} _{-8.2}	30.5 ^{+8.1} _{-7.0}	91.8 ^{+11.9} _{-10.9}	26.3 ^{+6.6} _{-5.5}	37.6 ^{+7.8} _{-6.7}	27.9 ^{+7.6} _{-6.5}	61.3 ^{+9.4} _{-8.3}
516	146.4 ^{+14.3} _{-13.2}	103.8 ^{+11.6} _{-10.5}	42.6 ^{+9.1} _{-8.0}	147.3 ^{+14.4} _{-13.3}	35.2 ^{+7.3} _{-6.2}	88.8 ^{+10.9} _{-9.9}	23.3 ^{+7.5} _{-6.4}	104.8 ^{+11.7} _{-10.6}
517	153.6 ^{+13.5} _{-12.5}	100.2 ^{+11.1} _{-10.0}	53.4 ^{+8.5} _{-7.4}	155.5 ^{+13.6} _{-12.6}	36.5 ^{+7.1} _{-6.1}	81.4 ^{+10.1} _{-9.0}	37.6 ^{+7.3} _{-6.2}	102.1 ^{+11.2} _{-10.1}
518	56.1 ^{+8.7} _{-7.7}	19.2 ^{+5.6} _{-4.4}	36.9 ^{+7.3} _{-6.2}	56.0 ^{+8.7} _{-7.7}	0.5 ^{+2.3} _{-0.8}	26.2 ^{+6.3} _{-5.2}	29.3 ^{+6.6} _{-5.5}	19.1 ^{+5.6} _{-4.4}
519	62.3 ^{+10.7} _{-9.6}	17.6 ^{+6.1} _{-5.0}	44.6 ^{+9.3} _{-8.2}	63.2 ^{+10.8} _{-9.7}	-0.7 ^{+3.2} _{-2.0}	22.4 ^{+6.5} _{-5.4}	41.5 ^{+8.9} _{-7.8}	18.6 ^{+6.3} _{-5.2}
520	29.0 ^{+10.6} _{-9.6}	2.2 ^{+5.7} _{-4.6}	26.8 ^{+9.4} _{-8.4}	30.5 ^{+10.8} _{-9.7}	1.9 ^{+4.7} _{-3.5}	7.8 ^{+5.9} _{-4.8}	20.9 ^{+8.7} _{-7.7}	3.7 ^{+6.0} _{-4.9}
521	25.1 ^{+6.5} _{-5.4}	15.5 ^{+5.2} _{-4.1}	9.6 ^{+4.6} _{-3.4}	25.0 ^{+6.5} _{-5.4}	4.4 ^{+3.4} _{-2.2}	11.6 ^{+4.7} _{-3.6}	9.0 ^{+4.4} _{-3.3}	15.4 ^{+5.2} _{-4.1}
522	27.9 ^{+7.3} _{-6.2}	19.5 ^{+5.8} _{-4.7}	8.4 ^{+5.1} _{-4.0}	27.5 ^{+7.3} _{-6.2}	4.4 ^{+3.6} _{-2.4}	14.8 ^{+5.2} _{-4.1}	8.3 ^{+5.0} _{-3.9}	19.1 ^{+5.8} _{-4.7}
523	66.9 ^{+9.9} _{-8.8}	44.2 ^{+7.9} _{-6.8}	22.7 ^{+6.7} _{-5.6}	66.5 ^{+9.9} _{-8.8}	10.4 ^{+4.6} _{-3.4}	42.7 ^{+7.8} _{-6.7}	13.4 ^{+5.7} _{-4.6}	43.9 ^{+7.9} _{-6.8}
524	7.3 ^{+4.6} _{-3.4}	5.6 ^{+3.8} _{-2.6}	1.7 ^{+3.4} _{-2.2}	7.3 ^{+4.6} _{-3.4}	-0.6 ^{+1.9} _{-0.0}	6.6 ^{+4.0} _{-2.8}	1.3 ^{+3.2} _{-1.9}	5.6 ^{+3.8} _{-2.6}
525	36.8 ^{+9.9} _{-8.8}	29.4 ^{+7.4} _{-6.4}	7.4 ^{+7.2} _{-6.1}	38.7 ^{+10.0} _{-9.0}	10.9 ^{+5.3} _{-4.1}	19.7 ^{+6.6} _{-5.5}	8.1 ^{+6.8} _{-5.7}	31.3 ^{+7.7} _{-6.6}
526	29.2 ^{+9.6} _{-8.5}	19.2 ^{+6.6} _{-5.5}	10.0 ^{+7.6} _{-6.5}	29.3 ^{+9.7} _{-8.6}	9.0 ^{+5.0} _{-3.9}	13.7 ^{+6.1} _{-4.9}	6.6 ^{+6.9} _{-5.8}	19.3 ^{+6.7} _{-5.6}
527	39.2 ^{+11.9} _{-10.9}	11.1 ^{+6.9} _{-5.8}	28.1 ^{+10.2} _{-9.2}	39.2 ^{+12.0} _{-11.0}	6.1 ^{+5.5} _{-4.3}	7.8 ^{+6.2} _{-5.1}	25.3 ^{+9.7} _{-8.6}	11.1 ^{+7.1} _{-6.0}
528	1227.2 ^{+36.7} _{-35.6}	359.7 ^{+20.3} _{-19.2}	867.5 ^{+31.0} _{-30.0}	1227.5 ^{+36.7} _{-35.7}	26.3 ^{+6.8} _{-5.7}	507.0 ^{+23.8} _{-22.8}	694.2 ^{+27.9} _{-26.8}	360.0 ^{+20.3} _{-19.3}
529	20.4 ^{+6.9} _{-5.8}	7.8 ^{+4.3} _{-3.1}	12.6 ^{+6.0} _{-4.8}	23.1 ^{+7.1} _{-6.0}	4.8 ^{+3.6} _{-2.4}	8.5 ^{+4.5} _{-3.3}	9.8 ^{+5.5} _{-4.4}	10.5 ^{+4.7} _{-3.6}
530	903.6 ^{+31.4} _{-30.4}	657.5 ^{+26.8} _{-25.8}	246.1 ^{+17.2} _{-16.2}	917.2 ^{+31.7} _{-30.6}	266.9 ^{+17.5} _{-16.4}	470.0 ^{+22.8} _{-21.8}	180.3 ^{+14.9} _{-13.9}	671.1 ^{+27.0} _{-26.0}
531	22.5 ^{+6.1} _{-5.0}	9.3 ^{+4.3} _{-3.1}	13.3 ^{+5.0} _{-3.8}	22.5 ^{+6.1} _{-5.0}	1.6 ^{+2.7} _{-1.3}	7.4 ^{+4.0} _{-2.8}	13.4 ^{+5.0} _{-3.8}	9.2 ^{+4.3} _{-3.1}
532	85.9 ^{+11.0} _{-10.0}	53.4 ^{+8.6} _{-7.5}	32.5 ^{+7.6} _{-6.5}	86.7 ^{+11.1} _{-10.0}	12.2 ^{+4.9} _{-3.7}	51.4 ^{+8.5} _{-7.4}	23.1 ^{+6.7} _{-5.6}	54.2 ^{+8.7} _{-7.6}
533	417.6 ^{+22.3} _{-21.2}	278.7 ^{+18.0} _{-17.0}	138.8 ^{+13.8} _{-12.8}	420.2 ^{+22.4} _{-21.3}	95.2 ^{+11.1} _{-10.0}	224.3 ^{+16.3} _{-15.3}	100.7 ^{+12.0} _{-11.0}	281.4 ^{+18.1} _{-17.0}
534	93.9 ^{+10.9} _{-9.8}	27.2 ^{+6.4} _{-5.3}	66.7 ^{+9.4} _{-8.3}	93.8 ^{+10.9} _{-9.8}	0.6 ^{+2.3} _{-0.8}	41.1 ^{+7.5} _{-6.5}	52.1 ^{+8.4} _{-7.3}	27.1 ^{+6.4} _{-5.3}
535	106.8 ^{+13.1} _{-12.1}	97.9 ^{+12.3} _{-11.3}	8.9 ^{+5.3} _{-4.2}	108.7 ^{+13.2} _{-12.2}	50.8 ^{+9.7} _{-8.6}	53.6 ^{+8.9} _{-7.9}	4.3 ^{+4.6} _{-3.4}	99.8 ^{+12.5} _{-11.4}
536	56.8 ^{+10.4} _{-9.4}	36.8 ^{+7.7} _{-6.6}	20.0 ^{+7.7} _{-6.6}	57.4 ^{+10.5} _{-9.5}	13.7 ^{+5.4} _{-4.2}	26.3 ^{+6.9} _{-5.8}	17.4 ^{+7.2} _{-6.1}	37.3 ^{+7.9} _{-6.8}
537	90.0 ^{+13.5} _{-12.5}	8.6 ^{+6.4} _{-5.3}	81.4 ^{+12.3} _{-11.3}	87.9 ^{+13.6} _{-12.5}	-1.5 ^{+4.4} _{-3.3}	12.4 ^{+6.4} _{-5.3}	77.0 ^{+11.9} _{-10.8}	6.6 ^{+6.4} _{-5.3}
538	169.6 ^{+16.3} _{-15.2}	74.8 ^{+10.6} _{-9.6}	94.8 ^{+12.9} _{-11.8}	168.7 ^{+16.3} _{-15.2}	2.8 ^{+4.9} _{-3.7}	86.0 ^{+11.0} _{-10.0}	79.9 ^{+12.0} _{-10.9}	74.0 ^{+10.7} _{-9.6}
539	131.7 ^{+14.3} _{-13.2}	128.6 ^{+13.4} _{-12.3}	3.1 ^{+5.9} _{-4.8}	131.1 ^{+14.3} _{-13.2}	83.0 ^{+11.0} _{-10.0}	49.0 ^{+8.7} _{-7.6}	-0.9 ^{+5.2} _{-4.1}	128.0 ^{+13.4} _{-12.3}
540	56.9 ^{+10.2} _{-9.2}	11.5 ^{+5.6} _{-4.4}	45.4 ^{+9.1} _{-8.0}	56.6 ^{+10.3} _{-9.2}	0.8 ^{+3.7} _{-2.5}	18.6 ^{+6.1} _{-4.9}	37.2 ^{+8.4} _{-7.3}	11.2 ^{+5.7} _{-4.6}

Table 5—Continued

Source No	<i>net_cnts</i> [1] [0.5–8.0keV]	<i>net_cnts</i> [2] [0.5–2.0keV]	<i>net_cnts</i> [3] [2.0–8.0keV]	<i>net_cnts</i> [4] [0.35–8.0keV]	<i>net_cnts</i> [5] [0.35–1.1keV]	<i>net_cnts</i> [6] [1.1–2.6keV]	<i>net_cnts</i> [7] [2.6–8.0keV]	<i>net_cnts</i> [8] [0.35–2.0keV]
541	23.3 ^{+6.9} _{-5.8}	20.8 ^{+6.5} _{-5.4}	2.6 ^{+3.4} _{-2.2}	24.3 ^{+7.0} _{-5.9}	9.1 ^{+4.9} _{-3.7}	14.3 ^{+5.4} _{-4.2}	0.9 ^{+3.0} _{-1.7}	21.7 ^{+6.6} _{-5.5}
542	27.8 ^{+8.7} _{-7.6}	33.0 ^{+8.4} _{-7.3}	-5.2 ^{+3.1} _{-1.9}	28.4 ^{+8.7} _{-7.6}	26.8 ^{+7.5} _{-6.4}	5.1 ^{+4.8} _{-3.7}	-3.4 ^{+3.1} _{-1.8}	33.6 ^{+8.5} _{-7.4}
543	42.8 ^{+8.1} _{-7.0}	15.4 ^{+5.2} _{-4.1}	27.4 ^{+6.7} _{-5.6}	42.6 ^{+8.1} _{-7.0}	5.0 ^{+3.6} _{-2.4}	13.9 ^{+5.0} _{-3.8}	23.8 ^{+6.4} _{-5.3}	15.2 ^{+5.2} _{-4.1}
544	257.1 ^{+17.4} _{-16.4}	45.2 ^{+8.0} _{-6.9}	211.9 ^{+15.9} _{-14.8}	257.0 ^{+17.4} _{-16.4}	5.7 ^{+3.8} _{-2.6}	72.3 ^{+9.7} _{-8.6}	179.0 ^{+14.7} _{-13.6}	45.1 ^{+8.0} _{-6.9}
545	38.6 ^{+9.3} _{-8.3}	21.6 ^{+7.3} _{-6.2}	17.1 ^{+6.5} _{-5.4}	38.2 ^{+9.3} _{-8.3}	14.7 ^{+6.3} _{-5.2}	7.1 ^{+4.9} _{-3.8}	16.4 ^{+6.3} _{-5.2}	21.1 ^{+7.3} _{-6.2}
546	325.1 ^{+19.9} _{-18.8}	123.8 ^{+12.6} _{-11.5}	201.2 ^{+15.9} _{-14.9}	327.7 ^{+19.9} _{-18.9}	5.5 ^{+4.3} _{-3.1}	167.3 ^{+14.3} _{-13.2}	154.8 ^{+14.2} _{-13.1}	126.5 ^{+12.7} _{-11.6}
547	24.5 ^{+9.1} _{-8.1}	2.4 ^{+4.8} _{-3.7}	22.1 ^{+8.2} _{-7.2}	24.5 ^{+9.2} _{-8.1}	1.0 ^{+3.8} _{-2.7}	4.6 ^{+4.9} _{-3.8}	18.9 ^{+7.7} _{-6.7}	2.3 ^{+4.9} _{-3.8}
548	54.0 ^{+8.6} _{-7.5}	35.0 ^{+7.1} _{-6.0}	18.9 ^{+5.7} _{-4.5}	54.9 ^{+8.7} _{-7.6}	7.5 ^{+4.0} _{-2.8}	30.0 ^{+6.6} _{-5.5}	17.4 ^{+5.4} _{-4.3}	36.0 ^{+7.1} _{-6.1}
549	34.5 ^{+10.4} _{-9.4}	25.8 ^{+7.4} _{-6.3}	8.7 ^{+7.9} _{-6.9}	36.4 ^{+10.6} _{-9.5}	29.6 ^{+7.2} _{-6.1}	-2.7 ^{+4.3} _{-3.2}	9.5 ^{+7.6} _{-6.5}	27.6 ^{+7.7} _{-6.6}
550	21.5 ^{+6.9} _{-5.8}	5.8 ^{+4.1} _{-3.0}	15.7 ^{+6.1} _{-5.0}	21.1 ^{+6.9} _{-5.8}	0.4 ^{+2.7} _{-1.3}	7.8 ^{+4.4} _{-3.3}	12.9 ^{+5.7} _{-4.6}	5.4 ^{+4.1} _{-3.0}
551	5.8 ^{+5.7} _{-4.6}	6.5 ^{+4.5} _{-3.3}	-0.7 ^{+4.4} _{-3.2}	6.5 ^{+5.8} _{-4.7}	5.7 ^{+4.0} _{-2.8}	1.6 ^{+3.6} _{-2.4}	-0.8 ^{+4.0} _{-2.8}	7.2 ^{+4.6} _{-3.4}
552	1802.4 ^{+44.1} _{-43.1}	1024.9 ^{+33.3} _{-32.3}	777.5 ^{+29.6} _{-28.6}	1806.7 ^{+44.2} _{-43.2}	236.7 ^{+16.7} _{-15.7}	978.6 ^{+32.5} _{-31.5}	591.4 ^{+26.0} _{-25.0}	1029.1 ^{+33.4} _{-32.4}
553	390.4 ^{+21.1} _{-20.1}	21.3 ^{+6.2} _{-5.1}	369.1 ^{+20.5} _{-19.4}	391.0 ^{+21.2} _{-20.1}	5.3 ^{+4.0} _{-2.8}	57.6 ^{+8.9} _{-7.8}	328.1 ^{+19.4} _{-18.3}	21.9 ^{+6.3} _{-5.2}
554	41.4 ^{+10.0} _{-8.9}	15.5 ^{+6.1} _{-5.0}	25.8 ^{+8.4} _{-7.3}	41.1 ^{+10.0} _{-9.0}	-1.6 ^{+3.3} _{-2.0}	25.0 ^{+7.0} _{-6.0}	17.7 ^{+7.4} _{-6.3}	15.3 ^{+6.2} _{-5.1}
555	48.2 ^{+9.1} _{-8.0}	21.1 ^{+6.2} _{-5.1}	27.2 ^{+7.3} _{-6.2}	49.1 ^{+9.2} _{-8.1}	6.8 ^{+4.1} _{-3.0}	18.5 ^{+5.9} _{-4.8}	23.9 ^{+6.9} _{-5.8}	22.0 ^{+6.3} _{-5.2}
556	11.0 ^{+5.7} _{-4.6}	4.2 ^{+3.8} _{-2.6}	6.8 ^{+4.9} _{-3.7}	10.6 ^{+5.7} _{-4.6}	3.2 ^{+3.4} _{-2.2}	0.3 ^{+3.0} _{-1.7}	7.0 ^{+4.7} _{-3.6}	3.8 ^{+3.8} _{-2.6}
557	23.8 ^{+6.8} _{-5.7}	2.5 ^{+3.2} _{-1.9}	21.3 ^{+6.4} _{-5.3}	23.7 ^{+6.8} _{-5.7}	0.6 ^{+2.3} _{-0.8}	8.1 ^{+4.3} _{-3.1}	15.0 ^{+5.7} _{-4.6}	2.4 ^{+3.2} _{-1.9}
558	23.9 ^{+7.2} _{-6.1}	3.6 ^{+4.0} _{-2.8}	20.2 ^{+6.5} _{-5.4}	24.3 ^{+7.3} _{-6.2}	-0.7 ^{+2.7} _{-1.3}	8.2 ^{+4.6} _{-3.4}	16.8 ^{+6.0} _{-4.9}	4.0 ^{+4.2} _{-3.0}
559	65.0 ^{+11.6} _{-10.6}	27.1 ^{+7.3} _{-6.2}	37.9 ^{+9.6} _{-8.5}	68.0 ^{+11.8} _{-10.7}	3.0 ^{+4.0} _{-2.8}	34.8 ^{+7.9} _{-6.8}	30.2 ^{+8.8} _{-7.8}	30.1 ^{+7.6} _{-6.5}
560	806.5 ^{+29.8} _{-28.7}	564.9 ^{+24.9} _{-23.9}	241.6 ^{+17.0} _{-16.0}	813.8 ^{+29.9} _{-28.9}	205.6 ^{+15.5} _{-14.5}	419.7 ^{+21.6} _{-20.6}	188.5 ^{+15.2} _{-14.1}	572.2 ^{+25.1} _{-24.1}
561	3923.7 ^{+64.1} _{-63.1}	2681.2 ^{+53.1} _{-52.0}	1242.5 ^{+36.7} _{-35.7}	3968.9 ^{+64.5} _{-63.5}	916.0 ^{+31.5} _{-30.4}	2152.1 ^{+47.6} _{-46.6}	900.8 ^{+31.5} _{-30.4}	2726.4 ^{+53.5} _{-52.5}
562	27.2 ^{+6.7} _{-5.6}	8.9 ^{+4.3} _{-3.1}	18.3 ^{+5.8} _{-4.7}	26.9 ^{+6.7} _{-5.6}	1.2 ^{+2.7} _{-1.3}	12.2 ^{+4.7} _{-3.6}	13.6 ^{+5.2} _{-4.1}	8.7 ^{+4.3} _{-3.1}
563	27.0 ^{+7.7} _{-6.6}	6.0 ^{+4.3} _{-3.1}	21.0 ^{+6.9} _{-5.8}	27.5 ^{+7.8} _{-6.7}	-0.7 ^{+2.7} _{-1.3}	10.2 ^{+4.9} _{-3.7}	18.0 ^{+6.4} _{-5.3}	6.5 ^{+4.5} _{-3.3}
564	127.4 ^{+13.3} _{-12.3}	93.5 ^{+11.0} _{-10.0}	33.9 ^{+8.2} _{-7.1}	129.1 ^{+13.4} _{-12.4}	32.9 ^{+7.1} _{-6.0}	71.0 ^{+9.8} _{-8.7}	25.2 ^{+7.4} _{-6.3}	95.2 ^{+11.1} _{-10.1}
565	340.1 ^{+19.7} _{-18.7}	219.0 ^{+15.9} _{-14.9}	121.1 ^{+12.4} _{-11.3}	343.0 ^{+19.8} _{-18.8}	78.7 ^{+10.0} _{-8.9}	174.7 ^{+14.4} _{-13.3}	89.6 ^{+10.8} _{-9.7}	221.8 ^{+16.0} _{-15.0}
566	19.7 ^{+6.3} _{-5.2}	8.1 ^{+4.3} _{-3.1}	11.5 ^{+5.2} _{-4.1}	19.3 ^{+6.3} _{-5.2}	2.5 ^{+3.2} _{-1.9}	8.4 ^{+4.3} _{-3.1}	8.3 ^{+4.7} _{-3.6}	7.7 ^{+4.3} _{-3.1}
567	19.6 ^{+8.3} _{-7.3}	12.6 ^{+5.7} _{-4.6}	7.0 ^{+6.7} _{-5.6}	21.5 ^{+8.5} _{-7.5}	9.5 ^{+4.9} _{-3.7}	4.3 ^{+4.8} _{-3.6}	7.7 ^{+6.4} _{-5.3}	14.5 ^{+6.0} _{-4.9}

Table 5—Continued

Source No	<i>net_cnts</i> [1] [0.5–8.0keV]	<i>net_cnts</i> [2] [0.5–2.0keV]	<i>net_cnts</i> [3] [2.0–8.0keV]	<i>net_cnts</i> [4] [0.35–8.0keV]	<i>net_cnts</i> [5] [0.35–1.1keV]	<i>net_cnts</i> [6] [1.1–2.6keV]	<i>net_cnts</i> [7] [2.6–8.0keV]	<i>net_cnts</i> [8] [0.35–2.0keV]
568	11.6 ^{+8.0} _{-6.9}	12.0 ^{+5.7} _{-4.6}	-0.4 ^{+6.2} _{-5.1}	11.1 ^{+8.1} _{-7.0}	7.1 ^{+4.8} _{-3.6}	6.0 ^{+4.9} _{-3.8}	-2.0 ^{+5.7} _{-4.6}	11.5 ^{+5.8} _{-4.7}
569	21.7 ^{+7.6} _{-6.5}	5.0 ^{+4.3} _{-3.2}	16.8 ^{+6.7} _{-5.6}	21.4 ^{+7.6} _{-6.5}	3.2 ^{+3.6} _{-2.4}	6.0 ^{+4.3} _{-3.1}	12.3 ^{+6.2} _{-5.0}	4.6 ^{+4.3} _{-3.2}
570	35.2 ^{+10.7} _{-9.6}	33.4 ^{+8.0} _{-6.9}	1.8 ^{+7.7} _{-6.6}	36.1 ^{+10.8} _{-9.7}	26.4 ^{+7.0} _{-5.9}	5.6 ^{+5.5} _{-4.4}	4.1 ^{+7.4} _{-6.4}	34.3 ^{+8.2} _{-7.1}
571	106.4 ^{+12.1} _{-11.1}	69.6 ^{+9.7} _{-8.6}	36.8 ^{+8.0} _{-6.9}	107.9 ^{+12.2} _{-11.2}	25.7 ^{+6.4} _{-5.3}	55.3 ^{+8.8} _{-7.7}	26.8 ^{+7.1} _{-6.0}	71.1 ^{+9.8} _{-8.7}
572	141.2 ^{+16.4} _{-15.4}	140.1 ^{+14.0} _{-12.9}	1.1 ^{+9.3} _{-8.3}	144.3 ^{+16.6} _{-15.6}	120.3 ^{+12.8} _{-11.7}	18.3 ^{+7.6} _{-6.5}	5.7 ^{+9.0} _{-8.0}	143.3 ^{+14.2} _{-13.2}
573	110.9 ^{+12.8} _{-11.7}	63.2 ^{+9.5} _{-8.4}	47.7 ^{+9.3} _{-8.2}	110.9 ^{+12.8} _{-11.8}	5.9 ^{+4.3} _{-3.2}	63.7 ^{+9.4} _{-8.4}	41.3 ^{+8.7} _{-7.6}	63.2 ^{+9.5} _{-8.4}
574	65.0 ^{+10.7} _{-9.6}	25.3 ^{+6.9} _{-5.8}	39.7 ^{+8.8} _{-7.7}	64.2 ^{+10.7} _{-9.6}	-1.4 ^{+3.0} _{-1.7}	35.4 ^{+7.6} _{-6.5}	30.2 ^{+7.9} _{-6.9}	24.5 ^{+6.9} _{-5.8}
575	93.3 ^{+11.8} _{-10.7}	36.5 ^{+7.6} _{-6.5}	56.9 ^{+9.6} _{-8.5}	92.5 ^{+11.8} _{-10.7}	1.4 ^{+3.2} _{-2.0}	41.7 ^{+7.9} _{-6.9}	49.5 ^{+9.1} _{-8.0}	35.7 ^{+7.6} _{-6.5}
576	149.4 ^{+14.1} _{-13.1}	93.3 ^{+11.0} _{-9.9}	56.1 ^{+9.6} _{-8.5}	150.2 ^{+14.2} _{-13.1}	27.9 ^{+6.6} _{-5.5}	78.0 ^{+10.2} _{-9.1}	44.3 ^{+8.7} _{-7.6}	94.1 ^{+11.0} _{-10.0}
577	274.9 ^{+18.2} _{-17.2}	174.8 ^{+14.4} _{-13.4}	100.1 ^{+11.9} _{-10.8}	277.7 ^{+18.3} _{-17.3}	46.2 ^{+8.0} _{-6.9}	150.6 ^{+13.5} _{-12.5}	80.8 ^{+10.8} _{-9.8}	177.6 ^{+14.5} _{-13.5}
578	12.8 ^{+5.8} _{-4.7}	5.1 ^{+4.0} _{-2.8}	7.7 ^{+4.9} _{-3.7}	12.7 ^{+5.8} _{-4.7}	0.3 ^{+2.7} _{-1.3}	6.7 ^{+4.1} _{-3.0}	5.6 ^{+4.5} _{-3.3}	4.9 ^{+4.0} _{-2.8}
579	513.7 ^{+24.0} _{-23.0}	326.6 ^{+19.2} _{-18.2}	187.1 ^{+15.1} _{-14.1}	520.2 ^{+24.2} _{-23.1}	117.2 ^{+11.9} _{-10.9}	271.4 ^{+17.6} _{-16.6}	131.6 ^{+12.9} _{-11.9}	333.1 ^{+19.4} _{-18.4}
580	6.5 ^{+3.8} _{-2.6}	4.8 ^{+3.4} _{-2.2}	1.7 ^{+2.7} _{-1.3}	6.5 ^{+3.8} _{-2.6}	1.9 ^{+2.7} _{-1.3}	2.9 ^{+2.9} _{-1.6}	1.7 ^{+2.7} _{-1.3}	4.8 ^{+3.4} _{-2.2}
581	35.4 ^{+8.3} _{-7.2}	13.3 ^{+5.2} _{-4.1}	22.1 ^{+7.0} _{-5.9}	35.0 ^{+8.3} _{-7.2}	1.2 ^{+3.0} _{-1.7}	20.1 ^{+6.0} _{-4.9}	13.6 ^{+6.0} _{-4.9}	12.9 ^{+5.2} _{-4.1}
582	27.5 ^{+7.3} _{-6.2}	16.9 ^{+5.6} _{-4.5}	10.6 ^{+5.4} _{-4.3}	27.5 ^{+7.3} _{-6.2}	5.0 ^{+3.6} _{-2.4}	14.8 ^{+5.4} _{-4.2}	7.7 ^{+4.9} _{-3.7}	16.9 ^{+5.6} _{-4.5}
583	52.3 ^{+8.7} _{-7.7}	5.1 ^{+3.8} _{-2.6}	47.2 ^{+8.3} _{-7.2}	53.2 ^{+8.8} _{-7.7}	3.0 ^{+3.2} _{-1.9}	6.4 ^{+4.0} _{-2.8}	43.9 ^{+8.0} _{-6.9}	6.0 ^{+4.0} _{-2.8}
584	11.4 ^{+4.6} _{-3.4}	2.8 ^{+2.9} _{-1.6}	8.6 ^{+4.1} _{-2.9}	11.4 ^{+4.6} _{-3.4}	0.9 ^{+2.3} _{-0.8}	1.9 ^{+2.7} _{-1.3}	8.6 ^{+4.1} _{-2.9}	2.8 ^{+2.9} _{-1.6}
585	282.5 ^{+18.4} _{-17.4}	258.8 ^{+17.3} _{-16.2}	23.7 ^{+7.3} _{-6.2}	287.1 ^{+18.6} _{-17.5}	151.4 ^{+13.5} _{-12.4}	127.0 ^{+12.5} _{-11.4}	8.7 ^{+5.8} _{-4.7}	263.4 ^{+17.4} _{-16.4}
586	105.7 ^{+12.2} _{-11.1}	68.0 ^{+9.6} _{-8.5}	37.7 ^{+8.2} _{-7.1}	107.1 ^{+12.3} _{-11.2}	15.2 ^{+5.4} _{-4.2}	62.7 ^{+9.3} _{-8.2}	29.2 ^{+7.5} _{-6.4}	69.4 ^{+9.7} _{-8.7}
587	271.6 ^{+17.7} _{-16.7}	163.1 ^{+13.9} _{-12.9}	108.5 ^{+11.6} _{-10.6}	274.4 ^{+17.8} _{-16.8}	29.4 ^{+6.7} _{-5.5}	168.0 ^{+14.1} _{-13.0}	77.0 ^{+10.0} _{-8.9}	165.9 ^{+14.0} _{-13.0}
588	19.3 ^{+5.6} _{-4.4}	7.9 ^{+4.0} _{-2.8}	11.5 ^{+4.6} _{-3.4}	19.3 ^{+5.6} _{-4.4}	1.9 ^{+2.7} _{-1.3}	7.9 ^{+4.0} _{-2.8}	9.5 ^{+4.3} _{-3.1}	7.8 ^{+4.0} _{-2.8}
589	831.1 ^{+30.2} _{-29.2}	565.1 ^{+24.9} _{-23.9}	266.0 ^{+17.8} _{-16.8}	834.7 ^{+30.3} _{-29.3}	195.1 ^{+15.1} _{-14.0}	468.4 ^{+22.8} _{-21.8}	171.1 ^{+14.6} _{-13.6}	568.7 ^{+25.0} _{-24.0}
590	12.0 ^{+6.6} _{-5.5}	8.5 ^{+4.7} _{-3.6}	3.5 ^{+5.3} _{-4.2}	12.6 ^{+6.7} _{-5.6}	1.7 ^{+3.2} _{-1.9}	7.4 ^{+4.6} _{-3.5}	3.5 ^{+5.0} _{-3.9}	9.0 ^{+4.9} _{-3.7}
591	27.5 ^{+8.1} _{-7.0}	17.0 ^{+5.7} _{-4.6}	10.5 ^{+6.4} _{-5.3}	26.6 ^{+8.1} _{-7.0}	1.0 ^{+3.3} _{-2.0}	21.8 ^{+6.2} _{-5.1}	3.8 ^{+5.4} _{-4.3}	16.1 ^{+5.7} _{-4.6}
592	44.5 ^{+10.2} _{-9.1}	24.6 ^{+7.0} _{-5.9}	19.9 ^{+8.0} _{-6.9}	43.1 ^{+10.2} _{-9.1}	3.3 ^{+4.1} _{-2.9}	19.0 ^{+6.7} _{-5.6}	20.8 ^{+7.7} _{-6.6}	23.2 ^{+7.0} _{-5.9}
593	132.3 ^{+13.8} _{-12.7}	87.7 ^{+10.8} _{-9.8}	44.7 ^{+9.2} _{-8.2}	131.4 ^{+13.8} _{-12.7}	26.4 ^{+6.7} _{-5.6}	81.2 ^{+10.5} _{-9.5}	23.8 ^{+7.5} _{-6.4}	86.8 ^{+10.8} _{-9.8}
594	84.9 ^{+10.3} _{-9.3}	61.6 ^{+8.9} _{-7.9}	23.3 ^{+6.0} _{-4.9}	84.9 ^{+10.3} _{-9.3}	16.8 ^{+5.2} _{-4.1}	55.7 ^{+8.5} _{-7.5}	12.4 ^{+4.7} _{-3.6}	61.6 ^{+8.9} _{-7.9}

Table 5—Continued

Source No	<i>net_cnts</i> [1] [0.5–8.0keV]	<i>net_cnts</i> [2] [0.5–2.0keV]	<i>net_cnts</i> [3] [2.0–8.0keV]	<i>net_cnts</i> [4] [0.35–8.0keV]	<i>net_cnts</i> [5] [0.35–1.1keV]	<i>net_cnts</i> [6] [1.1–2.6keV]	<i>net_cnts</i> [7] [2.6–8.0keV]	<i>net_cnts</i> [8] [0.35–2.0keV]
595	144.5 ^{+13.2} _{-12.2}	106.6 ^{+11.4} _{-10.4}	37.9 ^{+7.5} _{-6.4}	144.3 ^{+13.2} _{-12.2}	37.3 ^{+7.2} _{-6.1}	78.8 ^{+10.0} _{-8.9}	28.3 ^{+6.6} _{-5.5}	106.4 ^{+11.4} _{-10.4}
596	41.8 ^{+7.6} _{-6.5}	21.8 ^{+5.8} _{-4.7}	20.1 ^{+5.7} _{-4.5}	41.8 ^{+7.6} _{-6.5}	5.9 ^{+3.6} _{-2.4}	20.7 ^{+5.7} _{-4.5}	15.2 ^{+5.1} _{-4.0}	21.7 ^{+5.8} _{-4.7}
597	46.6 ^{+8.3} _{-7.3}	8.0 ^{+4.3} _{-3.1}	38.6 ^{+7.6} _{-6.5}	47.2 ^{+8.4} _{-7.3}	1.3 ^{+3.0} _{-1.6}	7.6 ^{+4.1} _{-2.9}	38.2 ^{+7.6} _{-6.5}	8.6 ^{+4.4} _{-3.3}
598	28.3 ^{+6.5} _{-5.4}	18.5 ^{+5.4} _{-4.3}	9.8 ^{+4.4} _{-3.3}	28.3 ^{+6.5} _{-5.4}	3.7 ^{+3.2} _{-1.9}	18.7 ^{+5.4} _{-4.3}	5.9 ^{+3.8} _{-2.6}	18.5 ^{+5.4} _{-4.3}
599	30.1 ^{+8.3} _{-7.2}	8.2 ^{+4.8} _{-3.6}	21.9 ^{+7.3} _{-6.2}	29.6 ^{+8.3} _{-7.2}	-0.3 ^{+2.7} _{-1.3}	12.3 ^{+5.4} _{-4.3}	17.6 ^{+6.7} _{-5.6}	7.7 ^{+4.8} _{-3.6}
600	1014.3 ^{+33.0} _{-32.0}	642.7 ^{+26.4} _{-25.4}	371.6 ^{+20.4} _{-19.4}	1021.2 ^{+33.1} _{-32.1}	212.4 ^{+15.7} _{-14.6}	529.6 ^{+24.1} _{-23.1}	279.2 ^{+17.9} _{-16.9}	649.6 ^{+26.6} _{-25.6}
601	345.8 ^{+20.5} _{-19.4}	187.9 ^{+15.1} _{-14.1}	157.9 ^{+14.4} _{-13.4}	349.1 ^{+20.6} _{-19.5}	53.2 ^{+8.7} _{-7.6}	165.0 ^{+14.2} _{-13.2}	130.9 ^{+13.3} _{-12.2}	191.2 ^{+15.2} _{-14.2}
602	16.8 ^{+5.3} _{-4.2}	8.7 ^{+4.1} _{-2.9}	8.1 ^{+4.1} _{-2.9}	16.8 ^{+5.3} _{-4.2}	1.8 ^{+2.7} _{-1.3}	8.7 ^{+4.1} _{-2.9}	6.2 ^{+3.8} _{-2.6}	8.6 ^{+4.1} _{-2.9}
603	29.7 ^{+8.1} _{-7.0}	16.4 ^{+6.0} _{-4.8}	13.2 ^{+6.2} _{-5.1}	30.2 ^{+8.2} _{-7.1}	4.6 ^{+4.0} _{-2.8}	13.8 ^{+5.5} _{-4.4}	11.8 ^{+5.9} _{-4.8}	17.0 ^{+6.1} _{-4.9}
604	8.0 ^{+4.1} _{-2.9}	2.8 ^{+2.9} _{-1.6}	5.2 ^{+3.6} _{-2.4}	8.0 ^{+4.1} _{-2.9}	-0.1 ^{+1.9} _{-0.0}	3.8 ^{+3.2} _{-1.9}	4.3 ^{+3.4} _{-2.2}	2.8 ^{+2.9} _{-1.6}
605	14.0 ^{+5.2} _{-4.1}	6.2 ^{+3.8} _{-2.6}	7.8 ^{+4.3} _{-3.1}	14.0 ^{+5.2} _{-4.1}	0.6 ^{+2.3} _{-0.8}	5.4 ^{+3.6} _{-2.4}	8.0 ^{+4.3} _{-3.1}	6.1 ^{+3.8} _{-2.6}
606	60.9 ^{+9.0} _{-7.9}	22.4 ^{+5.9} _{-4.8}	38.5 ^{+7.4} _{-6.3}	60.8 ^{+9.0} _{-7.9}	-0.4 ^{+1.9} _{-0.0}	28.5 ^{+6.5} _{-5.4}	32.7 ^{+6.9} _{-5.8}	22.4 ^{+5.9} _{-4.8}
607	39.7 ^{+8.4} _{-7.3}	5.0 ^{+4.2} _{-3.0}	34.7 ^{+7.7} _{-6.6}	38.9 ^{+8.4} _{-7.3}	-2.9 ^{+2.0} _{-0.0}	16.1 ^{+5.5} _{-4.4}	25.7 ^{+6.9} _{-5.8}	4.2 ^{+4.2} _{-3.0}
608	202.9 ^{+15.6} _{-14.6}	137.8 ^{+12.9} _{-11.9}	65.2 ^{+9.6} _{-8.5}	202.5 ^{+15.6} _{-14.6}	21.2 ^{+5.9} _{-4.8}	138.4 ^{+12.9} _{-11.9}	42.9 ^{+8.1} _{-7.0}	137.3 ^{+12.9} _{-11.9}
609	14.7 ^{+5.5} _{-4.3}	10.9 ^{+4.6} _{-3.4}	3.8 ^{+3.8} _{-2.6}	15.4 ^{+5.6} _{-4.5}	5.1 ^{+3.6} _{-2.4}	8.0 ^{+4.1} _{-2.9}	2.2 ^{+3.4} _{-2.2}	11.6 ^{+4.7} _{-3.6}
610	40.1 ^{+10.8} _{-9.8}	24.8 ^{+7.8} _{-6.7}	15.3 ^{+8.2} _{-7.1}	39.5 ^{+10.8} _{-9.8}	7.8 ^{+4.6} _{-3.5}	20.4 ^{+7.6} _{-6.5}	11.2 ^{+7.5} _{-6.4}	24.2 ^{+7.8} _{-6.7}
611	8.7 ^{+4.3} _{-3.1}	0.7 ^{+2.3} _{-0.8}	7.9 ^{+4.1} _{-2.9}	8.7 ^{+4.3} _{-3.1}	-0.1 ^{+1.9} _{-0.0}	2.6 ^{+2.9} _{-1.6}	6.1 ^{+3.8} _{-2.6}	0.7 ^{+2.3} _{-0.8}
612	25935.1 ^{+162.7} _{-161.7}	14808.2 ^{+123.1} _{-122.0}	11127.0 ^{+107.1} _{-106.0}	26021.9 ^{+163.0} _{-162.0}	3694.2 ^{+62.0} _{-60.9}	13903.2 ^{+119.3} _{-118.3}	8424.5 ^{+93.3} _{-92.3}	14895.0 ^{+123.4} _{-122.4}
613	361.6 ^{+21.4} _{-20.3}	239.9 ^{+16.9} _{-15.9}	121.6 ^{+13.8} _{-12.7}	366.3 ^{+21.6} _{-20.5}	84.5 ^{+10.6} _{-9.6}	180.6 ^{+15.0} _{-13.9}	101.2 ^{+12.7} _{-11.6}	244.7 ^{+17.2} _{-16.1}
614	34.1 ^{+7.2} _{-6.1}	19.3 ^{+5.6} _{-4.4}	14.8 ^{+5.2} _{-4.1}	33.9 ^{+7.2} _{-6.1}	1.6 ^{+2.7} _{-1.3}	22.3 ^{+5.9} _{-4.8}	10.1 ^{+4.6} _{-3.4}	19.2 ^{+5.6} _{-4.4}
615	28.4 ^{+6.7} _{-5.6}	23.6 ^{+6.1} _{-5.0}	4.8 ^{+3.8} _{-2.6}	28.0 ^{+6.7} _{-5.6}	3.9 ^{+3.4} _{-2.2}	22.8 ^{+6.0} _{-4.9}	1.2 ^{+3.0} _{-1.7}	23.2 ^{+6.1} _{-5.0}
616	26.5 ^{+8.4} _{-7.3}	5.3 ^{+4.5} _{-3.3}	21.2 ^{+7.6} _{-6.5}	25.5 ^{+8.4} _{-7.4}	-2.4 ^{+2.4} _{-1.0}	12.2 ^{+5.5} _{-4.4}	15.7 ^{+6.8} _{-5.8}	4.3 ^{+4.5} _{-3.3}
617	28.1 ^{+7.1} _{-6.0}	13.9 ^{+5.1} _{-4.0}	14.2 ^{+5.6} _{-4.5}	27.6 ^{+7.1} _{-6.0}	3.6 ^{+3.4} _{-2.2}	14.2 ^{+5.1} _{-4.0}	9.9 ^{+5.0} _{-3.9}	13.5 ^{+5.1} _{-4.0}
618	122.6 ^{+13.5} _{-12.5}	68.1 ^{+9.8} _{-8.7}	54.5 ^{+10.0} _{-8.9}	124.4 ^{+13.7} _{-12.6}	24.6 ^{+6.3} _{-5.2}	54.9 ^{+9.0} _{-7.9}	44.9 ^{+9.3} _{-8.2}	69.9 ^{+10.0} _{-8.9}
619	96.0 ^{+12.0} _{-10.9}	62.6 ^{+9.5} _{-8.4}	33.4 ^{+8.0} _{-6.9}	96.7 ^{+12.1} _{-11.0}	19.4 ^{+6.1} _{-5.0}	56.4 ^{+8.9} _{-7.8}	20.8 ^{+6.9} _{-5.8}	63.3 ^{+9.7} _{-8.6}
620	16.4 ^{+6.3} _{-5.1}	-0.2 ^{+2.7} _{-1.4}	16.6 ^{+6.0} _{-4.9}	16.0 ^{+6.3} _{-5.1}	-1.3 ^{+1.9} _{-0.0}	2.7 ^{+3.4} _{-2.2}	14.6 ^{+5.7} _{-4.6}	-0.7 ^{+2.7} _{-1.4}
621	73.5 ^{+10.4} _{-9.3}	18.1 ^{+5.7} _{-4.6}	55.4 ^{+9.2} _{-8.1}	73.4 ^{+10.4} _{-9.3}	-1.4 ^{+1.9} _{-0.0}	33.8 ^{+7.2} _{-6.1}	41.0 ^{+8.1} _{-7.0}	18.0 ^{+5.7} _{-4.6}

Table 5—Continued

Source No	<i>net_cnts</i> [1] [0.5–8.0keV]	<i>net_cnts</i> [2] [0.5–2.0keV]	<i>net_cnts</i> [3] [2.0–8.0keV]	<i>net_cnts</i> [4] [0.35–8.0keV]	<i>net_cnts</i> [5] [0.35–1.1keV]	<i>net_cnts</i> [6] [1.1–2.6keV]	<i>net_cnts</i> [7] [2.6–8.0keV]	<i>net_cnts</i> [8] [0.35–2.0keV]
622	114.8 ^{+13.9} _{-12.9}	30.0 ^{+7.6} _{-6.5}	84.8 ^{+12.2} _{-11.1}	116.3 ^{+14.0} _{-13.0}	5.8 ^{+4.5} _{-3.4}	41.9 ^{+8.5} _{-7.4}	68.5 ^{+11.1} _{-10.1}	31.5 ^{+7.7} _{-6.6}
623	55.1 ^{+10.3} _{-9.2}	29.6 ^{+7.2} _{-6.1}	25.4 ^{+8.0} _{-6.9}	57.7 ^{+10.5} _{-9.4}	11.6 ^{+5.0} _{-3.9}	34.6 ^{+7.5} _{-6.4}	11.5 ^{+6.7} _{-5.6}	32.3 ^{+7.5} _{-6.4}
624	21.6 ^{+6.9} _{-5.8}	4.5 ^{+4.0} _{-2.8}	17.2 ^{+6.1} _{-5.0}	21.2 ^{+6.9} _{-5.8}	-2.2 ^{+1.9} _{-0.0}	6.3 ^{+4.2} _{-3.0}	17.1 ^{+6.0} _{-4.9}	4.1 ^{+4.0} _{-2.8}
625	26.2 ^{+7.2} _{-6.1}	18.5 ^{+5.8} _{-4.7}	7.7 ^{+5.0} _{-3.9}	26.9 ^{+7.3} _{-6.2}	5.9 ^{+4.0} _{-2.8}	15.3 ^{+5.4} _{-4.2}	5.7 ^{+4.6} _{-3.5}	19.2 ^{+5.9} _{-4.8}
626	82.7 ^{+10.3} _{-9.3}	57.2 ^{+8.7} _{-7.6}	25.5 ^{+6.4} _{-5.3}	83.6 ^{+10.4} _{-9.3}	11.6 ^{+4.6} _{-3.4}	51.3 ^{+8.3} _{-7.2}	20.8 ^{+5.9} _{-4.8}	58.1 ^{+8.7} _{-7.7}
627	30.6 ^{+7.9} _{-6.9}	22.5 ^{+6.3} _{-5.2}	8.1 ^{+5.6} _{-4.4}	30.4 ^{+7.9} _{-6.9}	10.5 ^{+4.7} _{-3.6}	16.0 ^{+5.6} _{-4.5}	3.8 ^{+4.8} _{-3.7}	22.3 ^{+6.3} _{-5.2}
628	60.6 ^{+9.7} _{-8.6}	1.5 ^{+3.5} _{-2.2}	59.2 ^{+9.4} _{-8.3}	60.0 ^{+9.7} _{-8.6}	-1.0 ^{+2.4} _{-0.9}	4.4 ^{+4.0} _{-2.8}	56.6 ^{+9.2} _{-8.1}	0.8 ^{+3.5} _{-2.2}
629	16.4 ^{+5.7} _{-4.6}	2.5 ^{+3.2} _{-1.9}	13.9 ^{+5.2} _{-4.1}	16.2 ^{+5.7} _{-4.6}	-1.0 ^{+1.9} _{-0.0}	4.7 ^{+3.6} _{-2.4}	12.5 ^{+5.0} _{-3.8}	2.2 ^{+3.2} _{-1.9}
630	179.2 ^{+16.2} _{-15.2}	93.4 ^{+11.3} _{-10.2}	85.8 ^{+12.3} _{-11.2}	178.4 ^{+16.3} _{-15.2}	18.7 ^{+6.1} _{-4.9}	93.4 ^{+11.5} _{-10.4}	66.2 ^{+11.0} _{-9.9}	92.6 ^{+11.3} _{-10.3}
631	32.3 ^{+10.7} _{-9.6}	26.3 ^{+7.6} _{-6.5}	6.0 ^{+8.2} _{-7.1}	32.0 ^{+10.7} _{-9.7}	4.5 ^{+4.5} _{-3.3}	26.1 ^{+7.6} _{-6.5}	1.5 ^{+7.4} _{-6.3}	26.0 ^{+7.6} _{-6.6}
632	29.6 ^{+7.0} _{-5.9}	16.8 ^{+5.3} _{-4.2}	12.8 ^{+5.2} _{-4.1}	29.4 ^{+7.0} _{-5.9}	3.5 ^{+3.2} _{-1.9}	16.2 ^{+5.3} _{-4.2}	9.7 ^{+4.7} _{-3.6}	16.6 ^{+5.3} _{-4.2}
633	146.8 ^{+14.2} _{-13.2}	87.3 ^{+10.7} _{-9.7}	59.4 ^{+10.0} _{-8.9}	146.8 ^{+14.3} _{-13.2}	19.7 ^{+5.9} _{-4.8}	82.9 ^{+10.5} _{-9.5}	44.1 ^{+8.9} _{-7.8}	87.3 ^{+10.8} _{-9.7}
634	21.5 ^{+7.7} _{-6.6}	9.6 ^{+5.0} _{-3.9}	11.9 ^{+6.4} _{-5.3}	20.6 ^{+7.7} _{-6.6}	2.4 ^{+3.7} _{-2.4}	11.0 ^{+5.2} _{-4.0}	7.1 ^{+5.7} _{-4.6}	8.7 ^{+5.0} _{-3.9}
635	550.6 ^{+25.1} _{-24.1}	377.1 ^{+20.7} _{-19.7}	173.4 ^{+14.9} _{-13.9}	554.1 ^{+25.2} _{-24.2}	121.8 ^{+12.3} _{-11.2}	305.1 ^{+18.8} _{-17.7}	127.2 ^{+13.0} _{-11.9}	380.7 ^{+20.8} _{-19.8}
636	20.3 ^{+9.3} _{-8.3}	13.4 ^{+6.3} _{-5.2}	6.9 ^{+7.5} _{-6.4}	20.3 ^{+9.4} _{-8.3}	3.2 ^{+4.4} _{-3.2}	9.0 ^{+5.8} _{-4.6}	8.1 ^{+7.2} _{-6.1}	13.4 ^{+6.4} _{-5.3}
637	22.8 ^{+6.7} _{-5.6}	9.8 ^{+4.6} _{-3.4}	13.0 ^{+5.5} _{-4.4}	22.5 ^{+6.7} _{-5.6}	-1.2 ^{+1.9} _{-0.0}	16.8 ^{+5.5} _{-4.3}	6.9 ^{+4.6} _{-3.5}	9.5 ^{+4.6} _{-3.4}
638	24.8 ^{+6.8} _{-5.7}	11.3 ^{+4.7} _{-3.6}	13.5 ^{+5.5} _{-4.4}	24.6 ^{+6.8} _{-5.7}	1.0 ^{+2.7} _{-1.3}	15.5 ^{+5.2} _{-4.1}	8.1 ^{+4.7} _{-3.6}	11.1 ^{+4.7} _{-3.6}
639	145.3 ^{+13.6} _{-12.5}	72.7 ^{+9.8} _{-8.7}	72.6 ^{+10.0} _{-9.0}	144.6 ^{+13.6} _{-12.5}	13.8 ^{+5.1} _{-4.0}	74.9 ^{+9.9} _{-8.8}	55.9 ^{+9.0} _{-7.9}	72.0 ^{+9.8} _{-8.7}
640	105.6 ^{+12.3} _{-11.2}	94.1 ^{+11.0} _{-10.0}	11.5 ^{+6.2} _{-5.1}	105.8 ^{+12.3} _{-11.3}	67.5 ^{+9.4} _{-8.4}	28.8 ^{+6.9} _{-5.8}	9.5 ^{+5.9} _{-4.7}	94.4 ^{+11.1} _{-10.0}
641	29.9 ^{+9.5} _{-8.5}	7.4 ^{+5.5} _{-4.3}	22.6 ^{+8.3} _{-7.2}	30.9 ^{+9.6} _{-8.6}	3.0 ^{+4.2} _{-3.0}	5.4 ^{+5.1} _{-4.0}	22.5 ^{+8.0} _{-6.9}	8.3 ^{+5.7} _{-4.6}
642	31.6 ^{+7.6} _{-6.5}	2.4 ^{+3.4} _{-2.2}	29.2 ^{+7.2} _{-6.1}	32.4 ^{+7.7} _{-6.6}	0.1 ^{+2.4} _{-0.9}	9.9 ^{+4.8} _{-3.6}	22.5 ^{+6.5} _{-5.4}	3.2 ^{+3.6} _{-2.4}
643	32.0 ^{+9.2} _{-8.1}	11.1 ^{+5.6} _{-4.4}	20.9 ^{+7.9} _{-6.8}	32.5 ^{+9.3} _{-8.2}	3.0 ^{+3.9} _{-2.7}	10.1 ^{+5.4} _{-4.3}	19.4 ^{+7.5} _{-6.4}	11.6 ^{+5.7} _{-4.5}
644	23.8 ^{+7.1} _{-6.0}	12.9 ^{+5.0} _{-3.9}	10.9 ^{+5.7} _{-4.5}	24.4 ^{+7.2} _{-6.1}	3.7 ^{+3.4} _{-2.2}	15.2 ^{+5.4} _{-4.2}	5.5 ^{+4.8} _{-3.7}	13.5 ^{+5.1} _{-4.0}
645	46.8 ^{+9.0} _{-7.9}	16.8 ^{+5.7} _{-4.6}	30.0 ^{+7.5} _{-6.4}	46.5 ^{+9.0} _{-7.9}	4.3 ^{+3.6} _{-2.4}	22.0 ^{+6.2} _{-5.1}	20.2 ^{+6.6} _{-5.5}	16.5 ^{+5.7} _{-4.6}
646	13.2 ^{+5.4} _{-4.3}	11.3 ^{+4.7} _{-3.6}	1.9 ^{+3.5} _{-2.2}	13.9 ^{+5.5} _{-4.4}	7.0 ^{+4.0} _{-2.8}	7.3 ^{+4.2} _{-3.0}	-0.4 ^{+2.7} _{-1.4}	12.0 ^{+4.9} _{-3.7}
647	887.7 ^{+31.3} _{-30.3}	551.6 ^{+24.7} _{-23.7}	336.1 ^{+19.9} _{-18.8}	890.1 ^{+31.3} _{-30.3}	169.7 ^{+14.2} _{-13.2}	491.6 ^{+23.4} _{-22.4}	228.7 ^{+16.7} _{-15.6}	554.0 ^{+24.8} _{-23.7}
648	190.7 ^{+16.1} _{-15.1}	86.2 ^{+10.9} _{-9.8}	104.5 ^{+12.5} _{-11.4}	189.7 ^{+16.2} _{-15.1}	8.5 ^{+5.0} _{-3.8}	105.3 ^{+11.7} _{-10.6}	75.9 ^{+11.1} _{-10.0}	85.2 ^{+10.9} _{-9.8}

Table 5—Continued

Source No	<i>net_cnts</i> [1] [0.5–8.0keV]	<i>net_cnts</i> [2] [0.5–2.0keV]	<i>net_cnts</i> [3] [2.0–8.0keV]	<i>net_cnts</i> [4] [0.35–8.0keV]	<i>net_cnts</i> [5] [0.35–1.1keV]	<i>net_cnts</i> [6] [1.1–2.6keV]	<i>net_cnts</i> [7] [2.6–8.0keV]	<i>net_cnts</i> [8] [0.35–2.0keV]
649	26.9 ^{+7.4} _{-6.3}	14.4 ^{+5.5} _{-4.4}	12.5 ^{+5.6} _{-4.4}	27.1 ^{+7.5} _{-6.4}	6.4 ^{+4.4} _{-3.2}	8.4 ^{+4.5} _{-3.3}	12.2 ^{+5.5} _{-4.3}	14.6 ^{+5.7} _{-4.5}
650	41.5 ^{+8.2} _{-7.1}	13.4 ^{+5.0} _{-3.9}	28.1 ^{+7.1} _{-6.0}	41.2 ^{+8.2} _{-7.1}	4.1 ^{+3.4} _{-2.2}	13.9 ^{+5.1} _{-4.0}	23.2 ^{+6.5} _{-5.4}	13.1 ^{+5.0} _{-3.9}
651	11.2 ^{+7.3} _{-6.3}	8.1 ^{+5.0} _{-3.9}	3.1 ^{+6.0} _{-4.9}	14.4 ^{+7.7} _{-6.6}	7.4 ^{+4.5} _{-3.3}	5.9 ^{+4.8} _{-3.6}	1.1 ^{+5.4} _{-4.3}	11.3 ^{+5.5} _{-4.4}
652	32.0 ^{+8.1} _{-7.1}	19.5 ^{+5.9} _{-4.8}	12.5 ^{+6.2} _{-5.1}	31.8 ^{+8.1} _{-7.1}	2.6 ^{+3.2} _{-2.0}	20.5 ^{+6.1} _{-5.0}	8.7 ^{+5.6} _{-4.5}	19.3 ^{+5.9} _{-4.8}
653	111.4 ^{+12.6} _{-11.5}	86.5 ^{+10.7} _{-9.6}	24.8 ^{+7.4} _{-6.3}	112.1 ^{+12.6} _{-11.5}	55.3 ^{+8.7} _{-7.6}	36.3 ^{+7.5} _{-6.4}	20.6 ^{+6.9} _{-5.8}	87.3 ^{+10.7} _{-9.6}
654	74.7 ^{+11.9} _{-10.9}	30.6 ^{+7.4} _{-6.3}	44.0 ^{+9.9} _{-8.8}	76.2 ^{+12.1} _{-11.0}	5.5 ^{+4.5} _{-3.4}	34.2 ^{+7.7} _{-6.6}	36.6 ^{+9.2} _{-8.1}	32.2 ^{+7.7} _{-6.6}
655	24.9 ^{+7.7} _{-6.6}	4.8 ^{+4.2} _{-3.0}	20.1 ^{+7.0} _{-5.9}	26.7 ^{+7.9} _{-6.8}	4.8 ^{+3.6} _{-2.4}	10.1 ^{+4.9} _{-3.8}	11.9 ^{+6.2} _{-5.0}	6.6 ^{+4.5} _{-3.4}
656	50.5 ^{+9.1} _{-8.0}	37.8 ^{+7.5} _{-6.4}	12.7 ^{+5.8} _{-4.7}	50.3 ^{+9.1} _{-8.0}	8.6 ^{+4.3} _{-3.1}	31.3 ^{+7.0} _{-5.8}	10.5 ^{+5.5} _{-4.4}	37.6 ^{+7.5} _{-6.4}
657	53.5 ^{+9.8} _{-8.7}	27.2 ^{+6.9} _{-5.8}	26.3 ^{+7.6} _{-6.5}	53.6 ^{+9.9} _{-8.8}	3.9 ^{+3.9} _{-2.7}	32.2 ^{+7.2} _{-6.1}	17.6 ^{+6.7} _{-5.6}	27.3 ^{+7.0} _{-5.9}
658	20.3 ^{+8.3} _{-7.2}	17.7 ^{+6.1} _{-5.0}	2.7 ^{+6.3} _{-5.2}	20.3 ^{+8.4} _{-7.3}	0.1 ^{+3.5} _{-2.3}	16.7 ^{+6.0} _{-4.9}	3.5 ^{+5.9} _{-4.8}	17.7 ^{+6.2} _{-5.1}
659	24.8 ^{+7.6} _{-6.5}	15.1 ^{+5.5} _{-4.4}	9.7 ^{+5.9} _{-4.7}	25.1 ^{+7.7} _{-6.7}	3.4 ^{+3.9} _{-2.7}	13.9 ^{+5.4} _{-4.3}	7.8 ^{+5.4} _{-4.3}	15.4 ^{+5.8} _{-4.6}
660	16.9 ^{+5.9} _{-4.8}	12.3 ^{+4.7} _{-3.6}	4.6 ^{+4.4} _{-3.2}	16.6 ^{+6.0} _{-4.8}	1.6 ^{+2.7} _{-1.3}	9.5 ^{+4.5} _{-3.3}	5.5 ^{+4.4} _{-3.2}	12.0 ^{+4.7} _{-3.6}
661	83.7 ^{+11.1} _{-10.0}	26.1 ^{+6.8} _{-5.6}	57.7 ^{+9.3} _{-8.2}	85.6 ^{+11.2} _{-10.1}	2.4 ^{+3.8} _{-2.5}	34.6 ^{+7.3} _{-6.2}	48.6 ^{+8.7} _{-7.6}	27.9 ^{+7.0} _{-5.9}
662	23.3 ^{+8.1} _{-7.0}	19.8 ^{+6.4} _{-5.2}	3.5 ^{+5.8} _{-4.7}	23.7 ^{+8.3} _{-7.2}	7.7 ^{+4.7} _{-3.5}	14.7 ^{+5.8} _{-4.6}	1.3 ^{+5.3} _{-4.2}	20.2 ^{+6.6} _{-5.5}

[†]Uncertainties are given on a 90% confidence level.

Table 6. Merged photon flux ($\text{photons}/\text{cm}^2/\text{s}$) in different energy bands.

Source No	$flux[1]$ [0.5–8.0keV]	$flux[2]$ [0.5–2.0keV]	$flux[3]$ [2.0–8.0keV]	$flux[4]$ [0.35–8.0keV]	$flux[5]$ [0.35–1.1keV]	$flux[6]$ [1.1–2.6keV]	$flux[7]$ [2.6–8.0keV]	$flux[8]$ [0.35–2.0keV]
1	4.10e–06	1.82e–06	1.87e–06	4.16e–06	7.65e–07	1.61e–06	1.40e–06	1.98e–06
2	1.54e–06	6.39e–07	7.53e–07	1.57e–06	4.57e–07	5.09e–07	6.03e–07	7.00e–07
3	5.81e–06	2.46e–06	2.76e–06	5.98e–06	2.11e–06	2.00e–06	1.98e–06	2.74e–06
4	2.45e–06	1.42e–06	6.21e–07	2.49e–06	1.25e–06	1.08e–06	2.29e–07	1.56e–06
5	2.63e–06	1.08e–06	1.30e–06	2.71e–06	5.81e–07	9.49e–07	1.03e–06	1.21e–06
6	3.93e–06	2.89e–06	7.45e–08	4.09e–06	3.87e–06	1.48e–06	−1.46e–07	3.24e–06
7	8.71e–07	3.37e–07	4.58e–07	8.81e–07	6.30e–08	2.95e–07	4.26e–07	3.64e–07
8	7.41e–07	6.63e–07	−1.47e–07	7.51e–07	1.60e–06	1.02e–07	−1.70e–07	7.23e–07
9	4.42e–07	3.08e–07	3.19e–08	4.78e–07	3.13e–07	1.76e–07	4.60e–08	3.59e–07
10	4.34e–05	1.38e–05	2.74e–05	4.44e–05	8.83e–06	1.25e–05	2.27e–05	1.53e–05
11	4.63e–07	3.69e–07	−3.46e–08	4.66e–07	3.84e–07	1.81e–07	−1.73e–08	3.99e–07
12	1.81e–06	9.86e–07	5.47e–07	1.83e–06	7.84e–07	7.75e–07	2.50e–07	1.06e–06
13	1.63e–06	4.30e–07	1.15e–06	1.65e–06	1.99e–07	4.19e–07	9.82e–07	4.62e–07
14	1.71e–06	8.32e–07	6.66e–07	1.73e–06	4.87e–07	5.85e–07	6.40e–07	9.03e–07
15	2.36e–06	1.20e–06	8.36e–07	2.46e–06	1.01e–06	8.55e–07	7.02e–07	1.36e–06
16	1.05e–05	4.66e–06	4.64e–06	1.07e–05	2.87e–06	3.57e–06	4.02e–06	5.10e–06
17	5.51e–07	1.67e–07	3.58e–07	5.49e–07	2.16e–08	1.86e–07	2.73e–07	1.73e–07
18	1.04e–06	5.18e–07	3.79e–07	1.07e–06	3.03e–07	3.94e–07	3.30e–07	5.77e–07
19	6.76e–07	3.40e–07	2.39e–07	6.85e–07	3.52e–07	1.89e–07	2.22e–07	3.69e–07
20	8.42e–07	5.60e–07	1.34e–07	9.16e–07	1.25e–06	1.45e–07	1.06e–07	6.62e–07
21	1.25e–06	5.47e–07	5.61e–07	1.27e–06	4.89e–07	3.81e–07	4.55e–07	5.95e–07
22	1.69e–06	1.11e–06	2.43e–07	1.76e–06	1.51e–06	5.73e–07	1.35e–07	1.24e–06
23	5.94e–07	2.68e–07	2.58e–07	6.10e–07	1.79e–07	1.83e–07	2.57e–07	2.97e–07
24	1.66e–06	8.26e–07	6.29e–07	1.69e–06	4.92e–07	7.00e–07	4.11e–07	9.02e–07
25	2.19e–06	9.95e–07	9.35e–07	2.23e–06	7.44e–07	7.60e–07	7.15e–07	1.08e–06
26	1.42e–06	5.76e–07	7.14e–07	1.45e–06	3.39e–07	5.39e–07	4.87e–07	6.36e–07
27	7.99e–07	2.26e–07	5.42e–07	7.90e–07	4.21e–08	2.26e–07	4.55e–07	2.28e–07

Table 6—Continued

Source No	<i>flux</i> [1] [0.5–8.0keV]	<i>flux</i> [2] [0.5–2.0keV]	<i>flux</i> [3] [2.0–8.0keV]	<i>flux</i> [4] [0.35–8.0keV]	<i>flux</i> [5] [0.35–1.1keV]	<i>flux</i> [6] [1.1–2.6keV]	<i>flux</i> [7] [2.6–8.0keV]	<i>flux</i> [8] [0.35–2.0keV]
28	3.69e–06	2.01e–06	1.11e–06	3.75e–06	1.24e–06	1.43e–06	9.81e–07	2.19e–06
29	5.19e–06	2.64e–06	1.80e–06	5.27e–06	1.64e–06	2.27e–06	9.74e–07	2.88e–06
30	1.01e–06	4.08e–07	5.03e–07	1.01e–06	3.65e–07	2.91e–07	4.05e–07	4.34e–07
31	5.15e–07	2.96e–07	1.24e–07	5.23e–07	1.76e–07	2.12e–07	1.06e–07	3.23e–07
32	1.45e–06	5.51e–07	7.77e–07	1.48e–06	2.28e–07	5.35e–07	5.79e–07	6.09e–07
33	3.40e–06	1.58e–06	1.35e–06	3.46e–06	8.19e–07	1.36e–06	9.71e–07	1.73e–06
34	4.23e–07	8.55e–08	3.37e–07	4.29e–07	8.31e–08	4.24e–08	3.48e–07	9.27e–08
35	6.48e–05	3.28e–05	2.42e–05	6.65e–05	2.74e–05	2.40e–05	1.78e–05	3.63e–05
36	4.75e–07	1.84e–07	2.51e–07	5.40e–07	2.20e–07	1.52e–07	2.11e–07	2.46e–07
37	5.88e–05	3.15e–05	1.97e–05	6.02e–05	2.70e–05	2.21e–05	1.47e–05	3.47e–05
38	2.75e–06	1.04e–06	1.49e–06	2.79e–06	4.44e–07	1.03e–06	1.05e–06	1.13e–06
39	6.14e–07	2.50e–07	3.06e–07	6.15e–07	2.56e–08	1.99e–07	3.19e–07	2.66e–07
40	3.45e–06	1.55e–06	1.52e–06	3.51e–06	1.04e–06	1.38e–06	9.48e–07	1.70e–06
41	1.19e–06	1.27e–07	1.11e–06	1.22e–06	8.13e–08	1.23e–07	1.08e–06	1.43e–07
42	4.61e–07	1.76e–07	2.45e–07	4.80e–07	1.70e–07	1.14e–07	2.36e–07	2.02e–07
43	3.25e–07	2.27e–07	2.09e–08	3.29e–07	5.23e–07	2.62e–08	−1.26e–09	2.46e–07
44	7.49e–07	6.23e–08	7.28e–07	7.57e–07	3.31e–09	8.51e–08	6.84e–07	6.34e–08
45	2.03e–07	1.29e–07	3.25e–08	2.19e–07	1.02e–07	9.23e–08	2.44e–08	1.51e–07
46	2.60e–06	7.83e–07	1.70e–06	2.62e–06	9.61e–08	8.32e–07	1.39e–06	8.33e–07
47	5.73e–07	2.04e–07	3.29e–07	6.10e–07	1.59e–07	2.04e–07	2.31e–07	2.43e–07
48	1.61e–06	1.24e–06	7.13e–09	1.67e–06	2.49e–06	2.44e–07	−1.66e–08	1.39e–06
49	5.27e–07	1.71e–07	3.25e–07	5.60e–07	1.64e–07	1.71e–07	2.25e–07	2.05e–07
50	8.09e–07	2.71e–07	4.87e–07	8.79e–07	1.99e–07	2.56e–07	4.13e–07	3.40e–07
51	9.06e–07	4.38e–07	3.45e–07	9.11e–07	1.13e–07	3.68e–07	3.05e–07	4.69e–07
52	3.61e–07	2.22e–08	3.62e–07	3.77e–07	−2.09e–08	6.25e–08	3.19e–07	3.13e–08
53	5.27e–07	1.53e–07	3.51e–07	5.37e–07	3.85e–08	1.55e–07	3.06e–07	1.67e–07
54	4.32e–06	1.95e–06	1.87e–06	4.38e–06	1.65e–06	1.43e–06	1.44e–06	2.12e–06

Table 6—Continued

Source No	<i>flux</i> [1] [0.5–8.0keV]	<i>flux</i> [2] [0.5–2.0keV]	<i>flux</i> [3] [2.0–8.0keV]	<i>flux</i> [4] [0.35–8.0keV]	<i>flux</i> [5] [0.35–1.1keV]	<i>flux</i> [6] [1.1–2.6keV]	<i>flux</i> [7] [2.6–8.0keV]	<i>flux</i> [8] [0.35–2.0keV]
55	3.27e−07	1.92e−07	7.57e−08	3.23e−07	1.39e−07	1.60e−07	2.59e−09	2.02e−07
56	3.74e−07	1.84e−07	1.39e−07	4.04e−07	2.41e−07	1.04e−07	1.18e−07	2.19e−07
57	1.74e−07	9.98e−08	4.22e−08	1.77e−07	3.86e−08	7.51e−08	4.40e−08	1.09e−07
58	9.35e−07	4.49e−07	3.57e−07	9.49e−07	1.81e−07	3.62e−07	3.16e−07	4.89e−07
59	1.60e−06	9.84e−07	3.57e−07	1.65e−06	1.38e−06	4.29e−07	3.03e−07	1.09e−06
60	8.88e−07	3.92e−07	3.92e−07	8.96e−07	2.93e−07	2.91e−07	3.13e−07	4.22e−07
61	8.99e−07	3.23e−07	5.09e−07	9.11e−07	1.70e−07	2.76e−07	4.30e−07	3.49e−07
62	5.84e−07	6.09e−08	5.50e−07	6.08e−07	2.32e−08	7.00e−08	5.34e−07	7.68e−08
63	8.80e−06	3.38e−06	4.77e−06	9.02e−06	1.68e−06	3.24e−06	3.56e−06	3.74e−06
64	1.98e−05	9.43e−06	8.21e−06	2.03e−05	7.03e−06	7.13e−06	6.46e−06	1.04e−05
65	4.92e−07	2.23e−07	2.11e−07	4.95e−07	2.24e−07	1.24e−07	2.01e−07	2.39e−07
66	1.91e−07	1.29e−08	1.90e−07	1.93e−07	−5.25e−09	8.98e−08	6.46e−08	1.34e−08
67	1.88e−07	3.39e−08	1.56e−07	1.76e−07	−8.67e−08	5.94e−08	1.40e−07	2.41e−08
68	6.73e−06	3.31e−06	2.62e−06	6.88e−06	2.12e−06	2.75e−06	1.79e−06	3.64e−06
69	4.05e−07	3.01e−07	3.07e−09	4.00e−07	2.82e−07	1.76e−07	−2.22e−08	3.19e−07
70	9.44e−07	8.02e−07	−9.78e−08	9.55e−07	1.35e−06	2.20e−07	−1.06e−07	8.71e−07
71	7.61e−07	2.04e−07	5.31e−07	7.75e−07	5.87e−08	1.86e−07	5.02e−07	2.23e−07
72	3.72e−07	2.24e−07	7.50e−08	4.04e−07	5.14e−07	4.48e−08	5.34e−08	2.64e−07
73	5.93e−07	1.37e−07	4.47e−07	6.04e−07	−3.94e−09	2.01e−07	3.29e−07	1.50e−07
74	2.70e−06	1.38e−06	9.71e−07	2.76e−06	7.16e−07	1.09e−06	8.11e−07	1.52e−06
75	4.62e−07	1.16e−07	3.35e−07	4.65e−07	7.10e−08	1.34e−07	2.41e−07	1.22e−07
76	5.11e−06	1.87e−06	2.83e−06	5.23e−06	5.09e−07	1.94e−06	2.14e−06	2.07e−06
77	5.36e−07	7.07e−08	4.83e−07	5.37e−07	3.65e−08	8.87e−08	4.16e−07	6.95e−08
78	8.01e−07	2.00e−08	8.46e−07	8.07e−07	7.44e−08	2.73e−08	7.96e−07	1.49e−08
79	4.46e−07	1.01e−07	3.40e−07	4.51e−07	1.02e−07	1.06e−07	2.54e−07	1.07e−07
80	1.06e−07	3.24e−08	6.83e−08	1.08e−07	3.78e−08	1.44e−08	6.99e−08	3.52e−08
81	1.06e−07	3.24e−08	6.82e−08	1.08e−07	−2.17e−09	2.98e−08	6.98e−08	3.51e−08

Table 6—Continued

Source No	$flux[1]$ [0.5–8.0keV]	$flux[2]$ [0.5–2.0keV]	$flux[3]$ [2.0–8.0keV]	$flux[4]$ [0.35–8.0keV]	$flux[5]$ [0.35–1.1keV]	$flux[6]$ [1.1–2.6keV]	$flux[7]$ [2.6–8.0keV]	$flux[8]$ [0.35–2.0keV]
82	4.25e–07	2.34e–07	1.18e–07	4.32e–07	1.57e–07	1.98e–07	4.42e–08	2.56e–07
83	6.51e–07	1.22e–07	5.33e–07	6.60e–07	4.43e–08	1.51e–07	4.42e–07	1.31e–07
84	2.95e–07	1.56e–07	9.24e–08	3.27e–07	5.97e–08	1.55e–07	6.00e–08	1.92e–07
85	3.60e–07	6.31e–08	3.01e–07	3.66e–07	2.98e–08	7.23e–08	2.62e–07	6.90e–08
86	2.65e–07	8.59e–08	1.63e–07	2.69e–07	1.31e–07	5.93e–08	1.14e–07	9.33e–08
87	2.86e–07	9.74e–08	1.69e–07	2.99e–07	6.51e–08	7.50e–08	1.62e–07	1.13e–07
88	1.72e–06	1.27e–06	7.55e–08	1.79e–06	2.59e–06	2.58e–07	4.71e–08	1.42e–06
89	6.72e–07	3.73e–07	1.84e–07	6.81e–07	3.94e–07	2.17e–07	1.43e–07	4.06e–07
90	8.49e–06	4.36e–06	2.90e–06	8.71e–06	3.50e–06	3.27e–06	1.97e–06	4.82e–06
91	4.31e–07	1.43e–07	2.61e–07	4.32e–07	5.24e–08	1.08e–07	2.60e–07	1.50e–07
92	6.78e–07	3.75e–07	1.88e–07	6.76e–07	3.08e–07	2.61e–07	1.14e–07	3.98e–07
93	1.68e–06	7.56e–07	7.26e–07	1.71e–06	5.40e–07	6.51e–07	4.51e–07	8.25e–07
94	1.03e–06	7.95e–07	−2.01e–09	1.04e–06	1.62e–06	9.07e–08	2.37e–08	8.61e–07
95	3.13e–07	1.69e–07	9.41e–08	3.18e–07	1.28e–07	1.22e–07	6.60e–08	1.84e–07
96	5.85e–07	1.51e–07	4.17e–07	5.95e–07	−3.09e–09	2.16e–07	2.93e–07	1.64e–07
97	4.50e–07	4.72e–08	4.24e–07	4.58e–07	7.45e–09	7.22e–08	3.76e–07	5.13e–08
98	4.64e–07	8.33e–08	3.85e–07	4.94e–07	4.86e–08	1.26e–07	2.98e–07	1.08e–07
99	1.33e–06	5.31e–07	6.68e–07	1.38e–06	2.34e–07	4.57e–07	5.97e–07	6.01e–07
100	3.68e–06	2.83e–06	2.08e–08	3.88e–06	6.31e–06	4.84e–07	−1.27e–08	3.21e–06
101	2.10e–07	1.14e–07	6.26e–08	2.05e–07	1.21e–07	7.79e–08	2.20e–08	1.17e–07
102	6.88e–05	5.27e–05	9.34e–07	7.12e–05	1.05e–04	1.18e–05	2.82e–07	5.85e–05
103	1.30e–06	4.00e–07	8.40e–07	1.33e–06	1.51e–07	3.64e–07	7.46e–07	4.35e–07
104	3.41e–07	1.98e–07	8.08e–08	3.45e–07	−2.08e–08	2.14e–07	2.98e–08	2.14e–07
105	1.85e–06	8.86e–07	7.43e–07	1.88e–06	5.13e–07	7.34e–07	5.33e–07	9.63e–07
106	3.11e–07	4.49e–08	2.75e–07	3.13e–07	6.81e–08	3.66e–08	2.41e–07	4.61e–08
107	4.65e–07	2.59e–07	1.28e–07	4.66e–07	8.29e–08	2.09e–07	1.10e–07	2.77e–07
108	1.22e–06	2.16e–07	1.01e–06	1.23e–06	−4.86e–08	3.11e–07	8.41e–07	2.26e–07

Table 6—Continued

Source No	$flux[1]$ [0.5–8.0keV]	$flux[2]$ [0.5–2.0keV]	$flux[3]$ [2.0–8.0keV]	$flux[4]$ [0.35–8.0keV]	$flux[5]$ [0.35–1.1keV]	$flux[6]$ [1.1–2.6keV]	$flux[7]$ [2.6–8.0keV]	$flux[8]$ [0.35–2.0keV]
109	9.08e–07	4.56e–08	9.27e–07	9.15e–07	–6.35e–09	5.12e–08	9.20e–07	4.18e–08
110	9.63e–08	–8.59e–09	1.18e–07	1.02e–07	–3.98e–08	2.47e–08	9.36e–08	–6.15e–09
111	4.35e–07	1.56e–08	4.54e–07	4.27e–07	–6.10e–08	9.40e–08	3.45e–07	4.31e–09
112	1.55e–06	8.05e–07	5.06e–07	1.61e–06	7.70e–07	5.67e–07	3.43e–07	9.05e–07
113	5.56e–04	2.98e–04	1.83e–04	5.67e–04	1.83e–04	2.43e–04	1.20e–04	3.27e–04
114	2.34e–07	1.11e–07	9.29e–08	2.56e–07	1.18e–07	1.12e–07	2.13e–08	1.35e–07
115	5.29e–07	3.15e–07	1.09e–07	5.38e–07	2.10e–07	2.19e–07	8.84e–08	3.44e–07
116	7.06e–07	1.23e–07	5.91e–07	7.12e–07	–5.87e–08	2.35e–07	4.12e–07	1.28e–07
117	3.27e–07	8.54e–08	2.32e–07	3.49e–07	4.81e–08	6.16e–08	2.50e–07	1.06e–07
118	3.13e–07	1.56e–07	1.12e–07	3.18e–07	2.79e–07	5.66e–08	8.32e–08	1.70e–07
119	6.00e–07	4.33e–07	2.86e–08	6.03e–07	6.54e–07	1.74e–07	6.92e–09	4.66e–07
120	1.92e–07	9.52e–08	7.01e–08	1.86e–07	2.04e–08	7.98e–08	5.68e–08	9.64e–08
121	8.38e–07	2.79e–07	5.04e–07	8.50e–07	1.26e–07	2.74e–07	3.92e–07	3.02e–07
122	4.61e–06	2.07e–06	1.98e–06	4.69e–06	9.15e–07	1.74e–06	1.65e–06	2.26e–06
123	1.19e–06	3.10e–07	8.50e–07	1.21e–06	6.37e–08	3.61e–07	6.80e–07	3.34e–07
124	1.77e–06	3.10e–07	1.48e–06	1.79e–06	–1.10e–08	4.12e–07	1.27e–06	3.28e–07
125	1.64e–06	7.37e–07	7.01e–07	1.67e–06	4.93e–07	6.13e–07	4.91e–07	8.06e–07
126	6.79e–07	3.03e–07	2.96e–07	7.03e–07	2.48e–07	2.34e–07	2.26e–07	3.41e–07
127	1.19e–06	1.71e–07	1.05e–06	1.21e–06	–1.99e–07	2.71e–07	9.76e–07	1.85e–07
128	2.01e–07	4.06e–08	1.61e–07	2.09e–07	5.19e–08	3.71e–08	1.35e–07	4.73e–08
129	4.38e–07	1.16e–07	3.09e–07	4.45e–07	1.29e–07	1.19e–07	2.08e–07	1.26e–07
130	7.46e–07	3.03e–07	3.70e–07	7.73e–07	1.39e–07	2.60e–07	3.25e–07	3.42e–07
131	5.84e–07	1.05e–08	6.26e–07	5.87e–07	–1.32e–08	4.41e–08	5.80e–07	5.63e–09
132	3.71e–06	1.52e–06	1.80e–06	3.77e–06	5.31e–07	1.42e–06	1.40e–06	1.66e–06
133	8.39e–06	3.88e–06	3.47e–06	8.56e–06	2.42e–06	3.30e–06	2.38e–06	4.25e–06
134	2.95e–06	1.25e–06	1.38e–06	3.03e–06	9.17e–07	9.69e–07	1.12e–06	1.38e–06
135	5.27e–07	2.14e–07	2.60e–07	5.67e–07	1.54e–07	2.12e–07	1.70e–07	2.58e–07

Table 6—Continued

Source No	$flux[1]$ [0.5–8.0keV]	$flux[2]$ [0.5–2.0keV]	$flux[3]$ [2.0–8.0keV]	$flux[4]$ [0.35–8.0keV]	$flux[5]$ [0.35–1.1keV]	$flux[6]$ [1.1–2.6keV]	$flux[7]$ [2.6–8.0keV]	$flux[8]$ [0.35–2.0keV]
136	7.05e–07	2.60e–07	3.89e–07	7.15e–07	1.76e–07	2.43e–07	2.68e–07	2.81e–07
137	2.22e–07	1.52e–07	1.84e–08	2.38e–07	1.54e–07	9.20e–08	1.29e–08	1.76e–07
138	2.40e–06	1.14e–06	9.59e–07	2.44e–06	7.20e–07	9.62e–07	6.32e–07	1.24e–06
139	9.41e–07	7.30e–07	–4.94e–08	9.80e–07	1.50e–06	1.20e–07	–4.45e–08	8.16e–07
140	9.76e–07	3.43e–07	5.70e–07	9.97e–07	–3.30e–08	4.20e–07	3.94e–07	3.79e–07
141	2.06e–06	1.56e–07	2.03e–06	2.11e–06	1.55e–07	1.63e–07	1.95e–06	1.78e–07
142	1.59e–06	6.40e–07	7.91e–07	1.61e–06	3.38e–07	5.83e–07	5.74e–07	6.95e–07
143	5.02e–06	7.00e–07	4.46e–06	5.11e–06	1.53e–07	9.44e–07	3.91e–06	7.62e–07
144	1.79e–06	1.00e–06	4.95e–07	1.81e–06	5.28e–07	7.87e–07	3.57e–07	1.09e–06
145	3.28e–07	1.30e–07	1.66e–07	3.30e–07	1.36e–07	8.03e–08	1.42e–07	1.39e–07
146	3.18e–07	8.09e–10	3.47e–07	3.15e–07	2.74e–08	4.54e–10	3.29e–07	–6.19e–09
147	5.68e–07	3.24e–07	1.44e–07	5.73e–07	1.71e–07	2.63e–07	8.17e–08	3.49e–07
148	3.08e–07	4.43e–08	2.73e–07	3.19e–07	1.72e–08	5.86e–08	2.41e–07	5.28e–08
149	1.77e–06	1.39e–06	–8.42e–08	1.82e–06	2.94e–06	2.50e–07	–5.27e–08	1.53e–06
150	1.05e–06	3.15e–08	1.10e–06	1.06e–06	–1.21e–08	1.23e–07	9.61e–07	2.79e–08
151	2.95e–07	1.83e–07	5.12e–08	3.12e–07	1.22e–07	1.40e–07	3.13e–08	2.10e–07
152	2.75e–06	1.03e–06	1.50e–06	2.80e–06	3.15e–07	9.03e–07	1.36e–06	1.12e–06
153	1.08e–06	7.98e–07	5.23e–08	1.09e–06	1.30e–06	2.62e–07	4.24e–08	8.68e–07
154	9.86e–06	4.93e–06	3.66e–06	1.01e–05	4.27e–06	3.50e–06	2.82e–06	5.47e–06
155	5.63e–06	2.50e–06	2.56e–06	5.80e–06	1.51e–06	2.13e–06	1.94e–06	2.78e–06
156	4.55e–07	5.16e–08	4.22e–07	4.61e–07	–3.41e–08	8.26e–08	3.86e–07	5.48e–08
157	3.18e–07	1.43e–07	1.36e–07	3.17e–07	7.40e–08	1.45e–07	5.76e–08	1.51e–07
158	2.68e–04	1.29e–04	1.04e–04	2.74e–04	9.05e–05	1.01e–04	7.60e–05	1.42e–04
159	9.28e–06	4.24e–06	3.96e–06	9.44e–06	2.89e–06	3.45e–06	2.87e–06	4.63e–06
160	2.92e–07	1.81e–07	5.19e–08	2.94e–07	6.26e–08	1.62e–07	1.11e–08	1.96e–07
161	7.70e–07	3.36e–07	3.46e–07	7.88e–07	2.43e–07	2.72e–07	2.58e–07	3.71e–07
162	4.81e–06	3.24e–07	4.79e–06	4.90e–06	2.19e–07	4.79e–07	4.43e–06	3.50e–07

Table 6—Continued

Source No	$flux[1]$ [0.5–8.0keV]	$flux[2]$ [0.5–2.0keV]	$flux[3]$ [2.0–8.0keV]	$flux[4]$ [0.35–8.0keV]	$flux[5]$ [0.35–1.1keV]	$flux[6]$ [1.1–2.6keV]	$flux[7]$ [2.6–8.0keV]	$flux[8]$ [0.35–2.0keV]
163	2.08e–05	1.25e–05	5.00e–06	2.14e–05	1.21e–05	8.41e–06	3.12e–06	1.39e–05
164	2.91e–07	1.50e–07	9.75e–08	2.87e–07	1.14e–07	8.34e–08	1.07e–07	1.57e–07
165	8.28e–07	3.92e–07	3.27e–07	8.55e–07	2.81e–07	2.75e–07	3.05e–07	4.38e–07
166	1.27e–06	5.90e–07	5.19e–07	1.29e–06	4.73e–07	4.37e–07	3.91e–07	6.42e–07
167	1.97e–07	2.90e–08	1.73e–07	1.93e–07	−8.08e–09	2.69e–08	1.71e–07	2.55e–08
168	3.46e–07	9.41e–08	2.41e–07	3.50e–07	1.12e–08	1.24e–07	1.66e–07	1.01e–07
169	5.44e–07	2.63e–07	2.09e–07	5.70e–07	1.47e–07	1.84e–07	2.27e–07	3.01e–07
170	5.96e–07	1.75e–07	3.94e–07	6.55e–07	1.41e–07	1.56e–07	3.71e–07	2.30e–07
171	1.94e–07	1.39e–07	7.07e–09	1.97e–07	1.70e–07	6.01e–08	1.35e–08	1.52e–07
172	5.01e–07	5.65e–08	4.65e–07	5.01e–07	−4.17e–08	5.28e–08	4.85e–07	5.43e–08
173	1.62e–07	3.73e–08	1.22e–07	1.69e–07	−2.51e–08	9.27e–08	4.23e–08	4.41e–08
174	3.78e–07	1.22e–07	2.34e–07	4.28e–07	1.76e–07	9.22e–08	2.08e–07	1.67e–07
175	1.83e–06	1.18e–06	2.64e–07	1.91e–06	1.72e–06	5.49e–07	1.55e–07	1.33e–06
176	1.40e–06	1.08e–06	7.97e–09	1.46e–06	2.25e–06	1.69e–07	5.73e–08	1.20e–06
177	7.14e–07	1.11e–07	6.18e–07	7.21e–07	1.27e–07	6.84e–08	6.01e–07	1.16e–07
178	3.97e–07	1.83e–07	1.65e–07	4.11e–07	1.86e–07	1.23e–07	1.30e–07	2.05e–07
179	2.22e–06	1.01e–06	9.68e–07	2.22e–06	1.75e–07	9.55e–07	7.01e–07	1.07e–06
180	6.79e–04	3.08e–04	3.04e–04	6.96e–04	2.44e–04	2.37e–04	2.34e–04	3.40e–04
181	2.38e–06	1.22e–06	8.10e–07	2.46e–06	1.22e–06	8.00e–07	6.26e–07	1.36e–06
182	2.77e–07	1.33e–07	1.07e–07	2.99e–07	9.06e–08	1.13e–07	8.36e–08	1.59e–07
183	2.28e–06	1.74e–06	2.97e–08	2.40e–06	3.47e–06	4.39e–07	1.15e–09	1.97e–06
184	1.28e–05	9.73e–06	9.23e–08	1.33e–05	1.92e–05	2.10e–06	2.47e–08	1.09e–05
185	2.40e–07	1.16e–07	9.05e–08	2.44e–07	−4.95e–09	1.21e–07	6.75e–08	1.27e–07
186	3.96e–06	1.68e–06	1.86e–06	4.04e–06	1.13e–06	1.41e–06	1.38e–06	1.84e–06
187	1.18e–05	5.87e–06	4.49e–06	1.21e–05	5.26e–06	4.17e–06	3.36e–06	6.49e–06
188	7.37e–06	5.52e–06	2.69e–07	7.66e–06	1.13e–05	1.24e–06	1.24e–07	6.17e–06
189	5.08e–07	1.83e–07	2.85e–07	5.56e–07	1.80e–07	1.92e–07	1.76e–07	2.31e–07

Table 6—Continued

Source No	$flux[1]$ [0.5–8.0keV]	$flux[2]$ [0.5–2.0keV]	$flux[3]$ [2.0–8.0keV]	$flux[4]$ [0.35–8.0keV]	$flux[5]$ [0.35–1.1keV]	$flux[6]$ [1.1–2.6keV]	$flux[7]$ [2.6–8.0keV]	$flux[8]$ [0.35–2.0keV]
190	3.07e–06	1.64e–06	9.49e–07	3.14e–06	1.64e–06	1.08e–06	6.46e–07	1.80e–06
191	1.58e–07	−1.30e–08	1.92e–07	1.56e–07	−2.70e–08	−9.30e–09	2.04e–07	−1.78e–08
192	3.97e–07	2.14e–07	1.19e–07	3.92e–07	6.85e–08	1.79e–07	8.53e–08	2.24e–07
193	1.50e–06	5.27e–07	8.65e–07	1.55e–06	2.36e–07	5.10e–07	7.00e–07	5.97e–07
194	5.51e–07	2.84e–07	1.83e–07	5.56e–07	1.70e–07	1.94e–07	1.81e–07	3.07e–07
195	1.05e–05	2.69e–06	7.57e–06	1.07e–05	5.67e–07	3.12e–06	6.18e–06	2.96e–06
196	3.85e–07	1.92e–07	1.36e–07	4.00e–07	1.36e–07	1.49e–07	1.03e–07	2.16e–07
197	1.72e–05	1.30e–05	2.67e–07	1.78e–05	2.29e–05	3.94e–06	1.40e–07	1.44e–05
198	2.64e–07	6.93e–08	1.87e–07	2.78e–07	1.23e–07	4.15e–08	1.61e–07	8.31e–08
199	9.40e–07	2.34e–07	6.85e–07	9.53e–07	3.68e–10	3.08e–07	5.23e–07	2.53e–07
200	3.85e–07	9.88e–08	2.75e–07	3.89e–07	−4.37e–08	1.38e–07	2.20e–07	1.06e–07
201	2.21e–07	1.07e–07	8.32e–08	2.13e–07	4.86e–08	8.03e–08	6.92e–08	1.08e–07
202	4.45e–07	1.72e–07	2.32e–07	4.68e–07	1.02e–07	1.63e–07	1.76e–07	2.00e–07
203	3.31e–07	1.23e–08	3.45e–07	3.22e–07	−8.33e–08	5.72e–08	3.06e–07	1.48e–09
204	3.12e–07	1.32e–07	1.46e–07	3.25e–07	9.92e–08	9.14e–08	1.42e–07	1.50e–07
205	3.79e–07	1.64e–07	1.73e–07	3.94e–07	1.67e–07	9.58e–08	1.72e–07	1.86e–07
206	4.81e–06	2.31e–06	1.89e–06	4.95e–06	1.82e–06	1.78e–06	1.38e–06	2.57e–06
207	8.32e–07	3.69e–08	8.58e–07	8.48e–07	2.34e–08	9.87e–08	7.50e–07	4.05e–08
208	2.97e–07	1.71e–07	7.18e–08	3.05e–07	1.71e–07	1.33e–07	7.77e–09	1.89e–07
209	3.73e–07	4.07e–08	3.48e–07	3.72e–07	2.19e–08	1.50e–07	1.41e–07	3.79e–08
210	2.10e–06	9.77e–07	8.54e–07	2.14e–06	6.84e–07	7.72e–07	6.37e–07	1.08e–06
211	3.72e–07	1.97e–07	1.18e–07	3.87e–07	1.25e–07	1.34e–07	1.24e–07	2.22e–07
212	2.79e–07	1.55e–07	7.74e–08	2.78e–07	1.27e–07	9.95e–08	6.07e–08	1.64e–07
213	3.92e–07	1.01e–07	2.80e–07	3.92e–07	1.02e–07	5.69e–08	2.74e–07	1.05e–07
214	7.94e–07	3.54e–08	8.17e–07	8.02e–07	2.22e–08	8.34e–08	7.24e–07	3.28e–08
215	2.45e–06	1.03e–06	1.17e–06	2.52e–06	5.62e–07	8.91e–07	9.18e–07	1.14e–06
216	3.76e–07	1.39e–07	2.07e–07	3.87e–07	5.10e–08	1.54e–07	1.33e–07	1.55e–07

Table 6—Continued

Source No	<i>flux</i> [1] [0.5–8.0keV]	<i>flux</i> [2] [0.5–2.0keV]	<i>flux</i> [3] [2.0–8.0keV]	<i>flux</i> [4] [0.35–8.0keV]	<i>flux</i> [5] [0.35–1.1keV]	<i>flux</i> [6] [1.1–2.6keV]	<i>flux</i> [7] [2.6–8.0keV]	<i>flux</i> [8] [0.35–2.0keV]
217	2.50e–07	7.49e–08	1.64e–07	2.54e–07	–3.92e–09	5.03e–08	1.95e–07	8.12e–08
218	1.55e–07	2.70e–08	1.30e–07	1.71e–07	6.24e–08	4.70e–08	7.11e–08	4.01e–08
219	5.66e–07	1.87e–07	3.43e–07	5.78e–07	9.97e–08	1.52e–07	3.16e–07	2.06e–07
220	2.92e–07	3.38e–08	2.70e–07	2.94e–07	–2.19e–08	6.80e–08	2.21e–07	3.46e–08
221	1.17e–05	4.67e–06	6.03e–06	1.19e–05	2.49e–06	4.11e–06	4.76e–06	5.11e–06
222	3.99e–07	1.37e–07	2.35e–07	4.21e–07	1.26e–07	1.21e–07	1.83e–07	1.61e–07
223	2.29e–07	1.29e–07	6.14e–08	2.34e–07	8.10e–08	7.82e–08	7.74e–08	1.42e–07
224	3.80e–06	1.55e–06	1.87e–06	3.89e–06	7.18e–07	1.35e–06	1.55e–06	1.71e–06
225	3.77e–04	2.00e–04	1.26e–04	3.85e–04	1.41e–04	1.56e–04	8.48e–05	2.20e–04
226	4.76e–07	1.51e–07	2.99e–07	4.80e–07	1.42e–07	6.63e–08	3.32e–07	1.62e–07
227	2.50e–07	1.06e–07	1.17e–07	2.45e–07	4.48e–08	1.04e–07	6.67e–08	1.09e–07
228	1.15e–06	6.25e–07	3.31e–07	1.18e–06	5.27e–07	4.21e–07	2.65e–07	6.92e–07
229	7.57e–07	3.58e–07	3.05e–07	7.66e–07	1.81e–07	2.85e–07	2.54e–07	3.87e–07
230	1.76e–07	4.10e–08	1.32e–07	1.92e–07	5.56e–08	2.65e–08	1.33e–07	5.51e–08
231	1.01e–06	3.12e–07	6.43e–07	1.04e–06	2.40e–07	2.36e–07	6.03e–07	3.53e–07
232	2.50e–07	7.15e–08	1.69e–07	2.45e–07	–2.83e–08	8.34e–08	1.45e–07	7.04e–08
233	2.07e–06	1.05e–06	7.07e–07	2.11e–06	7.78e–07	8.24e–07	4.52e–07	1.16e–06
234	1.34e–06	1.82e–07	1.19e–06	1.37e–06	4.20e–09	3.48e–07	9.11e–07	2.07e–07
235	5.70e–07	1.23e–07	4.42e–07	5.82e–07	5.24e–08	1.49e–07	3.55e–07	1.36e–07
236	6.10e–06	4.51e–06	2.71e–07	6.31e–06	7.29e–06	1.57e–06	2.23e–07	5.01e–06
237	5.79e–06	2.74e–06	2.30e–06	5.93e–06	1.88e–06	2.23e–06	1.61e–06	3.03e–06
238	2.13e–06	8.96e–07	1.01e–06	2.18e–06	3.94e–07	7.84e–07	8.18e–07	9.83e–07
239	1.37e–07	1.39e–08	1.29e–07	1.48e–07	3.18e–08	2.77e–08	9.60e–08	2.19e–08
240	9.90e–07	4.26e–07	4.52e–07	1.02e–06	1.57e–07	3.83e–07	3.68e–07	4.72e–07
241	7.03e–07	2.19e–07	4.46e–07	7.27e–07	1.08e–08	2.77e–07	3.20e–07	2.48e–07
242	1.17e–06	7.79e–07	1.52e–07	1.25e–06	1.84e–06	9.55e–08	2.33e–07	9.01e–07
243	2.37e–07	4.55e–08	1.93e–07	2.51e–07	2.64e–09	6.74e–08	1.59e–07	5.73e–08

Table 6—Continued

Source No	$flux[1]$ [0.5–8.0keV]	$flux[2]$ [0.5–2.0keV]	$flux[3]$ [2.0–8.0keV]	$flux[4]$ [0.35–8.0keV]	$flux[5]$ [0.35–1.1keV]	$flux[6]$ [1.1–2.6keV]	$flux[7]$ [2.6–8.0keV]	$flux[8]$ [0.35–2.0keV]
244	3.85e–07	1.50e–07	2.02e–07	3.87e–07	1.14e–07	1.14e–07	1.67e–07	1.60e–07
245	7.59e–07	6.29e–07	−5.85e–08	8.01e–07	9.61e–07	2.37e–07	−4.71e–08	7.12e–07
246	2.99e–07	1.54e–07	1.03e–07	2.97e–07	7.06e–08	1.38e–07	5.28e–08	1.62e–07
247	7.62e–07	1.49e–07	6.15e–07	7.79e–07	5.90e–08	1.97e–07	4.87e–07	1.65e–07
248	9.98e–06	5.02e–06	3.69e–06	1.02e–05	4.06e–06	3.60e–06	2.91e–06	5.54e–06
249	6.74e–07	4.30e–07	1.27e–07	7.17e–07	8.87e–07	9.82e–08	1.25e–07	4.95e–07
250	1.28e–06	3.76e–07	8.46e–07	1.30e–06	1.56e–07	4.24e–07	6.16e–07	4.10e–07
251	6.70e–07	1.39e–07	5.28e–07	6.79e–07	7.37e–08	1.44e–07	4.56e–07	1.50e–07
252	9.76e–07	1.78e–07	8.07e–07	9.95e–07	−2.06e–08	2.79e–07	6.29e–07	1.95e–07
253	5.84e–07	2.48e–07	2.75e–07	5.89e–07	8.24e–08	2.30e–07	2.08e–07	2.66e–07
254	3.97e–07	2.11e–07	1.24e–07	3.99e–07	1.56e–08	2.09e–07	7.49e–08	2.26e–07
255	5.84e–06	2.88e–06	2.17e–06	6.00e–06	2.04e–06	2.16e–06	1.74e–06	3.19e–06
256	1.08e–06	5.01e–07	4.48e–07	1.11e–06	3.11e–07	3.95e–07	3.72e–07	5.58e–07
257	2.60e–07	1.21e–07	1.07e–07	2.58e–07	5.83e–08	8.48e–08	1.06e–07	1.27e–07
258	2.96e–07	1.35e–07	1.25e–07	3.04e–07	9.28e–08	9.31e–08	1.21e–07	1.50e–07
259	9.01e–07	3.74e–07	4.38e–07	9.29e–07	2.35e–07	3.04e–07	3.68e–07	4.18e–07
260	1.22e–06	9.02e–07	6.39e–08	1.22e–06	7.51e–07	7.65e–07	−3.20e–07	9.70e–07
261	2.04e–07	1.33e–07	2.75e–08	2.06e–07	1.52e–07	7.46e–08	9.61e–09	1.44e–07
262	3.99e–06	1.70e–06	1.86e–06	4.06e–06	1.06e–06	1.45e–06	1.38e–06	1.86e–06
263	1.05e–05	4.34e–06	5.14e–06	1.08e–05	2.65e–06	3.60e–06	4.17e–06	4.79e–06
264	1.10e–05	3.13e–06	7.49e–06	1.12e–05	1.75e–06	3.00e–06	6.25e–06	3.45e–06
265	3.86e–07	6.89e–08	3.21e–07	3.84e–07	4.52e–08	8.94e–08	2.43e–07	6.80e–08
266	7.22e–07	3.44e–07	2.85e–07	7.43e–07	1.44e–07	2.97e–07	2.26e–07	3.82e–07
267	1.35e–07	5.28e–08	6.97e–08	1.42e–07	8.94e–08	2.39e–08	6.30e–08	6.16e–08
268	2.81e–06	1.25e–06	1.24e–06	2.88e–06	8.72e–07	1.00e–06	9.44e–07	1.38e–06
269	1.00e–06	5.21e–07	3.30e–07	1.02e–06	5.29e–07	3.71e–07	1.74e–07	5.68e–07
270	6.07e–07	3.07e–07	2.27e–07	6.16e–07	6.31e–07	8.08e–08	1.91e–07	3.35e–07

Table 6—Continued

Source No	$flux[1]$ [0.5–8.0keV]	$flux[2]$ [0.5–2.0keV]	$flux[3]$ [2.0–8.0keV]	$flux[4]$ [0.35–8.0keV]	$flux[5]$ [0.35–1.1keV]	$flux[6]$ [1.1–2.6keV]	$flux[7]$ [2.6–8.0keV]	$flux[8]$ [0.35–2.0keV]
271	2.51e–07	1.31e–07	8.15e–08	2.50e–07	3.83e–08	9.89e–08	8.42e–08	1.39e–07
272	1.42e–06	9.13e–07	2.10e–07	1.45e–06	6.66e–07	6.38e–07	1.13e–07	9.99e–07
273	2.93e–07	1.86e–08	2.93e–07	3.08e–07	−1.52e–09	5.96e–08	2.38e–07	2.83e–08
274	3.28e–06	9.60e–07	2.17e–06	3.34e–06	4.41e–07	8.42e–07	1.98e–06	1.05e–06
275	4.07e–06	2.03e–06	1.47e–06	4.17e–06	1.40e–06	1.50e–06	1.22e–06	2.24e–06
276	5.11e–08	4.72e–11	5.59e–08	4.00e–08	−5.07e–08	9.92e–09	5.71e–08	−9.54e–09
277	2.84e–06	1.31e–06	1.21e–06	2.90e–06	5.34e–07	1.18e–06	9.14e–07	1.44e–06
278	1.94e–06	1.27e–06	2.23e–07	2.03e–06	1.62e–06	6.28e–07	1.63e–07	1.44e–06
279	9.55e–06	6.90e–06	5.24e–07	9.93e–06	1.22e–05	2.19e–06	2.12e–07	7.71e–06
280	1.02e–06	1.60e–07	8.80e–07	1.04e–06	−1.39e–08	2.44e–07	7.38e–07	1.79e–07
281	6.62e–06	1.98e–06	4.33e–06	6.76e–06	3.78e–07	2.21e–06	3.45e–06	2.18e–06
282	6.16e–06	2.96e–06	2.43e–06	6.30e–06	2.62e–06	2.25e–06	1.63e–06	3.26e–06
283	2.86e–06	1.25e–06	1.29e–06	2.93e–06	6.94e–07	1.03e–06	1.06e–06	1.38e–06
284	5.23e–07	2.72e–08	5.31e–07	5.26e–07	5.20e–08	2.84e–08	4.98e–07	2.47e–08
285	2.32e–06	1.09e–06	9.31e–07	2.37e–06	2.55e–07	9.72e–07	7.98e–07	1.20e–06
286	3.20e–07	3.56e–08	2.98e–07	3.24e–07	7.58e–08	1.39e–08	2.88e–07	3.70e–08
287	7.09e–06	5.24e–06	2.55e–07	7.36e–06	1.09e–05	1.09e–06	1.50e–07	5.84e–06
288	4.02e–07	3.56e–07	−6.40e–08	4.42e–07	4.72e–07	1.80e–07	−7.63e–08	4.17e–07
289	2.65e–07	1.67e–07	4.45e–08	2.77e–07	1.82e–07	1.16e–07	1.07e–09	1.88e–07
290	3.19e–07	1.75e–08	3.24e–07	3.09e–07	−2.99e–08	5.22e–08	2.67e–07	5.70e–09
291	1.88e–06	7.59e–07	9.67e–07	1.96e–06	1.50e–06	3.13e–07	8.60e–07	8.62e–07
292	3.73e–07	1.76e–07	1.48e–07	4.27e–07	1.59e–07	1.53e–07	1.15e–07	2.30e–07
293	6.07e–07	2.28e–07	3.29e–07	6.23e–07	1.74e–07	1.68e–07	2.96e–07	2.53e–07
294	3.38e–07	4.73e–08	3.00e–07	3.56e–07	9.30e–08	5.66e–08	2.40e–07	6.14e–08
295	1.07e–06	4.05e–07	5.82e–07	1.10e–06	1.87e–07	4.13e–07	3.95e–07	4.44e–07
296	2.11e–07	7.24e–08	1.24e–07	2.20e–07	4.24e–08	8.95e–08	6.45e–08	8.32e–08
297	8.64e–07	3.48e–07	4.31e–07	8.76e–07	1.91e–07	2.60e–07	4.06e–07	3.78e–07

Table 6—Continued

Source No	<i>flux</i> [1] [0.5–8.0keV]	<i>flux</i> [2] [0.5–2.0keV]	<i>flux</i> [3] [2.0–8.0keV]	<i>flux</i> [4] [0.35–8.0keV]	<i>flux</i> [5] [0.35–1.1keV]	<i>flux</i> [6] [1.1–2.6keV]	<i>flux</i> [7] [2.6–8.0keV]	<i>flux</i> [8] [0.35–2.0keV]
298	2.16e–06	1.65e–06	–4.85e–08	2.24e–06	3.42e–06	3.28e–07	–4.03e–08	1.84e–06
299	1.26e–05	5.93e–06	5.24e–06	1.29e–05	4.56e–06	4.50e–06	4.05e–06	6.55e–06
300	2.61e–07	8.58e–08	1.60e–07	2.58e–07	4.98e–08	9.14e–08	9.89e–08	8.73e–08
301	5.17e–06	2.67e–06	1.73e–06	5.28e–06	2.28e–06	1.90e–06	1.24e–06	2.93e–06
302	3.69e–07	3.07e–07	–4.73e–08	3.66e–07	2.98e–07	1.57e–07	–3.88e–08	3.28e–07
303	4.93e–07	1.78e–07	2.79e–07	4.90e–07	1.32e–07	1.46e–07	2.14e–07	1.84e–07
304	5.24e–07	1.85e–07	3.02e–07	5.58e–07	1.19e–07	1.91e–07	2.19e–07	2.21e–07
305	8.43e–07	2.90e–07	4.93e–07	8.55e–07	7.04e–08	2.81e–07	4.19e–07	3.15e–07
306	7.75e–07	3.92e–07	2.73e–07	7.75e–07	–5.19e–08	4.24e–07	1.59e–07	4.17e–07
307	1.05e–06	3.87e–07	5.89e–07	1.08e–06	1.87e–07	3.92e–07	4.10e–07	4.26e–07
308	3.09e–06	2.23e–06	2.10e–07	3.22e–06	4.49e–06	4.49e–07	2.06e–07	2.51e–06
309	7.43e–06	3.62e–06	2.82e–06	7.61e–06	2.51e–06	2.93e–06	1.92e–06	3.99e–06
310	7.31e–07	6.26e–08	7.08e–07	7.38e–07	5.31e–08	7.91e–08	6.45e–07	6.37e–08
311	1.99e–07	1.78e–08	1.92e–07	1.99e–07	1.01e–08	1.33e–08	1.89e–07	1.61e–08
312	4.67e–06	2.12e–06	2.00e–06	4.74e–06	1.22e–06	1.76e–06	1.52e–06	2.31e–06
313	1.07e–07	1.29e–07	–7.31e–08	1.05e–07	3.85e–08	9.51e–08	–6.92e–08	1.38e–07
314	2.29e–07	1.44e–07	3.89e–08	2.29e–07	1.20e–07	9.81e–08	1.50e–08	1.54e–07
315	2.51e–07	8.44e–08	1.51e–07	2.61e–07	1.26e–07	3.19e–08	1.58e–07	9.62e–08
316	5.90e–06	2.75e–06	2.44e–06	6.05e–06	2.02e–06	2.17e–06	1.80e–06	3.04e–06
317	5.36e–07	2.20e–07	2.61e–07	5.45e–07	9.50e–08	1.87e–07	2.24e–07	2.41e–07
318	4.20e–03	2.07e–03	1.66e–03	4.28e–03	1.31e–03	1.71e–03	1.18e–03	2.28e–03
319	2.51e–07	1.35e–07	7.09e–08	2.55e–07	1.14e–07	1.10e–07	1.91e–08	1.47e–07
320	9.13e–06	4.78e–06	3.19e–06	9.38e–06	4.14e–06	3.35e–06	2.44e–06	5.29e–06
321	1.24e–07	–7.45e–10	1.37e–07	1.16e–07	–5.15e–08	2.50e–08	1.14e–07	–9.30e–09
322	3.57e–07	2.39e–07	3.96e–08	3.75e–07	2.60e–07	1.48e–07	8.54e–09	2.71e–07
323	1.57e–06	7.04e–07	6.91e–07	1.60e–06	3.47e–07	5.91e–07	5.49e–07	7.64e–07
324	3.42e–07	1.64e–07	1.33e–07	3.46e–07	1.87e–07	1.04e–07	9.27e–08	1.77e–07

Table 6—Continued

Source No	<i>flux</i> [1] [0.5–8.0keV]	<i>flux</i> [2] [0.5–2.0keV]	<i>flux</i> [3] [2.0–8.0keV]	<i>flux</i> [4] [0.35–8.0keV]	<i>flux</i> [5] [0.35–1.1keV]	<i>flux</i> [6] [1.1–2.6keV]	<i>flux</i> [7] [2.6–8.0keV]	<i>flux</i> [8] [0.35–2.0keV]
325	5.12e–07	2.83e–07	1.41e–07	5.07e–07	4.84e–07	1.02e–07	8.75e–08	2.98e–07
326	1.43e–06	4.37e–07	9.21e–07	1.41e–06	2.36e–07	3.04e–07	8.95e–07	4.43e–07
327	8.31e–07	3.41e–07	4.07e–07	8.48e–07	1.67e–07	3.06e–07	3.12e–07	3.73e–07
328	5.24e–07	4.47e–07	–6.18e–08	5.44e–07	9.23e–07	8.59e–08	–7.19e–08	4.97e–07
329	4.05e–07	1.99e–07	1.49e–07	4.03e–07	7.11e–08	1.82e–07	9.08e–08	2.10e–07
330	2.99e–07	1.15e–07	1.57e–07	3.10e–07	1.29e–07	8.37e–08	1.21e–07	1.30e–07
331	6.40e–07	2.16e–07	3.84e–07	6.47e–07	1.24e–07	2.63e–07	1.91e–07	2.32e–07
332	6.08e–07	4.66e–07	9.00e–10	6.03e–07	1.02e–06	5.02e–08	–2.21e–09	4.97e–07
333	8.10e–07	4.61e–07	2.04e–07	8.29e–07	3.77e–07	3.20e–07	1.40e–07	5.08e–07
334	1.22e–05	9.29e–06	9.70e–08	1.26e–05	1.87e–05	1.97e–06	–6.11e–08	1.04e–05
335	1.35e–06	6.03e–07	5.98e–07	1.42e–06	2.91e–07	5.55e–07	4.43e–07	6.88e–07
336	1.40e–06	1.69e–07	1.28e–06	1.42e–06	9.03e–08	2.05e–07	1.15e–06	1.79e–07
337	3.73e–07	6.61e–08	3.12e–07	3.71e–07	–4.28e–08	8.68e–08	2.86e–07	6.52e–08
338	3.93e–07	1.87e–07	1.55e–07	3.95e–07	1.42e–07	1.46e–07	1.02e–07	2.00e–07
339	3.64e–06	2.15e–06	8.31e–07	3.72e–06	1.79e–06	1.32e–06	8.24e–07	2.36e–06
340	2.73e–07	9.46e–08	1.58e–07	2.83e–07	2.05e–08	1.09e–07	1.13e–07	1.08e–07
341	2.18e–07	7.93e–08	1.22e–07	2.21e–07	7.93e–08	7.16e–08	7.49e–08	8.63e–08
342	2.45e–06	8.87e–07	1.38e–06	2.50e–06	3.38e–07	8.46e–07	1.11e–06	9.74e–07
343	1.64e–07	5.61e–08	9.68e–08	1.70e–07	6.56e–08	5.27e–08	5.80e–08	6.35e–08
344	3.00e–07	1.20e–07	1.52e–07	3.15e–07	1.19e–07	9.14e–08	1.21e–07	1.39e–07
345	3.37e–07	1.67e–07	1.25e–07	3.48e–07	3.01e–07	6.87e–08	9.39e–08	1.87e–07
346	2.57e–06	8.18e–07	1.62e–06	2.65e–06	2.84e–07	8.80e–07	1.24e–06	9.20e–07
347	1.45e–05	6.95e–06	5.81e–06	1.48e–05	5.04e–06	5.38e–06	4.40e–06	7.67e–06
348	5.29e–06	2.11e–06	2.74e–06	5.44e–06	1.65e–06	1.73e–06	2.12e–06	2.35e–06
349	2.99e–07	2.41e–07	–1.62e–08	3.16e–07	4.37e–07	5.70e–08	–2.93e–09	2.73e–07
350	1.74e–07	1.57e–07	–4.04e–08	1.66e–07	9.19e–08	1.29e–07	–8.94e–08	1.63e–07
351	4.03e–07	8.06e–08	3.22e–07	4.06e–07	–3.95e–08	9.92e–08	3.01e–07	8.48e–08

Table 6—Continued

Source No	<i>flux</i> [1] [0.5–8.0keV]	<i>flux</i> [2] [0.5–2.0keV]	<i>flux</i> [3] [2.0–8.0keV]	<i>flux</i> [4] [0.35–8.0keV]	<i>flux</i> [5] [0.35–1.1keV]	<i>flux</i> [6] [1.1–2.6keV]	<i>flux</i> [7] [2.6–8.0keV]	<i>flux</i> [8] [0.35–2.0keV]
352	1.97e–06	9.23e–07	7.87e–07	2.03e–06	7.54e–07	6.68e–07	6.39e–07	1.03e–06
353	6.40e–07	3.50e–07	1.89e–07	6.52e–07	2.08e–07	2.72e–07	1.35e–07	3.83e–07
354	7.41e–07	1.39e–07	6.06e–07	8.28e–07	2.23e–07	1.15e–07	5.89e–07	2.11e–07
355	4.23e–07	1.76e–07	2.05e–07	4.23e–07	1.24e–07	1.27e–07	1.77e–07	1.86e–07
356	2.50e–06	1.25e–07	2.54e–06	2.53e–06	−1.03e–08	2.21e–07	2.39e–06	1.25e–07
357	3.37e–07	2.51e–07	1.06e–08	3.48e–07	5.67e–07	3.87e–08	−9.91e–09	2.78e–07
358	4.00e–07	7.48e–08	3.28e–07	4.11e–07	9.58e–08	3.92e–08	3.26e–07	8.43e–08
359	1.99e–07	9.77e–09	2.04e–07	1.97e–07	−6.51e–09	−7.73e–09	2.33e–07	6.09e–09
360	2.56e–07	1.79e–07	2.25e–08	2.65e–07	3.67e–07	5.81e–08	−1.44e–08	2.00e–07
361	7.13e–07	1.57e–07	5.49e–07	7.16e–07	1.79e–08	1.82e–07	4.67e–07	1.64e–07
362	1.91e–06	1.45e–06	3.16e–08	2.02e–06	2.66e–06	4.34e–07	−1.90e–08	1.64e–06
363	1.88e–07	1.26e–07	2.07e–08	2.13e–07	1.81e–07	6.20e–08	2.12e–08	1.54e–07
364	2.07e–07	2.72e–08	1.87e–07	2.16e–07	6.73e–08	3.02e–08	1.46e–07	3.35e–08
365	7.18e–06	3.15e–06	3.29e–06	7.33e–06	1.82e–06	2.59e–06	2.65e–06	3.46e–06
366	1.06e–06	7.33e–07	1.18e–07	1.10e–06	1.25e–06	2.55e–07	9.04e–08	8.20e–07
367	6.32e–07	3.02e–07	2.46e–07	6.69e–07	2.18e–07	2.39e–07	1.99e–07	3.50e–07
368	1.32e–06	8.70e–07	1.61e–07	1.38e–06	1.31e–06	3.98e–07	5.61e–08	9.76e–07
369	5.01e–07	4.22e–08	4.87e–07	5.09e–07	3.21e–09	3.65e–08	4.96e–07	4.52e–08
370	1.17e–06	5.90e–07	4.10e–07	1.19e–06	4.28e–07	4.21e–07	3.40e–07	6.45e–07
371	1.48e–06	1.14e–06	−1.65e–09	1.52e–06	2.25e–06	2.55e–07	−4.17e–08	1.25e–06
372	8.62e–07	5.76e–07	1.22e–07	8.73e–07	7.00e–07	2.75e–07	1.04e–07	6.26e–07
373	9.22e–07	5.41e–07	2.16e–07	9.34e–07	3.34e–07	4.02e–07	1.49e–07	5.88e–07
374	3.42e–07	3.00e–07	−5.50e–08	3.54e–07	4.79e–07	1.10e–07	−6.76e–08	3.33e–07
375	4.34e–07	3.07e–07	1.79e–08	4.64e–07	6.52e–07	7.30e–08	−8.49e–09	3.53e–07
376	2.48e–07	1.19e–07	9.44e–08	2.70e–07	3.08e–07	5.04e–09	9.81e–08	1.44e–07
377	2.41e–07	1.61e–07	2.67e–08	2.39e–07	1.81e–07	7.18e–08	3.30e–08	1.71e–07
378	2.29e–07	5.13e–09	2.44e–07	2.25e–07	−5.91e–08	3.25e–08	2.28e–07	−1.08e–09

Table 6—Continued

Source No	$flux[1]$ [0.5–8.0keV]	$flux[2]$ [0.5–2.0keV]	$flux[3]$ [2.0–8.0keV]	$flux[4]$ [0.35–8.0keV]	$flux[5]$ [0.35–1.1keV]	$flux[6]$ [1.1–2.6keV]	$flux[7]$ [2.6–8.0keV]	$flux[8]$ [0.35–2.0keV]
379	4.44e–07	9.48e–08	3.47e–07	4.64e–07	5.13e–08	9.70e–08	3.14e–07	1.13e–07
380	2.22e–07	7.93e–08	1.27e–07	2.32e–07	3.92e–08	5.38e–08	1.40e–07	9.09e–08
381	5.56e–06	3.07e–06	1.66e–06	5.69e–06	1.93e–06	2.42e–06	1.11e–06	3.38e–06
382	1.25e–07	7.84e–08	2.09e–08	1.21e–07	2.81e–08	5.61e–08	2.08e–08	8.07e–08
383	1.93e–07	7.41e–08	1.01e–07	1.84e–07	7.86e–08	5.08e–08	6.84e–08	7.15e–08
384	2.11e–06	7.67e–07	1.18e–06	2.14e–06	4.75e–07	6.51e–07	9.62e–07	8.27e–07
385	6.85e–07	3.16e–07	2.92e–07	7.35e–07	6.65e–07	9.31e–08	2.54e–07	3.75e–07
386	2.77e–06	1.38e–06	1.03e–06	2.81e–06	9.25e–07	1.03e–06	8.18e–07	1.51e–06
387	1.11e–06	3.55e–07	6.95e–07	1.14e–06	1.97e–07	3.35e–07	5.67e–07	3.94e–07
388	1.17e–06	5.10e–07	5.35e–07	1.18e–06	3.14e–07	4.17e–07	4.08e–07	5.49e–07
389	1.12e–05	5.53e–06	4.37e–06	1.15e–05	4.11e–06	4.13e–06	3.43e–06	6.09e–06
390	8.02e–07	3.67e–07	3.35e–07	8.20e–07	2.06e–07	3.45e–07	1.91e–07	4.05e–07
391	3.34e–06	1.34e–06	1.72e–06	3.41e–06	5.31e–07	1.30e–06	1.26e–06	1.47e–06
392	9.42e–07	4.30e–07	4.01e–07	9.67e–07	3.00e–07	3.57e–07	2.81e–07	4.75e–07
393	6.12e–07	2.46e–07	3.08e–07	6.20e–07	−2.40e–09	2.56e–07	2.46e–07	2.66e–07
394	7.39e–07	3.38e–08	7.57e–07	7.50e–07	4.83e–08	4.99e–08	7.09e–07	3.43e–08
395	2.06e–06	1.05e–06	7.11e–07	2.13e–06	8.12e–07	8.13e–07	4.79e–07	1.17e–06
396	4.42e–06	8.17e–07	3.63e–06	4.49e–06	1.39e–07	1.04e–06	3.09e–06	8.89e–07
397	8.33e–07	3.86e–07	3.43e–07	8.46e–07	1.80e–07	3.19e–07	2.81e–07	4.20e–07
398	3.33e–06	7.80e–07	2.50e–06	3.41e–06	2.96e–07	8.11e–07	2.20e–06	8.70e–07
399	1.36e–06	5.85e–07	6.39e–07	1.49e–06	5.50e–07	4.87e–07	5.09e–07	7.25e–07
400	3.99e–07	1.82e–07	1.68e–07	4.04e–07	4.77e–08	1.70e–07	1.28e–07	1.97e–07
401	1.64e–06	3.78e–07	1.24e–06	1.71e–06	−3.43e–08	4.35e–07	1.15e–06	4.48e–07
402	2.36e–07	6.41e–08	1.64e–07	2.32e–07	5.25e–08	3.48e–08	1.64e–07	6.30e–08
403	2.00e–06	9.12e–07	8.57e–07	2.05e–06	9.07e–07	6.50e–07	6.47e–07	1.01e–06
404	5.18e–07	3.01e–07	1.39e–07	5.50e–07	7.76e–07	4.26e–08	1.01e–07	3.48e–07
405	4.66e–07	2.55e–07	1.33e–07	4.67e–07	1.47e–07	1.99e–07	8.57e–08	2.73e–07

Table 6—Continued

Source No	<i>flux</i> [1] [0.5–8.0keV]	<i>flux</i> [2] [0.5–2.0keV]	<i>flux</i> [3] [2.0–8.0keV]	<i>flux</i> [4] [0.35–8.0keV]	<i>flux</i> [5] [0.35–1.1keV]	<i>flux</i> [6] [1.1–2.6keV]	<i>flux</i> [7] [2.6–8.0keV]	<i>flux</i> [8] [0.35–2.0keV]
406	1.38e–07	8.45e–09	1.38e–07	1.44e–07	2.50e–08	2.94e–09	1.38e–07	1.18e–08
407	7.55e–07	1.61e–07	5.89e–07	7.84e–07	−3.30e–08	2.32e–07	4.81e–07	1.89e–07
408	3.26e–06	1.59e–06	1.23e–06	3.38e–06	1.39e–06	1.09e–06	1.07e–06	1.79e–06
409	1.85e–06	1.15e–06	3.51e–07	1.93e–06	1.64e–06	5.81e–07	2.20e–07	1.29e–06
410	4.79e–07	3.64e–08	4.72e–07	4.86e–07	8.07e–08	1.47e–08	4.61e–07	3.81e–08
411	8.09e–07	3.32e–07	3.98e–07	8.08e–07	1.10e–07	3.01e–07	3.09e–07	3.50e–07
412	4.13e–07	3.32e–08	4.03e–07	4.27e–07	−9.53e–09	9.28e–08	3.16e–07	4.10e–08
413	2.97e–07	2.38e–07	−1.43e–08	3.28e–07	5.87e–07	2.94e–08	−2.72e–08	2.82e–07
414	8.49e–07	2.07e–07	6.24e–07	8.64e–07	4.79e–08	2.34e–07	5.23e–07	2.26e–07
415	2.98e–06	1.48e–06	1.08e–06	3.08e–06	1.43e–06	1.05e–06	7.51e–07	1.66e–06
416	1.02e–06	1.86e–07	8.42e–07	1.03e–06	6.62e–08	2.37e–07	6.94e–07	2.01e–07
417	1.58e–06	1.18e–06	5.99e–08	1.66e–06	2.54e–06	2.26e–07	2.84e–08	1.33e–06
418	2.62e–07	1.11e–07	1.22e–07	2.61e–07	5.26e–08	8.42e–08	1.11e–07	1.16e–07
419	2.17e–06	9.17e–07	1.03e–06	2.23e–06	5.77e–07	7.83e–07	7.83e–07	1.02e–06
420	6.50e–07	2.43e–07	3.54e–07	6.62e–07	5.93e–08	2.54e–07	2.61e–07	2.65e–07
421	5.85e–06	2.86e–06	2.28e–06	5.95e–06	1.75e–06	2.35e–06	1.62e–06	3.12e–06
422	1.67e–07	7.99e–08	6.43e–08	1.69e–07	7.44e–08	5.77e–08	4.23e–08	8.70e–08
423	2.38e–06	1.15e–06	9.16e–07	2.46e–06	9.94e–07	8.21e–07	7.09e–07	1.27e–06
424	1.08e–05	5.33e–06	4.00e–06	1.11e–05	5.10e–06	3.56e–06	3.13e–06	5.88e–06
425	1.62e–07	6.10e–08	8.81e–08	1.57e–07	2.03e–09	5.33e–08	8.05e–08	6.04e–08
426	3.58e–07	1.42e–07	1.82e–07	3.57e–07	4.84e–08	9.66e–08	1.99e–07	1.49e–07
427	5.80e–06	4.30e–06	1.79e–07	6.07e–06	9.06e–06	8.01e–07	6.80e–08	4.83e–06
428	8.66e–07	1.03e–07	7.98e–07	8.82e–07	−3.62e–08	2.28e–07	6.03e–07	1.12e–07
429	2.24e–06	1.26e–06	6.05e–07	2.30e–06	1.18e–06	8.32e–07	4.18e–07	1.39e–06
430	2.97e–07	1.78e–07	6.39e–08	3.08e–07	1.22e–07	1.24e–07	5.53e–08	1.98e–07
431	3.27e–07	3.91e–08	3.01e–07	3.32e–07	−2.29e–08	9.99e–08	2.09e–07	4.19e–08
432	3.91e–07	7.73e–08	3.14e–07	3.99e–07	−2.02e–08	1.26e–07	2.37e–07	8.54e–08

Table 6—Continued

Source No	$flux[1]$ [0.5–8.0keV]	$flux[2]$ [0.5–2.0keV]	$flux[3]$ [2.0–8.0keV]	$flux[4]$ [0.35–8.0keV]	$flux[5]$ [0.35–1.1keV]	$flux[6]$ [1.1–2.6keV]	$flux[7]$ [2.6–8.0keV]	$flux[8]$ [0.35–2.0keV]
433	1.62e–06	1.00e–06	3.06e–07	1.69e–06	3.07e–07	8.11e–07	2.95e–07	1.13e–06
434	4.88e–07	2.34e–07	1.88e–07	5.02e–07	1.12e–07	2.27e–07	9.88e–08	2.60e–07
435	3.85e–07	1.81e–07	1.54e–07	3.90e–07	1.16e–07	1.42e–07	1.18e–07	1.96e–07
436	3.60e–07	6.60e–08	2.97e–07	3.83e–07	6.43e–08	9.39e–08	2.23e–07	8.54e–08
437	1.73e–07	9.52e–08	4.85e–08	1.81e–07	1.59e–07	3.71e–08	3.97e–08	1.08e–07
438	1.05e–06	6.80e–07	1.77e–07	1.11e–06	1.24e–06	1.67e–07	2.20e–07	7.74e–07
439	8.91e–07	3.87e–07	4.06e–07	8.95e–07	2.55e–07	3.06e–07	3.14e–07	4.14e–07
440	1.40e–06	7.55e–07	4.20e–07	1.43e–06	7.07e–07	5.25e–07	2.64e–07	8.29e–07
441	1.07e–06	4.76e–07	4.73e–07	1.07e–06	2.28e–07	3.34e–07	4.79e–07	5.08e–07
442	5.62e–07	1.50e–07	3.93e–07	5.83e–07	−1.85e–09	1.67e–07	3.58e–07	1.73e–07
443	2.48e–07	1.74e–07	2.09e–08	2.52e–07	4.31e–07	1.20e–08	1.33e–08	1.91e–07
444	1.42e–06	2.18e–07	1.23e–06	1.44e–06	7.73e–08	1.80e–07	1.23e–06	2.38e–07
445	2.38e–07	1.57e–07	2.71e–08	2.29e–07	1.44e–07	1.00e–07	−6.80e–09	1.61e–07
446	3.85e–07	1.70e–07	1.72e–07	3.85e–07	3.05e–08	1.85e–07	9.02e–08	1.80e–07
447	9.60e–07	3.04e–07	6.01e–07	9.90e–07	1.95e–07	2.55e–07	5.35e–07	3.42e–07
448	1.26e–06	9.52e–07	3.37e–08	1.35e–06	2.01e–06	2.65e–07	−8.86e–08	1.09e–06
449	2.71e–07	1.11e–07	1.32e–07	2.84e–07	1.08e–07	6.51e–08	1.36e–07	1.28e–07
450	4.28e–06	1.97e–06	1.83e–06	4.36e–06	9.72e–07	1.73e–06	1.34e–06	2.16e–06
451	3.13e–07	1.32e–07	1.47e–07	3.21e–07	5.33e–08	1.04e–07	1.44e–07	1.46e–07
452	2.18e–06	7.49e–07	1.29e–06	2.22e–06	1.36e–07	8.08e–07	9.77e–07	8.12e–07
453	4.97e–07	5.89e–08	4.58e–07	5.28e–07	2.65e–08	9.67e–08	4.00e–07	8.15e–08
454	4.04e–07	8.16e–08	3.22e–07	4.10e–07	5.64e–08	8.59e–08	2.71e–07	8.83e–08
455	3.27e–07	4.74e–08	2.89e–07	3.33e–07	3.59e–08	5.88e–08	2.44e–07	5.13e–08
456	9.16e–07	6.31e–07	1.04e–07	9.67e–07	1.42e–06	6.88e–08	1.30e–07	7.17e–07
457	1.43e–06	5.43e–07	7.70e–07	1.48e–06	3.94e–07	4.16e–07	6.94e–07	6.12e–07
458	3.08e–07	1.13e–07	1.72e–07	3.01e–07	1.22e–07	8.63e–08	1.12e–07	1.13e–07
459	1.13e–06	6.40e–07	3.11e–07	1.15e–06	2.61e–07	5.42e–07	1.98e–07	7.04e–07

Table 6—Continued

Source No	$flux[1]$ [0.5–8.0keV]	$flux[2]$ [0.5–2.0keV]	$flux[3]$ [2.0–8.0keV]	$flux[4]$ [0.35–8.0keV]	$flux[5]$ [0.35–1.1keV]	$flux[6]$ [1.1–2.6keV]	$flux[7]$ [2.6–8.0keV]	$flux[8]$ [0.35–2.0keV]
460	2.32e–07	8.01e–08	1.35e–07	2.46e–07	1.35e–08	1.12e–07	7.19e–08	9.52e–08
461	4.17e–07	1.39e–07	2.51e–07	4.45e–07	1.20e–07	1.02e–07	2.44e–07	1.69e–07
462	3.83e–06	2.48e–06	5.48e–07	4.03e–06	3.99e–06	1.13e–06	1.86e–07	2.81e–06
463	1.51e–07	1.93e–08	1.37e–07	1.48e–07	−3.86e–08	2.55e–08	1.42e–07	1.66e–08
464	2.96e–07	1.62e–07	8.32e–08	3.01e–07	7.64e–08	1.47e–07	3.61e–08	1.77e–07
465	1.64e–06	6.34e–07	8.62e–07	1.69e–06	3.32e–07	5.74e–07	6.77e–07	7.03e–07
466	2.11e–07	2.90e–08	1.89e–07	2.18e–07	1.67e–08	3.63e–08	1.68e–07	3.40e–08
467	6.52e–07	3.64e–07	1.79e–07	6.58e–07	2.89e–07	2.60e–07	1.13e–07	3.93e–07
468	1.12e–06	4.02e–07	6.36e–07	1.16e–06	1.90e–07	4.10e–07	4.72e–07	4.57e–07
469	7.41e–07	1.46e–07	5.96e–07	7.44e–07	9.69e–08	1.59e–07	4.89e–07	1.52e–07
470	3.92e–06	9.86e–07	2.84e–06	4.00e–06	1.05e–07	1.36e–06	2.03e–06	1.08e–06
471	1.50e–06	6.98e–07	6.07e–07	1.53e–06	5.36e–07	5.34e–07	4.56e–07	7.70e–07
472	2.13e–07	1.88e–08	2.06e–07	2.17e–07	−3.57e–08	4.50e–08	1.83e–07	2.02e–08
473	2.83e–07	1.62e–07	7.00e–08	2.82e–07	1.00e–07	1.06e–07	7.08e–08	1.73e–07
474	2.34e–07	1.13e–07	8.89e–08	2.30e–07	6.45e–08	8.10e–08	7.61e–08	1.17e–07
475	4.47e–07	7.81e–08	3.74e–07	4.68e–07	1.95e–08	1.21e–07	2.97e–07	9.55e–08
476	2.94e–07	1.78e–07	5.81e–08	2.99e–07	1.15e–07	1.31e–07	3.64e–08	1.94e–07
477	1.00e–07	2.32e–08	7.56e–08	9.57e–08	1.17e–08	8.76e–09	8.32e–08	2.03e–08
478	5.83e–07	3.79e–07	7.57e–08	6.59e–07	3.92e–07	2.47e–07	7.04e–08	4.67e–07
479	6.08e–07	3.19e–07	2.12e–07	5.92e–07	8.82e–07	−1.88e–08	1.87e–07	3.27e–07
480	8.99e–07	6.21e–07	9.89e–08	9.58e–07	1.26e–06	1.61e–07	6.39e–08	7.14e–07
481	1.02e–06	4.65e–07	4.27e–07	1.08e–06	4.08e–07	3.53e–07	3.43e–07	5.43e–07
482	3.03e–06	1.32e–06	1.37e–06	3.09e–06	9.18e–07	1.04e–06	1.08e–06	1.45e–06
483	1.86e–06	8.14e–07	8.34e–07	1.90e–06	4.60e–07	6.96e–07	6.27e–07	8.93e–07
484	4.43e–07	1.15e–07	3.16e–07	4.42e–07	−7.51e–09	1.30e–07	2.69e–07	1.19e–07
485	1.22e–06	4.12e–07	7.28e–07	1.26e–06	2.33e–07	3.73e–07	6.11e–07	4.64e–07
486	2.09e–07	1.41e–07	1.96e–08	2.04e–07	4.33e–08	1.28e–07	−2.00e–08	1.47e–07

Table 6—Continued

Source No	<i>flux</i> [1] [0.5–8.0keV]	<i>flux</i> [2] [0.5–2.0keV]	<i>flux</i> [3] [2.0–8.0keV]	<i>flux</i> [4] [0.35–8.0keV]	<i>flux</i> [5] [0.35–1.1keV]	<i>flux</i> [6] [1.1–2.6keV]	<i>flux</i> [7] [2.6–8.0keV]	<i>flux</i> [8] [0.35–2.0keV]
487	1.81e–06	7.49e–07	8.76e–07	1.84e–06	4.39e–07	7.16e–07	5.46e–07	8.19e–07
488	3.03e–06	1.62e–06	9.20e–07	3.08e–06	1.14e–06	1.22e–06	6.32e–07	1.77e–06
489	7.04e–07	9.14e–08	6.36e–07	7.17e–07	5.36e–08	1.40e–07	5.17e–07	9.94e–08
490	2.87e–07	1.51e–07	8.82e–08	2.90e–07	1.33e–07	1.16e–07	3.85e–08	1.63e–07
491	8.95e–06	4.62e–06	2.97e–06	9.16e–06	3.49e–06	3.43e–06	2.16e–06	5.09e–06
492	1.39e–04	7.14e–05	4.98e–05	1.43e–04	5.85e–05	5.17e–05	3.75e–05	7.89e–05
493	2.38e–06	1.28e–06	7.92e–07	2.43e–06	1.06e–06	9.50e–07	5.13e–07	1.40e–06
494	4.83e–07	2.52e–07	1.59e–07	4.90e–07	3.93e–08	2.18e–07	1.47e–07	2.74e–07
495	3.54e–07	1.78e–07	1.25e–07	3.69e–07	8.10e–08	1.73e–07	6.39e–08	2.02e–07
496	1.38e–07	1.02e–07	8.70e–11	1.34e–07	1.67e–07	3.52e–08	−1.28e–08	1.07e–07
497	3.36e–06	1.68e–06	1.19e–06	3.48e–06	1.67e–06	1.14e–06	8.64e–07	1.88e–06
498	2.59e–06	1.30e–06	9.21e–07	2.67e–06	1.42e–06	8.46e–07	6.59e–07	1.45e–06
499	1.47e–06	6.64e–07	6.20e–07	1.50e–06	4.46e–07	5.23e–07	4.77e–07	7.25e–07
500	2.66e–07	7.89e–08	1.75e–07	2.79e–07	1.67e–08	8.56e–08	1.51e–07	9.27e–08
501	9.20e–08	6.39e–08	5.12e–09	9.32e–08	7.50e–08	2.74e–08	7.52e–09	6.95e–08
502	7.42e–06	3.61e–06	2.78e–06	7.65e–06	3.16e–06	2.58e–06	2.11e–06	4.02e–06
503	1.17e–07	6.06e–08	3.68e–08	1.75e–07	2.23e–07	1.78e–08	1.98e–08	1.10e–07
504	7.69e–07	3.50e–07	3.24e–07	8.01e–07	2.14e–07	3.00e–07	2.42e–07	3.97e–07
505	1.32e–06	5.38e–07	6.47e–07	1.36e–06	5.06e–07	3.95e–07	5.24e–07	6.07e–07
506	2.25e–07	2.88e–09	2.42e–07	2.21e–07	3.75e–09	9.56e–09	2.24e–07	−3.49e–09
507	3.28e–06	1.39e–06	1.55e–06	3.37e–06	1.05e–06	1.12e–06	1.18e–06	1.54e–06
508	2.51e–07	6.22e–08	1.83e–07	2.50e–07	3.98e–08	4.52e–08	1.74e–07	6.32e–08
509	1.94e–07	8.18e–08	9.20e–08	1.80e–07	−3.60e–08	1.23e–07	9.69e–09	7.51e–08
510	4.95e–07	3.35e–07	4.90e–08	5.18e–07	6.25e–07	9.04e–08	4.52e–08	3.77e–07
511	5.05e–07	3.30e–07	6.59e–08	5.31e–07	7.54e–07	6.25e–08	4.42e–08	3.74e–07
512	1.51e–07	5.68e–08	8.17e–08	1.59e–07	9.55e–08	2.70e–08	7.23e–08	6.61e–08
513	3.19e–07	7.86e–08	2.33e–07	3.27e–07	−1.25e–08	8.92e–08	2.15e–07	8.84e–08

Table 6—Continued

Source No	<i>flux</i> [1] [0.5–8.0keV]	<i>flux</i> [2] [0.5–2.0keV]	<i>flux</i> [3] [2.0–8.0keV]	<i>flux</i> [4] [0.35–8.0keV]	<i>flux</i> [5] [0.35–1.1keV]	<i>flux</i> [6] [1.1–2.6keV]	<i>flux</i> [7] [2.6–8.0keV]	<i>flux</i> [8] [0.35–2.0keV]
514	2.49e–07	1.03e–07	1.22e–07	2.51e–07	4.53e–08	9.80e–08	8.30e–08	1.10e–07
515	7.53e–07	3.71e–07	2.76e–07	7.69e–07	4.02e–07	2.04e–07	2.57e–07	4.07e–07
516	1.20e–06	6.28e–07	3.82e–07	1.23e–06	5.37e–07	4.78e–07	2.13e–07	6.93e–07
517	2.50e–06	1.19e–06	9.58e–07	2.58e–06	1.03e–06	8.79e–07	6.86e–07	1.33e–06
518	1.13e–06	2.80e–07	8.24e–07	1.15e–06	1.67e–08	3.47e–07	6.67e–07	3.04e–07
519	6.17e–07	1.30e–07	4.85e–07	6.38e–07	−1.31e–08	1.46e–07	4.60e–07	1.49e–07
520	2.68e–07	1.48e–08	2.72e–07	2.87e–07	3.28e–08	4.70e–08	2.16e–07	2.78e–08
521	3.96e–07	1.79e–07	1.67e–07	4.02e–07	1.21e–07	1.21e–07	1.59e–07	1.94e–07
522	3.49e–07	1.81e–07	1.15e–07	3.50e–07	1.05e–07	1.22e–07	1.16e–07	1.94e–07
523	6.95e–07	3.40e–07	2.58e–07	7.04e–07	1.98e–07	2.94e–07	1.56e–07	3.69e–07
524	1.71e–07	9.82e–08	4.30e–08	1.73e–07	−2.75e–08	1.02e–07	3.50e–08	1.07e–07
525	2.95e–07	1.75e–07	6.51e–08	3.16e–07	1.64e–07	1.04e–07	7.28e–08	2.03e–07
526	2.33e–07	1.13e–07	8.72e–08	2.37e–07	1.34e–07	7.21e–08	5.86e–08	1.25e–07
527	2.76e–07	5.81e–08	2.17e–07	2.81e–07	8.26e–08	3.61e–08	1.99e–07	6.36e–08
528	1.20e–05	2.70e–06	9.21e–06	1.23e–05	5.00e–07	3.38e–06	7.48e–06	2.96e–06
529	5.45e–07	1.56e–07	3.67e–07	6.28e–07	2.54e–07	1.49e–07	2.92e–07	2.30e–07
530	1.72e–05	9.63e–06	5.07e–06	1.78e–05	9.82e–06	6.12e–06	3.77e–06	1.07e–05
531	3.69e–07	1.11e–07	2.39e–07	3.75e–07	4.64e–08	8.01e–08	2.47e–07	1.20e–07
532	1.19e–06	5.50e–07	4.91e–07	1.22e–06	3.24e–07	4.67e–07	3.56e–07	6.10e–07
533	4.18e–06	2.12e–06	1.51e–06	4.29e–06	1.83e–06	1.51e–06	1.11e–06	2.34e–06
534	1.61e–06	3.40e–07	1.26e–06	1.64e–06	1.72e–08	4.65e–07	1.00e–06	3.70e–07
535	1.34e–06	9.24e–07	1.22e–07	1.38e–06	1.17e–06	4.55e–07	5.92e–08	1.03e–06
536	4.81e–07	2.31e–07	1.86e–07	4.94e–07	2.20e–07	1.47e–07	1.64e–07	2.57e–07
537	7.49e–07	5.32e–08	7.42e–07	7.45e–07	−2.38e–08	6.79e–08	7.17e–07	4.43e–08
538	1.63e–06	5.33e–07	9.96e–07	1.65e–06	5.18e–08	5.43e–07	8.57e–07	5.77e–07
539	1.41e–06	1.06e–06	3.55e–08	1.43e–06	1.69e–06	3.59e–07	−1.08e–08	1.15e–06
540	1.03e–06	1.55e–07	9.03e–07	1.05e–06	2.79e–08	2.20e–07	7.57e–07	1.65e–07

Table 6—Continued

Source No	<i>flux</i> [1] [0.5–8.0keV]	<i>flux</i> [2] [0.5–2.0keV]	<i>flux</i> [3] [2.0–8.0keV]	<i>flux</i> [4] [0.35–8.0keV]	<i>flux</i> [5] [0.35–1.1keV]	<i>flux</i> [6] [1.1–2.6keV]	<i>flux</i> [7] [2.6–8.0keV]	<i>flux</i> [8] [0.35–2.0keV]
541	3.71e−07	2.43e−07	4.51e−08	3.94e−07	2.56e−07	1.52e−07	1.53e−08	2.78e−07
542	3.65e−07	3.19e−07	−7.50e−08	3.80e−07	6.34e−07	4.40e−08	−5.06e−08	3.56e−07
543	6.96e−07	1.84e−07	4.90e−07	7.07e−07	1.46e−07	1.50e−07	4.33e−07	1.99e−07
544	2.91e−06	3.79e−07	2.63e−06	2.96e−06	1.19e−07	5.41e−07	2.26e−06	4.14e−07
545	4.91e−07	2.02e−07	2.38e−07	4.94e−07	3.38e−07	5.95e−08	2.34e−07	2.16e−07
546	1.21e−05	3.41e−06	8.21e−06	1.24e−05	4.05e−07	4.04e−06	6.47e−06	3.81e−06
547	2.90e−07	2.07e−08	2.87e−07	2.95e−07	2.26e−08	3.54e−08	2.50e−07	2.24e−08
548	1.09e−06	5.21e−07	4.19e−07	1.13e−06	2.74e−07	4.01e−07	3.92e−07	5.85e−07
549	5.47e−07	3.14e−07	1.49e−07	5.86e−07	8.94e−07	−2.96e−08	1.64e−07	3.67e−07
550	2.63e−07	5.25e−08	2.10e−07	2.63e−07	8.28e−09	6.33e−08	1.76e−07	5.37e−08
551	5.69e−08	4.73e−08	−7.42e−09	6.51e−08	1.05e−07	1.03e−08	−8.95e−09	5.74e−08
552	1.78e−05	7.75e−06	8.32e−06	1.82e−05	4.57e−06	6.55e−06	6.43e−06	8.51e−06
553	4.78e−06	1.93e−07	4.95e−06	4.87e−06	1.19e−07	4.67e−07	4.49e−06	2.17e−07
554	3.53e−07	9.89e−08	2.41e−07	3.57e−07	−2.60e−08	1.40e−07	1.69e−07	1.06e−07
555	5.96e−07	1.94e−07	3.67e−07	6.19e−07	1.62e−07	1.51e−07	3.29e−07	2.22e−07
556	1.18e−07	3.34e−08	8.01e−08	1.16e−07	6.38e−08	2.27e−09	8.48e−08	3.28e−08
557	5.77e−07	4.47e−08	5.66e−07	5.86e−07	2.69e−08	1.30e−07	4.06e−07	4.72e−08
558	2.48e−07	2.79e−08	2.31e−07	2.57e−07	−1.41e−08	5.61e−08	1.96e−07	3.37e−08
559	8.25e−07	2.54e−07	5.27e−07	8.79e−07	7.19e−08	2.89e−07	4.29e−07	3.09e−07
560	7.87e−06	4.13e−06	2.58e−06	8.09e−06	3.79e−06	2.73e−06	2.05e−06	4.57e−06
561	9.70e−05	4.89e−05	3.37e−05	9.99e−05	4.35e−05	3.47e−05	2.50e−05	5.44e−05
562	4.47e−07	1.08e−07	3.30e−07	4.51e−07	3.45e−08	1.33e−07	2.50e−07	1.15e−07
563	3.66e−07	6.00e−08	3.13e−07	3.80e−07	−1.75e−08	9.07e−08	2.74e−07	7.06e−08
564	2.40e−06	1.32e−06	6.96e−07	2.47e−06	1.24e−06	8.76e−07	5.28e−07	1.47e−06
565	5.71e−06	2.71e−06	2.24e−06	5.87e−06	2.41e−06	1.93e−06	1.69e−06	3.00e−06
566	3.39e−07	1.03e−07	2.19e−07	3.38e−07	7.84e−08	9.55e−08	1.61e−07	1.07e−07
567	2.61e−07	1.24e−07	1.03e−07	2.91e−07	2.39e−07	3.73e−08	1.14e−07	1.56e−07

Table 6—Continued

Source No	<i>flux</i> [1] [0.5–8.0keV]	<i>flux</i> [2] [0.5–2.0keV]	<i>flux</i> [3] [2.0–8.0keV]	<i>flux</i> [4] [0.35–8.0keV]	<i>flux</i> [5] [0.35–1.1keV]	<i>flux</i> [6] [1.1–2.6keV]	<i>flux</i> [7] [2.6–8.0keV]	<i>flux</i> [8] [0.35–2.0keV]
568	1.57e–07	1.21e–07	–6.03e–09	1.53e–07	1.84e–07	5.40e–08	–3.09e–08	1.27e–07
569	2.44e–07	4.15e–08	2.06e–07	2.45e–07	6.79e–08	4.43e–08	1.54e–07	4.23e–08
570	3.28e–07	2.41e–07	1.82e–08	3.43e–07	4.87e–07	3.57e–08	4.15e–08	2.71e–07
571	1.10e–06	5.35e–07	4.15e–07	1.13e–06	5.00e–07	3.78e–07	3.09e–07	5.97e–07
572	1.33e–06	1.01e–06	1.11e–08	1.38e–06	2.22e–06	1.17e–07	5.90e–08	1.14e–06
573	1.55e–06	6.52e–07	7.31e–07	1.58e–06	1.53e–07	5.84e–07	6.46e–07	7.13e–07
574	1.36e–06	3.96e–07	9.08e–07	1.37e–06	–5.74e–08	4.92e–07	7.04e–07	4.20e–07
575	1.24e–06	3.64e–07	8.25e–07	1.25e–06	3.52e–08	3.66e–07	7.33e–07	3.89e–07
576	2.57e–06	1.18e–06	1.06e–06	2.63e–06	8.91e–07	8.77e–07	8.53e–07	1.30e–06
577	4.65e–06	2.18e–06	1.86e–06	4.79e–06	1.47e–06	1.67e–06	1.53e–06	2.43e–06
578	2.06e–07	5.99e–08	1.37e–07	2.07e–07	9.89e–09	7.11e–08	1.01e–07	6.35e–08
579	5.71e–06	2.66e–06	2.29e–06	5.89e–06	2.42e–06	1.97e–06	1.65e–06	2.97e–06
580	3.17e–07	1.69e–07	9.11e–08	3.21e–07	1.51e–07	9.30e–08	9.47e–08	1.84e–07
581	5.89e–07	1.65e–07	4.01e–07	5.92e–07	3.86e–08	2.20e–07	2.53e–07	1.74e–07
582	4.43e–07	2.00e–07	1.88e–07	4.51e–07	1.46e–07	1.57e–07	1.39e–07	2.19e–07
583	8.36e–07	5.96e–08	8.29e–07	8.67e–07	8.53e–08	6.78e–08	7.85e–07	7.72e–08
584	2.72e–07	4.96e–08	2.24e–07	2.76e–07	3.74e–08	2.97e–08	2.29e–07	5.37e–08
585	4.10e–06	2.86e–06	3.73e–07	4.24e–06	4.16e–06	1.25e–06	1.39e–07	3.18e–06
586	1.33e–06	6.32e–07	5.19e–07	1.37e–06	3.57e–07	5.19e–07	4.09e–07	7.05e–07
587	1.63e–05	7.05e–06	7.19e–06	1.67e–05	3.17e–06	6.50e–06	5.22e–06	7.84e–06
588	4.63e–07	1.39e–07	3.02e–07	4.71e–07	8.07e–08	1.25e–07	2.56e–07	1.51e–07
589	1.22e–05	6.30e–06	4.25e–06	1.25e–05	5.42e–06	4.66e–06	2.78e–06	6.94e–06
590	2.03e–07	1.07e–07	6.50e–08	2.16e–07	5.60e–08	8.19e–08	6.50e–08	1.24e–07
591	1.40e–06	6.55e–07	5.83e–07	1.39e–06	1.06e–07	7.27e–07	2.16e–07	6.81e–07
592	5.96e–07	2.48e–07	2.90e–07	5.89e–07	8.94e–08	1.67e–07	3.10e–07	2.56e–07
593	1.33e–06	6.59e–07	4.93e–07	1.35e–06	5.13e–07	5.40e–07	2.68e–07	7.14e–07
594	2.04e–06	1.10e–06	6.14e–07	2.08e–06	7.32e–07	8.93e–07	3.33e–07	1.20e–06

Table 6—Continued

Source No	<i>flux</i> [1] [0.5–8.0keV]	<i>flux</i> [2] [0.5–2.0keV]	<i>flux</i> [3] [2.0–8.0keV]	<i>flux</i> [4] [0.35–8.0keV]	<i>flux</i> [5] [0.35–1.1keV]	<i>flux</i> [6] [1.1–2.6keV]	<i>flux</i> [7] [2.6–8.0keV]	<i>flux</i> [8] [0.35–2.0keV]
595	3.63e–06	1.98e–06	1.04e–06	3.69e–06	1.73e–06	1.31e–06	7.93e–07	2.16e–06
596	1.02e–06	3.90e–07	5.37e–07	1.04e–06	2.54e–07	3.34e–07	4.16e–07	4.25e–07
597	7.99e–07	1.02e–07	7.25e–07	8.24e–07	4.24e–08	8.59e–08	7.33e–07	1.19e–07
598	7.03e–07	3.39e–07	2.68e–07	7.15e–07	1.66e–07	3.07e–07	1.64e–07	3.70e–07
599	4.39e–07	8.89e–08	3.50e–07	4.40e–07	−7.12e–09	1.18e–07	2.88e–07	9.15e–08
600	3.13e–05	1.47e–05	1.25e–05	3.21e–05	1.25e–05	1.07e–05	9.62e–06	1.63e–05
601	3.61e–06	1.46e–06	1.80e–06	3.71e–06	1.08e–06	1.13e–06	1.52e–06	1.63e–06
602	4.17e–07	1.59e–07	2.21e–07	4.24e–07	7.98e–08	1.44e–07	1.73e–07	1.74e–07
603	4.98e–07	2.04e–07	2.44e–07	5.17e–07	1.45e–07	1.52e–07	2.22e–07	2.30e–07
604	2.87e–07	7.34e–08	2.06e–07	2.91e–07	−5.93e–09	8.88e–08	1.74e–07	7.96e–08
605	4.53e–07	1.49e–07	2.77e–07	4.60e–07	3.36e–08	1.16e–07	2.89e–07	1.61e–07
606	2.01e–06	5.47e–07	1.40e–06	2.05e–06	−2.12e–08	6.21e–07	1.21e–06	5.97e–07
607	1.09e–06	1.03e–07	1.04e–06	1.09e–06	−1.59e–07	2.91e–07	7.90e–07	9.43e–08
608	3.53e–06	1.77e–06	1.24e–06	3.59e–06	6.86e–07	1.59e–06	8.35e–07	1.93e–06
609	3.70e–07	2.04e–07	1.04e–07	3.96e–07	2.44e–07	1.34e–07	6.31e–08	2.38e–07
610	2.09e–06	9.74e–07	8.73e–07	2.10e–06	8.58e–07	6.94e–07	6.56e–07	1.04e–06
611	2.50e–07	1.54e–08	2.51e–07	2.54e–07	−5.26e–09	5.05e–08	1.97e–07	1.64e–08
612	8.02e–04	3.48e–04	3.73e–04	8.20e–04	2.47e–04	2.80e–04	2.90e–04	3.83e–04
613	4.13e–06	2.05e–06	1.52e–06	4.27e–06	1.91e–06	1.36e–06	1.29e–06	2.29e–06
614	8.39e–07	3.54e–07	3.98e–07	8.52e–07	7.43e–08	3.63e–07	2.77e–07	3.84e–07
615	1.52e–06	9.09e–07	2.84e–07	1.53e–06	3.65e–07	7.94e–07	7.32e–08	9.75e–07
616	4.82e–07	7.13e–08	4.23e–07	4.72e–07	−8.50e–08	1.45e–07	3.20e–07	6.27e–08
617	5.18e–07	1.89e–07	2.87e–07	5.19e–07	1.22e–07	1.72e–07	2.05e–07	2.00e–07
618	6.38e–06	2.69e–06	3.08e–06	6.60e–06	2.75e–06	1.86e–06	2.60e–06	3.02e–06
619	5.70e–06	2.70e–06	2.19e–06	5.85e–06	2.21e–06	2.14e–06	1.40e–06	2.99e–06
620	4.41e–07	−4.58e–09	4.88e–07	4.37e–07	−6.68e–08	4.73e–08	4.37e–07	−1.45e–08
621	2.14e–06	3.95e–07	1.77e–06	2.18e–06	−8.05e–08	6.45e–07	1.34e–06	4.30e–07

Table 6—Continued

Source No	<i>flux</i> [1] [0.5–8.0keV]	<i>flux</i> [2] [0.5–2.0keV]	<i>flux</i> [3] [2.0–8.0keV]	<i>flux</i> [4] [0.35–8.0keV]	<i>flux</i> [5] [0.35–1.1keV]	<i>flux</i> [6] [1.1–2.6keV]	<i>flux</i> [7] [2.6–8.0keV]	<i>flux</i> [8] [0.35–2.0keV]
622	1.34e–06	2.61e–07	1.08e–06	1.38e–06	1.35e–07	3.19e–07	8.93e–07	3.00e–07
623	9.53e–07	3.79e–07	4.83e–07	1.02e–06	3.85e–07	3.91e–07	2.23e–07	4.52e–07
624	3.90e–07	5.95e–08	3.40e–07	3.90e–07	−7.46e–08	7.50e–08	3.46e–07	5.96e–08
625	4.70e–07	2.46e–07	1.52e–07	4.92e–07	1.98e–07	1.81e–07	1.14e–07	2.79e–07
626	2.22e–06	1.14e–06	7.50e–07	2.29e–06	5.83e–07	9.11e–07	6.23e–07	1.27e–06
627	5.36e–07	2.92e–07	1.55e–07	5.41e–07	3.51e–07	1.84e–07	7.47e–08	3.16e–07
628	1.08e–06	1.96e–08	1.15e–06	1.09e–06	−3.45e–08	5.10e–08	1.13e–06	1.21e–08
629	4.63e–07	5.14e–08	4.31e–07	4.65e–07	−5.42e–08	8.77e–08	3.94e–07	5.11e–08
630	2.44e–06	9.48e–07	1.28e–06	2.47e–06	5.09e–07	8.29e–07	1.01e–06	1.03e–06
631	4.46e–07	2.71e–07	9.08e–08	4.50e–07	1.24e–07	2.35e–07	2.26e–08	2.94e–07
632	8.11e–07	3.42e–07	3.84e–07	8.20e–07	1.82e–07	2.94e–07	2.95e–07	3.70e–07
633	3.95e–06	1.74e–06	1.75e–06	4.02e–06	1.02e–06	1.45e–06	1.33e–06	1.90e–06
634	8.23e–07	2.73e–07	4.98e–07	8.02e–07	1.87e–07	2.72e–07	3.07e–07	2.70e–07
635	9.96e–06	5.06e–06	3.44e–06	1.02e–05	4.26e–06	3.61e–06	2.58e–06	5.59e–06
636	3.58e–07	1.76e–07	1.33e–07	3.65e–07	1.12e–07	1.03e–07	1.60e–07	1.92e–07
637	5.95e–07	1.90e–07	3.72e–07	5.99e–07	−6.22e–08	2.90e–07	2.02e–07	2.03e–07
638	8.97e–07	3.05e–07	5.34e–07	9.07e–07	6.87e–08	3.69e–07	3.27e–07	3.28e–07
639	3.78e–06	1.41e–06	2.06e–06	3.83e–06	6.93e–07	1.28e–06	1.62e–06	1.53e–06
640	2.87e–06	1.92e–06	3.40e–07	2.93e–06	3.74e–06	5.12e–07	2.89e–07	2.11e–06
641	5.59e–07	1.03e–07	4.61e–07	5.88e–07	1.13e–07	6.58e–08	4.69e–07	1.27e–07
642	8.32e–07	4.76e–08	8.38e–07	8.69e–07	3.85e–09	1.71e–07	6.60e–07	6.94e–08
643	6.47e–07	1.67e–07	4.63e–07	6.69e–07	1.22e–07	1.33e–07	4.39e–07	1.91e–07
644	6.37e–07	2.59e–07	3.19e–07	6.66e–07	1.98e–07	2.68e–07	1.63e–07	2.96e–07
645	1.23e–06	3.30e–07	8.63e–07	1.25e–06	2.24e–07	3.82e–07	5.93e–07	3.56e–07
646	7.33e–07	4.55e–07	1.15e–07	7.87e–07	6.86e–07	2.65e–07	−2.78e–08	5.28e–07
647	2.62e–05	1.22e–05	1.08e–05	2.68e–05	1.01e–05	9.49e–06	7.54e–06	1.34e–05
648	6.83e–06	2.30e–06	4.09e–06	6.92e–06	6.20e–07	2.44e–06	3.04e–06	2.49e–06

Table 6—Continued

Source No	<i>flux</i> [1] [0.5–8.0keV]	<i>flux</i> [2] [0.5–2.0keV]	<i>flux</i> [3] [2.0–8.0keV]	<i>flux</i> [4] [0.35–8.0keV]	<i>flux</i> [5] [0.35–1.1keV]	<i>flux</i> [6] [1.1–2.6keV]	<i>flux</i> [7] [2.6–8.0keV]	<i>flux</i> [8] [0.35–2.0keV]
649	1.83e–06	7.09e–07	9.41e–07	1.87e–06	8.14e–07	3.68e–07	9.40e–07	7.83e–07
650	2.31e–06	5.37e–07	1.73e–06	2.34e–06	4.13e–07	5.00e–07	1.46e–06	5.74e–07
651	3.43e–07	1.83e–07	1.05e–07	4.48e–07	4.41e–07	1.16e–07	3.85e–08	2.78e–07
652	8.65e–07	3.97e–07	3.68e–07	8.74e–07	1.44e–07	3.63e–07	2.61e–07	4.29e–07
653	7.15e–06	4.20e–06	1.73e–06	7.33e–06	7.77e–06	1.51e–06	1.47e–06	4.64e–06
654	1.40e–06	4.29e–07	9.03e–07	1.46e–06	2.07e–07	4.17e–07	7.68e–07	4.94e–07
655	7.12e–07	1.03e–07	6.27e–07	7.80e–07	2.83e–07	1.89e–07	3.78e–07	1.56e–07
656	2.78e–06	1.56e–06	7.65e–07	2.82e–06	9.50e–07	1.13e–06	6.42e–07	1.70e–06
657	1.85e–06	6.90e–07	9.99e–07	1.89e–06	2.62e–07	7.18e–07	6.82e–07	7.60e–07
658	6.25e–07	4.03e–07	9.02e–08	6.37e–07	9.21e–09	3.32e–07	1.21e–07	4.41e–07
659	1.43e–06	6.34e–07	6.20e–07	1.48e–06	3.75e–07	5.16e–07	5.07e–07	7.07e–07
660	2.62e–06	1.42e–06	7.77e–07	2.61e–06	5.03e–07	9.51e–07	9.53e–07	1.52e–06
661	4.78e–06	1.08e–06	3.63e–06	4.98e–06	2.61e–07	1.27e–06	3.14e–06	1.27e–06
662	1.40e–06	8.79e–07	2.29e–07	1.45e–06	9.35e–07	5.66e–07	8.99e–08	9.82e–07

Table 7. Best-fit results for sources with 8 or more spectral groups.

No.	Source ID	Best-fit ^a model	N_H^b (10^{22} cm^{-2})	Γ	kT (keV)	Norm ^c	DOF ^d	χ_{red}^2	L_X (0.35–2.0keV) ^e ($10^{35} \text{ erg s}^{-1}$)	L_X (0.35–8.0keV) ^f
3	013229.23+303618.6	pow	$0.01^{+0.00}_{-0.00}$	$1.37^{+0.00}_{-0.00}$	—	$2.54e-06^{+0.00e+00}_{-0.00e+00}$	5	0.96	$4.51^{+0.37}_{-4.43}$	$15.61^{+2.03}_{-15.53}$
6	013230.54+303618.0	vappec	$0.01^{+0.00}_{-0.00}$	—	$1.05^{+0.00}_{-0.00}$	$8.40e-06^{+0.00e+00}_{-0.00e+00}$	5	0.94	$4.84^{+0.38}_{-2.89}$	$5.62^{+0.47}_{-2.36}$
10	013236.84+303229.0	pow	$0.45^{+0.23}_{-0.20}$	$1.07^{+0.14}_{-0.13}$	—	$1.73e-05^{+3.28e-06}_{-5.70e-07}$	76	1.64	$31.61^{+1.53}_{-1.49}$	$150.34^{+8.29}_{-9.09}$
13	013241.32+303217.7	pow	$0.50^{+1.91}_{-0.50}$	$0.83^{+0.84}_{-0.58}$	—	$5.33e-07^{+2.83e-07}_{-2.83e-07}$	7	1.51	$1.01^{+0.37}_{-0.37}$	$6.31^{+5.89}_{-5.89}$
14	013242.07+303329.0	pow	$0.50^{+1.42}_{-0.50}$	$2.10^{+1.71}_{-0.91}$	—	$1.43e-06^{+4.25e-06}_{-8.29e-07}$	5	1.15	$2.58^{+0.43}_{-1.23}$	$4.78^{+1.11}_{-3.39}$
15	013242.46+304815.0	pow	$0.19^{+0.76}_{-0.19}$	$1.82^{+0.81}_{-0.49}$	—	$1.56e-06^{+1.62e-06}_{-5.70e-07}$	5	0.95	$2.76^{+0.53}_{-0.73}$	$6.31^{+0.71}_{-1.89}$
16	013243.41+303506.2	pow	$0.34^{+0.00}_{-0.00}$	$1.67^{+0.00}_{-0.00}$	—	$6.17e-06^{+0.00e+00}_{-0.00e+00}$	21	2.04	$10.87^{+0.73}_{-0.99}$	$28.20^{+2.94}_{-2.80}$
22	013247.71+304711.1	vappec	$0.56^{+0.00}_{-0.00}$	—	$0.77^{+0.00}_{-0.00}$	$5.61e-06^{+0.00e+00}_{-0.00e+00}$	7	1.62	$3.57^{+0.24}_{-1.05}$	$3.83^{+0.31}_{-1.02}$
25	013249.39+303829.6	pow	$0.01^{+0.00}_{-0.00}$	$1.44^{+0.00}_{-0.00}$	—	$1.01e-06^{+0.00e+00}_{-0.00e+00}$	5	0.90	$1.78^{+0.25}_{-1.75}$	$5.74^{+0.96}_{-5.71}$
26	013249.63+303250.7	pow	$0.48^{+1.41}_{-0.48}$	$1.62^{+0.98}_{-0.66}$	—	$8.86e-07^{+1.64e-06}_{-4.63e-07}$	7	0.77	$1.56^{+0.13}_{-0.51}$	$4.24^{+1.01}_{-2.99}$
28	013249.87+305018.9	pow	$0.60^{+0.89}_{-0.59}$	$2.31^{+1.32}_{-0.79}$	—	$3.72e-06^{+2.75e-06}_{-1.96e-06}$	5	1.70	$6.88^{+0.70}_{-1.37}$	$11.17^{+1.65}_{-4.80}$
29	013250.71+303035.3	pow	$0.67^{+0.64}_{-0.45}$	$2.36^{+0.62}_{-0.50}$	—	$5.75e-06^{+4.50e-06}_{-2.32e-06}$	7	0.98	$10.71^{+0.60}_{-1.02}$	$16.93^{+1.41}_{-3.88}$
33	013252.50+304023.9	pow	$0.66^{+1.06}_{-0.66}$	$2.02^{+1.05}_{-0.76}$	—	$3.08e-06^{+5.12e-06}_{-1.78e-06}$	5	0.39	$5.51^{+0.66}_{-1.41}$	$10.81^{+2.71}_{-3.80}$
35	013253.56+303814.8	pow	$0.10^{+0.07}_{-0.07}$	$1.74^{+0.09}_{-0.09}$	—	$3.85e-05^{+3.69e-06}_{-3.31e-06}$	133	0.94	$67.79^{+2.87}_{-2.83}$	$166.11^{+7.06}_{-5.02}$
37	013253.89+303311.8	pow	$0.17^{+0.05}_{-0.06}$	$1.95^{+0.08}_{-0.07}$	—	$4.15e-05^{+3.13e-06}_{-2.86e-06}$	167	0.91	$73.85^{+2.41}_{-2.10}$	$152.32^{+4.35}_{-4.88}$
38	013253.90+305017.8	pow	$0.63^{+1.25}_{-0.63}$	$1.55^{+0.90}_{-0.69}$	—	$1.78e-06^{+2.93e-06}_{-9.91e-07}$	5	0.50	$3.14^{+0.52}_{-1.33}$	$9.09^{+1.54}_{-3.71}$
40	013255.33+304215.8	pow	$0.14^{+0.00}_{-0.00}$	$1.65^{+0.00}_{-0.00}$	—	$1.86e-06^{+0.00e+00}_{-0.00e+00}$	6	2.45	$3.28^{+0.52}_{-0.55}$	$8.69^{+1.71}_{-2.18}$
41	013255.45+304842.3	pow	$3.33^{+0.00}_{-0.00}$	$0.44^{+1.40}_{-1.07}$	—	$3.81e-07^{+2.78e-06}_{-3.81e-07}$	5	0.62	$0.78^{+0.11}_{-0.18}$	$7.86^{+3.51}_{-6.76}$
48	013257.07+303927.0	vappec	$0.01^{+0.00}_{-0.00}$	—	$0.67^{+0.00}_{-0.00}$	$3.20e-06^{+0.00e+00}_{-0.00e+00}$	5	2.73	$2.05^{+0.04}_{-2.01}$	$2.15^{+0.25}_{-2.10}$
54	013259.67+305326.4	pow	$0.01^{+0.00}_{-0.00}$	$1.49^{+0.00}_{-0.00}$	—	$2.09e-06^{+0.00e+00}_{-0.00e+00}$	6	0.80	$3.70^{+0.13}_{-3.63}$	$11.35^{+1.28}_{-11.27}$
63	013301.03+304043.1	pow	$0.81^{+0.48}_{-0.35}$	$1.55^{+0.90}_{-0.69}$	—	$6.26e-06^{+2.60e-06}_{-1.72e-06}$	23	0.70	$11.04^{+0.45}_{-0.68}$	$31.88^{+3.01}_{-2.75}$
64	013301.93+303158.1	pow	$0.14^{+0.13}_{-0.11}$	$1.57^{+0.14}_{-0.13}$	—	$1.09e-05^{+1.74e-06}_{-1.44e-06}$	65	0.96	$19.13^{+1.23}_{-1.12}$	$54.43^{+3.56}_{-3.55}$
68	013303.55+303903.8	vappec	$0.42^{+0.22}_{-0.17}$	—	$3.75^{+1.20}_{-0.84}$	$1.84e-05^{+3.04e-06}_{-2.37e-06}$	34	0.76	$8.25^{+0.37}_{-0.36}$	$17.75^{+1.14}_{-1.56}$
74	013304.78+304124.1	pow	$0.59^{+0.63}_{-0.44}$	$2.13^{+0.64}_{-0.50}$	—	$2.61e-06^{+2.14e-06}_{-1.07e-06}$	7	0.88	$4.72^{+0.47}_{-0.47}$	$8.59^{+1.38}_{-1.39}$
76	013305.14+303001.4	pow	$1.36^{+1.20}_{-0.76}$	$1.66^{+0.55}_{-0.45}$	—	$4.43e-06^{+4.53e-06}_{-2.01e-06}$	7	1.47	$7.81^{+0.39}_{-0.60}$	$20.37^{+1.99}_{-3.91}$
78	013305.79+303804.7	pow	$9.87^{+0.00}_{-0.00}$	$1.29^{+0.00}_{-0.00}$	—	$1.05e-06^{+0.00e+00}_{-0.00e+00}$	5	2.57	$1.88^{+0.03}_{-0.03}$	$7.02^{+0.58}_{-3.96}$
88	013307.96+303219.5	vappec	$0.01^{+0.00}_{-0.00}$	—	$0.70^{+0.00}_{-0.00}$	$3.41e-06^{+0.00e+00}_{-0.00e+00}$	5	3.72	$2.20^{+0.05}_{-0.06}$	$2.31^{+0.15}_{-2.26}$
90	013308.35+304803.4	pow	$0.20^{+0.22}_{-0.17}$	$2.00^{+0.25}_{-0.24}$	—	$5.83e-06^{+1.63e-06}_{-1.20e-06}$	27	1.30	$10.40^{+1.03}_{-0.77}$	$20.75^{+2.05}_{-1.79}$
93	013309.10+303422.5	pow	$0.01^{+0.00}_{-0.00}$	$1.48^{+0.00}_{-0.00}$	—	$8.00e-07^{+0.00e+00}_{-0.00e+00}$	5	0.81	$1.41^{+0.07}_{-1.39}$	$4.37^{+0.71}_{-4.34}$
100	013311.09+303943.7	vappec	$0.01^{+0.00}_{-0.00}$	—	$0.55^{+0.00}_{-0.00}$	$8.73e-06^{+0.00e+00}_{-0.00e+00}$	18	4.50	$5.23^{+0.07}_{-5.10}$	$5.36^{+0.17}_{-5.24}$
102	013311.75+303841.5	vappec	$0.01^{+0.00}_{-0.00}$	—	$0.55^{+0.00}_{-0.00}$	$1.85e-04^{+0.00e+00}_{-0.00e+00}$	96	4.54	$110.63^{+1.52}_{-105.58}$	$113.54^{+0.83}_{-107.32}$
109	013314.32+304236.7	pow	$9.93^{+9.93}_{-8.27}$	$0.73^{+0.63}_{-0.70}$	—	$5.95e-07^{+1.57e-07}_{-5.95e-07}$	5	1.44	$1.14^{+0.04}_{-0.04}$	$8.04^{+5.57}_{-5.57}$
112	013315.10+304453.0	pow	$0.16^{+0.00}_{-0.16}$	$2.11^{+0.68}_{-0.43}$	—	$1.14e-06^{+8.42e-07}_{-3.78e-07}$	5	0.84	$2.05^{+0.32}_{-0.37}$	$3.77^{+0.72}_{-0.97}$
113	013315.16+305318.2	pow	$0.92^{+0.00}_{-0.00}$	$2.62^{+0.00}_{-0.00}$	—	$8.43e-04^{+0.00e+00}_{-0.00e+00}$	241	2.03	$1652.25^{+6.24}_{-6.21}$	$2298.20^{+15.37}_{-13.14}$

Table 7—Continued

No.	Source ID	Best-fit ^a model	N_H^b (10^{22} cm $^{-2}$)	Γ	kT (keV)	Norm ^c	DOF ^d	χ^2_{red}	L_X (0.35–2.0keV) ^e (10^{35} erg s $^{-1}$)	L_X (0.35–8.0keV) ^f (10^{35} erg s $^{-1}$)
122	013317.91+305236.3	pow	$0.61^{+0.68}_{-0.52}$	$1.72^{+0.58}_{-0.50}$	—	$3.39e-06^{+2.81e-06}_{-1.49e-06}$	5	0.85	$5.97^{+0.47}_{-0.85}$	$14.85^{+2.73}_{-3.62}$
123	013317.94+304900.1	pow	$1.63^{+2.56}_{-1.49}$	$1.27^{+0.98}_{-0.78}$	—	$7.91e-07^{+2.02e-06}_{-7.91e-07}$	5	0.78	$1.42^{+0.15}_{-0.47}$	$5.41^{+0.47}_{-4.26}$
124	013318.33+304200.6	pow	$3.12^{+2.22}_{-1.47}$	$1.28^{+0.59}_{-0.49}$	—	$1.48e-06^{+1.99e-06}_{-7.63e-07}$	11	1.11	$2.64^{+0.08}_{-0.27}$	$9.98^{+0.80}_{-2.93}$
132	013319.06+305205.0	pow	$1.74^{+1.37}_{-1.02}$	$2.02^{+0.85}_{-0.70}$	—	$4.73e-06^{+7.56e-06}_{-2.75e-06}$	5	1.52	$8.46^{+0.24}_{-1.12}$	$16.55^{+1.56}_{-6.18}$
133	013319.61+302847.8	pow	$0.62^{+0.31}_{-0.25}$	$2.01^{+0.28}_{-0.25}$	—	$7.56e-06^{+2.49e-06}_{-1.79e-06}$	25	0.45	$13.50^{+0.61}_{-0.60}$	$26.67^{+1.50}_{-2.52}$
134	013319.91+305102.0	pow	$0.13^{+0.60}_{-0.13}$	$1.38^{+0.48}_{-0.32}$	—	$1.39e-06^{+9.89e-07}_{-4.24e-07}$	5	1.08	$2.47^{+0.39}_{-0.64}$	$8.46^{+1.55}_{-2.34}$
138	013320.95+302648.8	pow	$0.25^{+1.11}_{-0.25}$	$1.79^{+0.72}_{-0.43}$	—	$1.47e-06^{+2.00e-06}_{-5.69e-07}$	6	1.63	$2.59^{+0.32}_{-0.60}$	$6.09^{+1.30}_{-2.40}$
141	013321.70+303858.4	pow	$0.01^{+0.00}_{-0.00}$	$-0.79^{+0.79}_{-0.79}$	—	$9.72e-08^{+0.00e+00}_{-0.00e+00}$	12	1.79	$0.29^{+0.01}_{-0.29}$	$14.62^{+0.57}_{-14.61}$
142	013321.94+303923.0	pow	$0.50^{+0.61}_{-0.44}$	$1.58^{+0.47}_{-0.41}$	—	$1.02e-06^{+6.82e-07}_{-3.93e-07}$	7	0.51	$1.81^{+0.21}_{-0.23}$	$5.09^{+0.69}_{-1.04}$
143	013321.94+305520.6	pow	$3.74^{+2.60}_{-1.77}$	$1.20^{+0.63}_{-0.55}$	—	$4.06e-06^{+6.33e-06}_{-2.28e-06}$	9	1.19	$7.30^{+0.21}_{-0.61}$	$30.28^{+2.10}_{-17.06}$
152	013323.65+302607.0	pow	$0.21^{+0.00}_{-0.00}$	$0.95^{+0.00}_{-0.00}$	—	$9.15e-07^{+0.00e+00}_{-0.00e+00}$	5	2.13	$1.70^{+0.21}_{-0.71}$	$9.22^{+1.78}_{-2.33}$
154	013323.93+303517.5	pow	$0.01^{+0.00}_{-0.00}$	$1.64^{+0.00}_{-0.00}$	—	$5.17e-06^{+0.00e+00}_{-0.00e+00}$	67	0.92	$9.10^{+0.14}_{-8.91}$	$24.22^{+1.23}_{-24.03}$
155	013323.94+304820.4	pow	$0.54^{+0.32}_{-0.26}$	$1.73^{+0.27}_{-0.25}$	—	$4.07e-06^{+1.36e-06}_{-9.79e-07}$	24	1.01	$7.17^{+0.42}_{-0.26}$	$17.69^{+1.86}_{-1.88}$
158	013324.40+304402.4	pow	$0.38^{+0.03}_{-0.02}$	$1.90^{+0.03}_{-0.02}$	—	$2.06e-04^{+6.15e-06}_{-5.92e-06}$	241	1.58	$365.08^{+1.95}_{-2.68}$	$779.40^{+8.48}_{-10.35}$
159	013324.46+302504.5	pow	$0.18^{+0.29}_{-0.18}$	$1.59^{+0.28}_{-0.26}$	—	$5.16e-06^{+1.79e-06}_{-1.24e-06}$	19	0.87	$9.09^{+0.03}_{-1.05}$	$25.41^{+2.58}_{-2.87}$
161	013324.88+304536.0	pow	$0.54^{+1.55}_{-0.54}$	$1.72^{+0.99}_{-0.65}$	—	$5.52e-07^{+1.13e-06}_{-2.96e-07}$	5	0.56	$0.97^{+0.19}_{-0.38}$	$2.41^{+0.51}_{-1.23}$
162	013324.90+305508.9	pow	$9.91^{+9.91}_{-3.25}$	$1.67^{+0.36}_{-0.34}$	—	$1.12e-05^{+2.80e-06}_{-6.93e-06}$	8	1.08	$19.67^{+0.48}_{-0.48}$	$51.00^{+23.31}_{-23.31}$
163	013325.38+305814.8	pow	$0.21^{+0.17}_{-0.14}$	$2.43^{+0.25}_{-0.21}$	—	$1.85e-05^{+4.27e-06}_{-3.22e-06}$	40	1.28	$34.98^{+2.87}_{-2.12}$	$53.13^{+3.84}_{-4.16}$
165	013325.48+303619.1	pow	$0.35^{+0.75}_{-0.35}$	$1.70^{+0.78}_{-0.56}$	—	$5.45e-07^{+5.52e-07}_{-2.40e-07}$	6	0.47	$0.96^{+0.14}_{-0.19}$	$2.42^{+0.57}_{-0.62}$
166	013325.54+304440.7	pow	$0.14^{+0.48}_{-0.14}$	$1.68^{+0.55}_{-0.37}$	—	$7.43e-07^{+4.92e-07}_{-2.30e-07}$	5	0.75	$1.31^{+0.21}_{-0.36}$	$3.38^{+0.36}_{-0.75}$
175	013327.76+304647.3	pow	$0.19^{+0.00}_{-0.00}$	$3.25^{+0.00}_{-0.00}$	—	$1.95e-06^{+0.00e+00}_{-0.00e+00}$	9	1.20	$4.60^{+0.43}_{-0.54}$	$5.28^{+0.76}_{-0.86}$
176	013328.08+303135.0	vapec	$0.01^{+0.00}_{-0.00}$	—	$0.59^{+0.00}_{-0.00}$	$3.81e-06^{+0.00e+00}_{-0.00e+00}$	5	1.84	$2.32^{+0.19}_{-0.27}$	$2.40^{+0.04}_{-2.35}$
180	013328.69+302723.6	pow	$0.07^{+0.02}_{-0.02}$	$1.46^{+0.02}_{-0.02}$	—	$3.51e-04^{+7.90e-06}_{-7.69e-06}$	244	1.58	$620.07^{+8.31}_{-7.32}$	$1958.87^{+24.47}_{-20.71}$
181	013328.72+304322.5	pow	$0.01^{+0.00}_{-0.00}$	$1.73^{+0.00}_{-0.00}$	—	$1.29e-06^{+0.00e+00}_{-0.00e+00}$	15	0.91	$2.28^{+0.05}_{-0.23}$	$5.53^{+0.35}_{-5.48}$
183	013328.96+304743.5	vapec	$0.01^{+0.00}_{-0.00}$	—	$0.33^{+0.00}_{-0.00}$	$1.11e-05^{+0.00e+00}_{-0.00e+00}$	11	2.29	$4.44^{+0.29}_{-4.30}$	$4.46^{+0.24}_{-4.32}$
184	013329.04+304216.9	vapec	$0.01^{+0.00}_{-0.00}$	—	$0.56^{+0.00}_{-0.00}$	$3.23e-05^{+0.00e+00}_{-0.00e+00}$	54	2.30	$19.44^{+0.34}_{-19.00}$	$20.00^{+0.02}_{-19.55}$
186	013329.29+304537.4	pow	$0.24^{+0.26}_{-0.21}$	$1.47^{+0.24}_{-0.22}$	—	$2.12e-06^{+6.31e-07}_{-4.66e-07}$	26	0.53	$3.74^{+0.36}_{-0.28}$	$11.69^{+1.04}_{-1.34}$
187	013329.29+304508.4	pow	$0.06^{+0.09}_{-0.06}$	$1.71^{+0.13}_{-0.11}$	—	$6.77e-06^{+8.41e-07}_{-6.93e-07}$	80	0.85	$11.92^{+0.73}_{-0.74}$	$29.77^{+1.36}_{-2.18}$
188	013329.45+304910.7	vapec	$0.01^{+0.00}_{-0.00}$	—	$0.56^{+0.00}_{-0.00}$	$1.79e-05^{+0.00e+00}_{-0.00e+00}$	34	2.85	$10.75^{+0.23}_{-10.50}$	$11.04^{+0.06}_{-10.79}$
190	013329.83+305118.0	pow	$0.06^{+0.32}_{-0.06}$	$1.93^{+0.45}_{-0.26}$	—	$1.90e-06^{+8.81e-07}_{-3.96e-07}$	8	1.27	$3.37^{+0.51}_{-0.84}$	$7.06^{+1.26}_{-1.46}$
193	013330.40+304641.9	pow	$1.44^{+1.50}_{-0.98}$	$1.61^{+0.78}_{-0.62}$	—	$1.25e-06^{+1.98e-06}_{-6.80e-07}$	7	1.53	$2.20^{+0.11}_{-0.30}$	$6.04^{+0.82}_{-0.82}$
195	013330.64+303404.1	pow	$2.27^{+0.37}_{-0.43}$	$1.44^{+0.16}_{-0.15}$	—	$9.28e-06^{+2.39e-06}_{-1.77e-06}$	98	0.85	$16.41^{+0.19}_{-0.25}$	$52.65^{+1.58}_{-3.17}$
197	013331.25+303333.4	vapec	$0.01^{+0.00}_{-0.00}$	—	$0.60^{+0.00}_{-0.00}$	$3.90e-05^{+0.00e+00}_{-0.00e+00}$	74	5.79	$23.98^{+0.43}_{-23.44}$	$24.81^{+0.10}_{-24.27}$
199	013331.30+304928.2	vapec	$3.70^{+3.01}_{-2.03}$	—	$3.93^{+3.93}_{-2.31}$	$5.81e-06^{+8.90e-06}_{-2.74e-06}$	5	0.40	$2.60^{+0.09}_{-0.35}$	$5.71^{+0.34}_{-3.00}$

Table 7—Continued

No.	Source ID	Best-fit ^a model	N_H^b (10^{22} cm^{-2})	Γ	kT (keV)	Norm ^c	DOF ^d	χ^2_{red}	L_X (0.35–2.0keV) ^e ($10^{35} \text{ erg s}^{-1}$)	L_X (0.35–8.0keV) ^f ($10^{35} \text{ erg s}^{-1}$)
206	013331.99+305741.0	pow	$0.25^{+0.51}_{-0.25}$	$1.74^{+0.52}_{-0.41}$	—	$3.07e-06^{+2.00e-06}_{-1.06e-06}$	7	0.84	$5.41^{+0.70}_{-1.41}$	$13.22^{+2.51}_{-2.95}$
207	013332.19+303656.8	vapec	$9.91^{+0.00}_{-0.00}$	—	$4.26^{+0.00}_{-0.00}$	$9.41e-06^{+0.00e+00}_{-0.00e+00}$	5	0.45	$4.20^{+0.11}_{-0.11}$	$9.57^{+3.80}_{-3.80}$
210	013332.23+303955.5	pow	$0.31^{+0.38}_{-0.27}$	$1.78^{+0.36}_{-0.30}$	—	$1.40e-06^{+6.00e-07}_{-3.91e-07}$	15	1.14	$2.47^{+0.25}_{-0.21}$	$5.82^{+0.94}_{-0.83}$
214	013332.81+304633.3	pow	$8.58^{+8.58}_{-5.68}$	$1.34^{+0.78}_{-1.09}$	—	$1.17e-06^{+1.10e-06}_{-1.17e-06}$	5	0.44	$2.07^{+0.04}_{-0.08}$	$7.36^{+0.12}_{-4.21}$
215	013332.89+304916.3	pow	$0.67^{+0.87}_{-0.58}$	$1.61^{+0.59}_{-0.49}$	—	$1.72e-06^{+1.59e-06}_{-7.53e-07}$	7	0.54	$3.03^{+0.30}_{-0.37}$	$8.31^{+1.37}_{-1.64}$
221	013333.71+303109.6	pow	$0.41^{+0.19}_{-0.16}$	$1.39^{+0.15}_{-0.14}$	—	$6.28e-06^{+1.16e-06}_{-9.44e-07}$	72	0.96	$11.15^{+0.38}_{-0.43}$	$37.70^{+2.42}_{-1.95}$
224	013334.12+303714.9	pow	$0.65^{+0.39}_{-0.31}$	$1.54^{+0.28}_{-0.25}$	—	$2.41e-06^{+9.03e-07}_{-6.21e-07}$	27	1.25	$4.25^{+0.20}_{-0.20}$	$12.39^{+0.88}_{-1.14}$
225	013334.13+303211.3	pow	$0.63^{+0.00}_{-0.00}$	$2.39^{+0.00}_{-0.00}$	—	$4.36e-04^{+0.00e+00}_{-0.00e+00}$	242	4.30	$815.89^{+3.18}_{-2.53}$	$1266.70^{+6.67}_{-7.85}$
228	013334.54+303556.1	pow	$0.01^{+0.00}_{-0.00}$	$1.87^{+0.00}_{-0.00}$	—	$6.75e-07^{+0.00e+00}_{-0.00e+00}$	6	0.71	$1.20^{+0.07}_{-0.17}$	$2.62^{+0.24}_{-2.59}$
233	013335.50+303729.3	pow	$0.43^{+0.29}_{-0.21}$	$2.09^{+0.42}_{-0.36}$	—	$1.73e-06^{+5.15e-07}_{-5.48e-06}$	14	0.90	$3.12^{+0.30}_{-0.23}$	$5.81^{+0.65}_{-0.84}$
234	013335.65+302632.2	pow	$4.21^{+4.21}_{-2.79}$	$1.45^{+1.10}_{-0.90}$	—	$1.52e-06^{+1.52e-06}_{-9.85e-06}$	5	0.98	$2.69^{+0.11}_{-0.33}$	$8.56^{+5.45}_{-0.14}$
235	013335.83+304655.4	pow	$3.90^{+3.90}_{-2.94}$	$2.00^{+1.77}_{-1.23}$	—	$1.09e-06^{+1.09e-06}_{-1.09e-06}$	6	0.86	$1.94^{+0.20}_{-0.20}$	$3.85^{+1.83}_{-1.33}$
236	013335.90+303627.4	vapec	$0.01^{+0.00}_{-0.00}$	—	$0.77^{+0.00}_{-0.00}$	$1.25e-05^{+0.00e+00}_{-0.00e+00}$	41	2.26	$7.98^{+0.08}_{-7.81}$	$8.55^{+0.13}_{-8.38}$
237	013336.04+303332.9	pow	$0.44^{+0.25}_{-0.20}$	$1.92^{+0.21}_{-0.19}$	—	$4.43e-06^{+1.14e-06}_{-8.42e-07}$	48	0.93	$7.86^{+0.26}_{-0.25}$	$16.62^{+0.82}_{-0.76}$
238	013336.40+303742.7	pow	$0.56^{+0.49}_{-0.37}$	$1.52^{+0.37}_{-0.32}$	—	$1.32e-06^{+4.19e-07}_{-4.19e-07}$	14	0.96	$2.33^{+0.18}_{-0.18}$	$6.93^{+0.89}_{-0.89}$
240	013336.70+303729.6	pow	$0.84^{+1.03}_{-0.72}$	$1.72^{+0.81}_{-0.64}$	—	$7.80e-07^{+1.02e-06}_{-4.10e-07}$	5	0.98	$1.38^{+0.15}_{-0.53}$	$3.41^{+0.44}_{-0.85}$
241	013336.84+304757.3	vapec	$3.88^{+3.06}_{-1.90}$	—	$2.15^{+3.79}_{-1.04}$	$6.46e-06^{+3.60e-06}_{-3.60e-06}$	5	0.24	$2.93^{+0.06}_{-0.33}$	$4.84^{+0.20}_{-1.87}$
245	013337.08+303253.5	vapec	$1.78^{+1.11}_{-0.66}$	—	$0.16^{+0.13}_{-0.05}$	$5.55e-04^{+2.52e-02}_{-5.55e-04}$	6	0.43	$112.13^{+0.00}_{-1.00}$	$112.14^{+0.02}_{-1.01}$
248	013337.52+304718.7	pow	$0.11^{+0.10}_{-0.08}$	$1.74^{+0.13}_{-0.12}$	—	$6.01e-06^{+7.95e-07}_{-6.84e-07}$	81	0.75	$10.60^{+0.87}_{-0.64}$	$25.92^{+1.46}_{-1.36}$
249	013337.75+304009.1	vapec	$0.01^{+0.00}_{-0.00}$	—	$0.68^{+0.00}_{-0.00}$	$1.40e-06^{+0.00e+00}_{-0.00e+00}$	5	1.42	$0.90^{+0.12}_{-0.88}$	$0.94^{+0.04}_{-0.92}$
250	013337.90+303837.2	pow	$2.09^{+0.00}_{-0.00}$	$1.80^{+0.00}_{-0.00}$	—	$1.44e-06^{+0.00e+00}_{-0.00e+00}$	7	2.38	$2.54^{+0.10}_{-0.27}$	$5.89^{+0.82}_{-1.42}$
251	013337.96+304023.8	pow	$0.01^{+0.00}_{-0.00}$	$0.01^{+0.00}_{-0.00}$	—	$8.99e-08^{+0.00e+00}_{-0.00e+00}$	5	0.30	$0.20^{+0.00}_{-0.20}$	$3.56^{+0.20}_{-3.56}$
252	013337.99+304035.6	pow	$3.94^{+3.56}_{-2.53}$	$1.58^{+1.21}_{-0.94}$	—	$1.21e-06^{+7.95e-07}_{-1.21e-06}$	5	1.93	$2.13^{+0.08}_{-0.27}$	$6.02^{+0.37}_{-3.67}$
255	013338.50+302851.2	pow	$0.24^{+0.21}_{-0.18}$	$1.78^{+0.24}_{-0.22}$	—	$3.70e-06^{+9.95e-07}_{-7.50e-07}$	29	1.20	$6.52^{+0.55}_{-0.52}$	$15.41^{+1.55}_{-1.51}$
256	013338.53+302750.1	pow	$0.50^{+0.84}_{-0.50}$	$1.84^{+0.83}_{-0.63}$	—	$8.14e-07^{+9.27e-07}_{-4.07e-07}$	6	0.80	$1.44^{+0.19}_{-0.30}$	$3.23^{+1.07}_{-1.09}$
259	013338.97+302734.8	pow	$0.22^{+1.11}_{-0.22}$	$1.34^{+0.83}_{-0.48}$	—	$4.36e-07^{+6.19e-07}_{-1.86e-07}$	5	0.55	$0.78^{+0.22}_{-0.40}$	$2.77^{+0.76}_{-1.15}$
262	013339.22+304049.9	pow	$0.14^{+0.29}_{-0.14}$	$1.38^{+0.26}_{-0.22}$	—	$1.87e-06^{+6.28e-07}_{-3.98e-07}$	27	1.11	$3.31^{+0.32}_{-0.33}$	$11.34^{+0.86}_{-1.37}$
263	013339.40+305347.6	pow	$0.22^{+0.27}_{-0.22}$	$1.29^{+0.25}_{-0.24}$	—	$4.73e-06^{+1.52e-06}_{-1.13e-06}$	22	1.22	$8.45^{+0.74}_{-0.83}$	$31.76^{+3.41}_{-4.02}$
264	013339.46+302140.8	pow	$0.35^{+0.87}_{-0.35}$	$0.89^{+0.43}_{-0.35}$	—	$3.90e-06^{+2.90e-06}_{-1.42e-06}$	9	0.54	$7.29^{+1.04}_{-1.65}$	$42.65^{+6.40}_{-9.89}$
266	013339.79+304350.3	pow	$1.35^{+1.59}_{-0.96}$	$2.46^{+1.24}_{-0.83}$	—	$1.13e-06^{+2.58e-06}_{-6.71e-07}$	5	1.13	$2.14^{+0.10}_{-0.32}$	$3.20^{+0.46}_{-1.48}$
268	013340.09+304323.1	pow	$0.21^{+0.33}_{-0.21}$	$1.53^{+0.30}_{-0.26}$	—	$1.57e-06^{+5.90e-07}_{-3.98e-07}$	19	0.39	$2.76^{+0.28}_{-0.25}$	$8.13^{+0.83}_{-1.00}$
272	013340.81+303524.2	pow	$1.08^{+0.00}_{-0.00}$	$3.55^{+0.00}_{-0.00}$	—	$3.41e-06^{+0.00e+00}_{-0.00e+00}$	10	0.85	$9.04^{+0.08}_{-0.32}$	$9.88^{+0.31}_{-0.50}$
274	013341.26+303213.4	pow	$0.01^{+0.40}_{-0.01}$	$0.53^{+0.26}_{-0.15}$	—	$7.39e-07^{+2.88e-07}_{-1.18e-07}$	22	0.94	$1.48^{+0.12}_{-0.33}$	$13.29^{+2.39}_{-1.63}$
275	013341.35+305607.9	pow	$0.21^{+0.45}_{-0.21}$	$1.78^{+0.60}_{-0.43}$	—	$2.57e-06^{+1.77e-06}_{-9.01e-07}$	6	1.14	$4.53^{+0.72}_{-1.02}$	$10.71^{+1.69}_{-1.96}$

Table 7—Continued

No.	Source ID	Best-fit ^a model	N_H^b (10^{22} cm $^{-2}$)	Γ	kT (keV)	Norm ^c	DOF ^d	χ_{red}^2	L_X (0.35–2.0keV) ^e (10^{35} erg s $^{-1}$)	L_X (0.35–8.0keV) ^f (10^{35} erg s $^{-1}$)
277	013341.56+304136.4	pow	$1.11^{+0.55}_{-0.42}$	$2.13^{+0.38}_{-0.33}$	—	$3.38e-06^{+1.74e-06}_{-1.06e-06}$	18	0.83	$6.10^{+0.16}_{-0.23}$	$11.08^{+0.84}_{-1.12}$
278	013341.62+303220.1	vapec	$0.01^{+0.00}_{-0.00}$	—	$1.26^{+0.00}_{-0.00}$	$4.11e-06^{+0.00e+00}_{-0.00e+00}$	7	2.11	$2.14^{+0.03}_{-2.10}$	$2.69^{+0.09}_{-2.64}$
279	013341.90+303848.8	vapec	$0.01^{+0.00}_{-0.00}$	—	$0.74^{+0.00}_{-0.00}$	$2.01e-05^{+0.00e+00}_{-0.00e+00}$	54	1.82	$12.86^{+0.26}_{-12.59}$	$13.68^{+0.07}_{-13.41}$
280	013342.05+304852.6	pow	$2.61^{+4.17}_{-2.61}$	$0.68^{+1.33}_{-1.05}$	—	$3.95e-07^{+2.11e-06}_{-3.95e-07}$	5	1.43	$0.77^{+0.06}_{-0.21}$	$5.71^{+0.91}_{-4.85}$
281	013342.54+304253.3	pow	$1.74^{+0.48}_{-0.40}$	$1.57^{+0.23}_{-0.20}$	—	$5.93e-06^{+2.00e-06}_{-1.42e-06}$	44	0.88	$10.45^{+0.23}_{-0.21}$	$29.60^{+1.54}_{-2.02}$
282	013342.55+305750.1	pow	$0.26^{+0.43}_{-0.26}$	$1.78^{+0.42}_{-0.36}$	—	$4.07e-06^{+2.07e-06}_{-1.28e-06}$	10	0.77	$7.17^{+1.12}_{-0.91}$	$16.88^{+2.84}_{-2.86}$
283	013342.77+304642.5	pow	$0.53^{+0.37}_{-0.30}$	$1.61^{+0.31}_{-0.29}$	—	$1.82e-06^{+4.95e-07}_{-4.95e-07}$	19	1.33	$3.21^{+0.17}_{-0.21}$	$8.83^{+1.00}_{-0.95}$
285	013342.97+305341.7	pow	$1.28^{+0.00}_{-0.00}$	$2.14^{+0.00}_{-0.00}$	—	$2.50e-06^{+0.00e+00}_{-0.00e+00}$	5	4.61	$4.53^{+0.15}_{-0.72}$	$8.15^{+0.73}_{-2.14}$
287	013343.39+304630.6	vapec	$0.01^{+0.00}_{-0.00}$	—	$0.48^{+0.00}_{-0.00}$	$2.18e-05^{+0.00e+00}_{-0.00e+00}$	42	1.40	$11.89^{+0.19}_{-11.59}$	$12.10^{+0.01}_{-11.81}$
295	013345.38+302833.8	pow	$0.83^{+1.44}_{-0.83}$	$1.50^{+0.91}_{-0.75}$	—	$6.73e-07^{+1.16e-06}_{-4.03e-07}$	7	1.24	$1.19^{+0.11}_{-0.38}$	$3.62^{+0.73}_{-2.00}$
298	013346.54+305430.8	vapec	$0.01^{+0.00}_{-0.00}$	—	$0.49^{+0.00}_{-0.00}$	$6.41e-06^{+0.00e+00}_{-0.00e+00}$	5	2.10	$3.52^{+0.13}_{-3.44}$	$3.59^{+0.31}_{-3.50}$
299	013346.56+303748.7	pow	$0.10^{+0.10}_{-0.08}$	$1.58^{+0.11}_{-0.11}$	—	$6.77e-06^{+8.20e-07}_{-7.15e-07}$	97	0.96	$11.92^{+0.63}_{-0.61}$	$33.73^{+3.01}_{-1.39}$
301	013346.81+305452.8	vapec	$1.51^{+0.00}_{-0.00}$	—	$1.05^{+0.00}_{-0.00}$	$2.87e-05^{+0.00e+00}_{-0.00e+00}$	9	2.86	$16.46^{+0.45}_{-1.10}$	$19.16^{+0.84}_{-2.05}$
305	013347.83+303249.2	pow	$1.00^{+1.41}_{-0.94}$	$1.35^{+0.76}_{-0.65}$	—	$5.25e-07^{+7.82e-07}_{-2.99e-07}$	5	0.70	$0.93^{+0.11}_{-0.19}$	$3.29^{+0.81}_{-1.71}$
308	013348.50+303307.8	vapec	$0.01^{+0.00}_{-0.00}$	—	$0.63^{+0.00}_{-0.00}$	$6.67e-06^{+0.00e+00}_{-0.00e+00}$	16	3.34	$4.18^{+0.13}_{-4.09}$	$4.35^{+0.06}_{-4.26}$
309	013348.91+302946.7	pow	$0.51^{+0.20}_{-0.17}$	$2.06^{+0.21}_{-0.20}$	—	$6.48e-06^{+1.50e-06}_{-1.17e-06}$	39	0.69	$11.63^{+0.34}_{-0.32}$	$22.18^{+1.32}_{-1.40}$
310	013349.00+304758.7	pow	$8.86^{+8.86}_{-6.74}$	$1.31^{+0.74}_{-1.19}$	—	$9.78e-07^{+9.00e-07}_{-9.78e-07}$	6	1.10	$1.75^{+0.06}_{-0.07}$	$6.43^{+0.56}_{-3.71}$
312	013349.78+305631.7	pow	$0.52^{+0.66}_{-0.47}$	$1.84^{+0.54}_{-0.46}$	—	$3.67e-06^{+2.72e-06}_{-1.47e-06}$	6	0.30	$6.48^{+0.60}_{-0.65}$	$14.58^{+1.91}_{-3.28}$
316	013350.50+303821.4	pow	$0.25^{+0.21}_{-0.17}$	$1.75^{+0.21}_{-0.20}$	—	$3.73e-06^{+9.12e-07}_{-7.01e-07}$	34	0.98	$6.58^{+0.39}_{-0.39}$	$16.00^{+1.14}_{-1.35}$
318	013350.89+303936.6	pow	$0.67^{+0.00}_{-0.00}$	$2.11^{+0.00}_{-0.00}$	—	$4.30e-03^{+0.00e+00}_{-0.00e+00}$	243	3.39	$7757.19^{+15.72}_{-19.15}$	$14315.10^{+48.70}_{-48.30}$
320	013352.12+302706.5	vapec	$0.04^{+0.12}_{-0.04}$	—	$4.67^{+1.60}_{-1.14}$	$1.99e-05^{+2.44e-06}_{-1.66e-06}$	41	0.83	$8.85^{+0.52}_{-0.84}$	$20.89^{+1.78}_{-2.52}$
323	013352.35+302651.6	pow	$0.54^{+0.81}_{-0.53}$	$1.77^{+0.62}_{-0.50}$	—	$1.20e-06^{+1.09e-06}_{-5.32e-07}$	5	0.26	$2.12^{+0.26}_{-0.28}$	$5.03^{+0.76}_{-1.21}$
327	013353.69+303605.6	pow	$0.74^{+1.02}_{-0.67}$	$1.78^{+0.71}_{-0.58}$	—	$6.77e-07^{+3.34e-07}_{-3.34e-07}$	5	0.61	$1.20^{+0.12}_{-0.41}$	$2.82^{+0.47}_{-1.01}$
332	013354.69+304518.4	vapec	$0.01^{+0.00}_{-0.00}$	—	$0.30^{+0.00}_{-0.00}$	$3.73e-06^{+0.00e+00}_{-0.00e+00}$	6	0.64	$1.41^{+0.05}_{-1.36}$	$1.41^{+0.07}_{-1.36}$
333	013354.76+304722.8	pow	$0.68^{+0.78}_{-0.53}$	$2.70^{+1.03}_{-0.73}$	—	$1.08e-06^{+1.29e-06}_{-5.30e-07}$	5	0.50	$2.16^{+0.11}_{-0.39}$	$2.90^{+0.27}_{-0.97}$
334	013354.91+303310.9	vapec	$0.01^{+0.00}_{-0.00}$	—	$0.44^{+0.00}_{-0.00}$	$3.98e-05^{+0.00e+00}_{-0.00e+00}$	59	2.73	$20.43^{+0.08}_{-19.90}$	$20.70^{+0.37}_{-20.17}$
335	013355.14+303108.3	pow	$1.16^{+0.81}_{-0.60}$	$2.18^{+0.65}_{-0.54}$	—	$1.70e-06^{+1.50e-06}_{-7.39e-07}$	7	0.41	$3.09^{+0.11}_{-0.41}$	$5.44^{+0.72}_{-1.19}$
336	013355.21+303010.1	pow	$7.10^{+7.10}_{-3.79}$	$1.83^{+0.90}_{-0.88}$	—	$3.24e-06^{+6.40e-06}_{-3.24e-06}$	5	1.74	$5.74^{+0.09}_{-0.26}$	$12.97^{+0.62}_{-5.88}$
339	013355.39+302343.7	vapec	$0.01^{+0.00}_{-0.00}$	—	$2.36^{+0.00}_{-0.00}$	$8.61e-06^{+0.00e+00}_{-0.00e+00}$	5	1.01	$3.89^{+0.29}_{-3.82}$	$6.73^{+0.03}_{-6.65}$
342	013356.06+303024.7	pow	$1.11^{+0.93}_{-0.66}$	$1.46^{+0.48}_{-0.41}$	—	$1.68e-06^{+1.37e-06}_{-6.87e-07}$	12	1.22	$2.97^{+0.16}_{-0.23}$	$9.40^{+0.96}_{-1.56}$
346	013356.53+302305.2	pow	$2.21^{+2.02}_{-1.43}$	$1.83^{+0.97}_{-0.79}$	—	$3.25e-06^{+7.12e-06}_{-3.25e-06}$	5	0.21	$5.75^{+0.20}_{-1.19}$	$13.03^{+1.65}_{-6.94}$
347	013356.77+303729.7	pow	$0.32^{+0.11}_{-0.10}$	$1.80^{+0.11}_{-0.11}$	—	$9.98e-06^{+1.23e-06}_{-1.07e-06}$	108	0.84	$17.62^{+0.67}_{-0.47}$	$41.03^{+1.73}_{-1.78}$
348	013356.82+303706.7	pow	$0.01^{+0.00}_{-0.00}$	$1.15^{+0.00}_{-0.00}$	—	$2.01e-06^{+0.00e+00}_{-0.00e+00}$	42	0.95	$3.63^{+0.17}_{-3.57}$	$15.87^{+0.58}_{-15.80}$
352	013357.19+305135.3	pow	$0.01^{+0.00}_{-0.00}$	$1.51^{+0.00}_{-0.00}$	—	$9.35e-07^{+0.00e+00}_{-0.00e+00}$	6	1.26	$1.65^{+0.01}_{-1.62}$	$4.96^{+0.82}_{-4.93}$

Table 7—Continued

No.	Source ID	Best-fit ^a model	N_H^b (10^{22} cm $^{-2}$)	Γ	kT (keV)	Norm ^c	DOF ^d	χ_{red}^2	L_X (0.35–2.0keV) ^e (10^{35} erg s $^{-1}$)	L_X (0.35–8.0keV) ^f (10^{35} erg s $^{-1}$)
356	013358.03+303201.2	pow	$9.96^{+9.96}_{-3.33}$	$1.16^{+0.31}_{-0.29}$	—	$2.94e-06^{+6.58e-05}_{-1.63e-06}$	17	1.21	$5.31^{+0.17}_{-0.17}$	$22.86^{+13.66}_{-13.66}$
361	013358.43+304827.7	pow	$2.94^{+3.36}_{-2.30}$	$1.27^{+1.15}_{-0.93}$	—	$5.61e-07^{+1.96e-06}_{-5.61e-07}$	6	1.48	$1.00^{+0.05}_{-0.20}$	$3.86^{+0.40}_{-2.81}$
362	013358.50+303332.2	vpec	$0.01^{+0.00}_{-0.00}$	—	$0.69^{+0.00}_{-0.00}$	$3.39e-06^{+0.00e+00}_{-0.00e+00}$	13	4.29	$2.18^{+0.03}_{-2.13}$	$2.29^{+0.06}_{-2.25}$
365	013358.83+305004.2	pow	$0.41^{+0.20}_{-0.17}$	$1.57^{+0.20}_{-0.19}$	—	$4.38e-06^{+1.04e-06}_{-8.18e-07}$	40	1.04	$7.72^{+0.35}_{-0.38}$	$21.98^{+1.48}_{-1.52}$
366	013359.02+303425.2	pow	$0.01^{+0.00}_{-0.00}$	$3.90^{+0.00}_{-0.00}$	—	$8.83e-07^{+0.00e+00}_{-0.00e+00}$	5	3.39	$2.74^{+0.17}_{-2.59}$	$2.88^{+0.13}_{-2.74}$
368	013359.47+303101.0	vpec	$0.01^{+0.00}_{-0.00}$	—	$1.17^{+0.00}_{-0.00}$	$2.84e-06^{+0.00e+00}_{-0.00e+00}$	5	1.30	$1.54^{+0.05}_{-1.51}$	$1.87^{+0.09}_{-1.84}$
370	013400.28+303057.2	pow	$0.27^{+0.55}_{-0.27}$	$1.90^{+0.70}_{-0.50}$	—	$8.32e-07^{+6.63e-07}_{-3.15e-07}$	5	0.63	$1.48^{+0.19}_{-0.24}$	$3.17^{+0.73}_{-0.78}$
371	013400.30+304219.3	vpec	$0.01^{+0.00}_{-0.00}$	—	$0.64^{+0.00}_{-0.00}$	$3.68e-06^{+0.00e+00}_{-0.00e+00}$	8	1.11	$2.31^{+0.00}_{-2.26}$	$2.41^{+0.11}_{-2.36}$
372	013400.31+304724.0	pow	$0.01^{+0.00}_{-0.00}$	$2.56^{+0.00}_{-0.00}$	—	$6.10e-07^{+0.00e+00}_{-0.00e+00}$	6	0.76	$1.18^{+0.04}_{-1.14}$	$1.69^{+0.30}_{-1.65}$
381	013401.12+303136.9	pow	$0.80^{+0.24}_{-0.24}$	$2.59^{+0.29}_{-0.26}$	—	$7.48e-06^{+1.67e-06}_{-3.39e-07}$	40	0.91	$14.55^{+0.24}_{-0.43}$	$20.56^{+0.81}_{-1.82}$
384	013401.16+303242.3	pow	$0.20^{+0.45}_{-0.20}$	$1.15^{+0.31}_{-0.26}$	—	$8.74e-07^{+2.29e-07}_{-7.52e-07}$	16	0.77	$1.58^{+0.19}_{-0.23}$	$6.90^{+0.89}_{-0.89}$
386	013401.63+304829.7	pow	$0.24^{+0.24}_{-0.24}$	$1.79^{+0.34}_{-0.28}$	—	$1.82e-06^{+4.74e-07}_{-4.74e-07}$	20	0.87	$3.21^{+0.40}_{-0.29}$	$7.52^{+0.80}_{-0.86}$
387	013401.66+303517.0	pow	$0.50^{+0.99}_{-0.50}$	$1.08^{+0.52}_{-0.44}$	—	$4.91e-07^{+4.41e-07}_{-2.12e-07}$	6	0.50	$0.90^{+0.15}_{-0.32}$	$4.19^{+0.70}_{-1.28}$
388	013401.69+303221.5	pow	$0.40^{+0.38}_{-0.40}$	$1.69^{+0.33}_{-0.44}$	—	$8.01e-07^{+5.50e-07}_{-3.05e-07}$	7	0.31	$1.41^{+0.13}_{-0.14}$	$3.61^{+0.51}_{-0.75}$
389	013402.03+303004.8	pow	$0.15^{+0.14}_{-0.12}$	$1.67^{+0.16}_{-0.15}$	—	$6.53e-06^{+9.51e-07}_{-9.51e-07}$	54	1.11	$11.50^{+0.98}_{-0.75}$	$29.88^{+2.18}_{-1.93}$
390	013402.10+304702.7	vpec	$0.66^{+1.36}_{-0.54}$	—	$3.06^{+5.72}_{-1.80}$	$2.58e-06^{+3.04e-06}_{-8.78e-07}$	5	0.56	$1.16^{+0.16}_{-0.23}$	$2.27^{+0.31}_{-0.70}$
391	013402.37+303136.2	pow	$1.05^{+0.55}_{-0.44}$	$1.74^{+0.33}_{-0.30}$	—	$2.87e-06^{+1.39e-06}_{-8.69e-07}$	26	1.06	$5.05^{+0.16}_{-0.22}$	$12.36^{+0.76}_{-0.96}$
392	013402.41+302940.4	pow	$0.14^{+0.89}_{-0.14}$	$1.58^{+0.88}_{-0.45}$	—	$5.10e-07^{+6.59e-07}_{-1.94e-07}$	5	0.55	$0.90^{+0.13}_{-0.46}$	$2.53^{+0.48}_{-1.00}$
394	013402.71+303052.7	pow	$9.95^{+9.95}_{-6.61}$	$1.71^{+0.75}_{-0.82}$	—	$1.78e-06^{+9.85e-05}_{-1.78e-06}$	5	1.49	$3.14^{+0.07}_{-0.07}$	$7.88^{+3.51}_{-3.51}$
395	013402.82+305412.4	pow	$0.58^{+0.51}_{-0.39}$	$2.30^{+0.63}_{-0.50}$	—	$2.15e-06^{+1.48e-06}_{-8.09e-07}$	8	0.42	$3.96^{+0.22}_{-0.37}$	$6.49^{+0.79}_{-0.99}$
396	013402.83+304940.5	pow	$2.55^{+1.05}_{-0.83}$	$1.03^{+0.32}_{-0.29}$	—	$2.64e-06^{+1.56e-06}_{-9.28e-07}$	28	0.85	$4.84^{+0.12}_{-0.22}$	$24.12^{+1.47}_{-2.83}$
397	013402.85+303439.0	pow	$0.51^{+1.23}_{-0.51}$	$1.59^{+0.89}_{-0.61}$	—	$5.12e-07^{+8.24e-07}_{-2.57e-07}$	5	1.93	$0.90^{+0.12}_{-0.21}$	$2.51^{+0.47}_{-1.13}$
398	013402.86+304151.2	pow	$1.30^{+0.89}_{-0.67}$	$0.80^{+0.35}_{-0.32}$	—	$1.29e-06^{+4.08e-07}_{-4.65e-07}$	21	0.91	$2.44^{+0.19}_{-0.21}$	$15.91^{+1.33}_{-2.03}$
403	013403.49+305641.3	pow	$0.01^{+0.00}_{-0.00}$	$1.57^{+0.00}_{-0.00}$	—	$1.03e-06^{+0.00e+00}_{-0.00e+00}$	5	0.63	$1.82^{+0.29}_{-1.78}$	$5.18^{+1.24}_{-5.15}$
408	013405.05+305557.2	pow	$0.11^{+0.53}_{-0.11}$	$1.70^{+0.64}_{-0.36}$	—	$1.91e-06^{+1.47e-06}_{-5.85e-07}$	5	0.67	$3.37^{+0.54}_{-1.07}$	$8.51^{+1.91}_{-2.09}$
411	013407.42+303121.0	pow	$0.74^{+1.51}_{-0.74}$	$1.68^{+1.02}_{-0.73}$	—	$6.19e-07^{+2.0e-06}_{-3.51e-07}$	5	0.29	$1.09^{+0.12}_{-0.37}$	$2.80^{+0.46}_{-2.16}$
414	013407.63+303902.4	pow	$3.50^{+3.21}_{-2.14}$	$1.74^{+1.05}_{-0.84}$	—	$1.22e-06^{+3.76e-06}_{-1.22e-06}$	5	0.62	$2.15^{+0.03}_{-0.29}$	$5.28^{+0.39}_{-2.66}$
415	013407.81+303553.9	pow	$0.06^{+0.20}_{-0.06}$	$1.88^{+0.28}_{-0.20}$	—	$1.77e-06^{+4.92e-07}_{-2.92e-07}$	22	1.36	$3.14^{+0.25}_{-0.49}$	$6.83^{+0.78}_{-0.81}$
416	013408.32+303851.7	pow	$4.66^{+4.66}_{-2.47}$	$1.78^{+0.99}_{-0.82}$	—	$1.81e-06^{+5.17e-06}_{-1.81e-06}$	5	0.71	$3.20^{+0.08}_{-0.29}$	$7.53^{+0.60}_{-3.95}$
417	013408.36+304633.2	vpec	$0.01^{+0.00}_{-0.00}$	—	$0.28^{+0.00}_{-0.00}$	$1.05e-05^{+0.00e+00}_{-5.95e-07}$	12	1.56	$3.69^{+0.04}_{-3.56}$	$3.70^{+0.01}_{-3.57}$
419	013409.65+303259.8	pow	$0.34^{+0.42}_{-0.31}$	$1.52^{+0.36}_{-0.32}$	—	$1.28e-06^{+5.95e-07}_{-3.83e-07}$	15	0.32	$2.25^{+0.19}_{-0.20}$	$6.71^{+0.88}_{-0.88}$
420	013409.70+303612.3	pow	$1.99^{+2.01}_{-1.28}$	$2.17^{+1.03}_{-0.78}$	—	$1.06e-06^{+6.59e-07}_{-1.64e-06}$	5	0.21	$1.92^{+0.06}_{-0.37}$	$3.40^{+0.31}_{-1.39}$
421	013409.91+305045.3	pow	$0.70^{+0.26}_{-0.23}$	$2.08^{+0.25}_{-0.24}$	—	$5.63e-06^{+1.22e-06}_{-1.22e-06}$	30	1.00	$10.12^{+0.32}_{-0.32}$	$19.04^{+1.20}_{-1.21}$
423	013410.42+305346.2	pow	$0.01^{+0.00}_{-0.00}$	$1.56^{+0.00}_{-0.00}$	—	$1.20e-06^{+0.00e+00}_{-0.00e+00}$	7	0.74	$2.11^{+0.15}_{-2.07}$	$6.07^{+0.56}_{-6.03}$

Table 7—Continued

No.	Source ID	Best-fit ^a model	N_H^b (10^{22} cm $^{-2}$)	Γ	kT (keV)	Norm ^c	DOF ^d	χ_{red}^2	L_X (0.35–2.0keV) ^e (10^{35} erg s $^{-1}$)	L_X (0.35–8.0keV) ^f (10^{35} erg s $^{-1}$)
424	013410.51+303946.4	pow	$0.01^{+0.00}_{-0.00}$	$1.71^{+0.00}_{-0.00}$	—	$5.78e-06^{+0.00e+00}_{-0.00e+00}$	86	1.03	$10.18^{+0.14}_{-9.96}$	$25.58^{+1.11}_{-25.35}$
427	013410.69+304224.0	vapec	$0.01^{+0.00}_{-0.00}$	—	$0.31^{+0.00}_{-0.00}$	$3.11e-05^{+0.00e+00}_{-0.00e+00}$	37	1.93	$11.81^{+0.16}_{-11.42}$	$11.85^{+0.15}_{-11.46}$
428	013410.78+305010.2	pow	$0.78^{+0.00}_{-0.00}$	$-0.08^{+0.08}_{-0.08}$	—	$1.05e-07^{+0.00e+00}_{-0.00e+00}$	6	1.57	$0.24^{+0.07}_{-0.16}$	$4.81^{+0.78}_{-4.65}$
429	013410.84+302455.8	pow	$0.22^{+0.56}_{-0.22}$	$2.24^{+0.76}_{-0.51}$	—	$1.85e-06^{+1.58e-06}_{-7.03e-07}$	5	0.37	$3.38^{+0.69}_{-0.69}$	$5.72^{+1.03}_{-1.54}$
439	013414.42+303303.8	pow	$0.01^{+0.00}_{-0.00}$	$1.48^{+0.00}_{-0.00}$	—	$3.97e-07^{+0.00e+00}_{-0.00e+00}$	7	1.16	$0.70^{+0.04}_{-0.69}$	$2.17^{+0.33}_{-2.16}$
440	013414.83+303412.3	pow	$0.24^{+0.38}_{-0.24}$	$2.18^{+0.57}_{-0.44}$	—	$1.12e-06^{+6.06e-07}_{-3.61e-07}$	9	0.76	$2.04^{+0.24}_{-0.25}$	$3.58^{+0.67}_{-0.61}$
448	013416.50+305156.5	vapec	$0.01^{+0.00}_{-0.00}$	—	$0.59^{+0.00}_{-0.00}$	$2.68e-06^{+0.00e+00}_{-0.00e+00}$	5	4.02	$1.64^{+0.15}_{-1.60}$	$1.69^{+0.07}_{-1.65}$
450	013416.76+305101.8	vapec	$0.68^{+0.30}_{-0.24}$	—	$4.34^{+2.48}_{-1.19}$	$1.25e-05^{+2.55e-06}_{-1.96e-06}$	22	1.11	$5.57^{+0.20}_{-0.29}$	$12.78^{+0.82}_{-2.79}$
452	013417.08+303426.6	vapec	$1.76^{+0.76}_{-0.63}$	—	$5.14^{+8.33}_{-3.06}$	$8.53e-06^{+3.19e-06}_{-1.94e-06}$	14	0.53	$3.77^{+0.14}_{-0.18}$	$9.24^{+0.48}_{-3.50}$
456	013417.61+304123.3	vapec	$0.01^{+0.00}_{-0.00}$	—	$0.70^{+0.00}_{-0.00}$	$2.02e-06^{+0.00e+00}_{-0.00e+00}$	5	2.35	$1.30^{+0.00}_{-1.27}$	$1.36^{+0.01}_{-1.34}$
462	013418.22+302446.1	vapec	$0.29^{+0.00}_{-0.00}$	—	$0.81^{+0.00}_{-0.00}$	$1.06e-05^{+0.00e+00}_{-0.00e+00}$	5	1.05	$6.73^{+0.53}_{-1.47}$	$7.27^{+0.61}_{-1.81}$
465	013419.32+304942.4	pow	$0.89^{+1.46}_{-0.76}$	$1.58^{+0.72}_{-0.53}$	—	$1.21e-06^{+1.77e-06}_{-5.92e-07}$	6	0.82	$2.14^{+0.19}_{-0.33}$	$6.03^{+1.03}_{-1.60}$
467	013419.77+303718.9	pow	$0.47^{+0.90}_{-0.47}$	$2.57^{+1.57}_{-0.89}$	—	$6.93e-07^{+2.23e-06}_{-3.64e-07}$	6	0.94	$1.34^{+0.18}_{-0.40}$	$1.91^{+0.37}_{-0.79}$
468	013420.91+303319.0	pow	$0.36^{+1.03}_{-0.36}$	$1.17^{+0.69}_{-0.51}$	—	$4.84e-07^{+1.80e-07}_{-2.25e-07}$	5	1.15	$0.87^{+0.15}_{-0.35}$	$3.74^{+0.82}_{-1.52}$
470	013421.09+304932.3	vapec	$4.84^{+1.42}_{-1.07}$	—	$2.19^{+1.03}_{-0.59}$	$3.95e-05^{+1.32e-05}_{-1.32e-05}$	16	1.22	$17.87^{+0.20}_{-0.24}$	$29.82^{+1.15}_{-2.93}$
471	013421.15+303930.7	pow	$0.20^{+0.52}_{-0.20}$	$1.67^{+0.45}_{-0.34}$	—	$8.86e-07^{+5.30e-07}_{-2.59e-07}$	10	1.11	$1.56^{+0.16}_{-0.26}$	$4.07^{+0.61}_{-0.67}$
481	013423.68+303833.2	pow	$0.16^{+0.00}_{-0.00}$	$1.59^{+0.00}_{-0.00}$	—	$5.23e-07^{+0.00e+00}_{-0.00e+00}$	5	2.42	$0.92^{+0.18}_{-0.35}$	$2.56^{+0.54}_{-0.72}$
482	013423.86+303847.6	pow	$0.29^{+0.30}_{-0.23}$	$1.56^{+0.30}_{-0.27}$	—	$1.74e-06^{+6.12e-07}_{-4.37e-07}$	20	0.79	$3.07^{+0.29}_{-0.28}$	$8.82^{+1.21}_{-0.96}$
483	013424.55+304307.1	pow	$0.60^{+0.82}_{-0.51}$	$1.72^{+0.54}_{-0.43}$	—	$1.33e-06^{+1.18e-06}_{-5.32e-07}$	11	1.16	$2.34^{+0.19}_{-0.19}$	$5.83^{+0.75}_{-0.81}$
485	013424.79+303914.1	pow	$0.44^{+0.95}_{-0.44}$	$1.04^{+0.56}_{-0.46}$	—	$5.06e-07^{+4.80e-07}_{-2.21e-07}$	5	0.81	$0.93^{+0.11}_{-0.21}$	$4.57^{+1.07}_{-1.39}$
487	013424.94+302539.6	pow	$0.24^{+0.84}_{-0.24}$	$1.50^{+0.80}_{-0.51}$	—	$9.21e-07^{+1.06e-06}_{-4.05e-07}$	5	1.33	$1.63^{+0.29}_{-0.82}$	$4.95^{+1.61}_{-2.24}$
488	013425.33+304159.7	pow	$0.28^{+0.28}_{-0.21}$	$2.11^{+0.33}_{-0.29}$	—	$2.34e-06^{+8.29e-07}_{-5.62e-07}$	21	1.07	$4.22^{+0.38}_{-0.27}$	$7.78^{+0.79}_{-0.90}$
491	013425.75+302817.9	pow	$0.23^{+0.31}_{-0.21}$	$1.91^{+0.30}_{-0.25}$	—	$6.04e-06^{+2.20e-06}_{-1.46e-06}$	19	1.17	$10.72^{+1.06}_{-0.87}$	$22.72^{+2.28}_{-2.49}$
492	013425.80+305518.1	pow	$0.19^{+0.04}_{-0.04}$	$1.87^{+0.06}_{-0.05}$	—	$9.50e-05^{+5.23e-06}_{-4.89e-06}$	238	1.00	$168.33^{+3.82}_{-3.06}$	$368.12^{+8.25}_{-7.57}$
493	013425.87+303316.8	pow	$0.24^{+0.40}_{-0.24}$	$2.21^{+0.60}_{-0.47}$	—	$1.95e-06^{+1.14e-06}_{-6.51e-07}$	9	1.28	$3.56^{+0.54}_{-0.49}$	$6.13^{+0.95}_{-1.23}$
497	013426.53+304446.2	pow	$0.02^{+0.20}_{-0.02}$	$1.83^{+0.29}_{-0.17}$	—	$1.89e-06^{+5.36e-07}_{-2.39e-07}$	22	1.26	$3.34^{+0.34}_{-0.81}$	$7.55^{+0.55}_{-0.92}$
498	013426.56+303738.1	pow	$0.01^{+0.00}_{-0.00}$	$1.90^{+0.00}_{-0.00}$	—	$1.50e-06^{+0.00e+00}_{-0.00e+00}$	15	1.17	$2.66^{+0.21}_{-2.60}$	$5.68^{+0.26}_{-5.62}$
499	013426.71+304812.8	pow	$0.65^{+0.88}_{-0.58}$	$1.85^{+0.67}_{-0.56}$	—	$1.23e-06^{+1.28e-06}_{-5.95e-07}$	5	0.19	$2.17^{+0.23}_{-0.34}$	$4.86^{+0.78}_{-1.15}$
502	013426.98+304313.4	pow	$0.04^{+0.13}_{-0.04}$	$1.67^{+0.17}_{-0.13}$	—	$4.02e-06^{+7.05e-07}_{-4.48e-07}$	47	0.71	$7.08^{+0.39}_{-0.67}$	$18.40^{+1.39}_{-1.61}$
504	013427.28+304421.9	pow	$0.83^{+1.42}_{-0.79}$	$1.96^{+1.04}_{-0.74}$	—	$7.11e-07^{+1.38e-06}_{-4.03e-07}$	5	0.73	$1.27^{+0.12}_{-0.26}$	$2.59^{+0.58}_{-1.03}$
507	013428.21+303248.0	pow	$0.17^{+0.39}_{-0.17}$	$1.46^{+0.34}_{-0.28}$	—	$1.71e-06^{+7.62e-07}_{-4.61e-07}$	11	0.42	$3.02^{+0.33}_{-0.43}$	$9.54^{+1.10}_{-1.45}$
515	013429.01+304249.7	pow	$0.01^{+0.00}_{-0.00}$	$1.70^{+0.00}_{-0.00}$	—	$3.31e-07^{+0.00e+00}_{-0.00e+00}$	6	2.45	$0.58^{+0.06}_{-0.57}$	$1.48^{+0.32}_{-1.47}$
516	013429.10+304212.9	vapec	$0.01^{+0.00}_{-0.00}$	—	$3.71^{+0.00}_{-0.00}$	$2.54e-06^{+0.00e+00}_{-0.00e+00}$	5	0.97	$1.14^{+0.06}_{-1.12}$	$2.44^{+0.19}_{-2.41}$
517	013429.74+305026.3	pow	$0.01^{+0.00}_{-0.00}$	$1.60^{+0.00}_{-0.00}$	—	$1.25e-06^{+0.00e+00}_{-0.00e+00}$	6	1.18	$2.21^{+0.20}_{-2.16}$	$6.07^{+0.73}_{-6.02}$

Table 7—Continued

No.	Source ID	Best-fit ^a model	N_H^b (10^{22} cm $^{-2}$)	Γ	kT (keV)	Norm ^c	DOF ^d	χ_{red}^2	L_X (0.35–2.0keV) ^e (10^{35} erg s $^{-1}$)	L_X (0.35–8.0keV) ^f
528	013432.02+303454.1	vapc	$3.02^{+0.62}_{-0.36}$	—	$10.87^{+6.62}_{-4.41}$	$5.13e-05^{+8.36e-06}_{-1.70e-06}$	66	1.38	$20.70^{+0.26}_{-0.74}$	$63.50^{+1.36}_{-12.38}$
530	013432.16+305158.7	pow	$0.01^{+0.00}_{-0.00}$	$1.95^{+0.00}_{-0.00}$	—	$1.03e-05^{+0.00e+00}_{-0.00e+00}$	46	1.48	$18.32^{+0.10}_{-17.88}$	$37.74^{+0.90}_{-37.28}$
532	013432.26+303201.2	vapc	$0.62^{+1.20}_{-0.57}$	—	$3.26^{+8.53}_{-1.76}$	$3.62e-06^{+3.51e-06}_{-1.35e-06}$	6	0.52	$1.63^{+0.28}_{-0.82}$	$3.29^{+0.52}_{-1.72}$
533	013432.56+303436.8	pow	$0.24^{+0.24}_{-0.19}$	$1.90^{+0.31}_{-0.28}$	—	$2.86e-06^{+9.22e-07}_{-6.78e-07}$	21	1.16	$5.06^{+0.38}_{-0.40}$	$10.84^{+1.32}_{-1.25}$
534	013432.59+305035.4	pow	$1.89^{+2.43}_{-1.60}$	$1.17^{+0.90}_{-0.77}$	—	$9.77e-07^{+2.34e-06}_{-9.77e-07}$	5	1.39	$1.76^{+0.07}_{-0.54}$	$7.54^{+0.85}_{-5.99}$
535	013432.60+304704.1	pow	$0.01^{+0.00}_{-0.00}$	$2.90^{+0.00}_{-0.00}$	—	$1.15e-06^{+0.00e+00}_{-0.00e+00}$	5	0.21	$2.41^{+0.06}_{-2.29}$	$3.03^{+0.28}_{-2.91}$
537	013432.74+303930.1	pow	$3.01^{+0.00}_{-0.00}$	$-0.31^{+0.31}_{-0.31}$	—	$8.80e-08^{+0.00e+00}_{-0.00e+00}$	5	0.64	$0.22^{+0.05}_{-0.07}$	$5.85^{+0.14}_{-5.42}$
538	013432.98+303857.4	pow	$3.14^{+2.06}_{-1.53}$	$2.03^{+0.89}_{-0.72}$	—	$2.93e-06^{+5.73e-06}_{-1.79e-06}$	6	1.01	$5.24^{+0.14}_{-0.69}$	$10.17^{+0.69}_{-5.02}$
539	013433.02+304639.1	vapc	$0.43^{+0.40}_{-0.43}$	—	$0.43^{+0.15}_{-0.14}$	$8.17e-06^{+1.52e-05}_{-5.07e-06}$	6	1.83	$4.12^{+0.14}_{-1.74}$	$4.17^{+0.12}_{-1.78}$
544	013435.06+304439.3	pow	$0.79^{+0.00}_{-0.00}$	$0.14^{+0.00}_{-0.00}$	—	$4.56e-07^{+0.00e+00}_{-2.31e-05}$	12	2.74	$1.00^{+0.15}_{-0.17}$	$14.84^{+1.16}_{-5.48}$
546	013435.14+305646.1	pow	$3.73^{+1.22}_{-1.09}$	$2.16^{+0.48}_{-0.43}$	—	$2.71e-05^{+2.31e-05}_{-1.18e-05}$	15	0.56	$49.20^{+0.47}_{-1.28}$	$87.41^{+3.48}_{-8.60}$
552	013436.04+303450.0	pow	$0.43^{+0.15}_{-0.13}$	$1.62^{+0.12}_{-0.12}$	—	$1.15e-05^{+1.45e-06}_{-1.45e-06}$	90	0.83	$20.22^{+0.54}_{-0.54}$	$55.07^{+2.44}_{-2.44}$
553	013436.43+304713.8	pow	$9.93^{+0.00}_{-0.00}$	$1.42^{+0.00}_{-0.00}$	—	$7.91e-06^{+0.00e+00}_{-0.00e+00}$	20	1.43	$14.02^{+0.39}_{-0.39}$	$46.13^{+24.45}_{-24.45}$
560	013438.72+304539.3	pow	$0.05^{+0.15}_{-0.05}$	$1.78^{+0.21}_{-0.13}$	—	$4.44e-06^{+9.66e-07}_{-5.31e-07}$	41	1.32	$7.83^{+0.46}_{-1.07}$	$18.43^{+1.33}_{-1.89}$
561	013438.83+305504.4	pow	$0.11^{+0.06}_{-0.06}$	$1.87^{+0.08}_{-0.08}$	—	$6.03e-05^{+5.03e-06}_{-4.56e-06}$	151	1.12	$106.69^{+4.68}_{-4.01}$	$234.40^{+8.61}_{-9.49}$
564	013439.69+302950.7	pow	$0.15^{+0.15}_{-0.15}$	$2.17^{+0.74}_{-0.42}$	—	$1.86e-06^{+1.46e-06}_{-5.88e-07}$	5	0.27	$3.38^{+0.56}_{-0.85}$	$5.97^{+0.88}_{-1.65}$
565	013439.84+305144.3	pow	$0.01^{+0.00}_{-0.00}$	$1.55^{+0.00}_{-0.00}$	—	$2.88e-06^{+0.00e+00}_{-0.00e+00}$	16	0.39	$5.08^{+0.34}_{-4.98}$	$14.66^{+0.89}_{-14.56}$
571	013440.81+304410.2	pow	$0.05^{+0.55}_{-0.05}$	$1.70^{+0.65}_{-0.35}$	—	$6.07e-07^{+4.80e-07}_{-1.62e-07}$	6	0.85	$1.07^{+0.16}_{-0.47}$	$2.70^{+0.67}_{-0.85}$
572	013441.10+304328.3	vapc	$0.01^{+0.00}_{-0.00}$	—	$0.38^{+0.00}_{-0.00}$	$5.49e-06^{+0.00e+00}_{-0.00e+00}$	5	1.57	$2.48^{+0.10}_{-2.41}$	$2.50^{+0.12}_{-2.43}$
573	013441.26+303516.4	pow	$0.81^{+1.15}_{-0.78}$	$1.53^{+0.83}_{-0.67}$	—	$1.01e-06^{+1.43e-06}_{-5.57e-07}$	5	1.61	$1.78^{+0.24}_{-0.63}$	$5.29^{+0.85}_{-1.64}$
575	013441.43+303415.7	pow	$2.56^{+2.40}_{-1.68}$	$1.60^{+0.96}_{-0.79}$	—	$1.25e-06^{+2.86e-06}_{-1.25e-06}$	7	1.38	$2.21^{+0.11}_{-0.44}$	$6.12^{+0.89}_{-4.01}$
576	013442.07+305228.8	pow	$0.36^{+0.56}_{-0.36}$	$1.73^{+0.59}_{-0.49}$	—	$1.73e-06^{+1.29e-06}_{-7.00e-07}$	5	0.35	$3.05^{+0.33}_{-0.47}$	$7.54^{+1.22}_{-1.44}$
577	013442.43+305249.5	pow	$0.37^{+0.36}_{-0.28}$	$1.76^{+0.38}_{-0.33}$	—	$3.11e-06^{+1.39e-06}_{-9.20e-07}$	14	0.93	$5.49^{+0.42}_{-0.43}$	$13.23^{+1.42}_{-2.07}$
579	013442.79+304505.6	pow	$0.01^{+0.00}_{-0.00}$	$1.57^{+0.00}_{-0.00}$	—	$2.77e-06^{+0.00e+00}_{-0.00e+00}$	27	1.23	$4.88^{+0.26}_{-4.79}$	$13.84^{+0.86}_{-13.74}$
585	013444.23+304920.3	vapc	$0.48^{+0.39}_{-0.41}$	—	$0.72^{+0.11}_{-0.15}$	$1.42e-05^{+1.15e-05}_{-6.42e-06}$	13	1.65	$9.09^{+0.54}_{-0.76}$	$9.62^{+0.63}_{-1.02}$
586	013444.38+304702.9	vapc	$0.59^{+0.78}_{-0.50}$	—	$3.87^{+11.33}_{-2.01}$	$3.90e-06^{+2.48e-06}_{-1.24e-06}$	5	0.27	$1.75^{+0.23}_{-0.25}$	$3.81^{+0.42}_{-1.26}$
587	013444.62+305535.0	vapc	$0.97^{+0.45}_{-0.35}$	—	$3.58^{+2.33}_{-1.08}$	$5.45e-05^{+1.62e-05}_{-1.18e-05}$	13	0.66	$24.48^{+0.89}_{-1.50}$	$51.58^{+4.18}_{-9.47}$
589	013444.99+304927.7	pow	$0.17^{+0.15}_{-0.13}$	$1.94^{+0.20}_{-0.18}$	—	$8.27e-06^{+1.71e-06}_{-1.36e-06}$	43	0.93	$14.70^{+0.89}_{-0.80}$	$30.52^{+2.36}_{-2.15}$
593	013446.78+304448.9	pow	$0.02^{+0.50}_{-0.02}$	$1.88^{+0.69}_{-0.33}$	—	$7.68e-07^{+6.03e-07}_{-1.68e-07}$	5	1.91	$1.36^{+0.11}_{-0.61}$	$2.97^{+0.53}_{-0.94}$
594	013447.35+304001.3	pow	$0.66^{+0.77}_{-0.53}$	$2.47^{+0.86}_{-0.65}$	—	$2.37e-06^{+2.64e-06}_{-1.15e-06}$	7	0.51	$4.50^{+0.39}_{-0.63}$	$6.72^{+0.81}_{-3.19}$
595	013447.62+303514.3	pow	$0.01^{+0.00}_{-0.00}$	$1.89^{+0.00}_{-0.00}$	—	$2.09e-06^{+2.74e-06}_{-0.90e+00}$	6	1.06	$3.71^{+0.34}_{-0.34}$	$8.00^{+6.24}_{-7.91}$
600	013449.00+303328.6	pow	$0.09^{+0.13}_{-0.09}$	$1.64^{+0.16}_{-0.14}$	—	$1.68e-05^{+2.29e-06}_{-0.00e+00}$	53	1.11	$29.62^{+3.30}_{-2.17}$	$78.74^{+4.64}_{-6.09}$
601	013449.04+304446.8	pow	$0.01^{+0.00}_{-0.00}$	$1.10^{+0.00}_{-0.00}$	—	$1.27e-06^{+0.00e+00}_{-0.00e+00}$	17	1.44	$2.32^{+0.13}_{-0.28}$	$10.70^{+1.06}_{-10.67}$
608	013451.10+304356.7	vapc	$0.85^{+0.00}_{-0.00}$	—	$2.52^{+0.00}_{-0.00}$	$1.20e-05^{+0.00e+00}_{-0.00e+00}$	8	2.15	$5.44^{+0.31}_{-0.26}$	$9.69^{+0.78}_{-1.91}$

Table 7—Continued

No.	Source ID	Best-fit ^a model	N_H^b (10^{22} cm^{-2})	Γ	kT (keV)	Norm ^c	DOF ^d	χ^2_{red}	L_X (0.35–2.0keV) ^e ($10^{35} \text{ erg s}^{-1}$)	L_X (0.35–8.0keV) ^f ($10^{35} \text{ erg s}^{-1}$)
612	013451.85+302909.7	pow	$0.28^{+0.03}_{-0.03}$	$1.54^{+0.03}_{-0.03}$	—	$4.71e-04^{+1.61e-05}_{-1.54e-05}$	238	1.04	$830.87^{+9.56}_{-8.44}$	$2423.76^{+33.84}_{-31.81}$
613	013451.94+304615.8	pow	$0.01^{+0.00}_{-0.00}$	$1.64^{+0.00}_{-0.00}$	—	$2.04e-06^{+0.00e+00}_{-0.00e+00}$	17	1.80	$3.60^{+0.03}_{-3.52}$	$9.60^{+0.95}_{-9.52}$
618	013452.89+302809.5	pow	$0.01^{+0.00}_{-0.00}$	$1.34^{+0.00}_{-0.00}$	—	$2.83e-06^{+0.00e+00}_{-0.00e+00}$	5	0.79	$5.04^{+0.19}_{-4.95}$	$17.93^{+2.04}_{-17.84}$
619	013453.25+305717.7	pow	$0.14^{+0.71}_{-0.14}$	$1.87^{+0.86}_{-0.47}$	—	$3.42e-06^{+3.70e-06}_{-1.23e-06}$	7	1.01	$6.06^{+0.57}_{-3.22}$	$13.33^{+3.77}_{-6.30}$
621	013454.94+303248.9	pow	$4.00^{+4.00}_{-2.79}$	$1.79^{+1.34}_{-1.06}$	—	$3.37e-06^{+1.78e-05}_{-3.37e-06}$	5	0.83	$5.95^{+0.22}_{-0.66}$	$13.91^{+1.53}_{-7.53}$
622	013455.30+304624.3	pow	$2.10^{+3.09}_{-2.01}$	$0.90^{+1.05}_{-0.87}$	—	$6.41e-07^{+2.01e-06}_{-6.41e-07}$	5	0.91	$1.20^{+0.09}_{-0.34}$	$6.92^{+1.16}_{-5.77}$
626	013457.21+303825.5	pow	$0.78^{+0.94}_{-0.67}$	$2.20^{+1.04}_{-0.76}$	—	$2.31e-06^{+3.47e-06}_{-1.28e-06}$	6	0.82	$4.21^{+0.30}_{-0.73}$	$7.31^{+0.94}_{-2.60}$
630	013458.51+304707.1	pow	$0.37^{+0.71}_{-0.37}$	$1.28^{+0.52}_{-0.43}$	—	$1.20e-06^{+9.28e-07}_{-4.76e-07}$	6	0.86	$2.15^{+0.20}_{-0.49}$	$8.12^{+1.44}_{-2.00}$
633	013500.54+305028.7	pow	$0.33^{+0.70}_{-0.33}$	$1.62^{+0.60}_{-0.46}$	—	$2.47e-06^{+2.12e-06}_{-9.77e-07}$	5	0.28	$4.35^{+0.77}_{-0.63}$	$11.78^{+1.91}_{-2.84}$
635	013500.97+304348.1	pow	$0.10^{+0.19}_{-0.19}$	$1.81^{+0.24}_{-0.21}$	—	$5.96e-06^{+1.52e-06}_{-1.05e-06}$	28	0.94	$10.53^{+1.05}_{-1.11}$	$24.32^{+1.80}_{-2.77}$
639	013502.80+303710.8	pow	$0.71^{+0.85}_{-0.58}$	$1.66^{+0.54}_{-0.45}$	—	$2.73e-06^{+2.31e-06}_{-1.18e-06}$	6	1.17	$4.81^{+0.66}_{-0.66}$	$12.57^{+1.97}_{-2.70}$
640	013503.04+303340.7	vapec	$0.01^{+0.00}_{-0.00}$	—	$0.74^{+0.00}_{-0.00}$	$5.84e-06^{+0.00e+00}_{-0.00e+00}$	5	2.07	$3.73^{+0.06}_{-3.66}$	$3.97^{+0.05}_{-3.89}$
647	013504.99+303445.5	pow	$0.18^{+0.18}_{-0.15}$	$1.70^{+0.19}_{-0.18}$	—	$1.55e-05^{+3.39e-06}_{-2.66e-06}$	46	1.02	$27.22^{+2.39}_{-6.69}$	$68.78^{+5.62}_{-5.34}$
648	013505.66+305006.4	pow	$2.32^{+1.37}_{-1.03}$	$2.06^{+0.68}_{-0.57}$	—	$1.07e-05^{+1.32e-05}_{-5.51e-06}$	7	0.39	$19.29^{+0.32}_{-1.94}$	$36.61^{+2.83}_{-8.11}$
653	013508.44+303150.4	pow	$0.01^{+0.00}_{-0.00}$	$3.29^{+0.00}_{-0.00}$	—	$5.72e-06^{+0.00e+00}_{-0.00e+00}$	5	3.43	$13.66^{+0.14}_{-13.07}$	$15.57^{+0.35}_{-14.98}$
661	013517.47+304446.7	pow	$1.53^{+3.71}_{-1.53}$	$1.00^{+1.15}_{-0.83}$	—	$2.28e-06^{+9.28e-06}_{-2.28e-06}$	5	0.97	$4.20^{+0.50}_{-1.27}$	$21.65^{+5.73}_{-18.26}$

^aThe best-fit model is either a **powerlaw** or a **vapec** model, depending which one has the lower χ^2_{red} . ^bThis is the column density internal to M33. The Galactic N_H was fixed at $0.06 \times 10^{22} \text{ cm}^{-2}$ (Dickey & Lockman 1990). ^cNormalization constant of the fit. For the **powerlaw** and the **vapec** model, the units are photons $\text{keV}^{-1} \text{ cm}^{-2} \text{ s}^{-1}$ at 1 keV and cm^{-5} , respectively. ^dDegrees of freedom. ^eand ^fabsorption-corrected X-ray luminosities assume a distance to M33 of $D = 817 \text{ kpc}$ (Freedman et al. 2001). All uncertainties are given at a 90% confidence level.

Table 8. Refined Spectral Fit Results for Bright Sources

Source ID	Source No.	Total Counts	N_H^a (10^{22} cm $^{-2}$)	diskbb		Γ	pow Norm b ($\times 10^{-4}$)	$\chi_{\text{red}}^2/\text{DOF}$	deabsorbed L_X^d	
				kT (keV)	Norm b				(0.35 – 2.0 keV) (erg s $^{-1}$)	(0.35 – 8.0 keV) (erg s $^{-1}$)
013350.89+303936.6	318	163938	0.28 $^{+0.06}_{-0.05}$	0.95 $^{+0.04}_{-0.04}$	60.5 $^{+3.4}_{-3.8}$	1.20 $^{+0.29}_{-0.40}$	5.61 $^{+4.40}_{-3.11}$	1.02/237	(5.43 $^{+0.02}_{-0.12}$) $\times 10^{38}$	(1.18 $^{+0.04}_{-0.24}$) $\times 10^{39}$
013328.69+302723.6	180	47082	0.00 $^{+0.01}_{-0.00}$	1.50 $^{+0.36}_{-0.26}$	6.48 $^{+2.13}_{-1.54}$	1.37 $^{+0.10}_{-0.06}$	2.28 $^{+0.16}_{-0.16}$	1.35/241	(6.54 $^{+0.05}_{-0.62}$) $\times 10^{37}$	(1.96 $^{+0.02}_{-0.16}$) $\times 10^{38}$
013324.40+304402.4	158	33863	0.22 $^{+0.06}_{-0.06}$	1.21 $^{+0.24}_{-0.16}$	7.00 $^{+2.52}_{-1.82}$	1.81 $^{+0.21}_{-0.18}$	1.11 $^{+0.21}_{-0.25}$	1.21/239	(3.51 $^{+0.03}_{-0.33}$) $\times 10^{37}$	(7.51 $^{+0.09}_{-0.98}$) $\times 10^{37}$
013451.85+302909.7	612	26303	0.29 $^{+0.14}_{-0.09}$	2.62 $^{+0.39}_{-0.39}$	3.63 $^{+1.30}_{-1.15}$	1.94 $^{+0.76}_{-0.76}$	3.43 $^{+0.63}_{-0.47}$	0.99/236	(1.03 $^{+0.13}_{-0.13}$) $\times 10^{38}$	(2.59 $^{+0.59}_{-0.17}$) $\times 10^{38}$
013315.16+305318.2	113	23117	0.53 $^{+0.11}_{-0.11}$	0.92 $^{+0.07}_{-0.07}$	22.6 $^{+4.4}_{-3.4}$	2.51 $^{+0.34}_{-0.34}$	2.74 $^{+0.98}_{-1.05}$	1.13/239	(1.17 $^{+0.01}_{-0.06}$) $\times 10^{38}$	(1.79 $^{+0.03}_{-0.14}$) $\times 10^{38}$
013425.80+305518.1	492	9064	0.19 $^{+0.04}_{-0.04}$	–	–	1.87 $^{+0.05}_{-0.05}$	0.95 $^{+0.05}_{-0.05}$	1.00/238	(2.08 $^{+0.05}_{-0.07}$) $\times 10^{37}$	(4.09 $^{+0.10}_{-0.10}$) $\times 10^{37}$
013253.89+303311.8	37	4891	0.17 $^{+0.06}_{-0.05}$	–	–	1.95 $^{+0.08}_{-0.08}$	0.42 $^{+0.03}_{-0.03}$	0.91/167	(9.18 $^{+0.39}_{-0.34}$) $\times 10^{36}$	(1.82 $^{+0.07}_{-0.07}$) $\times 10^{37}$
013438.83+305504.4	561	4044	0.11 $^{+0.06}_{-0.06}$	–	–	1.87 $^{+0.08}_{-0.08}$	0.60 $^{+0.05}_{-0.05}$	1.12/151	(1.32 $^{+0.07}_{-0.07}$) $\times 10^{37}$	(2.60 $^{+0.11}_{-0.13}$) $\times 10^{37}$
013253.56+303814.8	35	2808	0.09 $^{+0.07}_{-0.07}$	–	–	1.72 $^{+0.10}_{-0.09}$	0.38 $^{+0.04}_{-0.03}$	0.95/132	(8.16 $^{+0.43}_{-0.40}$) $\times 10^{36}$	(1.82 $^{+0.10}_{-0.07}$) $\times 10^{37}$
013356.77+303729.7	347	2434	0.31 $^{+0.11}_{-0.10}$	–	–	1.78 $^{+0.12}_{-0.11}$	0.10 $^{+0.01}_{-0.01}$	0.84/107	(2.12 $^{+0.10}_{-0.12}$) $\times 10^{36}$	(4.51 $^{+0.20}_{-0.17}$) $\times 10^{36}$
013346.56+303748.7	299	2195	0.11 $^{+0.10}_{-0.09}$	–	–	1.58 $^{+0.12}_{-0.11}$	0.07 $^{+0.01}_{-0.01}$	0.98/96	(1.44 $^{+0.08}_{-0.09}$) $\times 10^{36}$	(3.62 $^{+0.19}_{-0.19}$) $\times 10^{36}$

^aColumn density internal to M33. The Galactic N_H was fixed at 0.06×10^{22} cm $^{-2}$ (Dickey & Lockman 1990). ^b Normalization constant for the disk blackbody model **diskbb** in units of (km), where the normalization is $R_{in}(\cos\theta)^{1/2}$ with R_{in} being the inner disk radius and θ being the inclination angle (assuming a distance to M33 of $D = 817$ kpc). ^c Normalization constant for the non-thermal model **pow** in units of photons keV $^{-1}$ cm $^{-2}$ s $^{-1}$ at 1 keV. ^d Deabsorbed X-ray luminosities assume a distance to M33 of 817 kpc (Freedman et al. 2001). All uncertainties are given at a 90% confidence level.

Table 9. Cross-referenced source list.

Source ID ^a (1)	Src. No. (2)	FLC No. (3)	XMM No. (4)	G05 No. (5)	Extent (6)	Variability			$S_{H\alpha}$ ($10^{-17} \text{ erg s}^{-1} \text{ cm}^{-2} \text{ arcsec}^{-2}$) (10)	Source type (11)	Comments (12)
						η (7)	ξ (8)	$\frac{flux_{max}}{flux_{min}}$ (9)			
013224.55+303322.3	1	1	30,28	—	0	—	—	—	-0.187	—	—
013227.18+303521.0	2	2	—,—	—	0	—	—	—	2.157	—	—
013229.23+303618.6	3	3	35,35	—	0	—	—	—	16.261	Galaxy,2MASS-3086, USNO-7682	—
013229.31+304514.0	4	4	37,36	—	0	—	—	—	-0.692	—	pos. uncertain
013230.28+303548.1	5	5	—,—	—	0	—	—	—	1.456	non-stellar	—
013230.54+303618.0	6	6	39,—	—	0	—	—	—	31.397	FS,2MASS-3043, USNO-7490	—
013232.83+304027.9	7	7	—,—	—	0	0.9	8.95e-01	2.0 ± 1.9	2.913	—	—
013233.76+304726.7	8	—	—,—	—	0	—	—	—	2.711	2MASS-3183, USNO-8154	—
013236.34+304045.4	9	—	—,—	—	0	0.1	—	1.1 ± 1.1	0.779	—	—
013236.84+303229.0	10	8	47,44	—	0	—	—	—	-0.408	XRB,USNO-7375	PMH2004-47 (PMH04)
013240.62+303721.2	11	—	—,—	—	0	0.5	—	1.4 ± 1.1	1.296	USNO-5598	—
013240.86+303550.3	12	9	56,51	—	0	0.5	4.23e-01	1.2 ± 0.4	-0.637	stellar	—
013241.32+303217.7	13	10	—,—	—	0	—	—	—	1.289	XRB,XRT-1, USNO-6704	trans. source
013242.07+303329.0	14	11	—,—	—	0	—	—	—	0.065	Galaxy,USNO-6222	—
013242.46+304815.0	15	12	58,—	—	0	—	—	—	-0.581	Galaxy	ZKH08
013243.41+303506.2	16	13	60,54	—	0	0.9	8.16e-01	1.1 ± 0.1	3.17	QSO/AGN	—
013244.17+303559.7	17	14	—,—	—	0	2.3	2.61e-02	8.1 ± 12.7	60.645	—	—
013244.77+303037.4	18	—	—,—	—	0	—	—	—	-0.961	—	—
013245.06+303911.3	19	15	64,57	—	0	1.3	—	2.0 ± 1.2	207.383	—	—
013246.72+303437.7	20	16	68,61	—	0	0.8	3.33e-01	1.5 ± 0.9	6.797	L10-005,USNO-5070	—
013247.65+304414.7	21	17	69,62	—	0	0.1	7.42e-01	1.0 ± 0.4	0.192	—	—
013247.71+304711.1	22	18	—,—	—	0	—	2.00e-10	—	0.672	stellar,2MASS-2725, USNO-5821	—
013248.66+303441.3	23	19	—,—	—	0	1.4	9.89e-01	2.8 ± 2.6	3.843	—	—
013249.08+304253.5	24	20	—,—	—	2	1.7	9.69e-02	1.8 ± 0.7	-0.513	Galaxy	ZKH08
013249.39+303829.6	25	21	70,64	—	0	0.7	5.80e-01	1.2 ± 0.3	1.669	—	—
013249.63+303250.7	26	22	—,—	—	0	—	—	—	0.856	—	—
013249.84+303102.3	27	—	—,—	—	0	—	—	—	-0.357	—	—

Table 9—Continued

Source ID ^a (1)	Src. No. (2)	FLC No. (3)	XMM No. (4)	G05 No. (5)	Extent (6)	Variability			$S_{H\alpha}$ ($10^{-17} \text{ erg s}^{-1} \text{ cm}^{-2} \text{ arcsec}^{-2}$) (10) (11)	Source type (12)	Comments
						η (7)	ξ (8)	$\frac{flux_{max}}{flux_{min}}$ (9)			
013249.87+305018.9	28	23	71,65	—	0	—	—	—	-0.395	—	—
013250.71+303035.3	29	24	72,66	—	0	0.0	1.59e-01	1.0±0.2	0.625	QSO/AGN	—
013250.71+303144.1	30	—	73,67	—	0	1.3	1.49e-01	1.9±1.0	0.079	—	—
013250.86+304252.8	31	25	—,—	—	0	0.6	—	1.4±0.9	0.456	—	—
013251.87+305132.6	32	—	—,—	—	0	—	—	—	-0.238	—	—
013252.50+304023.9	33	26	80,—	—	0	0.3	5.52e-01	1.1±0.3	2.949	—	—
013253.20+303809.1	34	—	—,—	—	0	0.0	—	1.0±0.8	9.93	—	—
013253.56+303814.8	35	27	83,75	3	2	4.3	4.60e-02	1.2±0.0	6.237	QSO/AGN,X-1	—
013253.82+304732.6	36	—	—,—	—	0	0.2	—	1.3±1.6	-0.018	—	—
013253.89+303311.8	37	28	85,76	4	2	7.2	2.42e-03	1.4±0.1	0.898	QSO/AGN,X-2, USNO-4424	—
013253.90+305017.8	38	29	84,—	—	0	—	—	—	1.295	—	—
013255.06+305038.9	39	—	—,—	—	0	—	—	—	0.238	—	—
013255.33+304215.8	40	30	87,77	—	2	1.1	6.44e-01	1.2±0.2	0.06	—	—
013255.45+304842.3	41	31	—,—	—	0	—	—	—	-0.509	—	—
013255.66+304557.8	42	—	—,—	—	0	1.5	—	3.1±2.9	0.309	—	—
013255.74+303712.1	43	—	—,—	—	0	2.4	—	62.9±642.0	—	FS,2MASS-2128	—
013256.03+303559.8	44	32	—,—	5	0	3.6	7.47e-01	9.9±12.3	10.511	Galaxy	—
013256.20+303547.6	45	—	—,—	—	0	1.4	—	—	27.629	—	—
013256.94+302633.9	46	33	91,81	—	0	—	—	—	-2.787	Galaxy,USNO-7382	pos. uncertain
013257.07+303222.8	47	34	—,—	—	0	0.1	—	1.1±0.9	7.701	—	—
013257.07+303927.0	48	35	93,83	—	2	0.0	1.71e-01	—	219.594	L10-011,USNO-2576	—
013257.51+304314.8	49	36	—,—	—	0	1.2	—	2.0±1.3	-0.547	—	—
013258.16+304936.2	50	37	—,—	—	0	1.7	2.25e-01	2.7±1.8	-0.08	—	—
013258.17+303056.2	51	—	95,85	—	0	0.6	—	1.4±0.9	5.575	—	—
013258.54+303547.1	52	—	—,86	—	0	1.1	—	2.8±2.6	15.786	—	—
013258.63+304059.4	53	—	—,—	—	0	0.0	—	1.0±0.6	1.392	—	—
013259.67+305326.4	54	38	96,—	—	0	—	—	—	-0.136	USNO-7506	—
013259.71+304718.8	55	—	—,—	—	0	1.4	—	15.4±94.3	0.04	—	—
013300.07+303957.2	56	39	—,—	—	0	0.5	—	1.4±0.9	2.624	—	—
013300.12+304136.6	57	—	—,—	—	0	1.8	—	—	3.072	—	—
013300.19+304009.5	58	40	—,—	—	0	1.1	5.46e-01	1.9±1.4	7.764	—	—
013300.42+304408.1	59	41	98,88	—	2	0.0	4.15e-01	1.0±0.3	10.7	L10-013	pos. uncertain

Table 9—Continued

Source ID ^a	Src.	FLC	XMM	G05	Extent	Variability			$S_{H\alpha}$	Source type	Comments
	No.	No.	No.	No.	(6)	η	ξ	$\frac{flux_{max}}{flux_{min}}$	(10 ⁻¹⁷ erg s ⁻¹ cm ⁻² arcsec ⁻²)	(11)	(12)
(1)	(2)	(3)	(4)	(5)	(6)	(7)	(8)	(9)	(10)		
013300.43+303133.4	60	—	—,—	—	0	1.2	—	1.9±1.0	4.773	—	—
013300.88+303424.8	61	42	99,—	—	0	2.4	5.05e-01	4.2±3.5	75.497	—	—
013300.88+304520.8	62	43	—,—	—	0	0.5	9.70e-01	1.3±0.8	0.127	—	—
013301.03+304043.1	63	44	100,89	—	2	0.3	3.64e-01	1.0±0.1	2.974	stellar,USNO-2054	—
013301.93+303158.1	64	45	102,91	—	2	2.2	1.43e-01	1.2±0.1	9.713	QSO/AGN	—
013302.33+304643.1	65	46	—,—	—	0	1.4	—	2.8±2.7	0.05	Galaxy	—
013302.41+304328.6	66	—	—,—	—	0	0.6	—	1.9±2.5	2.381	—	—
013303.52+303827.3	67	—	—,—	—	0	0.9	—	2.5±2.6	1.243	—	—
013303.55+303903.8	68	47	104,95	—	2	4.9	3.81e-01	1.9±0.3	1.779	USNO-1636	—
013303.68+304043.9	69	48	105,—	—	0	0.9	—	2.2±2.4	0.115	QSO/AGN	—
013304.03+303953.6	70	49	106,—	—	2	0.5	9.31e-01	1.3±0.6	112.839	L10-018	—
013304.15+304006.7	71	50	—,—	—	0	0.4	—	1.3±1.0	1.697	—	—
013304.36+303112.1	72	—	—,—	—	0	0.6	—	1.7±1.4	21.707	2MASS-2341	—
013304.53+303903.7	73	51	—,—	—	0	1.2	—	4.7±12.0	1.126	stellar	—
013304.78+304124.1	74	52	108,—	—	2	0.6	4.51e-02	1.1±0.2	0.415	—	—
013304.90+302835.6	75	—	—,—	—	0	0.7	—	1.7±1.4	0.658	—	—
013305.14+303001.4	76	53	110,97	—	0	0.1	5.36e-02	1.0±0.2	7.697	XRB	PMH04
013305.62+303840.4	77	54	—,—	—	0	0.0	—	1.0±0.7	2.108	—	—
013305.79+303804.7	78	55	112,99	—	0	0.7	3.00e-01	1.5±0.9	1.101	—	—
013306.22+305109.2	79	—	—,—	—	0	1.4	—	3.3±3.3	0.133	—	—
013306.82+303909.7	80	—	—,—	—	0	1.2	—	—	12.553	—	—
013307.06+303910.4	81	—	—,—	—	0	1.2	—	—	16.052	—	—
013307.39+303912.3	82	56	—,—	—	0	1.3	—	2.4±1.7	15.083	—	—
013307.51+305343.5	83	—	—,—	—	0	0.7	—	1.5±0.9	0.083	—	—
013307.72+305235.5	84	—	—,—	—	0	0.1	—	1.1±1.1	0.183	—	—
013307.77+302827.0	85	—	—,—	—	0	1.3	—	3.4±3.8	5.148	—	—
013307.81+303044.6	86	—	—,—	—	0	0.3	—	1.4±1.4	11.69	—	—
013307.90+303316.1	87	—	—,—	—	0	1.1	—	2.9±3.0	13.773	—	—
013307.96+303219.5	88	57	114,102	—	2	0.4	8.73e-02	1.1±0.3	5.544	—	—
013308.23+305047.5	89	—	—,—	—	0	0.8	—	1.6±0.9	-0.03	—	—
013308.35+304803.4	90	58	116,101	6	0	4.7	1.16e-02	2.1±0.4	1.932	—	—
013308.50+303134.7	91	—	—,—	—	0	0.6	—	1.4±0.8	10.8	—	—
013308.80+304525.4	92	59	—,—	—	2	2.1	—	6.8±7.1	5.91	—	—

Table 9—Continued

Source ID ^a (1)	Src. No. (2)	FLC No. (3)	XMM No. (4)	G05 No. (5)	Extent (6)	Variability			$S_{H\alpha}$ ($10^{-17} \text{ erg s}^{-1} \text{ cm}^{-2} \text{ arcsec}^{-2}$) (10) (11)	Source type (12)	Comments
						η (7)	ξ (8)	$\frac{flux_{max}}{flux_{min}}$ (9)			
013309.10+303422.5	93	60	–,–	–	0	6.1	5.25e-02	7.3±3.1	5.545	–	–
013310.17+304221.9	94	61	118,105	–	2	1.2	7.92e-01	1.7±0.8	11.361	L10-022	–
013310.51+303539.9	95	–	–,–	–	0	1.1	–	3.2±4.1	0.55	–	–
013310.56+304228.5	96	62	–,–	–	0	0.1	–	1.1±0.7	2.215	–	–
013310.72+303734.6	97	63	–,–	–	0	1.2	–	2.5±1.8	2.129	–	–
013310.92+303741.7	98	64	–,–	–	0	1.1	–	3.6±4.4	3.444	Galaxy	affected by adjacent source
013311.08+304929.7	99	65	–,–	–	0	0.9	4.76e-01	1.4±0.5	7.416	–	–
013311.09+303943.7	100	66	120,107	–	1	0.5	8.44e-01	1.1±0.2	28.263	L10-023	–
013311.67+303858.8	101	–	–,–	–	0	1.4	–	4.7±7.4	558.145	–	–
013311.75+303841.5	102	67	121,108	–	1	1.6	3.05e-01	1.1±0.0	120.899	L10-025,X-3	–
013312.31+305504.5	103	–	–,109	–	0	3.0	2.38e-02	5.4±3.5	0.77	–	–
013313.12+305150.4	104	–	–,–	–	0	1.5	–	5.4±9.8	0.415	non-stellar	–
013313.48+305709.6	105	68	123,110	–	0	–	–	–	4.993	Galaxy,2MASS-3338, USNO-8971	pos. uncertain
013313.82+304530.5	106	–	–,–	–	0	0.5	–	1.7±2.3	54.634	–	–
013313.86+303552.2	107	69	–,–	–	0	0.4	–	1.3±0.8	1.638	–	–
013314.17+302459.0	108	70	–,–	–	0	1.4	1.58e-01	1.8±0.8	-0.354	stellar	–
013314.32+304236.7	109	71	–,–	–	0	2.3	9.81e-01	2.9±1.3	1.891	–	–
013314.68+304012.2	110	–	–,–	–	0	1.2	–	40.4±989.0	3.998	USNO-0626	–
013315.05+304059.4	111	72	–,–	–	0	0.7	–	3.8±9.8	1.717	–	–
013315.10+304453.0	112	73	124,112	8	0	2.7	7.10e-02	2.4±0.9	45.333	non-stellar	–
013315.16+305318.2	113	74	125,113	7	1	0.6	1.48e-02	1.0±0.0	142.037	XRB?,USNO-5969, X-4,2MASS-2746	–
013315.18+304138.0	114	–	–,–	–	0	0.4	–	2.3±5.1	85.993	–	–
013315.22+304937.9	115	–	–,–	–	0	1.6	–	2.8±2.1	1.538	–	–
013315.58+302418.2	116	–	–,–	–	0	1.1	4.36e-01	2.1±1.5	-0.285	–	–
013316.21+302934.1	117	–	–,–	–	0	0.5	–	2.8±8.4	2.419	–	–
013316.30+302823.8	118	–	–,–	–	0	0.5	–	1.7±2.2	3.042	non-stellar	–
013316.69+302429.4	119	–	128,–	–	0	0.3	–	1.2±0.8	-0.999	FS,2MASS-2911, USNO-6840	–
013317.29+303530.4	120	–	–,–	–	0	1.3	–	–	5.62	–	–
013317.30+303308.9	121	75	–,–	–	0	3.0	2.21e-01	4.2±2.2	8.303	–	–

Table 9—Continued

Source ID ^a	Src.	FLC	XMM	G05	Extent	Variability			$S_{H\alpha}$	Source type	Comments
	No.	No.	No.	No.	(6)	η	ξ	$\frac{flux_{max}}{flux_{min}}$	($10^{-17} \text{ erg s}^{-1} \text{ cm}^{-2} \text{ arcsec}^{-2}$)	(11)	(12)
(1)	(2)	(3)	(4)	(5)	(6)	(7)	(8)	(9)	(10)		
013317.91+305236.3	122	76	130,116	—	0	0.2	1.06e-02	1.1±0.2	4.19	—	—
013317.94+304900.1	123	77	—,—	—	0	0.8	2.17e-01	1.3±0.4	1.742	—	—
013318.33+304200.6	124	78	—,—	—	0	2.7	9.63e-04	3.2±1.9	1.241	—	—
013318.34+302840.4	125	—	131,—	—	0	0.2	3.25e-11	1.0±0.3	2.109	—	—
013318.45+304716.5	126	79	—,—	—	0	0.5	—	1.3±0.7	9.181	—	—
013318.70+302934.0	127	81	132,—	—	0	—	2.18e-01	—	9.997	non-stellar	trans. source?
013318.71+303736.5	128	80	—,—	—	0	1.8	—	—	2.704	Galaxy	—
013318.79+305241.0	129	—	—,—	—	0	0.5	—	1.5±1.2	2.192	—	—
013318.87+303229.9	130	82	—,—	—	0	0.7	—	1.4±0.8	3.055	stellar	—
013318.91+304546.0	131	—	—,—	—	0	1.0	—	1.9±1.4	1.474	—	—
013319.06+305205.0	132	83	133,—	—	0	1.4	5.88e-01	1.4±0.3	2.7	QSO/AGN	—
013319.61+302847.8	133	84	135,118	—	0	4.2	1.83e-01	1.7±0.2	-0.42	QSO/AGN	—
013319.91+305102.0	134	85	136,—	—	0	2.2	8.76e-02	1.6±0.3	1.423	—	—
013320.33+305241.6	135	—	—,—	—	0	0.3	—	1.2±0.8	0.81	—	—
013320.80+302948.0	136	86	—,—	—	0	3.0	—	—	5.062	—	—
013320.83+304335.6	137	—	—,—	—	0	1.3	—	16.0±110.7	4.684	—	—
013320.95+302648.8	138	87	—,—	—	0	0.4	1.20e-01	1.1±0.3	-0.326	Galaxy	—
013321.34+305218.9	139	88	137,—	—	0	0.2	3.67e-02	1.1±0.4	1.87	—	—
013321.48+302309.8	140	—	—,—	—	0	—	—	—	2.67	—	—
013321.70+303858.4	141	89	138,119	10	0	2.9	1.28e-01	2.2±0.6	4.1	Galaxy,2MASS-0976, USNO-0296	—
013321.94+303923.0	142	90	139,—	11	0	2.1	3.34e-01	2.3±0.9	0.557	—	—
013321.94+305520.6	143	91	141,—	—	0	1.1	3.66e-01	1.2±0.2	0.202	USNO-6915	—
013322.24+302445.6	144	92	—,—	—	0	0.7	1.45e-02	1.2±0.4	1.102	—	—
013322.33+304011.2	145	—	—,—	—	0	1.7	—	5.4±8.3	3.688	—	—
013322.45+304224.1	146	—	—,—	—	0	1.1	—	4.0±7.2	4.891	non-stellar	—
013322.48+302942.6	147	93	—,—	—	0	0.2	—	1.1±0.8	2.359	—	—
013322.92+304010.3	148	—	—,—	—	0	1.0	—	3.9±7.9	1.09	—	—
013323.11+305653.9	149	94	142,—	—	0	—	—	—	—	FS,2MASS-3150, USNO-8016	—
013323.62+305001.2	150	—	—,—	—	0	1.3	5.22e-02	1.8±0.8	3.197	—	—
013323.65+302607.0	151	95	—,—	—	0	1.1	3.07e-01	1.3±0.3	3.985	—	—
013323.65+303426.6	152	—	—,—	—	0	2.1	—	24.6±93.0	-1.055	stellar,USNO-0629	—

Table 9—Continued

Source ID ^a (1)	Src. No. (2)	FLC No. (3)	XMM No. (4)	G05 No. (5)	Extent (6)	Variability			$S_{H\alpha}$ ($10^{-17} \text{ erg s}^{-1} \text{ cm}^{-2} \text{ arcsec}^{-2}$) (10)	Source type (11)	Comments (12)
						η	ξ	$\frac{\text{flux}_{\text{max}}}{\text{flux}_{\text{min}}}$ (9)			
013323.84+302613.5	153	96	144,–	–	0	0.4	1.31e-01	1.2±0.5	80.499	L10-032,USNO-5009	–
013323.93+303517.5	154	97	145,121	12	2	11.3	2.20e-03	7.6±2.2	1.311	Galaxy	–
013323.94+304820.4	155	98	146,122	13	1	1.7	3.36e-01	1.3±0.2	1.582	–	–
013324.07+304347.3	156	99	–,–	–	0	1.5	6.45e-01	–	2.033	–	–
013324.15+303503.4	157	100	–,–	–	0	0.9	–	5.7±15.7	1.002	–	–
013324.40+304402.4	158	101	147,124	14	0	8.8	5.28e-03	1.2±0.0	3.559	XRB?,X-5	–
013324.46+302504.5	159	102	148,123	–	0	4.4	1.25e-01	1.7±0.2	1.337	–	–
013324.49+305346.6	160	–	–,–	–	0	1.3	–	4.4±7.3	1.489	–	–
013324.88+304536.0	161	103	–,–	–	0	2.1	4.70e-01	3.8±3.2	2.507	–	–
013324.90+305508.9	162	104	149,125	–	0	0.3	3.65e-01	1.1±0.2	0.773	USNO-6572	–
013325.38+305814.8	163	105	150,126	–	2	–	–	–	1.534	–	–
013325.39+304246.1	164	–	–,–	–	0	1.3	–	–	8.575	–	–
013325.48+303619.1	165	106	151,127	16	0	2.3	2.24e-01	3.2±1.4	0.726	–	–
013325.54+304440.7	166	107	–,–	17	0	2.1	3.20e-02	2.3±1.0	0.622	–	–
013325.56+303647.7	167	–	–,–	–	0	2.1	–	–	0.235	–	–
013326.05+304119.2	168	–	–,–	19	0	1.7	5.08e-01	–	2.994	–	–
013326.28+305639.8	169	–	–,–	–	0	0.5	–	1.5±1.2	-0.488	–	–
013326.36+305533.1	170	–	–,–	–	0	0.8	5.33e-01	1.6±1.0	0.943	–	–
013326.50+304535.7	171	–	–,–	–	0	1.5	–	23.0±208.5	6.131	FS,2MASS-1348, USNO-0675	–
013326.92+305012.5	172	–	–,–	–	0	1.2	–	2.4±1.9	0.464	–	–
013327.20+303119.8	173	–	–,–	–	0	1.0	–	2.0±1.4	9.008	–	–
013327.20+304911.4	174	–	–,–	–	0	0.9	–	2.8±3.4	1.24	–	–
013327.76+304647.3	175	108	152,128	21	0	1.5	8.00e-04	1.5±0.4	0.673	FS,2MASS-1495, USNO-0930	–
013328.08+303135.0	176	109	153,129	22	2	0.2	5.89e-02	1.0±0.3	51.757	L10-034	–
013328.18+302518.0	177	–	–,–	–	0	0.6	8.36e-01	1.4±0.7	-0.475	–	–
013328.43+304221.3	178	–	–,–	–	0	3.4	6.28e-01	220.7±7217.3	7.892	–	trans. source?
013328.63+305930.9	179	110	–,–	–	0	–	–	–	–	–	–
013328.69+302723.6	180	111	155,131	–	1	3.9	3.46e-02	1.0±0.0	0.011	XRB?,X-6	–
013328.72+304322.5	181	112	154,–	23	0	3.2	1.12e-01	2.3±0.6	4.062	–	–
013328.76+303309.3	182	–	–,–	–	0	0.8	–	2.1±2.0	7.361	–	–
013328.96+304743.5	183	113	156,132	24	2	0.5	2.91e-01	1.1±0.2	36.631	L10-035,2MASS-1622,	–

Table 9—Continued

Source ID ^a (1)	Src. No. (2)	FLC No. (3)	XMM No. (4)	G05 No. (5)	Extent (6)	Variability			$S_{H\alpha}$ ($10^{-17} \text{ erg s}^{-1} \text{ cm}^{-2} \text{ arcsec}^{-2}$) (10) (11)	Source type (12)	Comments
						η (7)	ξ (8)	$\frac{\text{flux}_{\text{max}}}{\text{flux}_{\text{min}}}$ (9)			
USNO-1182											
013329.04+304216.9	184	114	158,133	25	1	4.0	1.62e-01	1.6±0.2	570.348	L10-036,USNO-0162	affected by adjacent source
013329.16+305134.9	185	—	—,—	—	0	0.1	—	1.1±1.1	0.535	—	—
013329.29+304508.4	186	116	159,136	26	2	5.4	1.71e-01	1.9±0.2	2.798	—	—
013329.29+304537.4	187	115	160,137	27	0	3.7	2.28e-02	2.2±0.5	2.517	—	—
013329.45+304910.7	188	117	161,138	28	1	0.9	2.74e-01	1.1±0.1	13.226	L10-037	—
013329.61+304521.8	189	—	—,—	—	0	1.7	—	3.8±3.4	2.625	—	—
013329.83+305118.0	190	118	162,139	—	0	7.3	1.69e-01	4.5±1.0	1.049	QSO/AGN	—
013330.10+303456.7	191	—	—,—	—	0	1.3	—	—	5.769	—	—
013330.19+304255.6	192	119	—,—	—	0	2.0	—	6.9±10.9	5.377	stellar	—
013330.40+304641.9	193	120	—,—	—	0	2.3	8.10e-02	2.2±0.7	3.456	—	—
013330.43+305503.6	194	—	—,—	—	0	0.3	—	1.2±0.8	0.208	—	—
013330.64+303404.1	195	121	163,141	29	1	9.2	2.59e-02	2.8±0.3	7.265	—	—
013330.82+303455.2	196	122	—,—	—	0	1.0	—	7.0±33.5	8.96	stellar	—
013331.25+303333.4	197	123	164,142	31	1	4.2	8.95e-02	1.5±0.1	929.424	L10-039,X-14	—
013331.26+304445.7	198	—	—,—	—	0	1.4	—	18.2±138.1	0.235	—	—
013331.30+304928.2	199	125	—,—	—	0	1.7	5.89e-01	2.0±0.8	1.13	—	—
013331.32+303402.2	200	124	—,—	—	0	0.9	—	2.1±1.9	11.417	—	—
013331.37+303816.9	201	—	—,—	—	0	1.1	—	4.2±7.5	13.709	—	—
013331.39+303737.4	202	126	—,—	32	0	2.3	—	10.9±18.2	3.427	stellar	—
013331.64+303042.9	203	—	—,—	—	0	1.1	—	5.1±13.2	2.57	non-stellar	—
013331.72+303556.1	204	—	—,—	—	0	1.5	—	—	-2.625	—	—
013331.86+304011.7	205	127	—,—	—	0	1.9	—	12.0±44.4	-2.379	—	—
013331.99+305741.0	206	128	165,144	—	0	—	—	—	-0.262	QSO/AGN	—
013332.19+303656.8	207	129	—,—	33	0	2.1	5.39e-02	3.2±1.7	-0.07	stellar	—
013332.20+304446.7	208	—	—,—	—	0	1.6	—	8.1±17.0	-0.992	2MASS-1023	—
013332.22+302448.8	209	—	—,—	—	0	0.0	—	1.0±0.9	0.467	—	—
013332.23+303955.5	210	130	166,145	—	0	5.6	3.54e-02	20.0±33.2	-2.202	XRT-2	trans. source
013332.41+304824.5	211	—	—,—	—	0	0.1	—	1.1±1.0	3.735	—	—
013332.57+303617.4	212	—	—,—	—	0	1.8	—	90.4±2922.0	-0.744	—	—
013332.71+303339.3	213	—	—,—	—	0	1.3	—	7.4±21.6	26.969	—	—
013332.81+304633.3	214	131	—,—	—	0	2.1	3.08e-01	4.4±5.6	1.395	—	—

Table 9—Continued

Source ID ^a	Src.	FLC	XMM	G05	Extent	Variability			$S_{H\alpha}$	Source type	Comments
	No.	No.	No.	No.	(6)	η	ξ	$\frac{flux_{max}}{flux_{min}}$	(10 ⁻¹⁷ erg s ⁻¹ cm ⁻² arcsec ⁻²)	(11)	(12)
(1)	(2)	(3)	(4)	(5)	(6)	(7)	(8)	(9)	(10)	(11)	(12)
013332.89+304916.3	215	132	167,146	34	0	1.5	—	2.0±0.9	1.128	—	—
013333.00+304618.5	216	133	—,—	—	0	1.6	—	—	0.978	—	—
013333.07+305009.8	217	—	—,—	—	0	0.9	—	4.1±11.0	2.161	—	—
013333.13+305155.5	218	—	—,—	—	0	1.0	—	3.5±5.8	0.558	—	—
013333.28+304932.5	219	—	—,—	—	0	0.9	—	3.7±9.3	6.739	—	—
013333.43+302739.8	220	—	—,—	—	0	1.9	—	—	-0.634	—	—
013333.71+303109.6	221	134	168,147	35	2	9.6	3.08e-03	3.4±0.6	10.5	non-stellar	—
013333.93+302943.9	222	135	—,—	—	0	0.5	7.50e-01	6.0±63.0	2.965	—	—
013334.04+304710.1	223	—	—,—	—	0	0.3	—	1.3±1.1	131.657	USNO-0817	—
013334.12+303714.9	224	136	172,153	38	0	4.5	4.59e-03	2.5±0.6	3.903	stellar	—
013334.13+303211.3	225	137	171,150	37	1	44.2	<1.0e-15	2.2±0.0	835.426	XRB,X-7,UIT128	PMH04,MPH06
013334.24+302616.6	226	—	—,—	—	0	—	—	—	-1.992	USNO-4412	—
013334.51+304555.0	227	—	—,—	—	0	1.5	—	73.2±2480.4	1.08	—	—
013334.54+303556.1	228	138	174,—	39	0	1.3	3.36e-01	2.0±0.9	4.68	XRB	PMH04
013334.93+302711.4	229	139	—,—	—	0	0.5	1.62e-01	2.0±4.5	0.263	—	—
013335.02+304404.7	230	—	—,—	—	0	1.6	—	—	-0.915	—	—
013335.02+304931.8	231	140	176,—	—	0	0.8	—	—	6.476	2MASS-1806, USNO-1821	—
013335.45+305231.4	232	—	—,—	—	0	0.3	—	1.2±0.8	0.776	—	—
013335.50+303729.3	233	141	—,—	41	0	2.7	3.19e-01	2.3±0.9	1.316	—	—
013335.65+302632.2	234	142	177,—	—	0	0.5	1.01e-07	1.7±1.5	0.253	—	—
013335.83+304655.4	235	143	—,—	42	0	0.9	—	1.9±1.2	1.757	—	—
013335.90+303627.4	236	144	179,154	43	2	3.4	5.53e-02	1.7±0.2	884.723	L10-045	—
013336.04+303332.9	237	145	178,—	44	0	7.7	1.26e-02	3.8±0.7	8.666	—	—
013336.40+303742.7	238	146	180,155	45	0	8.4	3.16e-03	12.5±5.1	2.673	non-stellar	—
013336.51+304722.8	239	—	—,—	—	0	1.0	—	—	1.761	—	—
013336.70+303729.6	240	147	—,—	46	0	3.6	6.55e-02	9.5±12.3	0.783	—	—
013336.84+304757.3	241	148	—,—	—	0	1.3	5.56e-01	2.7±2.5	3.033	—	—
013336.91+302321.5	242	150	182,156	—	0	—	—	—	—	FS,2MASS-2864, USNO-6579	—
013336.91+304641.4	243	—	—,—	—	0	1.1	—	6.6±20.5	1.126	—	—
013336.99+302618.2	244	—	—,—	—	0	0.9	—	2.1±1.7	-0.485	—	—
013337.08+303253.5	245	149	181,—	—	2	0.8	3.49e-02	3.8±4.5	30.793	L10-046	—

167

Table 9—Continued

Source ID ^a (1)	Src. No. (2)	FLC No. (3)	XMM No. (4)	G05 No. (5)	Extent (6)	Variability			$S_{H\alpha}$ ($10^{-17} \text{ erg s}^{-1} \text{ cm}^{-2} \text{ arcsec}^{-2}$) (10) (11)	Source type (12)	Comments
						η	ξ	$\frac{flux_{max}}{flux_{min}}$ (9)			
013337.12+302558.5	246	—	—,—	—	0	2.1	7.75e-01	29.9±178.3	0.415	—	—
013337.39+305232.9	247	151	—,—	—	0	0.8	—	1.5±0.7	-0.394	non-stellar, USNO-3934	—
013337.52+304718.7	248	152	183,158	47	1	11.0	5.24e-02	3.4±0.4	2.346	QSO/AGN	—
013337.75+304009.1	249	153	—,—	48	0	0.6	1.91e-01	1.6±1.2	13.73	L10-047	—
013337.90+303837.2	250	154	—,—	49	0	3.9	2.97e-02	7.3±5.8	5.189	stellar	—
013337.96+304023.8	251	155	—,—	50	0	1.7	3.24e-01	2.7±1.6	14.046	—	—
013337.99+304035.6	252	156	—,—	51	0	2.6	1.95e-02	4.7±3.2	10.501	—	—
013337.99+304926.0	253	157	—,—	—	0	1.6	7.19e-01	3.5±2.8	2.057	—	—
013338.15+305407.6	254	—	—,—	—	0	1.4	—	3.4±3.7	0.356	—	—
013338.50+302851.2	255	159	186,—	—	0	3.9	2.15e-01	1.7±0.3	10.433	USNO-2193	—
013338.53+302750.1	256	158	185,159	—	0	3.7	4.44e-01	5.3±3.4	-0.039	—	—
013338.56+302829.7	257	—	—,—	—	0	1.9	—	—	5.802	—	—
013338.62+304343.7	258	160	—,—	—	0	0.9	—	2.5±3.2	0.099	—	—
013338.97+302734.8	259	162	—,—	—	0	1.4	2.07e-01	2.0±1.0	0.434	—	—
013339.01+302115.0	260	161	—,—	—	0	—	—	—	—	XRT-3,2MASS-3215, USNO-8296	trans. source
013339.18+303216.5	261	—	—,—	—	0	0.6	—	—	25.298	2MASS-1305	—
013339.22+304049.9	262	163	187,160	52	0	3.6	5.49e-02	2.4±0.5	12.594	—	—
013339.40+305347.6	263	164	188,161	—	0	5.1	2.73e-01	1.8±0.2	-0.916	—	—
013339.46+302140.8	264	165	189,162	—	0	—	—	—	12.37	—	—
013339.62+302745.7	265	166	—,—	—	0	2.1	7.12e-01	8.8±15.2	-0.699	—	—
013339.79+304350.3	266	167	—,—	53	0	3.0	6.81e-01	5.7±4.4	-0.437	—	—
013339.97+304015.4	267	—	—,—	—	0	2.7	—	—	13.108	non-stellar, 2MASS-0267	—
013340.09+304323.1	268	168	190,163	54	0	2.6	1.52e-01	1.8±0.4	1.401	—	—
013340.15+305352.5	269	169	—,—	—	0	1.1	4.92e-01	1.6±0.7	0.105	—	—
013340.66+303940.8	270	—	—,—	—	0	2.3	6.46e-02	5.5±5.7	27.614	L10-049	—
013340.75+304408.8	271	—	—,—	—	0	0.9	—	3.5±5.4	4.066	—	—
013340.81+303524.2	272	170	—,—	55	0	0.7	2.01e-01	2.2±1.9	12.868	—	—
013341.02+305322.2	273	—	—,—	—	0	1.0	—	2.1±1.7	0.203	—	—
013341.26+303213.4	274	171	—,—	—	0	5.1	5.20e-02	27.9±124.3	73.182	XRB,XRT-4	trans. source
013341.35+305607.9	275	172	192,167	—	0	2.2	5.85e-01	1.5±0.3	0.34	QSO/AGN	—

Table 9—Continued

Source ID ^a	Src.	FLC	XMM	G05	Extent	Variability			$S_{H\alpha}$	Source type	Comments
	No.	No.	No.	No.	(6)	η	ξ	$\frac{flux_{max}}{flux_{min}}$	(10 ⁻¹⁷ erg s ⁻¹ cm ⁻² arcsec ⁻²)	(11)	(12)
(1)	(2)	(3)	(4)	(5)	(6)	(7)	(8)	(9)	(10)	(11)	(12)
013341.47+303815.9	276	—	—,—	57	0	2.0	—	—	44.351	—	—
013341.56+304136.4	277	173	193,—	59	2	3.6	1.18e-01	2.3±0.7	41.132	—	—
013341.62+303220.1	278	174	194,168	58	0	2.2	3.08e-01	11.2±46.2	24.914	FS,2MASS-1241	—
013341.90+303848.8	279	175	196,170	60	2	8.6	6.57e-33	2.7±0.4	102.667	FS,2MASS-0220	—
013342.05+304852.6	280	176	—,—	—	0	1.6	4.08e-01	2.2±1.1	2.332	—	—
013342.54+304253.3	281	177	197,171	61	0	10.3	1.51e-01	5.8±1.6	1.514	XRB	PMH04,MPH06
013342.55+305750.1	282	178	198,172	—	0	—	—	—	-0.78	—	—
013342.77+304642.5	283	179	—,—	62	0	2.2	4.69e-03	1.7±0.4	1.412	—	—
013342.85+302826.6	284	—	—,—	—	0	1.0	—	—	1.4	non-stellar	—
013342.97+305341.7	285	180	199,—	—	0	0.5	1.15e-01	1.1±0.3	1.403	—	—
013343.30+304724.5	286	—	—,—	—	0	0.6	—	2.1±2.8	11.258	—	—
013343.39+304630.6	287	181	200,173	63	2	2.8	3.09e-02	1.9±0.6	—	FS,2MASS-1133, USNO-0448	—
013343.48+304103.7	288	—	—,—	64	2	1.7	8.37e-01	—	40.272	L10-056	—
013343.76+305313.2	289	—	—,—	—	0	0.3	—	1.4±1.2	10.862	—	—
013343.98+304955.5	290	—	—,—	—	0	1.7	—	—	0.934	—	—
013344.17+302205.4	291	182	201,—	—	0	—	—	—	13.232	—	—, position uncertain
013344.41+305437.1	292	—	—,—	—	0	0.8	—	1.9±1.6	-0.088	—	—
013345.21+302933.9	293	183	—,—	—	0	2.5	9.72e-01	3.7±2.4	2.678	—	—
013345.24+304135.0	294	184	—,—	—	0	4.3	9.34e-01	—	19.286	stellar	trans. source?
013345.38+302833.8	295	185	203,—	—	0	2.4	5.33e-01	2.7±1.2	0.057	—	—
013346.29+303251.6	296	—	—,—	—	0	0.5	—	—	24.319	—	—
013346.48+305223.0	297	186	—,—	—	0	1.8	9.26e-01	2.3±1.2	1.363	—	—
013346.54+305430.8	298	187	204,174	—	0	0.6	6.84e-01	1.2±0.3	—	FS,2MASS-2616, USNO-5296	—
013346.56+303748.7	299	188	205,175	68	1	11.8	2.33e-01	3.1±0.4	13.177	QSO/AGN?	variable
013346.78+304318.0	300	—	—,—	69	0	1.0	—	3.3±3.8	11.948	—	—
013346.81+305452.8	301	189	206,176	—	0	4.6	1.18e-02	2.1±0.4	-99.371	FS	—
013347.20+303045.1	302	190	—,—	—	0	0.6	—	—	3.317	stellar	—
013347.50+305403.8	303	—	—,—	—	0	0.5	—	1.6±1.7	38.425	USNO-4889	—
013347.56+304042.9	304	—	—,—	70	0	0.3	—	1.2±0.8	5.352	—	—
013347.83+303249.2	305	192	—,—	—	0	2.2	2.57e-01	2.9±1.5	63.677	—	—

Table 9—Continued

Source ID ^a	Src.	FLC	XMM	G05	Extent	Variability			$S_{H\alpha}$	Source type	Comments
	No.	No.	No.	No.	(6)	η	ξ	$\frac{flux_{max}}{flux_{min}}$	($10^{-17} \text{ erg s}^{-1} \text{ cm}^{-2} \text{ arcsec}^{-2}$)		
(1)	(2)	(3)	(4)	(5)					(10)		
013347.91+305516.2	306	—	—,—	—	0	0.2	6.48e-02	1.1±0.6	4.101	—	—
013348.46+302406.0	307	194	—,—	—	0	0.8	1.74e-01	3.3±9.1	-1.116	—	—
013348.50+303307.8	308	193	207,178	71	2	2.4	1.51e-01	1.7±0.4	82.277	L10-061	—
013348.91+302946.7	309	195	208,179	—	0	1.3	1.65e-02	1.5±0.4	2.202	—	—
013349.00+304758.7	310	196	—,—	—	0	1.7	—	2.7±1.6	1.926	—	—
013349.27+303249.8	311	—	—,—	—	0	1.0	—	—	12.443	—	—
013349.78+305631.7	312	197	209,181	—	0	—	—	—	41.813	non-stellar, USNO-6917	—
013350.05+305023.3	313	—	—,—	—	0	1.1	—	—	0.969	—	—
013350.49+302705.8	314	—	—,—	—	0	0.4	—	—	0.455	—	—
013350.50+303821.4	315	198	—,—	73	2	5.5	4.50e-01	2.5±0.5	11.965	stellar	—
013350.50+304858.7	316	—	—,—	—	0	1.7	—	—	2.248	—	—
013350.74+303245.4	317	199	—,—	—	0	1.0	—	—	6.813	—	—
013350.89+303936.6	318	200	211,182	74	1	—	—	—	—	XRB,X-8,nucleus, 2MASS-0000	PMH04, pile-up in 1730,F1e1/2
013351.13+303823.7	319	—	—,—	—	0	0.3	—	1.5±1.9	17.647	—	—
013352.12+302706.5	320	201	212,184	—	2	7.0	5.31e-02	2.2±0.3	0.554	USNO-3336	—
013352.13+303844.5	321	—	—,—	—	0	0.4	—	1.4±1.1	45.908	—	—
013352.27+303029.9	322	202	—,—	—	0	1.2	1.16e-01	—	1.397	—	—
013352.35+302651.6	323	203	—,—	—	0	1.6	4.31e-01	4.2±2.3	0.382	—	—
013352.63+302825.2	324	—	—,—	—	0	0.8	—	3.5±9.7	—	stellar	trans. source?
013353.32+304015.8	325	—	—,—	76	0	0.8	—	—	—	FS,2MASS-0066	—
013353.53+305719.9	326	—	—,—	—	0	—	—	—	14.235	USNO-7524	pos. uncertain
013353.69+303605.6	327	204	—,—	78	0	1.6	4.73e-02	2.9±2.3	8.762	stellar	—
013354.28+303347.8	328	—	213,—	—	0	1.2	9.14e-02	2.6±2.7	47.16	L10-069	—
013354.47+303414.5	329	205	—,—	—	0	0.7	—	—	15.788	stellar	—
013354.52+303523.7	330	—	—,—	80	0	2.3	—	—	56.482	—	—
013354.64+302549.0	331	206	—,—	—	0	0.2	—	1.4±2.2	0.986	—	—
013354.69+304518.4	332	208	214,187	81	2	1.8	1.53e-01	4.6±5.3	173.539	L10-070	—
013354.76+304722.8	333	207	—,—	—	0	2.9	1.81e-01	6.3±8.2	3.2	—	—
013354.91+303310.9	334	209	215,186	82	1	3.1	2.10e-01	1.3±0.1	577.4	L10-071,X-13	—
013355.14+303108.3	335	210	—,—	—	0	1.0	3.97e-02	2.6±1.8	2.379	stellar	—
013355.21+303010.1	336	211	—,—	—	0	1.8	5.67e-02	5.9±14.3	0.391	—	—

Table 9—Continued

Source ID ^a	Src.	FLC	XMM	G05	Extent	Variability			$S_{H\alpha}$	Source type	Comments
	No.	No.	No.	No.	(6)	η	ξ	$\frac{flux_{max}}{flux_{min}}$	(10 ⁻¹⁷ erg s ⁻¹ cm ⁻² arcsec ⁻²)	(11)	(12)
(1)	(2)	(3)	(4)	(5)					(10)		
013355.24+303528.6	337	—	—,—	83	0	0.4	—	3.6 ± 7.1	44.381	—	—
013355.30+303134.6	338	—	—,—	—	0	2.2	—	22.1 ± 75.2	4.181	—	—
013355.39+302343.7	339	212	216,188	—	0	1.5	$3.27e-01$	2.2 ± 0.9	-1.372	QSO/AGN,USNO-6082	—
013355.75+303924.9	340	213	—,—	85	0	1.8	—	—	8.123	—	—
013356.02+304404.7	341	—	—,—	—	0	1.8	—	8.6 ± 19.2	2.569	—	—
013356.06+303024.7	342	214	217,—	—	0	2.3	$1.00e-02$	1.8 ± 0.4	0.954	—	—
013356.23+304935.6	343	—	—,—	—	0	1.6	—	26.5 ± 216.5	1.575	—	—
013356.28+304535.7	344	—	—,—	—	0	1.8	—	5.9 ± 8.7	151.109	—	—
013356.32+302928.2	345	—	—,—	—	0	0.2	—	2.2 ± 5.7	0.57	Galaxy,2MASS-1759, USNO-1625	—
013356.53+302305.2	346	215	221,190	—	0	0.2	$1.49e-01$	1.2 ± 0.8	0.023	—	—
013356.77+303729.7	347	216	218,191	88	2	5.7	$6.45e-03$	5.9 ± 1.5	18.532	QSO/AGN?	—
013356.82+303706.7	348	217	219,192	87	1	2.4	$7.82e-02$	2.5 ± 0.7	10.268	XRB	HP01
013356.96+303458.6	349	—	220,—	90	0	0.7	$4.67e-01$	—	56.834	L10-074	—
013357.13+302849.3	350	218	—,—	—	0	0.7	—	—	15.741	—	—
013357.15+302634.1	351	219	—,—	—	0	0.7	—	3.8 ± 4.5	1.449	—	—
013357.19+305135.3	352	220	222,193	91	0	4.2	$5.56e-02$	3.8 ± 1.4	3.078	—	—
013357.79+302956.6	353	221	—,—	—	0	0.7	$8.15e-01$	2.7 ± 6.5	2.269	—	—
013357.97+305610.2	354	—	—,—	—	0	—	—	—	0.448	—	—
013358.01+304039.1	355	—	—,—	—	0	1.7	$8.60e-01$	—	8.86	—	—
013358.03+303201.2	356	222	224,—	93	0	3.5	$2.95e-01$	2.5 ± 0.7	17.755	non-stellar	—
013358.07+303754.5	357	—	—,—	92	0	1.2	$2.67e-01$	—	105.959	L10-078	—
013358.23+303438.2	358	223	—,—	94	2	1.1	—	3.7 ± 4.8	17.667	stellar	—
013358.38+303219.8	359	224	—,—	—	0	0.5	—	—	48.617	—	—
013358.42+303624.2	360	—	—,—	97	0	1.0	—	35.7 ± 308.9	44.785	L10-080	—
013358.43+304827.7	361	225	—,—	95	0	2.6	$7.43e-01$	3.5 ± 1.7	13.169	—	—
013358.50+303332.2	362	226	225,194	96	2	1.3	$3.10e-02$	2.4 ± 2.5	32.13	L10-081	—
013358.65+304228.5	363	—	—,—	—	0	1.0	—	3.2 ± 4.8	35.076	—	—
013358.72+304538.0	364	—	—,—	—	0	1.8	—	—	6.593	—	—
013358.83+305004.2	365	227	226,195	98	2	8.4	7.46e-15	3.0 ± 0.4	0.64	2MASS-1842	—
013359.02+303425.2	366	228	227,196	99	2	1.9	$2.72e-01$	2.4 ± 1.3	41.194	L10-083	—
013359.05+303143.6	367	229	—,—	—	0	0.6	$2.06e-01$	2.7 ± 2.9	15.164	—	—
013359.47+303101.0	368	230	—,—	100	0	1.1	$1.32e-02$	3.3 ± 2.4	12.072	FS,2MASS-1503,	—

Table 9—Continued

Source ID ^a (1)	Src. No. (2)	FLC No. (3)	XMM No. (4)	G05 No. (5)	Extent (6)	Variability			$S_{H\alpha}$ ($10^{-17} \text{ erg s}^{-1} \text{ cm}^{-2} \text{ arcsec}^{-2}$) (10)	Source type (11)	Comments (12)
	No. (7)	ξ (8)	$\frac{\text{flux}_{\text{max}}}{\text{flux}_{\text{min}}}$ (9)								
USNO-0941											
013400.19+305216.2	369	231	-,-	102	0	1.7	-	6.5 ± 9.9	8.41	-	-
013400.28+303057.2	370	233	228,-	101	0	1.6	2.12×10^{-1}	2.0 ± 1.0	6.969	-	-
013400.30+304219.3	371	234	230,197	103	2	1.1	4.72×10^{-2}	1.5 ± 0.6	29.23	L10-084	-
013400.31+304724.0	372	232	-,-	-	0	1.0	1.68×10^{-2}	1.8 ± 1.0	24.138	L10-085	-
013400.37+302400.6	373	235	-,-	-	0	0.1	9.22×10^{-2}	1.2 ± 1.5	-0.152	-	-
013400.60+304904.1	374	236	231,-	-	0	1.1	4.74×10^{-1}	2.1 ± 1.5	11.669	L10-086	-
013400.61+305202.3	375	237	-,-	104	0	1.3	-	3.0 ± 3.0	4.909	-	-
013400.65+305019.5	376	-	-,-	-	0	1.0	-	4.9 ± 15.1	1.468	-	-
013400.75+303944.9	377	-	-,-	-	0	1.1	-	5.3 ± 9.3	11.75	-	-
013400.91+303812.9	378	-	-,-	-	0	1.5	-	-	55.882	-	-
013400.97+304107.5	379	238	-,-	106	0	1.1	-	2.9 ± 3.4	4.884	-	-
013401.03+303445.0	380	-	-,-	-	0	2.7	2.52×10^{-1}	-	21.468	-	-
013401.12+303136.9	381	239	233,198	108	2	1.1	5.97×10^{-4}	1.5 ± 0.5	9.698	non-stellar	-
013401.12+303710.7	382	-	-,-	-	0	1.7	-	-	25.81	-	-
013401.12+305153.7	383	-	-,-	-	0	2.4	-	-	1.841	-	trans. source?
013401.16+303242.3	384	240	232,-	-	0	4.2	8.92×10^{-4}	4.6 ± 2.7	22.486	stellar	-
013401.34+303520.2	385	-	-,-	107	0	1.4	4.49×10^{-1}	4.6 ± 9.8	16.286	L10-087	-
013401.63+304829.7	386	241	-,-	-	2	6.4	3.25×10^{-2}	16.0 ± 16.2	2.015	XRT-5	trans. source
013401.66+303517.0	387	242	-,-	109	0	1.6	8.81×10^{-2}	2.6 ± 2.1	18.343	-	-
013401.69+303221.5	388	243	-,-	-	0	1.1	1.22×10^{-1}	5.3 ± 7.1	5.58	-	-
013402.03+303004.8	389	244	234,199	110	1	6.1	1.89×10^{-2}	1.9 ± 0.2	2.118	non-stellar,2MASS-1677, USNO-1379	-
013402.10+304702.7	390	245	-,-	-	0	1.4	1.69×10^{-1}	2.8 ± 2.8	5.65	stellar	-
013402.37+303136.2	391	246	-,-	-	2	1.3	4.13×10^{-1}	2.0 ± 0.8	4.3	-	-
013402.41+302940.4	392	247	-,-	-	0	1.0	7.56×10^{-2}	3.5 ± 2.7	0.271	-	-
013402.44+304040.5	393	248	-,-	111	0	1.5	4.16×10^{-1}	3.0 ± 2.7	13.34	stellar,2MASS-0298	GC (ZKH08)
013402.71+303052.7	394	250	-,-	-	0	0.3	5.78×10^{-1}	1.8 ± 4.4	13.872	-	-
013402.82+305412.4	395	252	-,-	113	0	3.4	6.40×10^{-1}	2.6 ± 0.8	2.093	-	-
013402.83+304940.5	396	251	235,-	112	2	5.9	9.49×10^{-4}	3.3 ± 0.8	1.869	-	-
013402.85+303439.0	397	253	-,-	114	0	2.3	8.39×10^{-1}	3.6 ± 2.3	17.918	-	-
013402.86+304151.2	398	254	236,-	115	0	4.2	6.72×10^{-3}	2.7 ± 0.7	5.22	stellar	-
013402.92+302042.6	399	249	-,-	-	0	-	-	-	-	-	pos. uncertain

Table 9—Continued

Source ID ^a	Src.	FLC	XMM	G05	Extent	Variability			$S_{H\alpha}$ ($10^{-17} \text{ erg s}^{-1} \text{ cm}^{-2} \text{ arcsec}^{-2}$)	Source type	Comments
	No.	No.	No.	No.	(6)	η	ξ	$\frac{\text{flux}_{\text{max}}}{\text{flux}_{\text{min}}}$ (9)			
(1)	(2)	(3)	(4)	(5)	(6)	(7)	(8)				
013403.06+302821.5	400	255	-,-	-	0	0.9	-	11.1 ± 14.5	0.931	stellar	-
013403.28+305815.8	401	256	-,-	-	0	-	-	-	0.124	-	pos. uncertain
013403.34+304618.2	402	-	-,-	-	0	0.7	-	6.0 ± 23.4	6.278	-	-
013403.49+305641.3	403	257	237,200	-	0	-	-	-	1.004	USNO-7210	-
013404.26+303257.0	404	-	-,-	-	0	1.3	1.15×10^{-2}	-	7.985	L10-091	-
013404.43+304153.4	405	-	-,-	119	0	1.0	-	2.8 ± 3.3	10.545	-	-
013404.48+304520.8	406	-	-,-	-	0	1.2	-	-	3.537	-	-
013404.71+302227.9	407	-	-,-	-	0	0.2	8.11×10^{-1}	1.3 ± 1.2	0.064	-	-
013405.05+305557.2	408	258	238,202	-	0	-	-	-	0.832	-	-
013405.68+302239.2	409	259	240,203	-	0	0.7	4.97×10^{-1}	1.7 ± 1.0	13.786	FS,2MASS-2978, USNO-7167	-
013406.58+305105.9	410	-	-,-	-	0	1.4	8.70×10^{-1}	3.3 ± 3.8	1.248	-	-
013407.42+303121.0	411	260	-,-	-	0	1.6	-	2.3 ± 1.1	1.73	-	-
013407.50+303249.4	412	262	-,-	-	0	0.7	-	-	2.623	-	-
013407.50+303708.0	413	261	-,-	121	0	1.4	2.68×10^{-1}	4.4 ± 5.8	15.271	L10-093	-
013407.63+303902.4	414	263	-,-	122	0	1.1	2.20×10^{-1}	1.6 ± 0.8	25.113	stellar	-
013407.81+303553.9	415	264	243,204	123	0	2.5	5.80×10^{-2}	1.8 ± 0.4	6.612	-	-
013408.32+303851.7	416	265	-,-	124	0	0.9	8.13×10^{-1}	1.6 ± 1.0	7.256	-	-
013408.36+304633.2	417	266	244,205	125	2	1.8	2.54×10^{-2}	1.8 ± 0.6	34.069	L10-094	-
013409.22+304848.3	418	-	-,-	-	0	1.0	-	4.2 ± 9.3	3.851	-	-
013409.65+303259.8	419	267	246	127	0	1.8	8.72×10^{-3}	2.9 ± 3.0	4.634	-	-
013409.70+303612.3	420	268	-,-	-	0	0.7	6.52×10^{-1}	-	7.034	-	-
013409.91+305045.3	421	269	-,208	128	1	6.5	1.41×10^{-1}	2.4 ± 0.3	-0.169	-	-
013410.03+302856.2	422	-	-,-	-	0	0.2	-	2.5 ± 6.5	0.355	-	-
013410.42+305346.2	423	270	248,209	131	0	2.3	2.21×10^{-1}	1.7 ± 0.4	8.245	stellar	-
013410.51+303946.4	424	271	249,210	132	0	8.4	6.89×10^{-4}	2.8 ± 0.3	4.996	stellar	-
013410.54+303218.8	425	-	247,207	129	0	0.3	-	-	2.547	-	-
013410.69+304224.0	426	272	250,211	133	2	3.0	1.31×10^{-1}	1.6 ± 0.2	362.455	L10-096	-
013410.69+305123.1	427	-	-,-	-	0	1.3	-	43.0 ± 1031.9	1.45	-	-
013410.78+305010.2	428	273	-,-	134	0	0.9	-	1.7 ± 1.0	0.889	stellar	-
013410.84+302455.8	429	274	-,-	-	0	2.8	6.91×10^{-1}	4.7 ± 1.6	-	FS,USNO-5620	-
013411.33+303432.2	430	275	-,-	-	0	0.8	-	7.3 ± 12.8	68.437	-	-
013411.80+304437.2	431	-	-,-	-	0	1.6	-	5.8 ± 10.5	7.612	-	-

Table 9—Continued

Source ID ^a	Src. No.	FLC No.	XMM No.	G05 No.	Extent (6)	Variability	η	ξ	$\frac{flux_{max}}{flux_{min}}$ (9)	$S_{H\alpha}$ ($10^{-17} \text{ erg s}^{-1} \text{ cm}^{-2} \text{ arcsec}^{-2}$) (10)	Source type (11)	Comments (12)
(1)	(2)	(3)	(4)	(5)	(6)	(7)	(8)					
013412.46+304447.4	432	277	–,–	–	0	1.5	–	5.4±8.2	7.687	–	–	–
013412.54+302222.0	433	276	–,–	–	0	–	–	–	0.421	Galaxy	–	–
013412.93+303555.1	434	278	251,213	137	0	1.3	–	–	11.211	–	–	–
013413.41+303546.2	435	–	–,–	–	0	1.0	–	–	7.268	–	–	–
013413.81+304423.3	436	–	–,–	–	0	2.0	–	10.8±24.4	7.823	–	–	–
013413.98+303706.6	437	–	–,214	–	0	0.5	–	–	32.566	–	–	–
013414.40+305351.9	438	–	252,–	138	0	1.9	4.84e-01	2.4±1.2	24.1	L10-105	–	–
013414.42+303303.8	439	279	–,–	–	0	1.2	8.21e-01	4.1±3.1	8.918	stellar	–	–
013414.83+303412.3	440	281	254,216	140	0	1.3	2.20e-01	1.6±0.6	28.571	PWN?	–	–
013414.92+305731.1	441	280	–,–	–	0	–	–	–	0.873	Galaxy,2MASS-3221, USNO-8341	–	–
013415.07+304748.8	442	282	–,–	141	0	0.4	–	1.2±0.7	7.88	–	–	–
013415.56+303259.9	443	–	–,–	–	0	0.9	6.35e-01	13.1±31.0	29.985	L10-107	–	–
013415.72+302745.4	444	283	255,217	–	0	1.4	6.00e-02	4.7±11.4	1.296	Galaxy,2MASS-2326, USNO-3733	–	–
013416.09+305025.6	445	–	–,–	–	0	0.9	–	2.6±3.1	1.318	–	–	–
013416.18+303808.9	446	284	–,–	–	0	2.1	9.92e-02	–	14.976	–	–	–
013416.32+305403.7	447	285	–,–	143	0	1.6	8.44e-01	2.0±0.9	1.036	–	–	–
013416.50+305156.5	448	286	256,220	142	0	1.4	–	3.3±3.2	2465.98	stellar,2MASS-2399, USNO-4125	–	–
013416.68+304410.7	449	–	–,–	144	0	2.1	–	12.2±40.2	2.31	–	–	–
013416.76+305101.8	450	287	258,219	145	2	2.4	3.93e-01	1.5±0.3	0.571	–	–	–
013416.87+304544.2	451	288	–,–	–	0	0.8	–	4.2±13.3	2.605	–	–	–
013417.08+303426.6	452	289	259,222	146	0	1.9	8.08e-02	1.7±0.5	28.364	stellar	–	–
013417.16+302616.5	453	290	–,–	–	0	0.8	–	–	-0.365	–	–	–
013417.17+304843.8	454	–	–,221	147	0	1.8	–	3.4±2.6	58.907	–	–	–
013417.56+302823.9	455	–	–,–	–	0	0.6	–	–	1.237	Galaxy,USNO-3396	–	–
013417.61+304123.3	456	–	–,–	148	0	2.8	2.71e-01	7.2±9.8	24.662	L10-111	–	–
013417.62+305649.8	457	291	–,–	–	0	–	–	–	0.973	2MASS-3122,USNO-7866	–	–
013417.65+303723.3	458	292	–,–	–	0	0.9	–	–	59.243	–	–	–
013417.77+305848.9	459	–	261,–	–	0	–	–	–	–	USNO-9606	–	–
013418.01+304208.9	460	–	–,–	–	0	0.9	–	–	2.417	–	–	–
013418.16+303516.0	461	293	–,–	–	0	0.8	–	6.9±10.0	8.346	stellar	–	–

Table 9—Continued

Source ID ^a	Src.	FLC	XMM	G05	Extent	Variability			$S_{H\alpha}$	Source type	Comments
	No.	No.	No.	No.	(6)	η	ξ	$\frac{flux_{max}}{flux_{min}}$	(10 ⁻¹⁷ erg s ⁻¹ cm ⁻² arcsec ⁻²)	(11)	(12)
(1)	(2)	(3)	(4)	(5)		(7)	(8)	(9)	(10)		
013418.22+302446.1	462	294	262,224	—	0	1.6	9.36e-02	2.1±0.8	-3.035	FS,2MASS-2775	—
013418.58+304710.1	463	—	—,—	—	0	0.5	—	2.3±3.4	5.053	—	—
013419.17+302907.1	464	—	—,—	—	0	0.5	—	—	0.811	—	—
013419.32+304942.4	465	295	265,—	150	0	2.2	8.43e-01	2.1±0.8	2.668	—	—
013419.71+304111.8	466	—	—,—	—	0	1.3	—	25.4±209.8	2.144	—	—
013419.77+303718.9	467	296	—,—	152	0	1.3	5.85e-01	—	6.403	—	—
013420.91+303319.0	468	—	—,—	—	0	8.5	5.21e-02	—	14.135	—	—
013420.96+305002.7	469	297	—,—	154	0	2.1	1.19e-01	2.5±1.3	2.089	—	—
013421.09+304932.3	470	298	268,230	156	0	2.0	6.54e-02	1.5±0.4	2.407	—	—
013421.15+303930.7	471	299	269,229	155	0	2.2	7.25e-01	2.4±1.2	2.401	—	—
013421.25+304335.4	472	300	—,—	—	0	3.0	—	—	76.03	stellar	trans. source?
013421.30+304051.8	473	—	—,—	—	0	1.7	—	25.1±212.8	4.842	—	—
013421.43+304449.0	474	301	—,—	157	0	1.4	—	4.2±5.6	7.883	—	—
013421.83+303618.2	475	302	—,—	—	0	0.8	—	—	2.155	stellar	—
013422.01+302915.4	476	—	—,—	—	0	2.0	—	15.4±57.7	1.488	—	—
013422.68+304623.9	477	—	—,—	—	0	1.2	—	—	6.6	—	—
013422.68+305504.1	478	—	—,—	—	0	2.1	9.44e-01	4.1±3.9	4.282	—	—
013423.22+302524.8	479	—	—,—	—	0	0.4	1.85e-01	2.4±4.1	6.863	L10-115	—
013423.27+305423.9	480	—	270,—	159	0	2.1	4.82e-02	4.5±4.6	7.532	L10-116	—
013423.68+303833.2	481	303	—,—	160	0	2.5	4.06e-02	3.8±2.8	0.467	—	—
013423.86+303847.6	482	304	272,231	161	0	1.8	1.17e-02	1.7±0.5	2.859	stellar	—
013424.55+304307.1	483	305	273,233	164	0	1.6	1.70e-01	1.8±0.7	2.378	—	—
013424.67+304022.0	484	306	—,—	—	0	1.4	—	—	1.498	—	—
013424.79+303914.1	485	307	—,—	166	0	0.7	3.71e-01	1.4±0.7	1.379	—	—
013424.85+303543.5	486	—	—,—	—	0	0.5	—	5.4±11.7	1.464	—	—
013424.94+302539.6	487	308	275,—	—	0	1.0	5.65e-01	2.1±1.2	-0.925	—	—
013425.33+304159.7	488	309	276,235	167	0	6.9	1.92e-01	7.5±3.7	1.384	—	—
013425.38+303131.5	489	310	—,—	—	0	0.9	8.36e-01	3.4±3.1	0.825	—	—
013425.43+305159.6	490	—	—,—	—	0	1.0	—	2.6±2.7	1.458	stellar,2MASS-2540, USNO-4858	—
013425.75+302817.9	491	311	277,237	168	0	1.6	4.59e-01	1.2±0.1	0.123	—	—
013425.80+305518.1	492	313	278,238	169	2	38.7	5.14e-02	3.0±0.1	-3.663	QSO/AGN?,X-9b, 2MASS-3001,	variable

Table 9—Continued

Source ID ^a (1)	Src. No. (2)	FLC No. (3)	XMM No. (4)	G05 No. (5)	Extent (6)	Variability			$S_{H\alpha}$ ($10^{-17} \text{ erg s}^{-1} \text{ cm}^{-2} \text{ arcsec}^{-2}$) (10)	Source type (11)	Comments (12)
						η (7)	ξ (8)	$\frac{\text{flux}_{\text{max}}}{\text{flux}_{\text{min}}}$ (9)			
USNO-7296											
013425.87+303316.8	493	312	279,239	—	0	2.0	1.12e-01	3.9 ± 1.8	4.867	L10-119	—
013426.11+303216.5	494	314	—,—	—	0	0.8	—	7.5 ± 11.1	0.197	—	—
013426.14+303726.6	495	315	—,—	—	0	1.8	—	—	0.377	—	—
013426.32+304324.8	496	—	—,—	—	0	1.7	—	—	2.761	—	—
013426.53+304446.2	497	316	282,240	171	0	2.8	1.13e-01	1.7 ± 0.3	11.539	—	—
013426.56+303738.1	498	317	283,243	172	0	2.1	4.56e-01	1.6 ± 0.4	0.642	—	—
013426.71+304812.8	499	318	284,242	173	0	0.2	1.82e-01	1.1 ± 0.3	5.607	non-stellar	—
013426.80+304050.4	500	—	—,—	—	0	1.4	—	256.7 ± 25412.6	3.778	—	—
013426.82+304803.6	501	—	—,—	—	0	1.4	—	—	4.224	—	—
013426.98+304313.4	502	319	286,244	174	0	4.3	2.27e-01	1.8 ± 0.2	2.938	—	—
013427.22+305151.9	503	—	—,—	—	0	1.7	—	146.2 ± 6480.3	4.842	—	—
013427.28+304421.9	504	320	—,—	175	0	1.6	1.97e-01	2.2 ± 1.2	7.349	—	—
013427.61+302921.0	505	321	—,—	—	0	0.3	7.65e-01	1.7 ± 4.2	0.062	—	—
013427.88+304138.1	506	—	—,—	—	0	1.0	—	9.0 ± 43.3	5.588	—	—
013428.21+303248.0	507	322	288,247	176	0	1.1	4.20e-01	1.3 ± 0.4	0.532	—	—
013428.24+304319.4	508	—	—,—	—	0	1.4	—	5.4 ± 9.9	2.168	—	—
013428.33+303653.3	509	—	—,—	—	0	1.2	—	—	1.501	—	—
013428.48+303301.5	510	323	—,—	—	0	1.0	—	—	—	FS,2MASS-1797, USNO-1775	—
013428.59+305548.1	511	—	—,—	—	0	—	4.50e-01	—	0.359	stellar	GC (ZKH08)
013428.69+304054.3	512	—	—,—	—	0	1.1	—	—	15.833	—	—
013428.87+303450.0	513	324	—,—	—	0	0.4	—	—	0.914	—	—
013428.94+303251.1	514	—	—,—	—	0	0.7	—	—	0.257	—	—
013429.01+304249.7	515	325	—,—	177	0	2.5	7.47e-01	3.4 ± 2.0	1.975	2MASS-1497	—
013429.10+304212.9	516	326	290,—	178	0	1.6	1.03e-01	1.8 ± 0.7	2.091	—	—
013429.74+305026.3	517	327	292,249	179	0	4.2	4.24e-01	2.7 ± 0.7	0.485	—	—
013429.95+305107.4	518	328	—,—	181	0	1.8	8.86e-03	2.7 ± 2.0	0.504	—	—
013430.14+303511.7	519	329	—,—	—	0	1.7	3.48e-01	2.9 ± 1.9	3.819	—	—
013430.36+303937.1	520	—	—,—	—	0	1.0	—	—	1.539	—	—
013430.49+305042.4	521	330	—,—	182	0	1.1	—	2.4 ± 2.1	1.49	—	—
013430.61+303259.7	522	331	—,—	—	0	1.1	—	2.5 ± 2.3	0.194	—	—
013430.91+304510.1	523	332	—,—	183	0	0.6	—	1.4 ± 0.7	1.255	—	—

Table 9—Continued

Source ID ^a	Src.	FLC	XMM	G05	Extent	Variability			$S_{H\alpha}$	Source type	Comments
	No.	No.	No.	No.	(6)	η	ξ	$\frac{flux_{max}}{flux_{min}}$	(10 ⁻¹⁷ erg s ⁻¹ cm ⁻² arcsec ⁻²)		
(1)	(2)	(3)	(4)	(5)	(6)	(7)	(8)	(9)	(10)	(11)	(12)
013431.62+302927.1	524	—	-,250	—	0	0.6	—	—	0.794	—	—
013431.71+304128.0	525	—	-,—	—	0	0.7	—	2.1±2.3	9.282	—	—
013431.86+304110.1	526	—	-,—	—	0	1.1	—	8.8±51.3	7.828	—	—
013431.87+304011.7	527	—	-,—	—	0	1.3	—	4.6±7.3	3.231	—	—
013432.02+303454.1	528	333	293,251	184	2	2.6	4.20e-02	1.3±0.1	2.546	—	—
013432.11+302538.6	529	—	-,—	—	0	0.8	—	1.7±1.2	-0.428	—	—
013432.16+305158.7	530	334	294,252	185	2	5.7	8.09e-02	1.9±0.3	-0.255	Galaxy,2MASS-2670, USNO-5534	—
013432.23+304958.9	531	—	-,—	187	0	1.6	—	3.9±4.3	2.029	—	—
013432.26+303201.2	532	335	-,—	186	0	1.3	1.41e-01	5.4±4.7	0.65	—	—
013432.56+303436.8	533	336	296,—	190	2	1.3	3.23e-01	1.8±0.6	0.804	—	—
013432.59+305035.4	534	338	295,—	189	0	1.0	6.45e-02	1.4±0.4	0.982	—	—
013432.60+304704.1	535	339	299,254	—	2	1.6	1.18e-01	1.7±0.6	5558.595	stellar,2MASS-2020	star cluster in NGC604
013432.65+304318.5	536	337	-,—	—	0	2.9	6.68e-02	—	3.184	—	—
013432.74+303930.1	537	340	-,—	188	0	0.5	—	1.3±0.7	1.544	—	—
013432.98+303857.4	538	341	298,—	—	0	1.1	1.41e-02	1.4±0.4	1.048	—	—
013433.02+304639.1	539	342	-,—	191	2	1.6	3.37e-01	2.0±0.8	502.389	L10-124	—
013433.64+305459.6	540	—	-,—	192	0	—	3.61e-01	—	0.153	—	—
013433.88+304652.7	541	—	-,—	—	0	2.3	—	20.3±73.8	1057.658	—	diffuse X-ray em. in NGC604
013434.30+304701.7	542	—	-,—	—	0	2.4	—	—	622.693	—	diffuse X-ray em. in NGC604
013434.60+305132.5	543	—	-,—	—	0	1.3	5.97e-01	1.9±0.9	-0.076	—	—
013435.06+304439.3	544	343	303,—	197	0	2.6	8.77e-02	2.0±0.5	7.226	—	—
013435.09+304712.0	545	—	-,—	198	0	1.2	—	2.6±2.3	113.57	—	diffuse X-ray em. in NGC604
013435.14+305646.1	546	—	304,258	200	0	—	—	—	18.529	2MASS-3389, USNO-9246	—
013435.32+303726.9	547	—	-,—	—	0	0.2	—	1.2±1.3	1.059	—	—
013435.38+304946.7	548	344	-,—	201	0	1.4	1.83e-01	2.2±1.6	1.994	—	—
013435.40+305212.6	549	—	-,—	202	0	0.4	1.07e-01	1.4±1.0	2.24	L10-125	—
013435.50+303352.4	550	—	-,—	—	0	0.8	—	—	0.505	—	—

Table 9—Continued

Source ID ^a	Src.	FLC	XMM	G05	Extent	Variability			$S_{H\alpha}$	Source type	Comments
	No.	No.	No.	No.	(6)	η	ξ	$\frac{flux_{max}}{flux_{min}}$	($10^{-17} \text{ erg s}^{-1} \text{ cm}^{-2} \text{ arcsec}^{-2}$)	(11)	(12)
(1)	(2)	(3)	(4)	(5)		(7)	(8)	(9)	(10)		
013436.01+304542.5	551	—	—,—	—	0	1.3	—	—	9.028	—	—
013436.04+303450.0	552	345	305,259	203	2	2.6	1.62e-02	1.6±0.2	2.166	—	—
013436.43+304713.8	553	346	306,260	204	0	5.0	8.63e-02	2.4±0.4	20.146	—	—
013436.67+304315.6	554	—	—,—	205	0	1.1	—	2.8±3.0	2.851	—	—
013436.76+303307.0	555	347	—,—	—	0	3.0	7.74e-01	11.6±22.2	1.237	—	—
013436.91+304552.3	556	—	—,—	—	0	0.9	—	9.6±68.9	8.666	—	—
013437.17+302927.7	557	348	—,—	—	0	0.9	—	5.1±5.8	-0.555	—	—
013437.53+304551.5	558	—	—,—	—	0	0.8	—	2.6±3.2	5.022	—	—
013437.74+303721.5	559	349	—,—	—	0	0.2	—	1.1±0.7	0.618	—	—
013438.72+304539.3	560	350	309,265	207	0	2.5	1.74e-02	1.3±0.2	4.612	—	—
013438.83+305504.4	561	351	310,266	208	0	11.9	1.23e-01	1.5±0.1	1.564	QSO/AGN,X-9a, USNO-8297	variable
013438.89+304117.4	562	—	—,—	210	0	2.2	4.49e-01	6.5±7.4	136.768	—	—
013439.66+304110.6	563	—	—,—	—	0	1.2	—	2.8±2.7	18.895	—	—
013439.69+302950.7	564	352	311,268	—	0	0.6	2.51e-04	1.6±0.9	-0.126	—	—
013439.84+305144.3	565	353	312,267	211	0	0.7	1.39e-01	1.1±0.2	5.002	QSO/AGN	—
013440.18+305050.6	566	—	—,—	—	0	1.6	—	6.8±11.9	1.69	—	—
013440.42+304154.5	567	—	—,—	—	0	2.6	—	—	59.568	—	—
013440.48+303954.9	568	—	—,—	—	0	0.9	—	3.3±5.4	3364.161	FS,2MASS-1853, USNO-1942	—
013440.63+304513.2	569	—	—,—	—	0	1.8	—	—	1.313	—	—
013440.73+304336.4	570	—	—,—	—	0	1.1	8.76e-01	4.0±8.6	118.794	L10-128,USNO-2442	contaminated by L10-129
013440.81+304410.2	571	354	—,—	212	0	2.2	4.45e-02	2.7±1.3	5.057	—	—
013441.10+304328.3	572	355	314,269	214	2	1.8	1.38e-01	2.0±0.9	106.161	L10-129	contaminated by L10-128
013441.26+303516.4	573	356	—,—	—	0	1.6	5.91e-01	1.7±0.6	1.046	—	—
013441.32+303921.8	574	—	315,—	—	0	2.5	2.40e-01	3.8±3.2	1.48	—	—
013441.43+303415.7	575	357	—,—	—	0	0.9	6.38e-02	1.5±0.7	-0.088	USNO-2946	—
013442.07+305228.8	576	358	317,271	216	0	1.8	2.33e-01	1.6±0.4	0.489	—	—
013442.43+305249.5	577	359	319,274	217	0	6.1	4.02e-02	2.8±0.5	-0.729	QSO/AGN	—
013442.70+304927.5	578	—	—,—	218	0	0.4	—	1.7±2.4	4.679	—	—
013442.79+304505.6	579	360	321,275	220	0	4.2	3.42e-01	2.0±0.3	1.225	—	—

| 178 |

Table 9—Continued

Source ID ^a (1)	Src. No. (2)	FLC No. (3)	XMM No. (4)	G05 No. (5)	Extent (6)	Variability			$S_{H\alpha}$ ($10^{-17} \text{ erg s}^{-1} \text{ cm}^{-2} \text{ arcsec}^{-2}$) (10)	Source type (11)	Comments (12)
						η (7)	ξ (8)	$\frac{\text{flux}_{\text{max}}}{\text{flux}_{\text{min}}}$ (9)			
013442.92+304459.8	580	—	—,—	—	0	—	—	—	1.139	—	—
013443.00+303423.0	581	—	—,—	—	0	0.8	—	1.5 ± 0.8	0.446	—	—
013443.12+304948.6	582	—	—,—	221	0	3.2	9.25 ± 0.01	—	-0.059	—	—
013443.41+304808.7	583	361	—,—	—	0	3.6	5.03 ± 0.02	18.3 ± 28.9	1.09	—	—
013444.02+303906.6	584	—	—,—	—	0	0.4	—	1.5 ± 1.4	0.309	—	—
013444.23+304920.3	585	362	—,—	223	2	4.8	3.36 ± 0.06	2.2 ± 0.4	85.209	FS,2MASS-2630, USNO-5348	—
013444.38+304702.9	586	363	—,—	222	0	2.3	4.85 ± 0.01	2.1 ± 0.7	6.981	—	—
013444.62+305535.0	587	—	322,276	224	0	—	1.79 ± 0.01	—	-0.336	—	—
013444.71+303732.9	588	—	—,—	—	0	0.6	—	1.5 ± 0.9	0.01	USNO-2664	—
013444.99+304927.7	589	364	323,277	—	2	3.6	2.24 ± 0.01	1.4 ± 0.1	1.215	XRB	PMH04
013445.34+303539.4	590	—	—,—	—	0	1.4	—	—	9.6	non-stellar	—
013445.62+302559.5	591	—	—,—	—	0	—	—	—	-0.593	—	pos. uncertain
013445.76+303138.8	592	365	—,—	—	0	0.8	5.08 ± 0.01	1.6 ± 1.0	0.147	—	—
013446.78+304448.9	593	366	—,—	226	0	3.8	4.35 ± 0.02	4.1 ± 1.9	1.25	—	—
013447.35+304001.3	594	367	326,282	227	0	1.4	5.28 ± 0.01	1.4 ± 0.4	0.778	—	—
013447.62+303514.3	595	368	327,280	—	0	0.4	1.63 ± 0.02	1.1 ± 0.2	0.578	—	—
013448.12+303714.4	596	369	329,—	—	0	0.0	5.93 ± 0.01	1.0 ± 0.4	0.703	—	—
013448.37+304313.2	597	370	—,—	—	0	2.2	7.14 ± 0.01	3.6 ± 2.5	0.574	—	—
013448.63+303627.0	598	—	—,—	—	0	1.2	—	1.9 ± 1.0	-0.041	—	—
013448.63+304706.7	599	—	—,—	229	0	1.0	—	2.2 ± 1.7	2.495	—	—
013449.00+303328.6	600	371	331,284	—	0	2.2	2.32 ± 0.02	1.2 ± 0.1	-1.036	USNO-4451	—
013449.04+304446.8	601	372	330,283	230	0	0.8	1.86 ± 0.01	1.2 ± 0.2	1.606	—	—
013449.36+303857.0	602	—	—,—	—	0	0.1	—	1.1 ± 0.8	-0.443	—	—
013449.51+305011.9	603	—	—,—	232	0	—	—	—	-0.702	—	—
013449.58+303935.0	604	—	—,—	—	0	0.3	—	1.6 ± 2.7	0.238	—	—
013450.35+303452.5	605	—	—,—	—	0	0.3	—	1.3 ± 1.1	0.578	—	—
013450.40+303545.3	606	373	333,—	—	0	0.5	1.36 ± 0.01	1.1 ± 0.4	1.779	—	—
013451.01+303226.5	607	—	—,—	—	0	1.1	5.81 ± 0.01	1.7 ± 0.8	-0.197	—	—
013451.10+304356.7	608	374	334,286	233	0	0.5	4.43 ± 0.01	1.1 ± 0.2	0.702	—	—
013451.31+303444.1	609	—	—,—	—	0	0.6	—	1.6 ± 1.3	-0.206	—	—
013451.37+302841.0	610	375	—,—	—	0	—	—	—	0.697	—	—
013451.73+303745.9	611	—	—,—	—	0	0.6	—	2.0 ± 2.3	-0.073	—	—

Table 9—Continued

Source ID ^a	Src.	FLC	XMM	G05	Extent	Variability			$S_{H\alpha}$	Source type	Comments
	No.	No.	No.	No.	(6)	η	ξ	$\frac{flux_{max}}{flux_{min}}$	($10^{-17} \text{ erg s}^{-1} \text{ cm}^{-2} \text{ arcsec}^{-2}$)	(11)	(12)
(1)	(2)	(3)	(4)	(5)		(7)	(8)	(9)	(10)		
013451.85+302909.7	612	376	335,288	—	0	12.5	6.62e-10	1.2 ± 0.1	0.176	XRB?,X-10	—
013451.94+304615.8	613	377	336,287	235	0	—	5.73e-02	—	1.126	non-stellar,USNO-5061	—
013452.00+303547.6	614	—	—,—	—	0	2.2	5.42e-01	3.0 ± 1.7	2.541	Galaxy,USNO-4258	—
013452.24+305309.2	615	—	—,—	236	0	—	1.74e-01	—	-1.233	stellar,USNO-8606	—
013452.34+305038.4	616	—	—,—	237	0	—	—	—	0.002	—	—
013452.52+304242.5	617	—	—,—	238	0	1.2	—	2.5 ± 2.3	3.076	—	—
013452.89+302809.5	618	378	337,289	—	0	—	—	—	—	FS,2MASS-3019, USNO-7388	—
013453.25+305717.7	619	—	338,290	239	0	—	—	—	-0.955	—	—
013453.81+303341.8	620	—	—,—	—	0	0.2	—	1.2 ± 1.0	0.902	—	—
013454.94+303248.9	621	379	—,—	—	0	0.1	8.42e-01	1.0 ± 0.3	0.117	—	—
013455.30+304624.3	622	380	—,—	241	0	—	2.64e-02	—	-0.03	—	—
013455.90+304814.5	623	381	—,—	242	0	—	—	—	0.146	—	—
013456.08+304237.9	624	—	—,—	—	0	1.8	—	51.1 ± 779.6	2.284	—	—
013456.26+304139.4	625	—	—,—	242	0	1.6	8.78e-01	3.2 ± 2.9	4.32	—	—
013457.21+303825.5	626	382	340,293	—	0	0.5	2.97e-01	1.1 ± 0.3	-1.216	QSO/AGN	—
013457.33+304319.4	627	—	—,—	246	0	0.5	—	1.4 ± 1.0	1.118	—	—
013457.76+304247.9	628	383	—,—	247	0	0.8	1.10e-01	1.4 ± 0.6	2.582	—	—
013458.06+303637.5	629	—	—,—	—	0	0.3	—	1.3 ± 1.0	0.013	—	—
013458.51+304707.1	630	384	341,294	248	0	—	9.77e-01	—	0.812	—	—
013459.25+304607.6	631	—	—,—	249	0	—	—	—	0.22	Galaxy,USNO-6196	—
013459.65+303833.6	632	385	—,—	—	0	0.2	—	1.1 ± 0.6	-0.575	—	—
013500.54+305028.7	633	386	342,295	250	0	—	2.07e-01	—	3.763	USNO-8197	—
013500.76+304952.7	634	—	343,296	—	0	—	—	—	1.324	USNO-7884	—
013500.97+304348.1	635	387	344,297	251	0	4.2	4.26e-02	1.6 ± 0.2	1.563	non-stellar,USNO-5859	—
013501.09+304847.4	636	—	—,—	—	0	—	—	—	0.141	—	—
013502.58+303849.8	637	—	—,—	—	0	1.5	—	2.7 ± 2.1	0.125	—	—
013502.70+303950.1	638	—	—,—	—	0	0.5	—	1.4 ± 0.8	4.776	—	—
013502.80+303710.8	639	388	348,300	—	0	2.8	1.05e-01	1.7 ± 0.3	4.963	—	—
013503.04+303340.7	640	389	349,301	—	0	—	—	—	32.367	FS,2MASS-2876, USNO-6648	—
013503.28+304559.1	641	—	—,—	—	0	—	—	—	-0.635	—	—
013503.46+304033.8	642	—	—,—	—	0	1.4	5.18e-01	2.1 ± 1.2	7.237	—	—

Table 9—Continued

Source ID ^a	Src.	FLC	XMM	G05	Extent	Variability			$S_{H\alpha}$	Source type	Comments
	No.	No.	No.	No.		η	ξ	$\frac{flux_{max}}{flux_{min}}$	($10^{-17} \text{ erg s}^{-1} \text{ cm}^{-2} \text{ arcsec}^{-2}$)	(11)	(12)
(1)	(2)	(3)	(4)	(5)	(6)	(7)	(8)	(9)	(10)	(11)	(12)
013504.54+304443.0	643	—	—,—	—	0	—	—	—	1.154	—	—
013504.72+304054.9	644	—	—,—	—	0	0.6	—	1.5 ± 0.9	3.949	—	—
013504.75+303919.1	645	—	—,—	—	0	0.1	6.63×10^{-2}	1.0 ± 0.4	0.276	—	—
013504.78+305034.5	646	—	—,—	253	0	—	—	—	0.456	—	pos. uncertain
013504.99+303445.5	647	390	350,302	—	0	1.2	2.20×10^{-3}	1.1 ± 0.1	-1.156	USNO-6681	—
013505.66+305006.4	648	391	351,304	254	0	—	1.17×10^{-1}	—	0.378	—	—
013505.83+305428.9	649	—	353,—	255	0	—	—	—	-0.508	—	—
013507.31+305208.8	650	—	355,306	256	0	—	—	—	0.103	—	—
013507.51+304636.5	651	—	—,—	—	0	—	—	—	-11.783	—	—
013507.75+304009.4	652	—	—,—	—	0	1.3	7.77×10^{-1}	2.0 ± 1.2	0.054	—	—
013508.44+303150.4	653	392	359,309	—	0	—	—	—	-0.418	FS	—
013509.10+304341.8	654	393	—,—	—	0	—	—	—	1.025	XRT-7	trans. source
013509.30+304108.4	655	—	—,—	—	0	—	4.28×10^{-2}	—	1.7	—	—
013509.55+303600.6	656	394	—,—	—	0	—	—	—	0.121	USNO-7190	—
013511.08+304256.9	657	—	—,—	257	0	—	—	—	1.146	—	—
013512.72+304515.8	658	—	367,—	258	0	—	—	—	1.996	—	—
013517.08+304409.3	659	—	—,—	259	0	—	—	—	—	—	—
013517.38+303601.5	660	—	376,321	260	0	—	—	—	—	—	pos. uncertain
013517.47+304446.7	661	—	377,322	261	0	—	—	—	—	—	—
013520.83+304237.0	662	—	—,—	—	0	—	—	—	—	—	pos. uncertain

(1)–(2): ChASeM33 source ID and number. (3)–(5): Matched source numbers in the FLC (Plucinsky et al. 2008), the *XMM-Newton* source catalogs from PMH04 and MPH06, and the *Chandra* source catalog from G05, respectively. (6): Estimate whether the source is possibly extended (=2), extended (=1), or not extended (=0). (7): η is the 5σ variability index and is sensitive to long-term variability. Sources with variability indices of $\eta \geq 5.0$ are highly likely to show long-term variability and are shown in boldface. (8): ξ is the KS probability of the source being constant within a single observation (short-term variability). Sources with KS probabilities of $\xi \leq 5.7 \times 10^{-7}$ are highly likely to show short-term variability and are shown in boldface (see section 3.4). (9): Variability factor expressed as the ratio of $flux_{max}/flux_{min}$ with 1σ uncertainties. (10): $H\alpha$ surface brightness measured from LGGS survey data (Massey et al. 2006) and extracted from circular regions with a radius of $2''$. Empty entries indicate that the source either did not lie inside the central LGGS field or is coincident with a foreground star. Any values $< 5 \times 10^{-17} \text{ erg cm}^{-2} \text{ s}^{-1} \text{ arcsec}^{-2}$ are probably consistent with zero. (11): Source classification and aliases using the USNO-b1.0 catalog (Monet et al. 2003) and the 2MASS catalog (Cutri et al. 2003). We discern the following types of sources: (a) foreground stars (FS), (b) stellar sources in M 33, (c) galaxies, (d) QSOs/AGN, (e) non-stellar sources, (f) SNRs (labeled 'L10-XXX'), (g) XRBs, and (h) transient sources (labeled 'XRT'). For the transients and the SNRs we use data from the ChASeM33 transient search (Williams et al. 2008) as well as from the ChASeM33 SNR catalog (Long et al. 2010). The classification of classes (a)–(e) is based on MMT follow-up spectroscopy and multi-wavelength data (see section 3.2). (12): Special remarks.

Table 10: Cross identifications of supersoft sources

Source ID	PMH04 Comments	Source ID	MPH06 Comments	Source ID	ChASeM33 Comments
52	01:32:38.01 +30:39:02.5	48	01:32:37.91 +30:39:03.7	–	not detected, at border of FOV
–		86	01:32:59.11 +30:35:45.5 only in one ObsID	–	not detected
–		92	01:33:01.94 +31:00:25.9 only in one ObsID	–	outside FOV
109	01:33:04.76 +30:21:07.0	96	01:33:04.75 +30:21:08.9 highly variable	–	outside FOV
–		130	01:33:28.65 +31:04:35.3 only in one ObsID	–	outside FOV
223	01:33:57.63 +30:33:20.3 diffuse emission, no point source	–		–	not detected
247	01:34:09.99 +30:32:21.0	207	01:34:09.87 +30:32:21.4 XRT 6 (Williams et al. 2008)	–	not detected
–		214	01:34:13.47 +30:37:10.1 only in one ObsID	–	not detected
–		264	01:34:38.58 +30:53:23.2 only in one ObsID	–	not detected
332	01:34:49.42 +30:48:09.5	285	01:34:49.35 +30:48:06.3	–	not detected
–		292	01:34:56.62 +30:56:03.0 only in one ObsID	–	not detected, at border of FOV
–		316	01:35:15.45 +30:39:17.9 only in one ObsID	–	not detected, at border of FOV

REFERENCES

- Alexander, D. M., et al. 2003, AJ, 126, 539
- Broos, P. S., Townsley, L. K., Getman, K., & Bauer, F. E. 2002, ACIS Extract, An ACIS Point Source Extraction Package (University Park: Pennsylvania State Univ.) http://www.astro.psu.edu/xray/docs/TARA/ae_users_guide.html
- Broos, P. S., Townsley, L. K., Feigelson, E. D., Getman, K. V., Bauer, F. E., & Garmire, G. P. 2010, ApJ, 714, 1582
- Capaccioli, M., della Valle, M., Rosino, L., & D'Onofrio, M. 1989, AJ, 97, 1622
- Cappelluti, N., et al. 2009, A&A, 497, 635
- Corbelli, E. 2003, MNRAS, 342, 199
- Cutri, R. M., et al. 2003, The IRSA 2MASS All-Sky Point Source Catalog, NASA/IPAC Infrared Science Archive. <http://irsa.ipac.caltech.edu/applications/Gator/>
- Dalton, W. W., & Sarazin, C. L. 1995, ApJ, 440, 280
- Dickey, J. M., & Lockman, F. J. 1990, ARA&A, 28, 215
- Dubus, G., & Rutledge, R. E. 2002, MNRAS, 336, 901
- Dubus, G., Charles, P. A., & Long, K. S. 2004, A&A, 425, 95
- Fabricant, D. G., Kurtz, M. J., Geller, M. J., Caldwell, N., Woods, D., & Dell'Antonio, I. 2008, PASP, 120, 1222
- Freedman, W. L., Madore, B. F., Gibson, B. K., Ferrarese, L., Kelson, D. D., Sakai, S., Mould, J. R., Kennicutt, R. C., Ford, H. C., Graham, J. A., Huchra, J. P., Hughes, S. M. G., Illingworth, G. D., Macri, L. M., & Stetson, P. B. 2001, ApJ, 553, 47
- Freeman, P. E., Kashyap, V., Rosner, R., & Lamb, D. Q. 2002, ApJS, 138, 185
- Gaetz, T. J., et al. 2007, ApJ, 663, 234
- Gehrels, N. 1986, ApJ, 303, 336
- Georgakakis, A., Nandra, K., Laird, E. S., Aird, J., & Trichas, M. 2008, MNRAS, 388, 1205
- Gilfanov, M. 2004, MNRAS, 349, 146

- Gordon, S. M., Kirshner, R. P., Long, K. S., Blair, W. P., Duric, N., & Smith, R. C. 1998, ApJS, 117, 89
- Grimm, H.-J., Gilfanov, M., & Sunyaev, R. 2002, A&A, 391, 923
- Grimm, H.-J., Gilfanov, M., & Sunyaev, R. 2003, MNRAS, 339, 793
- Grimm, H.-J., McDowell, J., Zezas, A., Kim, D.-W., & Fabbiano, G. 2005, ApJS, 161, 271 [G05]
- Haberl, F., & Pietsch, W. 2001, A&A, 373, 438 [HP01]
- Hammer, F., Puech, M., Chemin, L., Flores, H., & Lehnert, M. D. 2007, ApJ, 662, 322
- Harrison, F. A., Eckart, M. E., Mao, P. H., Helfand, D. J., & Stern, D. 2003, ApJ, 596, 944
- Hartman, J. D., Bersier, D., Stanek, K. Z., Beaulieu, J.-P., Kaluzny, J., Marquette, J.-B., Stetson, P. B., & Schwarzenberg-Czerny, A. 2006, MNRAS, 371, 1405
- Joye, W. A., & Mandel, E. 2003, Astronomical Data Analysis Software and Systems XII, 295, 489
- Kahabka, P., Pietsch, W., Filipović, M. D., & Haberl, F. 1999, A&AS, 136, 81
- Kim, M., et al. 2007, ApJS, 169, 401
- Kong, A. K. H., Garcia, M. R., Primini, F. A., Murray, S. S., Di Stefano, R., & McClintock, J. E. 2002, ApJ, 577, 738
- Kuntz, K., et al. 2011, in prep.
- Kuntz, K. D., & Snowden, S. L. 2010, ApJS, 188, 46
- La Parola, V., Damiani, F., Fabbiano, G., & Peres, G. 2003, ApJ, 583, 758
- Long, K. S., Dodorico, S., Charles, P. A., & Dopita, M. A. 1981, ApJ, 246, L61
- Long, K. S., Charles, P. A., Blair, W. P., & Gordon, S. M. 1996, ApJ, 466, 750
- Long, K. S., et al. 2010, ApJS, 187, 495 [L10]
- Markert, T. H., & Rallis, A. D. 1983, ApJ, 275, 571
- Massey, P., Olsen, K. A. G., Hodge, P. W., Strong, S. B., Jacoby, G. H., Schlingman, W., & Smith, R. C. 2006, AJ, 131, 2478

- McNeil, E. K. & Winkler, P. F. 2006, in Bull. AAS 39, 80
- Misanovic, Z., Pietsch, W., Haberl, F., Ehle, M., Hatzidimitriou, D., & Trinchieri, G. 2006, A&A, 448, 1247 [MPH06]
- Monet, D. G., et al. 2003, AJ, 125, 984
- Nandra, K., et al. 2005, MNRAS, 356, 568
- Newton, K. 1980, MNRAS, 190, 689
- Orosz, J.-A., et al. 2007, Nature, 449, 872
- Park, T., Kashyap, V. L., Siemiginowska, A., van Dyk, D. A., Zezas, A., Heinke, C., & Wargelin, B. J. 2006, ApJ, 652, 610
- Pence, W. D., Snowden, S. L., Mukai, K., & Kuntz, K. D. 2001, ApJ, 561, 189
- Pietsch, W., Misanovic, Z., Haberl, F., Hatzidimitriou, D., Ehle, M., & Trinchieri, G. 2004, A&A, 426, 11 [PMH04]
- Pietsch, W., Haberl, F., Sasaki, M., Gaetz, T. J., Plucinsky, P. P., Ghavamian, P., Long, K. S., & Pannuti, T. G. 2006, ApJ, 646, 420
- Pietsch, W., et al. 2009, ApJ, 694, 449
- Plucinsky, P. P., et al. 2008, ApJS, 174, 366
- Prestwich, A. H., Kilgard, R. E., Primini, F., McDowell, J. C., & Zezas, A. 2009, ApJ, 705, 1632
- Robitaille, T. P., & Whitney, B. A. 2010, ApJ, 710, L11
- Rosolowsky, E., & Simon, J. D. 2008, ApJ, 675, 1213
- Smith, L. F., Biermann, P., & Mezger, P. G. 1978, A&A, 66, 65
- Smith, R. K., Brickhouse, N. S., Liedahl, D. A., & Raymond, J. C. 2001, ApJ, 556, L91
- Sarajedini, A., & Mancone, C. L. 2007, AJ, 134, 447 [SM07]
- Schulman, E., & Bregman, J. N. 1995, ApJ, 441, 568
- Supper, R., Hasinger, G., Lewin, W. H. G., Magnier, E. A., van Paradijs, J., Pietsch, W., Read, A. M., & Trümper, J. 2001, A&A, 373, 63

- Trinchieri, G., Fabbiano, G., & Peres, G. 1988, ApJ, 325, 531
- Tüllmann, R., et al. 2008, ApJ, 685, 919
- Tüllmann, R., et al. 2009, ApJ, 707, 1361
- Verley, S., Corbelli, E., Giovanardi, C., & Hunt, L. K. 2009, A&A, 493, 453
- Weng, S.-S., Wang, J.-X., Gu, W.-M., & Lu, J.-F. 2009, PASJ, 61, 1287
- Williams, B. F., et al. 2008, ApJ, 680, 1120 [W08]
- Wilms, J., Allen, A., & McCray, R. 2000, ApJ, 542, 914
- Zaritsky, D., Elston, R., & Hill, J. M. 1989, AJ, 97, 97
- Zezas, A., Fabbiano, G., Baldi, A., Schweizer, F., King, A. R., Rots, A. H., & Ponman, T. J. 2007, ApJ, 661, 135
- Zloczewski, K., Kaluzny, J., & Hartman, J. 2008, Acta Astronomica, 58, 23 [ZKH08]